

**MASSIVELY PARALLEL TRANSPOSON  
MUTAGENESIS TO IDENTIFY  
RELATIONSHIPS BETWEEN BIOFILM  
FORMATION AND EFFLUX ACTIVITY IN  
ENTEROBACTERIACEAE**

Emma Rachel Holden

September 2021

60,395 words

A thesis submitted for the degree of Doctor of Philosophy

Quadram Institute Bioscience

University of East Anglia

"This copy of the thesis has been supplied on condition that anyone who consults it is understood to recognise that its copyright rests with the author and that use of any information derived therefrom must be in accordance with current UK Copyright Law. In addition, any quotation or extract must include full attribution."

**Abstract:**

Bacteria are usually found as part of structured, aggregated communities called biofilms. Progression through the biofilm life cycle requires temporally controlled gene expression to maximise fitness at each stage. Previous work identified that inhibition or deletion of efflux activity resulted in a severe reduction in biofilm formation, however the mechanism through which this occurs has not yet been described. In this work, I used TraDIS-*Xpress*; a massively parallel transposon mutagenesis approach to assay the impact of disruption or altered expression of all genes in the genome on biofilm formation and efflux activity in *Escherichia coli* and *Salmonella* Typhimurium. Pathways involved in biofilm formation in both species included fimbriae regulation and biosynthesis of flagella, nucleotides, curli and LPS. I identified genes with temporal contributions to biofilm fitness where their expression changed between being beneficial or detrimental depending on the stage at which they were expressed. Additionally, I characterised several genes in both *E. coli* and *S. Typhimurium* that had novel contributions to biofilm development. Efflux activity in both species was investigated in a similar way and identified genes involved in protein chaperoning, DNA housekeeping and signalling benefitted efflux in both species. Comparison of the genes and pathways involved in both biofilm development and efflux activity in both species revealed the importance of genes involved in DNA housekeeping, protein chaperoning, transcriptional regulation and stress responses. Overall, no one pathway was found to be the sole cause of the deficit in biofilm biomass seen in an efflux-deficient mutant. Therefore, it is most likely that disruption of efflux activity results in multiple pathways being altered, each of which impact biofilm matrix production to some degree. This work provides new insights into the requirements for successful biofilm formation through time and furthers our understanding of how biofilm development is affected by antimicrobial stress.

## **Acknowledgements**

A big thanks goes to my supervisor Mark Webber. Without his constant support, guidance, encouragement and trust I would not have started, let alone finished, this PhD. I will forever be thankful for the countless opportunities he has given me and for making me the researcher I am today. I also want to thank Eleftheria Trampari for her guidance and support, as well as passing on all her knowledge and skills in molecular biology, for which I will always be grateful. I feel extremely lucky to have worked alongside both Mark and Eleftheria, and even luckier to have found friends in them both. Special thanks go to John Wain, who's insight has been extremely valuable throughout the past four years.

I have been incredibly lucky to have worked with an amazing team of researchers during my PhD who have kept me going through everything: Heather, Maria, Iliana, Emma, Keith, Yasir, Nick, Rachel, Dheeraj, Nabil, Claire, Gaetan, and a special mention to my PhD brother and partner-in-crime Gregory Wickham. I'd also like to thank Jess Blair from the University of Birmingham for her support from the very beginning of my project. I want to thank everyone in the Quadram Institute and the Norwich Research Park who has helped me either with my science or just by cheering me up. There are far too many to name, as everyone has been so lovely, and I am grateful for them all.

Massive thanks to my family: to Mum and Dad, for their love, support, and for trying to understand my work; and to Ben for keeping me grounded in a way only a brother can. Thanks to all my friends from my time in Norwich, Bristol, Weston-super-mare, Cornwall, India, South Korea and Taiwan for keeping me going and distracting me from science when I needed it the most.

My time at the Quadram Institute has been so rewarding and so much fun. The people here have made these past four years so enjoyable, and I feel extremely fortunate to have worked alongside them.

## **Access Condition and Agreement**

Each deposit in UEA Digital Repository is protected by copyright and other intellectual property rights, and duplication or sale of all or part of any of the Data Collections is not permitted, except that material may be duplicated by you for your research use or for educational purposes in electronic or print form. You must obtain permission from the copyright holder, usually the author, for any other use. Exceptions only apply where a deposit may be explicitly provided under a stated licence, such as a Creative Commons licence or Open Government licence.

Electronic or print copies may not be offered, whether for sale or otherwise to anyone, unless explicitly stated under a Creative Commons or Open Government license. Unauthorised reproduction, editing or reformatting for resale purposes is explicitly prohibited (except where approved by the copyright holder themselves) and UEA reserves the right to take immediate 'take down' action on behalf of the copyright and/or rights holder if this Access condition of the UEA Digital Repository is breached. Any material in this database has been supplied on the understanding that it is copyright material and that no quotation from the material may be published without proper acknowledgement.



## Table of Contents

<b>1. CHAPTER 1: INTRODUCTION .....</b>	<b>24</b>
1.1. Biofilms .....	25
1.1.1. <i>S. Typhimurium</i> and <i>E. coli</i> biofilms .....	26
1.1.2. Curli .....	28
1.1.3. Cellulose .....	31
1.1.4. Other important components of the biofilm .....	33
1.2. Regulation of biofilm formation in <i>E. coli</i> and <i>S. Typhimurium</i> .....	33
1.2.1. Cyclic-di-GMP .....	33
1.2.2. RpoS/ $\sigma^S$ .....	35
1.2.3. EnvZ/OmpR .....	36
1.2.4. CpxA/CpxR .....	37
1.2.5. H-NS .....	38
1.2.6. IHF .....	39
1.2.7. Rcs .....	39
1.3. Efflux Pumps and their regulation .....	41
1.3.1. AcrAB-TolC .....	42
1.3.2. MarA, RamA and SoxS .....	43
1.4. How is biofilm formation affected by efflux activity? .....	45
1.4.1. EnvZ-OmpR .....	46
1.4.2. PdeC .....	46
1.4.3. TomB .....	47
1.5. Aims and Objectives .....	48
<b>2. CHAPTER 2: MATERIALS AND METHODS .....</b>	<b>49</b>
2.1. Bacteria .....	50
2.2. General microbiology techniques .....	52
2.3. Molecular Biology methods .....	52
2.3.1. PCR .....	52
2.3.2. Phenol-chloroform DNA Purification .....	53
2.3.3. Agarose gel electrophoresis .....	53
2.3.4. Digestions and ligations .....	54
2.3.5. Competent cells and transformations .....	54
2.3.6. Genomic DNA extraction .....	55
2.3.7. Constructing single gene deletion mutants and chromosomal integrations in <i>S. Typhimurium</i> .....	55
2.4. Plasmids .....	57
2.5. Primers .....	58
2.6. Antimicrobial susceptibility testing .....	68

2.7.	Biofilm assays .....	68
2.7.1.	Crystal violet biofilm assay .....	68
2.7.2.	Congo red and calcofluor biofilm assays .....	69
2.7.3.	Aggregation assay .....	69
2.7.4.	Bioflux .....	<b>Error! Bookmark not defined.</b>
2.8.	Growth kinetics .....	69
2.9.	Membrane permeability assays .....	69
2.10.	RT-PCR .....	70
2.11.	Competition assay .....	71
2.12.	$\beta$ -galactosidase assay .....	72
2.13.	<i>Galleria mellonella</i> infection model .....	72
2.14.	TraDIS .....	73
2.14.1.	Transposon mutant library creation .....	73
2.14.2.	TraDIS- <i>Xpress</i> experiments to investigate biofilm formation .....	74
2.14.3.	TraDIS- <i>Xpress</i> Experiments to investigate efflux activity .....	74
2.14.4.	Sequencing library preparation .....	75
2.14.5.	Data analysis .....	78
2.15.	Motility assay .....	79
2.16.	Statistical analyses .....	79
<b>3.</b>	<b>CHAPTER 3: CONSTRUCTING TOOLS AND MODELS FOR TRANSPOSON</b>	
	<b>MUTAGENESIS EXPERIMENTS.....</b>	<b>80</b>
3.1.	Introduction .....	81
3.2.	Aims .....	82
3.3.	Chromosomal integration of <i>lacIZ</i> into <i>S. Typhimurium</i> .....	82
3.4.	Confirming the fitness neutrality of <i>lacIZ</i> chromosomal insertion .....	86
3.4.1.	No difference in antimicrobial susceptibility between WT and WT:: <i>lacIZ</i> .....	86
3.4.2.	Biofilm formation unaffected by chromosomal integration of <i>lacIZ</i> .....	87
3.4.3.	Efflux activity appears unchanged with <i>lacIZ</i> integration into <i>S.</i> <i>Typhimurium</i> .....	89
3.4.4.	Equal competitive fitness between WT and WT:: <i>lacIZ</i> .....	90
3.4.5.	No change in pathogenicity between WT and WT:: <i>lacIZ</i> .....	91
3.5.	Constructing a transposon mutant library in <i>S. Typhimurium</i> :: <i>lacIZ</i> .....	92
3.6.	Defining the conditions for TraDIS- <i>Xpress</i> experiments to investigate biofilm formation and efflux activity .....	93
3.6.1.	Developing a model to investigate biofilm formation over time .....	93
3.6.2.	Selection of an appropriate substrate to investigate efflux activity .....	95
3.7.	Conclusions .....	96
<b>4.</b>	<b>CHAPTER 4: TEMPORALLY ESSENTIAL GENES FOR BIOFILM FORMATION</b>	
	<b>IN ESCHERICHIA COLI .....</b>	<b>98</b>

4.1.	Introduction .....	99
4.2.	Aims.....	100
4.3.	TraDIS- <i>Xpress</i> Method Validation .....	100
4.4.	Fimbriae expression and motility are important at all stages of biofilm formation. ....	102
4.4.1.	Type 1 fimbriae regulation.....	102
4.4.2.	Motility regulator <i>IrhA</i> and antitoxin <i>tomB</i> .....	107
4.5.	Regulatory genes are important in the early biofilm.....	110
4.5.1.	Transcriptional factors and transcriptional regulators. ....	110
4.5.2.	Genes of unknown function.....	110
4.6.	Biofilms sampled after 24 hours demonstrate both adhesion and matrix production are important.....	111
4.6.1.	DNA Housekeeping.....	111
4.6.2.	Curli biosynthesis and regulation.....	111
4.7.	The mature biofilm grown for 48 hours requires purine biosynthesis, matrix production, motility and solute transport.....	112
4.7.1.	Purine biosynthesis.....	112
4.7.2.	Flagella .....	113
4.7.3.	Transcriptional regulators.....	114
4.7.4.	Transmembrane transport.....	114
4.7.5.	Cell division.....	114
4.8.	Conclusions .....	115
<b>5.</b>	<b>CHAPTER 5: COMPARISON OF THE GENETIC BASIS OF BIOFILM FORMATION BETWEEN <i>SALMONELLA</i> TYPHIMURIUM AND <i>ESCHERICHIA COLI</i>.....</b>	<b>119</b>
5.1.	Introduction .....	120
5.2.	Aims.....	120
5.3.	Fimbriae regulation and biosynthesis of flagella, nucleotides, curli and LPS are involved in biofilm formation in both <i>S. Typhimurium</i> and <i>E. coli</i> .....	121
5.3.1.	Biofilm matrix .....	124
5.3.2.	Purine biosynthesis.....	124
5.3.3.	Transcriptional regulators and transcription factors .....	125
5.3.4.	LPS.....	125
5.3.5.	Transport .....	126
5.4.	DNA housekeeping, cell division and motility regulation are more important to biofilm fitness in <i>E. coli</i> compared to <i>S. Typhimurium</i> .....	128
5.5.	Genes involved in respiration, regulation of cellulose biosynthesis and ribosomal modification are more important to biofilm fitness in <i>S. Typhimurium</i> compared to <i>E. coli</i> .....	129

5.6.	Respiration is important for the fitness of the mature biofilm in <i>S. Typhimurium</i> .....	130
5.7.	Genes not previously implicated in biofilm formation .....	137
5.8.	Conclusions .....	139
<b>6.</b>	<b>CHAPTER 6: IDENTIFICATION OF GENES INVOLVED IN EFFLUX ACTIVITY AND ACRIFLAVINE SUSCEPTIBILITY IN <i>ESCHERICHIA COLI</i> AND <i>SALMONELLA TYPHIMURIUM</i>.....</b>	<b>141</b>
6.1.	Introduction .....	142
6.2.	Aims.....	143
6.3.	Validation of model efficacy through identification of genes known to be involved in efflux activity .....	143
6.3.1.	AcrAB-ToIC .....	148
6.3.2.	MarA, RamA and SoxS .....	151
6.3.3.	Other transmembrane transport systems .....	154
6.4.	Genes impacting efflux activity in <i>E. coli</i> and <i>S. Typhimurium</i> have roles in protein chaperoning, DNA housekeeping and signalling .....	157
6.4.1.	Protein chaperones .....	157
6.4.2.	Transcription factors and regulators .....	159
6.4.3.	Signalling .....	161
6.4.4.	DNA housekeeping .....	164
6.4.5.	Glutathione metabolism .....	166
6.4.6.	Respiration.....	168
6.4.7.	Ribosome modification.....	171
6.5.	Genes impacting acriflavine susceptibility in <i>E. coli</i> and <i>S. Typhimurium</i> have roles in cell envelope biogenesis, fimbriae expression and amino acid biosynthesis.....	172
6.5.1.	Peptidoglycan biosynthesis .....	172
6.5.2.	LPS.....	173
6.5.3.	Enterobacterial common antigen.....	174
6.5.4.	Fimbriae.....	177
6.5.5.	Amino acid biosynthesis.....	179
6.5.6.	DNA housekeeping .....	181
6.5.7.	Translation .....	183
6.5.8.	Motility.....	185
6.5.9.	Prophages .....	186
6.6.	Conclusions .....	186
<b>7.</b>	<b>CHAPTER 7: REGULATORY LINKS BETWEEN BIOFILM DEVELOPMENT AND EFFLUX ACTIVITY .....</b>	<b>188</b>
7.1.	Introduction .....	189

7.2.	Aims.....	189
7.3.	Identifying genes and pathways important in both biofilm development and efflux activity.....	190
7.4.	Nuo operon.....	192
7.4.1.	Hypothesis 1: Disruption of the proton gradient.....	192
7.4.2.	Hypothesis 2: Disruption of purine biosynthesis.....	196
7.5.	Disulphide bond oxidoreductase DsbA.....	198
7.5.1.	The role of <i>dsbA</i> in biofilm formation.....	198
7.5.2.	The role of <i>dsbA</i> in efflux activity.....	198
7.5.3.	Hypothesis 1: Disruption of <i>dsbA</i> affects outer membrane integrity.....	201
7.5.4.	Hypothesis 2: Disruption of <i>dsbA</i> reduces c-di-GMP degradation.....	201
7.6.	DNA housekeeping.....	202
7.6.1.	Macrodomain organiser MaoP.....	202
7.6.2.	DNA adenine methyltransferase Dam.....	205
7.7.	Transcription factors and regulators.....	207
7.7.1.	MarA, RamA and SoxS.....	207
7.7.2.	DksA and RpoS/ $\sigma^S$ .....	210
7.7.3.	Antitoxin component TomB.....	212
7.7.4.	Acid response regulator GadW.....	214
7.8.	Cell envelope biogenesis.....	214
7.9.	Intracellular signalling systems.....	218
7.9.1.	Response regulator OmpR.....	218
7.9.2.	Adenylate cyclase CyaA.....	218
7.10.	Fimbriae.....	221
7.11.	Motility.....	221
7.12.	Conclusions.....	221
<b>8.</b>	<b>CHAPTER 8: OVERALL DISCUSSION.....</b>	<b>224</b>
8.1.	Biofilms.....	225
8.2.	Efflux.....	226
8.3.	Links between biofilm formation and efflux activity.....	227
8.3.1.	DsbA.....	228
8.3.2.	MaoP.....	228
8.3.3.	The <i>nuo</i> operon.....	228
8.3.4.	MarA, RamA and SoxS.....	229
8.3.5.	TomB.....	229
8.3.6.	OmpR.....	230
8.4.	Looking to the future.....	230
<b>9.</b>	<b>REFERENCES.....</b>	<b>232</b>
<b>10.</b>	<b>APPENDICES.....</b>	<b>260</b>

10.1.	APPENDIX 1: Genes determined by TraDIS- <i>Xpress</i> to be important for biofilm formation in <i>E. coli</i> and <i>S. Typhimurium</i> (STM), and the phenotypes of deletion mutants relative to the wild type.....	260
10.2.	APPENDIX 2: Genes determined by TraDIS- <i>Xpress</i> to be important for efflux activity and acriflavine susceptibility in <i>E. coli</i> and <i>S. Typhimurium</i> (STM), and the phenotypes of deletion mutants relative to the wild type. ....	280
10.3.	APPENDIX 3: Mean insertion frequencies per gene in <i>E. coli</i> and <i>S. Typhimurium</i> for conditions treated with PA $\beta$ N or acriflavine compared to untreated controls.....	305
10.4.	APPENDIX 4: Genes implicated in both biofilm formation and efflux activity by the TraDIS- <i>Xpress</i> data and/or the phenotype of deletion mutants in <i>E. coli</i> and/or <i>S. Typhimurium</i> (STM).....	306
10.5.	APPENDIX 5: Biofilm and efflux phenotypes of all <i>E. coli</i> and <i>S. Typhimurium</i> deletion mutants relative to the wild type of each species.....	333

## List of Figures

<b>Figure 1.1:</b> Curli operon and products. Figure adapted from Van Gerven et al. (2015)....	30
<b>Figure 1.2:</b> Cellulose biosynthesis machinery. Adapted from figures from Thongsomboon et al. (2018) and Serra and Hengge (2019).....	32
<b>Figure 1.3:</b> Regulation of c-di-GMP metabolism and its effects on biofilm matrix production. Figure adapted from Hengge (2009) and Hengge (2020). ....	34
<b>Figure 1.4:</b> Two component signalling systems EnvZ/OmpR and CpxAR and their regulatory effects. ....	38
<b>Figure 1.5:</b> The Rcs phosphorylay and its effects on biofilm matrix production and motility. ....	41
<b>Figure 1.6:</b> Regulation of the genes encoding the AcrAB-TolC efflux system by local and global transcriptional regulators. ....	43
<b>Figure 2.1:</b> Chromosomal integration by gene doctoring, demonstrated through the integration of <i>lacI</i> Z into the intergenic region downstream of <i>glmS</i> . Figure adapted from (Lee et al., 2009).....	56
<b>Figure 2.2:</b> Layout of the TraDIS- <i>Xpress</i> experiments investigating biofilm formation (left) and efflux activity (right), detailing how samples were taken. ....	75
<b>Figure 2.3:</b> Tagmentation and Tn5 enrichment to prepare TraDIS- <i>Xpress</i> libraries for sequencing. ....	77
<b>Figure 3.1:</b> RT-PCR where the top panel is showing the absence of <i>lacI</i> RNA in WT <i>S. Typhimurium</i> and its presence in <i>S. Typhimurium::lacI</i> Z (WT:: <i>lacI</i> Z). The bottom panel a positive control measuring <i>gyrB</i> expression in both strains. A 1 kB DNA ladder is included in both panels. Three biological repeats were included for each strain.....	83
<b>Figure 3.2:</b> <i>S. Typhimurium::lacI</i> Z plated on LB agar supplemented with X-gal, <b>a)</b> with IPTG and <b>b)</b> without IPTG. Representative plates are shown from two biological and two technical replicates. ....	84
<b>Figure 3.3:</b> $\beta$ -galactosidase activity, as an indirect measurement of <i>lacI</i> activity in <i>S. Typhimurium::lacI</i> Z <b>a)</b> $\beta$ -galactosidase activity in <i>S. Typhimurium::lacI</i> Z when treated with IPTG, relative to <i>S. Typhimurium::lacI</i> Z without IPTG. <b>b)</b> $\beta$ -galactosidase activity in <i>E. coli</i> K-12, WT <i>S. Typhimurium</i> and <i>S. Typhimurium::lacI</i> Z with and without 1 mM IPTG, relative to WT <i>S. Typhimurium</i> without IPTG. For both graphs, points represent individual data points of relative $\beta$ -galactosidase activity for three biological replicates. Error bars show the mean and 95 % confidence intervals. A significant difference where $p < 0.05$ is denoted with an asterisks (*) or 'ns' (not significant). ....	85
<b>Figure 3.4:</b> Biofilm formation in WT <i>S. Typhimurium</i> and WT:: <i>lacI</i> Z. <b>a)</b> Biofilm biomass measured by crystal violet staining (OD <sub>590nm</sub> ) with and without PA $\beta$ N. The efflux mutant <i>tolC::cat</i> was included as a negative control. Points represent two biological and eight technical replicates and error bars denote 95% confidence intervals. <b>b)</b> Curli and cellulose	

production, measured by plating colonies on agar supplemented with Congo red and cellulose, respectively. Representative colonies from two biological and four technical replicates are shown.....88

**Figure 3.5:** Dye accumulation over 60 minutes in the presence and absence of the efflux inhibitor PA $\beta$ N, as an indication of efflux activity in WT *S. Typhimurium* and WT::*lacI*Z. The efflux mutant *toI*C::*cat* was included as a efflux-impaired control. Points represent mean values of 5 technical replicates and 2 biological replicates. Error bars show 95 % confidence intervals. ....89

**Figure 3.6:** *In vitro* competitive fitness assay between WT and WT::*lacI*Z. **a)** Points represent biological replicates, of which 15 were performed, and grey lines show pairwise comparisons between replicates at the start and after 24 hours coculture. Error bars denote 95% confidence intervals. **b)** A representative plate from 1 biological replicate showing CFU of WT *S. Typhimurium* (white) and WT::*lacI*Z (blue) after 24 hours coculture. ....90

**Figure 3.7:** Pathogenicity of WT *S. Typhimurium* and WT::*lacI*Z, in a *Galleria mellonella* infection model. Each treatment was completed with 10 larvae. The experimental error was 10% (1 larva). ....91

**Figure 3.8:** Insertion frequency across the *S. Typhimurium*::*lacI*Z genome on the forward (red) and reverse (blue) strands. Tracks show two independent sequencing library preparations. The GC content of the genome is shown in the inner track in grey, where peaks show areas rich in GC. Genes are shown in cyan. ....92

**Figure 3.9:** The model system used to determine the genes involved at different stages of the biofilm life cycle. Planktonic samples from the culture and biofilm samples from the beads were assayed from the same well over time. ....93

**Figure 3.10:** CFU of planktonic ( $\circ$ ) and biofilm ( $\bullet$ ) cells harvested from the biofilm model over time for the mutant library parent strains in **a)** *S. Typhimurium*::*lacI*Z (red) and **b)** *E. coli* BW25113 (green). Points represent biological replicates, of which 3 were performed, and error bars show 1 standard error. ....94

**Figure 4.1:** Mean insertion frequencies per gene in *E. coli* for each time point. Coloured points show mean insertion frequencies per gene in biofilm conditions (*x*-axis) compared to planktonic conditions (*y*-axis) for each time point. Black points show insertion frequencies per gene compared between identical replicates and show the experimental error. Replicates with and without promoter induction with IPTG are combined for analysis. ....100

**Figure 4.2:** Genes involved in biofilm formation over time in *E. coli*. Plus symbols (+) indicate genes that were beneficial for, and minus symbols (-) indicate genes that were detrimental to, biofilm fitness. ....101

**Figure 4.3:** Transposon insertion sites and frequencies in planktonic and biofilm conditions, mapped to a reference genome and plotted with BioTraDIS in Artemis. The



height of the peak can be used as a proxy for the mutant's 'fitness' in the condition. Red peaks indicate where the transposon-located promoter is facing left-to-right, and blue peaks show it facing right-to-left. **a)** Insertion sites in and around *fimB* and *fimE* in planktonic and biofilm conditions after 12- and 48-hours growth with and without promoter induction with IPTG. Leaky promoter expression is most likely responsible for the increased insertions upstream of *fimB* in conditions without IPTG. **b)** Insertion sites in and around *hdfR*, *lrhA* and *tomB* in planktonic and biofilm conditions after 24 hours growth. Conditions with and without IPTG have been combined. **c)** Insertion sites in and around *dksA* and *dsbA* in planktonic and biofilm conditions after 12- and 48-hours growth. Conditions with and without IPTG have been combined. For all plot files, one of two independent replicates is shown and y-axes have been normalised for all.....104

**Figure 4.4:** Phenotypic analysis of selected genes involved in biofilm formation. **a)** Biofilm biomass of single knockout mutants relative to wild type *E. coli*, measured by crystal violet staining. Two biological and a minimum of two technical replicates were performed for each mutant. **b)** Cell aggregation of single knockout mutants relative to wild type *E. coli*, measured by OD<sub>600 nm</sub> of the supernatant of unagitated cultures. Points show the ODs of three independent replicates. For both graphs, red points/bars distinguish between the two Keio collection mutants of each gene. Error bars show 95% confidence intervals, and the shaded area shows the 95% confidence interval of the wild type. Single asterisks (\*) represent a significant difference between one Keio mutant copy and the wild type, and double asterisks (\*\*) denote a significant difference between both Keio mutant copies and the wild type (Welch's *t*-test, *p* < 0.05). **c)** Colonies grown on agar supplemented with Congo red to compare curli biosynthesis between single knockout mutants and the wild type. Images are representative of 2 biological and 2 technical replicates. ....106

**Figure 4.5:** Biofilm formation of single knockout mutants on glass analysed under flow conditions after 12, 24 and 48 hours growth. **a)** Single knockout mutants selected for their effect on biofilm fitness. **b)** Single knockout mutants of genes not previously described to affect biofilm formation, to the best of our knowledge. 10x Magnification. Images are representative of two independent replicates. Scale bar indicates 10 µm. ....109

**Figure 4.6:** Summary of genes important for biofilm formation by *E. coli* at different stages of development. ....118

**Figure 5.1:** Mean insertion frequencies per gene in *S. Typhimurium* for each time point. Coloured points show mean insertion frequencies per gene in biofilm conditions (*x*-axis) compared to planktonic conditions (*y*-axis) for each time point. Black points show insertion frequencies per gene compared between identical replicates and show the experimental error. Replicates with and without promoter induction with IPTG are combined for analysis. ....121

**Figure 5.2:** Genes involved in biofilm formation over time in *S. Typhimurium*. **a)** Genes identified by TraDIS-*Xpress* to affect biofilm fitness in *S. Typhimurium* after 12-, 24- and

48-hours growth, relative to the planktonic conditions at each time point. Plus signs (+) indicate a gene's benefit to biofilm fitness and minus signs (-) indicate its detrimental effect on biofilm fitness. **b)** Pathways and genes that affect biofilm fitness in *E. coli* and *S. Typhimurium*. .....123

**Figure 5.3:** Biofilm formation in deletion mutants relative to wild type (WT) *S.*

*Typhimurium*. **a)** Biofilm biomass relative to the WT, measured by crystal violet staining (OD<sub>590 nm</sub>). Points show a minimum of two biological and eight technical replicates. The grey shaded area shows the 95% confidence interval of the wild type and error bars show 95% confidence intervals of the mutants. A significant difference in biofilm biomass to the wild type is indicated by asterisks: \* =  $p < 0.05$ ; \*\* =  $p < 0.01$ ; \*\*\* =  $p < 0.001$ ; \*\*\*\* =  $p < 0.0001$ . **b)** Mutants and the WT spotted on agar supplemented with Congo red and calcofluor, showing curli and cellulose production, respectively. For all images, colonies are representative images of two biological and two technical replicates. ....127

**Figure 5.4:** Mapped reads from TraDIS-*Xpress* data, plotted with BioTraDIS in Artemis, showing the location of transposon insertion sites in and around the *nuo* operon in **a)** *S. Typhimurium* and **b)** *E. coli* after 48 hours in growth in planktonic and biofilm conditions. The directionality of the transposon-located is indicated by colour, red denoting left-to-right and blue denoting right-to-left. Plofiles show one of two independent replicates and conditions with and without promoter induction with IPTG have been combined. **c)** Growth kinetics of wild type (WT),  $\Delta nuo$  and  $\Delta nuoB$  mutants in *S. Typhimurium* (left) and *E. coli* (right) over 24 hours. Points show the mean of two biological and eight technical replicates, and the shaded area denotes 95% confidence intervals for each strain. ....132

**Figure 5.5:** The effects of the *nuo* operon on biofilm formation in *E. coli* and *S.*

*Typhimurium*. **a)** Biofilm biomass of  $\Delta nuoB$  and  $\Delta nuo$  deletion mutants relative to wild type (WT) *E. coli* and *S. Typhimurium*. Points show a minimum of two biological and six technical replicates and error bars show 95% confidence intervals. Asterisks show a significant difference in biofilm biomass from the WT (Wilcoxon rank sum, \* =  $p < 0.05$ ; \*\* =  $p < 0.01$ ; \*\*\* =  $p < 0.001$ ; \*\*\*\* =  $p < 0.0001$ ). **b)** Curli and cellulose biosynthesis of  $\Delta nuoB$  and  $\Delta nuo$  mutants relative to their WTs. Images are representative of two biological and two technical replicates. **c)** Biofilm formation of WT *S. Typhimurium* and the  $\Delta nuo$  mutant on glass analysed under flow conditions after 12-, 24- and 48-hours growth. 20x Magnification. Scale bar indicates 10  $\mu\text{m}$ . ....134

**Figure 5.6:** The effect of environmental oxygen and the *nuo* operon on biofilm formation in *E. coli* and *S. Typhimurium*. **a)** Biofilm biomass of wild type and  $\Delta nuoB$  deletion mutants of *S. Typhimurium* and *E. coli* grown under various oxygen concentrations (0%, 5%, 10% and ambient ~20% oxygen). Points show biofilm biomass of a minimum of eight technical replicates and one biological replicate, and error bars denote 95% confidence intervals. Asterisks show a significant difference in biofilm biomass from the wild type (Wilcoxon rank sum, \* =  $p < 0.05$ ; \*\* =  $p < 0.01$ ; \*\*\* =  $p < 0.001$ ; \*\*\*\* =  $p < 0.0001$ ; ns = not

significant). **b)** Wild type and  $\Delta nuoB$  deletion mutants in *S. Typhimurium* and *E. coli* spotted on agar containing Congo red to highlight differences in curli biosynthesis when grown under various oxygen concentrations. Images are representative of four technical and two biological replicates. ....136

**Figure 5.7:** The effects of *STM14\_1074*, *yjiG* and *tyrT* on biofilm formation in *S. Typhimurium*. **a)** Biofilm biomass of  $\Delta STM14_1074$  and  $\Delta yjiG$  relative to wild type (WT) *S. Typhimurium*, and *S. Typhimurium* containing a plasmid overexpressing *tyrT* relative to the empty plasmid control. Points represent a minimum of six technical replicates across two biological replicates, and error bars show 95% confidence intervals. Asterisks show a significant difference in biofilm biomass from the wild type (Wilcoxon rank sum, \* =  $p < 0.05$ ; \*\* =  $p < 0.01$ ; \*\*\* =  $p < 0.001$ ; \*\*\*\* =  $p < 0.0001$ ; ns = not significant). **b)** Curli and cellulose biosynthesis of wild type *S. Typhimurium* and deletion mutants. Images are representative of two biological and two technical replicates. **c)** Biofilm formation of wild type *S. Typhimurium* and deletion mutants on glass analysed under flow conditions after 12-, 24- and 48-hours growth. 20x Magnification. Scale bar indicates 10  $\mu\text{m}$ .....138

**Figure 6.1:** Analysis of the pathways involved in efflux activity and acriflavine susceptibility in **a)** *E. coli* and **b)** *S. Typhimurium*. ....143

**Figure 6.2:** Dye accumulation in wild type *E. coli* and single gene deletion mutants from the Keio collection, where each copy of the deleted gene is separated by colour. Accumulation of resazurin (excitation 544 nm, emission 580 nm) was measured over 60 minutes and the area under the curve was plotted. Points represent each of 3 independent replicates. A single asterisks (\*) shows a significant difference (Welch's *t*-test,  $p < 0.05$ ) in dye accumulation between the wild type and one copy of the deletion mutant, where the orientation of the asterisks indicates whether this significant difference is in the first (left) or second (right) Keio mutant copy. The shaded area shows the 95% confidence interval of the wild type and error bars show 95% confidence intervals of deletion mutants. ....145

**Figure 6.3:** Fold change in MICs of acriflavine, azithromycin, cefotaxime and gentamycin in single deletion mutants from the Keio collection relative to wild type *E. coli*, measured by the **a)** broth and **b)** agar dilution methods. The shaded area shows an experimental error of 1-fold change and points show two independent replicates. ....146

**Figure 6.4:** Efflux activity in wild type (WT) *S. Typhimurium* and deletion mutants. **a)** Dye accumulation in deletion mutants and the WT. Accumulation of resazurin (excitation 544 nm, emission 580 nm) was measured over 100 minutes and the area under the curve was plotted. Points each of two biological and four technical replicates. Asterisks (\*) show a significant difference in dye accumulation between the wild type and the knockout mutant (Wilcoxon rank sum, \* =  $p < 0.05$ , \*\* =  $p < 0.01$ , \*\*\* =  $p < 0.001$ , \*\*\*\* =  $p < 0.0001$ ). The shaded area shows the 95% confidence interval of the wild type and error bars show 95% confidence intervals of mutants. **b)** Fold change in MICs of acriflavine, azithromycin,

cefotaxime and gentamycin in mutants relative to the WT, measured by the broth dilution method. The shaded area shows an experimental error of 1-fold change and points show two independent replicates. ....147

**Figure 6.5:** The effects of the AcrAB-TolC system on efflux activity in *E. coli* and *S. Typhimurium*. **a)** Mapped reads from TraDIS-*Xpress* data, plotted with BioTraDIS in Artemis, showing the location of transposon insertion sites in and around *acrAB*, *acrR* and *tolC* treated with subinhibitory concentrations of acriflavine and/or PA $\beta$ N in *E. coli* and *S. Typhimurium*. The height of the lines indicates the number of sequencing reads mapped to that locus and is used as a proxy for fitness. The colour of the lines indicates the direction that the transposon-located promoter faces, red denoting left-to-right and blue denoting right-to-left. Conditions with and without promoter induction with IPTG have been combined, and represent one of two independent replicates. **b)** Dye accumulation in the wild type and single gene deletion mutants in each species. Accumulation of resazurin (excitation 544 nm, emission 580 nm) was measured over 60 minutes in *E. coli* and 100 minutes in *S. Typhimurium* and the area under the curve was plotted. Points show 3 independent replicates. Asterisks (\*) show a significant difference (Welch's *t*-test,  $p < 0.05$ ) between the wild type and mutants. Colours discriminate between mutant copies. The shaded area shows the 95% confidence interval of the wild type and error bars show 95% confidence intervals of mutants. **c)** Fold change in MICs of acriflavine, azithromycin, cefotaxime and gentamycin in mutants relative to the wild type, measured by the broth dilution method (and the agar dilution method in *E. coli* shown in the middle panel). The shaded area shows an experimental error of 1-fold change and points show two independent replicates. ....150

**Figure 6.6:** The effects of *marA*, *ramA* and *soxS* on efflux activity in *E. coli* and *S. Typhimurium*. **a)** Mapped reads from TraDIS-*Xpress* data, plotted with BioTraDIS in Artemis, showing the location of transposon insertion sites in and around *marRA* and *soxRS* in *E. coli* and *ramRA* in *S. Typhimurium* treated with subinhibitory concentrations of acriflavine and/or PA $\beta$ N. The height of the lines indicates the number of sequencing reads mapped to that locus and is used as a proxy for fitness. The colour of the lines indicates the direction that the transposon-located promoter faces, red denoting left-to-right and blue denoting right-to-left. Conditions with and without promoter induction with IPTG have been combined, and represent one of two independent replicates. **b)** Dye accumulation in the wild type and single gene deletion mutants. Accumulation of resazurin (excitation 544 nm, emission 580 nm) was measured over 60 minutes and the area under the curve was plotted. Points show 3 independent replicates. Colours discriminate between mutant copies. The shaded area shows the 95% confidence interval of the wild type and error bars show 95% confidence intervals of mutants. **c)** Fold change in MICs of acriflavine, azithromycin, cefotaxime and gentamycin in *E. coli* and *S. Typhimurium* single deletion mutants relative to the wild type, measured by the broth dilution method (and the agar

dilution method in *E. coli* shown in the right-hand panel). The shaded area shows an experimental error of 1-fold change and points show two independent replicates. .... 153

**Figure 6.7:** The effects of genes involved in transmembrane transport on efflux activity in *E. coli*. **a)** Dye accumulation in the wild type and single gene deletion mutants.

Accumulation of resazurin (excitation 544 nm, emission 580 nm) was measured over 60 minutes and the area under the curve was plotted. Points show 3 independent replicates. Asterisks (\*) show a significant difference (Welch's *t*-test,  $p < 0.05$ ) between the wild type and mutants. Colours discriminate between mutant copies. The shaded area shows the 95% confidence interval of the wild type and error bars show 95% confidence intervals of mutants. **b)** Fold change in MICs of acriflavine, azithromycin, cefotaxime and gentamycin in mutants relative to each wild type, measured by the broth dilution (left) and agar dilution (right) methods. The shaded area shows an experimental error of 1-fold change and points show two independent replicates. .... 156

**Figure 6.8:** The effects of *skp* and *surA* on efflux activity in *E. coli*. **a)** Dye accumulation in the wild type and single gene deletion mutants. Accumulation of resazurin (excitation 544 nm, emission 580 nm) was measured over 60 minutes and the area under the curve was plotted. Points show 3 independent replicates. Asterisks (\*) show a significant difference (Welch's *t*-test,  $p < 0.05$ ) between the wild type and mutants. Colours discriminate

between mutant copies. The shaded area shows the 95% confidence interval of the wild type and error bars show 95% confidence intervals of mutants. **b)** Fold change in MICs of acriflavine, azithromycin, cefotaxime and gentamycin in mutants relative to each wild type, measured by the broth dilution (left) and agar dilution (right) methods. The shaded area shows an experimental error of 1-fold change and points show two independent replicates. .... 158

**Figure 6.9:** The effects of *dskA*, *gadW* and *crl* on efflux activity in *E. coli* and *S.*

*Typhimurium*. **a)** Dye accumulation in the wild type and single gene deletion mutants in each species. Accumulation of resazurin (excitation 544 nm, emission 580 nm) was measured over 60 minutes in *E. coli* and 100 minutes in *S. Typhimurium* and the area under the curve was plotted. Points show 3 independent replicates. Colours discriminate between mutant copies. The shaded area shows the 95% confidence interval of the wild type and error bars show 95% confidence intervals of mutants. **b)** Fold change in MICs of acriflavine, azithromycin, cefotaxime and gentamycin in mutants relative to each wild type, measured by the broth dilution method (and the agar dilution method in *E. coli* shown in the middle panel). The shaded area shows an experimental error of 1-fold change and points show two independent replicates. .... 160

**Figure 6.10:** The effects of genes involved in signalling on efflux activity in *E. coli* and *S. Typhimurium*. **a)** Dye accumulation in the wild type and single gene deletion mutants in each species. Accumulation of resazurin (excitation 544 nm, emission 580 nm) was measured over 60 minutes in *E. coli* and 100 minutes in *S. Typhimurium* and the area

under the curve was plotted. Points show 3 independent replicates. Colours discriminate between mutant copies. The shaded area shows the 95% confidence interval of the wild type and error bars show 95% confidence intervals of mutants. **b)** Fold change in MICs of acriflavine, azithromycin, cefotaxime and gentamycin in mutants relative to each wild type, measured by the broth dilution method (and the agar dilution method in *E. coli* shown in the middle panel). The shaded area shows an experimental error of 1-fold change and points show two independent replicates.....163

**Figure 6.11:** The effects of *dam* and *maoP* on efflux activity in *E. coli* and *S.*

*Typhimurium*. **a)** Dye accumulation in the wild type and single gene deletion mutants in each species. Accumulation of resazurin (excitation 544 nm, emission 580 nm) was measured over 60 minutes in *E. coli* and 100 minutes in *S. Typhimurium* and the area under the curve was plotted. Points show 3 independent replicates. Asterisks (\*) show a significant difference (Welch's *t*-test,  $p < 0.05$ ) between the wild type and mutants. Colours discriminate between mutant copies. The shaded area shows the 95% confidence interval of the wild type and error bars show 95% confidence intervals of mutants. **b)** Fold change in MICs of acriflavine, azithromycin, cefotaxime and gentamycin in mutants relative to each wild type, measured by the broth dilution method (and the agar dilution method in *E. coli* shown in the middle panel). The shaded area shows an experimental error of 1-fold change and points show two independent replicates. ....165

**Figure 6.12:** The effects of *gshB* and *pxpB* on efflux activity in *E. coli*. **a)** Dye

accumulation in the wild type and single gene deletion mutants. Accumulation of resazurin (excitation 544 nm, emission 580 nm) was measured over 60 minutes and the area under the curve was plotted. Points show 3 independent replicates. Colours discriminate between mutant copies. The shaded area shows the 95% confidence interval of the wild type and error bars show 95% confidence intervals of mutants. **b)** Fold change in MICs of acriflavine, azithromycin, cefotaxime and gentamycin in mutants relative to each wild type, measured by the broth dilution (left) and agar dilution (right) methods. The shaded area shows an experimental error of 1-fold change and points show two independent replicates. ....167

**Figure 6.13:** The effects of genes involved in respiration on efflux activity in *E. coli* and *S.*

*Typhimurium*. **a)** Dye accumulation in the wild type and single gene deletion mutants in each species. Accumulation of resazurin (excitation 544 nm, emission 580 nm) was measured over 60 minutes in *E. coli* and 100 minutes in *S. Typhimurium* and the area under the curve was plotted. Points show 3 independent replicates. Asterisks (\*) show a significant difference (Welch's *t*-test,  $p < 0.05$ ) between the wild type and mutants. Colours discriminate between mutant copies. The shaded area shows the 95% confidence interval of the wild type and error bars show 95% confidence intervals of mutants. **b)** Fold change in MICs of acriflavine, azithromycin, cefotaxime and gentamycin in mutants relative to each wild type, measured by the broth dilution method (and the agar dilution method in *E.*

*coli* shown in the middle panel). The shaded area shows an experimental error of 1-fold change and points show two independent replicates. ....170

**Figure 6.14:** The effects of *ychF* and *rimK* on efflux activity in *E. coli*. **a)** Dye accumulation in the wild type and single gene deletion mutants. Accumulation of resazurin (excitation 544 nm, emission 580 nm) was measured over 60 minutes and the area under the curve was plotted. Points show 3 independent replicates. Asterisks (\*) show a significant difference (Welch's *t*-test,  $p < 0.05$ ) between the wild type and mutants. Colours discriminate between mutant copies. The shaded area shows the 95% confidence interval of the wild type and error bars show 95% confidence intervals of mutants. **b)** Fold change in MICs of acriflavine, azithromycin, cefotaxime and gentamycin in mutants relative to each wild type, measured by the broth dilution (left) and agar dilution (right) methods. The shaded area shows an experimental error of 1-fold change and points show two independent replicates.....171

**Figure 6.15:** The effects of genes involved in cell envelope biogenesis on efflux activity in *E. coli* and *S. Typhimurium*. **a)** Dye accumulation in the wild type and single gene deletion mutants in each species. Accumulation of resazurin (excitation 544 nm, emission 580 nm) was measured over 60 minutes in *E. coli* and 100 minutes in *S. Typhimurium* and the area under the curve was plotted. Points show 3 independent replicates. Asterisks (\*) show a significant difference (Welch's *t*-test,  $p < 0.05$ ) between the wild type and mutants. Colours discriminate between mutant copies. The shaded area shows the 95% confidence interval of the wild type and error bars show 95% confidence intervals of mutants. **b)** Fold change in MICs of acriflavine, azithromycin, cefotaxime and gentamycin in mutants relative to each wild type, measured by the broth dilution method (and the agar dilution method in *E. coli* shown in the middle panel). The shaded area shows an experimental error of 1-fold change and points show two independent replicates .....176

**Figure 6.16:** The effects of fimbrial regulation on efflux activity in *E. coli*. **a)** Dye accumulation in the wild type and single gene deletion mutants. Accumulation of resazurin (excitation 544 nm, emission 580 nm) was measured over 60 minutes and the area under the curve was plotted. Points show 3 independent replicates. Asterisks (\*) show a significant difference (Welch's *t*-test,  $p < 0.05$ ) between the wild type and mutants. Colours discriminate between mutant copies. The shaded area shows the 95% confidence interval of the wild type and error bars show 95% confidence intervals of mutants. **b)** Fold change in MICs of acriflavine, azithromycin, cefotaxime and gentamycin in mutants relative to each wild type, measured by the broth dilution (left) and agar dilution (right) methods. The shaded area shows an experimental error of 1-fold change and points show two independent replicates.....178

**Figure 6.17:** The effects of *metL* and *leuL* on efflux activity in *E. coli*. **a)** Dye accumulation in the wild type and single gene deletion mutants. Accumulation of resazurin (excitation 544 nm, emission 580 nm) was measured over 60 minutes and the area under the curve

was plotted. Points show 3 independent replicates. Asterisks (\*) show a significant difference (Welch's *t*-test,  $p < 0.05$ ) between the wild type and mutants. Colours discriminate between mutant copies. The shaded area shows the 95% confidence interval of the wild type and error bars show 95% confidence intervals of mutants. **b)** Fold change in MICs of acriflavine, azithromycin, cefotaxime and gentamycin in mutants relative to each wild type, measured by the broth dilution (left) and agar dilution (right) methods. The shaded area shows an experimental error of 1-fold change and points show two independent replicates.....180

**Figure 6.18:** The effects of *yjhQ*, *rep* and *ybiB* on efflux activity in *E. coli*. **a)** Dye accumulation in the wild type and single gene deletion mutants. Accumulation of resazurin (excitation 544 nm, emission 580 nm) was measured over 60 minutes and the area under the curve was plotted. Points show 3 independent replicates. Colours discriminate between mutant copies. The shaded area shows the 95% confidence interval of the wild type and error bars show 95% confidence intervals of mutants. **b)** Fold change in MICs of acriflavine, azithromycin, cefotaxime and gentamycin in mutants relative to each wild type, measured by the broth dilution (left) and agar dilution (right) methods. The shaded area shows an experimental error of 1-fold change and points show two independent replicates. ....182

**Figure 6.19:** The effects of genes involved in translation on efflux activity in *E. coli* and *S. Typhimurium*. **a)** Dye accumulation in the wild type and single gene deletion mutants in each species. Accumulation of resazurin (excitation 544 nm, emission 580 nm) was measured over 60 minutes in *E. coli* and 100 minutes in *S. Typhimurium* and the area under the curve was plotted. Points show 3 independent replicates. Colours discriminate between mutant copies. The shaded area shows the 95% confidence interval of the wild type and error bars show 95% confidence intervals of mutants. **b)** Fold change in MICs of acriflavine, azithromycin, cefotaxime and gentamycin in mutants relative to each wild type, measured by the broth dilution method (and the agar dilution method in *E. coli* shown in the middle panel). The shaded area shows an experimental error of 1-fold change and points show two independent replicates.....184

**Figure 6.20:** The effects of motility regulators on efflux activity in *E. coli*. **a)** Dye accumulation in the wild type and single gene deletion mutants. Accumulation of resazurin (excitation 544 nm, emission 580 nm) was measured over 60 minutes and the area under the curve was plotted. Points show 3 independent replicates. Colours discriminate between mutant copies. The shaded area shows the 95% confidence interval of the wild type and error bars show 95% confidence intervals of mutants. **b)** Fold change in MICs of acriflavine, azithromycin, cefotaxime and gentamycin in mutants relative to each wild type, measured by the broth dilution (left) and agar dilution (right) methods. The shaded area shows an experimental error of 1-fold change and points show two independent replicates. ....185



**Figure 7.1:** Relative biofilm biomass plotted against relative dye accumulation in **a)** the first and **b)** second copies of deletion mutants from the Keio collection relative to wild type *E. coli*, and **c)** wild type *S. Typhimurium* and deletion mutants. The top-left quadrant of these graphs shows genes where biofilm biomass formation was reduced and drug accumulation was increased when deleted. Points show averages of two biological and two technical replicates (*E. coli* biofilm biomass data), three independent replicates (*E. coli* dye accumulation data) and two biological and four technical replicates (*S. Typhimurium* biofilm biomass data and dye accumulation data)..... 191

**Figure 7.2:** The effects of the *nuo* operon on biofilm formation, efflux activity and motility in *E. coli* and *S. Typhimurium*. **a)** Biofilm biomass of  $\Delta nuo$  mutants and the wild type (WT) of each species, measured by crystal violet staining (OD<sub>590 nm</sub>). Points show biofilm biomass for a minimum of two biological and six technical replicates. **b)** Curli biosynthesis of  $\Delta nuo$  mutants and relative to the WT of each species. Images are representative of four independent replicates. **c)** Dye accumulation in  $\Delta nuo$  mutants and the WT of each species. Accumulation of resazurin (excitation 544 nm, emission 580 nm) was measured over 60 minutes in *E. coli* and 100 minutes in *S. Typhimurium* and the area under the curve was plotted. Points show two biological and eight technical replicates. Both biofilm biomass and dye uptake were measured in stress free conditions (●) and with PA $\beta$ N (○). **d)** Fold change in MICs of acriflavine, azithromycin, cefotaxime and gentamycin in  $\Delta nuo$  mutants, relative to each WT, measured by the broth dilution method. The shaded area shows an experimental error of 1-fold change and points show two independent replicates. **e)** Swimming motility of  $\Delta nuo$  mutants and the WT of each species, measured by the diameter of the motile disk. Points show five independent replicates. For all graphs, error bars show 95% confidence intervals and asterisks (\*) show where there was a significant difference between the strains indicated (Mann–Whitney U test, ns = not significant; \* =  $p < 0.05$ ; \*\* =  $p < 0.01$ ; \*\*\* =  $p < 0.001$ ; \*\*\*\* =  $p < 0.0001$ ). ..... 195

**Figure 7.3:** Curli biosynthesis in *S. Typhimurium* and *E. coli* wild types and deletion mutants, in the presence and absence of inosine. Two out of four independent replicates are shown for each strain..... 197

**Figure 7.4:** The effects of *dsbA* on biofilm formation, efflux activity and motility in *S. Typhimurium*. **a)** Biofilm biomass of various deletion mutants and overexpression constructs in wild type (WT) *S. Typhimurium*, measured by crystal violet staining (OD<sub>590 nm</sub>). Points show two biological and four technical replicates. **b)** Curli and cellulose biosynthesis in  $\Delta dsbA$ , the WT overexpressing *dsbA* on a plasmid,  $\Delta tolC$  and  $\Delta pdeC$ , relative to the WT. Images are representative of four independent replicates. **c)** Dye accumulation in the WT,  $\Delta dsbA$ , the WT overexpressing *dsbA* on a plasmid and an empty plasmid control. Accumulation of resazurin (excitation 544 nm, emission 580 nm) was measured over 100 minutes and the area under the curve was plotted. Points show two biological and four technical replicates. Both biofilm biomass and dye uptake were

measured in stress-free conditions (purple) and with PA $\beta$ N (blue). **d)** Fold change in MICs of acriflavine, azithromycin, cefotaxime and gentamycin in  $\Delta dsbA$  relative to the WT, and the WT overexpressing *dsbA* on a plasmid relative to the plasmid control, measured by the broth dilution method. The shaded area shows an experimental error of 1-fold change and points show two independent replicates. **e)** Swimming motility of WT,  $\Delta dsbA$  and  $\Delta toIC$ , measured by the diameter of the motile disk. Points show five independent replicates. For all graphs, error bars show 95% confidence intervals and asterisks (\*) show where there was a significant difference between the strains indicated (Mann–Whitney U test, ns = not significant; \* =  $p < 0.05$ ; \*\* =  $p < 0.01$ ; \*\*\* =  $p < 0.001$ ; \*\*\*\* =  $p < 0.0001$ ). .....200

**Figure 7.5:** The effects of *maoP* on biofilm formation efflux activity and, motility in *S. Typhimurium*. **a)** Biofilm biomass of various deletion mutants and overexpression constructs in wild type (WT) *S. Typhimurium*, measured by crystal violet (OD<sub>590 nm</sub>). Points show two biological and four technical replicates. **b)** Curli and cellulose biosynthesis in  $\Delta maoP$ , the WT overexpressing *maoP* on a plasmid and  $\Delta toIC$ , relative to the WT. Images are representative of four independent replicates. **c)** Dye accumulation in the WT,  $\Delta maoP$ , the WT overexpressing *maoP* on a plasmid and the empty plasmid control. Accumulation of resazurin (excitation 544 nm, emission 580 nm) was measured over 100 minutes and the area under the curve was plotted. Points show two biological and four technical replicates. Both biofilm biomass and dye uptake were measured in stress-free conditions (purple) and with PA $\beta$ N (blue). **d)** Fold change in MICs of acriflavine, azithromycin, cefotaxime and gentamycin in  $\Delta maoP$  relative to the WT, and the WT overexpressing *maoP* on a plasmid relative to the plasmid control, measured by the broth dilution method. The shaded area shows an experimental error of 1-fold change and points show two independent replicates. For all graphs, error bars show 95% confidence intervals and asterisks (\*) show where there was a significant difference between the strains indicated (Mann–Whitney U test, ns = not significant; \* =  $p < 0.05$ ; \*\* =  $p < 0.01$ ; \*\*\* =  $p < 0.001$ ; \*\*\*\* =  $p < 0.0001$ ). .....204

**Figure 7.6:** The effects of *dam* on biofilm formation and efflux activity in *E. coli*. **a)** Biofilm biomass of  $\Delta dam$  and the wild type (WT), measured by crystal violet staining (OD<sub>590 nm</sub>). Points show two biological and four technical replicates. **b)** Curli biosynthesis in  $\Delta dam$  relative to the WT. Images are representative of four independent replicates. **c)** Dye accumulation in  $\Delta dam$  and the WT. Accumulation of resazurin (excitation 544 nm, emission 580 nm) was measured over 60 minutes and the area under the curve was plotted. Points show two biological and four technical replicates. Both biofilm biomass and dye uptake were measured in stress free conditions (●) and with PA $\beta$ N (○). **d)** Fold change in MICs of acriflavine, azithromycin, cefotaxime and gentamycin in  $\Delta dam$  relative to the WT, measured by the broth (left) and agar (right) dilution methods. The shaded area shows an experimental error of 1-fold change and points show two independent

replicates. For all graphs, error bars show 95% confidence intervals and asterisks (\*) show where there was a significant difference between the strains indicated (Mann–Whitney U test, ns = not significant; \* =  $p < 0.05$ ; \*\* =  $p < 0.01$ ; \*\*\* =  $p < 0.001$ ; \*\*\*\* =  $p < 0.0001$ ). .....206

**Figure 7.7:** The effects of *marA*, *ramA* and *soxS* on biofilm formation and efflux activity in *S. Typhimurium*. **a)** Biofilm biomass of *tolC::cat*, and strains overexpressing *marA*, *ramA* and *soxS* on plasmids, relative to wild type (WT) *S. Typhimurium*. Points represent two biological and eight technical replicates. **b)** Dye accumulation in the WT, *tolC::cat*, and strains overexpressing *marA*, *ramA* and *soxS* on plasmids. Accumulation of resazurin (excitation 544 nm, emission 580 nm) was measured over 100 minutes and the area under the curve was plotted. Points represent two biological and six technical replicates. Both biofilm biomass and dye uptake in strains overexpressing *marA*, *ramA* or *soxS* were compared to the plasmid controls, where expression was not induced with IPTG. Both biofilm biomass and dye uptake were measured in stress free conditions (●) and with PAβN (○). Error bars show 95% confidence intervals and asterisks (\*) show where there was a significant difference between the strains indicated (Mann–Whitney U test, ns = not significant; \* =  $p < 0.05$ ; \*\* =  $p < 0.01$ ; \*\*\* =  $p < 0.001$ ; \*\*\*\* =  $p < 0.0001$ ). .....209

**Figure 7.8:** The effects of *dksA* on biofilm formation and efflux activity in *E. coli*. **a)** Biofilm biomass of  $\Delta dksA$  and the wild type (WT), measured by crystal violet staining (OD<sub>590 nm</sub>). Points show two biological and four technical replicates. **b)** Curli biosynthesis in  $\Delta dksA$  relative to the WT. Images are representative of four independent replicates. **c)** Dye accumulation in  $\Delta dksA$  and the WT. Accumulation of resazurin (excitation 544 nm, emission 580 nm) was measured over 60 minutes and the area under the curve was plotted. Points show two biological and four technical replicates. Dye uptake was measured in stress free conditions (●) and with PAβN (○). **d)** Fold change in MICs of acriflavine, azithromycin, cefotaxime and gentamycin in  $\Delta dksA$  relative to the WT, measured by the broth (left) and agar (right) dilution methods. The shaded area shows an experimental error of 1-fold change and points show two independent replicates. For all graphs, error bars show 95% confidence intervals and asterisks (\*) show where there was a significant difference between the strains indicated (Mann–Whitney U test, ns = not significant; \* =  $p < 0.05$ ; \*\* =  $p < 0.01$ ; \*\*\* =  $p < 0.001$ ; \*\*\*\* =  $p < 0.0001$ ). .....211

**Figure 7.9:** The effects of *tomB* on biofilm formation and efflux activity in *E. coli*. **a)** Biofilm biomass of  $\Delta tomB$  and the wild type (WT), measured by crystal violet staining (OD<sub>590 nm</sub>). Points show two biological and four technical replicates. **b)** Curli biosynthesis in *E. coli* and *S. Typhimurium* wild types and  $\Delta tomB$  mutants., *E. coli*  $\Delta csgD$  and *S. Typhimurium*  $\Delta tolC$ , are included as curli-deficient controls. Images are representative of four technical and two biological replicates. **c)** Dye accumulation in  $\Delta tomB$  and the WT. Accumulation of resazurin (excitation 544 nm, emission 580 nm) was measured over 60 minutes and the area under the curve was plotted. Points show two biological and four technical replicates.

Both biofilm biomass and dye uptake were measured in stress free conditions (●) and with PAβN (○). **d)** Fold change in MICs of acriflavine, azithromycin, cefotaxime and gentamycin in  $\Delta dksA$  relative to the WT, measured by the broth (left) and agar (right) dilution methods. The shaded area shows an experimental error of 1-fold change and points show two independent replicates. For all graphs, error bars show 95% confidence intervals and asterisks (\*) show where there was a significant difference between the strains indicated (Mann–Whitney U test, ns = not significant; \* =  $p < 0.05$ ; \*\* =  $p < 0.01$ ; \*\*\* =  $p < 0.001$ ; \*\*\*\* =  $p < 0.0001$ ). .....213

**Figure 7.10:** The effects of genes involved in LPS biosynthesis on biofilm formation and efflux activity in *E. coli* and *S. Typhimurium*. **a)** Biofilm biomass of deletion mutants and the wild type (WT) of each species, measured by crystal violet staining (OD<sub>590 nm</sub>). Points show two biological and a minimum of six technical replicates. **b)** Curli biosynthesis in deletion mutants relative to the WT of each species. Images are representative of four independent replicates. **c)** Dye accumulation in deletion mutants and the WT of each species. Accumulation of resazurin (excitation 544 nm, emission 580 nm) was measured over 60 minutes in *E. coli* and 100 minutes in *S. Typhimurium* and the area under the curve was plotted. Points show two biological and four technical replicates. Both biofilm biomass and dye uptake was measured in stress free conditions (●) and with PAβN (○). **d)** Fold change in MICs of acriflavine, azithromycin, cefotaxime and gentamycin in deletion mutants relative to the WT of each species, measured by the broth dilution method. The shaded area shows an experimental error of 1-fold change and points show two independent replicates. For all graphs, error bars show 95% confidence intervals and asterisks (\*) show where there was a significant difference between wild type and the mutant indicated (Mann–Whitney U test, ns = not significant; \* =  $p < 0.05$ ; \*\* =  $p < 0.01$ ; \*\*\* =  $p < 0.001$ ; \*\*\*\* =  $p < 0.0001$ ). .....217

**Figure 7.11:** The effects of *ompR* and *cyaA* on biofilm formation and efflux activity in *E. coli* and *S. Typhimurium*. **a)** Biofilm biomass of  $\Delta ompR$  relative to wild type (WT) *E. coli* and  $\Delta cyaA$  relative to WT *S. Typhimurium*, measured by crystal violet staining (OD<sub>590 nm</sub>). Points show two biological and a minimum of four technical replicates. **b)** Curli biosynthesis of  $\Delta ompR$  and  $\Delta cyaA$  relative to the WT of each species. Images are representative of four technical and two biological replicates. **c)** Dye accumulation in  $\Delta ompR$ ,  $\Delta cyaA$  and the WT of each species. Accumulation of resazurin (excitation 544 nm, emission 580 nm) was measured over 60 minutes for *E. coli* and 100 minutes for *S. Typhimurium*, and the area under the curve was plotted. Points show two biological and four technical replicates. Both biofilm biomass and dye uptake were measured in stress free conditions (●) and with PAβN (○). **d)** Fold change in MICs of acriflavine, azithromycin, cefotaxime and gentamycin in  $\Delta dksA$  relative to the WT, measured by the broth (left) and agar (right) dilution methods. The shaded area shows an experimental error of 1-fold change and points show two independent replicates. For all graphs, error bars show 95%

confidence intervals and asterisks (\*) show where there was a significant difference between the strains indicated (Mann–Whitney U test, ns = not significant; \* =  $p < 0.05$ ; \*\* =  $p < 0.01$ ; \*\*\* =  $p < 0.001$ ; \*\*\*\* =  $p < 0.0001$ ).....220

## List of Tables

<b>Table 2.1:</b> Bacteria used in this work.....	51
<b>Table 2.2:</b> PCR programme .....	53
<b>Table 2.3:</b> Plasmids used in this work. ....	57
<b>Table 2.4:</b> Primers used in this work. Primers were synthesised by Sigma.....	58
<b>Table 3.1:</b> MIC ( $\mu\text{g}/\text{mL}$ ) of multiple antibiotics in <i>S. Typhimurium</i> and <i>S. Typhimurium::lacZ</i> . Values are the average of two biological replicates and the experimental error was a 1-fold change in MIC.....	86
<b>Table 3.2:</b> CFU per bead and gDNA per bead of <i>E. coli</i> BW2113 and <i>S. Typhimurium::lacZ</i> biofilms on beads over time. Values are the mean of 2 technical replicates. ....	95
<b>Table 3.3:</b> MIC ( $\mu\text{g}/\text{mL}$ ) of multiple antibiotics in <i>S. Typhimurium::lacZ</i> and <i>E. coli</i> BW25113, with and without efflux inhibition by 125 $\mu\text{g}/\text{mL}$ PA $\beta$ N. Two biological replicates per antibiotic per strain were completed. The experimental error was a fold change.....	96

# **1. CHAPTER 1: INTRODUCTION**

## 1.1. Biofilms

Most bacteria readily form aggregated multicellular communities called 'biofilms', and for many species this is the normal mode of life. Understanding how bacteria behave in a biofilm is therefore intrinsically important to our understanding of bacterial physiology, as well as being important in clinical, domestic and industrial contexts. Bacteria in nature rarely exist planktonically and are often found as part of multi-species communities with their associated extracellular matrix, aggregated together and often attached to a surface (Sasahara and Zottola, 1993, Kumar and Anand, 1998, Berlanga and Guerrero, 2016). When not attached to a surface, biofilms can form aggregates where cells are attached to one another (Kragh et al., 2016, Melaugh et al., 2016). Bacteria transition through a biofilm lifecycle, where planktonic cells adhere to a surface and start to aggregate, before the biofilm grows and matures with characteristic production of extracellular matrix before finally cells can disperse from the biofilm, becoming planktonic again, to colonise new surfaces (Berlanga and Guerrero, 2016, Mah and O'Toole, 2001).

One of the hallmarks of bacteria found in a biofilm is their resistance to a range of antibiotics, biocides, toxins and detergents, as compared to their planktonic counterparts. Changes in gene and protein expression, and in the physiology of biofilms with their low levels of metabolic activity, promote the formation of 'persister' cells (Bigger, 1944). These are dormant, non-dividing cells that tolerate a wide range of antimicrobials, allowing biofilms to be typically 10-1000-fold less sensitive to drugs (Mah and O'Toole, 2001, Hoyle and Costerton, 1991). An infection caused by biofilm-forming bacteria is rarely resolved with antibiotic chemotherapy alone due to decreased drug sensitivity, therefore infections persist after treatment and can result in worse patient outcomes. Biofilms can be found colonising catheters, artificial joints and skin wounds, and can prevent wound healing (Mah and O'Toole, 2001, Percival et al., 2012). Perhaps the most studied example of the clinical importance of antibiotic resistance in biofilms is *Pseudomonas* infections in patients with cystic fibrosis. Chronic *Pseudomonas* infections occur due to bacterial biofilms conferring resistance to phagocytosis by the body's immune system as well as decreased susceptibility to antibiotic treatments. These prolonged, persistent infections lead to a heightened antibody response and chronic inflammation in the lungs, which result in devastating lung damage and usually ultimately kill the patient (Alcalde-Rico et al., 2016, Høiby et al., 2010). We are becoming more aware of the importance of biofilm formation in any industry dependent on killing bacteria, including veterinary, pharmaceutical, agricultural industries and water treatment systems (Mah and O'Toole, 2001). Additionally, there are many useful applications of biofilms, including wastewater treatment and bioengineering applications (Flemming et al., 2016)

Whilst there are a number of common hallmarks of biofilms formed by different species (matrix production, slow metabolic rates and antimicrobial resistance, see Fux et al. (2005) for review), the specific genes involved in the regulation of these phenotypic changes vary in different species. Little is known about the details of complex regulatory networks controlling biofilm formation (Amores et al., 2017). There are various model organisms which have been the focus of detailed study to reveal mechanisms of biofilm formation, including *Pseudomonas* spp. (important due to its prevalence in infections in the lungs of patients with cystic fibrosis (Sriramulu et al., 2005, Høiby et al., 2010)), *Bacillus subtilis* (important as a colonising organism of plant roots (Branda et al., 2006, Mielich-Süss and Lopez, 2015)) and *Staphylococcus aureus* (where biofilms are common on implanted medical devices (Beenken et al., 2004, Resch et al., 2005)). The *Salmonella* biofilm has also been widely studied as a model foodborne pathogen, for example studies have investigated biofilms on plants in a tomato model (Cevallos-Cevallos et al., 2012, Shaw et al., 2011), on food processing materials such as metal and glass (Speranza et al., 2011, Prouty and Gunn, 2003) and the medical implications of chronic disease and carriage mediated through biofilms on gallstones (Crawford et al., 2010, Prouty and Gunn, 2003, Prouty et al., 2002) (See Steenackers et al. (2012) for review).

There is an interesting and complex relationship between biofilm formation and bacterial virulence. The changes in gene expression and metabolism that occur as part of biofilm formation can often result in reduced expression of virulence factors required for infection, such as the downregulation of SPI virulence genes in *Salmonella* biofilms *in vivo* (Desai et al., 2019). This results in reduced immediate pathogenicity through asymptomatic disease carriage. However, because of this reduced metabolic activity, biofilms can augment bacterial virulence by allowing persistence *in vivo*, resulting in long term asymptomatic disease carriage that is less susceptible to antimicrobial treatment. *Salmonella* biofilms have been observed growing on gall stones in humans with chronic but asymptomatic infections (Prouty et al., 2002). Studies in mice have found increased disease transmission from individuals with *Salmonella* biofilms on their gall stones as compared to infected mice without gall stones (Crawford et al., 2010). In some situations, production of a biofilm may offer a strategy to allow reproduction and dissemination of the pathogen without killing its host whilst in others acute pathology can directly result from the presence of a biofilm.

#### **1.1.1. S. Typhimurium and E. coli epidemiology**

The World Health Organisation estimated that there were 600 million cases and 420,000 deaths from foodborne illnesses in 2010 (WHO, 2015). A major cause of diarrhoeal disease, estimated to cause over half of these deaths, was nontyphoidal *Salmonella enterica* (WHO, 2015). Another major foodborne disease agent is *Escherichia coli*,



specifically enteropathogenic *E. coli* (EPEC) and enterotoxigenic *E. coli* (ETEC) (Aijuka and Buys, 2019, WHO, 2015). In the EU in 2018, the top three agents responsible for the most commonly reported human zoonoses were *Campylobacter* spp., *Salmonella* spp. and Shiga toxin-producing *E. coli* (EFSA and ECDC, 2019). It was calculated that nontyphoidal *Salmonella enterica* and EPEC were responsible for 18 million disability life adjusted years, a metric the WHO uses to determine disease burden (WHO, 2015). Non-invasive *Salmonella* and *E. coli* infections are associated with diarrhoea and vomiting, while more serious invasive nontyphoidal *Salmonella* infections, which can result in bacteraemia and meningitis, are more common in sub-Saharan Africa (Stanaway et al., 2019). The probability of serious complications increases with risk factors such as malnourishment, increased age, sickle-cell disease and co-infection with HIV (Stanaway et al., 2019, WHO, 2015). In the UK, it is estimated that 25% of the population suffers from an infectious intestinal disease each year, with 17 million cases per year (Tam et al., 2012). Up to 2010, reports of *Salmonella* infections were decreasing in England and Wales as well as across Europe, but since then the number of cases has remained constant (PHE, 2016, ECDC, 2020).

The main vectors of nontyphoidal *Salmonella* are eggs and egg products, with recent European outbreaks caused by contaminated eggs (2016), sesame paste (2016), infant formula (2017) and poultry products (2017) (ECDC, 2020). The two most common *Salmonella* serotypes in England and Wales are Enteritidis and Typhimurium, together accounting for just under 50% of all nontyphoidal salmonellosis reported in England in Wales in 2015 (PHE, 2016). These serotypes have a broad host range and can be found in beef, pork, poultry products, seafood, fruits and vegetables (Ferrari et al., 2019). Other relevant nontyphoidal *Salmonella* serotypes are Newport, Infantis and monophasic Typhimurium, where infections in the EU are mostly associated with poultry and pork (EFSA and ECDC, 2018). As well as meat sources, multiple *Salmonella* serotypes have also been identified in irrigation water, directly contaminating crops (Santiago et al., 2018). Invasive nontyphoidal *Salmonella* infections are most common in sub-Saharan Africa, mostly caused by *S. Typhimurium*, specifically ST313 which can result in a typhoid-like disease (Kingsley et al., 2009). *E. coli* is mostly transmitted through meat products and their processing environments (Osman et al., 2018, Nesse et al., 2014). Enterohaemorrhagic *E. coli* O157:H7 is a major cause of foodborne illness and is mostly found in bovine food products and product contaminated by waste from these environments (Lim et al., 2010).

### 1.1.2. *S. Typhimurium* and *E. coli* biofilms

Biofilms allow bacteria to persist on surfaces and make decontamination more difficult. As well as the food sources already mentioned, *Salmonella* biofilms have been found to form on abiotic surfaces in food processing environments, including slaughterhouses, kitchens, factories and animal feed processing environments (Steenackers et al., 2012, Vestby et al., 2009). Strains of *E. coli* found in sheep and cattle farming environments were found to form biofilms in a range of environments to facilitate their colonisation and persistence (Osman et al., 2018, Nesse et al., 2014). This is further complicated a decrease in antimicrobial susceptibility found in *Salmonella* Typhimurium isolated from the food chain, making infections more difficult to treat (Wang et al., 2019, Osman et al., 2018).

*E. coli* is also one of the best understood model organisms in modern molecular biology (Blount, 2015). *E. coli* K-12 was first isolated in Stanford in 1922 and is used regularly as a relatively safe, non-pathogenic lab strain. A major milestone in molecular microbiology using *E. coli* K-12 included the creation of the Keio collection; a library of single-gene deletion mutants of every non-essential gene in the *E. coli* genome, created to further the field of functional genomics and understand the role of every gene (Baba et al., 2006). Recent high-density transposon mutant libraries made in *E. coli* have been used to determine the genes and regulatory networks important for survival under any given stress condition (Yasir et al., 2020). Though there is some concern about the applicability of data generated from a laboratory-adapted non-pathogenic bacterial strain (Hobman et al., 2007), data generated by *E. coli* K-12 can still be used to identify genes important in a given phenotype with the option for relatively easy phenotypic validation via the available mutant libraries. In this thesis, data from *E. coli* was compared to that generated by *S. Typhimurium* to allow genes of generic importance in biofilm formation in Enterobacteriaceae to be identified. *S. Typhimurium* and *E. coli* biofilms have significant similarities and the organisms are closely related albeit having diverged 140 million years ago (Wirth et al., 2006). For both species, the most important extracellular components for biofilm formation, aggregation and adhesion have been shown to be curli and cellulose (Barnhart and Chapman, 2006).

### 1.1.3. Curli

Curli is an amyloid fibrous protein exposed on the cell surface and is a main component of the biofilm matrix in *E. coli* and *S. Typhimurium*, involved in adhesion and aggregation (See Barnhart and Chapman (2006) and Van Gerven et al. (2015) for review). It's production is essential for effective biofilm formation in *Salmonella*, as deletion of curli fibres has been shown to prevent biofilm formation (Jonas et al., 2007). Curli has also been implicated in virulence, as it has a role in adhering to host cells to facilitate host colonisation (Barnhart and Chapman, 2006, Bian et al., 2000)

Two divergently transcribed operons encode curli: *csgBAC* and *csgDEFG* (figure 1.1). The structural subunits of curli fibres are made up of CsgB and CsgA, where CsgB is a nucleator protein that directs the major subunit, CsgA, to polymerise to form curli fibres (Mao et al., 2019). CsgC interacts with CsgA in the periplasm to prevent its polymerisation and stop curli fibres from forming inside the cell, keeping CsgA in a form that can withstand degradation and facilitates its secretion (Evans et al., 2015). CsgG is an outer membrane protein that forms a pore, through which CsgA and CsgB are secreted, and interacts with CsgE and CsgF to stabilise CsgA and CsgB and facilitate efficient curli fibre formation (Loferer et al., 1997). CsgF is a surface-located protein associated with CsgG that is required for surface-associated CsgB-mediated nucleation of curli fibres. Inactivation of *csgF* results in detached polymerised curli fibres in the extracellular environment, suggesting the role of CsgF in the localisation of CsgB and CsgA (Nenninger et al., 2009). CsgE aids in the recruitment of CsgA to the CsgG pore for secretion and prevents lethal aggregation of curli subunits within the periplasm (Nenninger et al., 2011).

The transcriptional regulator, *csgD*, activates transcription of the *csgBAC* operon to increase curli production (Brombacher et al., 2006). As well as regulating curli fibre biosynthesis, CsgD positively regulates cellulose biosynthesis through increasing *adrA* expression, which encodes a diguanylate cyclase. AdrA drives the synthesis of the secondary messenger molecule c-di-GMP, which binds to and initiates transcription of the cellulose biosynthesis operon *bcsABZC* (Garcia et al., 2004, Römling et al., 2000). Expression of *adrA* alongside *csgD* has been shown to rescue biofilm formation when expressed in a poor biofilm-forming strain of *S. Typhimurium* (Garcia et al., 2004).

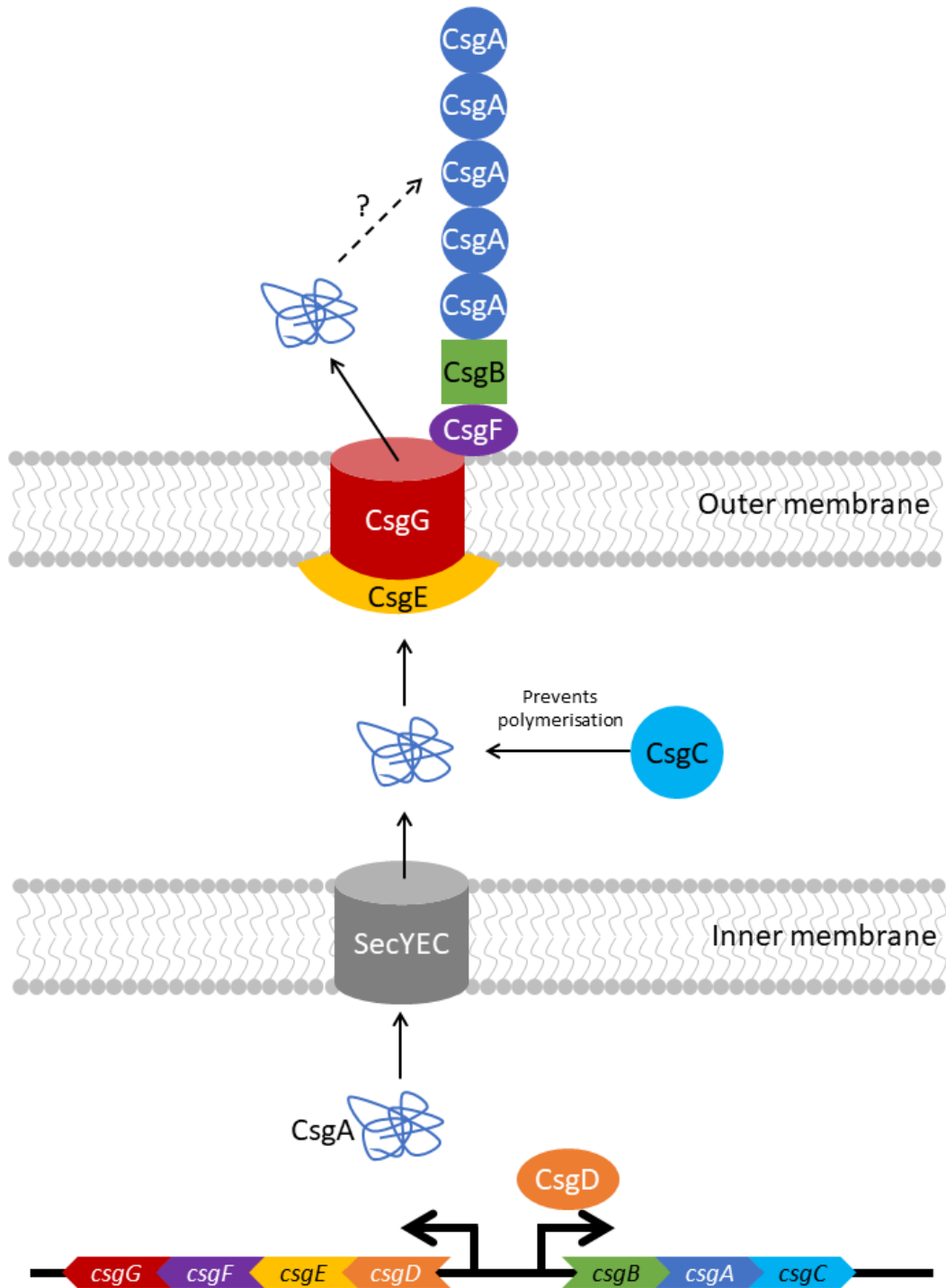


**Figure 1.1:** Curli operon and products. Figure adapted from Van Gerven et al. (2015).

#### 1.1.4. Cellulose

Cellulose is a polysaccharide that makes up a large part of the extracellular matrix of the biofilm for a wide range of bacterial species (See Serra and Hengge (2019) for review). The importance of cellulose in the biofilm may depend on environmental factors, as *S. Typhimurium* grown in the presence of cellulase could form biofilms on gallstones but not on glass surfaces (Prouty and Gunn, 2003). Disruption of the cellulose biosynthetic pathway prevented biofilm formation on tomatoes (Shaw et al., 2011) and images of biofilms formed by these mutants on glass slides revealed the formation of aggregates but not a confluent biofilm (Jonas et al., 2007). The importance of cellulose may also vary by serovar, as mutations and early stop codons have been identified in *Salmonella* Typhi in the operon encoding the cellulose biosynthetic machinery (Römling et al., 2003, Nuccio et al., 2014), and host-restricted serovars of *Salmonella enterica* were less able to form biofilms (Römling et al., 2003). There is a lack of evidence surrounding the contribution of cellulose to biofilm formation in *S. Typhi* and other host-restricted pathogens, which may be due to differences between their *in vivo* environment and lab model conditions. The role of curli in the biofilm matrix seems to be critical but the role of cellulose is less clear.

Cellulose biosynthesis is mediated by the constitutively-transcribed divergent operons *bcsRQABZC* and *bcsEFG* (Zogaj et al., 2001, Solano et al., 2002) (See Serra and Hengge (2019) and Whitney and Howell (2013) for review) (figure 1.2). The main catalytic protein is made up of two subunits, BcsA and BcsB, and sits in the inner membrane. The BcsA subunit has a cytoplasmic face that has a PilZ domain to bind c-di-GMP for activating cellulose biosynthesis (Ryjenkov et al., 2006, Morgan et al., 2014), and an active site for binding UDP-glucose, where glucose is transferred to the growing glucan chain (Lin et al., 1990). This chain is fed through a channel inside the BcsA-BcsB complex into the periplasm (Morgan et al., 2012). Once there, the periplasmic cellulase BcsZ breaks down long polysaccharide chains to allow efficient secretion and assembly outside of the cell (Mazur and Zimmer, 2011). Cellulose chains are secreted from the cell through BcsC, which is predicted to form a large outer membrane porin (Keiski et al., 2010).

Next to the BcsA-BcsB complex on the inner membrane sits the transmembrane protein BcsG which acts as a phosphoethanolamine (pEtN) transferase. As the growing cellulose chain is fed through BcsB into the periplasm, BcsG interacts with this chain to aid in the assembly of long, thick, straight cellulose filaments. Its activity is most probably regulated through its interaction with BcsF, which interacts with BcsE. In the inner membrane, BcsF sits next to and closely interacts with BcsG and BcsE, but its role is still undefined (Thongsomboon et al., 2018). BcsE is a cytosolic c-di-GMP-binding protein that is not essential for cellulose synthesis but required for optimal synthesis (Fang et al., 2014). Together, BcsEFG functions close to BcsA-BcsB and has been implicated in contributing

to BcsA-BcsB assembly or stability (Thongsomboon et al., 2018). Other essential components include BcsQ, which is a cytosolic protein determined to be involved in localising cellulose production at the poles and initiating cellulose-mediated cell-to-cell adhesion (Le Quéré and Ghigo, 2009). The role of BcsR is yet to be determined. It is known to be a small protein essential for cellulose secretion and is predicted to be cytosolic (Krasteva et al., 2017, Serra and Hengge, 2019).

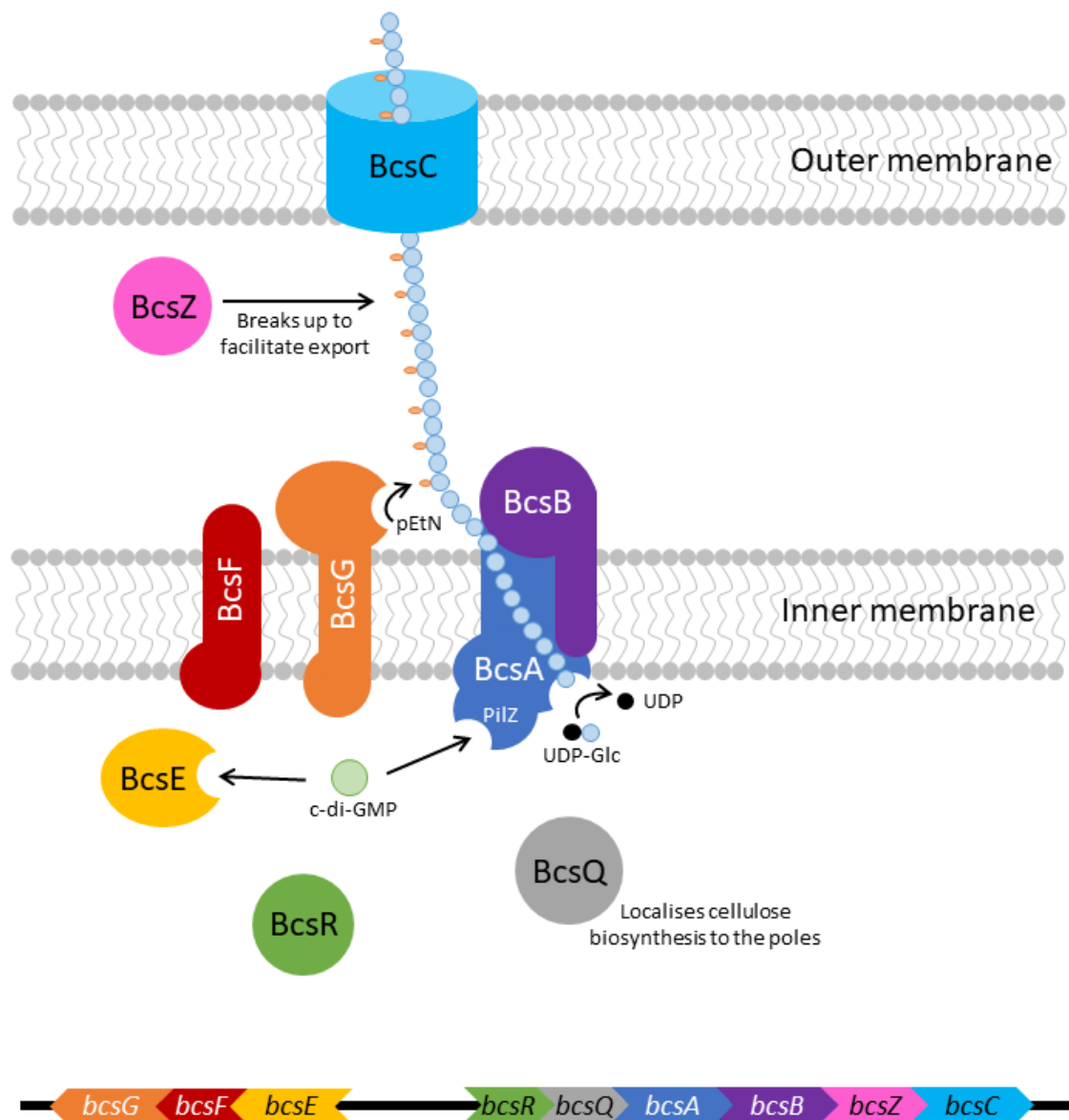


**Figure 1.2:** Cellulose biosynthesis machinery. Adapted from figures from Thongsomboon et al. (2018) and Serra and Hengge (2019).

### 1.1.5. Other important components of the biofilm

Extracellular DNA (eDNA) makes up an integral part of many bacterial biofilms (Tetz et al., 2009). Biofilms formed by *Pseudomonas aeruginosa* (Whitchurch et al., 2002), *Bacillus cereus* (Vilain et al., 2009) and a range of Gram-negative pathogens including *E. coli* (Tetz et al., 2009) could not grow in the presence of DNase, demonstrating the importance of eDNA in the biofilm matrix. Previous work in *Pseudomonas aeruginosa* revealed that DNA is released by explosive cell lysis, and that sustained eDNA release is required for microcolony formation (Hynen et al., 2020).

The curli transcriptional regulator CsgD also positively regulates the expression of *bapA*, encoding the large secreted protein BapA. It has been found to be important for bacterial aggregation, pellicle formation and thus biofilm formation, and makes up a considerable part of the *S. Typhimurium* biofilm (Latasa et al., 2005). However, the role of BapA role is not well understood, as microscopy studies have found no discernible difference in biofilm formation between a *bapA*-deficient strain and wild type *S. Typhimurium* (Jonas et al., 2007).

## 1.2. Regulation of biofilm formation in *E. coli* and *S. Typhimurium*

### 1.2.1. Cyclic-di-GMP

C-di-GMP is a secondary messenger molecule that binds to a wide range of effector proteins to regulate their activities, including biosynthesis of biofilm components (See Hengge (2009) for review). The levels of c-di-GMP in the cell are controlled by diguanylate cyclases containing GGDEF protein domains, responsible for c-di-GMP synthesis, and degraded by phosphodiesterases containing EAL protein domains (Simm et al., 2004) (figure 1.3). As previously outlined, c-di-GMP has a large role in regulating cellulose production through binding to BcsA and BcsE and activating its biosynthesis. C-di-GMP has also been implicated in modulating *csgD* expression, but the mechanism through which this acts is yet to be determined (Kader et al., 2006). It also affects motility via two mechanisms: c-di-GMP binding to YcgR reduces flagella motor direction and speed, and accumulation of extracellular cellulose (due to increased cellulose production via c-di-GMP) has been seen to prevent flagella rotation (Ryjenkov et al., 2006, Zorraquino et al., 2013). C-di-GMP has also been implicated in the stress response, through the *dosCP* system (previously *yddV-dos* operon). This consists of a diguanylate cyclase and a phosphodiesterase, respectively, and has been implicated in c-di-GMP regulation under oxygen stress. Changes in c-di-GMP homeostasis arise when each gene product binds oxygen at different rates. This results in reduced biofilm formation under low oxygen conditions (Tuckerman et al., 2009). A functional *yddV* gene is required for expression of the *csgBAC* operon, but not the *csgDEFG* operon (Tagliabue et al., 2010), suggesting that

c-di-GMP acts directly on expression of the curli subunits rather than their transcriptional regulator.

C-di-GMP seems to play an important role in the trade-off between virulence and biofilm formation, whereby the transition between planktonic and biofilm lifestyles involves attenuation. Increased intracellular levels of c-di-GMP in *S. Typhimurium* that promote biofilm formation have also been shown to inhibit intracellular invasion through reduced expression of the type III secretion system effector protein SipA, which is also inhibited by CsgD (Ahmad et al., 2011). An inverse relationship between biofilm and virulence has also been reported, whereby virulence can be increased at the expense of biofilm formation. Increased expression of the virulence factor MgtC occurs following intracellular invasion of *Salmonella* into host cells, which results in reduced cellulose biosynthesis via decreased transcription of *bcsA* and a reduction in c-di-GMP levels (Pontes et al., 2015). This demonstrates how bacteria can adapt and maximise their fitness in an environment through modulating intracellular levels of c-di-GMP.

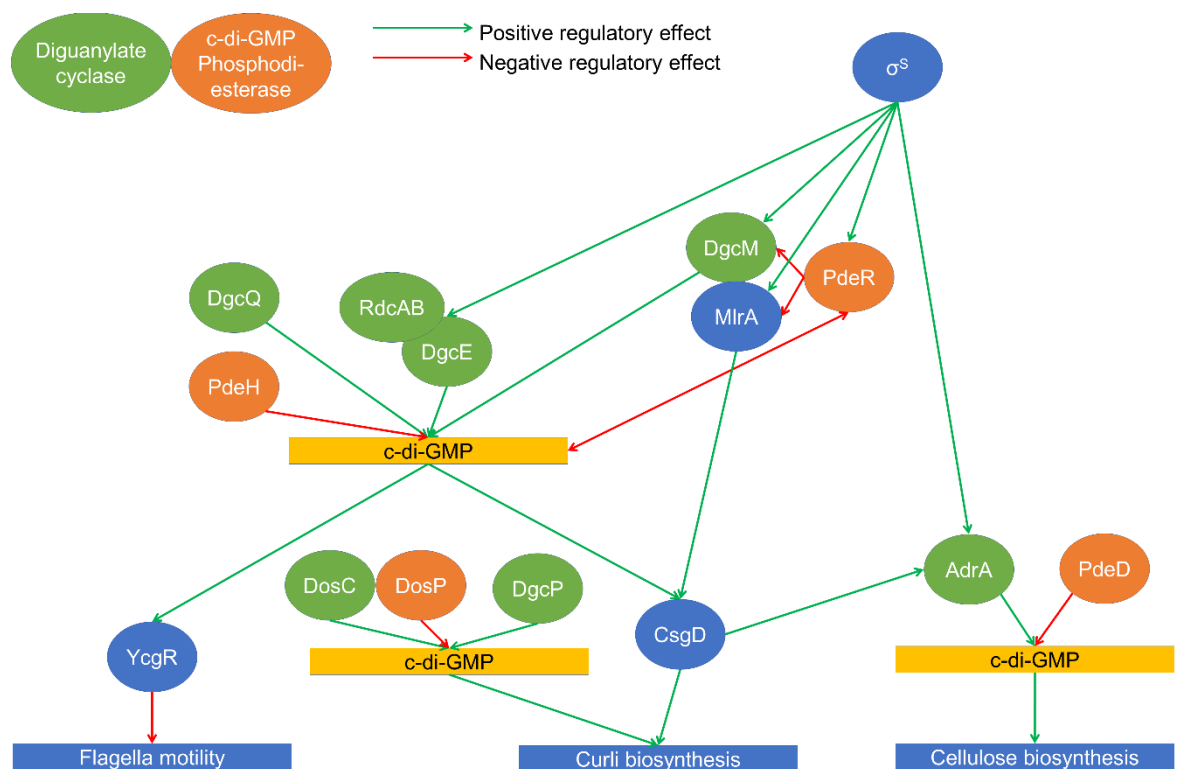


**Figure 1.3:** Regulation of c-di-GMP metabolism and its effects on biofilm matrix production. Figure adapted from Hengge (2009) and Hengge (2020).



### 1.2.2. RpoS/ $\sigma^S$

The sigma factor *rpoS* ( $\sigma^S$ ) is the master regulator of stationary phase genes, many of which are associated with the general stress response in Gram-negative bacteria (Suh et al., 1999, Xu et al., 2001). Its expression has been implicated in survival under antibiotic and toxin stress, expression of virulence factors, quorum sensing and biofilm formation (Trastoy et al., 2018). Many avirulent *E. coli* K-12 strains have amber mutations in *rpoS* that confer reduced virulence (Kaasen et al., 1992, Olsén et al., 1993) and *rpoS* mutants are responsible for attenuation in *S. Typhimurium* strains (Swords et al., 1997), implicating the role of  $\sigma^S$  in pathogenicity. Synthesis of  $\sigma^S$  is positively regulated by the alarmone (p)ppGpp and the transcription factor DksA, which themselves regulate the stringent response and the transition to stationary phase independently of *rpoS* (Girard et al., 2018, Gentry et al., 1993). Expression of (p)ppGpp is highly linked with decreased growth rate, persister cell formation and biofilm formation (Helaine and Kugelberg, 2014).

Expression of *rpoS* has been suggested to be essential for biofilm formation in *E. coli* (Tagliabue et al., 2010, Schembri et al., 2003, Römling et al., 1998a) and *S. Typhimurium* (Prouty and Gunn, 2003). An *rpoS* mutant was seen to have a different extracellular matrix to the wild type, suggesting that  $\sigma^S$  regulates matrix component production (Römling et al., 2000). This was found to be mediated through *rpoS*-dependent expression of *mlrA*, which activates *csgD* transcription (Brown et al., 2001). Expression of *rpoS* has also been found to positively regulate various genes known to synthesise and degrade c-di-GMP, thus promoting biofilm matrix production (Weber et al., 2006). However, *rpoS* has also been seen to negatively regulate initial adhesion during biofilm formation triggered by changes in osmolarity and overproduction of curli, resulting in increased transcription of *cpxR*, which represses transcription of *csgB* and *csgD* (Prigent-Combaret et al., 2001). This suggests that the effect of  $\sigma^S$  on biofilm formation is condition specific.

It is predicted the *rpoS* plays an important role in temperature-dependent curli expression, where expression of *csgD* is maximised at 30 °C relative to low expression at 37 °C (Olsén et al., 1993, Sokaribo et al., 2020). It was found that constitutive, *rpoS*-independent expression of *csgD* relieved temperature-dependent curli expression, either through point mutations in the *csgD* promoter (Römling et al., 1998b) or by increased levels of c-di-GMP (Kader et al., 2006). Temperature-dependent expression may be mediated through *rpoS*-regulated diguanylate cyclases *yaiC*, *ydaM* and *yddV* activated at lower temperatures, thereby increasing c-di-GMP and curli biosynthesis (Weber et al., 2006). There is conflicting evidence as to whether temperature regulation of curli acts on either the *csgD* promoter (Römling et al., 1998b) or the *csgBAC* promoter (Brombacher et al., 2006, Bougdour et al., 2004). The latter is consistent with the hypothesis that *rpoS*, along with

*crl*, are responsible for temperature regulation of curli biosynthesis. Crl is thought to be a secondary thermosensor which accumulates in the cell at 30 °C, but not 37 °C, and interacts directly with  $\sigma^S$  to activate curli biosynthesis via the *csgBAC* promoter (Bougdoor et al., 2004, Pratt and Silhavy, 1998). However, transcription of *csgBAC* remained temperature-dependent in an *E. coli* mutant with inactivated *rpoS* and *hns*, suggesting the existence of other mechanisms of temperature-controlled transcription (Bougdoor et al., 2004)

### 1.2.3. EnvZ/OmpR

The EnvZ/OmpR two-component regulatory system is made up of the sensor histidine kinase EnvZ and the transcriptional response regulator OmpR (figure 1.4). In response to osmotic or pH stress, EnvZ phosphorylates OmpR and dephosphorylates OmpR-P to regulate downstream gene expression (Cai and Inouye, 2002, Chakraborty and Kenney, 2018). Only *ompR* and *envZ* make up the operon *ompB* and are controlled by the same promoter. OmpR positively regulates biofilm formation through *csgD* activation by binding to the *csgD* promoter, thereby inducing production of biofilm matrix components (Gerstel and Römling, 2001, Römling et al., 1998a, Vidal et al., 1998). Curli biosynthesis is also regulated by pH, whereby expression of *csgD* increases as pH increases, however it is unclear whether this is sensed through EnvZ/OmpR or an alternative pathway. It is thought that pH-dependent curli expression is regulated through the *csgD* promoter, as a constitutive *csgD* promoter showed higher expression of CsgD at low pH and lower expression at high pH (Gerstel and Römling, 2001). OmpR also has a role in regulating motility through repressing flagella expression via *flhDC* in *E. coli* (Shin and Park, 1995). However, the opposite is true in *Yersinia enterocolitica*, where OmpR positively regulates *flhDC* and an *ompR* mutant was non motile (Raczkowska et al., 2011). This demonstrates that the regulome of OmpR and its effect on biofilm formation is complex and not broadly conserved.

The most well-understood regulatory pathway of OmpR is its effect on the expression of outer membrane porins OmpC and OmpF. Low levels of OmpR-P result in transcription of *ompF* and high levels of OmpR-P cause transcriptional repression of *ompF* and activate transcription of *ompC* (Cai and Inouye, 2002). OmpR also regulates OmpF through increasing the expression of *micF*, which is an anti-sense RNA that inhibits translation of *ompF* RNA (Aiba et al., 1987). OmpR also has a role in virulence, where it binds to and induces expression of SPI-2 regulators and effector genes (Garmendia et al., 2003, Xu and Hensel, 2010). Insertional inactivation of *ompR* resulted in attenuation on *S. Typhimurium* in a mouse model (Dorman et al., 1989). Although insertional inactivation of *ompC* and *ompF* had no effect on virulence of *S. Typhimurium* in a mouse model (Dorman

et al., 1989), deletion of *ompC* and *ompF* in avian pathogenic *E. coli* resulted in reduced adherence, colonisation and invasion in duck and mouse models (Hejair et al., 2017).

#### **1.2.4. CpxA/CpxR**

The CpxA/CpxR two-component regulatory system is made up of the membrane-associated sensory protein CpxA which phosphorylates and dephosphorylates the cytoplasmic transcriptional regulator CpxR in response to high osmolarity (Dong et al., 1993, Jubelin et al., 2005) (figure 1.4). The periplasmic protein CpxP prevents autophosphorylation of CpxA when the membrane is not under stress (Fleischer et al., 2007). The Cpx system has been implicated in positively regulating virulence gene expression (Nakayama and Watanabe, 1998), pili expression and assembly (Hung et al., 2001) and membrane protein folding (Duguay and Silhavy, 2004). Similar to the EnvZ/OmpR system, CpxR can regulate the membrane porins OmpC and OmpF, resulting in reduced expression of *ompF* and increased expression of *ompC* (Batchelor et al., 2005).

The Cpx system plays an important role in initial adhesion to abiotic surfaces, important for biofilm formation (Otto and Silhavy, 2002). In response to high osmolarity, CpxA phosphorylates CpxR, which binds to and represses transcription of *csgD* and *csgA* to prevent curli synthesis (Jubelin et al., 2005, Dorel et al., 1999). CpxA can also act to promote biofilm formation by dephosphorylating CpxR and thus allowing transcription of *csgA* (Dorel et al., 1999). However, its effect on curli expression is most likely secondary to other regulatory pathways, as inactivation of *cpxR* had no effect on biofilm matrix production, as seen through differences in Congo red morphology compared to wild type *S. Typhimurium* in conditions of high osmolarity (Gerstel and Romling, 2003).

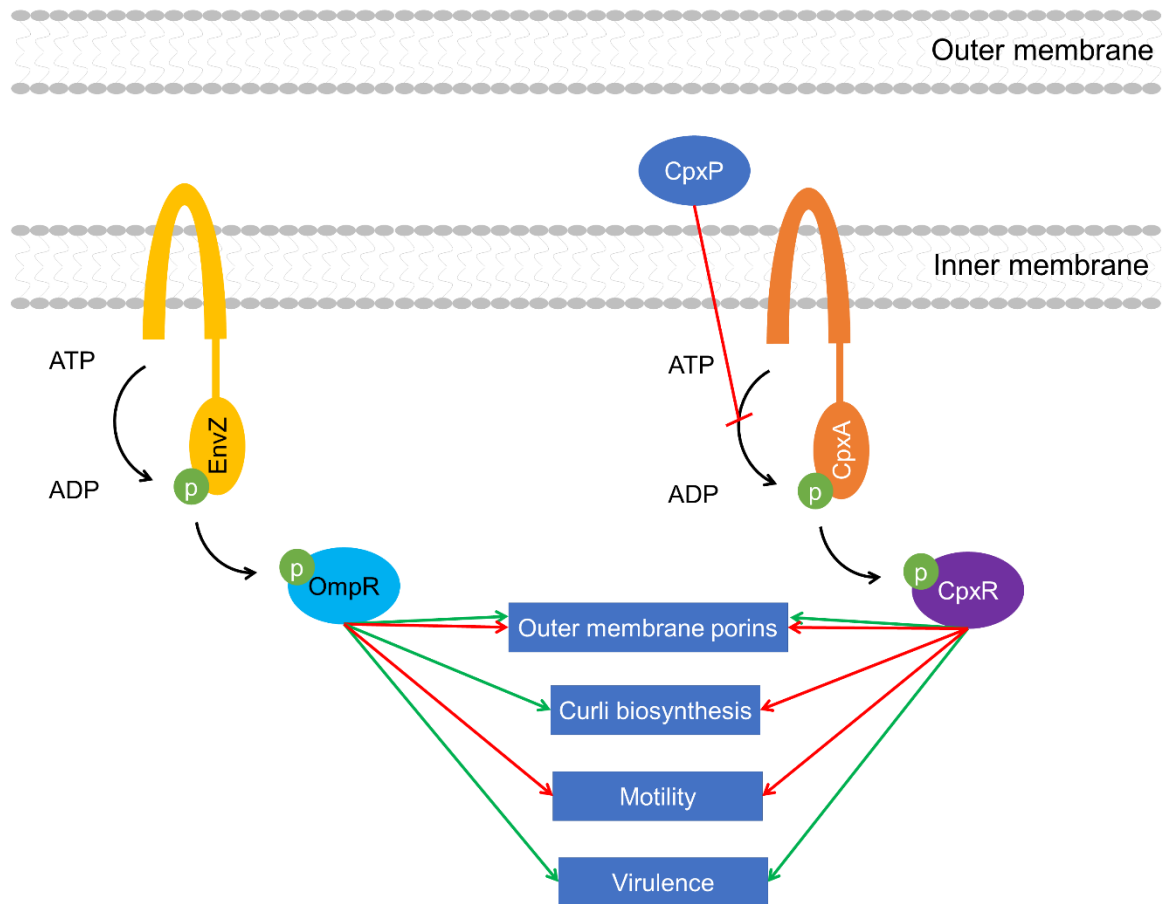


**Figure 1.4:** Two component signalling systems EnvZ/OmpR and CpxAR and their regulatory effects.

### 1.2.5. H-NS

Histone-like nucleoid structuring protein (H-NS) is a DNA binding protein involved in transcriptional regulation (Schroder and Wagner, 2002). It does not bind to specific DNA sequences, but does preferentially bind to bent DNA (Yamada et al., 1990). It has a role in many global regulatory networks and plays a key role in responding the stress and maintaining homeostasis in challenging conditions (Schroder and Wagner, 2002). Microarray analyses have implicated a role for H-NS in virulence regulation, stress responses, motility and growth (Müller et al., 2006).

The relationship between H-NS and biofilm formation is complex and differs between *E. coli* and *S. Typhimurium*. In *E. coli*, H-NS represses curli biosynthesis through repressing transcription of *csgA* (Weber et al., 2006, Olsén et al., 1993), however inactivation of H-NS in *S. Typhimurium* resulted in reduced curli expression through reduced expression of *csgD* (Gerstel et al., 2003). H-NS also negatively regulates *ompR* in *S. Typhimurium*, thereby repressing an activator of *csgD* expression (Bang et al., 2002). It plays an important role in growth phase-dependent regulation, where H-NS negatively regulates

*rpoS* expression in growing cells to prevent stationary phase-related gene expression (Weber et al., 2006, Lucchini et al., 2009).

#### 1.2.6. IHF

Integration host factor (IHF) is a histone-like DNA binding protein that binds at site-specific sequences and introduces a bend in the DNA (Goosen and van de Putte, 1995, Thompson and Landy, 1988). This aids in the recruitment of other machinery necessary for transcription. IHF and other histone-like proteins are necessary accessory factors in many other cellular processes, such as DNA replication, site-specific recombination and transcription (Goosen and van de Putte, 1995). There may be some redundancy between histone-like proteins, where the growth rate of *E. coli* mutants lacking IHF or HU (another small histone-like protein) was not impaired, but deletion of IHF, HU and H-NS was lethal for the cell (Yasuzawa et al., 1992). IHF plays an important role in virulence regulation in *S. Typhimurium*, where it positively regulates expression of type III secretion systems SPI-1 and SPI-2. Inactivation of *ihfA* or *ihfB* in this strain was seen to greatly reduce epithelial cell invasion (Mangan et al., 2006). It also has a role as a negative transcriptional regulator, through inhibiting expression of membrane porins *ompC* and *ompF*, as well as the *ompB* operon containing *envZ* and *ompR* (Huang et al., 1990, Tsui et al., 1991b).

An *ihfAB* mutant in *S. Typhimurium* exhibited reduced expression of known stationary phase genes, suggesting that IHF plays an important role in stationary phase-dependent and *rpoS*-dependent gene expression (Mangan et al., 2006). IHF has been implicated in regulating biofilm matrix production through directly binding to the *csgD* promoter to activate *csgD* transcription. It has been suggested to regulate biofilm formation in low oxygen conditions, where IHF activates *csgD* expression under oxygen stress (Gerstel et al., 2003, Gerstel and Romling, 2003, Gerstel and Römling, 2001). However, deletion of *ihfAB* resulted in reduced curli production, as seen through its Congo red morphology, regardless of oxygen stress (Gerstel et al., 2003).

#### 1.2.7. Rcs

The Rcs system is a complex signalling pathway involved in responding to extracellular stress and coordinating outer membrane protein synthesis, and was named for its role in regulating colanic acid capsule synthesis (See Wall et al. (2018) and Majdalani and Gottesman (2005) for review) (figure 1.5). The outer membrane protein RcsF senses stress in the outer membrane or periplasm and changes shape to interact with the inner membrane protein IgaA, which is a negative regulator of the Rcs phosphorelay. The mechanism of action of IgaA has recently been described, whereby it interacts with inner membrane protein RcsD, which then signals to another inner membrane protein RcsC to autophosphorylate (Wall et al., 2020). This phosphate is then passed to RcsD, which then

phosphorylates and thereby activates the cytosolic response regulator RcsB. Phosphorylated RcsB can homodimerise to transcriptionally regulate gene expression alone or heterodimerise with cytosolic auxiliary protein RcsA. RcsB has a different regulatory activity depending on its phosphorylation state and the availability of RcsA. H-NS can inhibit *rcaA* expression in *E. coli* to change the activity of RcsB transcriptional regulation (Majdalani and Gottesman, 2005). In the absence of RscC or RcsD, RcsB is constantly phosphorylated, suggesting that RcsC and RcsD also play a role in deactivating RcsB through dephosphorylation (Wall et al., 2018). The Rcs system has roles in regulating virulence in *Salmonella* (Mouslim et al., 2004), as well as regulating motility and biofilm formation (Majdalani and Gottesman, 2005).

Biofilm formation is affected in many ways by the Rcs system. RcsB-P positively regulates the production of the small RNA *rprA*, which affects biofilm formation by inhibiting *csgD* expression (Latasa et al., 2012), but also by activating *rpoS* expression, which positively regulates *csgD* expression downstream (Majdalani and Gottesman, 2005).

Phosphorylated RcsB has also been implicated in biofilm formation by reducing motility in conjunction with RcsA through inhibition of *flhDC* expression (Majdalani and Gottesman, 2005, Wall et al., 2018). Unphosphorylated RcsB allows *csgD* expression and biofilm matrix production, which may be why RcsC has been implicated as important for biofilm formation in *E. coli*, through its ability to dephosphorylate RcsB-P (Ferrières and Clarke, 2003, Latasa et al., 2012). The Rcs system has also been described to regulate biofilm formation through affecting c-di-GMP-dependent biofilm matrix production by repressing diguanylate cyclases responsible for c-di-GMP synthesis in *Yersinia pestis* (Fang et al., 2015). The causative agent of the black plague, *Yersinia pestis*, forms biofilms inside the flea gut to aid disease transmission and encodes a non-functional *rcaA*. However, the closely related *Yersinia pseudotuberculosis* expresses a functional *rcaA*, which inhibits biofilm formation. It has been found that the non-functional *rcaA* in *Y. pestis* allows expression of *hmsT*, a diguanylate cyclase responsible for c-di-GMP synthesis. Complementation of a functional *rcaA* in *Y. pestis* resulted in repression of *hmsD*, another diguanylate cyclase responsible for biofilm matrix production (Guo et al., 2015). The complex relationship between the Rcs system and biofilm formation is yet to be fully elucidated.

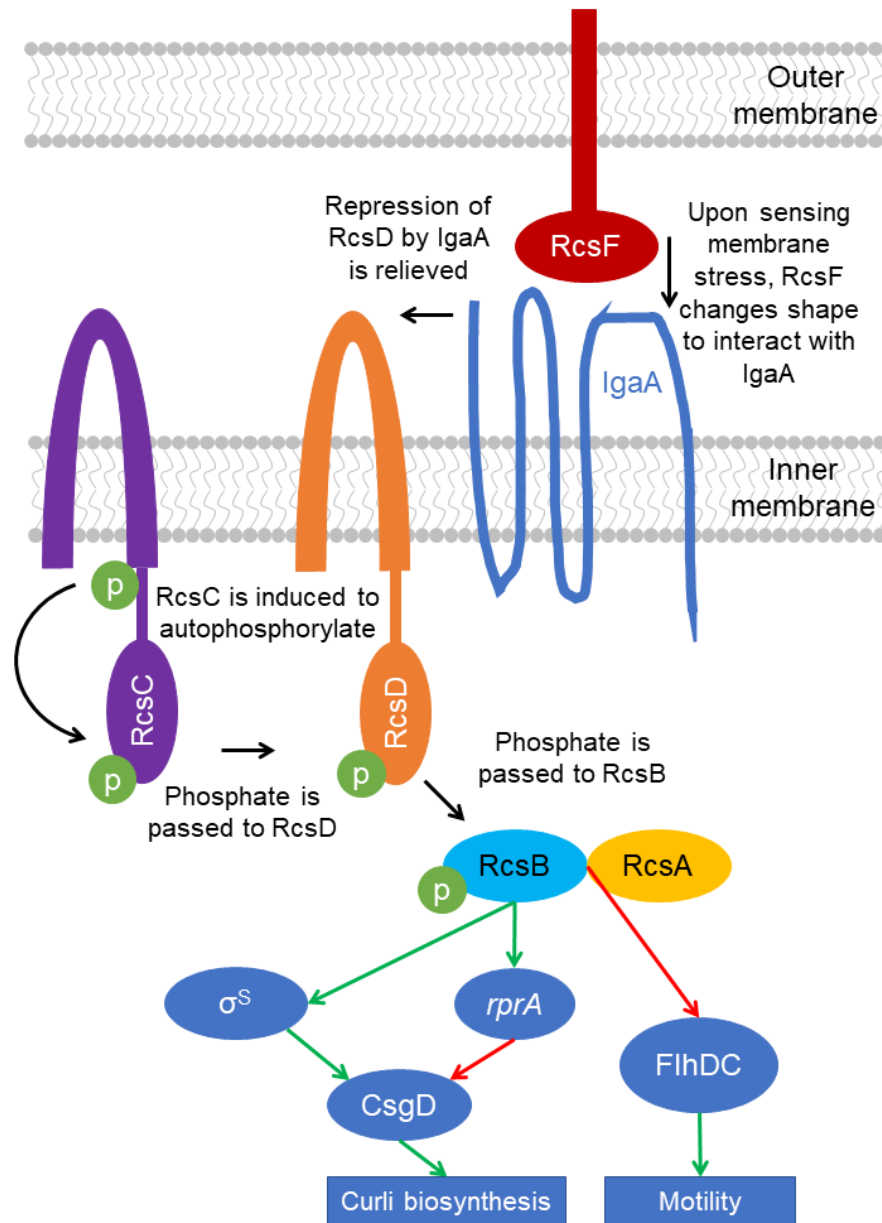


**Figure 1.5:** The Rcs phosphorylay and its effects on biofilm matrix production and motility.

### 1.3. Efflux Pumps and their regulation

Efflux pumps are complexes that sit on the cell membrane and actively remove compounds, toxins and dyes from the cell. They can export a wide range of antimicrobials from the cells, making efflux activity a major contributor to multi-drug resistance (Blair et al., 2015a, Sun et al., 2011). There are seven main families of bacterial efflux pumps. These include the ABC (ATP-binding cassette), MFS (Major facilitator superfamily), MATE (Multidrug and toxic compound extrusion), PACE (Proteobacterial antimicrobial compound efflux), SMR (Small multidrug resistance), AbgT (*p*-aminobenzoyl-glutamate transporter) and RND (Resistance-nodulation division) families (Chitsaz and Brown, 2017). All of these efflux pumps are powered by the proton motive force except the ABC family, which is powered by ATP hydrolysis (Webber and Piddock, 2003). The RND, MFS and MATE

families are clinically most important in contributing to resistance to antibiotics, with the RND family being the most important in Gram-negative bacteria (Blair et al., 2015a, Fahmy et al., 2016).

Whilst all cells carry efflux pump genes, drug-resistant mutants often show enhanced efflux activity. Mutations that result in decreased antibiotic susceptibility via efflux activity fall under two categories: those that increase the expression of efflux pump proteins and those that increase the efficiency of efflux substrate export by altering pump structure (Piddock, 2006a). Any mutation that results in the overexpression or upregulation of multi-drug resistance efflux pump genes can decrease susceptibility to multiple antibiotics (Bailey et al., 2010, Blair et al., 2015a). Efflux alone is often only responsible for a modest increase in MIC values, which are typically 2-8 fold higher in efflux mutants than for susceptible strains, but acts as a platform for other resistance mechanisms (Piddock, 2006b). For example, target site mutations in *gyrA* in *E. coli* confer resistance to fluoroquinolones, but these mutants become susceptible when efflux is inactivated (Oethinger et al., 2000, Kern et al., 2000). In *Campylobacter* spp., ribosomal mutations that confer decreased susceptibility to erythromycin and tylosin do not result in clinical resistance following inactivation of the AcrB homolog, CmeB (Cagliero et al., 2006).

### 1.3.1. AcrAB-TolC

The AcrAB-TolC efflux system is the prototypical RND efflux system in *Salmonella* and *E. coli*, and the most important in conferring resistance to antimicrobials (Baugh et al., 2012, Webber et al., 2009, Piddock, 2006a, Blair et al., 2015b). It exports a wide range of substrates, aided by two large multisite binding pockets within AcrB (Eicher et al., 2012, Blair et al., 2015b). The pump sits on the inner membrane and is a tripartite complex, made up of the homotrimer AcrB in the inner membrane, the outer membrane channel TolC and a periplasmic adaptor protein AcrA (Blair et al., 2015b). When any of these genes are deleted, mutants lack efflux activity (Pérez et al., 2012, Wang-Kan et al., 2017). This system also plays an important role in bacterial fitness and disease pathogenicity (Webber et al., 2009, Alcalde-Rico et al., 2016). Mutants with inactivated *acrA* or *acrB* demonstrated decreased motility, reduced growth (Webber et al., 2009), reduced invasive ability in vitro (Buckley et al., 2006, Webber et al., 2009, Blair et al., 2009) and reduced virulence in chicken, mice and *C. elegans* infection models (Bailey et al., 2010, Nishino et al., 2006, Buckley et al., 2006).

The expression of AcrAB is controlled by both local and global regulatory pathways that modulate efflux activity in response to environmental stress (figure 1.6). AcrR represses expression of *acrAB*, restricting expression to a basal level, and loss of function mutations in *acrR* result in constitutive overexpression of *acrAB* (Webber and Piddock, 2001).



Mutations in the repressor genes have been found to be an important route to conferring decreased susceptibility to antibiotics in *E. coli*, by allowing increased expression of the transcriptional regulators (Webber and Piddock, 2001).

### 1.3.2. MarA, RamA and SoxS

Expression of *acrA* and *acrB* is also controlled by MarA, RamA and SoxS (figure 1.6), which are members of the AraC/XylS family of transcriptional regulators in Enterobacteriaceae (Gallegos et al., 1997). They have a wide range of targets across the genome, influencing efflux activity, biofilm formation, quorum sensing, pathogenicity and motility (see Holden and Webber (2020) for review). Expression of *marA*, *ramA* and *soxS* can be quickly activated in response to a stimulus, and equally can be inhibited and gene products degraded to return to a baseline level.

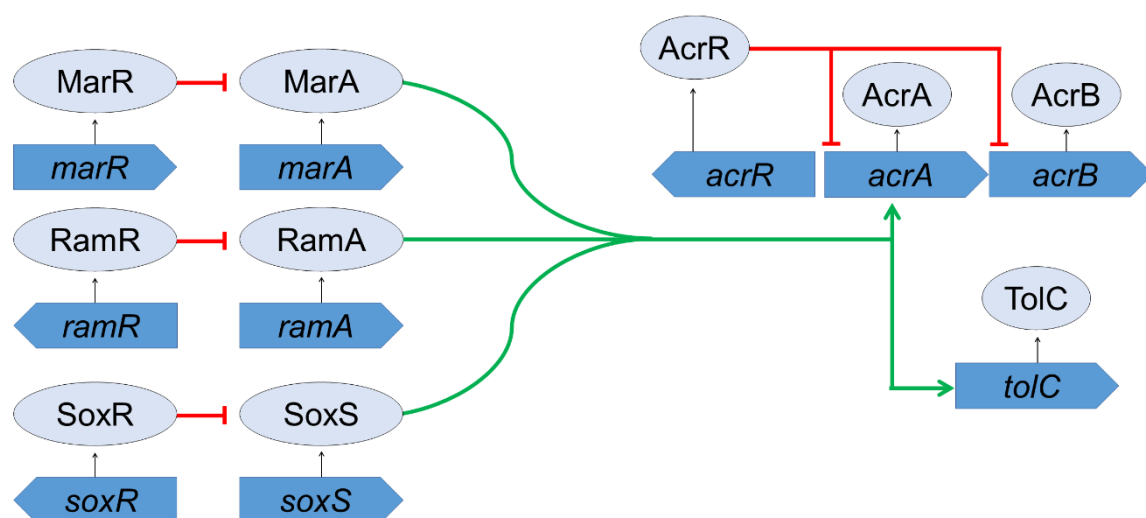


**Figure 1.6:** Regulation of the genes encoding the AcrAB-TolC efflux system by local and global transcriptional regulators.

Although MarA, RamA and SoxS activate overlapping regulatory networks, they retain some substrate specificity to provide a drug-specific response. Inhibition of *marA* expression by MarR was first seen with salicylic acid, which determined how substrate binding causes a conformational shape change in MarR that prevents binding to, and thus transcription of, *marA* (Alekshun and Levy, 1999b, Perera and Grove, 2010). As well as its involvement in antimicrobial activity, the *mar* regulon includes genes involved in lipid trafficking and DNA repair (Sharma et al., 2017). RamR is present in *Salmonella*, *Klebsiella* and other *Enterobacteriaceae* but not *E. coli*. It has been shown to be important in survival in the gut, as it binds to bile acids and indole and prevents it from binding to and inhibiting *ramA* expression (Abouzeed et al., 2008, Baucheron et al., 2014, Nikaido et al., 2011, Yamasaki et al., 2019). RamA also regulates some ribosomal, amino acid and

LPS biosynthetic pathways on top of regulating efflux activity (Bailey et al., 2010, De Majumdar et al., 2015). The SoxRS operon is involved initiation of transcription of genes that protect against oxidative stress (Dempse, 1996). SoxR contains a [2Fe-2S] cluster that is inactivated when oxidised by superoxides, nitric oxides and paraquat, which releases the inhibition of *soxS* transcription (Fujikawa et al., 2012).

Efflux regulation by the AraC/XylS family is conserved across Gram-negative bacteria, but the extent to which these genes regulate pump activity differs between organisms. MarA is the main regulator of efflux activity in *E. coli* and has been identified in many species of Enterobacteriaceae (Alekshun and Levy, 1999b, Abouzeed et al., 2008). RamA is not present in all Enterobacteriaceae and appears to overtake MarA to act as the main regulator of efflux activity in the species in which it is present. These include *Salmonella*, *Klebsiella*, *Enterobacter*, *Citrobacter* and some Enterobacteriaceae, but not *E. coli* (Blair et al., 2014, George et al., 1995, Sulavik et al., 1997). SoxS has a smaller but crucial role across these species (Oethinger et al., 1998, Pomposiello and Dempse, 2000). There is evidence that the relationship between transcriptional regulators and the pump genes is more complex than one-way activation, for example *ramA* was found to be highly overexpressed in *acrB* and *tolC* knockout mutants, demonstrating that the cell can somehow sense loss of efflux functions and attempts to restore efflux via these pathways (Webber et al., 2009).

Another transcriptional regulator in the AraC/XylS family that is not outlined in figure 1.6 is *rob*, which has been found to activate AcrAB when overexpressed at very high levels (Barchiesi et al., 2008). Rob is constitutively expressed and always present in the cell in high quantities, whereas levels of MarA, RamA and SoxS in the cell are low under basal conditions as described above (Bennik et al., 2000). Rob is regulated through a 'sequestration-dispersal' mechanism, where clustering of Rob prevents its C-terminal domain from binding to DNA and renders it inactive, but also prevents its degradation by Lon protease. When activated by an inducer, dispersal of Rob frees up the C-terminal domain to initiate transcription of target genes (Griffith et al., 2009). However, Rob has a moderate effect on transcription of target genes and needs to be overexpressed at very high levels in order to see a change in phenotype (Bennik et al., 2000). Overexpression of *marA*, *soxS* (Webber et al., 2005) and *ramA* (Rosenblum et al., 2011) has been identified in clinical isolates but not *rob* (Pidcock, 2006a).

#### 1.4. How is biofilm formation affected by efflux activity?

When efflux activity is genetically or chemically inactivated, bacteria cannot form normal biofilms (Baugh et al., 2012, Baugh et al., 2014, Alav et al., 2018, Fahmy et al., 2016, Kvist et al., 2008). These differences could not be attributed to any change in growth rate, cell surface hydrophobicity, quorum sensing or an effect on aggregation in *Salmonella* (Baugh et al., 2014, Baugh et al., 2012). Reduced biofilm formation in efflux mutants was found to be mediated through transcriptional repression of curli biosynthesis through *csgB* and *csgD*, rather than the inability to export or assemble curli (Baugh et al., 2014). Cellulose biosynthesis was unaffected. In addition to matrix biosynthesis, deletion or inhibition of efflux activity was reported to reduce persister cell formation in both liquid cultures and in biofilms (Byrd et al., 2021). The genetic basis for the regulatory link by which a change in efflux function is sensed and translated into repression of curli biosynthesis (and thereby compromised biofilm formation) is not yet clear. The relationship between efflux activity and biofilm formation is seen in a wide range of bacteria, including *A. baumannii*, *E. coli*, *P. aeruginosa*, *S. aureus* and *S. Typhimurium* (see Alav et al. (2018) for review). However, the exact genes and pathways linking biofilm formation and efflux activity are unknown.

Quorum sensing has been suggested as a possible mechanism linking efflux activity and biofilm formation, whereby efflux-deficient mutants are not able to export biofilm-promoting signalling molecules to other bacteria. There is a limited understanding of quorum sensing in *S. Typhimurium*, and no described quorum sensing molecule that affects biofilm formation (Blana et al., 2017, Prouty et al., 2002, Parsek and Greenberg, 2005, Perrett et al., 2009, Ahmer, 2004, Blanco et al., 2016). Additionally, efflux-deficient mutants grown in media pre-conditioned by wild type *S. Typhimurium* were not able to form biofilms, supporting the theory that this relationship is not mediated through quorum sensing (Baugh et al., 2014).

Both biofilm formation and efflux activity are influenced by regulatory networks that are conserved between species, therefore it is likely that it is these conserved pathways which mediate the relationship between efflux activity and biofilm formation. An inverse relationship between curli expression and the expression of *ramA* and *marA* was seen in colonies of *S. Typhimurium*, where curli is expressed by stationary-phase cells at the centre of the colony and the transcriptional regulators are expressed in growing cells at the perimeter (Holden and Webber, 2020). Transcriptome analysis of mutants lacking *acrB* or *tolC* found a marked over-expression of *ramA* in response to loss of efflux (Webber et al., 2009). Artificial overexpression of *ramA*, *marA* or *soxS* in wild-type cells resulted in reduced curli expression and decreased biofilm formation (Baugh, 2014). However, inactivation of these regulators in efflux mutants did not restore biofilm

formation, raising the question of whether they play a direct role in biofilm repression when efflux activity is lost. Recently, a direct link between MarA and biofilm formation in *E. coli* has been identified. MarA binds upstream of the *ycgZ-ymgABC* operon, which has a role in curli formation (Kettles et al., 2019). However, this was not sufficient to fully explain the link between efflux activity and biofilm formation, as inactivation of MarA (or RamA or SoxS) in *Salmonella* failed to rescue the biofilm deficit observed in efflux mutants (Baugh et al., 2014). Despite this, coordinated transcriptional regulation is the most likely explanation for the phenotypic link observed.

Previously, a small transposon mutant screen was used to try and 'rescue' biofilm formation in efflux mutants to determine whether inactivation of specific genes can rescue biofilm formation. A number of hits were obtained although no single gene was able to rescue biofilm formation across all efflux mutants (Baugh, 2014). The hits identified in this screen will now be described.

#### **1.4.1. EnvZ-OmpR**

A transposon mutagenesis experiment in efflux-deficient *S. Typhimurium* lacking TolC found that inactivation of *envZ* was able to rescue curli expression (Baugh, 2014). However, inactivation of *envZ* or *ompR* had no impact on biofilm formation in other efflux mutants, including *acrB* knockout mutants. OmpR is known to bind to and regulate expression of *csgD* (Gerstel et al., 2003), therefore modulating *ompR* expression would have a direct effect on biofilm regulation. OmpR can also negatively regulate *acrR* transcription, and directly binds to and activates *acrAB* transcription in *Yersinia enterocolitica* (Raczkowska et al., 2015). However, this does not explain how inactivation of efflux activity, especially through efflux pumps other than AcrAB, reduces transcription of curli biosynthesis genes. Overexpression of *ompR* is seen in *acrB* and *tolC* knockout mutants, suggesting that the EnvZ-OmpR system must somehow sense reduced efflux activity, but the mechanism through which this is regulated is unknown (Webber et al., 2009).

#### **1.4.2. PdeC**

There is some evidence that c-di-GMP may play a role in the relationship between efflux activity and biofilm formation through PdeC (formerly YjcC), which is a phosphodiesterase specific for breaking down c-di-GMP. The deletion of *soxS* in *Klebsiella pneumoniae* caused a decrease in *pdeC*, suggesting that *soxS* activates *pdeC*, thereby reducing c-di-GMP levels and impeding biofilm formation (Huang et al., 2013). Additionally, deletion of *pdeC* in *K. pneumoniae* resulted in a significant increase in biofilm formation and increased production of MrkA, which is important for *Klebsiella* biofilms (Huang et al., 2013). The mutagenesis experiment mentioned previously found that when the EmrAB

efflux pump was inactivated, biofilm formation could be restored to the levels of the wild type through interrupting the activity of *pdeC* (Baugh, 2014). This would reduce the breakdown of c-di-GMP and therefore result in prolonged promotion of biofilm matrix biosynthesis. However, cellulose biosynthesis remains unchanged when efflux activity is disrupted, (Baugh et al., 2012) suggesting that if c-di-GMP is important in the relationship between efflux activity and biofilm formation, it must be mediated through a pathway separate from that which affects cellulose biosynthesis.

### 1.4.3. TomB

Another gene highlighted in this genetic screen was *tomB* (previously *ybaJ*). Inactivation of *tomB* rescued biofilm formation in an *mdtK* efflux pump knockout mutant to the level of the wild type, but biofilm formation was only partially restored through *tomB* inactivation in a *toIC* mutant and not at all in an *acrB* mutant, suggesting that the relationship is not consistent across efflux pumps (Baugh, 2014). TomB acts as an antitoxin to Hha, which is a negative regulator of biofilm formation, and TomB, has been implicated in promoting biofilm formation through persister cell formation increasing cell aggregation and decreasing motility (Sharma and Bearson, 2013, Jaiswal et al., 2016, Barrios et al., 2006). It is therefore surprising that inactivation of *tomB* would rescue biofilm formation in efflux-deficient mutants. Additionally, overexpression of *hha*, as a result of the inactivation of *tomB*, should further impede biofilm formation through its interaction with H-NS, which has been implicated in transcriptional repression of *csgA* at high osmolarity (Olsén et al., 1993). Hha-like genes are restricted to Enterobacteriaceae, and because the relationship between efflux activity and biofilm formation is seen in other families of bacteria, this pathway alone cannot be responsible for the relationship observed (Madrid et al., 2007).

## 1.5. Aims and Objectives

This project aims to determine the genetic networks important for both biofilm formation, and control of efflux in *Salmonella* and *E. coli* and to investigate genes that govern the relationship between efflux activity and biofilm formation. A novel genetic screen, TraDIS-*Xpress*, was optimised to identify genes involved in biofilm formation and efflux activity in both species. From the gene lists generated by TraDIS-*Xpress*, hypotheses were made as to how they were co-regulated, and these were tested through inactivation and overexpression of highlighted genes and pathways. Because multiple transcriptional regulators and signalling systems have been found to affect biofilm development and curli biosynthesis, it was expected that multiple pathways would be highlighted by TraDIS-*Xpress* to affect biofilm formation and development following inactivation of efflux activity. Systems involved in sensing membrane stress, such as the EnvZ/OmpR and CpxAR two component signalling systems and the Rcs phosphorylay, were expected to be involved in sensing disruption of efflux activity and affecting curli biosynthesis. Stress response regulators MarA, RamA and SoxS were also expected to be identified in this study, as their overexpression following efflux inactivation has previously been found to affect biofilm formation (Baugh, 2014). RpoS, also involved in the stress response, was also expected to affect biofilm formation in response to stress. Overall, it was expected that the disruption of efflux activity would activate multiple stress response pathways, that in turn would result in transcriptional repression of curli biosynthesis and reduced biofilm biomass production.

## **2. CHAPTER 2: MATERIALS AND METHODS**

## 2.1. Bacteria

The bacterial strains used in the work covered in this thesis were mainly *Salmonella enterica* serovar Typhimurium strain 14028S and *Escherichia coli* strain BW25113, or mutants derived from them. Both were chosen as there is previous knowledge about their ability to form biofilms, their full genome sequences are available and both can be genetically manipulated.

*S. Typhimurium* 14028S has been widely used as a model organism in experiments investigating biofilm formation (Prouty and Gunn, 2003, Prouty et al., 2002, Garcia et al., 2004, Trampari et al., 2019) and efflux activity (Nikaido et al., 2011, Nishino et al., 2006, Sun et al., 2011, Webber et al., 2009). There is also a wealth of literature on the relationship between efflux activity and biofilm formation in this strain (Baugh, 2014, Baugh et al., 2012, Baugh et al., 2014). This strain was fully sequenced and characterised in 2010 (Jarvik et al., 2010).

*E. coli* strain BW25113 is a widely used model organism in molecular biology. It is the parent strain for the Keio collection, which is a library of single-gene deletion mutants of every non-essential gene in the genome, created to further the field of functional genomics (Baba et al., 2006). Additionally, previous TraDIS-*Xpress* experiments have been conducted in the same mutant library of *E. coli* BW25113 (Yasir et al., 2020), thereby providing data comparable to those generated in this project.



**Table 2.1:** Bacteria used in this work.

<b>Bacteria</b>	<b>Source</b>
<i>S. Typhimurium</i> 14028S (WT)	ATCC
WT+ <i>lacZ</i>	Made in house
<i>tolC::cat</i> (also referred to as $\Delta tolC$ )	(Nishino et al., 2006)
$\Delta acrB$	Made in house
$\Delta acrB \Delta tomB$	Made in house
$\Delta pdeC$	Made in house
$\Delta nuo$	Made in house
$\Delta nuoB$	Made in house
$\Delta STM14\_1074$	Made in house
$\Delta nirD$	Made in house
$\Delta pdeK$	Made in house
$\Delta infB$	Made in house
$\Delta rfbF$	Made in house
$\Delta crl$	Made in house
$\Delta cyaA$	Made in house
$\Delta dsbA$	Made in house
$\Delta maoP$	Made in house
$\Delta ramRA$	Made in house
<i>E. coli</i> TOP10 (DH10B)	(Durfee et al., 2008)
<i>E. coli</i> MG1655 (K-12)	ATCC
<i>E. coli</i> BW25113 (K-12)	(Grenier et al., 2014)
Keio collection mutants	(Baba et al., 2006)
<i>E. coli</i> MFDpir	(Ferrières et al., 2010)

## **2.2. General microbiology techniques**

Overnight cultures were grown in 5 mL LB broth and incubated for 16-24 hours at 37 °C with agitation of 250 rpm, unless otherwise stated. Bacteria were grown to mid-logarithmic growth phase by inoculating LB broth 1:100 with the relevant bacterial overnight culture and incubating the culture at 37 °C shaking at 200 rpm until the optical density (OD), measured at 600 nm, reached between 0.2 and 0.3. Cells were pelleted at 3,000 x g. Agar plates were incubated at 37 °C for 16-24 hours overnight, unless otherwise stated. Serial dilutions (1:10) were performed in a 96-well plate filled with 180 µL sterile PBS, and 20 µL of culture from the first well was mixed by pipetting before being transferred to the well below.

Anaerobic and microaerophilic work was performed in an anaerobic cabinet. Agar plates were placed in an anaerobic cabinet 48 hours prior to inoculation and the environmental oxygen was controlled using the Anoxomat® anaerobic culture system. Liquid cultures were set up in anaerobic LB broth in a 96-well plate, sealed with a gas permeable membrane (4TITUDE, 4TI-0516/96) and environmental oxygen was controlled using the atmospheric control unit attached to the FLUOstar Omega plate reader (BMG Labtech).

## **2.3. Molecular Biology methods**

### **2.3.1. PCR**

To amplify genes for chromosomal insertion, or to prepare alleles for sequencing, a 50 µL PCR reaction consisted of 25 µL NEBNext® Ultra™ II Q5® Master Mix (NEB, M0544S), 20 µL double distilled and deionised water (Sigma, W4502) and 2.5 µL of each primer (10mM). To check for the presence or absence of insertions into vectors or into the chromosome, 10 µL reactions were used with the same relative concentrations as described above, instead using the polymerase GoTaq® G2 Green Master Mix (Promega, M7822). Bacterial template DNA was added by picking a single bacterial colony from an LB agar plate and resuspending it in the reaction. Plasmid DNA was isolated from cells using the NucleoSpin® Plasmid kit (Macherey-Nagel, 740588.50) following the manufacturer's instructions, and 1-2 µL of plasmid DNA was added to the PCR reaction, adjusting the amount of water added to maintain the overall volume of the reaction. A Veriti thermocycler (ThermoFisher, 4375786) was used for all PCR reactions, following the protocol described in table 4. PCR products were stored short term at 4 °C or long term at -20 °C. Amplified DNA was cleaned up using NucleoSpin® Gel and PCR Clean-up kit (Macherey-Nagel, 740609.50), following the manufacturer's instructions.

**Table 2.2:** PCR programme

Step	Temperature	Duration
<b>Initial denaturation</b>	95 °C	1 or 3 minutes *
	25-35 cycles of:	
<b>Denaturation</b>	95 °C	30 seconds
<b>Annealing</b>	50-70 °C **	30 seconds
<b>Elongation</b>	72 °C	30 seconds per 1 kB of amplified product
<b>Final elongation</b>	72 °C	7 minutes
<b>Hold</b>	4 °C	

\* depending on if the template DNA was plasmid or a bacterial colony, respectively

\*\* depending on the annealing temperature of the primers used

### 2.3.2. Phenol-chloroform DNA Purification

Transposon DNA PCR amplifications were purified using phenol-chloroform. Transposon DNA was amplified in an 8-tube PCR strip in 50 µL reaction volumes. These reactions were pooled together into a sterile Eppendorf tube and 200 µL (0.5x volume) phenol-chloroform (Sigma, 77617) was added. This was centrifuged at 18,000 x g for 3 minutes and the top layer of liquid was added to a separate tube containing 40 µL 3M Sodium Acetate (Sigma, 567422) and 240 µL 10% isopropanol. This was then kept at -20 °C overnight and centrifuged again at 14 °C for 20 minutes, after which the supernatant was removed without disturbing the pellet. Following this, the pellet was rinsed with 300 µL 70% ethanol twice and centrifuged again to remove all liquid. The pellet was allowed to air-dry for 5 minutes, before being resuspended in 0.1x TE buffer. The concentration of DNA was measured using Qubit DNA Broad Range assay kit (ThermoFisher, Q32853), following the manufacturer's instructions.

### 2.3.3. Agarose gel electrophoresis

Agarose gel DNA electrophoresis was used to visualise and determine the size of PCR products and plasmids. Agarose gels were prepared at 0.8 % unless otherwise stated, and 5 µL of Midori Green Advance nucleic acid staining reagent (Nippon Genetics, MG04) was added per 50 µL of agarose gel. Gel loading dye (NEB, B7024S) was added to the DNA as per the manufacturer's instructions, unless PCR products were amplified with GoTaq® G2 Green Master Mix, where loading dye was already present in the master mix. For PCR products, 5 µL of reaction was loaded into a well, whereas this was between 5 and 20 µL for plasmid DNA. To measure band size, 5 µL of 1 kB DNA ladder (NEB, N3200S) was included in every run. Gels tanks were filled with 1x TBE (Severn Biotech, 20-6000-50) and were run at 120 V for 20 minutes unless otherwise stated.

#### **2.3.4. Digestions and ligations**

Digestions were performed in 20  $\mu$ L reactions consisting of 2  $\mu$ L CutSmart® buffer (NEB, B7204S), 2  $\mu$ L restriction enzyme, 6  $\mu$ L plasmid DNA and 10  $\mu$ L double distilled and deionised water. Reactions were incubated for at least 1 hour at 37 °C. Before ligation, digested plasmids were treated with alkaline phosphatase (Sigma, 04898133001) to discourage empty vector relegation. This was carried out using 20  $\mu$ L vector DNA, 2  $\mu$ L Alkaline phosphatase, 3  $\mu$ L Alkaline phosphatase buffer and 5  $\mu$ L double distilled and deionised water. This reaction was incubated for 30 minutes at 37 °C, and subsequently cleaned up using NucleoSpin® Gel and PCR Clean-up kit, following the manufacturer's instructions. Vectors and inserts were ligated in 10  $\mu$ L reactions consisting of 6  $\mu$ L insert DNA, 2  $\mu$ L vector DNA, 1  $\mu$ L T4 DNA Ligase (NEB, M0202S) and 1  $\mu$ L T4 DNA Ligase buffer. After 15 minutes at room temperature, ligations were ready for transformation.

#### **2.3.5. Competent cells and transformations**

To make cells chemically competent, cells were grown to mid- logarithmic growth phase as described previously and centrifuged at 3,000 x g. The pellet was washed three times, once with 12.5 mL 100 mM ice-cold sterile  $MgCl_2$ , then 25 mL 100 mM ice-cold sterile  $CaCl_2$  and finally 1 mL ice-cold sterile 100mM  $CaCl_2$  with 20% glycerol. From this, 50  $\mu$ L aliquots were made in sterile tubes and kept on ice. Aliquots that were not used on the same day were stored at -70 °C. For chemical transformations, 2  $\mu$ L of DNA was added to a 50  $\mu$ L aliquot of cells and left on ice for 10 minutes. Cells were then transferred to a 42 °C heat block for 2 minutes, and then were placed back on ice for 2 minutes. After this, 1 mL LB broth was added to each aliquot and cells were incubated at 37 °C for at least 1 hour. To select for successful transformants, 100  $\mu$ L of each transformation was plated on LB agar supplemented with the relevant antibiotics.

DNA was transformed into *S. Typhimurium* via electroporation. Cells were grown to mid- logarithmic growth phase as described previously and centrifuged at 3,000 x g. The pellet was washed three times, once with 12.5 mL and then with 25 mL ice-cold sterile double distilled and deionised water, and finally 600  $\mu$ L ice-cold sterile 10% glycerol. Aliquots were made in sterile Eppendorf tubes with 50  $\mu$ L cells and stored on ice until use. Fresh electrocompetent cells were made for every electroporation. Unless otherwise stated, 2  $\mu$ L DNA was added to 50  $\mu$ L aliquots and kept on ice. Cells were electroporated in prechilled sterile 2 mm electrode gap cuvettes (Geneflow, E6-0060) using a Bio-Rad GenePusler II set to 2.4 kV and 200  $\Omega$ . Cells were immediately recovered in 1 mL SOC media (NEB, B9020S), transferred to sterile tubes and incubated at 37 °C for at least 1 hour. Transformations were plated on LB agar supplemented with relevant antibiotics to select for successful transformants.

### 2.3.6. Genomic DNA extraction

Cell pellets were resuspended in 100  $\mu$ L lysis buffer, which was made with 10 mL TE buffer, 100  $\mu$ L 0.5 mg/mL lysozyme (Sigma, L6876) and 10  $\mu$ L 100 mg/mL RNase A (ThermoFisher, 12091021). This was incubated at 37 °C for 25 minutes, shaking at 1600 rpm in an Eppendorf Thermomixer<sup>®</sup>. Following this, 10 $\mu$ L lysing additive, made with 528  $\mu$ L TE buffer, 600  $\mu$ L 10% SDS, 60 $\mu$ L 20 mg/mL Proteinase K (ThermoFisher, AM2546) and 12  $\mu$ L 100 mg/mL RNase A, was added to each sample and was incubated at 65 °C for 15 minutes, shaking at 1600 rpm. To isolate the DNA, 50  $\mu$ L SPRI beads (Roche, 07983298001) was added to each sample, mixed thoroughly, and left to incubate at room temperature for 5 minutes. Tubes were then placed on the magnetic stand for 2 minutes until the supernatant was clear. The supernatant was discarded, and beads were rinsed twice with 100  $\mu$ L freshly made 80% ethanol. All ethanol was removed from the wells and tubes were left to air-dry for 15 minutes. Tubes were then removed from the magnetic stand and beads were resuspended in 50  $\mu$ L 10 mM Tris-HCl. After incubation at room temperature for 5 minutes, tubes were placed back onto the magnetic stand for 2 minutes until the supernatant went clear. The supernatant was collected and the concentration of DNA was measured using Qubit dsDNA Broad Range (ThermoFisher, Q32853) or High Sensitivity (ThermoFisher, Q32854) assay kits following the manufacturer's instructions.

### 2.3.7. Constructing single gene deletion mutants and chromosomal integrations in *S. Typhimurium*

Gene doctoring is a high-throughput recombineering technique that uses the  $\lambda$ -red recombinase system to specifically modify the genome (Lee et al., 2009). Single gene deletion mutants were constructed following the protocol described by Thomson et al. (2020). Regions homologous to the target gene were amplified and cloned into pDOC-GG, which was then introduced into electrocompetent *S. Typhimurium*. The  $\lambda$ -red recombinase system was then induced with arabinose, replacing the target gene with a tetracycline resistance cassette. Chromosomal integrations used a similar system with the related plasmid pDOC-K-glmS, used to insert transgenes into a site in the non-coding region downstream of *glmS* (Holden et al., 2020) (figure 2.1). This region is also used for Tn7 chromosomal insertions and has been reported to have no significant effect on fitness (Mitra et al., 2010, McKenzie and Craig, 2006, Choi et al., 2005). This was optimised and validated through the successful insertion of *lacZ* into the chromosome of *S. Typhimurium* (Chapter 3) (Holden et al., 2020). Gene deletions and complementations were confirmed with whole genome sequencing.

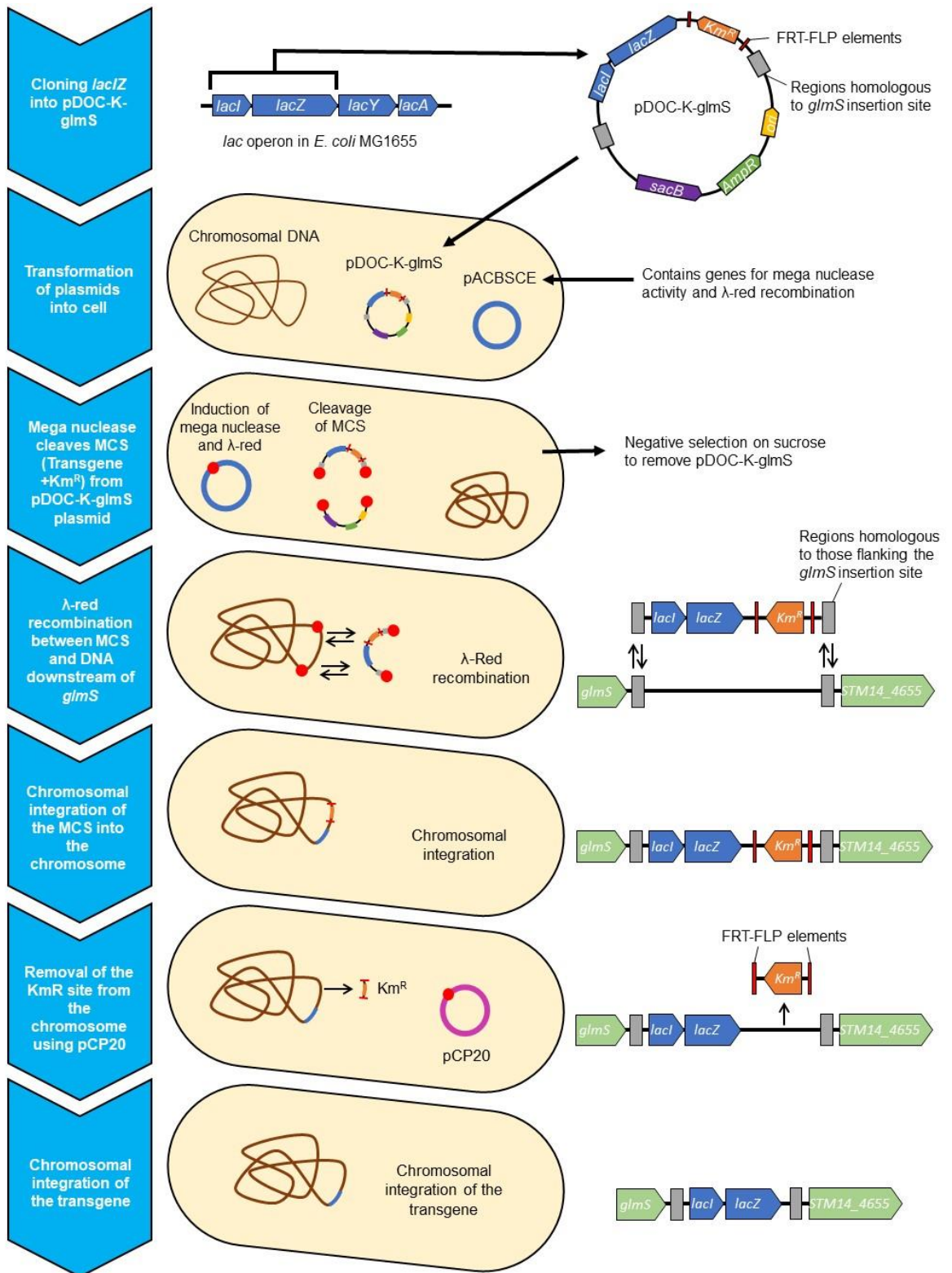


**Figure 2.1:** Chromosomal integration by gene doctoring, demonstrated through the integration of *lacI**Z* into the intergenic region downstream of *glmS*. Figure adapted from (Lee et al., 2009).

## 2.4. Plasmids

**Table 2.3:** Plasmids used in this work.

<b>Plasmid</b>	<b>Source</b>
pUC19	(Invitrogen, supplied with 18265017)
pDOC-K- <i>glmS</i>	(Holden et al., 2020)
pDOC-GG	(Thomson et al., 2020)
pACBSCE	(Holden et al., 2020, Lee et al., 2009)
pCP20	(Cherepanov and Wackernagel, 1995)
pTrc- <i>marA</i>	(Baugh, 2014)
pTrc- <i>ramA</i>	(Baugh, 2014)
pTrc- <i>soxS</i>	(Baugh, 2014)
pBR322/ <i>lac</i>	Made in house
pBR322/ <i>lac-tyrT</i>	Made in house
pJMA- <i>t5</i>	Gift from Nicholas Thomson, Quadram Institute, Norwich, UK
pJMA- <i>t5-dsbA</i>	Made in house
pJMA- <i>t5-maoP</i>	Made in house

## 2.5. Primers

**Table 2.4:** Primers used in this work. Primers were synthesised by Sigma.

Name	Sequence	Role
lac NotI For	AGATCCCTCAATAGCGGCCGCACCATCGAATGGCGCA	Amplify <i>lacZ</i> from <i>E. coli</i> MG1655
lacZ rev XhoI long	CCCAAGCTTCTCGAGTTATTTTTGACACCAGACCAACTGGT AATGGTAGCGACCGGCGCT	Amplify <i>lacZ</i> from <i>E. coli</i> MG1655
Kan_test_For	CGCAGCGCATCGCCTTCTATCG	Check integration of <i>lacZ</i> in pDOC-K-glmS
glms_test_Rev	CAGCGCCTGTCACAGCGCAC	Check integration of <i>lacZ</i> in pDOC-K-glmS
glms_out_Rev	AGCCAATGTGGATCTCTGGCTG	Check integration of <i>lacZ</i> in <i>S. Typhimurium</i> 14028S chromosome
glms_out_For	CCTGGGGCGTGCGATCAAT	Check integration of <i>lacZ</i> in <i>S. Typhimurium</i> 14028S chromosome
lac Part2 For	GCCCACACCAGTGGCGCGGCGACTTCCAGTTCAAC	Check integration of <i>lacZ</i> in <i>S. Typhimurium</i> 14028S chromosome
pDoc-K Rev	GGTTTTCCAGTCACGACGT	Check integration of <i>lacZ</i> in <i>S. Typhimurium</i> 14028S chromosome
glmS rev	ACGTGGCGCTGATTAAGGCACCGACGTTG	Check integration of <i>lacZ</i> in <i>S. Typhimurium</i> 14028S chromosome
lac mid rev	CGCCCAGTCGCGTACCGTCT	Used for RT-PCR of <i>lacI</i> to assay its expression in <i>S. Typhimurium</i> + <i>lacZ</i>



Internal lac rev	TGCCACCTCCAGTCTGGCCC	Used for RT-PCR of <i>lacI</i> to assay its expression in <i>S. Typhimurium</i> + <i>lacZ</i>
gyrB for	GGAAGGGGACTCCGCGGGCG	Used for RT-PCR of <i>gyrB</i> as a control
gyrB rev	CAGCGGCGGCTGCGCAATGT	Used for RT-PCR of <i>gyrB</i> as a control
Tn5Km-01	CTGTCTCTTATACACATCTTCTAGACAACC	Amplification of TnKm001-P <sub>tac</sub>
Tn5Km-06	TGGCGTCACCGAGAGGACTTTCAAGCTTCTG	Amplification of TnKm001-P <sub>tac</sub>
Tnp100	CTGTCTCTTATACACATCT	Mosaic end of transposon used for amplification of Tnp001
i7N701New	CAAGCAGAAGACGGCATAACGAGATTCGCCTTAGTGACTGG AGTTCAGACGTGTGCTCTTCCGATCTCGCGTTTTTCGTGC GCCGCTTCA	Illumina adapter-specific sequencing primer customised for DNA tagmented with the MuSeek enzyme, used to sequence DNA from the TraDIS- <i>Xpress</i> experiments.
i7N702New	CAAGCAGAAGACGGCATAACGAGATCTAGTACGGTGACTG GAGTTCAGACGTGTGCTCTTCCGATCTCGCGTTTTTCGTG CGCCGCTTCA	Illumina adapter-specific sequencing primer customised for DNA tagmented with the MuSeek enzyme, used to sequence DNA from the TraDIS- <i>Xpress</i> experiments.
i7N703New	CAAGCAGAAGACGGCATAACGAGATTTCTGCCTGTGACTGG AGTTCAGACGTGTGCTCTTCCGATCTCGCGTTTTTCGTGC GCCGCTTCA	Illumina adapter-specific sequencing primer customised for DNA tagmented with the MuSeek enzyme, used to sequence DNA from the TraDIS- <i>Xpress</i> experiments.
i7N704New	CAAGCAGAAGACGGCATAACGAGATGCTCAGGAGTGACTG GAGTTCAGACGTGTGCTCTTCCGATCTCGCGTTTTTCGTG CGCCGCTTCA	Illumina adapter-specific sequencing primer customised for DNA tagmented with the MuSeek enzyme, used to sequence DNA from the TraDIS- <i>Xpress</i> experiments.

i7N705New	CAAGCAGAAGACGGCATAACGAGATAGGAGTCCGTGACTG GAGTTCAGACGTGTGCTCTTCCGATCTCGCGTTTTTCGTG CGCCGCTTCA	Illumina adapter-specific sequencing primer customised for DNA tagmented with the MuSeek enzyme, used to sequence DNA from the TraDIS- <i>Xpress</i> experiments.
i7N706New	CAAGCAGAAGACGGCATAACGAGATCATGCCTAGTGACTG GAGTTCAGACGTGTGCTCTTCCGATCTCGCGTTTTTCGTG CGCCGCTTCA	Illumina adapter-specific sequencing primer customised for DNA tagmented with the MuSeek enzyme, used to sequence DNA from the TraDIS- <i>Xpress</i> experiments.
i7N707New	CAAGCAGAAGACGGCATAACGAGATGTAGAGAGGTGACTG GAGTTCAGACGTGTGCTCTTCCGATCTCGCGTTTTTCGTG CGCCGCTTCA	Illumina adapter-specific sequencing primer customised for DNA tagmented with the MuSeek enzyme, used to sequence DNA from the TraDIS- <i>Xpress</i> experiments.
i7N710New	CAAGCAGAAGACGGCATAACGAGATCAGCCTCGGTGACTG GAGTTCAGACGTGTGCTCTTCCGATCTCGCGTTTTTCGTG CGCCGCTTCA	Illumina adapter-specific sequencing primer customised for DNA tagmented with the MuSeek enzyme, used to sequence DNA from the TraDIS- <i>Xpress</i> experiments.
Tnp001P-i5S502-4	AATGATACGGCGACCACCGAGATCTACACCTCTCTATACA CTCTTTCCCTACACGACGCTCTTCCGATCTCTGACCAGGC ATGCCAGGGTTGAGATGTG	One of the four primers mixed to make the transposon-specific customised sequencing primer pool i5S502, for sequencing DNA from the TraDIS- <i>Xpress</i> experiments.
Tnp001P-i5S502-5	AATGATACGGCGACCACCGAGATCTACACCTCTCTATACA CTCTTTCCCTACACGACGCTCTTCCGATCTTGACATCAGG CATGCCAGGGTTGAGATGTG	One of the four primers mixed to make the transposon-specific customised sequencing primer pool i5S502, for sequencing DNA from the TraDIS- <i>Xpress</i> experiments.

Tnp001P-i5S502-6	AATGATACGGCGACCACCGAGATCTACACCTCTCTATACA CTCTTTCCCTACACGACGCTCTTCCGATCTGACTGAGCAG GCATGCCAGGGTTGAGATGTG	One of the four primers mixed to make the transposon-specific customised sequencing primer pool i5S502, for sequencing DNA from the TraDIS- <i>Xpress</i> experiments.
Tnp001P-i5S502-7	AATGATACGGCGACCACCGAGATCTACACCTCTCTATACA CTCTTTCCCTACACGACGCTCTTCCGATCTACTGTGTTTCAG GCATGCCAGGGTTGAGATGTG	One of the four primers mixed to make the transposon-specific customised sequencing primer pool i5S502, for sequencing DNA from the TraDIS- <i>Xpress</i> experiments.
Tnp001P-i5S503-4	AATGATACGGCGACCACCGAGATCTACACTATCCTCTACA CTCTTTCCCTACACGACGCTCTTCCGATCTCTGACCAGGC ATGCCAGGGTTGAGATGTG	One of the four primers mixed to make the transposon-specific customised sequencing primer pool i5S503, for sequencing DNA from the TraDIS- <i>Xpress</i> experiments.
Tnp001P-i5S503-5	AATGATACGGCGACCACCGAGATCTACACTATCCTCTACA CTCTTTCCCTACACGACGCTCTTCCGATCTTGACATCAGG CATGCCAGGGTTGAGATGTG	One of the four primers mixed to make the transposon-specific customised sequencing primer pool i5S503, for sequencing DNA from the TraDIS- <i>Xpress</i> experiments.
Tnp001P-i5S503-6	AATGATACGGCGACCACCGAGATCTACACTATCCTCTACA CTCTTTCCCTACACGACGCTCTTCCGATCTGACTGAGCAG GCATGCCAGGGTTGAGATGTG	One of the four primers mixed to make the transposon-specific customised sequencing primer pool i5S503, for sequencing DNA from the TraDIS- <i>Xpress</i> experiments.
Tnp001P-i5S503-7	AATGATACGGCGACCACCGAGATCTACACTATCCTCTACA CTCTTTCCCTACACGACGCTCTTCCGATCTACTGTGTTTCAG GCATGCCAGGGTTGAGATGTG	One of the four primers mixed to make the transposon-specific customised sequencing primer pool i5S503, for sequencing DNA from the TraDIS- <i>Xpress</i> experiments.
Tnp001P-i5S505-4	AATGATACGGCGACCACCGAGATCTACACGTAAGGAGACA CTCTTTCCCTACACGACGCTCTTCCGATCTCTGACCAGGC ATGCCAGGGTTGAGATGTG	One of the four primers mixed to make the transposon-specific customised sequencing primer pool i5S505, for sequencing DNA from the TraDIS- <i>Xpress</i> experiments.

Tnp001P-i5S505-5	AATGATACGGCGACCACCGAGATCTACACGTAAGGAGACA CTCTTTCCCTACACGACGCTCTTCCGATCTTGACATCAGG CATGCCAGGGTTGAGATGTG	One of the four primers mixed to make the transposon-specific customised sequencing primer pool i5S505, for sequencing DNA from the TraDIS- <i>Xpress</i> experiments.
Tnp001P-i5S505-6	AATGATACGGCGACCACCGAGATCTACACGTAAGGAGACA CTCTTTCCCTACACGACGCTCTTCCGATCTGACTGAGCAG GCATGCCAGGGTTGAGATGTG	One of the four primers mixed to make the transposon-specific customised sequencing primer pool i5S505, for sequencing DNA from the TraDIS- <i>Xpress</i> experiments.
Tnp001P-i5S505-7	AATGATACGGCGACCACCGAGATCTACACGTAAGGAGACA CTCTTTCCCTACACGACGCTCTTCCGATCTACTGTGTTGAG GCATGCCAGGGTTGAGATGTG	One of the four primers mixed to make the transposon-specific customised sequencing primer pool i5S505, for sequencing DNA from the TraDIS- <i>Xpress</i> experiments.
Tnp001P-i5S506	AATGATACGGCGACCACCGAGATCTACACACTGCATAACA CTCTTTCCCTACACGACGCTCTTCCGATCTCTGACCAGGC ATGCCAGGGTTGAGATGTG	Transposon-specific customised sequencing primer for sequencing transposon mutant library DNA
Tnp001P-i5S507	AATGATACGGCGACCACCGAGATCTACACAAGGAGTAACA CTCTTTCCCTACACGACGCTCTTCCGATCTTACCAGGCAT GCCAGGGTTGAGATGTG	Transposon-specific customised sequencing primer for sequencing DNA from the TraDIS- <i>Xpress</i> experiments.
Tnp001P-i5S508	AATGATACGGCGACCACCGAGATCTACACCTAAGCCTACA CTCTTTCCCTACACGACGCTCTTCCGATCTCCAGGCATGC CAGGGTTGAGATGTG	Transposon-specific customised sequencing primer for sequencing DNA from the TraDIS- <i>Xpress</i> experiments.
Tnp001P-i5S510	AATGATACGGCGACCACCGAGATCTACACCGTCTAATACA CTCTTTCCCTACACGACGCTCTTCCGATCTCTGACCAGGC ATGCCAGGGTTGAGATGTG	Transposon-specific customised sequencing primer for sequencing DNA from the TraDIS- <i>Xpress</i> experiments.

Tnp001P-i5S511	AATGATACGGCGACCACCGAGATCTACACTCTCTCCGACA CTCTTTCCCTACACGACGCTCTTCCGATCTTACCAGGCAT GCCAGGGTTGAGATGTG	Transposon-specific customised sequencing primer for sequencing DNA from the TraDIS- <i>Xpress</i> experiments.
pBR322 fwd plac SmaI XhoI NotI HindIII	GGAATCCCGGGGTCTCGAGGCGCGGCCGCGATAAGCTTT ATTGTTATCCGCTCACAATTCACACAACATACGAGCCGG AAGCATAAAGTGTAACGATAAGCTTTAATGCGGTAGTT	Amplification of the pBR322 backbone for the addition of the lac promoter, to create a plasmid with an inducible promoter upstream of the MCS (pBR322/ <i>lac</i> )
pBR322 rev XbaI EcoRI AvrII SmaI	GTAATCCCGGGTGCCTAGGAAGAATTCTTTCTAGATAAAA GGATCTAGGTGAAGATCC	Amplification of the pBR322 backbone for the addition of the lac promoter, to create a plasmid with an inducible promoter upstream of the MCS (pBR322/ <i>lac</i> )
tyrT EcoRI fwd	GGAAGCGGGCCAGTATTAAGCATTGAATTCTGGTGGGGTT C	Amplify <i>tyrT</i> from <i>S. Typhimurium</i> with restriction sites for insertion into pBR322/ <i>lac</i>
tyrT HindIII rev	GCATTGCTCATCGAGTTAACTACATCGCTGTAAAGCTTAAT GGTGGTGGG	
TcR rev	GATGACGATGAGCGCATTGTTAGATTTTCAT	For PCR and sequencing out from the tetracycline cassette in pBR322
TcR check fwd	ATGCCGGTACTGCCGGGCCTCTTGC	
TcR check rev	CTCCATGCACCGCGACGCAACGCGG	
tetR check fwd	GTAAACCCTCAAGCTCAGGGGAGTAAACA	For PCR and sequencing out from the tetracycline cassette in pDOC-GG
tetR check rev	GTAACGTAATTACCAATGCGATCTTTGTCG	
nuoB H1 fwd	CAAGGTCTCCCTACGCATGATATCGCGATTACGCTCA	Amplification of homologous regions adjacent to <i>nuoB</i> in <i>S. Typhimurium</i> for cloning into pDOC-GG to create the $\Delta$ <i>nuoB</i> deletion mutant
nuoB H1 rev	CGGGTCTCACTCCGCGCCTGTCGGCAGCAGCAC	
nuoB H2 fwd	GTAGGTCTCACGCTAATGCCTCGCGGTTAGCGTT	

nuoB H2 rev	GAAGGTCTCCTCGTCACTGGGCATTGCTATCTT	
nuoM H2 fwd	GGGGTCTCACGCTGCTAAGTATGTCCCTTATATTTACTCCT GCT	Amplification of a homologous region adjacent to <i>nuoM</i> in <i>S.</i> Typhimurium for cloning into pDOC-GG to create the $\Delta nuo$ deletion mutant
nuoM H2 rev	GGCTGGTCTCTTCGTTTTTGCAGGCAAAGGCCTGGTACTG	
1074 H1 fwd	GTGGGTCTCCCTACTCCGGCGGGGTGAAATCTTT	Amplification of homologous regions adjacent to <i>STM14_1074</i> in <i>S.</i> Typhimurium for cloning into pDOC-GG to create the $\Delta STM14_1074$ deletion mutant
1074 H1 rev	GGGGTCTCCCTCCTTAATCCTGGCCGTA CT TCT	
1074 H2 fwd	GTACGGTCTCTCGCTTCCACTGTGTTTAATAAACCGTCGT G	
1074 H2 rev	GGGGTCTCGTCGTGGCATAAACTGGCGAAAGGCCG	
yjiG H1 fwd	GTCGGGTCTCGCTACTGATAAGCGCCCGTGAGCATCC	Amplification of homologous regions adjacent to <i>yjiG</i> in <i>S.</i> Typhimurium for cloning into pDOC-GG to create the $\Delta yjiG$ deletion mutant
yjiG H1 rev	GCTGGTCTCTCTCCAAGGAGTTATCATGCCTGATTT	
yjiG H2 fwd	GTAGGTCTCTCGCTATGATTGGGCTCCTTGCGCAGG	
yjiG H2 rev	GTGGGTCTCATCGTGCACCGTCGGTTATCCTTTCTC	
nirD HR1 fwd	GTCGGGTCTCGCTACGCAGCCGATCTCGATCGCGACACG	Amplification of homologous regions adjacent to <i>nirD</i> in <i>S.</i> Typhimurium for cloning into pDOC-GG to create the $\Delta nirD$ deletion mutant
nirD HR1 rev	GCTGGTCTCTCTCCCGTTTTCTCCACCAGAGTGACC	
nirD HR2 fwd	GTAGGTCTCTCGCTTATTTTTGGGAGGCGCAACGCC	
nirD HR2 rev	GTGGGTCTCATCGTCCGACATAAGCCCCGGCCAT	
pdeK HR1 fwd	GTCGGGTCTCGCTACATGATAAGACCGATAATCAGCGCAA T	Amplification of homologous regions adjacent to <i>pdeK</i> in <i>S.</i> Typhimurium for cloning into pDOC-GG to create the $\Delta pdeK$ deletion mutant
pdeK HR1 rev	GCTGGTCTCTCTCCAAGGTCGCGCTTGTGCGAG	

pdeK HR2 fwd	GTAGGTCTCTCGCTTGTTTAATTGTTAACGAGCGGCTGAC G	
pdeK HR2 rev	GTGGGTCTCATCGTAACGGCGGGCGGCAGCAGCCA	
infB HR1 fwd	GTCGGGTCTCGCTACTGCCCGCTTTTACTGCGTCTTCATC T	Amplification of homologous regions adjacent to <i>infB</i> in <i>S.</i> Typhimurium for cloning into pDOC-GG to create the $\Delta infB$ deletion mutant
infB HR1 rev	GCTGGTCTCTCTCCCTTCGTCGTCTTTTGGGCCG	
infB HR2 fwd	GTAGGTCTCTCGCTCTGTTCCCTCCTGCTACAGTTTATTAC GC	
infB HR2 rev	GTGGGTCTCATCGTTTTGATATTGATGAAGAGTTCGCGACC G	
rfbF HR1 fwd	GTCGGGTCTCGCTACACTCACGATTGTCGTAGCACT	
rfbF HR1 rev	GCTGGTCTCTCTCCTAGATGATTGATAAAAATTTTTGGCAA GGTAAACG	
rfbF HR2 fwd	GTAGGTCTCTCGCTAATTATCCTCAATATTATTAGATGCGG TAAATGCATCAGAA	
rfbF HR2 rev	GTGGGTCTCATCGTTTTTTTTATTTCGTGAAAGTGACAGACCT ATAATCTTCC	
crl HR1 fwd	GTCGGGTCTCGCTACTGGCTTGCCTGGGGCCGGTG	Amplification of homologous regions adjacent to <i>crl</i> in <i>S.</i> Typhimurium for cloning into pDOC-GG to create the $\Delta crl$ deletion mutant
crl HR1 rev	GCTGGTCTCTCTCCGCGATCTCCTTTAATGAAGCAACTGT	
crl HR2 fwd	GTAGGTCTCTCGCTCCTGCTGCCATGCCTGATGG	
crl HR2 rev	GTGGGTCTCATCGTGCCGAAGCCTGGGCTACGGG	

cyaA HR1 fwd	GTCGGGTCTCGCTACGCGCAAGGGGACTTTGGCGT	Amplification of homologous regions adjacent to <i>cyaA</i> in <i>S. Typhimurium</i> for cloning into pDOC-GG to create the $\Delta cyaA$ deletion mutant
cyaA HR1 rev	GCTGGTCTCTCTCCACGTATCGCCTGATGTTGCT	
cyaA HR2 fwd	GTAGGTCTCTCGCTTGCTGCGCCGGGCAAAGCTG	
cyaA HR2 rev	GTGGGTCTCATCGTCATAATCATATTGATAAGAATAATGGC CGCACATG	
dsbA HR1 fwd	GTCGGGTCTCGCTACATTGAACCTTTACGCGCCATGCG	Amplification of homologous regions adjacent to <i>dsbA</i> in <i>S. Typhimurium</i> for cloning into pDOC-GG to create the $\Delta dsbA$ deletion mutant
dsbA HR1 rev	GCTGGTCTCTCTCCATCAACTCTCTCCGATTAATACATTGG CG	
dsbA HR2 fwd	GTAGGTCTCTCGCTAAGAACGCCGGTCACTGACCGGCGT TTTT	
dsbA HR2 rev	GTGGGTCTCATCGTCTTAATATTACGTTGTGTTACCCAAAC AACGATCG	
maoP HR1 fwd	GTCGGGTCTCGCTACCACTCCCATAAAGACGCGCTG	Amplification of homologous regions adjacent to <i>maoP</i> in <i>S. Typhimurium</i> for cloning into pDOC-GG to create the $\Delta maoP$ deletion mutant
maoP HR1 rev	GCTGGTCTCTCTCCCTGCACGCTCCTAATTCTTTG	
maoP HR2 fwd	GTAGGTCTCTCGCTAAAAAGGCGTAATGCCCTTTTTTTAC GC	
maoP HR2 rev	GTGGGTCTCATCGTCGTTTCTTGATCGTTTTGACCTTTTCGC	
STM <i>dsbA</i> fwd Bsal	GAGAGGGTCTCGCATGTCATGAAAAAGATTTGGCTGGCGC TG	Amplification of <i>dsbA</i> from <i>S. Typhimurium</i> for insertion into the overexpression vector pJMA <i>t5</i>
STM <i>dsbA</i> rev Bsal	GGGGGAATTGGAGACCTTTTTATTTTTTATCAACCAAATAT TTCACAGTATCAG	



STM maoP fwd Bsal	GAGAGGGTCTCGCATGGGATGGCGGAAAGCTTTACGAC	Amplification of <i>maoP</i> from <i>S. Typhimurium</i> for insertion into the overexpression vector pJMA <i>t5</i>
STM maoP rev Bsal	GGGGAATTGGAGACCTTATTAATCATCAGCTTCGGTGTA GTCTTCTGC	

## **2.6. Antimicrobial susceptibility testing**

Antibiotic susceptibility testing was used to determine the minimum inhibitory concentration (MIC) of a drug or substrate needed to prevent bacterial growth. This protocol is an adaptation of the EUCAST microbroth dilution method (EUCAST, 2021). All wells (except the first column) of a 96-well plate were filled with 50  $\mu\text{L}$  Muller Hinton (MH) broth. A stock of the required drug or substrate was made at double the maximum concentration required for the assay, and 50  $\mu\text{L}$  of this was added to the first and second columns of the plate. With a multichannel pipette, 50  $\mu\text{L}$  was taken from the second column and double-diluted across the plate to the 11<sup>th</sup> column, leaving the final column with just MH broth. Finally, a bacterial overnight culture was diluted 1:100 twice (to 1:10<sup>4</sup>) and 50  $\mu\text{L}$  of this culture was added to all wells. A gas permeable membrane was used to seal the top of the plate, and this was incubated at 37 °C overnight. The following day, the presence and absence of bacterial growth in each well was visible by eye and recorded. In some cases when this was more difficult to see, plates were centrifuged at 3,000 x g for 5 minutes to pellet the cells and the presence or absence of a pellet was used to determine at what concentration bacterial growth was inhibited. The MIC was determined to be the minimum concentration of antibiotic at which no bacterial growth was visible. Each substrate was tested in duplicate and two biological replicates were performed.

The agar dilution method was also used to investigate the MIC of a drug or substrate needed to prevent bacterial growth. Bacterial cultures were normalised to an OD<sub>600 nm</sub> of 0.1 and 5  $\mu\text{L}$  of culture was spotted onto Muller Hinton agar plates supplemented with antimicrobials at a range of concentrations. The concentration of antibiotic at which no growth was observed on the agar plate was recorded as its MIC.

## **2.7. Batch culture biofilm assays**

### **2.7.1. Crystal violet biofilm assay**

A crystal violet biofilm assay was performed to assess the differences in biofilm biomass production between bacterial strains. Bacterial overnight cultures were diluted 1:10<sup>4</sup> and 50  $\mu\text{L}$  of culture was added to a 96-well plate filled with 50  $\mu\text{L}$  LB broth without salt. The plate was covered with a gas permeable seal and incubated at 30 °C for 48 hours. After incubation, the plate was rinsed with a gentle stream of water to remove unattached cells, then turned upside-down on absorbent paper towel to drain residual water. To stain the biofilm, 200  $\mu\text{L}$  of 0.1 % crystal violet (Sigma, C0775) was added to each well and left for 10 minutes. The plate was rinsed again with water to remove all residual dye. To solubilise the stained biofilm, 200  $\mu\text{L}$  of 70 % ethanol was added to each well and absorbance was measured at 590 nm in a plate reader. This assay was repeated twice with eight technical replicates in each run.

### **2.7.2. Congo red and calcofluor biofilm assays**

Congo red binds to amyloid fibres and calcofluor binds to cellulose, and these dyes were used to measure curli and cellulose biosynthesis in the biofilm, respectively. LB agar without salt was supplemented with either 40 µg/mL Congo red dye (Sigma, C6277) or 200 µg/mL Calcofluor (Sigma, F3543). Plates were spotted with 10 µL of culture diluted to approximately  $10^7$  CFU/mL and were incubated at 30 °C for 48 hours. Four independent replicates were photographed and representative images are shown in this work.

### **2.7.3. Aggregation assay**

Cell aggregation was measured by leaving bacterial cultures (normalised to an OD<sub>600 nm</sub> of 3.0) on an unagitated surface at room temperature. After 24 hours, 100 µL from the top of the supernatant of each culture was removed by pipetting, diluted in PBS and measured in a plate reader at 600 nm. This assay was made up of three biological and two technical replicates per mutant copy.

### **2.8. Continuous culture biofilm assays**

Adhesion and biofilm architecture were investigated under flow conditions for several mutants using the Bioflux system. Flow cells were primed with LB broth without salt at 5 dyne/cm<sup>2</sup> and seeded with approximately  $10^7$  cells. The plate was left at room temperature for 3 hours to allow attachment, and subsequently incubated at 30 °C at a flow rate of 0.3 dyne/cm<sup>2</sup>. After 12, 24 and 48 hours, biofilms were visualised with an inverted light microscope and representative images at 4x, 10x, 20x and 40x magnification were taken at three locations of the flow cell. Experiments were performed in duplicate.

### **2.9. Growth kinetics**

Bacterial growth was measured over 24 hours to investigate differences in growth rate between strains. Overnight cultures were diluted to an OD<sub>600 nm</sub> of 0.1 and added to a 96-well plate sealed with a gas permeable membrane. Absorbance at 600 nm was measured every 15 minutes for 24 hours. Eight technical and two biological replicates were performed for this assay.

### **2.10. Membrane permeability assays**

Efflux activity can be inferred by determining the intracellular accumulation and extrusion of fluorescent efflux substrates in the presence and absence of an efflux inhibitor. Resazurin is a non-fluorescent blue dye that undergoes an irreversible redox reaction by

entering living cells, which transforms it into a fluorescent pink dye. Measuring this colour change over time gives an indication of membrane permeability. This was assayed in the presence and absence of the efflux pump inhibitor PA $\beta$ N to infer the efflux activity of each strain. Bacteria were grown to mid-logarithmic growth phase, as previously described. Pellets were resuspended in sterile PBS and OD<sub>600 nm</sub> was normalised for all strains. Bacteria were added to relevant wells of a 96-well plate alongside 10  $\mu$ g/mL resazurin and 125  $\mu$ g/mL PA $\beta$ N. A mutant lacking efflux pump protein TolC was also included as a control. Fluorescence was measured with a plate reader using an excitation wavelength of 544 nm and emission wavelength of 590 nm. Absorbance was also measured at 600 nm at each time point to correct for changes in cell density over time. Five technical and two biological replicates were performed for this assay.

### **2.11. RT-PCR**

RT-PCR was used to determine expression of genes of interest in selected conditions. RNA was isolated using the SV Total RNA Isolation System kit (Promega, Z3100) following a protocol optimised in house. A 4 % inoculum from a bacterial overnight culture was added to 50 mL LB broth in a 250 mL conical flask and incubated until cells reached mid-logarithmic growth phase. Bacteria were centrifuged at 3000 x g at 4 °C for 10 minutes, after which the pellet was resuspended in the residual supernatant left in the tube after the majority was tipped away. This was then transferred to sterile tubes and centrifuged for 1 minute at 18,000 x g in a microfuge. Pellets were resuspended in 100  $\mu$ L TE containing 50 mg/mL lysozyme and incubated at room temperature for 5 minutes with occasional agitation. From the SV Total RNA Isolation System kit, 75  $\mu$ L RNA Lysis Buffer was added and mixed by inversion several times, followed by 350  $\mu$ L RNA Dilution Buffer. Samples were heated at 70 °C for 3 minutes and centrifuged for 10 minutes. The supernatant was transferred to clean tubes and 200  $\mu$ L 95 % ethanol was added. This was transferred to the spin columns provided in the SV Total RNA Isolation System kit and centrifuged again for 30 seconds. Columns were washed with 600  $\mu$ L RNA Wash Solution and centrifuged to dry columns. After each spin, the eluate was discarded. DNase mix was prepared following the SV Total RNA Isolation System kit protocol and 50  $\mu$ L was added to each sample. After a 15 minutes incubation, 200  $\mu$ L DNase Stop Solution was added and samples were centrifuged for 30 seconds. Columns were washed with 600  $\mu$ L followed by 250  $\mu$ L of RNA Wash Solution, and then centrifuged again for 1 minute to dry. Columns were transferred to sterile microcentrifuge tubes and 100  $\mu$ L of nuclease-free water was added to each column. These were centrifuged for 2 minutes and immediately placed on ice. The quantity and quality of RNA was checked by running 2  $\mu$ L RNA on a 1.2 % agarose gel at 100 V for 10 minutes. RNA was quantified using a

NanoDrop Microvolume Spectrophotometer and diluted to 5 µg/µL with nuclease-free water.

To synthesise cDNA, 11 µL diluted RNA was added to 1 µL 50 ng/µL random hexamers (ThermoFisher, N8080127) and 1 µL 10 mM dNTP mix (ThermoFisher, R0191). This was heated at 65°C for 5 minutes and then immediately put on ice for at least 1 minute. The reverse transcriptase reaction mixture was prepared using 4 µL 5x SSIV Buffer, 1 µL 100 mM DTT and 1 µL 200 U/µL SuperScript™ IV Reverse Transcriptase (ThermoFisher, 18090010) per 1 sample. This mix was combined with the RNA mix and incubated at 23 °C for 10 minutes, 50-55 °C for 10 minutes and inactivated by heating at 80°C for 10 minutes. cDNA was stored at -20 °C until needed. PCR was then performed as described previously using relevant primers for the target gene.

## **2.12. Competition assay**

Competition assays were used to determine differences in relative fitness between two strains,. Bacterial overnights were diluted in PBS to OD<sub>600 nm</sub> of 1. Subsequently, 50 µL of each strain was added to universals containing 5 mL LB broth. To determine CFU at the beginning of the competition assay (time point 0), this coculture was serially diluted down a 96-well plate and 100 µL of each dilution was plated on LB agar supplemented with 20 µg/mL X-gal and 1 mM IPTG to facilitate blue-white screening. Universals were incubated at 37 °C with agitation for 24 hours (time point 24), at which time the cultures were serially diluted and 100 µL of the 1:10<sup>7</sup> and 1:10<sup>8</sup> dilutions were plated on LB with IPTG and X-gal. The CFU for each strain was counted and the percentage of each strain was compared between time points 0 and 24 with a paired *t*-test. Two biological and five technical replicates were carried out for this assay.

### 2.13. $\beta$ -galactosidase assay

A  $\beta$ -galactosidase assay measures the activity of the reporter gene LacZ. To measure  $\beta$ -galactosidase activity, bacteria were grown to mid-logarithmic growth phase in universals containing 5 mL LB, and the OD was measured at 650 nm. Cells were lysed by adding 3 drops of toluene (Sigma, 244511) and 3 drops of 1% Sodium deoxycholate (Sigma, D6750). Lysed bacteria were incubated at 37 °C with agitation for 10-15 minutes in universals without lids to allow evaporation of the toluene. Test tubes were placed in a water bath at 30 °C, into which 2 mL of Z-buffer with 0.4 g/L ONPG (Sigma, N1127) was added. Z-buffer was made with 0.75 g KCl, 0.25 g MgSO<sub>4</sub>·7H<sub>2</sub>O, 8.53 g Na<sub>2</sub>HPO<sub>4</sub>, 4.86 g NAH<sub>2</sub>PO<sub>4</sub> and 270  $\mu$ L  $\beta$ -mercaptoethanol in 1 L distilled water. To start the experiment, the time was recorded as 100  $\mu$ L lysate was added to a test tube, vortexed, and placed back into the water bath. When the solution began to turn yellow, the time was recorded and the reaction was stopped by adding 1 mL Na<sub>2</sub>CO<sub>3</sub>. The OD of this solution was recorded at 420 nm, and  $\beta$ -galactosidase activity was calculated using the following equation:

$$\beta - \text{galactosidase activity} = \frac{20,000 \times \text{OD}_{420}}{\text{OD}_{650} \times (t_1 - t_0)}$$

Where:

- $t_0$  = reaction start time
- $t_1$  = reaction stop time
- $\text{OD}_{650}$  = OD of cells at mid-logarithmic growth phase before lysis, measured at 650 nm
- $\text{OD}_{420}$  = OD of the yellow o-Nitrophenol produced when ONPG is broken down by  $\beta$ -galactosidase, measured at 420 nm

### 2.14. *Galleria mellonella* infection model

The *Galleria mellonella* infection model uses wax moth larvae to investigate the virulence of bacterial and fungal pathogens. It has previously been used with *S. Typhimurium* and has found similar results to murine models (Bender et al., 2013). Advantages of the *Galleria* model include its similarity to mammalian innate immune function, its low cost and ease of maintenance. Animal models provide a much more realistic environment to study how differences in gene expression *in vivo* affects disease pathology and pathogen virulence.

*Galleria mellonella* were sourced from livefoods.co.uk. Preliminary experiments with the wild type determined that the LD50 of *S. Typhimurium* was approximately  $1.5 \times 10^4$  CFU per inoculum. Relevant bacterial strains were grown overnight and diluted to an OD<sub>600 nm</sub>

of 1 in 100  $\mu\text{L}$  sterile PBS (approximately  $10^7$  CFU/mL). These were subsequently serially diluted down a 96-well plate in sterile PBS. To determine CFU per inoculum, 5  $\mu\text{L}$  from each dilution in the 96-well plate was spotted onto a square LB agar plate and colonies were counted the following day. Two technical replicates were plated per strain and CFU was counted the next day.

Larvae were injected with 10  $\mu\text{L}$  of culture diluted to approximately  $1.5 \times 10^4$  CFU per inoculum. Larvae were held between the thumb, index and middle fingers with their prolegs facing outwards. Hamilton needles (Sigma, 20779) were used to deliver the inoculum into the third right proleg. Needles were flushed twice with 70% ethanol and once with sterile PBS between inoculations. Ten larvae were infected per strain and were placed together on filter paper in a petri dish. Controls included ten uninfected larvae and ten larvae injected with PBS. Larvae were incubated at 37 °C and were checked three times per day, at which time survival was recorded.

## **2.15. TraDIS**

### **2.15.1. Transposon mutant library creation**

An *E. coli* BW25113 transposon mutant library used in this study has been described by Yasir et al. (2020). A transposon mutant library in *S. Typhimurium* was constructed following a similar protocol with the same Tn5 transposon encoding kanamycin resistance and an outward facing, IPTG-inducible promoter. Cells were grown to mid-logarithmic growth phase by adding 4 mL of a bacterial overnight culture to 400 mL 2xYT broth (Fisher, 15430675) supplemented with 0.7 mM EDTA (Sigma, 03690). Bacteria were grown to an OD<sub>600 nm</sub> between 0.2 and 0.25 and were centrifuged for 15 minutes at 3000 x g. The supernatant was discarded and pellets were washed and resuspended together in 25 mL 10 % glycerol. After 3 wash steps with 25 mL 10% glycerol, cells were resuspended in 600  $\mu\text{L}$  10% glycerol and 60  $\mu\text{L}$  aliquots were made in tubes on ice. These tubes contained 2  $\mu\text{L}$  water (Sigma), 2  $\mu\text{L}$  TypeOne Restriction Inhibitor (Cambio, TY0261H) and 0.4  $\mu\text{L}$  transposome. The transposome was made with 2  $\mu\text{L}$  transposon DNA (described by Yasir et al. (2020)) at a concentration of 100-150 ng/ $\mu\text{L}$ , 2  $\mu\text{L}$  100% glycerol and 4  $\mu\text{L}$  EZ-Tn5 transposase (Epicentre, TNP92110). Transposon DNA was amplified using the primers outlined in chapter 2.5 and cleaned up using phenol-chloroform. Electroporations were performed as previously described. Following a 2-hour recovery at 37 °C, five transformations were pooled and plated per bioassay plate (Sigma, CLS431111), containing LB agar supplemented with 50  $\mu\text{g}/\text{mL}$  kanamycin (Foremedium, KAN0005). A 1:100 dilution of each pool was plated on a smaller plate to aid in calculating the size of the mutant library. Plates were incubated at 37 °C overnight. The following day, the number of colonies per plate was calculated and the bacteria were resuspended from

the plate in LB broth. An equal volume of 100 % glycerol was added to this and 500  $\mu$ L aliquots were made in cryotubes for storage at -20 °C.

### **2.15.2. TraDIS-*Xpress* experiments to investigate biofilm formation**

To determine genes involved in biofilm formation, mutant libraries were added to glass beads. Approximately  $10^8$  cells from either transposon mutant library were added to 5 mL LB broth without salt in 6-well plates (Sigma, CLS3736). Glass beads (Sigma, 18406) were sterilised by autoclaving and 35 beads were added to each well with tweezers sterilised with 70 % ethanol. Plates were laid out as outlined in figure 2.2. One replicate was made up 70 beads shared across 2 wells of the 6-well plate. Half of the wells were treated with 1 mM IPTG to induce the transposon-located promoter. Cultures were incubated at 30 °C with light agitation at 60 rpm.

After incubation for 12, 24 and 48 hours, planktonic and biofilm samples were taken. For planktonic samples, 1 mL culture was taken from each well and added to a 96-well deep-well plate. For the biofilm samples, 70 beads were transferred with sterile tweezers to a 6-well plate containing 5 mL sterile PBS, with 35 beads per well. Beads were gently washed twice to remove planktonic cells. To resuspend the biofilm from the beads, six beads at-a-time were split between two 2 mL tubes (Fisher Scientific, 10031282) each containing 500  $\mu$ L sterile PBS, and vortexed for 15 seconds. All beads were vortexed in the same PBS, which was combined and added to the same 96-well deep-well plate as the planktonic samples. These cells were pelleted at 2100 x g for 5 minutes and stored at -20 °C ahead of DNA extraction.

To optimise the model, this method was performed using the transposon library parent strains *E. coli* BW25113 and *S. Typhimurium+lacI<sub>Z</sub>*. Only 6 beads were included in the optimisation experiments, which were sampled more regularly, at 6, 9, 12, 24 and 48 hours. Planktonic and biofilm samples were extracted in the same way, and CFU/mL over time was calculated by serially-diluting and spotting 10  $\mu$ L culture on square LB agar plates that were incubated at 37 °C overnight

### **2.15.3. TraDIS-*Xpress* Experiments to investigate efflux activity**

To determine genes involved in efflux activity, cells were exposed to acriflavine with or without the efflux inhibitor PA $\beta$ N, to differentiate the genes involved in efflux from those involved in acriflavine susceptibility alone. Approximately  $10^8$  cells from either transposon mutant library were added to 5 mL LB broth without salt in 6-well plates. Acriflavine (64  $\mu$ g/mL or 256  $\mu$ g/mL), 125  $\mu$ g/mL PA $\beta$ N or 1 mM IPTG were added to the corresponding wells, as outlined in figure 2.2. Plates were incubated at 30 °C with light agitation at 60



rpm. After 24 hours incubation, 2 mL culture was taken from the wells after 24 hours. More supernatant was taken for samples treated with acriflavine to capture all the surviving cells. This was added to a 96-well deep-well plate, pelleted at 2100 x g for 5 minutes, and stored at -20 °C.

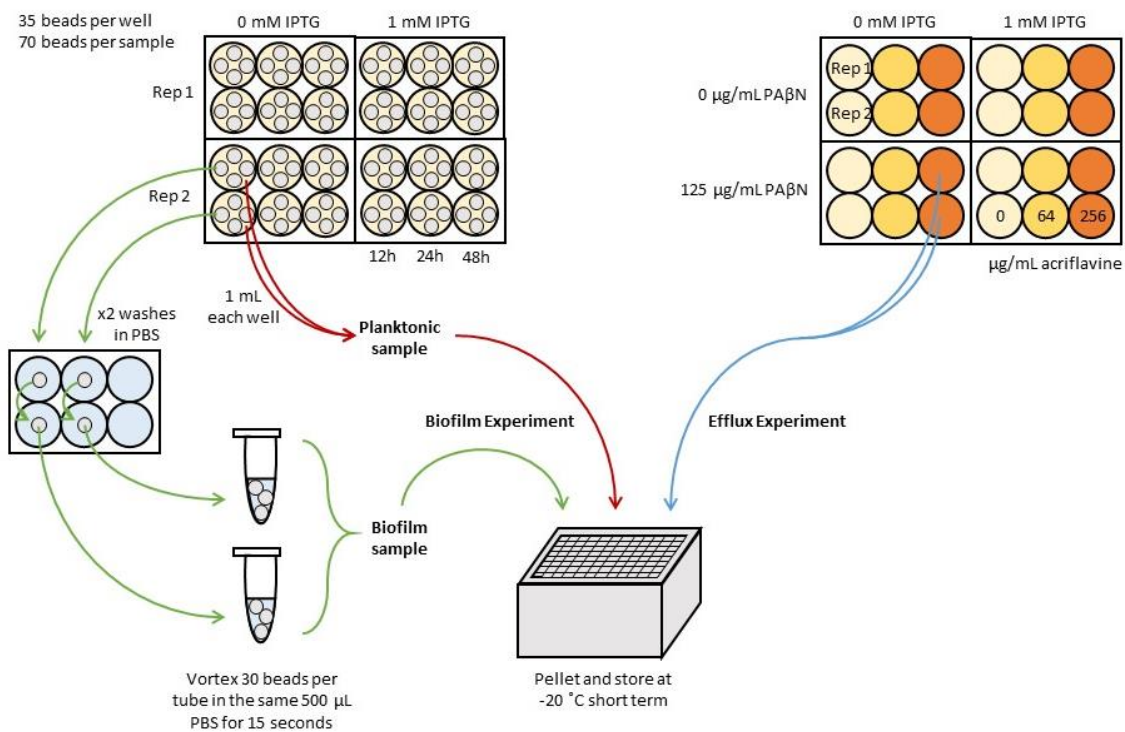


**Figure 2.2:** Layout of the TraDIS-*Xpress* experiments investigating biofilm formation (left) and efflux activity (right), detailing how samples were taken.

#### 2.15.4. Sequencing library preparation

Genomic DNA was prepared for sequencing using the MuSeek library preparation kit (ThermoFisher, K1361) (figure 2.3). Tagmentation uses MuA transposase to fragment the DNA, and requires 50 ng genomic DNA, 2.5 µL MuSeek Fragmentation Reaction Buffer and 0.5 µL MuSeek Enzyme Mix, mixed thoroughly on ice. Nuclease-free water from the same kit was added to each reaction to bring to total reaction volume to 30 µL. This was placed in a thermocycler at 30 °C for 5 minutes.

Tagmented DNA was purified by adding 45 µL (1.5x volume) of AMPure XP beads (Beckman Coulter, A63880) warmed to room temperature and mixed thoroughly. This was then transferred to a 96-well PCR plate, where it was incubated at room temperature for 5 minutes. The plate was placed on a magnetic stand for 2 minutes or until the supernatant was clear. This supernatant was removed, with care taken not to disrupt the magnetic beads. Whilst on the magnetic stand, the beads were washed twice with 200 µL freshly-

made 80% ethanol. All ethanol was removed from the plate and it was left to air-dry for 10 minutes. The plate was removed from the magnetic stand and 20  $\mu$ L elution buffer was mixed with the beads and incubated at room temperature for 2 minutes. The plate was placed back onto the magnetic stand, left for 2 minutes for the supernatant to clear, and 15  $\mu$ L of this supernatant was transferred to PCR strips.

For Tn5 fragment enrichment, this DNA was mixed 25  $\mu$ L NEBNext® High-Fidelity 2X PCR Master Mix (NEB, M0541S) and 5  $\mu$ L of customised i7 and i5 index primers. The i7 indices were customised to recognise the MuSeek adapters, and the i5 indices were customised to recognise the transposon-located tag, so that only fragments containing transposons were amplified. This reaction underwent the following PCR protocol:

- 72°C for 3 minutes
- 98°C for 30 seconds
- 28 cycles of:
  - 98°C for 10 seconds
  - 63°C for 30 seconds
  - 72°C for 60 seconds
- Hold at 10°C

The resulting PCR product was purified as above, using 30  $\mu$ L AMPure XP beads. DNA was eluted in 35  $\mu$ L elution buffer and 30  $\mu$ L eluate was transferred to a fresh 96-well PCR plate. This was quantified using Qubit DNA High Sensitivity assay kit and prepared for sequencing following protocol A from the Illumina NextSeq Denature and Dilute Libraries Guide (Illumina, version 13). Samples were sequenced on a NextSeq 500 using a NextSeq 500/550 High Output v2 kit (75 cycles) (Illumina, 20024906).

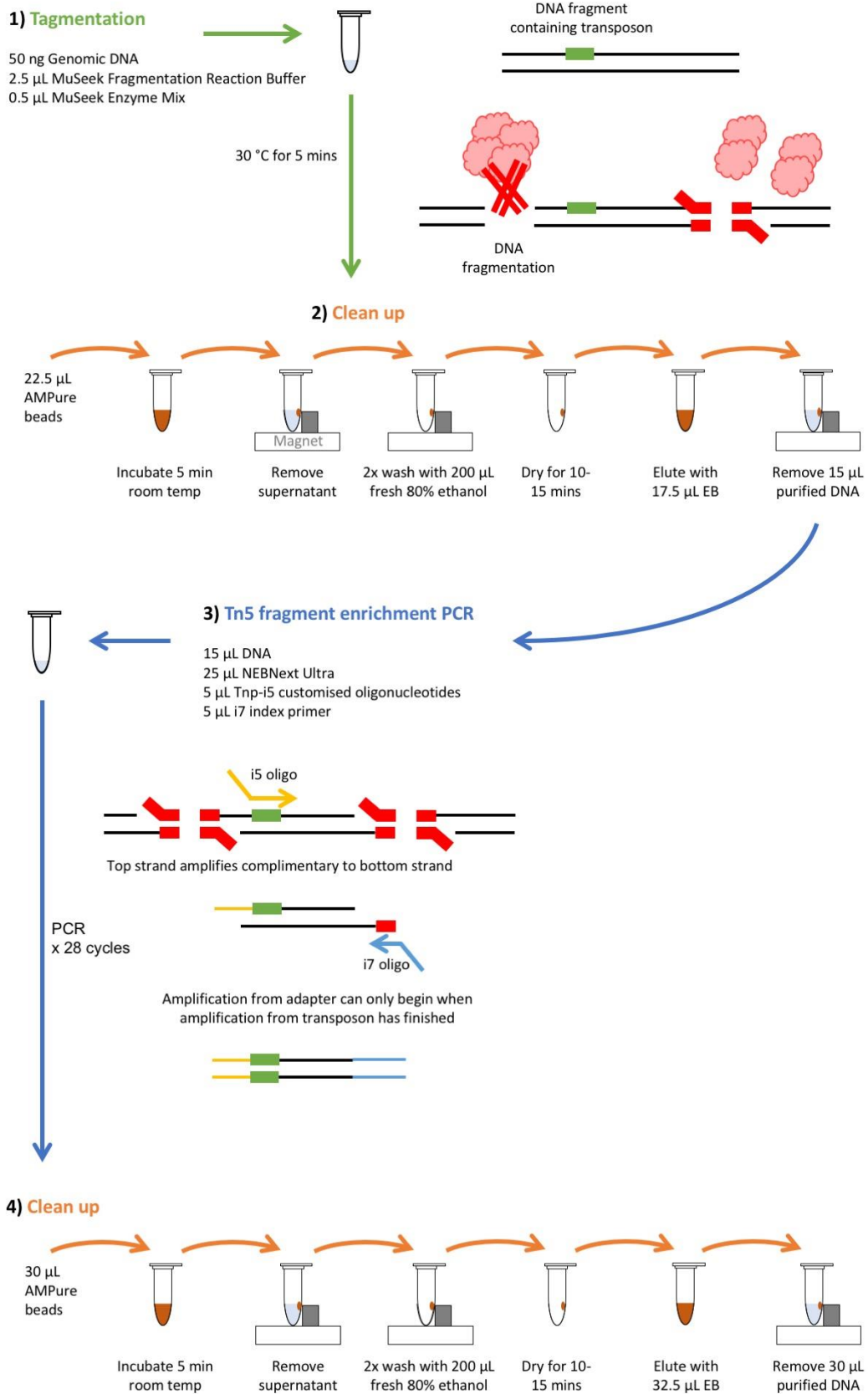


**Figure 2.3:** Tagmentation and Tn5 enrichment to prepare TraDIS-*Xpress* libraries for sequencing.

### 2.15.5. Data analysis

Sequencing generated FastQ files that were aligned to a reference genome and analysed using BioTraDIS (version 1.4.3) (Barquist et al., 2016) using SMALT (version 0.7.6).

Reference genomes used were CP009273 for *E. coli* BW25113 (Grenier et al., 2014) and CP001363 for *S. Typhimurium* ATCC 14028S (Jarvik et al., 2010), which was manipulated to add the *lacZ* operon from *E. coli* MG1655. BioTraDIS was used to aligned sequencing reads that contained the transposon tag sequence to the reference genome to create plot files. There parameters used were:

- Mapping quality cutoff score (m) = 0
- Custom k-mer value for SMALT mapping (smalt\_k) = 13
- Custom step size for SMALT mapping (smalt\_s) = 1
- Custom y parameter for SMALT mapping (smalt\_y) = 0.8
- Custom r parameter for SMALT mapping (smalt\_r) = 0

Multiple analysis techniques were used to determine the essentiality of genes between the control and test replicates. The first analysis step involved comparing insertion frequency per gene between the test and control conditions. The number of insertions per gene was identified using `tradis_gene_insert_sites` within the BioTraDIS toolkit. For each control and test condition being compared, the insertion frequency for each gene in each replicate was plotted against each other to determine the experiment variation between replicates. Underneath this variation in a different colour, the mean insertion frequencies per gene for both replicates were determined and the control condition was plotted against the test condition. Any data point that fell outside the experimental variation demonstrated a notable difference in insertion frequency in that gene between the control and test conditions, and these genes were recorded.

Files created from this were then analysed further using `tradis_comparison.R` (also part of the BioTraDIS toolkit) to determine significant differences in insertion frequencies per gene between control and test conditions. Genes with a *q*-value (*p*-value corrected for false discovery rate) below 0.05 were recorded as significantly different between control and test conditions.

Finally, plot files for all replicates were visually examined in Artemis (version 17.0.1) (Carver et al., 2011) to determined differences between control and test conditions. This highlighted where transposon insertions between genes affected their expression due to the outwards-facing promoter. These were not identified in previous analyses that only examined and compared insertions within genes. Manual scrutiny of the plot files determined whether an increased insertion frequency within a gene was due to that gene's activity or the transposon-located promoter activity affecting the expression of

neighbouring genes. These analyses generated a gene list for each condition where data showed a difference in gene essentiality between stressed and unstressed control conditions.

### **2.16. Motility assay**

Motility agar and plates were made following the protocol described in Thomson and Pallen (2020). Bacterial overnight cultures were diluted to an OD<sub>600 nm</sub> of 0.1 and 1 uL of culture was inoculated in the middle of the agar plate piercing the agar halfway. There were five replicates per strain to account for variation in motility. Plates were incubated at 37 °C overnight and the diameter of the motile disk was measured.

### **2.17. Statistical analyses**

The statistical tests used in this study are reported in the text alongside the significance values. To determine whether insertion of *lacIZ* into *S. Typhimurium* resulted in a different phenotype from the wild type, TOSTs (two one-sided *t*-tests) were used to determine equivalence rather than significant difference. Wilcoxon rank sum tests were used on data that was non-parametric made up of independent samples. A Welch's *t*-test was used on normally distributed data with unequal variances.

**3. CHAPTER 3: CONSTRUCTING TOOLS  
AND MODELS FOR TRANSPOSON  
MUTAGENESIS EXPERIMENTS**

### 3.1. Introduction

The first step in the process of determining the link between efflux activity and biofilm formation was to identify the genes and pathways involved in each. This was done using TraDIS (Transposon Directed Insertion-site Sequencing), a large-scale parallel transposon mutagenesis screen for highlighting the genes and networks required for survival under a given stress. This method was first successfully used to determine the genes essential in bile tolerance in *Salmonella* Typhi (Langridge et al., 2009), and has since been used to determine the essential genes for the survival and reproduction of other pathogens (Wong et al., 2016, Goodall et al., 2018).

A limitation of the traditional TraDIS methodology was its inability to assay essential genes, as it relies heavily on insertional inactivation. This was resolved with the recent development of TraDIS-*Xpress*, which integrates an outwards-facing inducible promoter into the transposon. (Yasir et al., 2020). Insertions upstream of essential genes allow investigation into how their overexpression affects fitness. Insertions downstream of essential genes may induce the production of antisense RNA that represses their translation, thereby downregulating a gene without inactivating it completely. Outward-facing promoters have been used previously in Tn-seq to determine essential genes in *Staphylococcus aureus*, with various promoters of different strengths used to investigate varied expression (Santiago et al., 2015). TraDIS-*Xpress* employs the use of a titratable *lac* promoter, which achieves varied levels of promoter strength with different concentrations of inducer. Like the *lac* promoter, expression from the *lac* promoter can be prevented by the *lac* repressor, LacI, binding to the *lac* operator upstream of the promoter and preventing its induction. To relieve this repression, the anti-inducer isopropyl  $\beta$ -D-1-thiogalactopyranoside (IPTG) binds to LacI and reduces its affinity for the *lac* operator, thereby allowing controlled promoter induction (Lewis, 2005). Varying the concentration of IPTG results in a concurrent varied level of promoter expression.

This system has been used in *E. coli* to assay genes important for survival following triclosan exposure (Yasir et al., 2020), however the *S. Typhimurium* genome does not contain a *lac* repressor or any gene that acts in the same way. To resolve this, the *lac* repressor *lacI* was amplified from *E. coli* and integrated into the *S. Typhimurium* chromosome. Downstream of *lacI* sits *lacZ*, encoding  $\beta$ -galactosidase, which is widely used as a reporter gene to assay promoter activity (MacGregor et al., 1991). This was also integrated into the *S. Typhimurium* chromosome downstream of *lacI*, as the inclusion of this reporter gene provided a simple and quick method to test whether *lacI* could affect *lac* promoter activity when expressed in its non-native host, *S. Typhimurium*. Following this, it was important to determine that this chromosomal insertion had no effect on overall fitness, efflux activity or biofilm formation that would prevent this strain from being used as

a proxy for the wild type in our experiments. Once this was confirmed, a transposon mutant library was constructed in this strain for use in TraDIS-*Xpress* experiments.

### 3.2. Aims

- To integrate *lacZ* into the chromosome of *Salmonella* Typhimurium 14028S
- To optimise a novel method of integrating transgenes into bacterial chromosomes
- To confirm that this novel method of chromosomal integration has no effect on bacterial fitness
- To confirm that *lacI* is expressed in *S. Typhimurium::lacZ* strain, and that the addition of IPTG allows control over the expression of genes repressed by *lacI*
- To construct a transposon mutant library in *S. Typhimurium::lacZ*

### 3.3. Chromosomal integration of *lacZ* into *S. Typhimurium*

The genes *lacI* and *lacZ* were integrated into the chromosome of *S. Typhimurium* using gene doctoring, as described by Holden et al. (2020). These genes were amplified from *E. coli* MG1655 using the relevant primers as listed in chapter 2.5. The assembly of *lacZ* inside pDOC-K-*glmS* was confirmed by PCR and Sanger sequencing, and successful chromosomal integration at the *glmS* site was confirmed by PCR, Sanger sequencing and whole genome sequencing (Illumina NextSeq). This strain will henceforth be referred to as *S. Typhimurium::lacZ* or WT::*lacZ*. The transcription of *lacI* RNA in *S. Typhimurium::lacZ* was confirmed using RT-PCR (figure 3.1). cDNA from WT *S. Typhimurium* and *S. Typhimurium::lacZ* was amplified with primers specific for *lacI*, with *gyrB* included as a positive control for both strains.



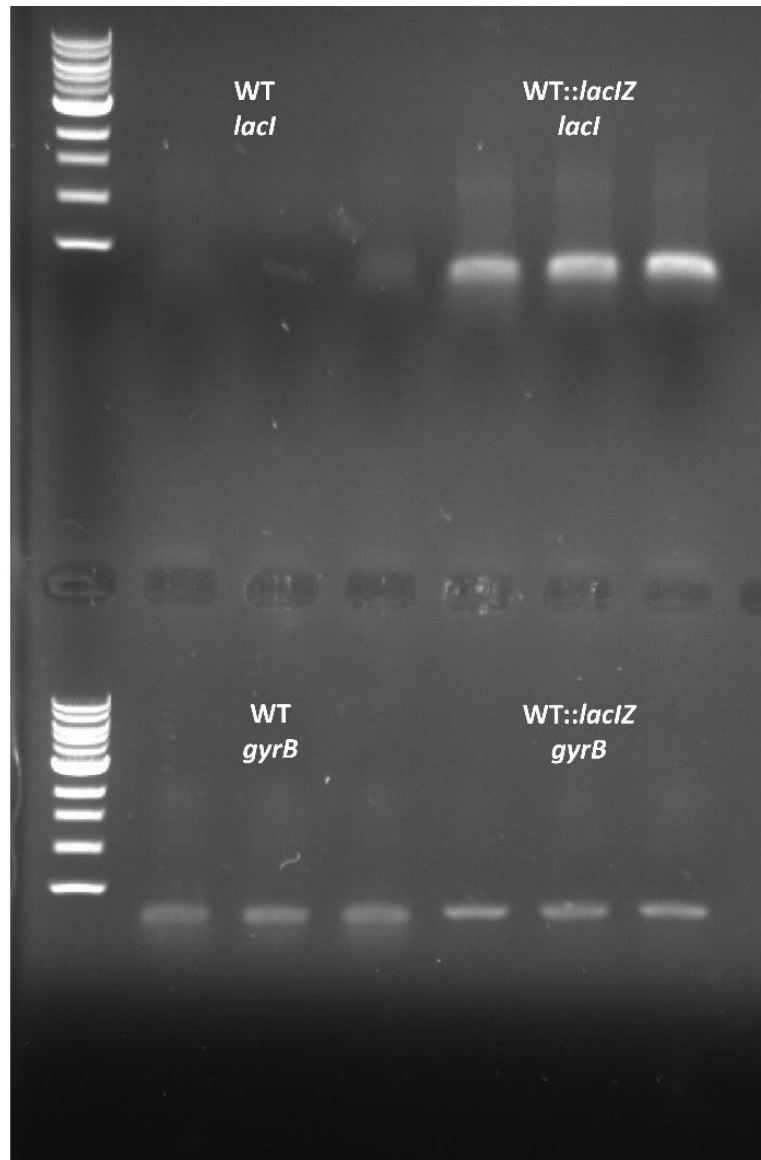


**Figure 3.1:** RT-PCR where the top panel is showing the absence of *lacI* RNA in WT *S. Typhimurium* and its presence in *S. Typhimurium*::*lacIZ* (WT::*lacIZ*). The bottom panel a positive control measuring *gyrB* expression in both strains. A 1 kb DNA ladder is included in both panels. Three biological repeats were included for each strain.

To phenotypically demonstrate *lacIZ* activity in *S. Typhimurium*::*lacIZ*, this strain was plated on LB agar supplemented with X-gal with and without 1 mM IPTG. Figure 3.2 demonstrates that the addition of IPTG allows expression of *lacZ*, which makes colonies appear blue on agar supplemented with X-gal.

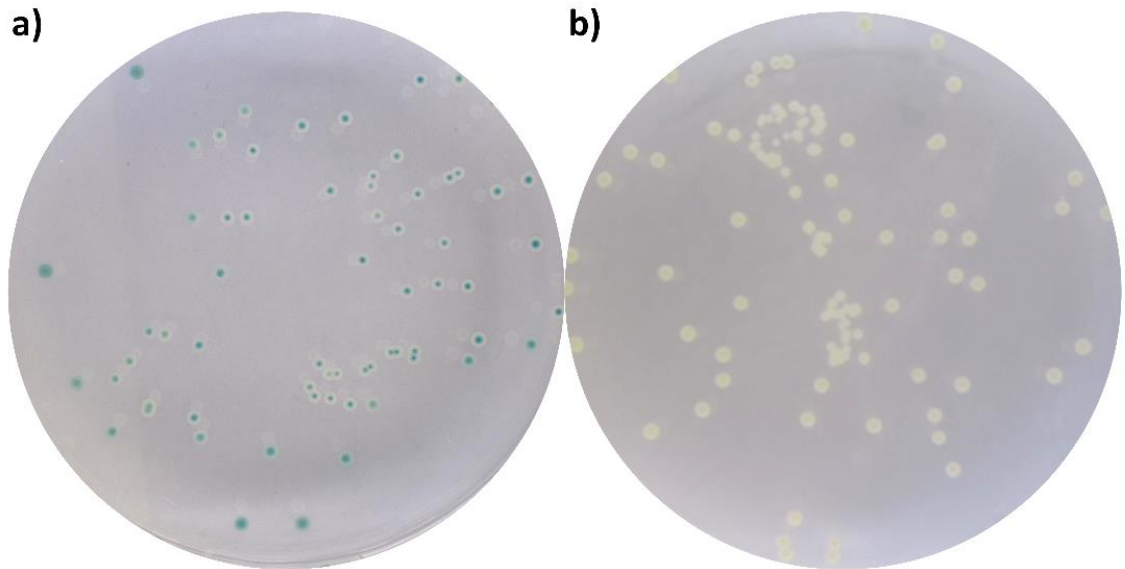


**Figure 3.2:** *S. Typhimurium::lacZ* plated on LB agar supplemented with X-gal, **a)** with IPTG and **b)** without IPTG. Representative plates are shown from two biological and two technical replicates.

A widely used method to assay promoter activity involves introducing *lacZ* downstream of the promoter in question and measuring  $\beta$ -galactosidase activity (MacGregor et al., 1991). This was undertaken in *S. Typhimurium::lacZ* to investigate whether LacI produced in its non-native host could facilitate titratable control of the *lac* promoter, and if so how much IPTG would need to be added to achieve stepwise increases in promoter activity at practical intervals. Figure 3.3a shows a stepwise increase  $\beta$ -galactosidase activity with increasing concentrations of IPTG. The addition of up to 10  $\mu\text{g}/\text{mL}$  IPTG did not cause a significant increase in  $\beta$ -galactosidase activity relative to untreated *S. Typhimurium::lacZ* (Welch's t-test,  $p = 0.119$ ), but a significant difference was seen with concentrations of 15  $\mu\text{g}/\text{mL}$  and above (Welch's t-test, 15  $\mu\text{g}/\text{mL}$  IPTG,  $p = 0.005$ ). This shows that 15-40  $\mu\text{g}/\text{mL}$  IPTG induces a moderate level of promoter expression, and 100  $\mu\text{g}/\text{mL}$  or above induces a high level of promoter expression. Concentrations of IPTG higher than 100  $\mu\text{g}/\text{mL}$  did not result in a significant stepwise increase in  $\beta$ -galactosidase activity (Welch's  $t$ -test, 1000 relative to 100  $\mu\text{g}/\text{mL}$ ,  $p = 0.239$ ; 10,000 relative to 100  $\mu\text{g}/\text{mL}$ ,  $p = 0.764$ ). This suggests that 100  $\mu\text{g}/\text{mL}$  IPTG is sufficient to induce maximum promoter activity. Previous TraDIS-*Xpress* experiments with the BW25113 library used 1 mM IPTG (equivalent to 238.31  $\text{g}/\text{mL}$ ), which was more than sufficient to induce promoter expression in the *S. Typhimurium::lacZ* library.

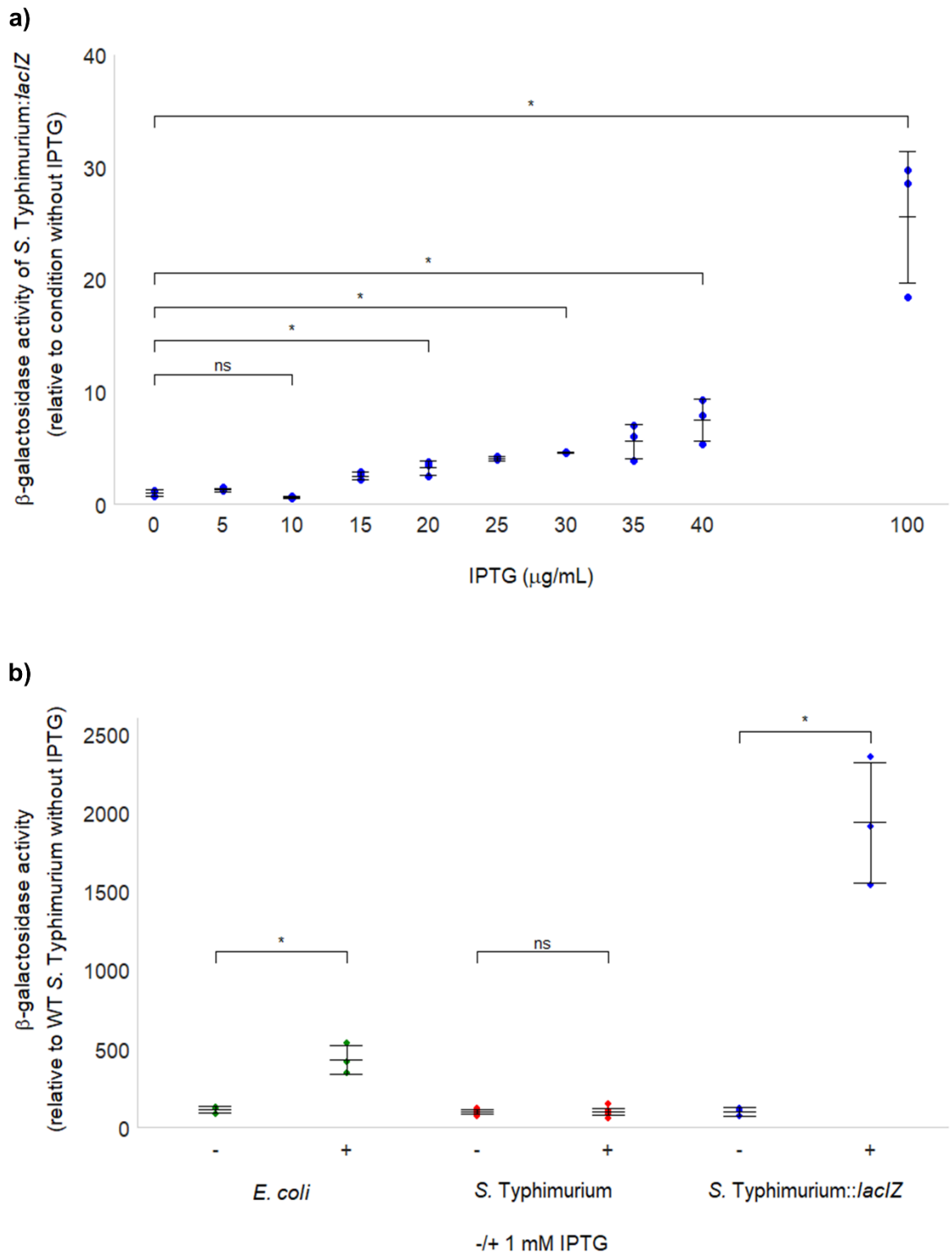


**Figure 3.3:**  $\beta$ -galactosidase activity, as an indirect measurement of *lacI* activity in *S. Typhimurium::lacZ* **a)**  $\beta$ -galactosidase activity in *S. Typhimurium::lacZ* when treated with IPTG, relative to *S. Typhimurium::lacZ* without IPTG. **b)**  $\beta$ -galactosidase activity in *E. coli* K-12, WT *S. Typhimurium* and *S. Typhimurium::lacZ* with and without 1 mM IPTG, relative to WT *S. Typhimurium* without IPTG. For both graphs, points represent individual data points of relative  $\beta$ -galactosidase activity for three biological replicates. Error bars show the mean and 95 % confidence intervals. A significant difference where  $p < 0.05$  is denoted with an asterisks (\*) or 'ns' (not significant).

$\beta$ -galactosidase activity with and without IPTG was compared between *S. Typhimurium*, *S. Typhimurium::lacI<sub>Z</sub>* and *E. coli* K-12, from which *lacI<sub>Z</sub>* was initially cloned (figure 3.3b). In strains that expressed *lacI<sub>Z</sub>*,  $\beta$ -galactosidase activity increased with the addition of IPTG (Welch's *t*-test, *E. coli*,  $p = 0.025$ ; *S. Typhimurium::lacI<sub>Z</sub>*,  $p = 0.016$ ), and remained unchanged in wild type *S. Typhimurium* without *lacI<sub>Z</sub>* (Welch's *t*-test,  $p = 1$ ). This demonstrated that wild type *S. Typhimurium* had no background  $\beta$ -galactosidase activity, and that chromosomal integration of *lacI<sub>Z</sub>* was responsible for all of the  $\beta$ -galactosidase activity seen in this assay. There was also a significantly higher  $\beta$ -galactosidase activity in *S. Typhimurium::lacI<sub>Z</sub>* compared to *E. coli* (Welch's *t*-test,  $p = 0.019$ ), which may be due to the location that *lacI<sub>Z</sub>* was inserted into the chromosome in *S. Typhimurium::lacI<sub>Z</sub>*.

### 3.4. Confirming the fitness neutrality of *lacI<sub>Z</sub>* chromosomal insertion

It was necessary to confirm that the integration of *lacI<sub>Z</sub>* into the chromosome of *S. Typhimurium* did not affect its fitness in a way that would prevent it from being used as a proxy for the wild type in future experiments. Wild type *S. Typhimurium* and *S. Typhimurium::lacI<sub>Z</sub>* were investigated for any differences in antibiotic susceptibility, biofilm formation, efflux activity, competitive fitness and pathogenicity. It was established that the chromosomal insertion of *lacI<sub>Z</sub>* had no measurable effect on these phenotypes.

#### 3.4.1. No difference in antimicrobial susceptibility between WT and WT::*lacI<sub>Z</sub>*

Antimicrobial susceptibility testing was performed by microbroth dilution to examine whether the chromosomal integration of *lacI<sub>Z</sub>* had any effect on the antibiotic susceptibility of *S. Typhimurium* (Table 3.1). No significant difference in susceptibility to eight antibiotics was found between *S. Typhimurium* and *S. Typhimurium::lacI<sub>Z</sub>*.

**Table 3.1:** MIC ( $\mu\text{g/mL}$ ) of multiple antibiotics in *S. Typhimurium* and *S.*

*Typhimurium::lacI<sub>Z</sub>*. Values are the average of two biological replicates and the experimental error was a 1-fold change in MIC.

	<b>S. Typhimurium</b>	<b>S. Typhimurium::<i>lacI<sub>Z</sub></i></b>
Ampicillin	2	2
Azithromycin	4	4
Chloramphenicol	2	2
Ciprofloxacin	0.016	0.008
Cefotaxime	0.031	0.031
Kanamycin	4	2
Nalidixic acid	4	2
Tetracycline	0.5	0.5

### 3.4.2. Biofilm formation unaffected by chromosomal integration of *lacI*Z

Biofilm formation was unaffected by the chromosomal integration of *lacI*Z in *S. Typhimurium* (figure 3.4). This was confirmed by crystal violet biofilm assays, where biofilm biomass of the wild type was found to be equivalent to that of WT::*lacI*Z (TOST,  $p = 0.032$ ). This assay was also carried out with both strains treated with an efflux inhibitor to determine whether the relationship between efflux activity and biofilm formation was disrupted by the chromosomal integration of these genes. The efflux mutant *tolC::cat* was included as a control as it is known to have impaired biofilm formation (Baugh et al., 2012). When efflux was chemically impaired, biofilm biomass was equivalent in WT and WT::*lacI*Z (TOST,  $p = 0.029$ ). As well as investigating biofilm biomass, biofilm matrix composition was also investigated through plating each strain on agar supplemented with Congo red and calcofluor to examine curli and cellulose production, respectively. Colony morphology showed there was no visible difference in curli and cellulose biosynthesis between biofilms produced by WT and WT::*lacI*Z.

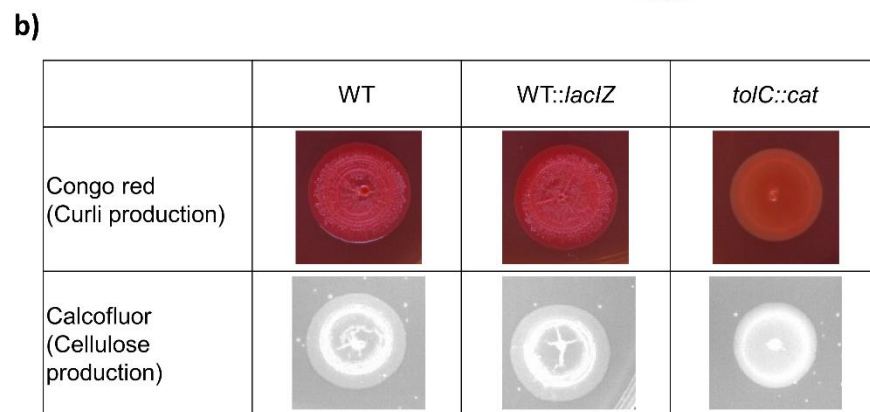
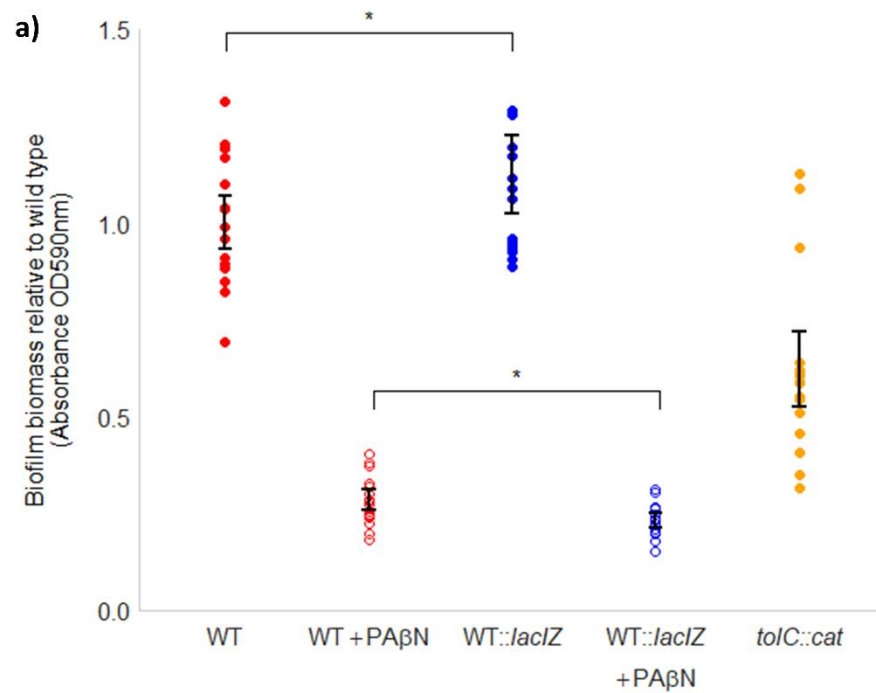


**Figure 3.4:** Biofilm formation in WT *S. Typhimurium* and WT::lacZ. **a)** Biofilm biomass measured by crystal violet staining (OD<sub>590nm</sub>) with and without PAβN. The efflux mutant *tolC::cat* was included as a negative control. Points represent two biological and eight technical replicates and error bars denote 95% confidence intervals. Statistical equivalence was determined using two one-sided *t*-tests (TOSTs), where an asterisks denotes a *p*-value below 0.05. **b)** Curli and cellulose production, measured by plating colonies on agar supplemented with Congo red and cellulose, respectively. Representative colonies from two biological and four technical replicates are shown.

### 3.4.3. Efflux activity appears unchanged with *lacI*Z integration into *S. Typhimurium*

Efflux activity was unchanged with the chromosomal integration of *lacI*Z in *S.*

*Typhimurium* (figure 3.5). This was determined by measuring the uptake of resazurin with and without chemical inhibition of efflux by PA $\beta$ N. The efflux mutant *tolC::cat* was included in both assays as a efflux-impaired control. Efflux activity in WT::*lacI*Z was found to be equivalent to the wild type in the absence (TOST of area under the curve,  $p = 0.011$ ) and presence of PA $\beta$ N (TOST of area under the curve,  $p = 0.017$ ).

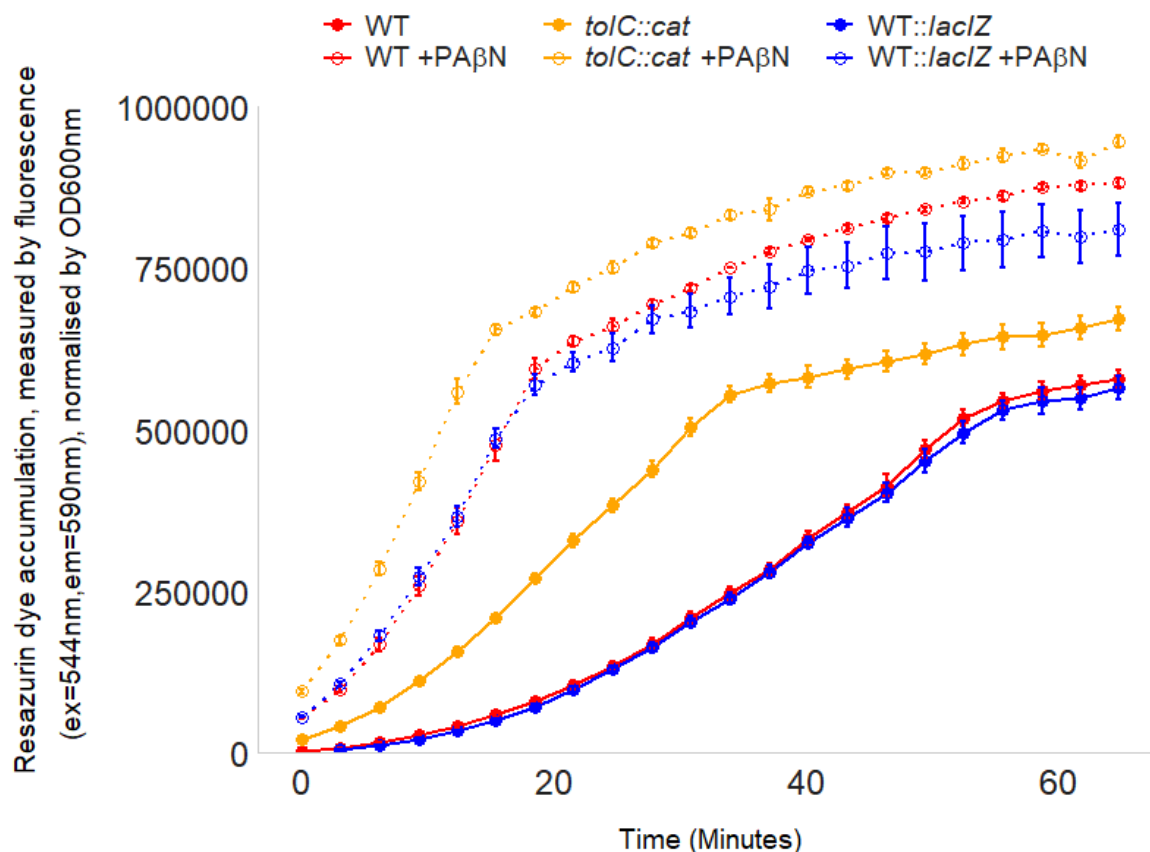


**Figure 3.5:** Dye accumulation over 60 minutes in the presence and absence of the efflux inhibitor PA $\beta$ N, as an indication of efflux activity in WT *S. Typhimurium* and WT::*lacI*Z. The efflux mutant *tolC::cat* was included as a efflux-impaired control. Points represent mean values of 5 technical replicates and 2 biological replicates. Error bars show 95 % confidence intervals.

### 3.4.4. Equal competitive fitness between WT and WT::*lacI*Z

Differences in fitness between bacteria can be measured with a competition assay, where strains are co-cultured and the relative abundance of each strain is measured over time. WT *S. Typhimurium* and WT::*lacI*Z were co-cultured for 24 hours (figure 3.6) and equivalence testing found there to be no change in the percentage of WT::*lacI*Z at the start and after 24 hours of co-culture with WT *S. Typhimurium* (Paired TOST,  $p = 0.047$ )

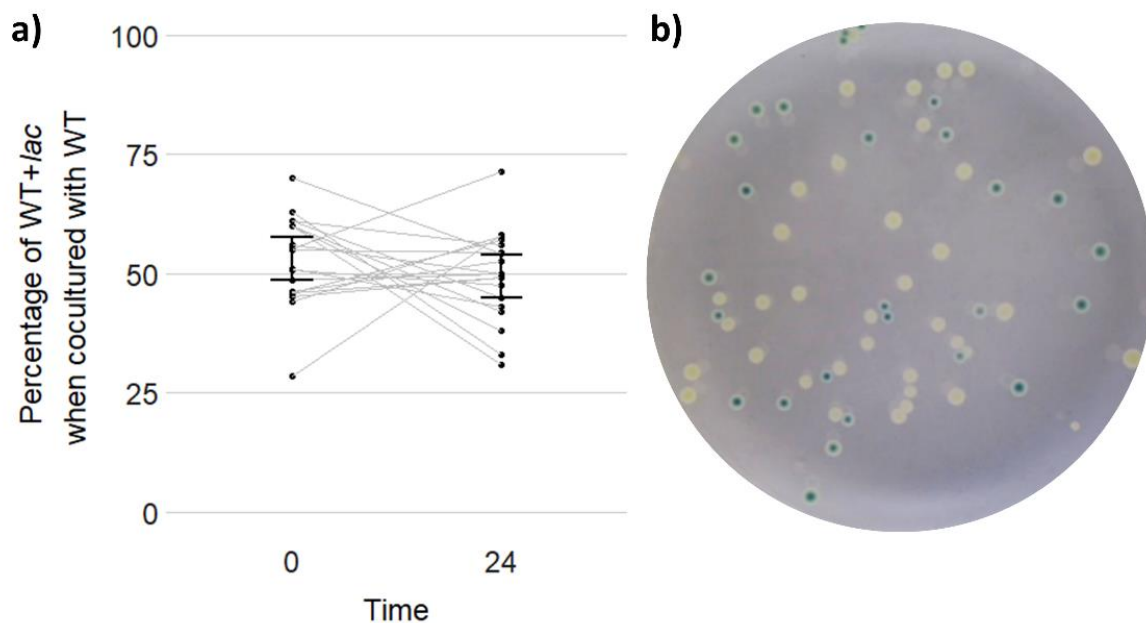


**Figure 3.6:** *In vitro* competitive fitness assay between WT and WT::*lacI*Z. **a)** Points represent biological replicates, of which 15 were performed, and grey lines show pairwise comparisons between replicates at the start and after 24 hours coculture. Error bars denote 95% confidence intervals. **b)** A representative plate from 1 biological replicate showing CFU of WT *S. Typhimurium* (white) and WT::*lacI*Z (blue) after 24 hours coculture.



### 3.4.5. No change in pathogenicity between WT and WT::*lacI*Z

The *Galleria mellonella* infection model was used to show that the chromosomal integration of *lacI*Z into *S. Typhimurium* had no effect on pathogenicity. Over a 48-hour period, both strains followed the same trend and there was no observable difference in their pathogenicity (figure 3.7).

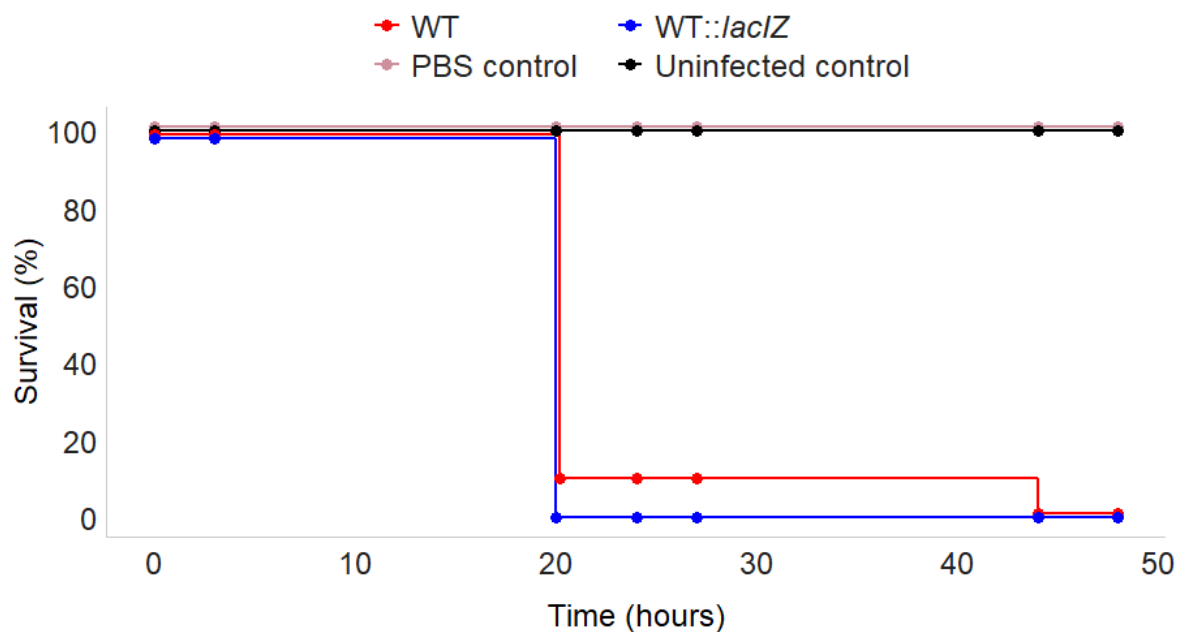


**Figure 3.7:** Pathogenicity of WT *S. Typhimurium* and WT::*lacI*Z, in a *Galleria mellonella* infection model. Each treatment was completed with 10 larvae. The experimental error was 10% (1 larva).

### 3.5. Constructing a transposon mutant library in *S. Typhimurium::lacZ*

A mutant library was created in *S. Typhimurium::lacZ* following the protocol outlined in chapter 2.14.1. Analysis of this library with the BioTraDIS toolkit (Barquist et al., 2016) found approximately 500,000 unique insertion sites, or one insertion every 10 base pairs and roughly 90 insertions per gene. Two independent replicates were sequenced and appeared almost identical, with insertions evenly spaced throughout the genome (figure 3.8).

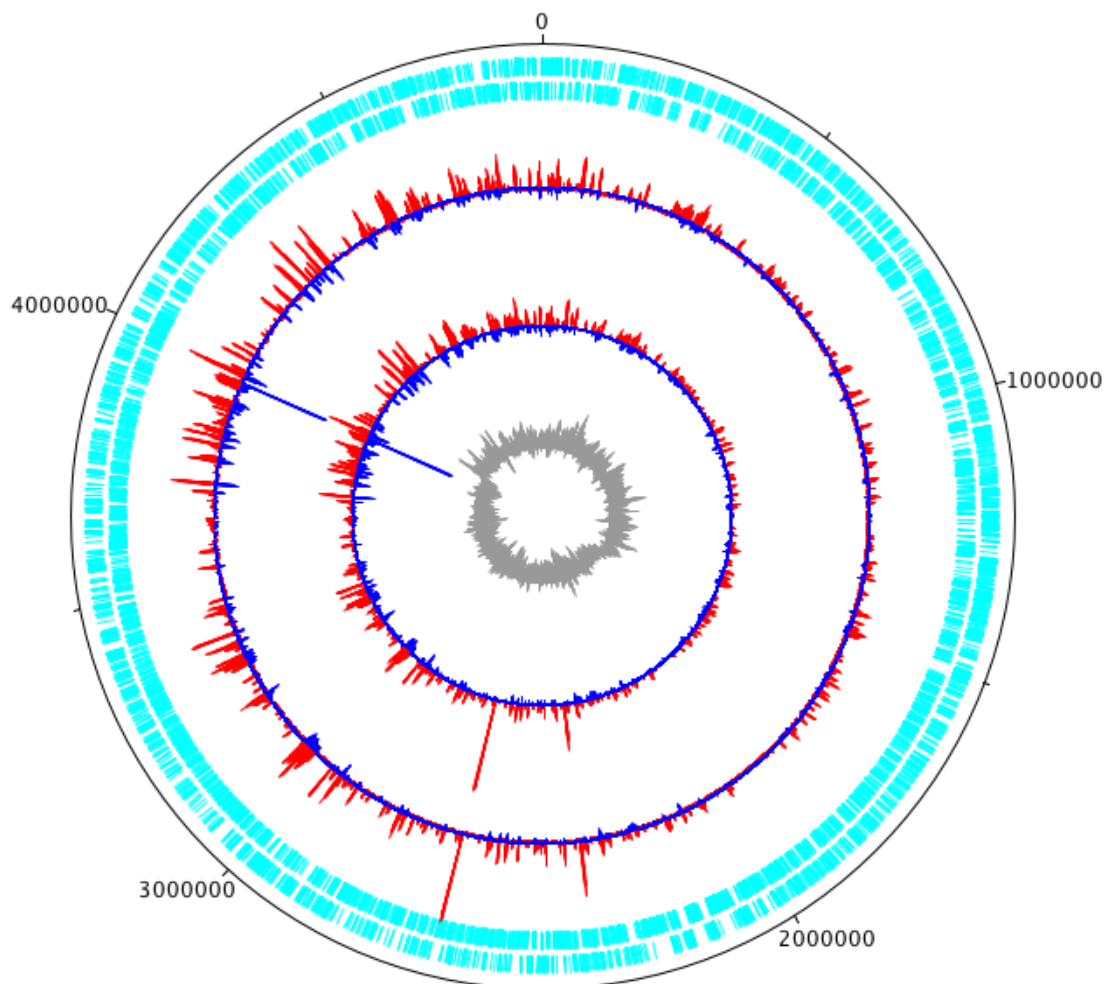


**Figure 3.8:** Insertion frequency across the *S. Typhimurium::lacZ* genome on the forward (red) and reverse (blue) strands. Tracks show two independent sequencing library preparations. The GC content of the genome is shown in the inner track in grey, where peaks show areas rich in GC. Genes are shown in cyan.

### 3.6. Defining the conditions for TraDIS-Xpress experiments to investigate biofilm formation and efflux activity

#### 3.6.1. Developing a model to investigate biofilm formation over time

To investigate the genes involved in biofilm formation, I designed a model to compare planktonic and biofilm cells and multiple time points throughout the biofilm life cycle. This involved growing biofilms on glass beads in 6-well plates and extracting planktonic samples and biofilm samples from the same culture (figure 3.9).

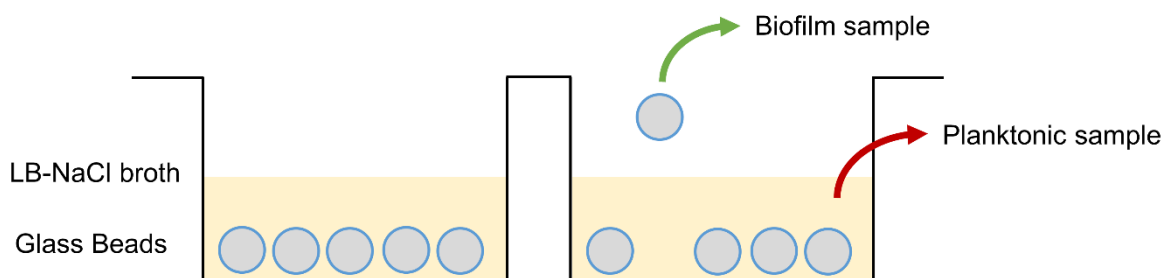


**Figure 3.9:** The model system used to determine the genes involved at different stages of the biofilm life cycle. Planktonic samples from the culture and biofilm samples from the beads were assayed from the same well over time.

Initial optimisation focused on the determining the number of cells that could be harvested from the biofilm formed on a glass bead over time for both transposon mutant library parent strains, *E. coli* BW25113 and *S. Typhimurium::lacZ*. Sampling the model at different times would determine genes involved at each stage of the biofilm life cycle, including initial biofilm attachment, biofilm maturation, and biofilm dispersal, rather than solely the genes required for maintenance of a mature biofilm.

For both species, approximately  $10^6$ - $10^7$  CFU could be harvested from a biofilm formed on a glass bead after 48 hours (figure 3.10). Interspecies differences in biofilm development were apparent, as a small biofilm of approximately  $10^4$  CFU per bead could be harvested after only 6 hours for *S. Typhimurium*, however it took 12 hours for an *E. coli* biofilm to reach this number of cells. The *E. coli* and *S. Typhimurium* transposon mutant libraries contain approximately 800,000 and 500,000 unique insertion mutants, respectively. Therefore in order to avoid a sampling bottleneck, at least this number of cells must be able to be isolated from the biofilm condition at all time points, to allow each of the mutants the opportunity to form a biofilm on the bead. An average of  $5.5 \times 10^5$  *E. coli* cells per bead were isolated at the 12 hour time point, which was fewer than the  $8 \times 10^5$  CFU necessary to avoid a sampling bottleneck. This was addressed by adding 70 beads to each replicate and removing the attached cells from them all to constitute one sample.

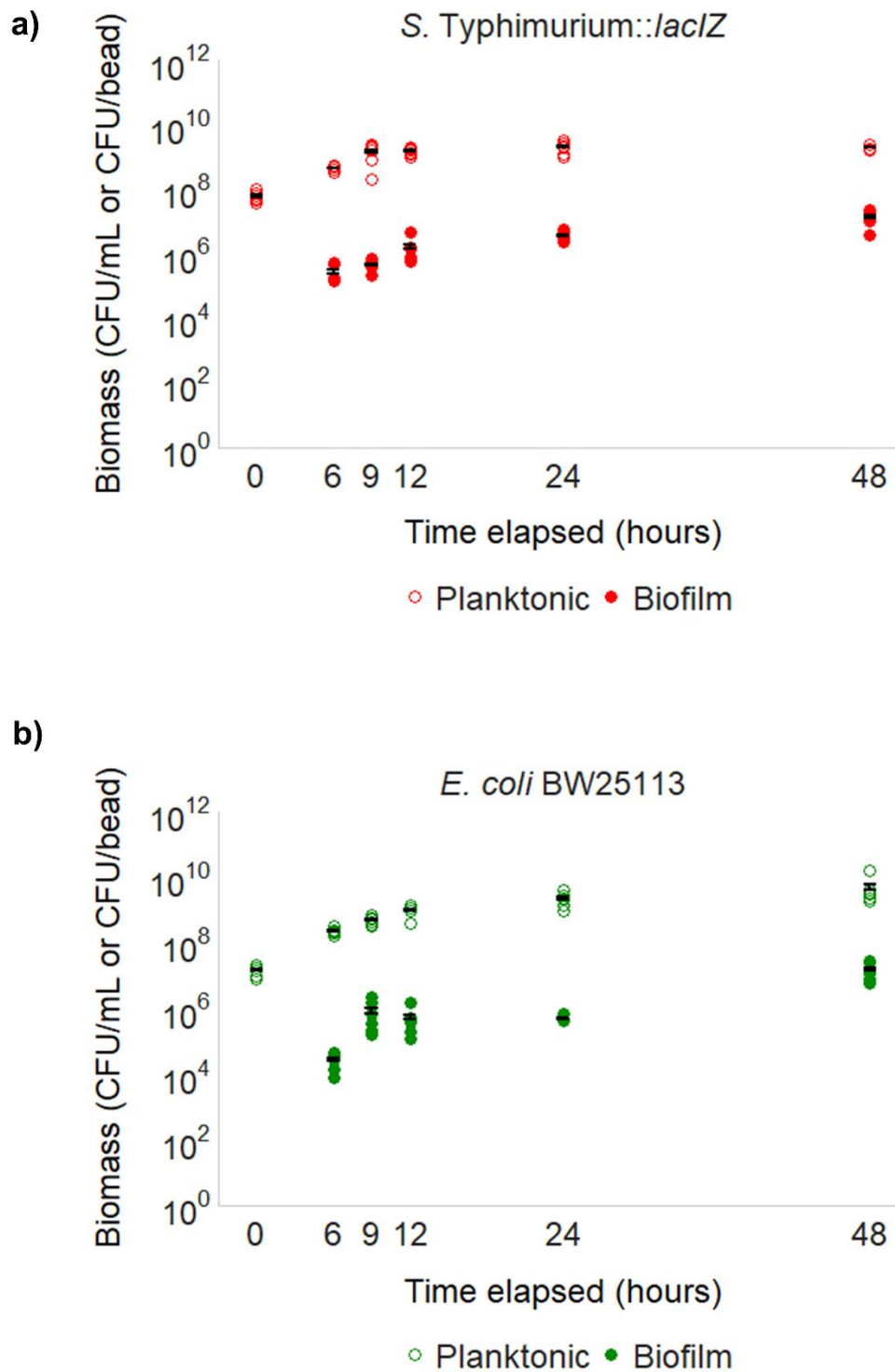


**Figure 3.10:** CFU of planktonic (○) and biofilm (●) cells harvested from the biofilm model over time for the mutant library parent strains in **a)** *S. Typhimurium::lacZ* (red) and **b)** *E. coli* BW25113 (green). Points represent biological replicates, of which 3 were performed, and error bars show 1 standard error.

At least 50 ng (1 ng/ $\mu$ L) DNA was required to prepare transposon mutant libraries for sequencing, so it was important to determine the number of beads that would need to be included in the model to not only carry enough cells to allow sufficient mutants to grow but to also get this amount of DNA. After wild type *E. coli* BW25113 and *S. Typhimurium::lacZ* had been growing on 30 glass beads for 12, 24 and 48 hours, the cells were removed from the bead, the CFU per bead was calculated, and the genomic DNA was extracted and quantified (table 3.2). In agreement with the previous experiment, a higher CFU could be isolated from *S. Typhimurium* biofilms compared to *E. coli* biofilms growing on the beads. Following this experiment, it was agreed that reducing the elution volume for DNA extraction to 10  $\mu$ L and using 70 beads per replicate would increase concentration of DNA isolated from the beads to an adequate amount for sequencing library preparation.

**Table 3.2:** CFU per bead and gDNA per bead of *E. coli* BW2113 and *S.*

*Typhimurium::lacZ* biofilms on beads over time. Values are the mean of 2 technical replicates.

Species	Time (hours)	Mean CFU per bead isolated from 30 beads	Mean gDNA (ng/ $\mu$ L) isolated from 30 beads	Volume needed for sequencing library preparation ( $\mu$ L)
<i>E. coli</i>	12	$5.53 \times 10^5$	0.249	> 200
	24	$5.10 \times 10^6$	1.732	28.87
	48	$1.57 \times 10^7$	2.930	17.06
<i>S. Typhimurium</i>	12	$1.63 \times 10^6$	0.728	68.73
	24	$3.63 \times 10^6$	7.065	7.077
	48	$1.4 \times 10^7$	13.850	3.610

There is the potential for a bottleneck to occur at the 12 hour sampling time point, where fewer than  $10^7$  cells could form a biofilm per bead out of the  $10^7$  CFU/ mL of transposon mutant library added to the culture. This was addressed through using 70 beads per replicate. Each cell has an equal chance to form a biofilm on the bead, with mutants competing with each other

### 3.6.2. Selection of an appropriate substrate to investigate efflux activity

Five chemicals were tested for potential use as an efflux substrate in TraDIS-*Xpress* experiments investigating efflux activity in *S. Typhimurium* and *E. coli* (Table 3.3).

Acriflavine and ethidium bromide are dyes that bind to DNA and inhibit cell functions (Lerman, 1963, Wainwright, 2001); ciprofloxacin inhibits DNA replication by targeting DNA gyrase and topoisomerases (Campoli-Richards et al., 1988); tetracycline prevents protein translation by binding blocking tRNA associated with the 30S ribosomal subunit (Maxwell, 1967) and chloramphenicol prevents protein synthesis through inhibiting protein chain elongation (Pestka, 1975). Kanamycin is not an efflux substrate and was included as a negative control. Susceptibility testing was undertaken in the presence and absence of the efflux inhibitor PA $\beta$ N to compare how the MIC of these drugs changed with or without functional efflux. From this experiment, acriflavine was chosen as the most suitable efflux substrate to use in TraDIS-*Xpress* experiments. This was because there was the largest difference in its MIC in cells with and without functional efflux. Treating bacteria with a combination of efflux substrate and efflux inhibitor will most likely reveal genes and pathways involved in efflux activity rather than substrate-specific responses.

**Table 3.3:** MIC ( $\mu\text{g/mL}$ ) of multiple antibiotics in *S. Typhimurium::lacZ* and *E. coli* BW25113, with and without efflux inhibition by 125  $\mu\text{g/mL}$  PA $\beta$ N. Two biological replicates per antibiotic per strain were completed. The experimental error was a fold change.

	<b><i>S. Typhimurium</i> 14028S::<i>lacZ</i></b>		<b><i>E. coli</i> BW25113</b>	
	<b>No efflux inhibition</b>	<b>Efflux inhibition (125 <math>\mu\text{g/mL}</math> PA<math>\beta</math>N)</b>	<b>No efflux inhibition</b>	<b>Efflux inhibition (125 <math>\mu\text{g/mL}</math> PA<math>\beta</math>N)</b>
Acriflavine	256	< 2	256	< 2
Ethidium bromide	128	64	128	32
Ciprofloxacin	0.01	< 0.0025	0.01	< 0.0025
Chloramphenicol	2	0.25	1	0.25
Tetracycline	1	0.25	0.5	0.12
Kanamycin	2	2	1	1

### 3.7. Conclusions

In this chapter, *S. Typhimurium* was modified through the chromosomal integration of *lacZ* to create a strain capable of controlling *tac* promoter activity. This insertion was proven to be fitness neutral and did not affect antibiotic susceptibility, biofilm formation, efflux activity, competitive fitness and pathogenicity of *S. Typhimurium*. No difference in susceptibility was found towards eight antibiotics following insertion of *lacZ*. The antibiotics tested had different mechanisms of action and different targets within the cell. Because there was no change in susceptibility, it can be assumed that the chromosomal integration of *lacZ* did not affect any major targets such as cell wall biosynthesis, DNA

replication machinery or protein synthesis machinery. Together, this supports the use of *S. Typhimurium::lacZ* as a proxy for the wild type in experiments investigating biofilm formation and efflux activity in *Salmonella*.

A transposon insertion library of approximately 500,000 mutants was created in this strain for use in TraDIS-*Xpress* experiments. This equates to roughly one insertion every 10 base pairs. Coverage of insertions was good across the genome. The high level of consistency between replicates is common for TraDIS data and reflects a low level of experimental error.

A model was developed to investigate biofilm formation over time, whereby planktonic and biofilm samples could grow alongside each other and be directly comparable. *E. coli* and *S. Typhimurium::lacZ* were grown on glass beads and harvested at intervals over 48 hours to determine the best conditions for investigating biofilm development. From this data, it was decided that the model would be sampled at 12, 24 and 48 hours to investigate biofilm formation over time. The yield of genomic DNA per bead was also investigated and optimised to retrieve as much DNA as possible.

This chapter describes the development of the tools and models necessary for the investigation of biofilm formation and efflux activity in *E. coli* and *S. Typhimurium*. With the construction of a transposon mutant library in *S. Typhimurium* and the development of models to investigate biofilm formation, the next chapters will focus on identifying and characterising the genes involved in biofilm formation over time.

**4. CHAPTER 4: TEMPORALLY  
ESSENTIAL GENES FOR BIOFILM  
FORMATION IN ESCHERICHIA COLI**



#### 4.1. Introduction

Biofilms complete a life cycle where cells aggregate, grow and produce a structured community before dispersing to seed biofilms in new environments. Progression through this life cycle requires controlled temporal and spatial gene expression to maximise fitness at each stage. Most previous studies focusing on identifying the genes and pathways required for biofilm formation in *E. coli* have concentrated on the mature biofilm rather than dissecting events across the life cycle. One study assessed biofilm formation using the Keio collection (Niba et al., 2008), and identified roles for many genes, although analysis was limited to the effect of inactivation of each gene (Aedo et al., 2019). Another study used a transcriptomic approach to identify 243 genes with altered expression in biofilms compared to in suspension over time (Domka et al., 2007). As well as analysing the role of genes within a strain, DNA microarrays have also been used to link the presence of different genes with biofilm capacity amongst large panels of isolates which has helped identify core and mobile genes linked to biofilm formation in *E. coli* (Schembri et al., 2003).

Large scale transposon mutagenesis experiments represent another high-throughput, sensitive whole genome approach to link phenotype to genotype (Puttamreddy et al., 2010, Goh et al., 2017, Nhu et al., 2018). In this chapter, I sought to investigate biofilm formation using TraDIS-*Xpress* to get a more detailed view of important genes than possible in the previous studies described above. DNA was extracted from biofilms formed by the transposon mutant library on glass beads, and for direct comparison was also harvested from the corresponding planktonic cultures from the same well at three time points through the biofilm life cycle. The location and frequency of transposon insertion sites was determined by sequencing and mapped to a reference genome. Differences in insertion frequency between biofilm and planktonic conditions suggested a difference in fitness between conditions for mutants at a site; for example, a gene was considered important for biofilm formation if it contained fewer insertions in biofilm conditions relative to the planktonic control. Predictions made by this approach were then tested in a range of assays which measure different aspects of biofilm formation using defined mutants from the Keio library (Baba et al., 2006), a collection of single knockout mutants in the same parent strain as the transposon mutant library.

This study identified 48 genes that affected the fitness of *E. coli* growing in a biofilm. By investigating the genes important across the biofilm life cycle, I was able to get a dynamic view of the main pathways with roles at different stages of biofilm development. These findings reinforced the importance of adhesion, motility and matrix production in the biofilm, and revealed roles for genes not previously implicated in biofilm formation. This included genes involved in cell division (*zapE* (Marteyn et al., 2014) and *truA* (Tsui et al.,

1991a)), DNA housekeeping (*maoP* (Valens et al., 2016)), and *yigZ* and *ykgJ*, the functions of which have not been elucidated. I identified clear requirements for some pathways at specific points of the biofilm life cycle, furthering our understanding of how biofilms fitness is affected over time.

#### 4.2. Aims

- To use TraDIS-*Xpress* to determine the genes involved in biofilm formation in *E. coli* at different points throughout the biofilm life cycle
- To characterise the roles of these genes at different stages in biofilm development

#### 4.3. TraDIS-*Xpress* Method Validation

Analysis of the TraDIS-*Xpress* data found that the variation in insertion frequency per gene between replicates was very low, indicating low experimental error (figure 4.1). There were 48 genes as candidates that considerably affected biofilm formation over time in *E. coli*: 42 were identified as being beneficial for biofilm fitness and 6 genes were predicted to be detrimental to biofilm fitness (figure 4.2 and Appendix 1). The main pathways that were consistently important in the biofilm through all the time points included type 1 fimbriae, curli biosynthesis and regulation of flagella (figure 4.2). All other loci identified affected biofilm formation at specific points in the life cycle.

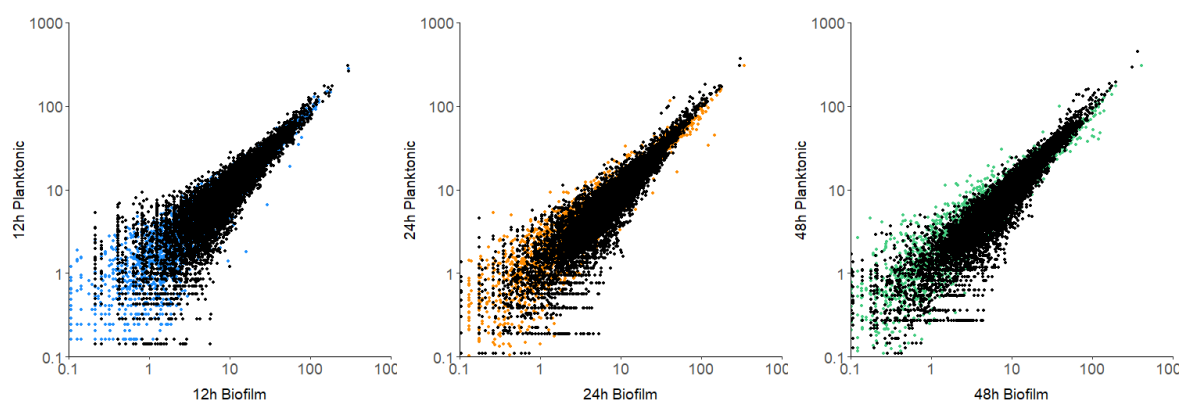


**Figure 4.1:** Mean insertion frequencies per gene in *E. coli* for each time point. Coloured points show mean insertion frequencies per gene in biofilm conditions (x-axis) compared to planktonic conditions (y-axis) for each time point. Black points show insertion frequencies per gene compared between identical replicates and show the experimental error. Replicates with and without promoter induction with IPTG are combined for analysis.

***E. coli***

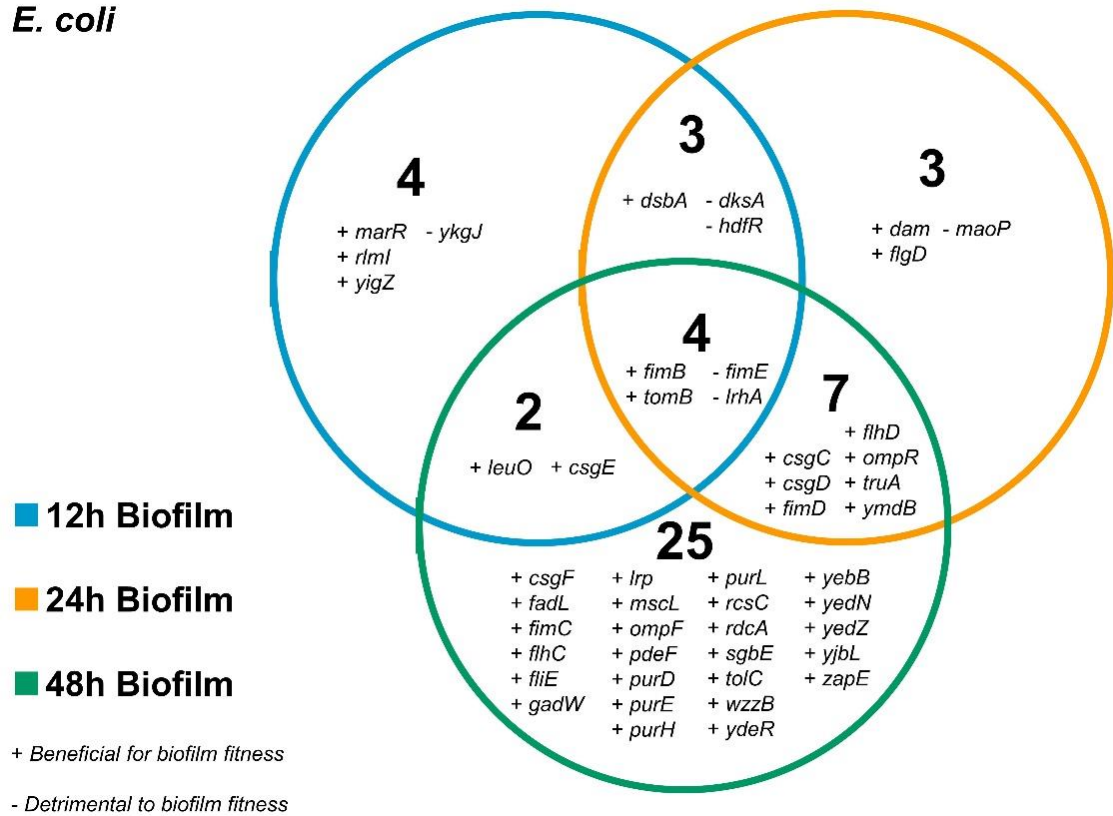


**Figure 4.2:** Genes involved in biofilm formation over time in *E. coli*. Plus symbols (+) indicate genes that were beneficial for, and minus symbols (-) indicate genes that were detrimental to, biofilm fitness.

#### **4.4. Fimbriae expression and motility are important at all stages of biofilm formation**

##### **4.4.1. Type 1 fimbriae regulation**

Only 4 genes were found to be important at all time points (figure 4.2). These included *fimB* and *fimE* involved in control of fimbriae expression, where deletion of *fimB* results in no fimbriated cells in a population, and deletion of *fimE* results in more fimbriated cells in a population relative to wild type culture (McClain et al., 1993). The recombinase gene *fimB* which helps mediate both 'ON-to-OFF' and 'OFF-to-ON' switching of fimbriae expression was beneficial for biofilm formation at all time points. There were fewer insertions within and more insertions upstream of *fimB* in biofilm conditions compared to planktonic conditions at all time points. This suggests that *fimB* expression was beneficial throughout biofilm development (figure 4.3a). In contrast, inactivation of *fimE*, responsible for only 'ON-to-OFF' fimbrial regulation (Klemm, 1986), increased biofilm fitness at all time points. Initially, there were only slightly more *fimE* mutants in biofilm conditions compared to planktonic at 12 hours, but this increased over time with a stark contrast seen between biofilm and planktonic conditions at the 24- and 48-hour time points (figure 4.3a). Biofilm biomass was measured by growing knockout mutants in a 96-well plate for 48 hours and staining the resulting biofilm with crystal violet. Cell aggregation was quantified by measuring the OD of the supernatant of cultures left unagitated for 24 hours. Deletion of *fimE* resulted in reduced biofilm biomass (figure 4.4a), contrary to the TraDIS-*Xpress* prediction, and both  $\Delta fimB$  and  $\Delta fimE$  mutants were deficient in cell aggregation (figure 4.4b). This finding supports previous work that reported the importance of fimbriae expression across all stages of biofilm development (Domka et al., 2007). Together, the TraDIS-*Xpress* and phenotypic data suggest that the ability to regulate fimbriae expression in a phase-dependent manner and the ability to present cells both with and without fimbriae is important for fitness of a biofilm throughout the life cycle.

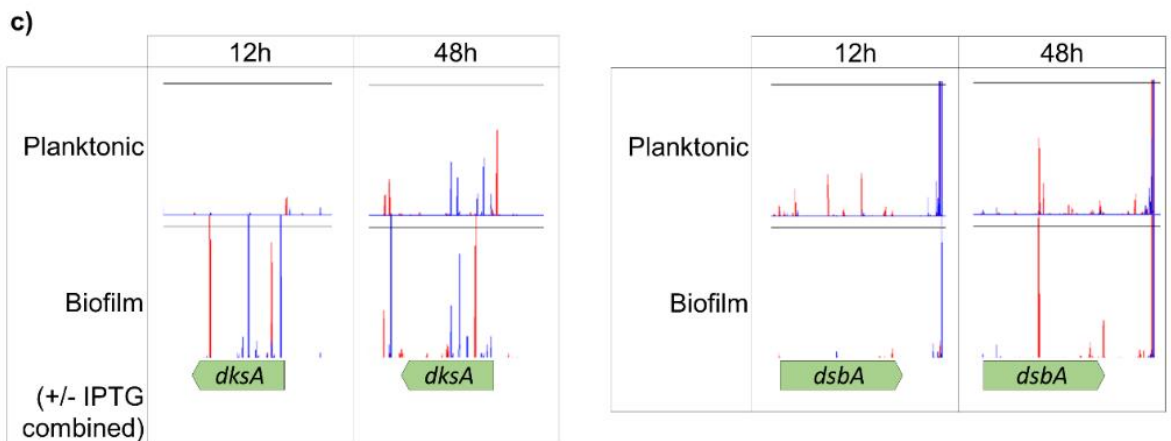
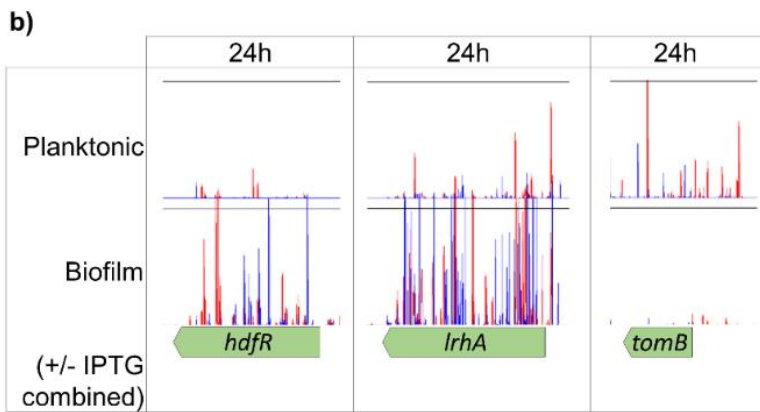
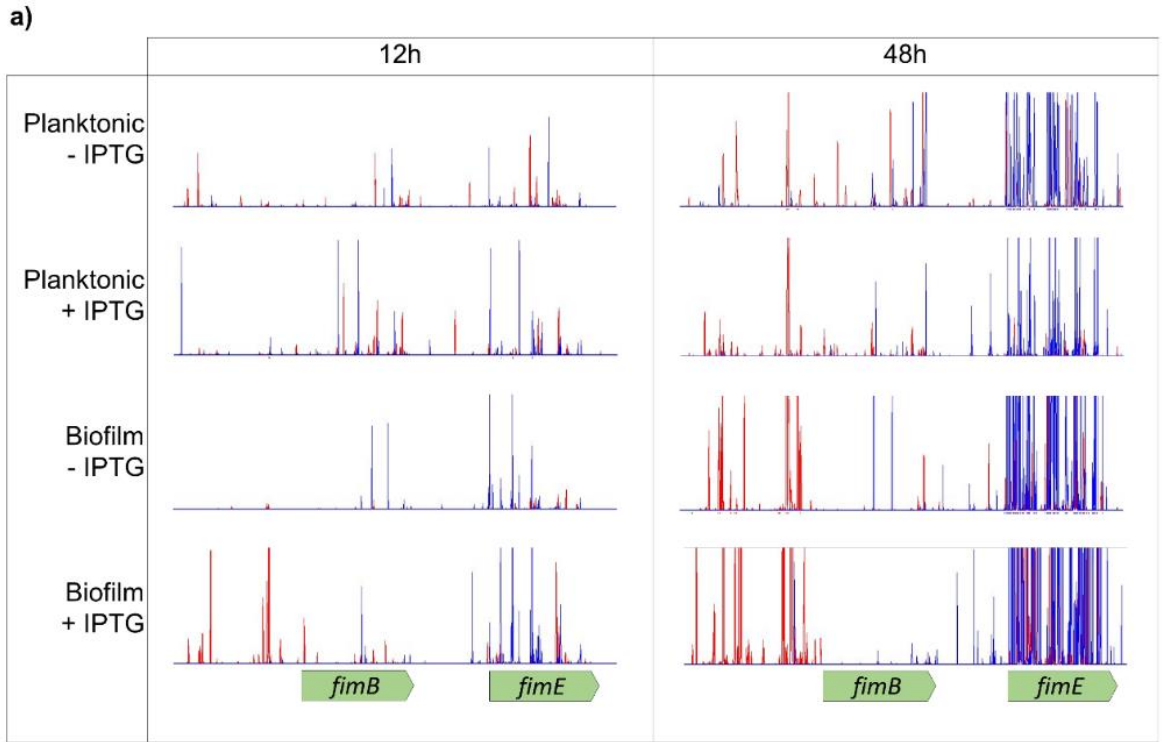
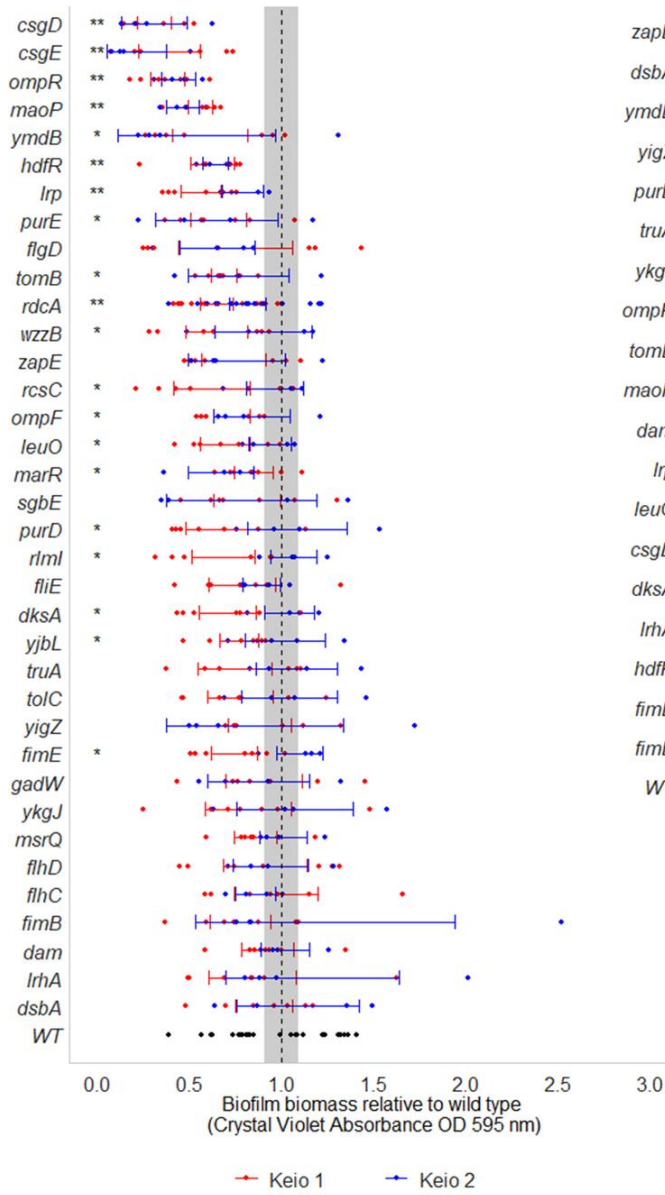
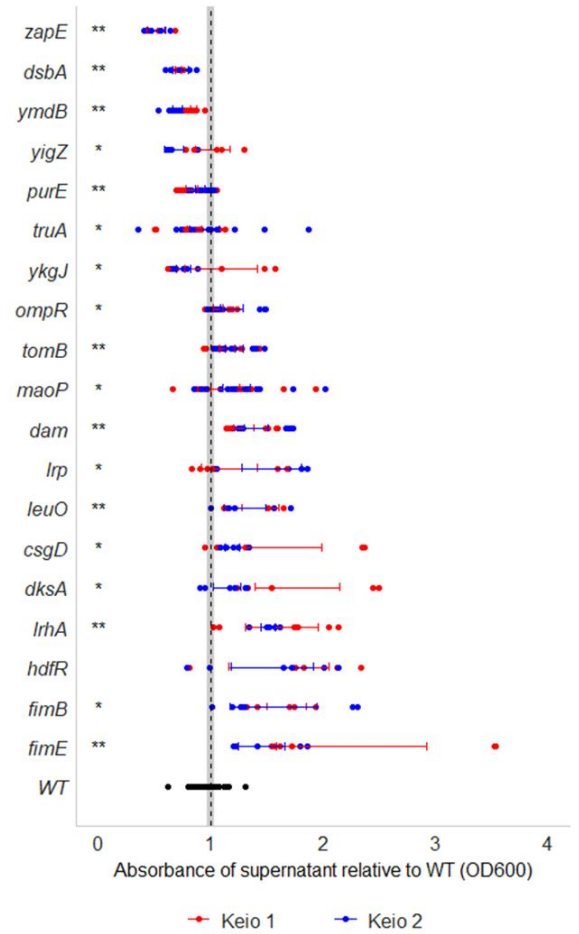


**Figure 4.3:** Transposon insertion sites and frequencies in planktonic and biofilm conditions, mapped to a reference genome and plotted with BioTraDIS in Artemis. The height of the peak can be used as a proxy for the mutant's 'fitness' in the condition. Red peaks indicate where the transposon-located promoter is facing left-to-right, and blue peaks show it facing right-to-left. **a)** Insertion sites in and around *fimB* and *fimE* in planktonic and biofilm conditions after 12- and 48-hours growth with and without promoter induction with IPTG. Leaky promoter expression is most likely responsible for the increased insertions upstream of *fimB* in conditions without IPTG. **b)** Insertion sites in and around *hdfR*, *lrhA* and *tomB* in planktonic and biofilm conditions after 24 hours growth. Conditions with and without IPTG have been combined. **c)** Insertion sites in and around *dksA* and *dsbA* in planktonic and biofilm conditions after 12- and 48-hours growth. Conditions with and without IPTG have been combined. For all plot files, one of two independent replicates is shown and y-axes have been normalised for all.

a)



b)



c)

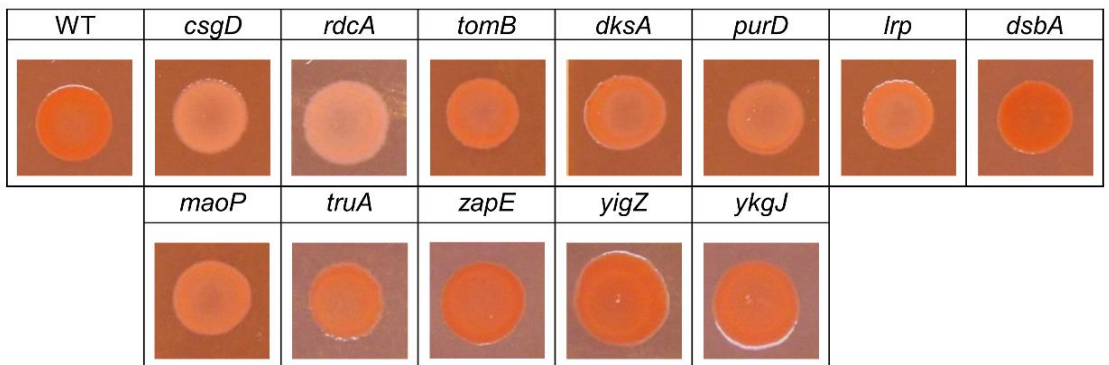


**Figure 4.4:** Phenotypic analysis of selected genes involved in biofilm formation. **a)** Biofilm biomass of single knockout mutants relative to wild type *E. coli*, measured by crystal violet staining. Two biological and a minimum of two technical replicates were performed for each mutant. **b)** Cell aggregation of single knockout mutants relative to wild type *E. coli*, measured by OD<sub>600 nm</sub> of the supernatant of unagitated cultures. Points show the ODs of three independent replicates. For both graphs, red points/bars distinguish between the two Keio collection mutants of each gene. Error bars show 95% confidence intervals, and the shaded area shows the 95% confidence interval of the wild type. Single asterisks (\*) represent a significant difference between one Keio mutant copy and the wild type, and double asterisks (\*\*) denote a significant difference between both Keio mutant copies and the wild type (Welch's *t*-test,  $p < 0.05$ ). **c)** Colonies grown on agar supplemented with Congo red to compare curli biosynthesis between single knockout mutants and the wild type. Images are representative of 2 biological and 2 technical replicates.



#### 4.4.2. Motility regulator *IrhA* and antitoxin *tomB*

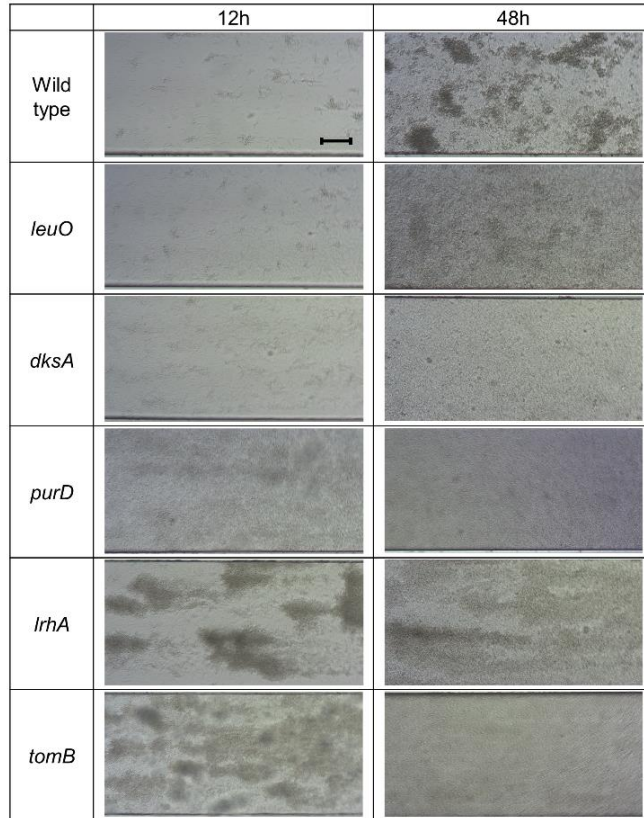
Disruption of *IrhA*, a regulator of motility and chemotaxis (Lehnen et al., 2002), was beneficial for biofilm formation at all time points (figure 4.3b). *IrhA* also has a role in type 1 fimbriae expression through activating expression of *fimE* (Blumer et al., 2005), but in addition represses flagella-mediated motility. Analysis of the  $\Delta IrhA$  biofilm showed initial formation of microcolonies occurred faster than the wild-type (figure 4.5a) but at later time points the biofilms formed by this mutant were less mature than seen with the wild-type. There was no significant change in biomass formed by this mutant (figure 4.4a) and mutants appeared less aggregative than the wild type (figure 4.4b). These data suggest that inactivation of *IrhA* impacts both adhesion and aggregation differently at distinct stages of the biofilm life cycle and may result in a benefit to early surface colonisation but with a cost to later maturation.

Expression of the Hha toxin attenuator *tomB* was also found to be consistently important for biofilm formation at 12, 24 and 48 hours (figure 4.3b). Consistent with this prediction, the  $\Delta tomB$  mutant biofilm had reduced cell aggregation, curli biosynthesis and biofilm biomass (figure 4.4 a,b,c). Studies on the effect of *tomB* on biofilm formation have focused on its toxin-antitoxin relationship with *hha*, which has been found to reduce expression of fimbrial subunit *fimA* and activate prophage lytic genes causing cell death (Garcia-Contreras et al., 2008). Deletion of *hha* was found to reduce motility through *flhDC* and increase curli production through *csgD* (Sharma and Bearson, 2013). TraDIS-*Xpress* showed no obvious benefit to biofilm fitness with insertional inactivation of *hha*, but this may not be visible in our data due to these mutants having a functional copy of *tomB* which would mask impacts from loss of *hha*.

Analysis of biofilms under flow conditions found that  $\Delta IrhA$  and  $\Delta tomB$  mutant biofilms had a similar appearance after 12 hours growth, with microcolonies visible which disappeared over time (figure 4.5a). The similarities in phenotypes could indicate both genes influence biofilms in a similar manner. The role of *IrhA* as a negative regulator of motility has been well documented (Lehnen et al., 2002, Blumer et al., 2005, Li et al., 2019), and expression of *tomB* has been seen to reduce motility through repression of *fliA* (Barrios et al., 2006). Although  $\Delta IrhA$  and  $\Delta tomB$  deletion mutants shared many similar phenotypes, TraDIS-*Xpress* data predicted that *tomB* was beneficial and *IrhA* was detrimental to biofilm formation at 12, 24 and 48 hours. Therefore, these genes may regulate the same pathways but in different ways. Previous studies on  $\Delta IrhA$  mutant biofilms have reported increased adhesion, aggregation and biomass compared to the wild type (Blumer et al., 2005). Although I found decreased aggregation in the  $\Delta IrhA$  mutant after 24 hours (figure 4.4), I also saw increased adhesion, aggregation and flow cell coverage at each time point in  $\Delta IrhA$  mutant biofilms grown under flow conditions relative to the wild type (figure 4.5a).

This supports the findings from the TraDIS-*Xpress* data, showing inactivation of *lrhA* was beneficial for biofilm fitness throughout biofilm development. This may be due to reduced induction of *fimE* by LrhA (Blumer et al., 2005), thereby allowing expression of type 1 fimbriae to facilitate adhesion. I have already described how expression of both *fimB* and *fimE* is necessary for optimal fitness of the mature biofilm, and the effect of *lrhA* on biofilm formation correlates with these findings, with reduced aggregation in  $\Delta lrhA$  biofilms after 24 hours (also seen in *fimB* and *fimE* mutants) and no microcolony formation under flow conditions at 24 and 48 hours. The importance of *lrhA* to biofilm formation clearly appears to be time dependent, with the most important role in early events.

a)



b)

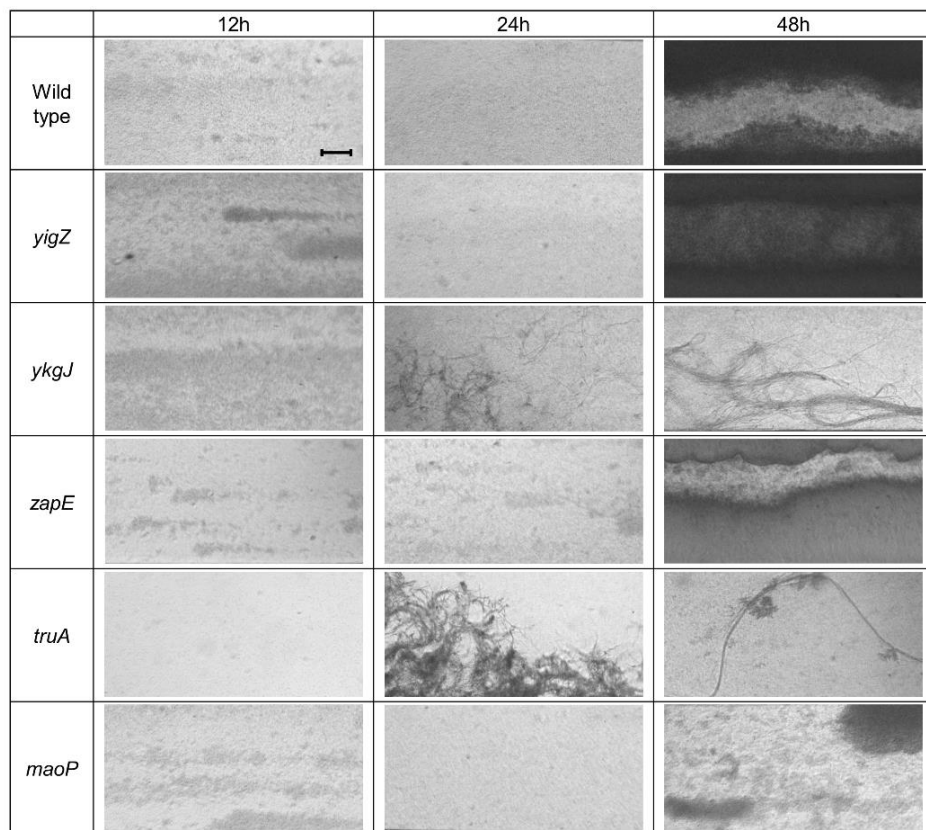


**Figure 4.5:** Biofilm formation of single knockout mutants on glass analysed under flow conditions after 12, 24 and 48 hours growth. **a)** Single knockout mutants selected for their effect on biofilm fitness. **b)** Single knockout mutants of genes not previously described to affect biofilm formation, to the best of our knowledge. 10x Magnification. Images are representative of two independent replicates. Scale bar indicates 10  $\mu$ m.

## 4.5. Regulatory genes are important in the early biofilm

### 4.5.1. Transcriptional factors and transcriptional regulators.

In the early biofilm, after 12 hours growth, only 13 genes were found to distinguish the planktonic and biofilm conditions. Of these, 9 had roles in transcriptional regulation. The TraDIS-*Xpress* data indicated that inactivation of transcriptional factor *dksA* promoted biofilm formation at the 12- and 24-hour time points but not in the mature biofilm (figure 4.3c). Supporting this, analysis of  $\Delta dksA$  mutant biofilms under flow conditions showed an initial benefit with increased adhesion at both the 12- and 24-hour time points, but reduced microcolony formation at the 48 hour time point, suggesting *dksA* affects biofilm initiation (figure 4.5a). Inactivation of  $\Delta dksA$  was also seen to reduce cell aggregation, curli biosynthesis and biofilm biomass (figure 4.4 a,b,c). The effect of *dksA* expression on biofilm formation has been extensively studied and it is known that the deletion of *dksA* increases fimbriae-dependent adhesion, but reduces motility (Magnusson et al., 2007) and curli production (Nhu et al., 2018, Smith et al., 2017, Hengge, 2020). This demonstrates the importance of controlled gene expression at different stages of the biofilm life cycle to optimise biofilm fitness.

In addition, the stress response regulator *marR* (Aleksun and Levy, 1999a) and the 23S rRNA methyltransferase *rmlI* (Herzberg et al., 2006) were both found to be beneficial for biofilm fitness at the 12 hour time point only, and reduced biofilm biomass was found in the corresponding deletion mutants (figure 4.4a). These genes have both previously been implicated in biofilm formation (Holden and Webber, 2020, Kettles et al., 2019, Herzberg et al., 2006), but the effect on early biofilm formation has not been described previously. Expression of *hdfR*, a negative regulator of motility (Ko and Park, 2000), was found to be detrimental to biofilm fitness in the early biofilm after 12- and 24-hours growth (figure 4.3b), and  $\Delta hdfR$  mutant biofilms had significantly reduced biomass (figure 4.4a).

### 4.5.2. Genes of unknown function

Two genes of unknown function, *yigZ* and *ykgJ* were found to affect biofilm formation at 12 hours. Fewer mutants were observed in *yigZ* in biofilm conditions relative to planktonic at 12 hours, indicating its importance in early biofilm formation. Reduced expression of *ykgJ* was beneficial for biofilm formation, with more transposon insertions in an antisense orientation to *ykgJ* present in biofilm conditions relative to planktonic. Although there were no differences seen between the wild type and *ykgJ* in biofilms grown under flow conditions for 12 hours, differences became apparent at the 24- and 48-hour time points, where the *ykgJ* mutant was significantly more filamented, which may suggest a role for *ykgJ* in cell division. For both *yigZ* and *ykgJ*, one mutant copy showed slightly increased aggregation relative to the wild type (figure 4.4b), but there were no differences observed in biofilm biomass, curli biosynthesis or adhesion (figures 4.4 a,c and figure 4.5b). YigZ is

a widely conserved protein, with homologues found in archaea and mammals, (Park et al., 2004) and YkgJ is predicted to be a ferredoxin, but further investigation into both of these genes is necessary to properly characterise their functions.

#### **4.6. Biofilms sampled after 24 hours demonstrate both adhesion and matrix production are important**

##### **4.6.1. DNA Housekeeping**

Two genes involved in DNA housekeeping were found to be involved in biofilm development after 24-hours growth. This included *dam*, encoding DNA methyltransferase (Szyf et al., 1984), insertional activation of which was not tolerated in the 24-hour biofilm, with  $\Delta dam$  mutants defective in aggregation compared to the wild type (figure 4.4b). Also, inactivation of *maoP*, involved in Ori macrodomain organisation (Valens et al., 2016), was predicted to confer a fitness advantage in the 24-hour biofilm compared to the planktonic condition. TraDIS-*Xpress* data showed more reads mapped to *maoP* in the biofilm conditions compared to the planktonic at 24 hours suggesting loss of this gene was beneficial. Phenotypic analysis of the  $\Delta maoP$  mutant biofilm did demonstrate a phenotype although in opposition to the prediction, *maoP* mutants were significantly deficient in biofilm biomass production, curli biosynthesis and one mutant displayed reduced aggregation (figure 4.4 a,c). After 48 hours growth under flow conditions, the  $\Delta maoP$  mutant biofilm was considerably less dense than the wild type (figure 4.5b). A homolog to *maoP* in *Yersinia pestis* was identified as having a role in adhesion and may positively regulate adhesin expression (Eichelberger et al., 2020). It is unclear why the defined mutants made less biofilm than the wild type when TraDIS-*Xpress* predicted expression of *maoP* was detrimental to biofilm formation. Chromosomal organisation of the Ori macrodomain requires both *maoP* and *maoS* (Valens et al., 2016) and it may be that deletion of *maoP* affects the interplay between these two genes. Further investigation into how chromosomal macrodomain organisation affects biofilm formation is warranted.

##### **4.6.2. Curli biosynthesis and regulation**

Curli biosynthesis became important by the 24 hour time point as no insertions mapped to *csgC*, encoding a curli subunit chaperone (Evans et al., 2015) and more transposon insertions mapped upstream of the curli biosynthesis regulator *csgD* (Barnhart and Chapman, 2006), predicting its increased expression benefitted biofilm formation. At the 48 hour time point, both genes were essential for biofilm formation, which was also the case for the known *csgD* regulator, *ompR* (Jubelin et al., 2005), supported by significantly reduced biofilm biomass and reduced aggregation in knockout mutants (figure 4.4 a,b).

There were fewer insertions detected within *dsbA* (encoding disulphide oxidoreductase (Lee et al., 2008)) in biofilms grown for 12- and 24-hours relative to planktonic culture (figure 4.3c). The role of *dsbA* in adhesion to abiotic surfaces and epithelial cells has previously been suggested (Lee et al., 2008, Bringer et al., 2007). Phenotypic validation of the  $\Delta dsbA$  mutant showed a red, dry and rough (*rdar*) phenotype on Congo red plates (figure 4.4c), indicative of increased curli biosynthesis. Cell aggregation in the  $\Delta dsbA$  mutant was significantly higher compared to the wild type, implying a role of *dsbA* in inhibiting cell-cell aggregation. This data showed that *dsbA* is important in the early biofilm, but its deletion appears to be beneficial to the formation of a mature biofilm, according to the Congo red and aggregation data. Expression of *dsbA* has been previously found to result in repression of the curli regulator *csgD* and curli subunit *csgA*, essential for optimal fitness of the mature biofilm (Anwar et al., 2014).

Various genes were expected to be identified by the model to confirm its efficacy, such as genes involved in curli biosynthesis, however there were some genes that were not detected by TraDIS-*Xpress* that are known to affect biofilm formation. Although many genes involved in curli biosynthesis were identified by our model, the gene encoding the main curli subunit, *csgA*, was not detected. This may be because TraDIS-*Xpress* experiments use a mutant library pool, where *CsgA* produced by the surrounding population is able to complement the  $\Delta csgA$  mutants (Hammar et al., 1996). Although this may be a potential limitation for studying a gene's role in biofilm formation, it is more representative of intercellular interactions in a non-clonal multispecies biofilm found outside the laboratory

#### **4.7. The mature biofilm grown for 48 hours requires purine biosynthesis, matrix production, motility and solute transport**

##### **4.7.1. Purine biosynthesis**

There were 38 genes found to be important for fitness of the mature biofilm after 48 hours growth, and 25 of these genes were identified as essential at this time point only. The major pathway implicated in biofilm formation at 48 hours was purine ribonucleotide biosynthesis, with four genes, *purD*, *purH*, *purL* and *purE* (Zhang et al., 2008b), found to be essential at this time point only. TraDIS-*Xpress* did not identify mutants in any of these genes in biofilms sampled at 48 hours, whereas several reads mapped to these loci under planktonic conditions, as well as under both biofilm and planktonic conditions earlier at 12 and 24 hours. Visualisation of a  $\Delta purD$  mutant biofilm under flow conditions saw poor biofilm formation and no microcolony formation at any time compared to the wild type (figure 4.5a). Additionally,  $\Delta purD$  and  $\Delta purE$  mutants were deficient in biofilm biomass production, curli biosynthesis, and  $\Delta purE$  also showed increased cell aggregation (figure

4.4 a,b,c), confirming an important role for purine biosynthesis in matrix production and curli biosynthesis in the mature biofilm.

Similar findings have previously been described in another transposon mutagenesis experiment in uropathogenic *E. coli* (Nhu et al., 2018). Inactivation of purine biosynthetic genes was also found to impair biofilm formation in *Bacillus cereus*, but this was thought to be due to reduced extracellular DNA in the biofilm matrix (Vilain et al., 2009). Extracellular DNA is thought to aid adhesion and has been found to be important in the biofilms of a wide range of bacterial species (Whitchurch et al., 2002, Tetz et al., 2009). These data suggest that purine biosynthesis is important in the mature biofilm rather than initial adhesion. A relationship between both purine and pyrimidine biosynthesis and biofilm matrix production has been reported, where their inactivation reduces curli biosynthesis (Nhu et al., 2018, Smith et al., 2017, Garavaglia et al., 2012). More recently, curli biosynthesis in a *purL* mutant was reported to be abrogated through addition of inosine, which is involved in the *de novo* purine biosynthetic pathway for production of adenosine monophosphate (AMP) and guanine monophosphate (GMP) (Cepas et al., 2020). This suggests that nucleotide production itself, rather than the regulatory effects of the genes involved, affects curli biosynthesis, supporting one hypothesis that disruption of the purine biosynthetic pathway may directly result in a reduction of cyclic-di-GMP. Additionally, two genes involved in c-di-GMP biosynthesis, *rcdA* and *pdeF* (Pfiffer et al., 2019), were identified to be important for biofilm formation at 48 hours. The effects of c-di-GMP on biofilm biomass production and curli biosynthesis have been thoroughly described (Nhu et al., 2018, Pfiffer et al., 2019). Quantification of intracellular c-di-GMP or further investigation of other c-di-GMP-dependent pathways in these mutants would uncover the relationship between these pathways and biofilm formation.

#### **4.7.2. Flagella**

The flagella master regulatory system *flhDC* was identified as important in the mature biofilm. Biofilms sampled after 48 hours saw fewer *flhC* mutants, while insertions interpreted as over-expressing *flhD* increased in numbers both at the 24- and 48-hour time points, compared to planktonic conditions. No mutants in *flgD* and *fliE*, encoding flagellar filament proteins, were identified at 24 and 48 hours, respectively. It has previously been shown that motility is important for initial biofilm formation (Pratt and Kolter, 1998, Wang et al., 2020), but this may not relate to biomass formation where no differences were seen for  $\Delta flhD$ ,  $\Delta flhC$ ,  $\Delta fliE$  and  $\Delta flgD$  mutants. Previous work has suggested that flagella filaments are important for initial attachment and adhesion (Wood et al., 2006) and the expression of flagella is important at all stages of the developing biofilm (Domka et al., 2007). I did not find this to be true, with the expression of flagella filaments only appearing to increase biofilm fitness in the mature biofilm grown for 48

hours, although I found that motility regulators *hdfR* and *lrhA* affected the fitness of the early biofilm. The relationship between motility and biofilm formation is complex. Although it is widely understood that motility is crucial for biofilm formation (Pratt and Kolter, 1998, Wang et al., 2020), there is also an inverse relationship between motility and expression of matrix components: when biofilm matrix production is induced, motility is repressed in a motile-to-sessile lifestyle transition (Pesavento et al., 2008, Fang and Gomelsky, 2010, Hengge, 2020). It appears that maintaining the ability to flexibly regulate production of flagella and motility, rather than their fixed expression or absence, is important for optimal biofilm fitness throughout biofilm development.

#### **4.7.3. Transcriptional regulators**

Various pleiotropic transcriptional regulators were also important in the mature biofilm. This included the H-NS antagonist *LeuO* (Shimada et al., 2011). Increased insertions upstream of *leuO* under biofilm conditions after 12 hours growth, as well as no *leuO* mutants in 48-hour biofilms, indicated it was beneficial to biofilm formation. A  $\Delta leuO$  mutant did not aggregate as well as the wild type, and one  $\Delta leuO$  mutant had reduced biofilm biomass (figure 4.4 a,b). The  $\Delta leuO$  mutant biofilm under flow conditions demonstrated an inability to form microcolonies after 48 hours growth (figure 4.5a). The leucine-responsive global regulator *lrp* (Kroner et al., 2019) and a transcriptional regulator responsible for survival under acid stress, *gadW* (Tramonti et al., 2008) were also found to have fewer mutants in the 48 hour biofilm compared to the planktonic condition, indicating their importance in the mature biofilm. Reduced biofilm biomass, aggregation and curli biosynthesis were observed for one copy of  $\Delta lrp$ , but no differences in biofilm formation or aggregation were seen for  $\Delta gadW$  mutant biofilms (figure 4.4 a,b,c).

#### **4.7.4. Transmembrane transport**

Inactivation of the outer membrane channels *mscL* (Sukharev et al., 1994), *toIC* (Morona et al., 1983) and *ompF* (Cai and Inouye, 2002) was not tolerated in the mature biofilm grown for 48 hours. This would indicate the importance of transport in the mature biofilm, however inactivation of *toIC* and *ompF* did not result in a change in biofilm biomass (figure 4.4a). Disruption of *toIC* has previously been found to reduce curli biosynthesis through transcriptional repression of *csgD* and *csgB*, however the mechanism behind this is unknown (Baugh et al., 2012).

#### **4.7.5. Cell division**

Two genes involved in cell division, *zapE* (Marteyn et al., 2014) and *truA* (Tsui et al., 1991a), were identified as important in the 48 hour biofilm. No mutants were seen in *zapE* in biofilms grown for 48 hours, suggesting its essentiality for biofilm formation at this stage. The  $\Delta zapE$  mutant had higher aggregation (figure 4.4 a,b,c) and considerably



reduced adhesion after 12 hours growth under flow conditions, relative to the wild type (figure 4.5b). The pseudouridine synthase *truA* (Hamma and Ferré-D'Amaré, 2006) was found to be essential in the mature biofilm grown for 24 and 48 hours. When grown under flow conditions, the  $\Delta truA$  mutant cells were extremely filamented in biofilms (figure 4.5b). Both *zapE* and *truA* have not before been implicated in biofilm formation. ZapE has been found to be required for growth under low oxygen conditions (Marteyn et al., 2014), which may explain why its expression was beneficial for the fitness of biofilms formed on beads submerged in growth media. Deletion of *truA* has previously been reported to result in filament formation and reduced cell division (Tsui et al., 1991a), and increased expression of *truA* was seen to benefit intracellular survival and survival under oxidative stress conditions (Yang et al., 2019). Filamentation has previously been suggested to provide a competitive advantage in adhesion and early biofilm formation, but filamented cells were outcompeted as the biofilm matured (Wucher et al., 2019). Our data suggests that temporal regulation of filamentation is important for optimal biofilm fitness over time, where filamentation may benefit biofilm initiation but reduce fitness as it matures.

#### **4.8. Conclusions**

In this chapter, I have characterised the essential genome of *E. coli* biofilms across the biofilm lifecycle by using the high throughput transposon mutagenesis screen TraDIS-*Xpress* (figure 4.6). The identification of genes and pathways already described to be involved in biofilm formation validates the efficacy of this experimental model. The early biofilm established 12 hours after inoculation was characterised by genes involved in adhesion. The 24-hour biofilm required both adhesion and matrix production, and after 48 hours genes involved in matrix production, cell division and purine biosynthesis were beneficial to biofilm fitness. In concordance with previous work identifying genes whose importance varies with time in the *E. coli* biofilm, I also found that control of fimbriae expression and motility remained important at each stage of the biofilm life cycle rather than just being involved in initial attachment (Domka et al., 2007).

As well as identifying how the presence or absence of genes affected biofilm formation, TraDIS-*Xpress* can determine how increased or reduced gene expression affects biofilm fitness. This could not be done with traditional transposon mutagenesis and provides a further depth to our understanding of how gene expression affects biofilm formation. TraDIS-*Xpress* was also able to identify genes not previously reported to be involved in biofilm formation, to our knowledge, including *yigZ*, *ykgJ*, *zapE*, *maoP* and *truA*.

Expression of *dsbA* and repression of *dksA* was found in this study to benefit early biofilm fitness. Based on previous studies and phenotypic analysis of knockout mutants in this

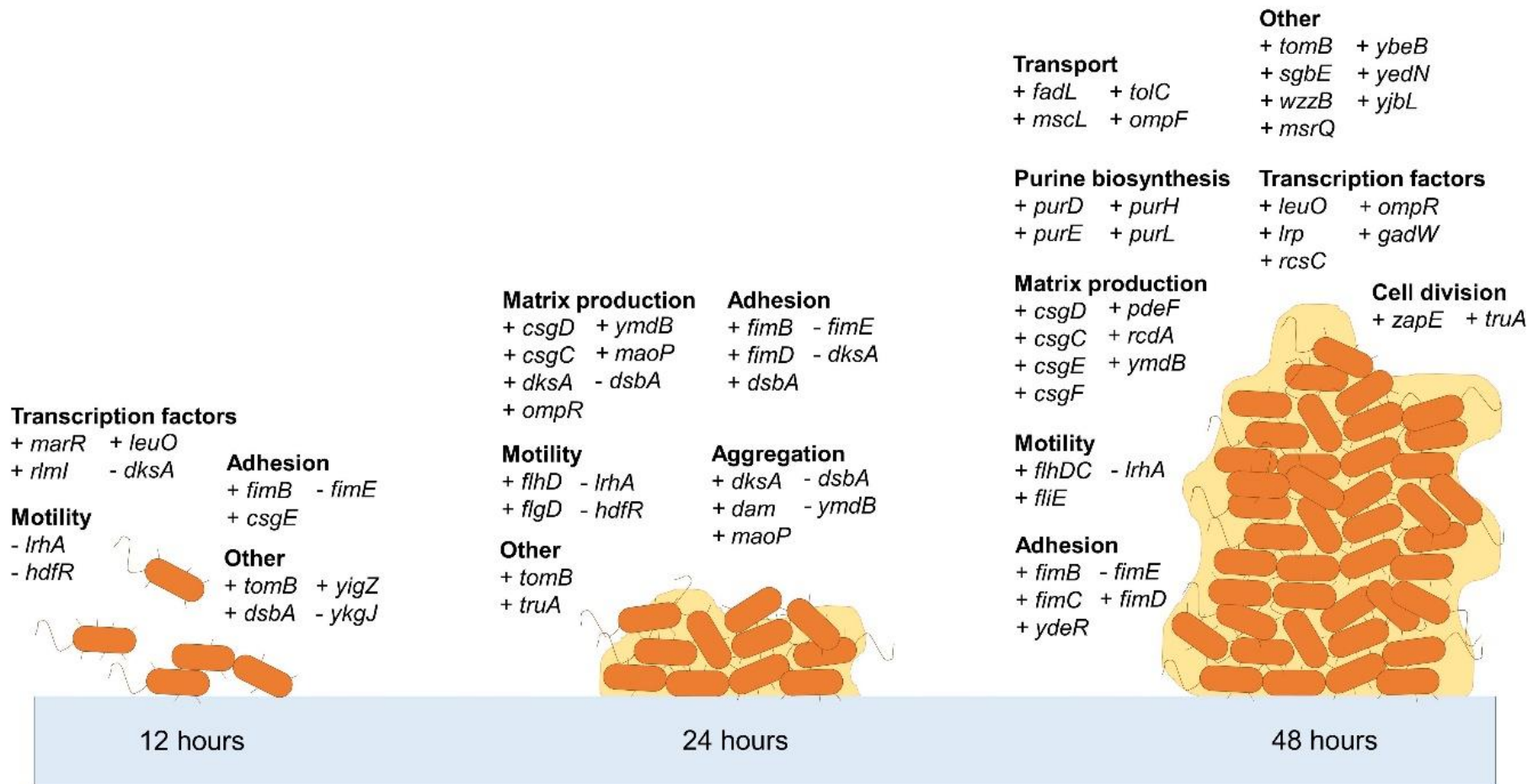
study, the increase in biofilm fitness seen may be due to increased adhesion in these mutants (Bringer et al., 2007, Magnusson et al., 2007). This study has highlighted the benefit of close temporal gene regulation in the biofilm, where the expression of certain genes can have a different effect on biofilm fitness at different stages of the biofilm life cycle. Deletion of *dsbA* was detrimental to the early biofilm, but increased curli expression and increased aggregation at the later time points. Conversely, the transcription factor *dksA* was detrimental in the early biofilm, whilst a *dksA* knockout biofilm had reduced biofilm biomass, reduced curli biosynthesis and reduced aggregation. These data show differential expression of important genes at different stages of the biofilm life cycle is essential for optimising biofilm fitness.

Previous genome-wide screens on *E. coli* biofilm formation have identified some of the same genes as this study (Nhu et al., 2018, Puttamreddy et al., 2010, Niba et al., 2008). The TraDIS-*Xpress* technology used here differentiates this work from other studies as I was able to predict the effect of changes in gene expression and gene essentiality over time. It identified that increased expression of 3 genes and reduced expression of 1 gene was beneficial for biofilm fitness. Differences between this work and previous studies may reflect biofilms being grown under different conditions on different surfaces, as these environmental factors greatly affect the pattern of gene expression and gene essentiality in the biofilm (Prouty and Gunn, 2003). To partially address this, both batch culture and continuous culture biofilm assays were used to better assess gene essentiality during biofilm formation. Biofilms grown in batch culture are affected by oxygen and nutrient starvation more than those grown with a continuous flow of fresh media, therefore the two methods can result in the same culture producing two very different biofilms responding to different environmental stimuli. In this chapter, the mutant library was grown on glass beads in batch culture, and future work could compare this to the same library grown on glass under continuous culture to determine similarities and differences in gene expression and essentiality between each condition.

Validation of the TraDIS-*Xpress* data was carried out using whole gene knockout mutants from the Keio collection, which differ from transposon insertion mutants. With an insertion an average every 6 base pairs, TraDIS-*Xpress* gives a more in-depth analysis of exactly which regions of the genes in question are important for a given phenotype (Yasir et al., 2020). TraDIS-*Xpress* experiments involve competition of each mutant against the rest of the pool, and this is very sensitive to changes in fitness. Whilst we chose a set of important biofilm-associated phenotypes for validation of our candidate genes using defined mutants, these are inevitably somewhat crude and cannot replicate the competition happening within the biofilms in the main experiments. Problems with the construction of the Keio collection have resulted in not all of the deletions being correct,

thereby complicating our phenotypic analysis (Aedo et al., 2019). It is likely we failed to identify the basis for a phenotypic impact of some of our candidate mutants in our limited validation conditions with whole gene inactivation mutants.

This chapter has revealed important time-specific roles for known and identified novel genes with roles in biofilm formation in *E. coli*. It has revealed that some pathways have a more important role in the mature biofilm than previously appreciated and identifies genes with time dependent conditional essentiality within the biofilm. It also describes potential new candidate genes essential for biofilm formation, which could be targeted for novel anti-biofilm therapies. Further work using high-density transposon mutant libraries in different bacterial species to highlight similarities and differences is likely to further our understanding of biofilm biology.



+ Beneficial for biofilm fitness

- Detrimental to biofilm fitness

**Figure 4.6:** Summary of genes important for biofilm formation by *E. coli* at different stages of development.

**5. CHAPTER 5: COMPARISON OF THE  
GENETIC BASIS OF BIOFILM  
FORMATION BETWEEN *SALMONELLA*  
*TYPHIMURIUM* AND *ESCHERICHIA*  
*COLI***

## 5.1. Introduction

*S. enterica* and *E. coli* are closely related, having diverged approximately 140 million years ago (Wirth et al., 2006), and share similarities in the biofilms formed as part of their life cycles. In 2018, *Salmonella* spp. and *E. coli* were among the causative agents behind the most commonly reported human zoonoses in the EU (EFSA and ECDC, 2019).

*Salmonella* biofilms have been found to form on abiotic surfaces in food processing environments, including slaughterhouses, kitchens, factories and animal feed processing environments (Steenackers et al., 2012, Vestby et al., 2009). Strains of *E. coli* found in sheep and cattle farming environments were found to form biofilms in a range of environments to facilitate their colonisation and persistence. There is a great need to further our understanding of biofilm formation in *Salmonella* spp. and *E. coli*, paving the way for the development of new methods to prevent biofilm contamination in food and agricultural industries. Although the two species are closely related, there are significant differences between them and comparison of the genes involved in biofilm formation in the two species will reveal core genes important in both, as well as species-specific differences. In this chapter, I used transposon mutagenesis experiments to investigate biofilm formation through time in *S. Typhimurium*, using the same approach as in the previous chapter with *E. coli*. These two experiments were designed to be directly comparable to highlight the similarities and differences in biofilm formation and fitness over time between the two species.

## 5.2. Aims

- To use TraDIS-*Xpress* to determine the genes involved in biofilm formation in *S. Typhimurium* at different points throughout the biofilm life cycle
- To highlight the similarities and differences in the genes and pathways involved in biofilm fitness between *S. Typhimurium* and *E. coli* over time
- To characterise the roles of these genes in *S. Typhimurium* at different stages of biofilm development

### 5.3. Fimbriae regulation and biosynthesis of flagella, nucleotides, curli and LPS are involved in biofilm formation in both *S. Typhimurium* and *E. coli*

Analysis of the TraDIS-*Xpress* data found 79 genes implicated in biofilm formation in *S. Typhimurium* (Appendix 1). The variation of insertion frequencies per gene between replicates was low for the *S. Typhimurium* TraDIS-*Xpress* data (figure 5.1), similar to the same experiment in *E. coli* in the previous chapter. This indicates a high degree of similarity between each replicate and suggests differences between the planktonic and biofilm conditions are less likely due to chance. Similar to the findings for *E. coli*, the pathways important for biofilm formation change over time as the biofilm develops. In *S. Typhimurium* biofilms after 12 hours growth, genes involved in adhesion, fimbriae expression, cellulose biosynthesis and amino acid biosynthesis were beneficial to biofilm fitness. As the biofilm matured, pathways such as protease activity, flagella biosynthesis, cAMP biosynthesis, the electron transport chain, purine biosynthesis, LPS biosynthesis, as well as various stress response transcriptional regulators and transcription factors affected the fitness of biofilms grown for 24 hours. After 48 hours growth, genes involved in biofilm matrix biosynthesis, fimbriae expression, flagella biosynthesis, respiration, transmembrane transport, LPS biosynthesis and ribosomal modification were beneficial to mature biofilm fitness in *S. Typhimurium* (figure 5.2a).

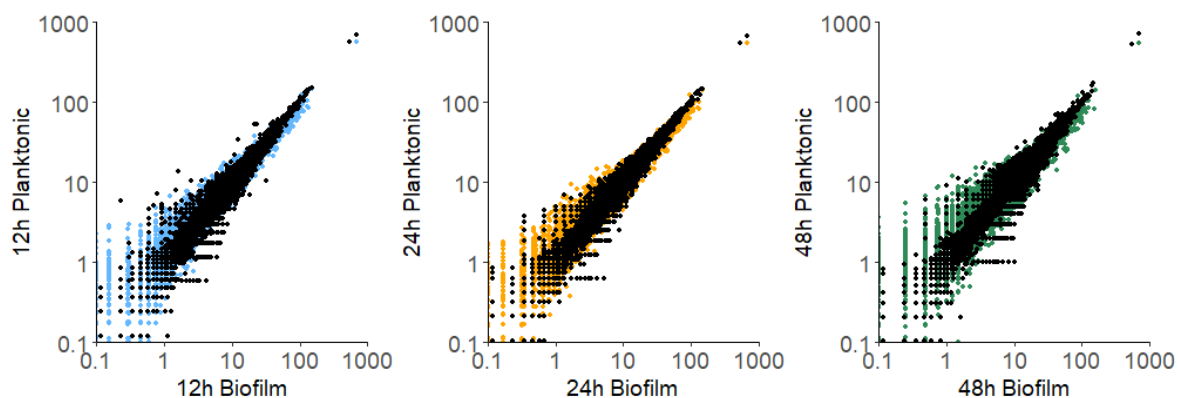


**Figure 5.1:** Mean insertion frequencies per gene in *S. Typhimurium* for each time point. Coloured points show mean insertion frequencies per gene in biofilm conditions (x-axis) compared to planktonic conditions (y-axis) for each time point. Black points show insertion frequencies per gene compared between identical replicates and show the experimental error. Replicates with and without promoter induction with IPTG are combined for analysis.

Pathways identified in both *E. coli* and *S. Typhimurium* biofilm formation include type I fimbriae regulation, flagella biosynthesis, purine biosynthesis, curli production, LPS biosynthesis, sugar utilisation, transmembrane transport and various similar transcriptional regulators (figure 5.2b).

Three genes were identified in both species at the same time points: these were *csgD*, *tolC* and *dsbA*. The curli biosynthesis regulator *csgD* was beneficial to biofilm formation in both species at 48 hours, but in *S. Typhimurium* the TraDIS-*Xpress* data showed more mutants upstream of *csgD*, indicating a fitness benefit to its overexpression, in the biofilm condition relative to the planktonic after 12 hours growth. This difference between *E. coli* and *S. Typhimurium* may be due to *csgD*-induced cellulose production (Römling et al., 2000) conferring a fitness benefit to the early *S. Typhimurium* biofilm, which is absent in *E. coli* K-12 due to disruption of the cellulose biosynthetic machinery (Serra et al., 2013). There were fewer insertions within *tolC* in biofilm conditions relative to planktonic after 48-hours growth in both species. Deletion of *tolC* has previously been shown to result in transcriptional repression of curli biosynthesis and loss of biofilm fitness (Baugh et al., 2014).

Insertional inactivation of *dsbA*, encoding a disulphide oxidoreductase (Lee et al., 2008), affected the fitness of both *E. coli* and *S. Typhimurium* biofilms after 12 hours growth, but in different ways. There were more insertions in *dsbA* in *S. Typhimurium* biofilm conditions at 12 hours, and fewer insertions in *E. coli* biofilms at 12 and 24 hours, relative to their planktonic conditions. In the previous chapter, it was suggested that in *E. coli*, *dsbA* had a positive effect on adhesion in the early biofilm and a detrimental effect on curli biosynthesis in the late biofilm. It seems that for *S. Typhimurium*, any fitness benefit to adhesion provided by *dsbA* does not outweigh the cost to curli biosynthesis or matrix production. Deletion of *dsbA* in *S. Typhimurium* resulted in increased curli biosynthesis, similar to that which was seen in *E. coli*, and additionally increased cellulose biosynthesis was seen compared to the wild type (figure 5.3b). It is possible that deletion of *dsbA* affects *csgD* in *S. Typhimurium*, but this hypothesis warrants further investigation.



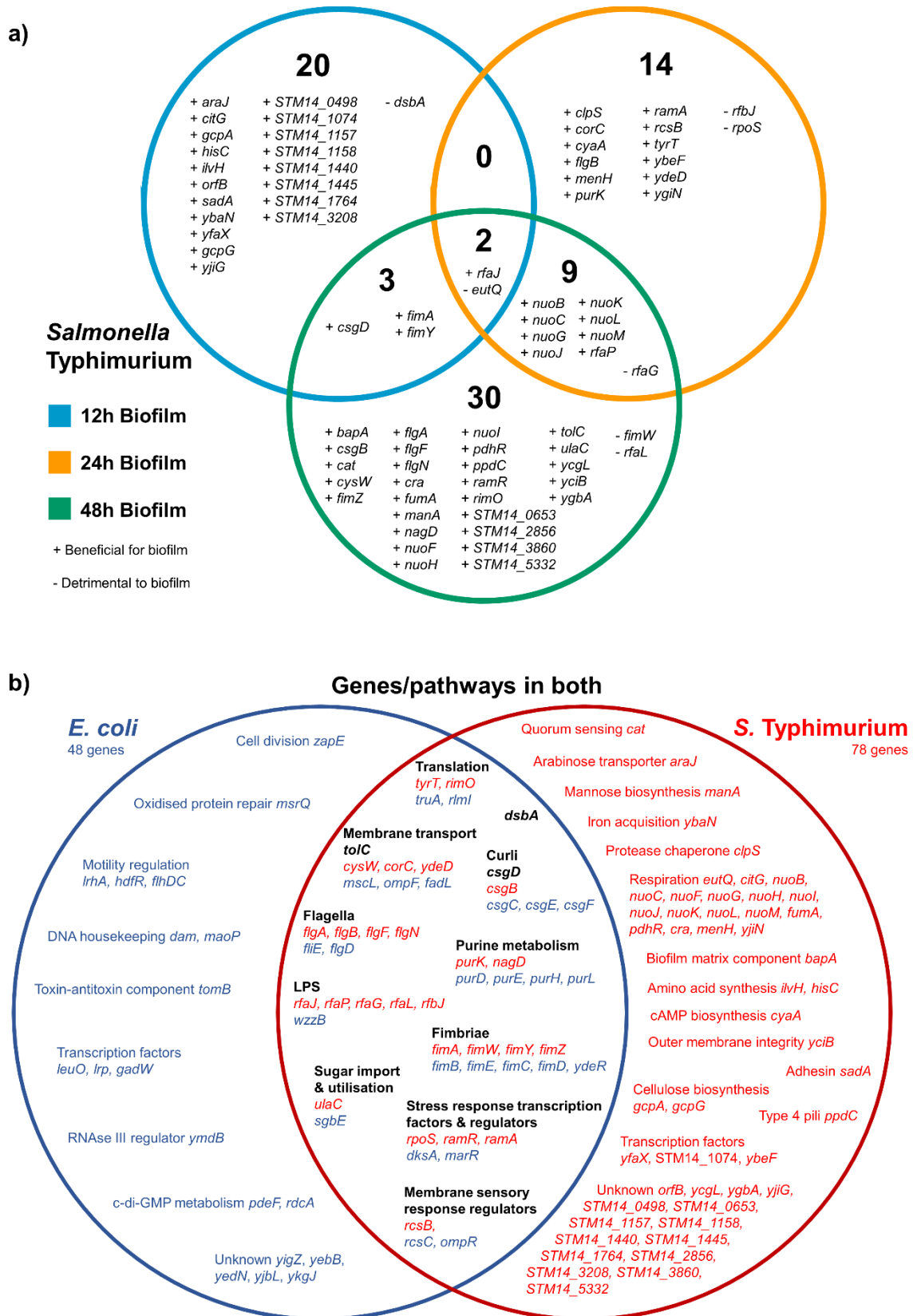


**Figure 5.2:** Genes involved in biofilm formation over time in *S. Typhimurium*. **a)** Genes identified by TraDIS-Xpress to affect biofilm fitness in *S. Typhimurium* after 12-, 24- and 48-hours growth, relative to the planktonic conditions at each time point. Plus signs (+) indicate a gene's benefit to biofilm fitness and minus signs (-) indicate its detrimental effect on biofilm fitness. **b)** Pathways and genes that affect biofilm fitness in *E. coli* and *S. Typhimurium*.

### 5.3.1. Biofilm matrix

Genes involved in curli biosynthesis and regulation were beneficial to biofilm formation in both species. Various genes identified here are known to affect curli biosynthesis through *csgD*. Increased expression of the adenylate cyclase *cyaA* (Roy and Danchin, 1982) was beneficial to biofilm development, with more insertions seen upstream of this gene in biofilm conditions grown for 24 hours relative to planktonic culture. Deletion of *cyaA* resulted in significantly reduced biofilm biomass and slightly reduced curli biosynthesis relative to the wild type (figure 5.3 a,b). cAMP is a secondary messenger molecule produced by *cyaA* that has been described to positively regulate *csgD* transcription (Hufnagel et al 2016), suggesting cAMP biosynthesis is beneficial to biofilm fitness through regulation of matrix production.

In biofilms grown for 48 hours, expression of *manA*, involved in the synthesis of polysaccharide GDP-mannose, was beneficial compared to planktonic cultures. In *Salmonella*, mannose is involved in the biosynthesis of LPS and colanic acid, both extracellular polysaccharides in the biofilm matrix (Li et al., 2017). Inactivation of *manA* in *Photobacterium luminescens* resulted in reduced biofilm biomass, pellicle formation and motility (Amos et al., 2011). Previous work in *S. Typhimurium* found that a *manA* deficient mutant was impaired in its colonisation of seedlings and mice due to deficiencies in O-antigen and colanic acid production (Kwan et al., 2018). However, because *manA* expression was only found here to be beneficial to biofilm fitness after 48 hours growth, this indicates a role in matrix biosynthesis in the mature biofilm rather than initial attachment.

### 5.3.2. Purine biosynthesis

Purine biosynthesis was important in the mature biofilm of both *E. coli* and *S. Typhimurium*. Four genes were identified to be important in purine biosynthesis in the *E. coli* biofilm at 48 hours, whereas the only gene identified in *S. Typhimurium* biofilm conditions was *purK*. Other studies have highlighted that inactivation of *purK*, as well as other genes involved in purine biosynthesis, disrupts curli biosynthesis (Nhu et al., 2018, Smith et al., 2017). We also found that expression of the nucleotide phosphatase *nagD* (Tremblay et al., 2006) was important for the fitness of the mature biofilm. Recent work on purine biosynthesis in *E. coli* found that curli biosynthesis could be rescued in a *purL* deletion mutant through the addition of inosine (Cepas et al., 2020), and it is possible that inosine released from *nagD*-mediated breakdown of IMP is important for curli biosynthesis in the mature biofilm.

### 5.3.3. Transcriptional regulators and transcription factors

Several similar transcriptional regulators were found to affect biofilm formation in both *E. coli* and *S. Typhimurium*. We found the global stress response regulators *ramR*, *ramA* and *marR* (Abouzeed et al., 2008, Alekshun and Levy, 1999a) were beneficial for biofilm fitness at different points in biofilm formation in *S. Typhimurium* and *E. coli*. There were fewer mutants mapped to *ramA* in biofilms grown for 24 hours and *ramR* in biofilms grown for 48 hours compared to planktonic conditions in *S. Typhimurium*, whereas *marR* was beneficial for biofilm fitness in *E. coli* after 12 hours. Deletion of *ramA* and *ramR* ( $\Delta ramRA$ ) in *S. Typhimurium* resulted in significantly increased biofilm biomass, and unchanged curli and cellulose biosynthesis relative to the wild type (figure 5.3 a,b). The relationship between *marA* and *ramA* and biofilm formation is extremely complex, where their overexpression results in significantly reduced biofilm biomass in *S. Typhimurium* (Holden and Webber, 2020). Further investigation is necessary to determine how these efflux regulators affect biofilm formation.

In biofilms grown for 24 hours, there were more insertions in *rpoS* in *S. Typhimurium* biofilms and more insertions in *dksA* in *E. coli* biofilms compared to planktonic conditions, both of which are transcription factors both involved in stationary phase regulation and both are responsive to the stress signalling molecule ppGpp (Brown et al., 2002). The Rcs phosphorelay, a multicomponent signalling system, was beneficial to biofilm fitness in both species, with more insertions upstream of the transcriptional regulator *rpsB*, conferring a fitness benefit to its overexpression, in *S. Typhimurium* biofilms grown for 24 hours and fewer mutants in sensory kinase *rpsC* in *E. coli* biofilms after 48 hours growth relative to planktonic culture.

### 5.3.4. LPS

Genes involved in LPS biosynthesis were identified as important in both *S. Typhimurium* and *E. coli* biofilm formation. In *S. Typhimurium*, five genes were identified across all measured time points of biofilm formation, in contrast to only one gene identified in *E. coli* biofilms after 48 hours growth. This may be because *E. coli* K-12 is known to be defective in O-antigen production (Stevenson et al., 1994). In *S. Typhimurium*, expression of *rfaJ* was beneficial for biofilm formation throughout the biofilm lifecycle after 12-, 24- and 48-hours growth, and *rfaP* was beneficial at the 24- and 48-hour time points. Both genes are involved in biosynthesis of the LPS core (Schnaitman and Klena, 1993). LPS is known to have a role in curli production and biofilm formation, where deleting genes involved in LPS inner core biosynthesis reduced curli production (Smith et al., 2017). A transposon mutagenesis study in *E. coli* O157:H7 found that insertions in *rfaJ* and *rfaP* homologs (*waaJ* and *waaP*), impaired biofilm formation (Puttamreddy et al., 2010), consistent with our findings that disruption of LPS biosynthesis is harmful to biofilm fitness.

Puttamreddy et al. (2010) found that disruption of *waaL* reduced biofilm formation, whereas we found the opposite was true for its homolog in *Salmonella*, *rfaL*, where insertional inactivation of *rfaL*, *rfaG* and *rfaJ* improved biofilm fitness in our study after 24- or 48-hours growth. Both *rfaJ* and *rfaL* are involved in O-antigen biosynthesis and ligation (Schnaitman and Klena, 1993). Previous work on O-antigen biosynthesis in *Salmonella* biofilms found that its disruption can be beneficial for biofilm biomass formation, as it can act as a surfactant that inhibits biofilm formation (Mireles et al., 2001). Other studies have reported the opposite to be true, that O-antigen biosynthesis is beneficial for biofilm fitness and disruption of *galE* reduced biofilm formation on biotic surfaces, but this may be due to its role in exopolysaccharide production rather than O-antigen biosynthesis (Prouty et al., 2002, Nesper et al., 2001). We tested the production of biofilm biomass, curli and cellulose of a mutant lacking *rfaF*, involved in O-antigen biosynthesis. There was no significant difference in biofilm biomass from the wild type, but there was a visibly less curli and cellulose biosynthesis in the *rfaF* mutant (figure 5.3 a,b). Although this particular gene was not highlighted by TraDIS-*Xpress* to affect biofilm fitness, it gives an indication as to how O-antigen biosynthesis benefits biofilm matrix production in *S. Typhimurium*. RfaG is involved in linking the inner and outer cores in LPS core biosynthesis (Schnaitman and Klena, 1993), and it has been reported that its deletion resulted in reduced curli biosynthesis (Anriany et al., 2006, Smith et al., 2017), but increased biofilm biomass and cellulose production relative to the wild type (Anriany et al., 2006). The differences seen between the TraDIS-*Xpress* data and the phenotypic characterisation of knockout mutants may be due to the former using a pool of mutants rather than the clonal population used in the latter. In a pool of mutants, 'cheaters' which would otherwise be unable to survive on their own can exploit others to survive and thrive. This is more representative of a multispecies heterogenic biofilm but complicates investigations into the roles of individual genes in the biofilm. Overall, the relationship between O-antigen biosynthesis and biofilm formation is complex and may vary due to differing environmental conditions across these studies.

### 5.3.5. Transport

Genes involved in transmembrane transport affected biofilm formation in both *S. Typhimurium* and *E. coli*. Genes involved in the import and degradation of L-ascorbate (*sgbE* in *E. coli* and *ulaC* in *S. Typhimurium*) were beneficial to the fitness of biofilms grown for 48 hours. Deletion of the *ulaC* homolog in *Streptococcus mutans* resulted in reduced biofilm matrix production when grown on media with L-ascorbate as the sole carbon source (Wu et al., 2016), suggesting L-ascorbate utilisation by the cell may be important for matrix production in *E. coli* and *S. Typhimurium* biofilms. Various transporters were found to only affect biofilm fitness in *S. Typhimurium*, with fewer

mutants in *corC* (Gibson et al., 1991) and *ydeD* (Dassler et al., 2000) after 24 hours growth, and *cysW* (Sirko et al., 1995) after 48 hours growth, in biofilm conditions relative to planktonic. Outer membrane integrity, maintained by *yciB* (Niba et al., 2008) appears to be important in the *S. Typhimurium* biofilm at 48 hours, containing fewer insertions compared to planktonic culture.

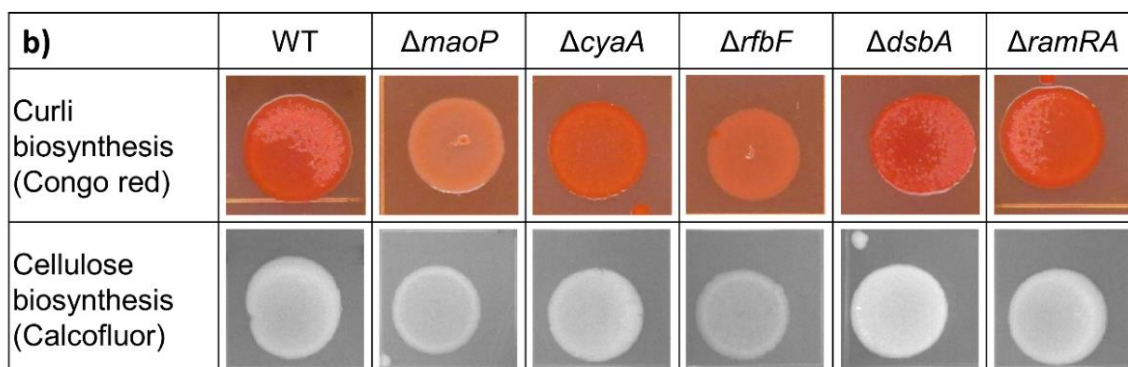
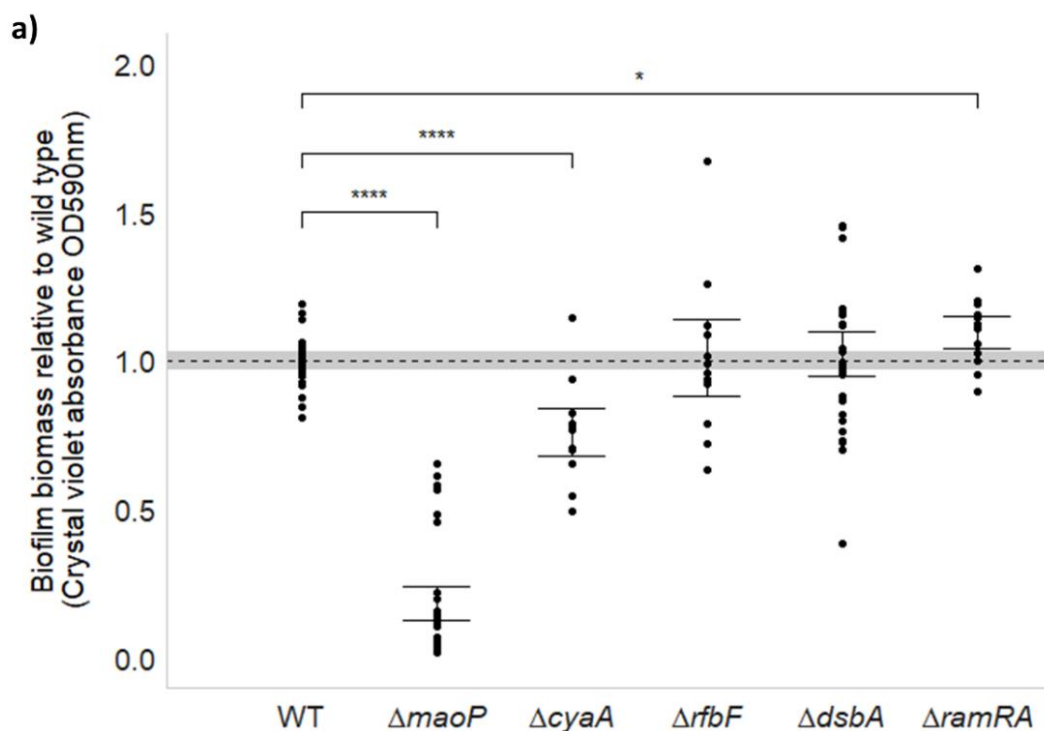


**Figure 5.3:** Biofilm formation in deletion mutants relative to wild type (WT) *S. Typhimurium*. **a)** Biofilm biomass relative to the WT, measured by crystal violet staining (OD<sub>590 nm</sub>). Points show a minimum of two biological and eight technical replicates. The grey shaded area shows the 95% confidence interval of the wild type and error bars show 95% confidence intervals of the mutants. A significant difference in biofilm biomass to the wild type is indicated by asterisks: \* =  $p < 0.05$ ; \*\* =  $p < 0.01$ ; \*\*\* =  $p < 0.001$ ; \*\*\*\* =  $p < 0.0001$ . **b)** Mutants and the WT spotted on agar supplemented with Congo red and calcofluor, showing curli and cellulose production, respectively. For all images, colonies are representative images of two biological and two technical replicates.

#### 5.4. DNA housekeeping, cell division and motility regulation are more important to biofilm fitness in *E. coli* compared to *S. Typhimurium*

Comparing the genes that affect biofilm formation in *S. Typhimurium* and *E. coli* revealed several differences between these species. TraDIS-*Xpress* identified genes involved in DNA housekeeping, cell division, c-di-GMP metabolism, motility regulation and anti-toxin production were important in biofilm fitness in *E. coli* but not *S. Typhimurium*.

In *E. coli* biofilms grown for 24 hours, DNA housekeeping genes *dam* and *maoP* were seen to have a significant effect on biofilm fitness, however no DNA housekeeping genes were identified by the TraDIS-*Xpress* data to affect the fitness of the *S. Typhimurium* biofilm. In the previous chapter, we identified a novel role of *maoP* in biofilm formation, demonstrating deletion of *maoP* resulted in a reduction in curli biosynthesis and biofilm biomass in *E. coli*. To further investigate the role of this gene on biofilm fitness, we disrupted the *maoP* homolog in *S. Typhimurium* and found it to have the same effect on biofilm formation in *S. Typhimurium* as in *E. coli*. In addition to a reduction in curli biosynthesis and biofilm biomass, deletion of *maoP* in *S. Typhimurium* also resulted in reduced cellulose biosynthesis, despite seeing no indication for this in the TraDIS-*Xpress* data (figure 5.3 a,b). We found the TraDIS-*Xpress* findings and the phenotypic characterisation of the  $\Delta$ *maoP* mutant disagreed with each other on how this gene affected fitness in *E. coli* biofilms. This demonstrates that differences in phenotype arise following insertional inactivation or whole gene deletion of *maoP*, and this may explain why insertional inactivation of *maoP* in *S. Typhimurium* had no effect on fitness in the biofilm. MaoP is involved in chromosomal macrodomain organisation, and differences in the TraDIS-*Xpress* data between *E. coli* and *S. Typhimurium* may be due to how chromosomal organisation is managed in each species. Very little is known about *maoP* and further investigation into its activity and regulation will clarify its role in biofilm development in both species.

Genes involved in flagella biosynthesis were important in both *E. coli* and *S. Typhimurium* biofilms grown for 24 and 48 hours. In *E. coli*, motility regulators *IrhA*, *hdfR* and *flhDC* were found to affect biofilm formation at different stages, but no regulators were identified in the data from *S. Typhimurium*.

In *E. coli*, antitoxin modulator *tomB* was found to benefit fitness in biofilms grown for 12, 24 and 48 hours, however the same relationship was not seen in *S. Typhimurium*. Phenotypically, deletion of *tomB* in *S. Typhimurium* is predicted to result in reduced curli biosynthesis in the same manner as demonstrated in *E. coli*. Previous work describes how deletion of *tomB* in *S. Typhimurium* rescued the deficit in biofilm biomass of a *mdtK* deletion mutant, and partially complemented that of a *tolC* deletion mutant (Baugh, 2014).

It is possible that in *S. Typhimurium*, *tomB* affects biofilm fitness in a more pronounced way when the cell is under efflux stress, relative to the effect on biofilm fitness seen in *E. coli*.

### **5.5. Genes involved in respiration, regulation of cellulose biosynthesis and ribosomal modification are more important to biofilm fitness in *S. Typhimurium* compared to *E. coli***

Pathways that were identified by TraDIS-*Xpress* to affect biofilm fitness in *S. Typhimurium* but not *E. coli* include amino acid biosynthesis, cellulose biosynthesis regulation, cyclic AMP biosynthesis, iron acquisition and protease activity.

Initial attachment and adhesion to surfaces is extremely important in early biofilm formation. Insertions upstream of cellulose biosynthetic regulatory genes *gcpA* and *gcpG* (Garcia et al., 2004), resulting in their overexpression, increased the fitness of biofilms after 12 hours growth. Both genes encode GGDEF domain-containing proteins involved in regulation of cellulose biosynthesis (Garcia et al., 2004). Cellulose has been identified as an essential component of the biofilm matrix for *Salmonella* when growing on glass (Prouty and Gunn, 2003). *E. coli* K-12 strains do not produce cellulose due to disruption of the cellulose biosynthetic machinery, specifically an early stop codon in *bcsQ* (Serra et al., 2013). The importance of these genes so early in the biofilm life cycle implies a role for cellulose in attachment and adhesion to surfaces. After 12 hours growth, more insertions were seen upstream of *sadA*, encoding a trimeric autotransporter adhesin (Raghunathan et al., 2011), in biofilm conditions relative to planktonic, indicating a fitness benefit from *sadA* overexpression. This is supported by previous work, which found that expression of *sadA* promoted biofilm formation, cell aggregation and adhesion to epithelial cells (Raghunathan et al., 2011). Arabinose has also been implicated in attachment and adhesion in the biofilm (Bahat-Samet et al., 2004). We found expression of the arabinose transporter *araJ* (Reeder and Schleif, 1991) to be important in the early biofilm, with fewer insertions seen in *araJ* in biofilm conditions relative to planktonic after 12 hours growth. This finding is supported by previous work describing upregulation of *araJ* in *E. coli* biofilms (May et al., 2009). Although the exact role of AraJ is unknown (Reeder and Schleif, 1991), it may be involved arabinose transport to regulate adhesion during biofilm development.

Amino acid biosynthesis was crucial for early biofilm formation in *S. Typhimurium*, with fewer insertions in *hisC* (Schembri et al., 2003) and *ilvH* (Squires et al., 1981) in biofilms grown for 12 hours relative to planktonic conditions. Increased expression of *hisC*, involved in histidine biosynthesis, has previously been seen in *E. coli* (Schembri et al.,

2003) and *Staphylococcus aureus* (Beenken et al., 2004) biofilms. IlvH is a small regulatory subunit involved in synthesising L-valine, L-leucine and L-isoleucine from pyruvate (Squires et al., 1981), and has been previously identified to have a relationship with biofilm formation, with reduced IlvH seen in *Pseudomonas aeruginosa* biofilms incubated for 18 hours (Coquet et al., 2006). IlvH has also been found to contain a potential c-di-GMP receptor (Fang et al., 2014), but further characterisation is needed to determine how this affects biofilm formation.

TraDIS-*Xpress* identified more insertions upstream of *rimO* in biofilm conditions relative to planktonic after 48 hours growth, suggesting that overexpression of *rimO* improved biofilm fitness. RimO methylthiolates ribosomal protein S12 (Anton et al., 2008). RimO has not previously been implicated in biofilm formation, but its target, ribosomal protein S12, has. Previous work found that decreased ribosomal performance caused by mutations in *rpsL*, encoding ribosomal protein S12, correlated with increased biofilm formation (Boehm et al., 2010). Overexpression of *rimO* in the mature biofilm may reduce ribosomal activity, thereby increasing the fitness of the mature biofilm. Boehm et al. (2010) also suggested that secondary messenger molecules ppGpp and c-di-GMP may play a role in modulating ribosomal performance, in addition to their well-understood role in biofilm matrix production. RimO has since been found to contain a potential c-di-GMP receptor (Fang et al., 2014). As c-di-GMP levels increase in the mature biofilm, its binding to RimO may activate methylthiolation of ribosomal protein S12, leading to reduced ribosomal activity and increased biofilm formation. Further investigation into this hypothesis may clarify the role of ribosomal activity and *rimO* in biofilm formation.

#### **5.6. Respiration is important for the fitness of the mature biofilm in *S. Typhimurium***

Aerobic respiration was critical for biofilm development in *S. Typhimurium*. We found 17 genes involved in the electron transport chain were important for the fitness of the growing and maturing biofilm after 24 and 48 hours. Overexpression of *fumA*, involved in the TCA cycle (Guest and Roberts, 1983), was beneficial for biofilm fitness at 48 hours. There were also fewer insertions in *pdhR* and *cra*, both involved in regulating the expression of genes involved in the TCA cycle and electron transport chain (Ogasawara et al., 2007, Saier and Ramseier, 1996). Both *pdhR* and *cra* have been associated with *csgD* promoter binding (Ogasawara et al., 2020) and may regulate curli biosynthesis.

Reduced expression of *eutQ* was beneficial for *Salmonella* biofilms at 12, 24 and 48 hours. EutQ is an acetate kinase, responsible for breaking down acetate to acetyl-phosphate during ethanolamine utilisation or pyruvate fermentation (Moore and Escalante-Semerena, 2016). Acetyl-phosphate can phosphorylate response regulators,



such as OmpR and RcsB in two component systems in place of their sensory histidine kinases (McCleary et al., 1993, Prüss et al., 2010). Deletion of genes involved in acetyl-phosphate production has been shown to have negative effects on flagella biosynthesis and positive effects on fimbriae biosynthesis (Prüss et al., 2010). Reduced expression of *eutQ* throughout the biofilm lifecycle may benefit biofilm formation through allowing response regulators to only be phosphorylated following sensory kinase stimulation, allowing the cell to respond to extracellular stimuli more sensitively. Deletion of *eutQ* has been found to result in a growth defect (Moore and Escalante-Semerena, 2016), which may explain why we see that reduced expression, rather than inactivation, of *eutQ* benefits the biofilm throughout its life cycle.

The *nuo* operon, encoding the type I NADH dehydrogenase in the electron transport chain (Archer and Elliott, 1995), contains 14 genes, ten of which we found had fewer mutants in the biofilm conditions relative to planktonic culture after 24- or 48-hours growth (figure 5.4a). In addition to this, there were also fewer insertions in *ygiN* and *menH*, involved in electron carrier biosynthesis and maintenance (Adams and Jia, 2005, Meganathan and Kwon, 2009), in biofilm conditions relative to planktonic after 24 hours growth. This suggests the effect on biofilm formation is due to the electron transport chain, rather than the NADH dehydrogenase itself.

Previous work found that the *nuo* operon was upregulated in *Acinetobacter baumannii* biofilms (Penesyan et al., 2019) and is essential for root colonisation by *Pseudomonas fluorescens* (Camacho Carvajal et al., 2002). Despite this conserved importance of the *nuo* operon in biofilm formation across many species, we did not identify a signal for the *nuo* operon in our previous investigations into biofilm formation in *E. coli*. A comparison of the TraDIS-*Xpress* plot files between *E. coli* and *S. Typhimurium* found this was due to considerably fewer mutants mapped to the planktonic condition in *E. coli* relative to *S. Typhimurium* (figure 5.4 a,b). Genes are identified as affecting biofilm formation if there is a substantial difference in insertion frequency between the planktonic and biofilm conditions. In *S. Typhimurium*, this difference is obvious, due to the higher number of mutants mapped to the *nuo* operon in the planktonic condition. However in *E. coli*, fewer mutants are mapped to the planktonic condition relative to *S. Typhimurium*, therefore the difference between planktonic and biofilm conditions in *E. coli* is less pronounced. I investigated whether the difference in mapped reads in planktonic culture between *S. Typhimurium* and *E. coli* was due to differences in fitness between the  $\Delta nuoB$  deletion mutants in each species in planktonic culture. The growth kinetics of the  $\Delta nuoB$  and  $\Delta nuo$  deletion mutants relative to the wild type were similar in both *S. Typhimurium* and *E. coli* (figure 5.4c), therefore the difference in mapped reads in the planktonic conditions between the two species is unlikely to be due to a more pronounced fitness imbalance in

*E. coli* compared to *S. Typhimurium*. There may be fewer mutants in the planktonic condition in *E. coli* due to chance, as transposon insertion is relatively random and this area of the genome may not have received as much coverage as other areas. This highlights a limitation of using TraDIS-*Xpress* to identify genes affecting fitness, but also highlights the benefit of comparing two similar transposon mutant libraries cultured under the same conditions.

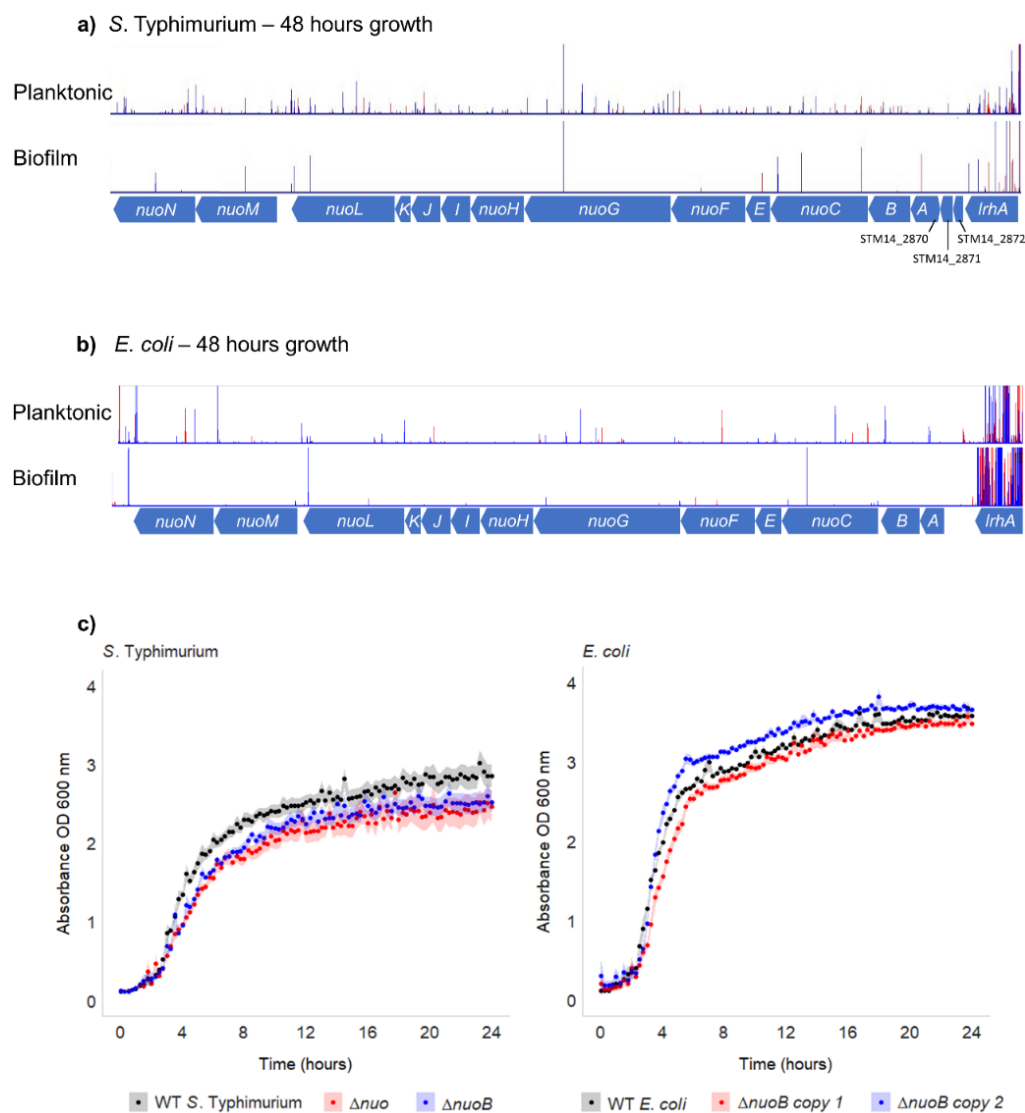


**Figure 5.4:** Mapped reads from TraDIS-*Xpress* data, plotted with BioTraDIS in Artemis, showing the location of transposon insertion sites in and around the *nuo* operon in **a)** *S. Typhimurium* and **b)** *E. coli* after 48 hours in growth in planktonic and biofilm conditions. The directionality of the transposon-located is indicated by colour, red denoting left-to-right and blue denoting right-to-left. Profiles show one of two independent replicates and conditions with and without promoter induction with IPTG have been combined. **c)** Growth kinetics of wild type (WT),  $\Delta nuo$  and  $\Delta nuoB$  mutants in *S. Typhimurium* (left) and *E. coli* (right) over 24 hours. Points show the mean of two biological and eight technical replicates, and the shaded area denotes 95% confidence intervals for each strain.

The effect of the *nuo* operon on biofilm formation was investigated in both *S. Typhimurium* and *E. coli*. In *S. Typhimurium*, I created two deletion mutants: one lacking *nuoB* and another where the majority of the *nuo* operon (from *nuoB* to *nuoN*) was deleted. Two  $\Delta nuoB$  deletion mutants in *E. coli* were retrieved from the Keio collection, and biofilm formation was tested in these mutants relative to the respective wild type for each species. Deletion of the *nuo* operon or *nuoB* resulted in significantly reduced biofilm biomass (Wilcoxon rank sum,  $p < 0.0001$ ) and curli biosynthesis relative to the wild type in both *S. Typhimurium* and *E. coli*, but cellulose biosynthesis was relatively unchanged in *S. Typhimurium* (figure 5.5 a,b). Analysis of *nuo*-deficient biofilms under flow conditions showed reduced adhesion after 12- and 24-hours growth and reduced biofilm biomass relative to wild type *S. Typhimurium* (figure 5.5c).

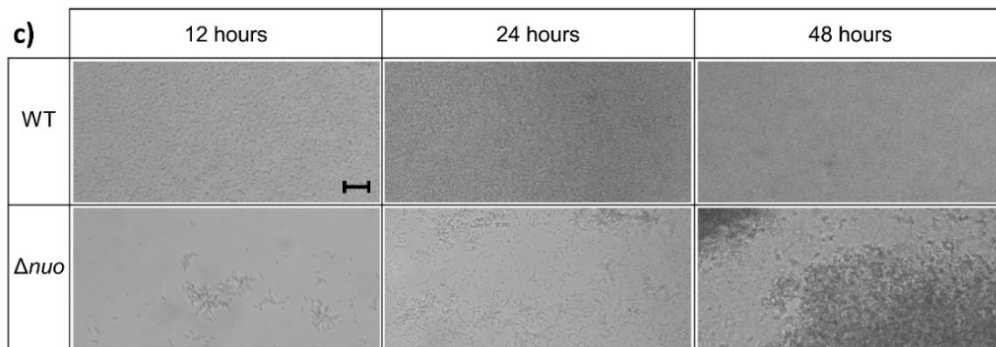
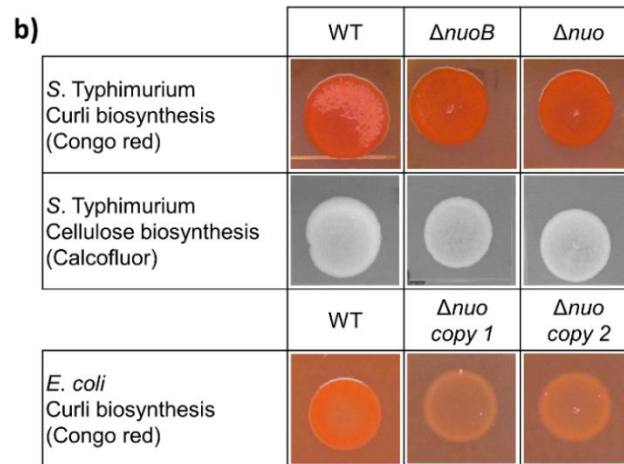
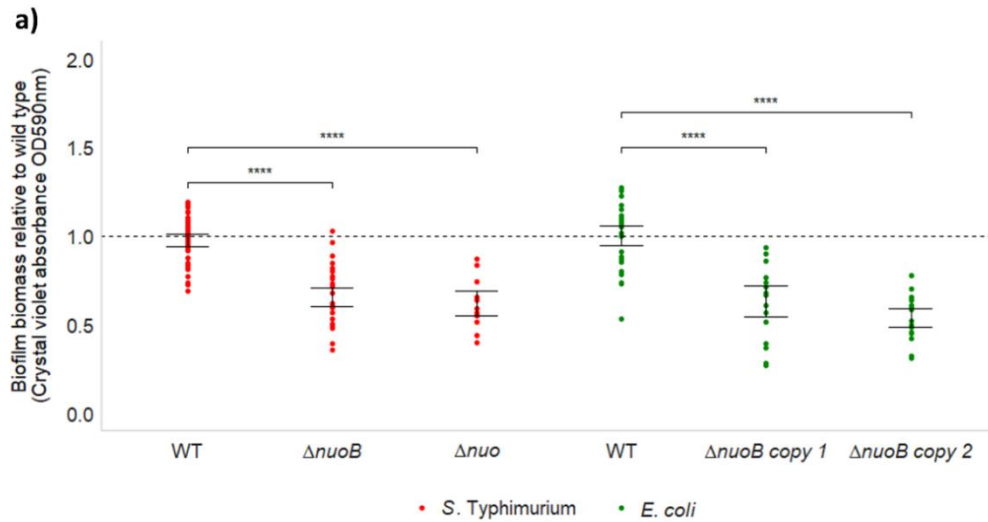


**Figure 5.5:** The effects of the *nuo* operon on biofilm formation in *E. coli* and *S. Typhimurium*. **a)** Biofilm biomass of  $\Delta nuoB$  and  $\Delta nuo$  deletion mutants relative to wild type (WT) *E. coli* and *S. Typhimurium*. Points show a minimum of two biological and six technical replicates and error bars show 95% confidence intervals. Asterisks show a significant difference in biofilm biomass from the WT (Wilcoxon rank sum, \* =  $p < 0.05$ ; \*\* =  $p < 0.01$ ; \*\*\* =  $p < 0.001$ ; \*\*\*\* =  $p < 0.0001$ ). **b)** Curli and cellulose biosynthesis of  $\Delta nuoB$  and  $\Delta nuo$  mutants relative to their WT. Images are representative of two biological and two technical replicates. **c)** Biofilm formation of WT *S. Typhimurium* and the  $\Delta nuo$  mutant on glass analysed under flow conditions after 12-, 24- and 48-hours growth. 20x Magnification. Scale bar indicates 10  $\mu\text{m}$ .

Because the *nuo* operon is involved in aerobic respiration, we investigated whether environmental oxygen affected biofilm formation in wild type *S. Typhimurium* and *E. coli* compared to the *nuoB*-deficient mutants in each species. These were grown under aerobic, anaerobic and microaerophilic conditions and biofilm biomass and curli biosynthesis was examined. Deletion of *nuoB* significantly reduced biofilm biomass (Wilcoxon rank sum,  $p < 0.001$ ) in anaerobic and ambient oxygen conditions in both *S. Typhimurium* and *E. coli* (figure 5.6a). There was no significant difference in biofilm biomass between wild type *S. Typhimurium* and  $\Delta nuoB$  under microaerophilic conditions (Wilcoxon rank sum; 5% O<sub>2</sub>,  $p = 0.130$ ; 10% O<sub>2</sub>,  $p = 0.721$ ) and only a slightly significant difference between wild type *E. coli* and  $\Delta nuoB$  under 5% oxygen (Wilcoxon rank sum; 5% O<sub>2</sub>,  $p = 0.0499$ ; 10% O<sub>2</sub>,  $p = 0.959$ ) (figure 5.6a). There was very little difference in curli biosynthesis between wild type *S. Typhimurium* and the  $\Delta nuoB$  mutant under anaerobic and microaerophilic conditions, with the biggest difference seen in aerobic conditions, where  $\Delta nuoB$  produced less curli than the wild type (figure 5.6b). In *E. coli*, curli biosynthesis appears to be reduced in  $\Delta nuoB$  relative to the wild type at all oxygen concentrations tested (figure 5.6b). From this, we can determine that the effect of the *nuo* operon on biofilm biomass, but not curli biosynthesis, is sensitive to environmental oxygen conditions in *S. Typhimurium* and *E. coli*.

The *nuo* operon affects biofilm biomass and curli biosynthesis, but the pathway through which this occurs is unclear. Previous work described how disruption of the *nuo* operon interrupts the oxidative pentose phosphate pathway and purine and pyrimidine biosynthesis (Claas et al., 2000), which has previously been reported to affect curli production (Cepas et al., 2020), however further investigation is needed to confirm whether this is the pathway through which the *nuo* operon affects curli biosynthesis. Additionally, the NADH dehydrogenase that the *nuo* operon encodes is a known proton pump and has a role in establishing a proton gradient between the cytoplasm and the periplasm (Bogachev et al., 1996). The proton gradient provides energy for ATP synthesis, efflux pump activity and flagella motion, all of which are known to affect biofilm formation (Baugh et al., 2012, Pesavento et al., 2008, Bosch et al., 2020). This will be investigated in a later chapter.

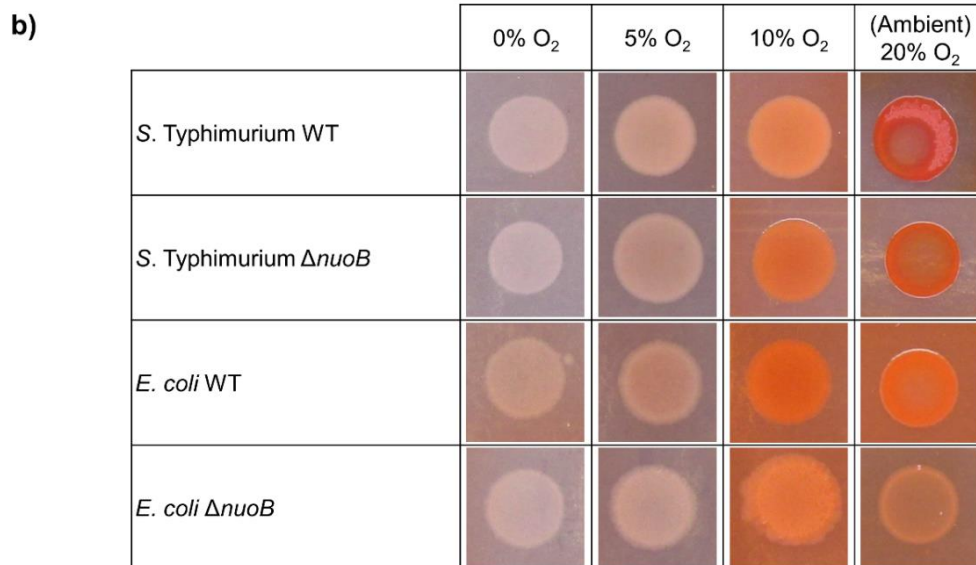
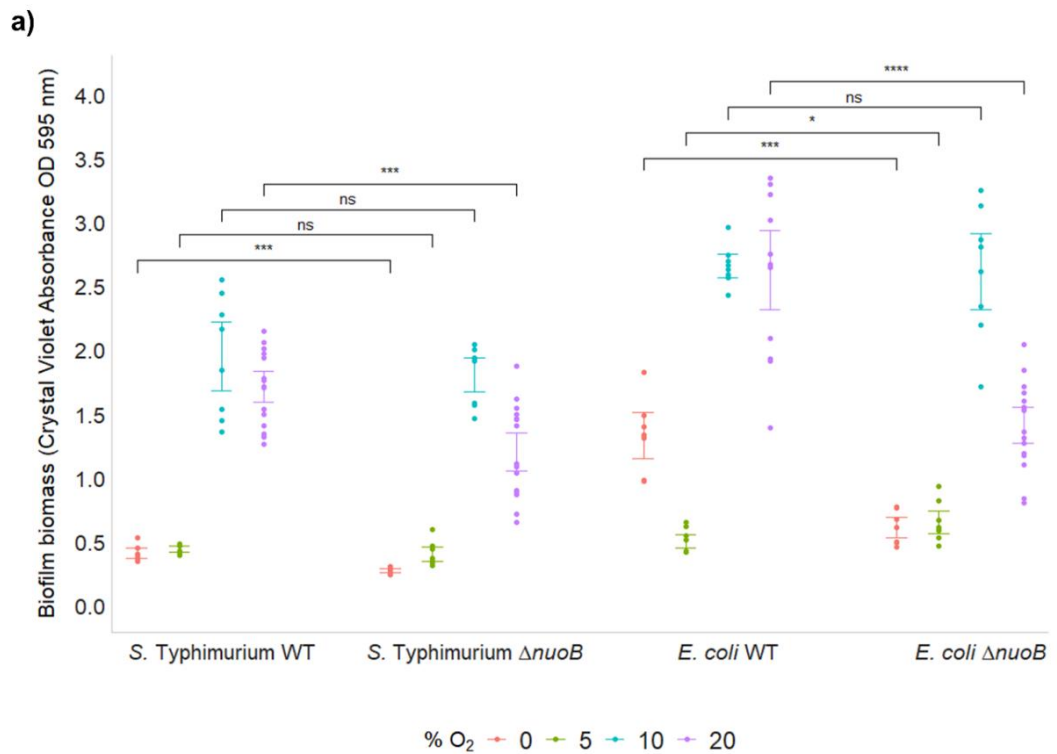


**Figure 5.6:** The effect of environmental oxygen and the *nuo* operon on biofilm formation in *E. coli* and *S. Typhimurium*. **a)** Biofilm biomass of wild type and  $\Delta nuoB$  deletion mutants of *S. Typhimurium* and *E. coli* grown under various oxygen concentrations (0%, 5%, 10% and ambient ~20% oxygen). Points show biofilm biomass of a minimum of eight technical replicates and one biological replicate, and error bars denote 95% confidence intervals. Asterisks show a significant difference in biofilm biomass from the wild type (Wilcoxon rank sum, \* =  $p < 0.05$ ; \*\* =  $p < 0.01$ ; \*\*\* =  $p < 0.001$ ; \*\*\*\* =  $p < 0.0001$ ; ns = not significant). **b)** Wild type and  $\Delta nuoB$  deletion mutants in *S. Typhimurium* and *E. coli* spotted on agar containing Congo red to highlight differences in curli biosynthesis when grown under various oxygen concentrations. Images are representative of four technical and two biological replicates.

## 5.7. Genes not previously implicated in biofilm formation

TraDIS-*Xpress* identified 21 genes that benefitted biofilm fitness that had not previously been linked to biofilm formation. These included *orfB*, *ybaN*, *yjiG*, STM14\_0498, STM14\_1074, STM14\_1157, STM14\_1158, STM14\_1440, STM14\_1445, STM14\_1764 and STM14\_3208 after 12 hours growth, *tyrT*, *ybeF*, *ybeX* and *ygiN* after 24 hours growth, and *ycgL*, *yliG*, STM14\_0653, STM14\_2049, STM14\_2856 and STM14\_3860 beneficial for biofilm formation after 48 hours growth.

Of these, we chose to investigate three genes that seemed to have the largest effect on fitness in biofilm conditions relative to planktonic conditions to characterise how they affected biofilm formation in *S. Typhimurium*. These included the genes encoding putative transcriptional regulator STM14\_1074 (Qin et al., 2016), inner membrane protein YjiG (Tang and Saier, 2014) and tyrosine tRNA TyrT (Winston et al., 1979). Analysis of the TraDIS-*Xpress* data found fewer mutants in both STM14\_1074 and *yjiG* in biofilms grown for 12 hours, relative to planktonic culture. This was supported by reduced adhesion in both mutants relative to the wild type after 12 hours growth under flow conditions (figure 5.7c).

There were more transposon insertions upstream of *tyrT* in the biofilm conditions relative to the planktonic conditions, indicating that overexpression of *tyrT* was beneficial to biofilm fitness after 24 hours growth. To investigate this, *tyrT* was inserted into the expression plasmid pBR322 under the IPTG-inducible *lac* operator (pBR322/*lac*) in *S. Typhimurium*::*lacI*Z (to control *lac* promoter activity), and its effect on biofilm formation was examined relative to an empty plasmid control. Overexpression of *tyrT* (pBR322/*lac-tyrT*) resulted in no significant change in biofilm biomass, cellulose biosynthesis or adhesion relative to the plasmid control (figure 5.7 a,b,c). Analysis of the colonies spotted on agar supplemented with Congo red revealed slightly increased curli biosynthesis, with more wrinkles visible in colonies overexpressing *tyrT* (indicative of *rdar* colony morphology), however this effect was only small. These three genes, *yjiG*, STM14\_1074 and *tyrT*, may also affect different aspects of biofilm development not measured in these phenotypic assays, however TraDIS-*Xpress* is extremely sensitive to variations in fitness and was able to predict the effect of these genes on the biofilm phenotype.

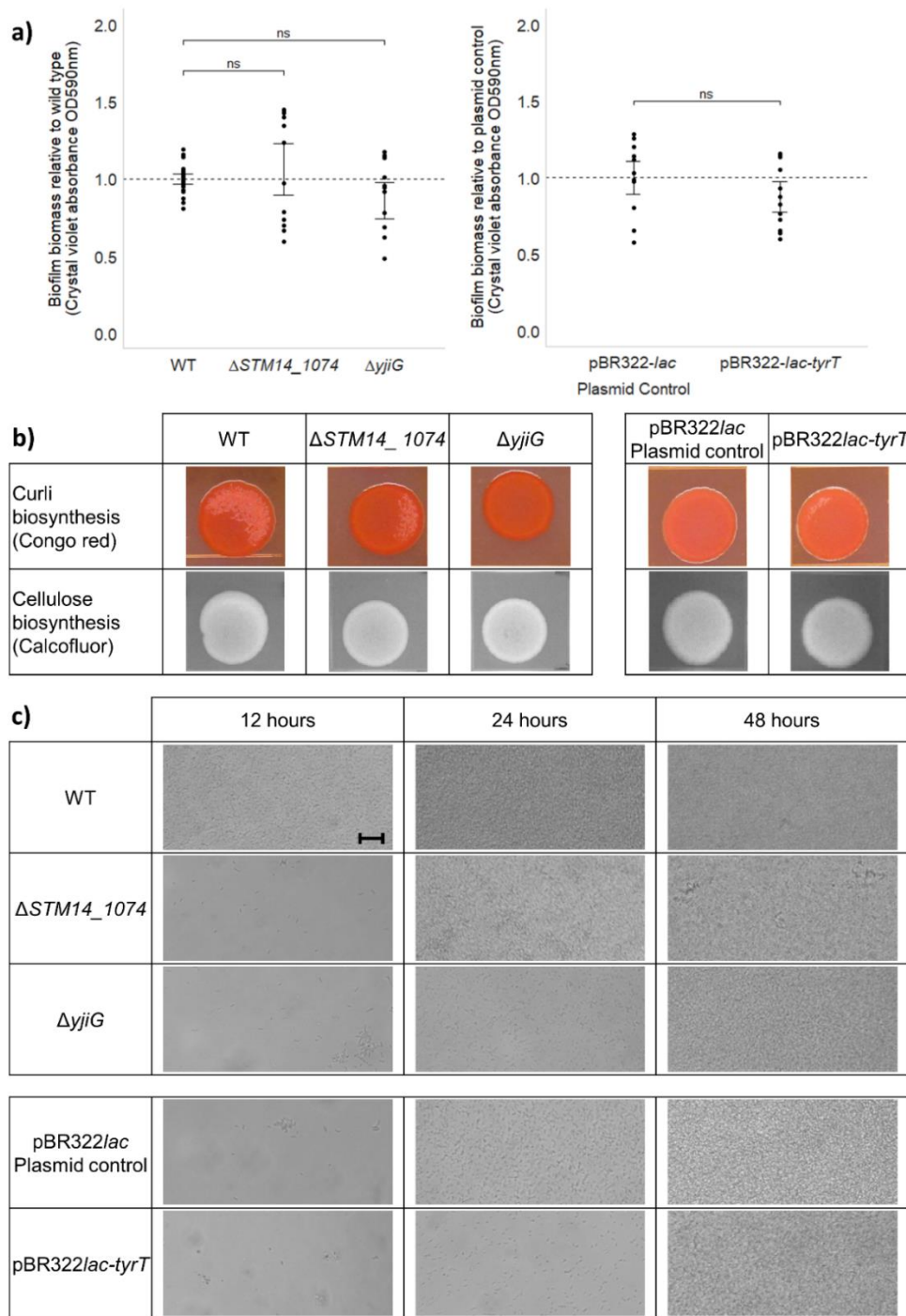


**Figure 5.7:** The effects of *STM14\_1074*, *yjiG* and *tyrT* on biofilm formation in *S. Typhimurium*. **a)** Biofilm biomass of  $\Delta STM14\_1074$  and  $\Delta yjiG$  relative to wild type (WT) *S. Typhimurium*, and *S. Typhimurium* containing a plasmid overexpressing *tyrT* relative to the empty plasmid control. Points represent a minimum of six technical replicates across two biological replicates, and error bars show 95% confidence intervals. Asterisks show a significant difference in biofilm biomass from the wild type (Wilcoxon rank sum, \* =  $p < 0.05$ ; \*\* =  $p < 0.01$ ; \*\*\* =  $p < 0.001$ ; \*\*\*\* =  $p < 0.0001$ ; ns = not significant). **b)** Curli and cellulose biosynthesis of wild type *S. Typhimurium* and deletion mutants. Images are representative of two biological and two technical replicates. **c)** Biofilm formation of wild type *S. Typhimurium* and deletion mutants on glass analysed under flow conditions after 12-, 24- and 48-hours growth. 20x Magnification. Scale bar indicates 10  $\mu\text{m}$ .



## 5.8. Conclusions

Here I described the genes that affect biofilm fitness in *S. Typhimurium* and compared the similarities and differences in gene essentiality and expression in biofilm formation to *E. coli*. Pathways identified to affect biofilm fitness in both species include type I fimbriae regulation, flagella biosynthesis, purine biosynthesis, curli production, LPS biosynthesis, sugar utilisation, transmembrane transport and various similar transcriptional regulators.

Pathways that affect biofilm fitness in *S. Typhimurium* but not *E. coli* include respiration, amino acid biosynthesis, cellulose biosynthesis regulation, cyclic AMP biosynthesis, iron acquisition and protease activity. This comparison between the two species revealed the importance of the electron transport chain in the fitness of the mature biofilm after 24- and 48-hours growth, where the contribution of the *nuo* operon to biofilm fitness was identified from the TraDIS-*Xpress* data. Phenotypic analyses supported this finding in both *S. Typhimurium* and *E. coli*, under both aerobic and anaerobic conditions. In chapter 7, I investigated pathways through which the deletion of the *nuo* operon may reduce curli biosynthesis. Comparing these results to other *E. coli* strains, *Salmonella* species and members of the Enterobacteriaceae family will deepen our understanding of the requirements for optimal biofilm fitness in these bacteria.

Additionally, I identified 21 genes that had not previously been associated with biofilm formation in *S. Typhimurium*, and further investigated how three of these genes affected biofilm formation. Deletion of *STM14\_1074* and *yjiG* were identified to reduce the fitness of the early biofilm, and were found to reduced adhesion to glass under flow conditions after 12 hours growth. Overexpression of *tyrT* improved the fitness of biofilms grown for 24 hours and resulted in a slight increase in curli biosynthesis. Further characterisation of these genes is necessary to determine the exact mechanism through which they affect adhesion and matrix production in the biofilm.

This comparison of gene essentiality and expression in the biofilm between *S. Typhimurium* and *E. coli* has revealed new information about biofilm fitness in both species, highlighting species-specific requirements as well as common pathways important in biofilm formation. To the best of my knowledge, this work is the first to determine the role of the *nuo* operon in biofilm formation in *S. Typhimurium* and *E. coli*, as well as the first to identify how 21 other genes not previous known to be involved in biofilm formation affect biofilm fitness in *S. Typhimurium*. This demonstrates the importance of comparing biofilm formation between difference species to develop a deeper understanding of the core requirements for biofilm formation.

This model system has successfully identified genes that affect biofilm fitness in two defined bacterial strains used frequently in the lab, paving the way for further investigations using species and strains isolated from the environment that have a real-world importance. These experiments used glass beads as a substrate on which biofilms could grow, but they can easily be replaced with other materials that are more relevant for other applications. This could also be used to test the efficacy of anti-biofilm agents, allowing the determination of the exact mechanism through which they affect biofilm fitness and how this may change over time.

Overall, this comparison of the requirements for optimal biofilm fitness between *S. Typhimurium* and *E. coli* sheds light on the species-specific differences in biofilm formation, but also deepens our understanding of the core requirements for biofilm formation across the Enterobacteriaceae family.

**6. CHAPTER 6: IDENTIFICATION OF  
GENES INVOLVED IN EFFLUX  
ACTIVITY AND ACRIFLAVINE  
SUSCEPTIBILITY IN *ESCHERICHIA  
COLI* AND *SALMONELLA  
TYPHIMURIUM***

## 6.1. Introduction

Bacterial efflux pumps are involved in the active transport of antimicrobials, metabolites and other compounds out of the cell (Blair et al., 2015a). Mutations that increase the expression of efflux pumps can result in reduced susceptibility to multiple antibiotics (Bailey et al., 2010, Blair et al., 2015a, Li et al., 1994, Blair et al., 2014). The most clinically important family of multidrug resistance efflux pumps in Enterobacteriaceae is the resistance nodulation division (RND) family, and more specifically, the AcrAB-TolC system (Blair et al., 2014). Homologs of AcrAB-TolC have been identified in many commensal and pathogenic bacteria (Pidcock, 2006a). This pump is negatively regulated locally by *acrR* and positively regulated globally by *marA* and *soxS* in *E. coli*, with the addition of *ramA* in *S. Typhimurium* (Okusu et al., 1996, Gallegos et al., 1997). As well as AcrAB, MarA, RamA, and SoxS can also regulate the expression of other efflux pumps, such as the RND pump AcrEF (Bailey et al., 2010) and a member of the multidrug and toxic compound extrusion (MATE) family, MdtK (Sun et al., 2011) in response to environmental stress.

TraDIS-*Xpress* was used to identify the genes that affected efflux activity. This was done by growing *E. coli* and *S. Typhimurium* transposon mutant libraries in the presence of subinhibitory and inhibitory concentrations of the efflux substrate acriflavine and comparing gene essentiality and expression to the unstressed control condition. To detangle the genes involved in efflux activity from the genes involved in acriflavine susceptibility, experiments were replicated for each concentration of acriflavine in the presence and absence of the efflux inhibitor PA $\beta$ N. Altogether, 67 genes in *E. coli* and 95 genes in *S. Typhimurium* were found to affect fitness in all conditions. Genes determined to affect efflux activity had roles in ribosome modification, respiration, glutathione metabolism, DNA housekeeping, cell signalling, transcriptional regulation and protein chaperones. Deletion mutants of several of these genes were tested for their effect on efflux activity, by measuring antimicrobial susceptibility and dye accumulation in the presence and absence of active efflux to validate the findings from TraDIS-*Xpress*. Additionally, pathways involved in acriflavine susceptibility (not efflux) were identified, furthering our knowledge of the mechanisms of acriflavine action and resistance. These included envelope biosynthesis, fimbriae expression, amino acid biosynthesis, DNA housekeeping, translation, motility and prophages. Overall, the work described in this chapter provides a broad overview of the genes that determine efflux activity and acriflavine susceptibility in *E. coli* and *S. Typhimurium* and demonstrates the overwhelming similarities in how both species response to drug stress.

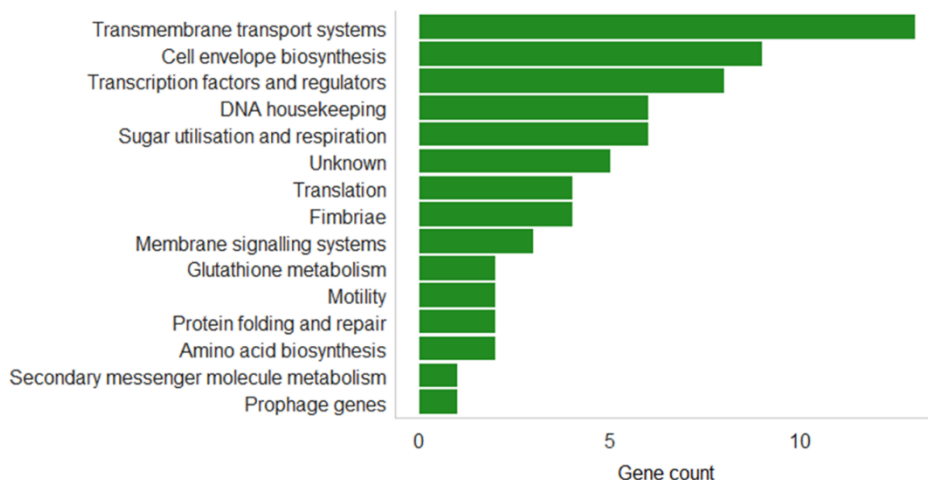
## 6.2. Aims

- To use TraDIS-*Xpress* to determine the genes involved in acriflavine susceptibility in the presence and absence of active efflux
- To detangle the genes involved in efflux activity from the genes involved in acriflavine susceptibility alone
- To phenotypically validate the roles of these genes in efflux activity

## 6.3. Validation of model efficacy through identification of genes known to be involved in efflux activity

Analysis of the TraDIS-*Xpress* data found a total of 67 genes in *E. coli* and 95 genes in *S. Typhimurium* affected fitness in all conditions - in the presence of acriflavine, PA $\beta$ N, and a combination of the two (Appendix 2). These were mostly involved in transmembrane transport, cell envelope biogenesis and transcription (figure 6.1). Insertion frequencies per gene between replicates was low, indicating low experimental error (Appendix 3).

### a) *E. coli*



### b) *S. Typhimurium*

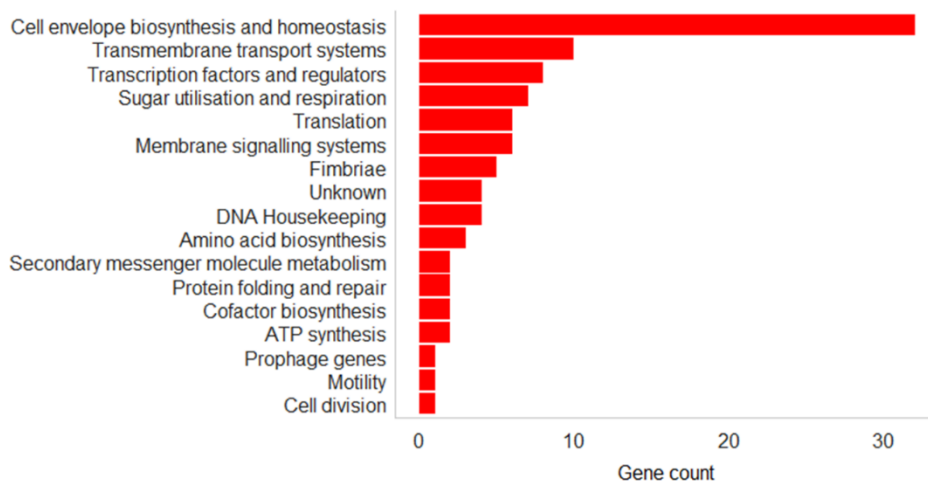


**Figure 6.1:** Analysis of the pathways involved in efflux activity and acriflavine susceptibility in **a) *E. coli*** and **b) *S. Typhimurium***.

To validate the predictions made by the TraDIS-*Xpress* data, dye accumulation (figure 6.2) and drug susceptibility (figure 6.3) were tested in various deletion mutants in *E. coli* and *S. Typhimurium* (figure 6.4). Drug susceptibility was tested using both broth and agar dilution methods, using antimicrobials including acriflavine, azithromycin and cefotaxime, all of which are substrates of RND efflux pumps, and non-efflux substrate gentamycin included as a control. Single gene deletion mutants in *E. coli* were retrieved from the Keio collection (Baba et al., 2006) and I constructed several deletion mutants in *S. Typhimurium*. Genes that appeared to affect efflux in both species were validated in the *E. coli* mutant alone. The largest difference in insertion frequencies between the stress conditions and unstressed controls were in genes encoding known efflux systems and their regulators, including *acrAB*, *acrR*, *marA* and *soxS*.

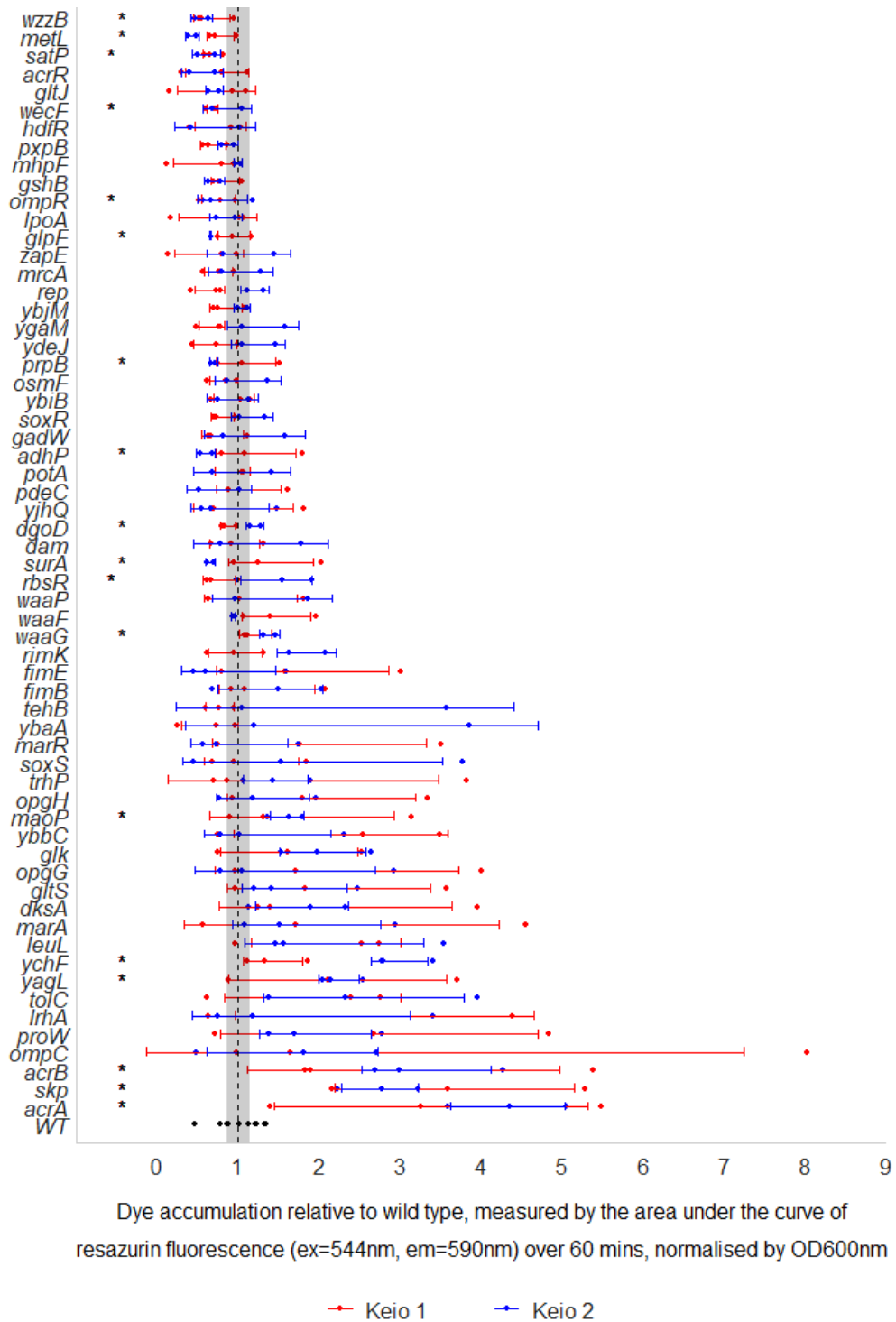


**Figure 6.2:** Dye accumulation in wild type *E. coli* and single gene deletion mutants from the Keio collection, where each copy of the deleted gene is separated by colour. Accumulation of resazurin (excitation 544 nm, emission 580 nm) was measured over 60 minutes and the area under the curve was plotted. Points represent each of 3 independent replicates. A singular asterisks (\*) shows a significant difference (Welch's *t*-test,  $p < 0.05$ ) in dye accumulation between the wild type and one copy of the deletion mutant, where the orientation of the asterisks indicates whether this significant difference is in the first (left) or second (right) Keio mutant copy. The shaded area shows the 95% confidence interval of the wild type and error bars show 95% confidence intervals of deletion mutants.

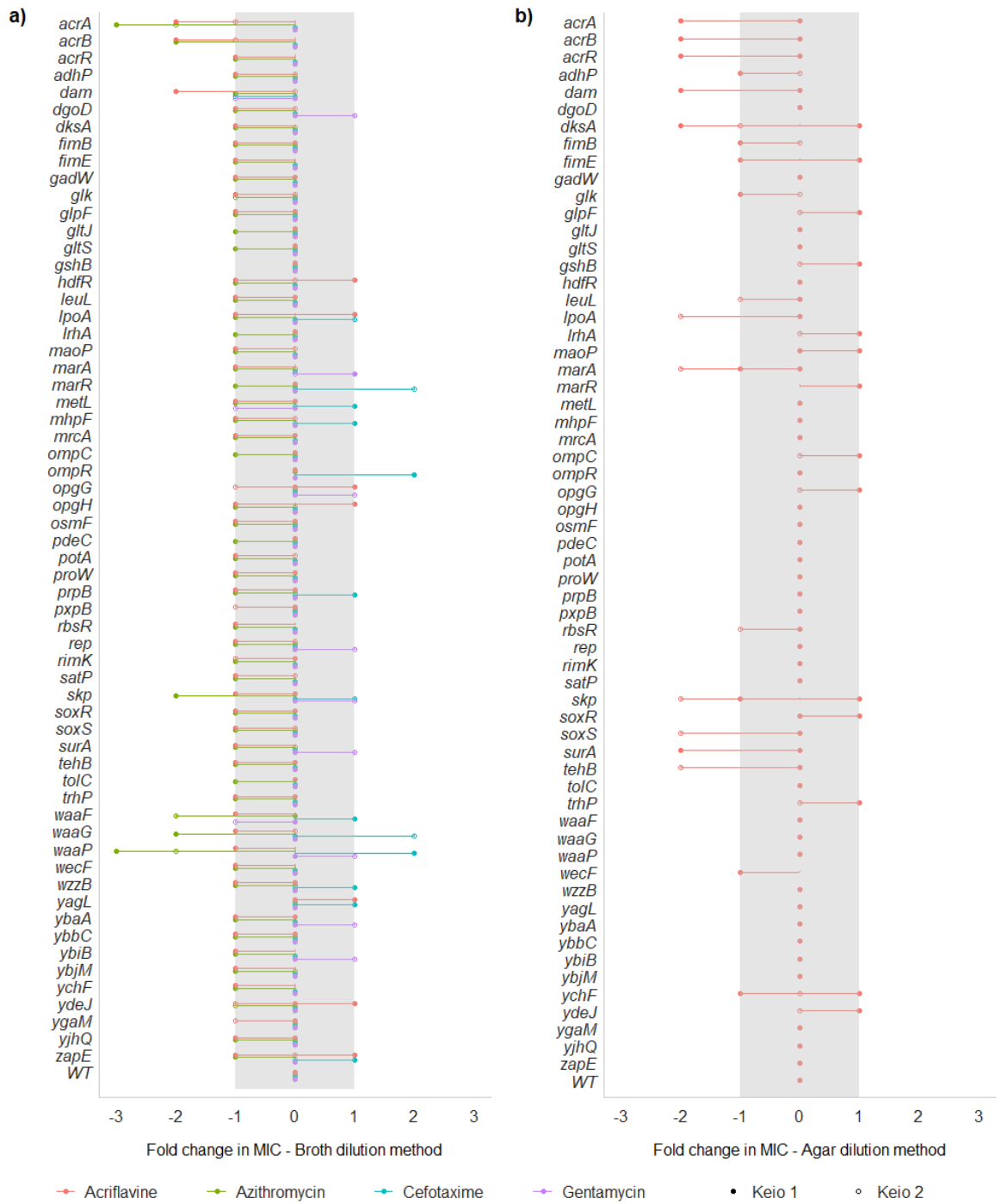


**Figure 6.3:** Fold change in MICs of acriflavine, azithromycin, cefotaxime and gentamycin in single deletion mutants from the Keio collection relative to wild type *E. coli*, measured by the **a)** broth and **b)** agar dilution methods. The shaded area shows an experimental error of 1-fold change and points show two independent replicates.



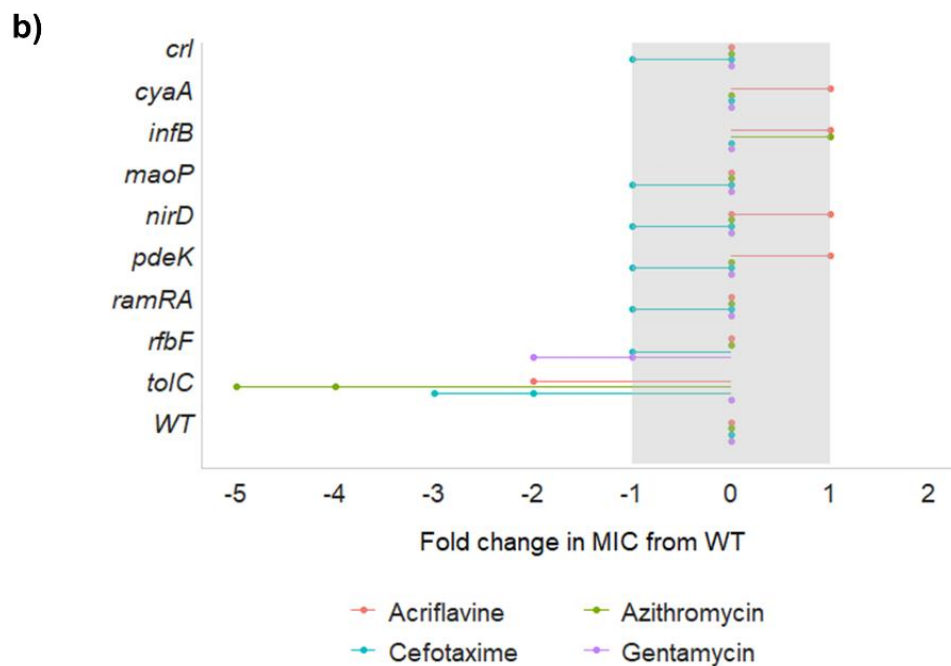
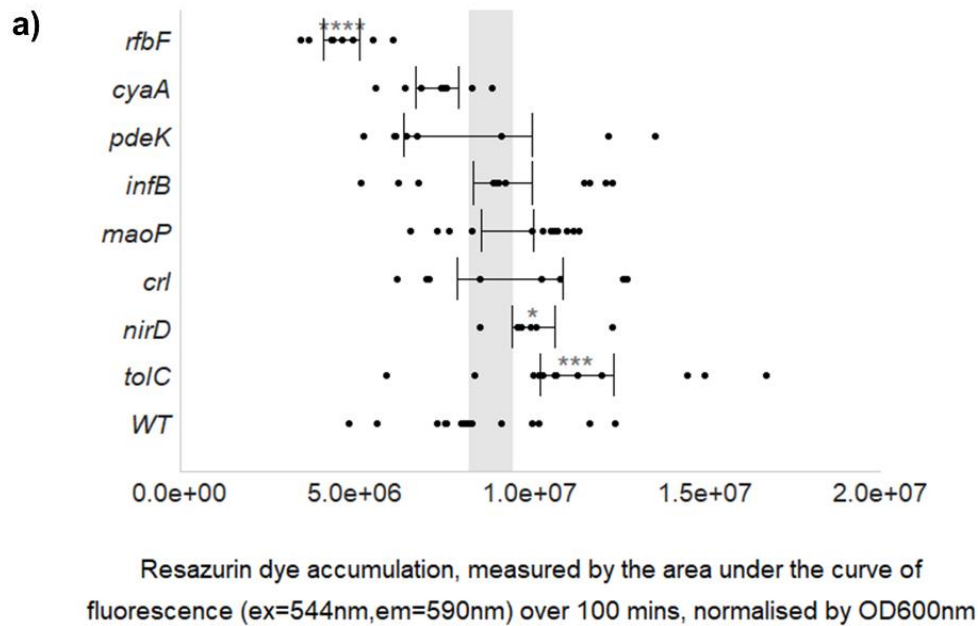


**Figure 6.4:** Efflux activity in wild type (WT) *S. Typhimurium* and deletion mutants. **a)** Dye accumulation in deletion mutants and the WT. Accumulation of resazurin (excitation 544 nm, emission 580 nm) was measured over 100 minutes and the area under the curve was plotted. Points each of two biological and four technical replicates. Asterisks (\*) show a significant difference in dye accumulation between the wild type and the knockout mutant (Wilcoxon rank sum, \* =  $p < 0.05$ , \*\* =  $p < 0.01$ , \*\*\* =  $p < 0.001$ , \*\*\*\* =  $p < 0.0001$ ). The shaded area shows the 95% confidence interval of the wild type and error bars show 95% confidence intervals of mutants. **b)** Fold change in MICs of acriflavine, azithromycin, cefotaxime and gentamycin in mutants relative to the WT, measured by the broth dilution method. The shaded area shows an experimental error of 1-fold change and points show two independent replicates.

### 6.3.1. AcrAB-TolC

The AcrAB-TolC efflux system is the main mechanism of resistance against acriflavine (Ma et al., 1995). In both *E. coli* and *S. Typhimurium*, fewer mutants mapped to *acrA*, *acrB* in the subinhibitory acriflavine condition relative to the unstressed control, and there were fewer mutants in *acrA*, *acrB* and *tolC* in the efflux-inhibited condition relative to the unstressed control (figure 6.5a). The local regulator of *acrAB* expression, *acrR*, had more transposon insertions in the condition stressed with a subinhibitory concentration of acriflavine in both *E. coli* and *S. Typhimurium*, relative to the unstressed controls (figure 6.5a). The difference in the insertions within *acrR* between the control and subinhibitory acriflavine conditions is very strong, showing the importance of this condition in identifying genes involved in efflux activity. This finding of genes involved in AcrAB-TolC efflux pump expression validates the efficacy of this model at identifying genes that affect efflux activity.

Deletion of either *acrA* or *acrB* in *E. coli* resulted in an increase in dye accumulation (figure 6.5b) and a significant increase in drug susceptibility (figure 6.5c). Increased dye uptake was seen in the  $\Delta tolC$  mutant and decreased dye uptake was seen in the  $\Delta acrR$  mutant in *E. coli*, but these were not significantly different from the wild type (figure 6.5b). Drug susceptibility was unchanged in the  $\Delta tolC$  mutant, and acriflavine susceptibility was increased in the  $\Delta acrR$  mutant when measured by agar dilution (figure 6.5c), despite previous studies reporting the contrary (Baucheron et al., 2004, Ricci et al., 2006, Okusu et al., 1996). This may reflect issues with the construction of these mutants in *E. coli*, as deletion of *tolC* in *S. Typhimurium* resulted in significantly increased dye accumulation and increased drug susceptibility as expected (figure 6.5 b,c).

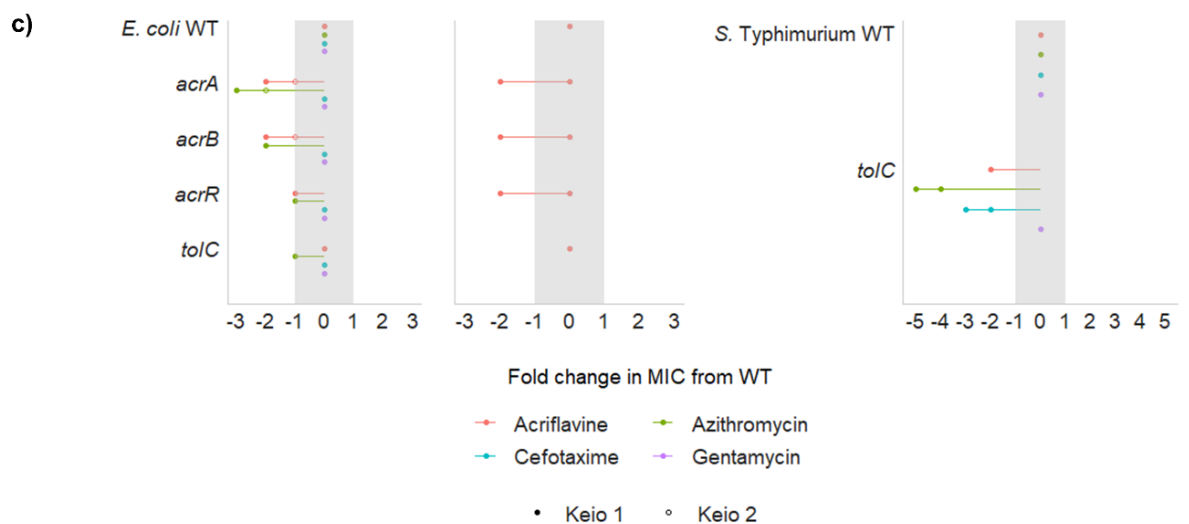
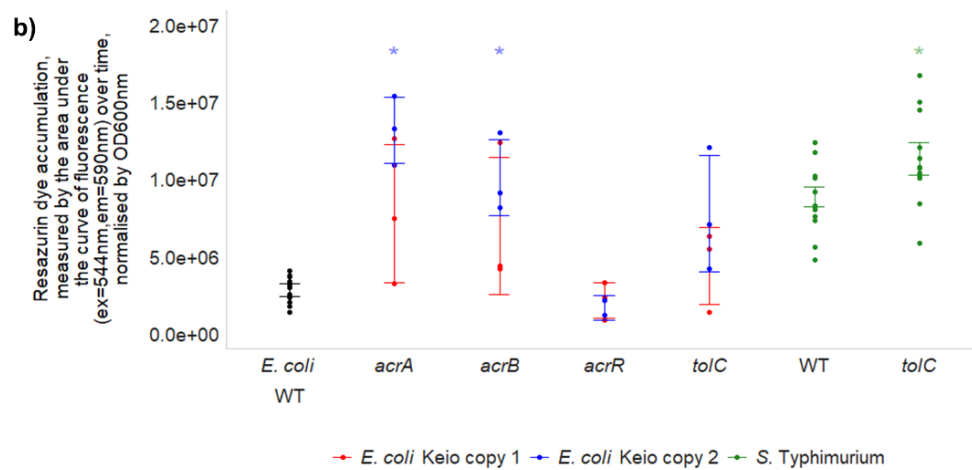
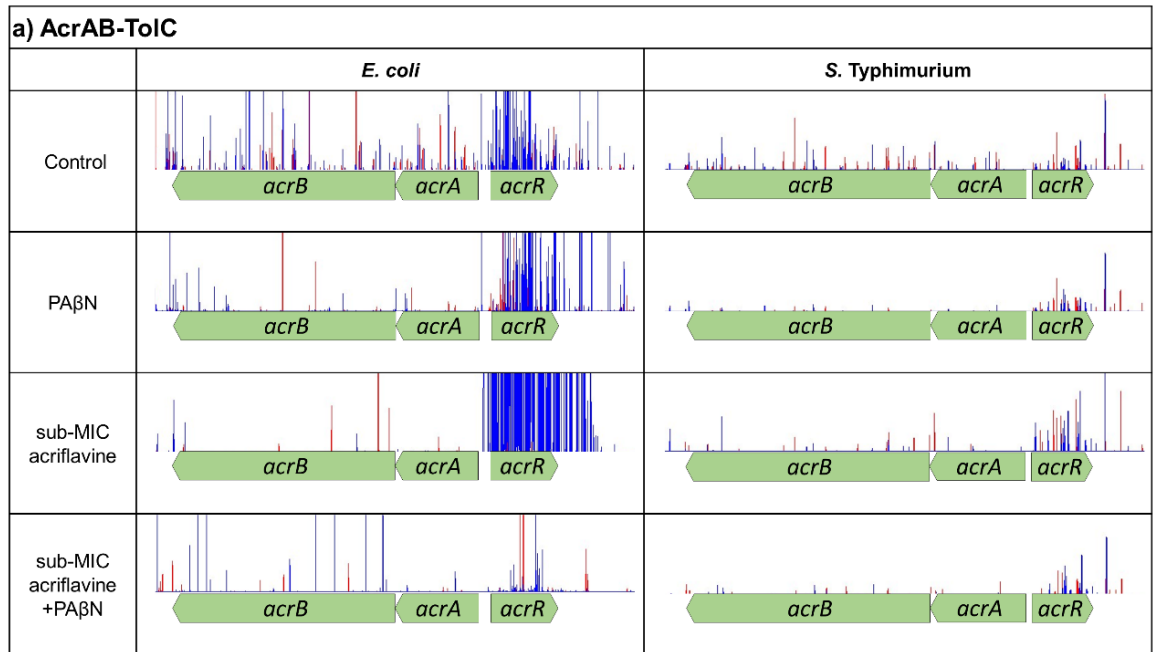


**Figure 6.5:** The effects of the AcrAB-TolC system on efflux activity in *E. coli* and *S. Typhimurium*. **a)** Mapped reads from TraDIS-*Xpress* data, plotted with BioTraDIS in Artemis, showing the location of transposon insertion sites in and around *acrAB*, *acrR* and *tolC* treated with subinhibitory concentrations of acriflavine and/or PA $\beta$ N in *E. coli* and *S. Typhimurium*. The height of the lines indicates the number of sequencing reads mapped to that locus and is used as a proxy for fitness. The colour of the lines indicates the direction that the transposon-located promoter faces, red denoting left-to-right and blue denoting right-to-left. Conditions with and without promoter induction with IPTG have been combined, and represent one of two independent replicates. **b)** Dye accumulation in the wild type and single gene deletion mutants in each species. Accumulation of resazurin (excitation 544 nm, emission 580 nm) was measured over 60 minutes in *E. coli* and 100 minutes in *S. Typhimurium* and the area under the curve was plotted. Points show 3 independent replicates. Asterisks (\*) show a significant difference (Welch's *t*-test,  $p < 0.05$ ) between the wild type and mutants. Colours discriminate between mutant copies. The shaded area shows the 95% confidence interval of the wild type and error bars show 95% confidence intervals of mutants. **c)** Fold change in MICs of acriflavine, azithromycin, cefotaxime and gentamycin in mutants relative to the wild type, measured by the broth dilution method (and the agar dilution method in *E. coli* shown in the middle panel). The shaded area shows an experimental error of 1-fold change and points show two independent replicates.

### 6.3.2. MarA, RamA and SoxS

The global transcriptional regulators *marA*, *ramA* and *soxS* play an essential role in regulating efflux pump expression in response to environmental stimuli (Holden and Webber, 2020). TraDIS-*Xpress* data from *E. coli* shows more insertions mapped upstream of and fewer insertions inside of both *marA* and *soxS* under subinhibitory concentrations of acriflavine relative to the unstressed control (figure 6.6a), demonstrating increased expression of these regulators is beneficial for fitness in these conditions. Expression of *marA*, *ramA* and *soxS* is negatively regulated by their local repressors *marR*, *ramR* and *soxR*. There were more mutants in *marR* and *soxR* in *E. coli* under subinhibitory concentrations of acriflavine relative to the unstressed control and relative to the condition treated with both PAβN and a subinhibitory concentration of acriflavine (figure 6.6a). This shows that disruption of *marR* or *soxR* is only beneficial for fitness in these conditions in the presence of active efflux, rather than a response to acriflavine alone. In *S. Typhimurium*, there are more insertions in *ramR* under subinhibitory concentrations of acriflavine relative to the unstressed control (figure 6.6a), suggesting that deletion of *ramR* is beneficial for in these conditions. The *ram* operon is the main regulator of antibiotic resistance in *S. Typhimurium*, which explains why disruption of *ramR*, rather than *marR* or *soxR*, is seen to affect fitness under antimicrobial stress.

Deletion of *marA*, *marR*, *soxS* or *soxR* in *E. coli* did not result in a significant change in dye accumulation (figure 6.6b), most probably due to the redundancy seen between these regulators (Holden and Webber, 2020). In *E. coli*, the  $\Delta marR$  mutant had a decreased in susceptibility to cefotaxime and the  $\Delta marA$  and  $\Delta soxS$  mutants had an increased susceptibility to acriflavine as measured by agar dilution (figure 6.6c). Drug susceptibility was unchanged for the  $\Delta soxR$  mutant in *E. coli* and the  $\Delta ramRA$  mutant in *S. Typhimurium* (figure 6.6c). Whilst there are clear overlaps in the phenotypes conferred by the genes controlled by MarA, RamA, and SoxS, MarA has often been found to be the most important transcriptional regulator for conferring AcrAB-TolC-mediated drug resistance in *E. coli* (Holden and Webber, 2020).

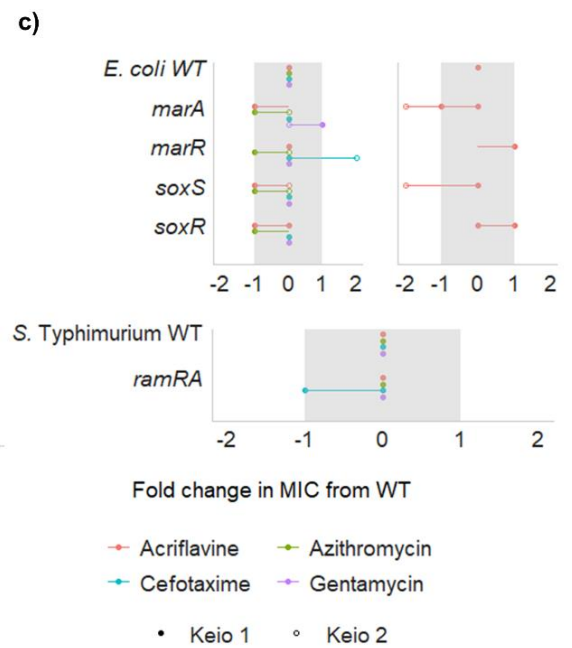
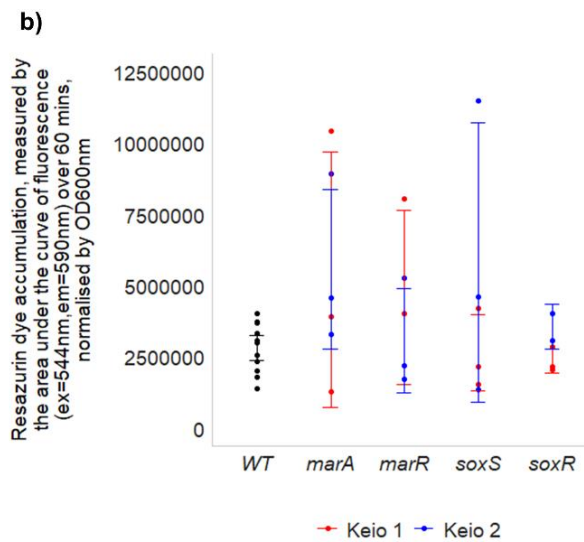
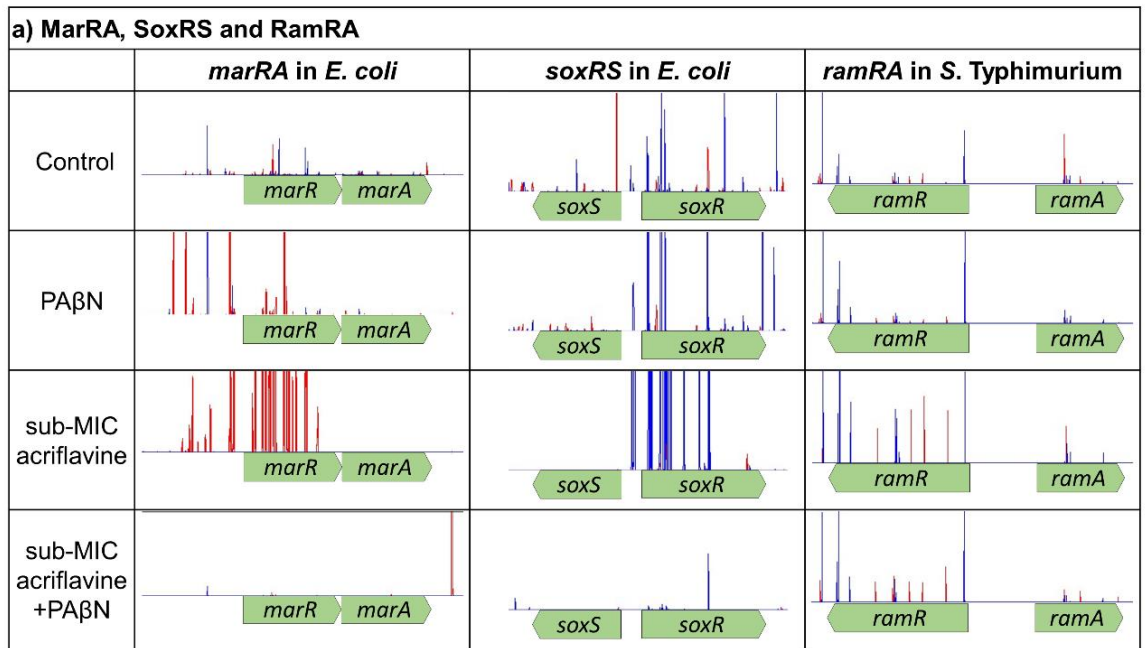


**Figure 6.6:** The effects of *marA*, *ramA* and *soxS* on efflux activity in *E. coli* and *S. Typhimurium*. **a)** Mapped reads from TraDIS-*Xpress* data, plotted with BioTraDIS in Artemis, showing the location of transposon insertion sites in and around *marRA* and *soxRS* in *E. coli* and *ramRA* in *S. Typhimurium* treated with subinhibitory concentrations of acriflavine and/or PA $\beta$ N. The height of the lines indicates the number of sequencing reads mapped to that locus and is used as a proxy for fitness. The colour of the lines indicates the direction that the transposon-located promoter faces, red denoting left-to-right and blue denoting right-to-left. Conditions with and without promoter induction with IPTG have been combined, and represent one of two independent replicates. **b)** Dye accumulation in the wild type and single gene deletion mutants. Accumulation of resazurin (excitation 544 nm, emission 580 nm) was measured over 60 minutes and the area under the curve was plotted. Points show 3 independent replicates. Colours discriminate between mutant copies. The shaded area shows the 95% confidence interval of the wild type and error bars show 95% confidence intervals of mutants. **c)** Fold change in MICs of acriflavine, azithromycin, cefotaxime and gentamycin in *E. coli* and *S. Typhimurium* single deletion mutants relative to the wild type, measured by the broth dilution method (and the agar dilution method in *E. coli* shown in the right-hand panel). The shaded area shows an experimental error of 1-fold change and points show two independent replicates.

### 6.3.3. Other transmembrane transport systems

In *S. Typhimurium*, *smvA* encodes an efflux pump important for acriflavine resistance (Villagra et al., 2008). Under subinhibitory concentrations of acriflavine, there were more insertions upstream and fewer insertions inside *smvA* relative to the unstressed control. This indicates that *smvA* is beneficial for fitness in the presence of subinhibitory concentrations of acriflavine, and overexpression of *smvA* increases fitness in these conditions.

Multiple transmembrane transport systems were seen to benefit fitness under subinhibitory concentrations of acriflavine. In *E. coli*, under subinhibitory concentrations of acriflavine relative to the unstressed control, there were fewer mutants mapped to *gltS* encoding a glutamate:sodium symporter (Kalman et al., 1991), *satP* encoding an acetate/succinate:H<sup>+</sup> symporter (Sá-Pessoa et al., 2013), and *osmF* (Lang et al., 2015), *potA* and *gltJ* (Moussatova et al., 2008), each encoding components of different ABC transport systems. There was no significant difference in dye uptake between the wild type and  $\Delta osmF$ ,  $\Delta gltJ$  or  $\Delta gltS$  mutants (figure 6.7a) and no difference in drug susceptibility was detected in any of these mutants (figure 6.7b). Deletion of *satP* caused a significant decrease in dye accumulation (figure 6.7a), contrary to what was predicted by TraDIS-*Xpress*, but no change in drug susceptibility (figure 6.7b). Deletion of these genes may cause a feedback loop that results in the overexpression of efflux regulators, which explains the significant decrease in dye accumulation under stress. There were also more insertions upstream of *proW*, encoding a glycine betaine ABC transporter membrane subunit, indicating its expression was beneficial for survival under subinhibitory concentrations of acriflavine relative to the unstressed control in *E. coli*. Deletion of *proW* resulted in a slightly increased dye uptake, although not significantly different from the wild type (figure 6.7a), however TraDIS-*Xpress* predicted *proW* overexpression would affect fitness rather than the gene's deletion, so its contribution to efflux cannot be ruled out. Overexpression of *xylH* was also seen to benefit efflux in *E. coli*, with more insertions upstream in conditions with subinhibitory concentrations of acriflavine and inhibited efflux, relative to the same concentration of acriflavine alone, indicating the role of *xylH* in efflux rather than survival under acriflavine alone. The genes encoding transmembrane transport systems that were seen to be beneficial for fitness in *S. Typhimurium* at inhibitory concentrations of acriflavine were *potD* encoding a spermidine preferential ABC transporter component (Kashiwagi et al., 1993) and *secM*, encoding a regulator of secretion through the Sec protein translocation pathway (Sarker and Oliver, 2002).

Various genes involved in transmembrane transport were seen to be detrimental to fitness in the presence of acriflavine. Under subinhibitory concentrations, more mutants mapped to *pitA*, encoding a phosphate:H<sup>+</sup> symporter (Harris et al., 2001) and *corA* encoding a



magnesium importer (Hmiel et al., 1986), relative to the unstressed control in *S. Typhimurium*. Under inhibitory concentrations of acriflavine, more mutants mapped to *glpF*, encoding a glycerol channel protein (Braun et al., 2000), relative to the unstressed control in *E. coli*. Deletion of *glpF* in *E. coli* resulted in a significant reduction in dye accumulation (figure 6.7a) but no change in acriflavine susceptibility (figure 6.7b). TraDIS-*Xpress* data showed that when efflux was inhibited with PA $\beta$ N, there were more insertions in *ompC*, encoding a major outer membrane porin, relative to the unstressed control in *E. coli*. Deletion of *ompC* resulted in a non-significant increase in dye accumulation (figure 6.7a) and no change in drug susceptibility (figure 6.7b). The gene encoding OmpR, involved in control of regulation of *ompC* and *ompF*, also had more insertions under subinhibitory concentrations of acriflavine relative to the control and relative to the condition treated with the same concentration of acriflavine plus the efflux inhibitor. This suggests a role for *ompR* in efflux rather than membrane permeability or acriflavine resistance in *E. coli*. We found deletion of *ompR* significantly reduced dye uptake (figure 6.7a) and reduced susceptibility to cefotaxime in *E. coli* (figure 6.7b). Previous studies have reported decreased susceptibility to cefoxitin and norfloxacin in an *ompR* deletion mutant (Ruiz and Levy, 2011), lending support to our finding that *ompR* may be detrimental to efflux activity.

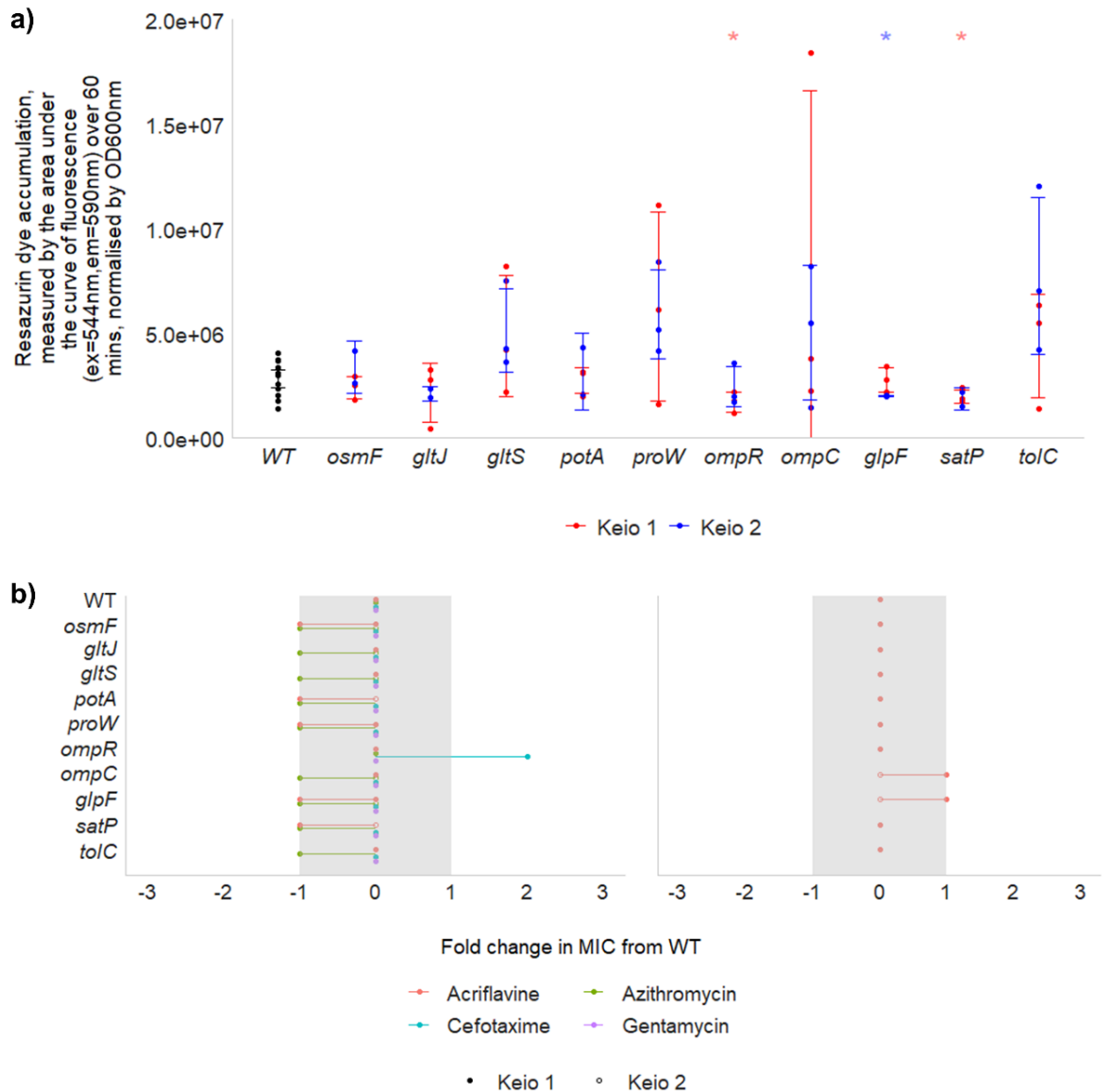


**Figure 6.7:** The effects of genes involved in transmembrane transport on efflux activity in *E. coli*. **a)** Dye accumulation in the wild type and single gene deletion mutants. Accumulation of resazurin (excitation 544 nm, emission 580 nm) was measured over 60 minutes and the area under the curve was plotted. Points show 3 independent replicates. Asterisks (\*) show a significant difference (Welch's *t*-test,  $p < 0.05$ ) between the wild type and mutants. Colours discriminate between mutant copies. The shaded area shows the 95% confidence interval of the wild type and error bars show 95% confidence intervals of mutants. **b)** Fold change in MICs of acriflavine, azithromycin, cefotaxime and gentamycin in mutants relative to each wild type, measured by the broth dilution (left) and agar dilution (right) methods. The shaded area shows an experimental error of 1-fold change and points show two independent replicates.

## 6.4. Genes impacting efflux activity in *E. coli* and *S. Typhimurium* have roles in protein chaperoning, DNA housekeeping and signalling

### 6.4.1. Protein chaperones

Chaperones involved in protein translocation and folding had a considerable effect on efflux activity. There were more mutants within *skp* in *E. coli* in conditions treated with PA $\beta$ N, and more mutants in *surA* when treated with a subinhibitory concentration of acriflavine, relative to unstressed controls. Deletion of *surA* significantly reduced dye uptake in *E. coli* (figure 6.8a), in accordance with the predictions made by TraDIS-*Xpress*. However, deletion of *skp* significantly increased dye uptake in *E. coli* (figure 6.8a). Susceptibility to acriflavine as measured by agar dilution was increased in both the  $\Delta$ *skp* and  $\Delta$ *surA* deletion mutants, and azithromycin susceptibility was increased in the  $\Delta$ *skp* mutant when measured by broth dilution (figure 6.8b). Deletion of *skp* resulted in a reduction in outer membrane porins OmpA, OmpC, OmpF and LamB (Chen and Henning, 1996), however *skp* does not affect TolC assembly (Werner et al., 2003). In *S. Typhimurium*, there were more insertions in *secB* when treated with either PA $\beta$ N or a subinhibitory concentration of acriflavine, relative to the unstressed control. SecB is involved in the correct folding of outer membrane proteins, such as *tolC* and *ompF* that affect membrane permeability (Baars et al., 2006). The TraDIS-*Xpress* data suggests that *skp*, *surA* and *secB* are detrimental for efflux activity, despite the phenotypic validation for the  $\Delta$ *skp* mutant suggesting otherwise, therefore further investigation into the role of these genes is needed to elucidate their relationship with efflux activity.

In *S. Typhimurium*, there were fewer insertions in *degS* when treated with PA $\beta$ N relative to the unstressed control. DegS is an inner membrane protease involved in the activation of  $\sigma^E$ , which governs the expression of genes involved in protein chaperoning, LPS biosynthesis and the envelope stress response (Alba and Gross, 2004). Many genes involved in cell envelope biogenesis have been highlighted by TraDIS-*Xpress* to affect fitness under acriflavine and PA $\beta$ N stress, as discussed in the next section, therefore protection of this regulator is consistent with these findings.

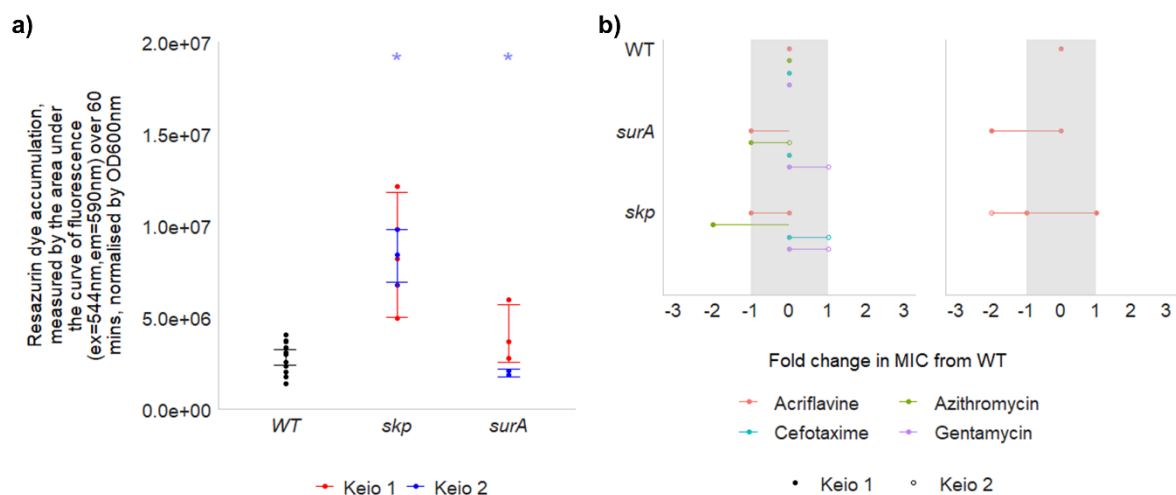


**Figure 6.8:** The effects of *skip* and *surA* on efflux activity in *E. coli*. **a)** Dye accumulation in the wild type and single gene deletion mutants. Accumulation of resazurin (excitation 544 nm, emission 580 nm) was measured over 60 minutes and the area under the curve was plotted. Points show 3 independent replicates. Asterisks (\*) show a significant difference (Welch's *t*-test,  $p < 0.05$ ) between the wild type and mutants. Colours discriminate between mutant copies. The shaded area shows the 95% confidence interval of the wild type and error bars show 95% confidence intervals of mutants. **b)** Fold change in MICs of acriflavine, azithromycin, cefotaxime and gentamycin in mutants relative to each wild type, measured by the broth dilution (left) and agar dilution (right) methods. The shaded area shows an experimental error of 1-fold change and points show two independent replicates.

#### 6.4.2. Transcription factors and regulators

In conditions treated with either PA $\beta$ N or subinhibitory concentrations of acriflavine, there were fewer insertions in *dskA* in *E. coli* and fewer insertions in *rpoS* in *S. Typhimurium*, relative to the unstressed controls of both libraries. Additionally, in *S. Typhimurium* under these same conditions, there were fewer insertions in *iraP*, involved in stabilisation of  $\sigma^S$  encoded by *rpoS* (Girard et al., 2018) and *crl*, which interacts with  $\sigma^S$  to increase transcription of the *rpoS* regulon in response to environmental stimuli (Bougdour et al., 2004). Deletion of *crl* in *S. Typhimurium* did not significantly affect dye uptake or drug susceptibility (figure 6.9 a,b). Both *dksA* and *rpoS* have previously been shown to affect the transcription of multiple transmembrane transport systems and their regulators (Wang et al., 2018, Dong and Schellhorn, 2009). Deletion of *dksA* in *E. coli* resulted in no change in dye uptake (figure 6.9a) but increased susceptibility to acriflavine (figure 6.9b). Increased expression of *marR*, resulting in repression of *marA*, has been reported in both  $\Delta dksA$  (Wang et al., 2018) and  $\Delta rpoS$  (Dong and Schellhorn, 2009) mutants, highlighting a possible mechanism through which *dksA* may affect efflux activity.

In *E. coli*, there were more insertions in *gadW* in conditions treated with PA $\beta$ N, and fewer insertions in *gadY* in conditions treated with both PA $\beta$ N and a subinhibitory concentration of acriflavine, relative to the wild type. The *gadXW* operon is involved in positive regulation of the principle acid resistance system, and *gadY* is a small regulatory RNA that stabilises the processing of *gadXW* mRNA (Tramonti et al., 2008). Deletion of *gadW* did not significantly affect dye accumulation or drug susceptibility in *E. coli* (figure 6.9 a,b). GadW may have been predicted to be detrimental to efflux activity by TraDIS-*Xpress* because it is negative regulator of the *gadXW* operon and *gadY*, thereby reducing induction of the acid resistance system. The relationship between this an efflux has not yet been confirmed.

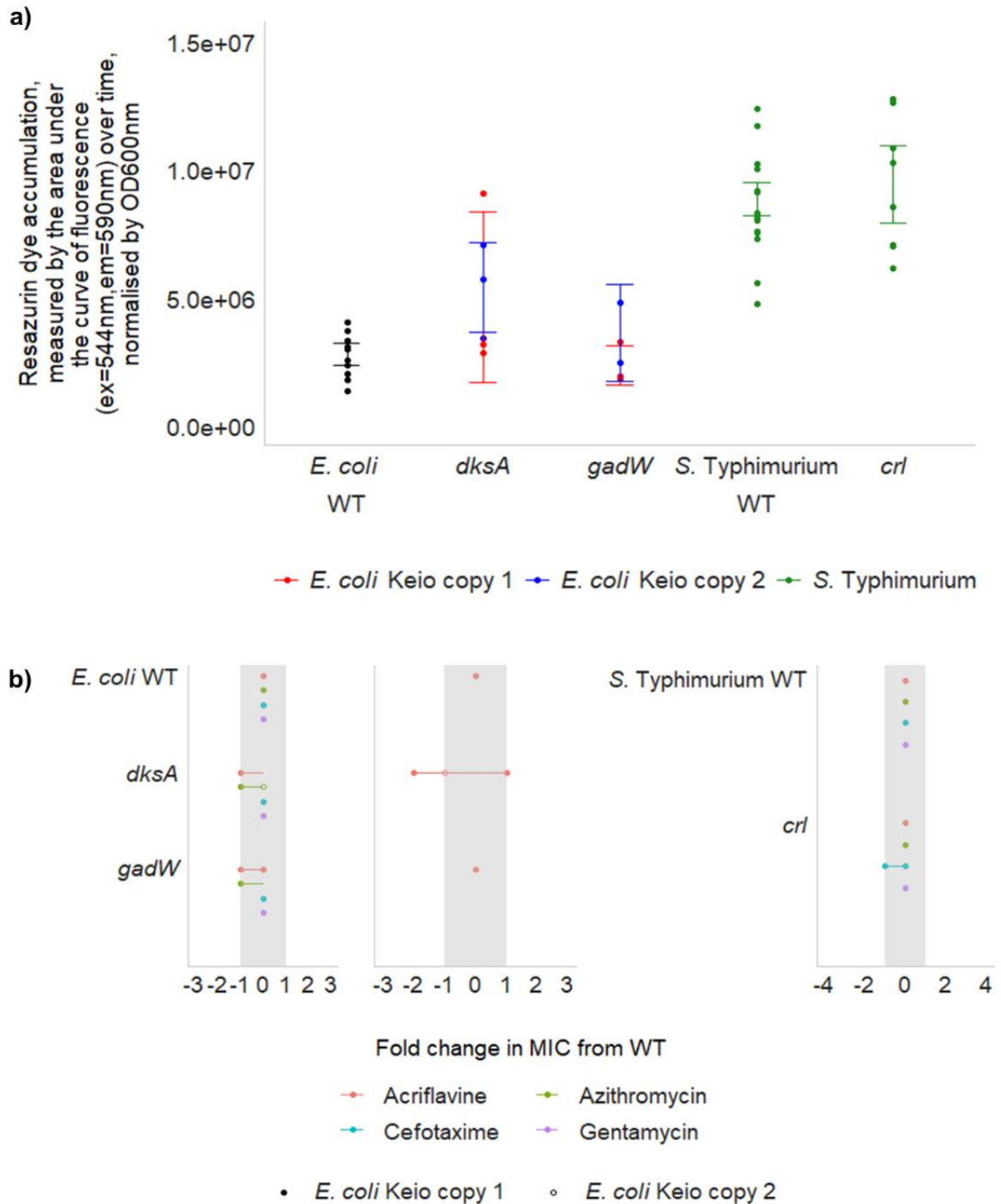


**Figure 6.9:** The effects of *dskA*, *gadW* and *crl* on efflux activity in *E. coli* and *S. Typhimurium*. **a)** Dye accumulation in the wild type and single gene deletion mutants in each species. Accumulation of resazurin (excitation 544 nm, emission 580 nm) was measured over 60 minutes in *E. coli* and 100 minutes in *S. Typhimurium* and the area under the curve was plotted. Points show 3 independent replicates. Colours discriminate between mutant copies. The shaded area shows the 95% confidence interval of the wild type and error bars show 95% confidence intervals of mutants. **b)** Fold change in MICs of acriflavine, azithromycin, cefotaxime and gentamycin in mutants relative to each wild type, measured by the broth dilution method (and the agar dilution method in *E. coli* shown in the middle panel). The shaded area shows an experimental error of 1-fold change and points show two independent replicates.

### 6.4.3. Signalling

Signalling systems involved in sensing environmental stresses and activating response regulators are extremely important in survival. CpxA is the sensory kinase component of the CpxAR two component system involved in maintaining the integrity of the cell envelope alongside the response regulator CpxR (Ruiz and Silhavy, 2005), and there were more insertions in *cpxA* under subinhibitory concentrations of acriflavine relative to the wild type in *S. Typhimurium*. The TraDIS-*Xpress* data suggests *cpxA* is deleterious for efflux activity in *S. Typhimurium*, however previous work has shown that the CpxAR system has a role in activating *marA* and *tolC* transcription (Weatherspoon-Griffin et al., 2014) and is important for survival when TolC-dependent efflux is inhibited (Rosner and Martin, 2013). It is possible that deletion of *cpxA* induces a membrane stress response that decreases acriflavine susceptibility.

There were fewer insertions in *phoP* and *phoQ*, encoding the PhoPQ two component sensory system (Kasahara et al., 1992), in *S. Typhimurium* treated with the efflux inhibitor relative to the unstressed control. The PhoPQ two component system has been reported to activate transcription of *tolC* (Zhang et al., 2008a), supporting our findings that *phoPQ* is important for efflux activity. Deletion of *phoPQ* in *Stenotrophomonas maltophilia* significantly increased susceptibility to a wide range of drugs (Lu et al., 2020), which may indicate that PhoPQ plays an important role in multidrug efflux in a number of species.

Biosynthesis of osmoregulated periplasmic glucans, achieved through *opgGH* (Bontemps-Gallo et al., 2017), seems to be detrimental for efflux activity in both *E. coli* and *S. Typhimurium*. There were more mutants mapped to both *opgG* and *opgH* in *E. coli* treated with PA $\beta$ N, relative to the unstressed control, and in *S. Typhimurium* treated with both PA $\beta$ N and subinhibitory concentrations of acriflavine, relative to acriflavine alone. Deletion of either *opgG* or *opgH* resulted in no significant change in dye uptake or drug susceptibility in *E. coli* (figure 6.10 a,b). Although the exact role of osmoregulated periplasmic glucans has not been elucidated, it has been suggested that they have a role in signalling, whereby their concentration in the periplasm may affect the activity of the EnvZ-OmpR and RcsCDB signalling systems (Bontemps-Gallo et al., 2013, Bontemps-Gallo et al., 2017).

Secondary messenger molecules play an important role in cell signalling. Cyclic-di-GMP phosphodiesterases were seen to effect efflux activity in both *E. coli* and *S. Typhimurium*. There were more insertions in *pdeC* in *E. coli* treated with inhibitory concentrations in acriflavine, and fewer mutants in *pdeK* in *S. Typhimurium* treated with PA $\beta$ N, relative to their unstressed controls. Deletion of *pdeC* in *E. coli* or *pdeK* in *S. Typhimurium* resulted no change in drug uptake or drug susceptibility (figure 6.10 a,b). A relationship between

*pdeC* and efflux activity has already been described, where expression of *pdeC* is reduced in a  $\Delta$ *soxS* mutant in *Klebsiella pneumoniae* (Huang et al., 2013). The gene responsible for cAMP biosynthesis, *cyaA* (Roy and Danchin, 1982), had more insertions in *S. Typhimurium* treated with subinhibitory concentrations of acriflavine relative to the unstressed control. Deletion of *cyaA* has been reported to reduce *marA*-mediated multidrug resistance in *E. coli* and resulted in significantly increased susceptibility to cefoxitin, norfloxacin, chloramphenicol and minocycline in a  $\Delta$ *marRA* background relative to a  $\Delta$ *marR* background (Ruiz and Levy, 2010). However the mechanism through which this occurs has not been reported, and its deletion had no significant effect on dye accumulation or drug susceptibility in *S. Typhimurium* (figure 6.10 a,b).



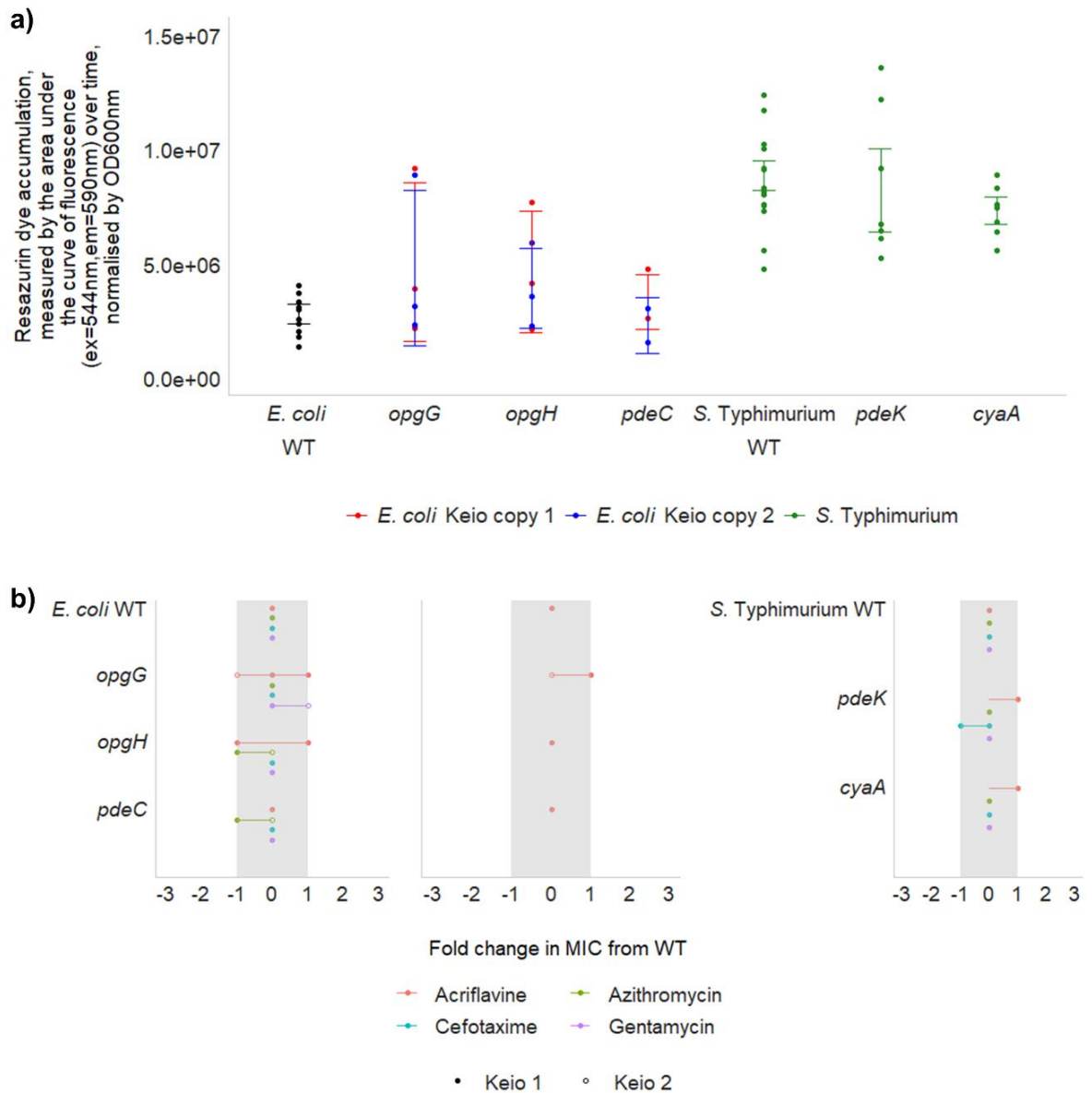


**Figure 6.10:** The effects of genes involved in signalling on efflux activity in *E. coli* and *S. Typhimurium*. **a)** Dye accumulation in the wild type and single gene deletion mutants in each species. Accumulation of resazurin (excitation 544 nm, emission 580 nm) was measured over 60 minutes in *E. coli* and 100 minutes in *S. Typhimurium* and the area under the curve was plotted. Points show 3 independent replicates. Colours discriminate between mutant copies. The shaded area shows the 95% confidence interval of the wild type and error bars show 95% confidence intervals of mutants. **b)** Fold change in MICs of acriflavine, azithromycin, cefotaxime and gentamycin in mutants relative to each wild type, measured by the broth dilution method (and the agar dilution method in *E. coli* shown in the middle panel). The shaded area shows an experimental error of 1-fold change and points show two independent replicates.

#### 6.4.4. DNA housekeeping

Two genes involved in DNA housekeeping were implicated in efflux activity by TraDIS-*Xpress*. There were fewer insertions in *dam*, encoding DNA adenine methyltransferase, in both *E. coli* and *S. Typhimurium* treated with subinhibitory concentrations of acriflavine relative to their unstressed controls. In *E. coli*, there were fewer insertions in *dam* in conditions treated with a subinhibitory concentration of acriflavine relative to conditions with both acriflavine and PA $\beta$ N, demonstrating the fitness benefit of *dam* only in conditions with functional efflux. Deletion of *dam* in *E. coli* resulted in increased susceptibility to acriflavine but no change in dye accumulation (figure 6.11 a,b). Multiple studies have suggested a link between *dam* and efflux activity (Motta et al., 2015, Adam et al., 2008), but a regulatory relationship has not yet been characterised. Previous work reported increased expression of *rpoS* and *marR* in a *dam* mutant relative to the wild type, but no change in expression of *acrAB*, *tolC* or *marA* involved in efflux activity (Hughes et al., 2020). However, other studies have reported reduced expression of *marR* (Løbner-Olesen et al., 2003) and increased expression of *marA* (Prieto et al., 2009) following deletion of *dam*. If DAM methylation affects expression of the *mar* operon, a phenotypic change in dye uptake may not be visible due to redundancy between the MarA, RamA and SoxS regulons (Holden and Webber, 2020). Additionally, *dam* regulates the expression of genes in the SOS regulon involved in DNA repair (Peterson et al., 1985, Cohen et al., 2016, Løbner-Olesen et al., 2003), and may affect drug susceptibility through multiple pathways.

There were fewer insertions in *maoP*, involved in chromosome organisation and orientation (Valens et al., 2016), when *E. coli* was treated with PA $\beta$ N relative to an unstressed control. Deletion of *maoP* in *E. coli* resulted in a significant increase in dye accumulation (figure 6.11a) but no change in drug susceptibility (figure 6.11b). However, dye uptake did not change following deletion of *maoP* in *S. Typhimurium* (figure 6.11 a). Previous work has found reduced expression of *maoP* in an *acrB*-deficient mutant relative to wild type *E. coli* (Ruiz and Levy, 2013), highlighting a regulatory pathway through which *maoP* expression and efflux activity may be linked.

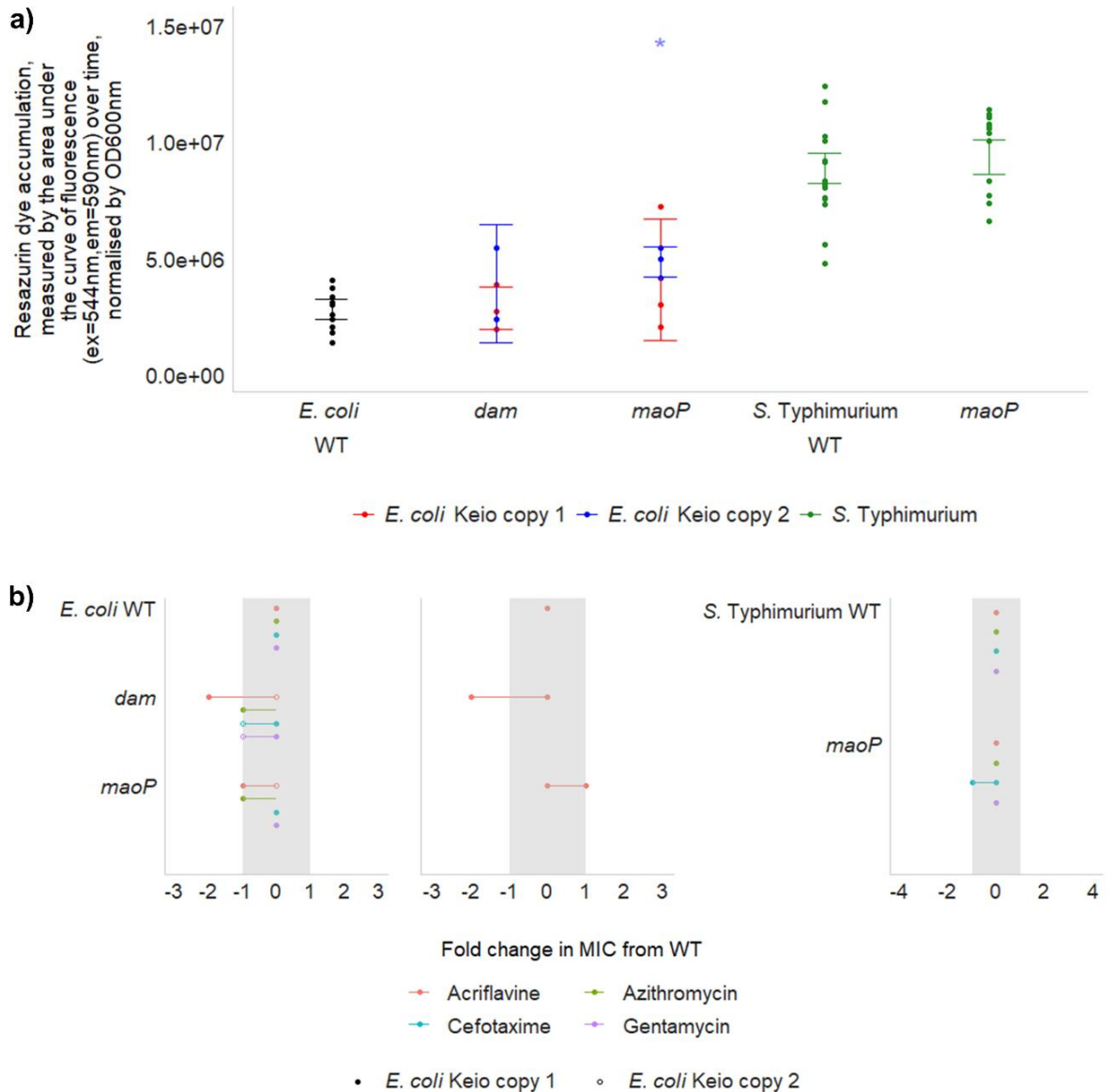


**Figure 6.11:** The effects of *dam* and *maoP* on efflux activity in *E. coli* and *S. Typhimurium*. **a)** Dye accumulation in the wild type and single gene deletion mutants in each species. Accumulation of resazurin (excitation 544 nm, emission 580 nm) was measured over 60 minutes in *E. coli* and 100 minutes in *S. Typhimurium* and the area under the curve was plotted. Points show 3 independent replicates. Asterisks (\*) show a significant difference (Welch's *t*-test,  $p < 0.05$ ) between the wild type and mutants. Colours discriminate between mutant copies. The shaded area shows the 95% confidence interval of the wild type and error bars show 95% confidence intervals of mutants. **b)** Fold change in MICs of acriflavine, azithromycin, cefotaxime and gentamycin in mutants relative to each wild type, measured by the broth dilution method (and the agar dilution method in *E. coli* shown in the middle panel). The shaded area shows an experimental error of 1-fold change and points show two independent replicates.

#### 6.4.5. Glutathione metabolism

Two genes involved in glutathione metabolism were implicated in efflux activity in *E. coli*. There were more mutants in *gshB*, involved in glutathione synthesis (Fuchs and Warner, 1975), in conditions treated with PA $\beta$ N relative to the unstressed control, and fewer mutants in *pxpB*, an 5-oxoprolinase responsible for breaking down glutathione to glutamate (Niehaus et al., 2017), in conditions treated with subinhibitory concentrations of acriflavine relative to the unstressed control and conditions with both PA $\beta$ N and acriflavine. Together, this suggests that glutathione is detrimental to efflux activity in *E. coli*. The *pxpABC* genes cluster with those encoding various transporters (Niehaus et al., 2017) and a role for the  $\gamma$ -glutamyl cycle in amino acid transport has previously been suggested (Orlowski and Meister, 1970), therefore it may be through this mechanism that glutathione metabolism affects efflux activity in *E. coli*. However, deletion of *gshB* or *pxpB* in *E. coli* had no effect on dye accumulation or drug susceptibility (figure 6.12 a,b), so any effect of glutathione metabolism on efflux activity may be small.

There were fewer insertions in *STM14\_1969* in *S. Typhimurium* treated with inhibitory concentrations of acriflavine, relative to conditions with both PA $\beta$ N and acriflavine and relative to an unstressed control. This gene is homologous to *frmR*, encoding a negative transcriptional regulator of *frmAB* involved in glutathione-dependent formaldehyde detoxification (Herring and Blattner, 2004). Repression of this pathway may be beneficial to efflux activity by maximising glutathione catabolism through the  $\gamma$ -glutamyl cycle.

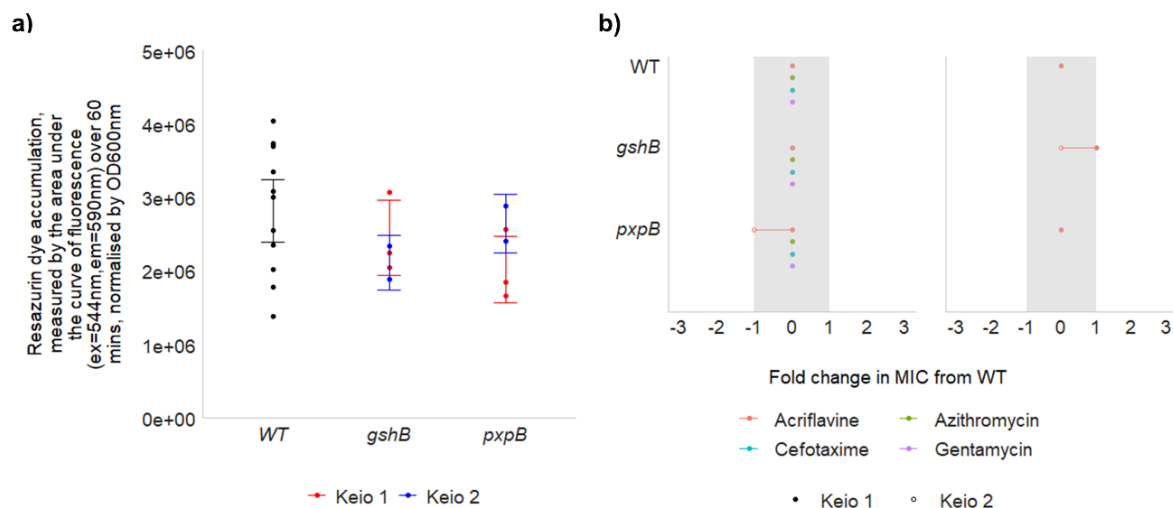


**Figure 6.12:** The effects of *gshB* and *pxpB* on efflux activity in *E. coli*. **a)** Dye accumulation in the wild type and single gene deletion mutants. Accumulation of resazurin (excitation 544 nm, emission 580 nm) was measured over 60 minutes and the area under the curve was plotted. Points show 3 independent replicates. Colours discriminate between mutant copies. The shaded area shows the 95% confidence interval of the wild type and error bars show 95% confidence intervals of mutants. **b)** Fold change in MICs of acriflavine, azithromycin, cefotaxime and gentamycin in mutants relative to each wild type, measured by the broth dilution (left) and agar dilution (right) methods. The shaded area shows an experimental error of 1-fold change and points show two independent replicates.

#### 6.4.6. Respiration

Genes involved in sugar degradation and respiration were beneficial for survival in *E. coli* and *S. Typhimurium* when under efflux stress. There were fewer insertions in *dgoD*, involved in D-galactonate degradation (Deacon and Cooper, 1977), and *adhP*, an alcohol dehydrogenase involved in mixed acid fermentation (Shafqat et al., 1999), in *E. coli* treated with subinhibitory concentrations of acriflavine relative to conditions with acriflavine and PA $\beta$ N, and relative to the unstressed control. This suggests a role for these genes in efflux activity, as they are beneficial to survival only when efflux is not inhibited. Similarly, there were fewer insertions in *prpB* in *E. coli*, and *citG* and *STM14\_0712* in *S. Typhimurium* when treated with inhibitory concentrations of acriflavine relative to conditions with acriflavine and PA $\beta$ N, and the unstressed controls. In *S. Typhimurium*, there were fewer mutants in *nagA* when treated with PA $\beta$ N relative to the unstressed control, and fewer mutants in *nirD* when treated with inhibitory concentrations of acriflavine, relative to the unstressed control. PrpB is involved in propionate catabolism to pyruvate (Brock et al., 2001), CitG is involved in citrate lyase activation (Schneider et al., 2000), STM14\_0712 has homology with the terminal electron transfer enzyme DmsC (Weiner et al., 1993), NagA is involved in catabolism of N-acetyl-D-glucosamine for use as a carbon source (Hall et al., 2007) and NirD is a nitrite reductase involved in anaerobic growth (Harborne et al., 1992). There was a significant increase in dye accumulation in the  $\Delta dgoD$  mutant and a significant decrease in the  $\Delta adhP$  and  $\Delta prpB$  mutants in *E. coli* (figure 6.13a). In *S. Typhimurium*, dye uptake was significantly increased in the *nirD* mutant relative to the wild type (figure 6.13a). However, there was no change in drug susceptibility when any of these genes were deleted (figure 6.13b). There is a relationship with efflux regulator RamA and both *adhP* and *nirD*: RamA has been shown to directly bind to and increase transcription of *adhP* in *Klebsiella pneumoniae* (De Majumdar et al., 2015), and expression of *nirD* was reduced when *ramA* was overexpressed (De Majumdar et al., 2015) and when *acrB* was disrupted (which leads to *ramA* overexpression) (Webber et al., 2009). The benefit of these genes to efflux activity is unclear from this regulatory relationship alone. Respiration generates ATP and a proton gradient to power efflux pumps, but the pathway through which these genes may impact efflux activity is not clear.

Two genes involved in ribose catabolism and transport were seen to be beneficial to efflux activity in the TraDIS-*Xpress* data from both *E. coli* and *S. Typhimurium*. There were more insertions upstream of *rbsK*, indicating a fitness benefit to its overexpression, in *S. Typhimurium* treated with subinhibitory concentrations of acriflavine relative to the unstressed control. In both *E. coli* and *S. Typhimurium*, there were fewer mutants mapped to the negative regulator of the ribose catabolism operon, *rbsR*, when treated with subinhibitory concentrations of acriflavine, relative to conditions with both PA $\beta$ N and acriflavine and relative to the unstressed control. Contrary to the prediction from the

TraDIS-*Xpress* data, deletion of *rbsR* resulted in significantly reduced dye accumulation in *E. coli* (figure 6.13a) and no change in drug susceptibility (figure 6.13b). RbsR is a negative regulator of the *rbs* operon, which encodes a D-ribose degradation and transport system (Lopilato et al., 1984) and is involved in regulating purine nucleotide biosynthesis and salvage (Shimada et al., 2013). Purine biosynthesis has previously been implicated in activation of the *acrAB* promoter, where cellular metabolites from this pathway induce efflux pump expression (Ruiz and Levy, 2013). Deletion of *rbsR* may increase ribose catabolism, resulting in a detrimental effect on efflux activity.

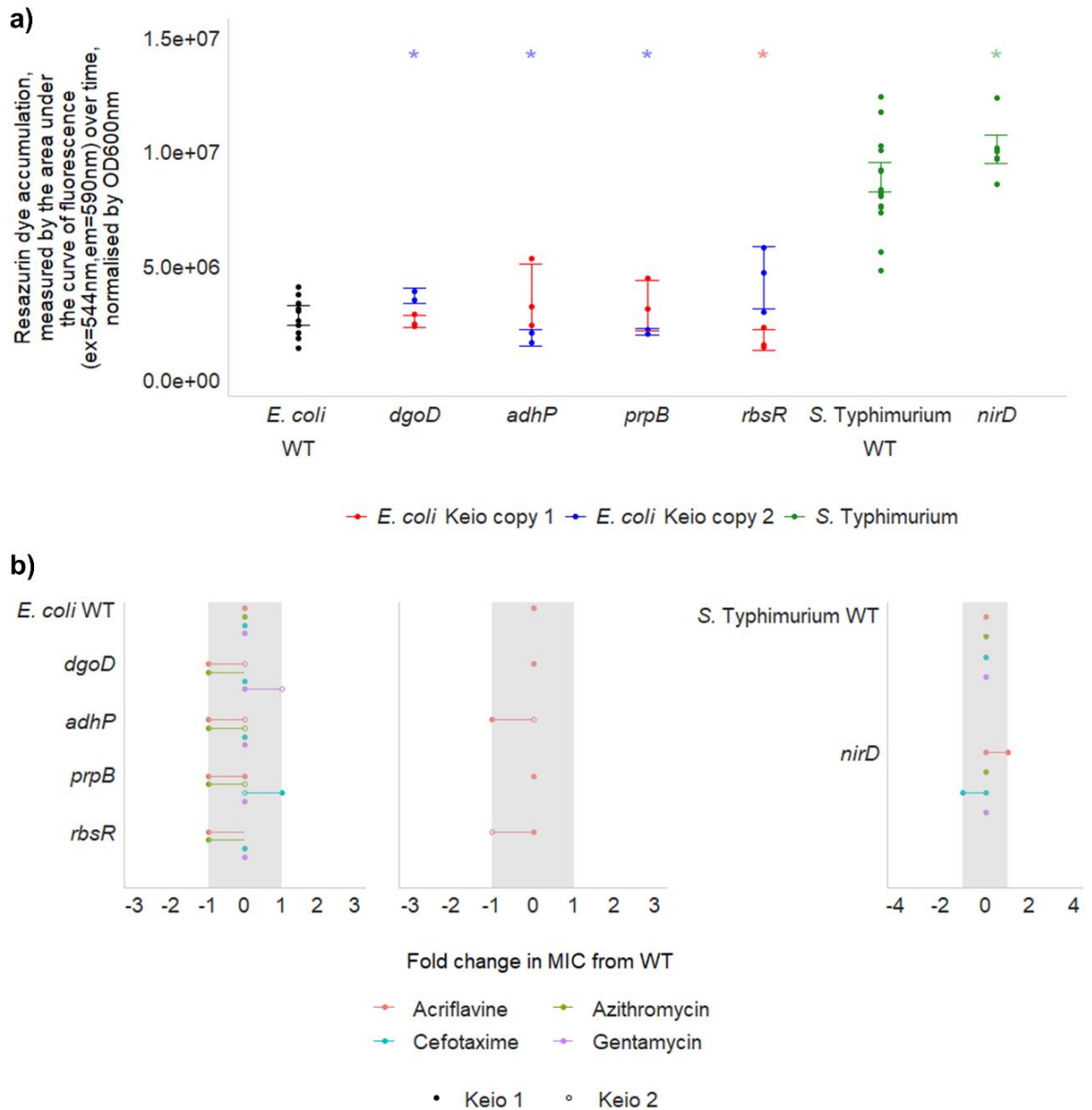


**Figure 6.13:** The effects of genes involved in respiration on efflux activity in *E. coli* and *S. Typhimurium*. **a)** Dye accumulation in the wild type and single gene deletion mutants in each species. Accumulation of resazurin (excitation 544 nm, emission 580 nm) was measured over 60 minutes in *E. coli* and 100 minutes in *S. Typhimurium* and the area under the curve was plotted. Points show 3 independent replicates. Asterisks (\*) show a significant difference (Welch's *t*-test,  $p < 0.05$ ) between the wild type and mutants. Colours discriminate between mutant copies. The shaded area shows the 95% confidence interval of the wild type and error bars show 95% confidence intervals of mutants. **b)** Fold change in MICs of acriflavine, azithromycin, cefotaxime and gentamycin in mutants relative to each wild type, measured by the broth dilution method (and the agar dilution method in *E. coli* shown in the middle panel). The shaded area shows an experimental error of 1-fold change and points show two independent replicates.



### 6.4.7. Ribosome modification

Genes involved in ribosomal modification were beneficial for fitness under efflux stress. The TraDIS-*Xpress* data showed fewer mutants in *ychF* in *E. coli* treated with subinhibitory concentrations of acriflavine relative to conditions with both acriflavine and PA $\beta$ N and relative to an unstressed control, suggesting *ychF* only benefits fitness when efflux is not inhibited. There was a significant increase in drug accumulation in the  $\Delta ychF$  mutant, but no change in drug susceptibility (figure 6.14 a,b). YchF is an ATPase that binds to the 50S and 70S ribosomal subunits and may have a role in regulating translation (Tomar et al., 2011). It has previously been implicated in survival under oxidative stress (Zorraquino et al., 2017), but its role in efflux activity requires further characterisation. There were also fewer insertions in *rimK*, involved in ribosomal modification (Kang et al., 1989), in *E. coli* treated with subinhibitory concentrations of acriflavine relative to the unstressed control. Dye uptake was increased in the  $\Delta rimK$  mutant relative to the wild type but not significantly and there was no change in drug susceptibility (figure 6.14 a,b). A reduction in *rimK* expression was reported in  $\Delta ramA$  mutant relative to wild type *S. Typhimurium* (Zheng et al., 2011), highlighting the relationship between ribosome modification and efflux activity.

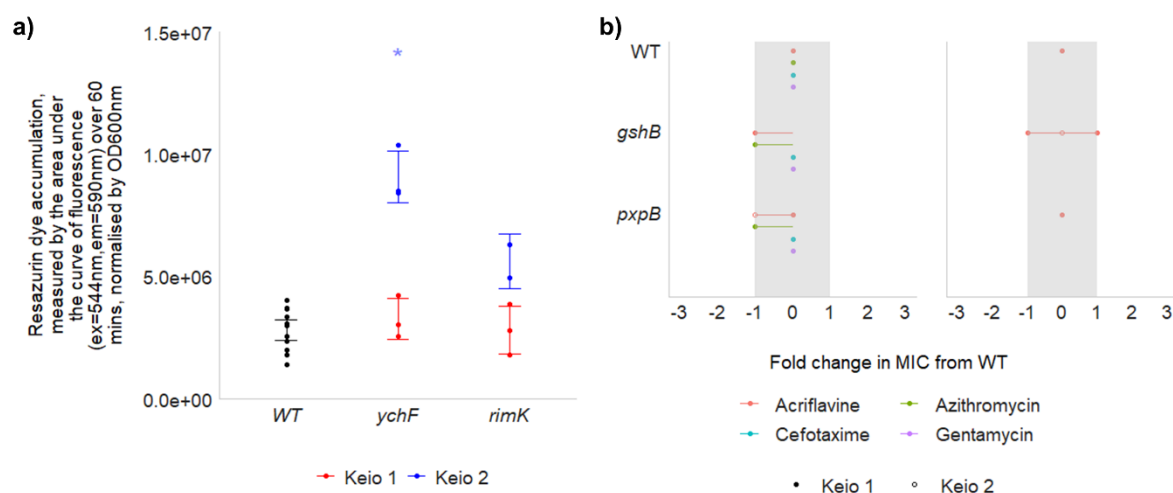


**Figure 6.14:** The effects of *ychF* and *rimK* on efflux activity in *E. coli*. **a)** Dye accumulation in the wild type and single gene deletion mutants. Accumulation of resazurin (excitation 544 nm, emission 580 nm) was measured over 60 minutes and the area under the curve was plotted. Points show 3 independent replicates. Asterisks (\*) show a significant difference (Welch's *t*-test,  $p < 0.05$ ) between the wild type and mutants. Colours discriminate between mutant copies. The shaded area shows the 95% confidence interval of the wild type and error bars show 95% confidence intervals of mutants. **b)** Fold change in MICs of acriflavine, azithromycin, cefotaxime and gentamycin in mutants relative to each wild type, measured by the broth dilution (left) and agar dilution (right) methods. The shaded area shows an experimental error of 1-fold change and points show two independent replicates.

## **6.5. Genes impacting acriflavine susceptibility in *E. coli* and *S. Typhimurium* have roles in cell envelope biogenesis, fimbriae expression and amino acid biosynthesis**

### **6.5.1. Peptidoglycan biosynthesis**

Peptidoglycan biosynthesis was extremely important for the fitness of both *E. coli* and *S. Typhimurium* under efflux stress. There were fewer insertions in the genes encoding penicillin binding proteins 1 and 2 (Suzuki et al., 1978), *mrcA* (PBP1) in *E. coli* and *mrcB* (PBP2) in *S. Typhimurium*, when treated with PA $\beta$ N relative to the unstressed controls. Under the same conditions in *E. coli*, there were also fewer insertions in *lpoA*, which encodes an outer membrane protein essential for PBP1 function (Typas et al., 2010). Deletion of *mrcA* or *lpoA* in *E. coli* did not affect dye accumulation (figure 6.15a), but there was a significant increase in acriflavine susceptibility in the  $\Delta$ *lpoA* mutant (figure 6.15b). Under inhibitory concentrations of acriflavine, some genes involved in peptidoglycan biosynthesis appeared detrimental to fitness. Relative to the unstressed control, there were more insertions in *ddlB* in *E. coli*, encoding a D-alanine—D-alanine ligase (Zawadzke et al., 1991), and *prc* in *S. Typhimurium*, encoding a protease with a role in PBP3 maturation and peptidoglycan biosynthesis regulation (Hara et al., 1991).

Genes involved in maintaining membrane integrity during cell division affected the fitness of *S. Typhimurium* when treated with acriflavine and PA $\beta$ N. There were more insertions in *zapE*, involved in Z-ring formation (Marteyn et al., 2014), when treated with a subinhibitory concentration of acriflavine relative to an unstressed control. When *zapE* was disrupted in *E. coli*, there was no change in dye uptake or drug susceptibility (figure 6.15 a,b). There were more insertions in four genes constituting the Tol-Pal system involved in maintaining cell membrane integrity during outer membrane invagination, *tolB*, *tolQ*, *tolA* and *tolR* (Gerding et al., 2007), under inhibitory concentrations of acriflavine relative to the unstressed control. This suggests that production of some components of cell division were detrimental to the survival of *S. Typhimurium* in the presence of acriflavine. However, there were fewer insertions in *nlpD* in conditions treated with PA $\beta$ N or subinhibitory concentrations of acriflavine relative to an unstressed control. NlpD activates amidases during cell division to break down peptidoglycan at the correct moment to maintain cell membrane integrity (Tsang et al., 2017). This strict regulation of cell division to maintain membrane integrity may be essential for optimising fitness under drug stresses, but it is doubtful whether this affects the function of efflux pumps.

### 6.5.2. LPS

LPS is made up of lipid A, which anchors the LPS into the membrane, an inner core, outer core and O-antigen (Wang et al., 2015). The TraDIS-*Xpress* data suggests genes involved in the biosynthesis of each of these components affects fitness differently under different stresses. Starting off with lipid A biosynthesis, there were more insertions upstream of *lpxD* in *E. coli* treated with PA $\beta$ N relative to the unstressed control, suggesting that increased expression of *lpxD*, was beneficial for fitness in the absence of active efflux. *LpxD* is an essential gene (Ma et al., 2020), where its inactivation is lethal to the cell. Previous work using TraDIS-*Xpress* has also identified *lpxD* to be beneficial for fitness when treated with triclosan, another efflux substrate (Yasir et al., 2020). Additionally, expression of *ramA* has been shown to affect lipid A biosynthesis through the *lpx* operon (De Majumdar et al., 2015), suggesting a pathway through which modulation of efflux activity may affect LPS biosynthesis.

Multiple genes involved in LPS core biosynthesis affected the fitness of both *E. coli* and *S. Typhimurium* differently. In *E. coli*, there were more insertions in *waaP* when treated with PA $\beta$ N and *waaG* when treated with inhibitory concentrations of acriflavine, relative to unstressed controls. There were also more mutants mapped to *waaF* when treated with subinhibitory concentrations of acriflavine and PA $\beta$ N, relative to acriflavine alone. Deletion of either *waaP*, *waaG* or *waaF* resulted in a significant increase azithromycin susceptibility and deletion of *waaP* or *waaG* resulted in decreased susceptibility to cefotaxime (figure 6.15b). Dye accumulation was significantly increased in the  $\Delta waaG$  mutant, but no change in dye accumulation was seen for the  $\Delta waaF$  or  $\Delta waaP$  mutants (figure 6.15a). In *S. Typhimurium*, *rfaJ* (homologous to *waaJ* in *E. coli*) and *rfaI* (homologous to *waaO* in *E. coli*) involved in outer core biosynthesis were beneficial to fitness. There were fewer mutants in *rfaJ*, and more mutants upstream of *rfaI* promoting increased expression, when treated with subinhibitory concentrations of acriflavine and PA $\beta$ N relative to acriflavine alone. Under the same condition, there were also fewer insertions in *rfaL* (homologous to *waaL* in *E. coli*), involved in connecting the O-antigen to the outer core (Ruan et al., 2012). This suggest that LPS core biosynthesis is beneficial for *S. Typhimurium* fitness in the presence of acriflavine without active efflux.

*E. coli* K-12 does not produce an O-antigen (Stevenson et al., 1994), but *S. Typhimurium* does. The *rfb* operon, involved in O-antigen production (Jiang et al., 1991). affected the fitness of *S. Typhimurium* differently under different stresses. There were fewer insertions in *rfbF*, *rfbG* and *rfbH* when treated with either PA $\beta$ N or subinhibitory concentrations of acriflavine, relative to an unstressed control. *RfbA* *rfbC*, *rfbI* and *rfbN* were all beneficial to survival in the absence of active efflux, with fewer mutants mapped to all these genes in conditions with PA $\beta$ N and subinhibitory concentrations of acriflavine relative to acriflavine

alone. However, when treated with inhibitory concentrations of acriflavine, there were more mutants in *rfaA*, *rfaK*, *rfaM*, *rfaU* and *rfaX*, relative to the unstressed control. The effect of O-antigen biosynthesis on efflux activity was investigated phenotypically in *S. Typhimurium* through an  $\Delta rfaF$  mutant. The significant reduction in dye accumulation seen in the  $\Delta rfaF$  mutant in the presence and absence of PA $\beta$ N was because the concentration of resazurin and PA $\beta$ N in this assay were lethal to this mutant (figure 6.15a). There was a significant increase in gentamycin susceptibility in the  $\Delta rfaF$  mutant, but drug susceptibility was unchanged for acriflavine, azithromycin and cefotaxime (figure 6.15b). Because gentamycin is not an efflux substrate, this suggests that LPS biosynthesis affects membrane permeability and drug susceptibility in a manner that is independent to efflux activity.

In *E. coli*, there were fewer mutants in *wzzB* when treated with subinhibitory concentrations of acriflavine relative to the unstressed control and relative to conditions treated with both acriflavine and PA $\beta$ N. Deletion of *wzzB* resulted in significantly reduced dye uptake in *E. coli* (figure 6.15a). WzzB has a role in regulating the length of the O-antigen (Franco et al., 1996), despite *E. coli* K-12 not producing an O-antigen. Instead, it is more likely that the fitness benefit provided by *wzzB* is due to its role in regulating the length of another outer membrane polysaccharide, enterobacterial common antigen (Leo et al., 2021).

### 6.5.3. Enterobacterial common antigen

Much like LPS, enterobacterial common antigen (ECA) is a surface-located outer membrane component but is restricted to the Enterobacteriaceae family. The TraDIS-*Xpress* findings suggest the relationship between ECA biosynthetic genes and efflux activity is complex, where ECA biosynthesis is beneficial for fitness when efflux is inhibited, but detrimental for survival in the presence of acriflavine. When treated with PA $\beta$ N, there were fewer insertions in *wecA*, *wecB*, *wecC* and *wecG* in *S. Typhimurium* relative to an unstressed control. This is supported by previous findings showing increased susceptibility to bile salts in *S. Typhimurium* following disruption of the ECA biosynthetic genes *wecD* or *wecA* (Ramos-Morales et al., 2003). Additionally, there were fewer mutants in *yhdP* in *S. Typhimurium* treated with PA $\beta$ N relative to the unstressed control, where YhdP is involved in maintaining the permeability of the outer membrane in response to cyclic ECA (Mitchell et al., 2018). Together, this suggests that ECA has an important role in membrane permeability and transmembrane transport. However, several genes involved in ECA biosynthesis were detrimental to fitness in the presence of acriflavine. In both *E. coli* and *S. Typhimurium*, there were more mutants in *wecF* when treated with subinhibitory concentrations of acriflavine relative to their unstressed controls. Under the same conditions, there were also more mutants in *wecC* and *wecE* in *E. coli*. In

*S. Typhimurium*, there were more insertions in *wzxE*, encoding an inner membrane transporter of the ECA chain (Islam and Lam, 2014), in conditions with either concentration of acriflavine. Biosynthesis and export of ECA seems to be detrimental to acriflavine tolerance in both *E. coli* and *S. Typhimurium*. Deletion of *wecF* reduced dye uptake (figure 6.15a), consistent with the TraDIS-*Xpress* findings that *wecF* was detrimental in the presence of acriflavine. Deletion of *wzxE* increased susceptibility to both nalidixic acid and amikacin (Girgis et al., 2009) and deletion of *wecE* has previously been shown to confer a slight increase in gentamycin susceptibility in *E. coli* (Tamae et al., 2008). As gentamycin is not an efflux substrate, this suggests that the changes in dye uptake and drug susceptibility that result in deletion of genes involved in ECA biosynthesis are not due to changes in efflux activity.

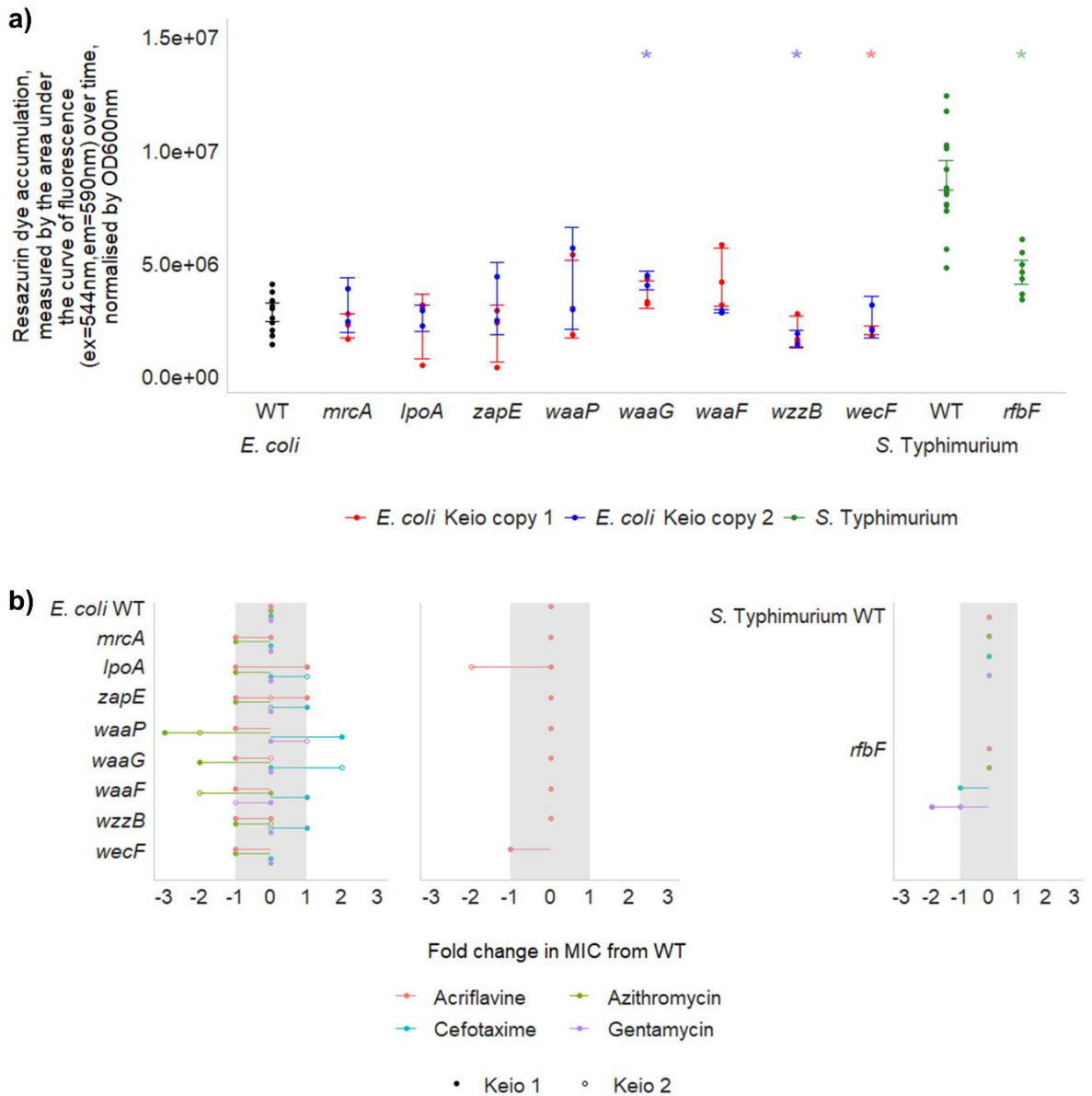


**Figure 6.15:** The effects of genes involved in cell envelope biogenesis on efflux activity in *E. coli* and *S. Typhimurium*. **a)** Dye accumulation in the wild type and single gene deletion mutants in each species. Accumulation of resazurin (excitation 544 nm, emission 580 nm) was measured over 60 minutes in *E. coli* and 100 minutes in *S. Typhimurium* and the area under the curve was plotted. Points show 3 independent replicates. Asterisks (\*) show a significant difference (Welch's *t*-test,  $p < 0.05$ ) between the wild type and mutants. Colours discriminate between mutant copies. The shaded area shows the 95% confidence interval of the wild type and error bars show 95% confidence intervals of mutants. **b)** Fold change in MICs of acriflavine, azithromycin, cefotaxime and gentamycin in mutants relative to each wild type, measured by the broth dilution method (and the agar dilution method in *E. coli* shown in the middle panel). The shaded area shows an experimental error of 1-fold change and points show two independent replicates

#### 6.5.4. Fimbriae

Type I fimbriae affected the fitness of both *E. coli* and *S. Typhimurium* when under efflux-related stresses. Genes involved in fimbriae biosynthesis, *fimC* and *fimD* (Allen et al., 2012), had more mutants in *E. coli* treated with inhibitory concentrations of acriflavine, and *fimF* had more mutants in *S. Typhimurium* treated with subinhibitory concentrations of acriflavine, relative to their unstressed controls.

The regulators of fimbriae biosynthesis were also seen to affect fitness. In *S. Typhimurium*, positive fimbrial regulators *fimZ* and *fimY* (Saini et al., 2009) had more insertions in conditions treated with subinhibitory concentrations of acriflavine, relative to the unstressed control. The negative fimbrial regulator, *fimW* (Saini et al., 2009), had fewer insertions in conditions treated with PA $\beta$ N or both concentrations of acriflavine, relative to the unstressed control. This indicates that expression of type I fimbriae is detrimental to survival under a range of efflux-related stresses. This is consistent with previous findings, showing genes encoding fimbrial subunits and regulators were also seen to be detrimental for the fitness of *E. coli* growing under high concentrations of triclosan, which is also an efflux substrate (Yasir et al., 2020).

In *E. coli*, the relationship between the fimbrial regulators and fitness in these conditions is more complex. Consistent with the findings in *S. Typhimurium*, there were more mutants in the positive fimbrial regulator *fimB* (Klemm, 1986) when treated with inhibitory concentrations of acriflavine and PA $\beta$ N relative to acriflavine alone, or when treated with PA $\beta$ N relative to the unstressed control. However, there were more insertions in *fimE* when treated with PA $\beta$ N relative to the unstressed control, and fewer insertions in *fimE* when treated with either concentration of acriflavine relative to the unstressed control. This may reflect differences between the two substrates used here to measure the genes involved in efflux activity, where expression of fimbriae increases susceptibility to acriflavine, but deletion of both regulators may be beneficial for fitness when efflux is inhibited. However, deletion of *fimB* or *fimE* in *E. coli* did not affect dye uptake or drug susceptibility (figure 6.16 a,b). Close regulation of type I fimbriae expression may be important to maximise fitness in response to specific environmental stressors.

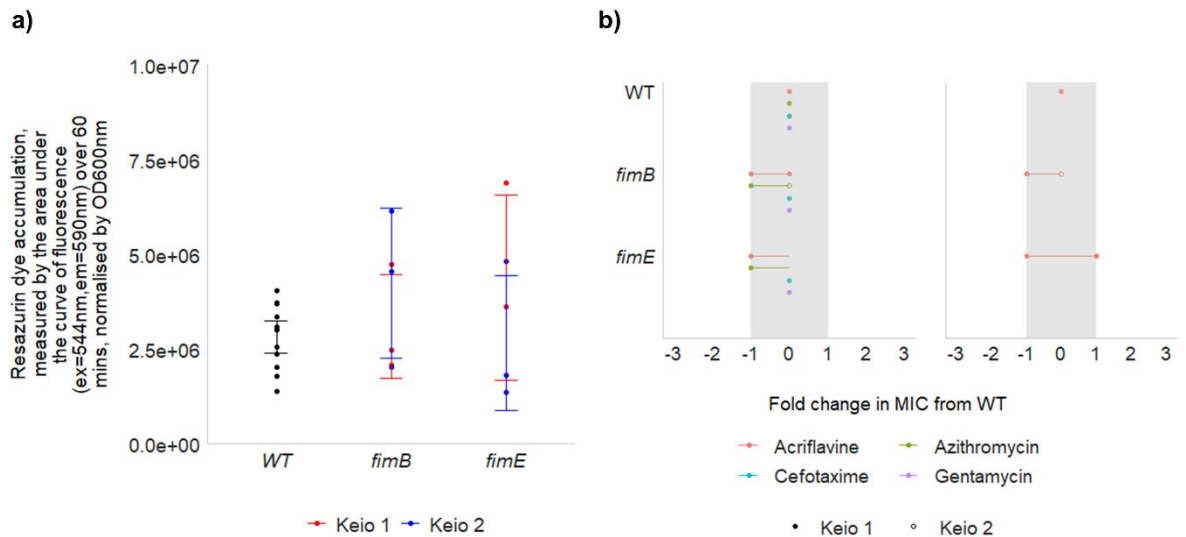


**Figure 6.16:** The effects of fimbrial regulation on efflux activity in *E. coli*. **a)** Dye accumulation in the wild type and single gene deletion mutants. Accumulation of resazurin (excitation 544 nm, emission 580 nm) was measured over 60 minutes and the area under the curve was plotted. Points show 3 independent replicates. Asterisks (\*) show a significant difference (Welch's *t*-test,  $p < 0.05$ ) between the wild type and mutants. Colours discriminate between mutant copies. The shaded area shows the 95% confidence interval of the wild type and error bars show 95% confidence intervals of mutants. **b)** Fold change in MICs of acriflavine, azithromycin, cefotaxime and gentamycin in mutants relative to each wild type, measured by the broth dilution (left) and agar dilution (right) methods. The shaded area shows an experimental error of 1-fold change and points show two independent replicates.



### 6.5.5. Amino acid biosynthesis

The gene encoding MetL, involved in the beginning of lysine and homoserine biosynthesis and indirectly involved in methionine and threonine biosynthesis (Thèze et al., 1974), was implicated in efflux activity in both *E. coli* and *S. Typhimurium*. There were more insertions in *metL* under inhibitory concentrations of acriflavine in *E. coli*, and under efflux inhibition in *S. Typhimurium*, relative to their unstressed controls. In *E. coli*, deletion of *metL* reduced dye accumulation but resulted in no change in drug susceptibility (figure 6.17 a,b). Deletion of *metL* has been reported to increase cefoxitin susceptibility in *E. coli*, and this was determined to be independent of *marA* (Ruiz and Levy, 2011, Ruiz and Levy, 2010). Leucine biosynthesis was also implicated in both *E. coli* and *S. Typhimurium*, with fewer mutants in *leuL* in *E. coli* treated with subinhibitory concentrations of acriflavine, and in *leuD* (Gemmill et al., 1983) in *S. Typhimurium* treated with inhibitory concentrations of acriflavine, relative to their unstressed controls. Deletion of *leuL* in *E. coli* resulted in no significant changes in dye accumulation or drug susceptibility (figure 6.17 a,b). Disruption of *argG* was implicated as detrimental for efflux activity in *S. Typhimurium*, with more mutants mapped to this gene when treated with subinhibitory concentrations of acriflavine relative to the unstressed control. Expression of *metL*, *argG* and *tolC* was identified to be beneficial for swarming motility in *E. coli*, alongside many other genes involved in cell envelope biogenesis and enterobacterial common antigen biosynthesis (Inoue et al., 2007). Together, this suggests genes involved in amino acid biosynthesis may have a role in cell envelope integrity and may affect membrane permeability and drug susceptibility through their role in envelope biosynthesis.

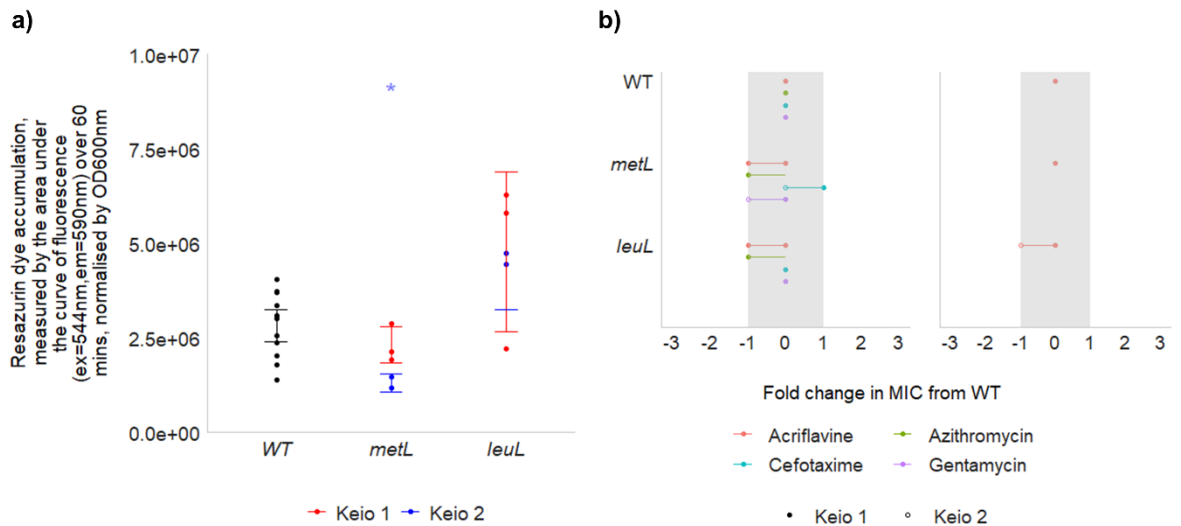


**Figure 6.17:** The effects of *metL* and *leuL* on efflux activity in *E. coli*. **a)** Dye accumulation in the wild type and single gene deletion mutants. Accumulation of resazurin (excitation 544 nm, emission 580 nm) was measured over 60 minutes and the area under the curve was plotted. Points show 3 independent replicates. Asterisks (\*) show a significant difference (Welch's *t*-test,  $p < 0.05$ ) between the wild type and mutants. Colours discriminate between mutant copies. The shaded area shows the 95% confidence interval of the wild type and error bars show 95% confidence intervals of mutants. **b)** Fold change in MICs of acriflavine, azithromycin, cefotaxime and gentamycin in mutants relative to each wild type, measured by the broth dilution (left) and agar dilution (right) methods. The shaded area shows an experimental error of 1-fold change and points show two independent replicates.

### 6.5.6. DNA housekeeping

Acriflavine binds to DNA (Lerman, 1963), therefore it was expected that genes involved in DNA repair would benefit survival under acriflavine stress, however the exact mechanism of acriflavine action is unknown. Various genes involved in supercoiling maintenance, replication, DNA repair and others induced by DNA damage affected fitness in *E. coli* and *S. Typhimurium* treated with acriflavine.

There were fewer mutants in *yjhQ* in *E. coli* treated with subinhibitory concentrations of acriflavine and PA $\beta$ N, relative to acriflavine alone. Expression of *yjhQ* relieves the toxicity of TopAI, an inhibitor of topoisomerase I (TopA) (Yamaguchi and Inouye, 2015), thereby preventing excess negative supercoiling of DNA. However, there were no differences in insertion frequency in *topAI* or *topA* in *E. coli* treated with subinhibitory concentrations of acriflavine and PA $\beta$ N, relative to acriflavine alone. Additionally, deletion of *yjhQ* resulted in no significant difference in dye uptake or drug susceptibility (figure 6.18 a,b). This suggests either that *yjhQ* may affect acriflavine susceptibility through a different means, or that YjhQ may affect multiple topoisomerase inhibitors that have functional redundancy and can complement each other's phenotype when one is disrupted.

The TraDIS-*Xpress* data suggested that ATP-dependent DNA helicase encoded by *rep* (Yarranton and Gefter, 1979) is detrimental to the fitness of *E. coli* without active efflux, as there were more insertions in *rep* in *E. coli* treated with PA $\beta$ N relative to the unstressed control. However, deletion of *rep* resulted in no change in dye accumulation or drug susceptibility (figure 6.18 a,b). Rep has a role in promoting DNA replication when the replisome is blocked by protein-DNA complexes (Guy et al., 2009), and it is perhaps this role that makes *rep* detrimental to fitness when acriflavine is bound to DNA.

There were fewer insertions in *hupA*, encoding the histone-like DNA-binding protein HU (Oberto et al., 2009), when *S. Typhimurium* was treated with PA $\beta$ N relative to the unstressed control. Deletion of *hupA* in *Salmonella spp.* has previously been reported to increase susceptibility to fluoroquinolones (Turner et al., 2020a) and bile (Langridge et al., 2009), both of which are efflux substrates. The HU regulon comprises of many genes involved in responding to acid stress, high osmolarity and SOS induction (Oberto et al., 2009), and any change in antimicrobial susceptibility may be due to any one of these affected pathways.

There were more insertions in *ybiB* in *E. coli* treated with subinhibitory concentrations of acriflavine relative to the unstressed control. Deletion of *ybiB* resulted in no change in dye accumulation or drug susceptibility (figure 6.18 a,b). Little is known about YbiB, except that it is a DNA binding molecule induced by DNA-damaging agents (Schneider et al.,

2015). Another DNA damage-induced gene, this time affecting *S. Typhimurim* fitness, is *dinI*, which had fewer mutants when treated with inhibitory concentrations of acriflavine relative to an unstressed control. *DinI* acts as a positive regulator of RecA activity (Lusetti et al., 2004), involved in repairing double-strand DNA breaks via homologous recombination, suggesting that DNA repair is beneficial for survival in the presence of acriflavine. However, two other genes involved in the same pathway were seen to have a negative effect on fitness in *S. Typhimurium* under the same conditions: There were more mutants in *recB* in conditions with inhibitory concentrations of acriflavine, and more mutants in *recC* when treated with either concentration of acriflavine, relative to unstressed controls. DNA damage repair via homologous recombination therefore may have a complex role in acriflavine susceptibility.

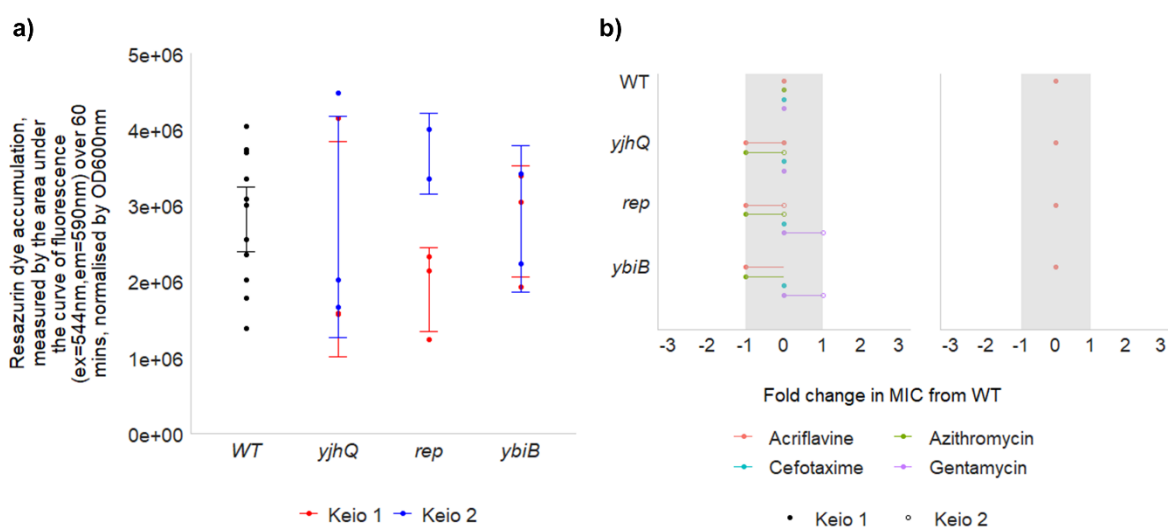


**Figure 6.18:** The effects of *yjhQ*, *rep* and *ybiB* on efflux activity in *E. coli*. **a)** Dye accumulation in the wild type and single gene deletion mutants. Accumulation of resazurin (excitation 544 nm, emission 580 nm) was measured over 60 minutes and the area under the curve was plotted. Points show 3 independent replicates. Colours discriminate between mutant copies. The shaded area shows the 95% confidence interval of the wild type and error bars show 95% confidence intervals of mutants. **b)** Fold change in MICs of acriflavine, azithromycin, cefotaxime and gentamycin in mutants relative to each wild type, measured by the broth dilution (left) and agar dilution (right) methods. The shaded area shows an experimental error of 1-fold change and points show two independent replicates.

### 6.5.7. Translation

Many antibiotics act by inhibiting translation (Kavčič et al., 2020). Whilst acriflavine is thought to target DNA, many genes involved in ribosome assembly and modification were highlighted by TraDIS-*Xpress* to be involved in acriflavine susceptibility. There were fewer insertions in *ygaM* and *trhP* in *E. coli* treated with subinhibitory concentrations of acriflavine relative to the unstressed control. YgaM is an inner membrane protein that binds to the ribosome (Yoshida et al., 2012) and TrhP is a peptidase involved in tRNA modification (Sakai et al., 2019). Deletion of either *ygaM* or *trhP* had no effect on dye uptake or drug susceptibility in *E. coli* (figure 6.19 a,b). Deletion of *trhP* has been reported to reduce expression of type 1 fimbriae and confer increased susceptibility to oxidative stress (Bessaiah et al., 2019), both of which affect drug susceptibility but may not directly affect efflux activity.

There were more insertions upstream of *infB* when *S. Typhimurium* was treated with subinhibitory concentrations of acriflavine relative to the unstressed control, suggesting increased expression of *infB* was beneficial for fitness in these conditions. Translation initiation factor B has also been reported to be beneficial for fitness under high triclosan concentrations (Yasir et al., 2020) and has a role in repairing DNA damage upon exposure to DNA damaging agents (Madison et al., 2012), however deletion of *infB* resulted in no change in dye uptake or drug susceptibility in *S. Typhimurium* (figure 6.19 a,b).

Several genes involved in translation were seen to negatively affect fitness in the presence of acriflavine. There were more insertions in both genes encoding elongation factor Tu, *tuf\_1* and *tuf\_2* (Weijland et al., 1992), in *S. Typhimurium* treated with subinhibitory concentrations of acriflavine relative to the wild type. Increased expression of elongation factor Tu was reported in *E. coli* exposed to a range of environmental stresses including starvation, radiation treatment and seawater (Muela et al., 2008), implicating elongation factor Tu in responding to stress, and not necessarily suggesting a role in efflux activity. Two genes involved in ribosome assembly were deleterious to fitness in the presence of acriflavine. There were more mutants in *bipA* and *deaD* in *S. Typhimurium* treated with subinhibitory concentrations of acriflavine relative to the unstressed control. BipA is involved in assembly of the 50S ribosomal subunit at low temperatures (Choi and Hwang, 2018), and DeaD is involved in ribosome assembly (Peil et al., 2008) and mRNA processing, where DeaD is required for activation of  $\sigma^S$  synthesis by DsrA at low temperatures (Resch et al., 2010). I previously identified *rpoS* expression to be beneficial for efflux activity, therefore the effects of *deaD* on fitness in the presence of acriflavine are likely not due to its relationship with  $\sigma^S$  activation.

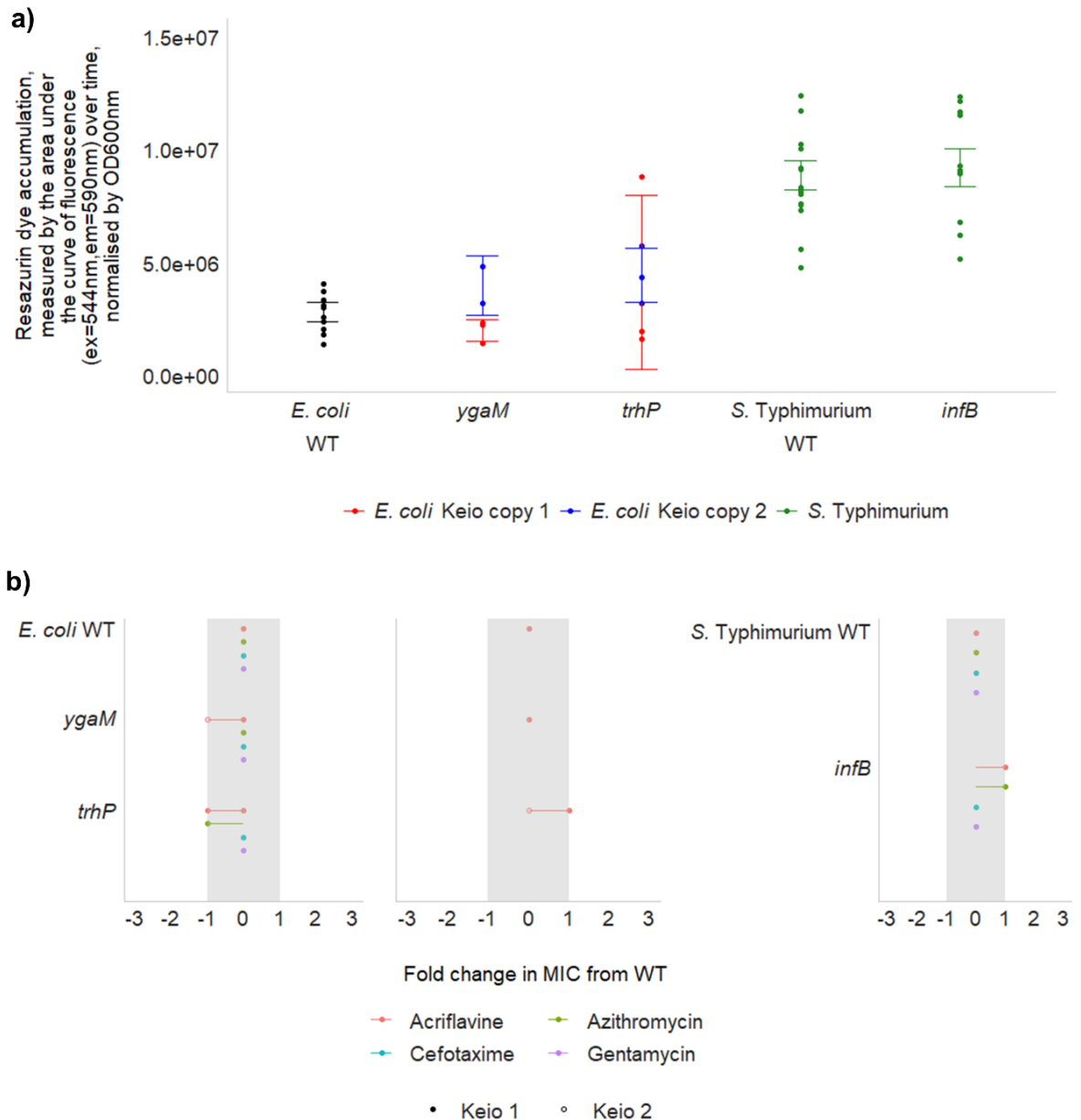


**Figure 6.19:** The effects of genes involved in translation on efflux activity in *E. coli* and *S. Typhimurium*. **a)** Dye accumulation in the wild type and single gene deletion mutants in each species. Accumulation of resazurin (excitation 544 nm, emission 580 nm) was measured over 60 minutes in *E. coli* and 100 minutes in *S. Typhimurium* and the area under the curve was plotted. Points show 3 independent replicates. Colours discriminate between mutant copies. The shaded area shows the 95% confidence interval of the wild type and error bars show 95% confidence intervals of mutants. **b)** Fold change in MICs of acriflavine, azithromycin, cefotaxime and gentamycin in mutants relative to each wild type, measured by the broth dilution method (and the agar dilution method in *E. coli* shown in the middle panel). The shaded area shows an experimental error of 1-fold change and points show two independent replicates.

### 6.5.8. Motility

Negatively motility regulators *hdfR* (Ko and Park, 2000) and *lrhA* (Lehnen et al., 2002) were found by TraDIS-*Xpress* to benefit efflux activity in *E. coli*, with fewer insertions in these genes in conditions treated with either PA $\beta$ N or subinhibitory concentrations of acriflavine, relative to the unstressed control. Genes involved in motility were only seen to affect to fitness of *E. coli* in these conditions and not *S. Typhimurium*. However, there was no change in dye accumulation or drug susceptibility (figure 6.20 a,b) in either of these mutants.

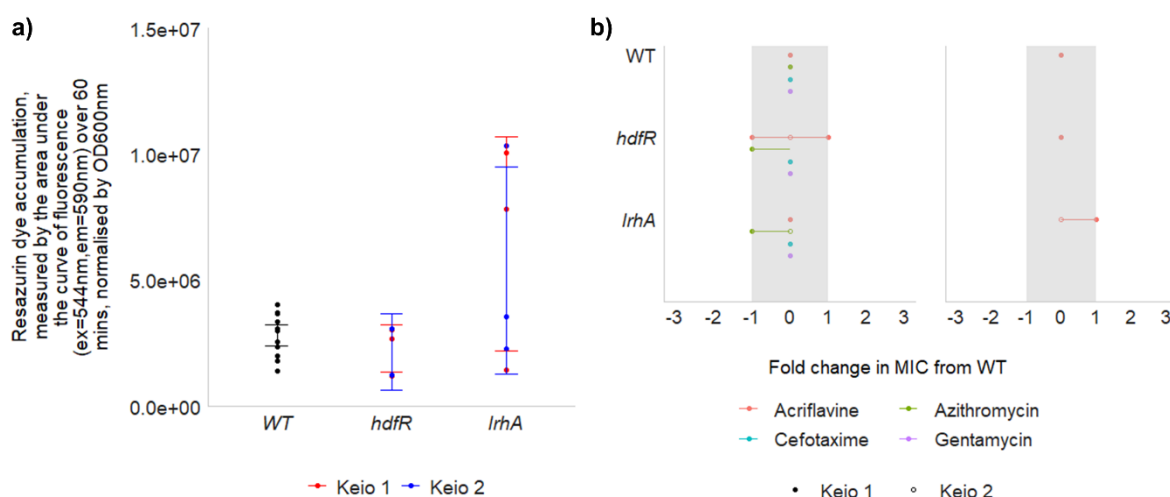


**Figure 6.20:** The effects of motility regulators on efflux activity in *E. coli*. **a)** Dye accumulation in the wild type and single gene deletion mutants. Accumulation of resazurin (excitation 544 nm, emission 580 nm) was measured over 60 minutes and the area under the curve was plotted. Points show 3 independent replicates. Colours discriminate between mutant copies. The shaded area shows the 95% confidence interval of the wild type and error bars show 95% confidence intervals of mutants. **b)** Fold change in MICs of acriflavine, azithromycin, cefotaxime and gentamycin in mutants relative to each wild type, measured by the broth dilution (left) and agar dilution (right) methods. The shaded area shows an experimental error of 1-fold change and points show two independent replicates.

### 6.5.9. Prophages

Analysis of the TraDIS-*Xpress* data found insertional inactivation of genes in prophages affected the survival of *E. coli* and *S. Typhimurium* when treated with acriflavine or PA $\beta$ N. There were more insertions downstream of *yagL* in *E. coli* treated with inhibitory concentrations of acriflavine relative to the unstressed control, where these insertions were driving the production of anti-sense RNA and reduced expression was beneficial for fitness. YagL is a prophage protein regulated by  $\sigma^S$  (Maciag et al., 2011), but little else is known about its function. Deletion of *yagL* in *E. coli* resulted in a significant increase in dye accumulation (figure 6.2 a,b) and no change in drug susceptibility (figure 6.3 a,b). There were more insertions in many genes in the Gifsy-3 prophage, from *STM14\_1418* to *STM14\_1483* (Figuroa-Bossi et al., 2001), when *S. Typhimurium* was treated with subinhibitory concentrations of acriflavine and PA $\beta$ N relative to acriflavine alone. Acriflavine is a DNA binding agent (Lerman, 1963), and previous work has suggested Gifsy-3 is induced by DNA damage (Frye et al., 2005). In the absence of active efflux, disruption of genes in Gifsy-3 seems to benefit survival, but overall this does not suggest the prophage is involved in efflux activity.

### 6.6. Conclusions

I used TraDIS-*Xpress* to identify genes involved in efflux activity in *E. coli* and *S. Typhimurium* by comparing the fitness of mutants treated with various concentrations of acriflavine in the presence and absence of the efflux inhibitor PA $\beta$ N. The validity of this method was supported through the identification of known efflux pumps and their regulators, as well as phenotypic validation of the data generated. By teasing apart the pathways involved in each condition, I have identified roles in efflux activity for genes involved in ribosome modification, respiration, glutathione metabolism, DNA housekeeping, signalling systems, transcription and protein chaperoning. Additionally, I identified pathways that affect the fitness of *E. coli* and *S. Typhimurium* in the presence of acriflavine independent of efflux activity, which include genes involved in envelope biosynthesis, fimbriae expression, amino acid biosynthesis, DNA housekeeping, translation, motility and prophages.

This investigation into efflux activity could be improved by repeating this experiment with other efflux substrates. Comparing and contrasting the effect of different antimicrobials on mutant fitness in the presence and absence of active efflux would create a more accurate picture of genes that affect efflux activity separate from those that affect fitness through different mechanisms. Additionally, comparing the data from conditions treated with acriflavine relative to other antimicrobials with known mechanisms of action and antibacterial targets may provide further insight into mechanisms of acriflavine action and



resistance. Further investigation into the genes and pathways highlighted in this study would benefit our understanding of the requirements for efflux activity and regulation.

PA $\beta$ N potentiates the effect of multiple antimicrobials by inhibiting RND efflux pumps (Lomovskaya et al., 2001), which are clinically the most important family at conferring multidrug resistance (Blair et al., 2015a). This model system could be exploited to find synergies between other antibiotics and antibiotic potentiators. TraDIS-*Xpress* has previously been used to identify mechanisms of trimethoprim action and resistance in *E. coli* and found a strong synergy with 3'-azido-3'-deoxythymidine (AZT), a known Tdk inhibitor and HIV drug (Turner et al., under review). Further work with a range of antibiotics and clinically important pathogens may revolutionise our knowledge of drug interactions and synergies to increase treatment efficacy and reduce development of resistance.

This chapter provides a broad overview of the requirements of efflux activity and acriflavine susceptibility in *E. coli* and *S. Typhimurium*. This was essential for the following chapter, which identified and characterised the genes and pathways important for both efflux activity and biofilm formation to further investigate the relationship between the two.

**7. CHAPTER 7: REGULATORY LINKS  
BETWEEN BIOFILM DEVELOPMENT  
AND EFFLUX ACTIVITY**

## 7.1. Introduction

Loss of efflux function has been shown to result in severely reduced biofilm formation in many bacterial species (Baugh et al., 2012, Baugh et al., 2014, Kvist et al., 2008, Alav et al., 2018). This has led to inhibition of efflux as an anti-biofilm strategy. However, a mechanistic understanding for why loss of efflux often results in loss of biofilm is lacking. Deletion of *toIC*, encoding the main channel protein for multiple RND efflux systems, results in reduced biofilm biomass that was linked to loss of curli biosynthesis in *E. coli* and *S. Typhimurium*, via transcriptional repression of *csgD* (Baugh et al., 2012, Baugh et al., 2014). The pathway through which inactivation of efflux causes reduced curli biosynthesis is however yet to be described.

I used TraDIS-*Xpress* to identify the genes involved in both biofilm development and in efflux activity in *E. coli* and *S. Typhimurium*. This revealed roles for genes involved in both pathways, including those involved in respiration, DNA housekeeping, transmembrane transport, translation, signalling systems, purine biosynthesis, transcriptional regulators and protein chaperones. In this chapter, I used the TraDIS-*Xpress* data and phenotypic validation performed in the previous chapters to formulate and test hypotheses as to how modulation of efflux activity affects biofilm development.

## 7.2. Aims

- To determine the pathways involved in both biofilm development and efflux activity in both *E. coli* and *S. Typhimurium*
- To discuss how these pathways affect biofilm development and efflux activity using the phenotypic findings of this study in conjunction with previously published work
- To formulate and test hypotheses on how individual genes affect biofilm development and efflux activity

### 7.3. Identifying genes and pathways important in both biofilm development and efflux activity

Analysis of the TraDIS-*Xpress* data identified 48 and 78 candidate genes involved in biofilm development in *E. coli* and *S. Typhimurium* respectively, and 67 and 99 candidate genes involved in efflux activity and acriflavine susceptibility. Of these, 24 candidate genes were identified between both species to affect biofilm development and efflux activity, including genes with roles in transmembrane transport, cell envelope biogenesis, intracellular signalling, fimbriae expression, transcriptional regulation, cell division and motility (Appendix 4). In concordance with previous work (Baugh et al., 2012, Baugh et al., 2014), *tolC* was identified to be important in both biofilm development and efflux activity in both *E. coli* and *S. Typhimurium*. There were fewer insertions in *tolC* in both species in biofilm conditions grown for 48 hours relative to the planktonic control and fewer insertions in *tolC* when both species were treated with PA $\beta$ N relative to the unstressed controls. Biofilm formation and efflux activity was measured for the genes highlighted in the previous chapters (Appendix 5). Figure 7.1 shows relative biofilm biomass plotted against relative dye accumulation to highlight genes that affected both biofilm development and efflux activity. Genes that stand out in this figure as positively affecting both biofilm development and efflux activity in *E. coli* are efflux pump components *acrA*, *acrB* and *proW*, purine biosynthetic genes *purD* and *purE*, macrodomain organiser *maoP* and antitoxin component *tomB* (figure 7.1a). In *S. Typhimurium*, the *nuo* operon can be seen to have a clear role in biofilm development and efflux activity, with deletion of *nuoB* or the *nuo* operon resulting in reduced biofilm biomass and increased dye accumulation (figure 7.1b). The roles of each of these systems in biofilm development and efflux activity will be discussed in greater detail.

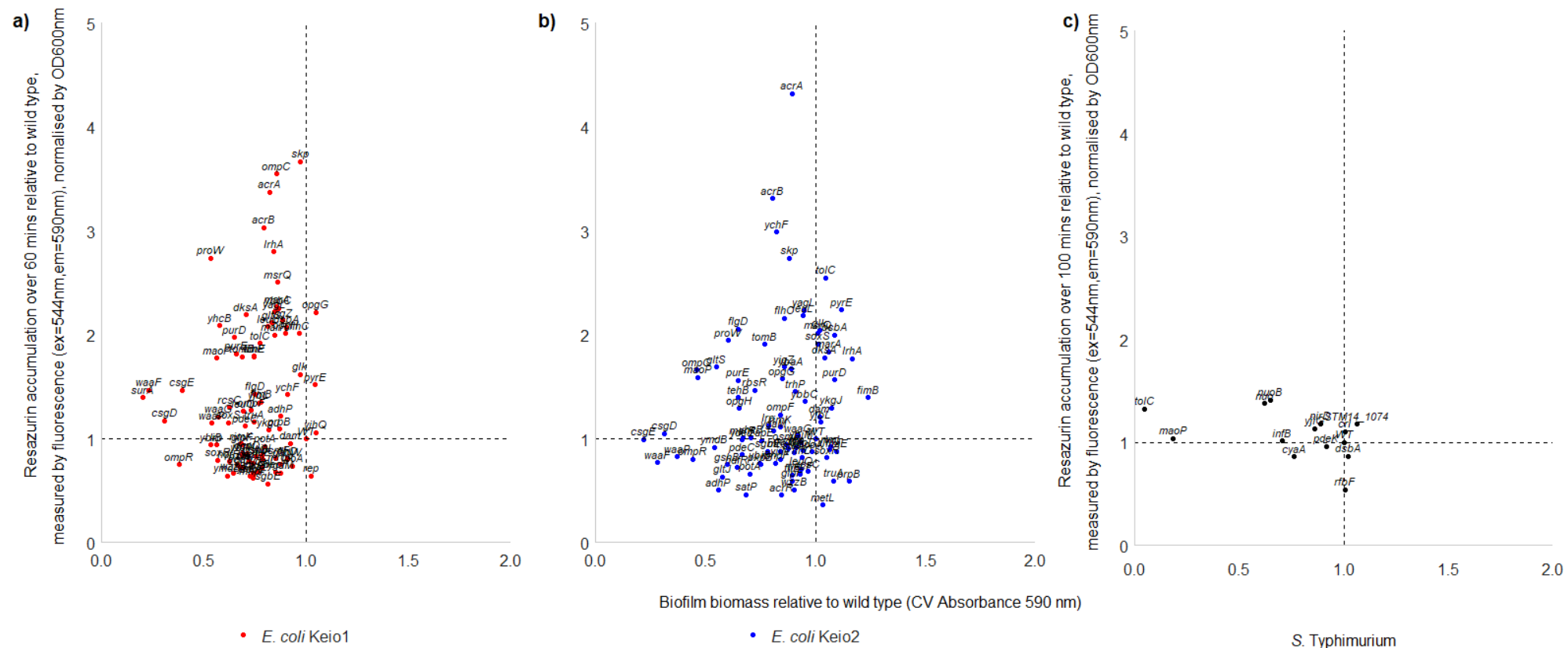


**Figure 7.1:** Relative biofilm biomass plotted against relative dye accumulation in **a)** the first and **b)** second copies of deletion mutants from the Keio collection relative to wild type *E. coli*, and **c)** wild type *S. Typhimurium* and deletion mutants. The top-left quadrant of these graphs shows genes where biofilm biomass formation was reduced and drug accumulation was increased when deleted. Points show averages of two biological and two technical replicates (*E. coli* biofilm biomass data), three independent replicates (*E. coli* dye accumulation data) and two biological and four technical replicates (*S. Typhimurium* biofilm biomass data and dye accumulation data).

## 7.4. Nuo operon

TraDIS-*Xpress* found that insertional inactivation of 10 out of the 14 genes in the *nuo* operon reduced the fitness of the *S. Typhimurium* biofilm grown for 24 and 48 hours, relative to the planktonic control. The *nuo* operon encodes the type I NADH dehydrogenase in the electron transport chain (Archer and Elliott, 1995). Deletion of *nuoB*, located at the start of the *nuo* operon, reduced biofilm biomass and curli biosynthesis in both *E. coli* (Appendix 5) and *S. Typhimurium* (figure 7.2 a,b). Additionally, deletion of *nuoB* and the *nuo* operon in *S. Typhimurium* significantly reduced efflux activity in a similar way to deletion of efflux channel *tolC* (figure 7.2c), and increased susceptibility of cefotaxime, as did deletion of *tolC* (figure 7.2d). I formulated two hypotheses as to how the *nuo* operon and the electron transport chain may play a role in biofilm development and efflux activity.

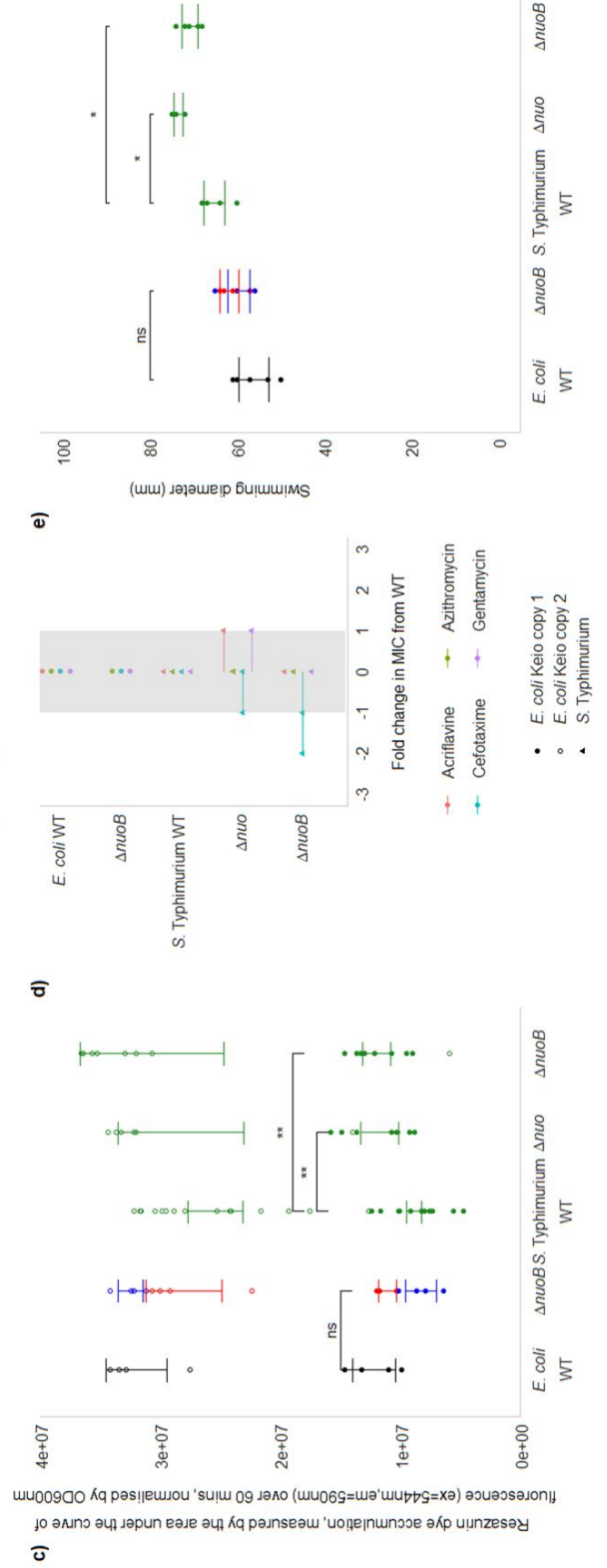
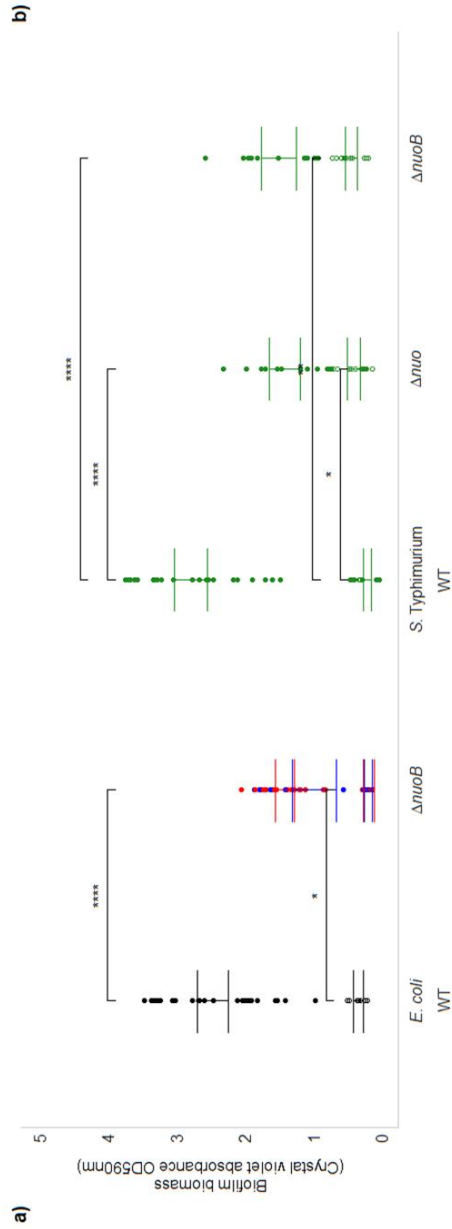
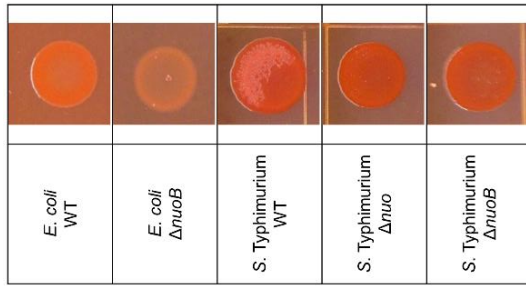
### 7.4.1. Hypothesis 1: Disruption of the proton gradient

Type I NADH dehydrogenase, encoded by the *nuo* operon, is the first component of the electron transport chain, involved in transferring electrons to ubiquinone and transporting protons across the inner membrane into the periplasm, maintaining the proton gradient (Archer and Elliott, 1995). The proton gradient has a role in powering ATP synthesis, flagella rotation and many efflux pumps. Therefore, disruption of the proton gradient through deletion of the *nuo* operon was predicted to reduce efflux activity. Efflux pumps are large transmembrane protein complexes, and their absence or inhibition may also result disruption of the proton gradient in a similar way to deletion of the *nuo* operon. Deletion of either the *nuo* operon or genes encoding efflux pump components resulted in reduced biofilm biomass and curli biosynthesis. I predicted that deletion or inhibition of efflux disrupts the proton gradient, activating stress response systems involved in preserving membrane integrity, one or some of which are involved in the transcriptional repression of curli biosynthesis.

When *acrB* was deleted in *S. Typhimurium*, reduced expression of genes involved in the anaerobic respiratory chain (with roles in producing the proton gradient) was reported (Webber et al., 2009). No change in expression of these genes was seen in an  $\Delta$ *acrA* deletion mutant (Webber et al., 2009), similar to the finding that curli production is only reduced in an  $\Delta$ *acrB* and not an  $\Delta$ *acrA* mutant (Baugh et al., 2012). One of the genes identified to have reduced expression in an  $\Delta$ *acrB* deletion mutant was *nirD*, which was also found in the TraDIS-*Xpress* experiments to benefit the fitness of *S. Typhimurium* growing under inhibitory acriflavine concentrations, relative to the unstressed control. Deletion of *nirD* did not have the same effect on biofilm biomass production or dye accumulation as deletion of *nuo* or *nuoB* in *S. Typhimurium* (Appendix 5), therefore

disruption of the proton gradient may affect biofilm development different depending on environmental conditions such as oxygen availability.

The integrity of the proton gradient was indirectly tested in the *nuo*, *nuoB* and *tolC* deletion mutants relative to wild type *S. Typhimurium* by measuring motility in these strains, as the proton gradient also powers flagella rotation as well as efflux activity. Deletion of *tolC* significantly reduced swimming motility compared to the wild type (figure 7.2e). This was consistent with my hypothesis that disruption of efflux systems disrupts the proton gradient. However, deletion of either *nuoB* or the *nuo* operon resulted in significantly increased swimming motility compared to the wild type (figure 7.2e). This was the opposite to what was predicted. The differences in swimming motility are only small and with only five replicates performed it is possible that these differences represent natural variation in swimming motility. If disruption of the *nuo* operon does result in an increase in swimming motility, it is possible that this may be independent of its effect on the proton gradient. A more direct method of measuring proton gradient integrity would be best to determine the effect of *nuo* operon disruption. Overall, it appears that disruption of efflux may affect the proton gradient, but the pathways through which this may or may not affect curli transcription are yet to be elucidated.



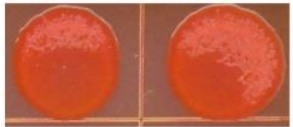
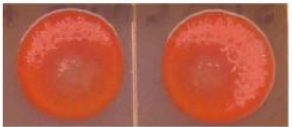


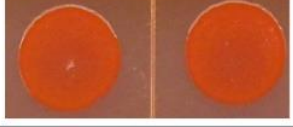
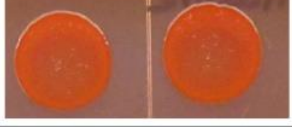


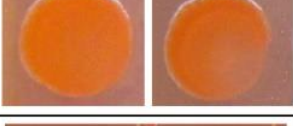
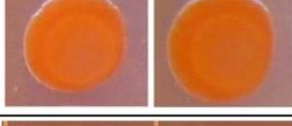










**Figure 7.2:** The effects of the *nuo* operon on biofilm formation, efflux activity and motility in *E. coli* and *S. Typhimurium*. **a)** Biofilm biomass of  $\Delta nuo$  mutants and the wild type (WT) of each species, measured by crystal violet staining (OD<sub>590 nm</sub>). Points show biofilm biomass for a minimum of two biological and six technical replicates. **b)** Curli biosynthesis of  $\Delta nuo$  mutants and relative to the WT of each species. Images are representative of four independent replicates. **c)** Dye accumulation in  $\Delta nuo$  mutants and the WT of each species. Accumulation of resazurin (excitation 544 nm, emission 580 nm) was measured over 60 minutes in *E. coli* and 100 minutes in *S. Typhimurium* and the area under the curve was plotted. Points show two biological and eight technical replicates. Both biofilm biomass and dye uptake were measured in stress free conditions (●) and with PA $\beta$ N (○). **d)** Fold change in MICs of acriflavine, azithromycin, cefotaxime and gentamycin in  $\Delta nuo$  mutants, relative to each WT, measured by the broth dilution method. The shaded area shows an experimental error of 1-fold change and points show two independent replicates. **e)** Swimming motility of  $\Delta nuo$  mutants and the WT of each species, measured by the diameter of the motile disk. Points show five independent replicates. For all graphs, error bars show 95% confidence intervals and asterisks (\*) show where there was a significant difference between the strains indicated (Mann–Whitney U test, ns = not significant; \* =  $p < 0.05$ ; \*\* =  $p < 0.01$ ; \*\*\* =  $p < 0.001$ ; \*\*\*\* =  $p < 0.0001$ ).

#### 7.4.2. Hypothesis 2: Disruption of purine biosynthesis

Deletion of *nuo* operon has previously been reported to interrupt the pentose phosphate pathway and reduce *purF*-independent thiamine synthesis (Claas et al., 2000). This pathway also includes genes involved in purine synthesis, such as *purD* and *purE* (Zhang et al., 2008b), which were both identified in the TraDIS-*Xpress* experiments to benefit the fitness of biofilms grown for 48 hours, relative to the planktonic control. Additionally, *rbsR* involved in regulating ribose metabolism and *de novo* purine biosynthesis (Lopilato et al., 1984), was implicated in efflux activity in both *E. coli* and *S. Typhimurium*. Therefore, purine biosynthesis may have a role in the relationship between biofilm development and efflux activity. I predicted that manipulation of efflux and the deletion of the *nuo* operon affect purine biosynthesis in the same manner, and that the reduction in curli biosynthesis seen in an efflux mutant was due to disruption of purine biosynthesis.

Inosine is a compound made in the purine biosynthetic pathway and is the first compound in the pathway to have a purine ring. Recently, it was described that the addition of inosine could rescue curli biosynthesis in a  $\Delta purL$  deletion mutant (Cepas et al., 2020). I was thought that the addition of inosine to  $\Delta nuo$ ,  $\Delta nuoB$  and  $\Delta tolC$  deletion mutants would determine whether disruption of purine biosynthesis was responsible for the reduced curli biosynthesis seen in these mutants. Mutants in nucleotide biosynthetic genes *purD*, *purE*, *pyrE* and *purL* in *E. coli* were included as experimental controls. The addition of inosine did not rescue curli biosynthesis in the  $\Delta nuo$ ,  $\Delta nuoB$  and  $\Delta tolC$  deletion mutants in *S. Typhimurium* (figure 7.3). The original study reported that 50  $\mu\text{g}/\text{mL}$  inosine rescued curli biosynthesis in a  $\Delta purL$  mutant, but in this study curli biosynthesis was only restored to wild type levels in the outer ring of the colony. Curli biosynthesis slightly increased in the  $\Delta purE$  and  $\Delta pyrE$  deletion mutants with the addition of inosine, but not back to wild type levels. Inosine appeared to have no effect on curli biosynthesis in a  $\Delta purD$  deletion mutant. Overall, this suggests that the transcriptional repression of curli biosynthesis in efflux-deficient strains is not mediated through deficiencies in the purine biosynthetic pathway. However, this method was not conclusive at determining that inosine could rescue curli biosynthesis in mutants defective in purine biosynthesis. It has previously been reported that *csgD* may positively regulate *gsk*, involved in adenosine, guanosine and inosine breakdown and salvage for *de novo* purine nucleotide synthesis (Brombacher et al., 2006). There may be a feedback loop that exists between curli and purine biosynthesis where both processes effect each other through multiple pathways, but efflux activity does not seem to affect this.

	Congo red	Congo red + 50 µg/mL Inosine
<i>S. Typhimurium</i> Wild type		
<i>S. Typhimurium</i> $\Delta nuoB$		
<i>S. Typhimurium</i> $\Delta nuo$		
<i>S. Typhimurium</i> $\Delta tolC$		
<i>E. coli</i> Wild type		
<i>E. coli</i> $\Delta purL$		
<i>E. coli</i> $\Delta purD$		
<i>E. coli</i> $\Delta purE$		
<i>E. coli</i> $\Delta pyrE$		

**Figure 7.3:** Curli biosynthesis in *S. Typhimurium* and *E. coli* wild types and deletion mutants, in the presence and absence of inosine. Two out of four independent replicates are shown for each strain.

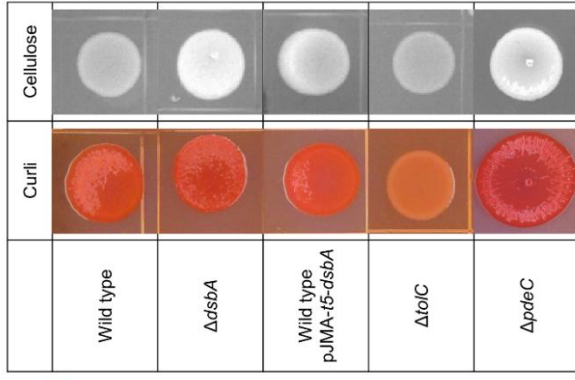
## **7.5. Disulphide bond oxidoreductase DsbA**

### **7.5.1. The role of *dsbA* in biofilm formation**

DsbA is a disulphide bond oxidoreductase involved in forming disulphide bonds in outer membrane proteins (Raina and Missiakas, 1997). TraDIS-*Xpress* found *dsbA* affected biofilm fitness in both *E. coli* and *S. Typhimurium*, albeit differently, where there were fewer insertions in *dsbA* in biofilm conditions after 12- and 24-hours growth relative to planktonic conditions in *E. coli*, but there were more insertions in *dsbA* in biofilm conditions after 12-hours growth relative to planktonic conditions in *S. Typhimurium*. In both species, deletion of *dsbA* resulted in increased curli biosynthesis but no change in overall biofilm biomass (Appendix 5, figure 7.4 a,b). DsbA may play a role in the assembly of adhesins (Lee et al., 2008, Bringer et al., 2007), which explains its importance in the early biofilm in *E. coli*. Previous work has described that an *E. coli* mutant deficient in *dsbA* did not express flagella or type I pili (Bringer et al., 2007), explaining the reduced adhesion seen in this mutant relative to wild type *E. coli*. This was supported by reduced motility in a  $\Delta dsbA$  mutant relative to wild type *E. coli* (figure 7.4e), most likely due to the role of *dsbA* in assembling outer membrane proteins, such as flagella (Dailey and Berg, 1993).

### **7.5.2. The role of *dsbA* in efflux activity**

TraDIS-*Xpress* suggested *dsbA* did not have a strong effect on the fitness of *E. coli* or *S. Typhimurium* when treated with PA $\beta$ N, acriflavine or a combination of the two. Analysis of efflux activity in the  $\Delta dsbA$  mutants found increased dye accumulation in *E. coli* relative to the wild type, suggestive of reduced efflux activity (Appendix 5). However in *S. Typhimurium*, the opposite was seen, where deletion of *dsbA* significantly reduced dye accumulation relative to the wild type (figure 7.4c). Deletion of *dsbA* in either species did not affect drug susceptibility (figure 7.4d). Overexpression of *dsbA* had no effect on dye accumulation or drug susceptibility in *S. Typhimurium* (figure 7.4 c,d). It is possible that *dsbA* does not affect efflux activity, and that its expression is increased in response to membrane stress with a role in reparation of outer membrane proteins.



**b)**

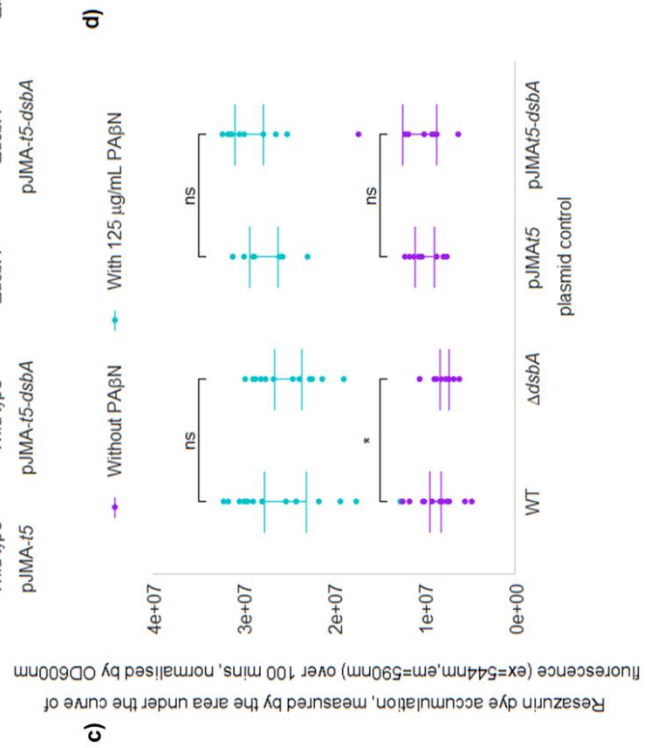
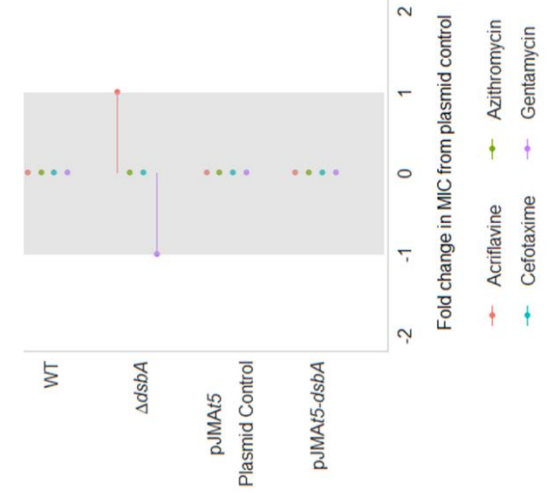
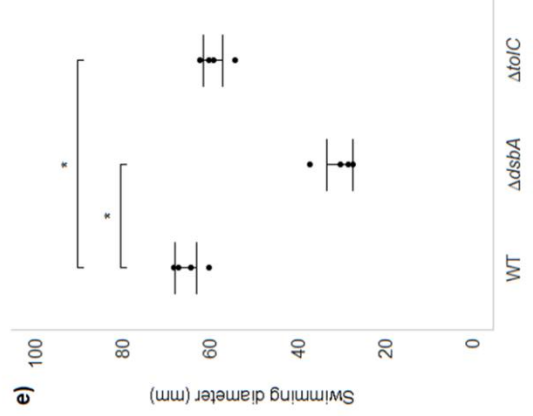
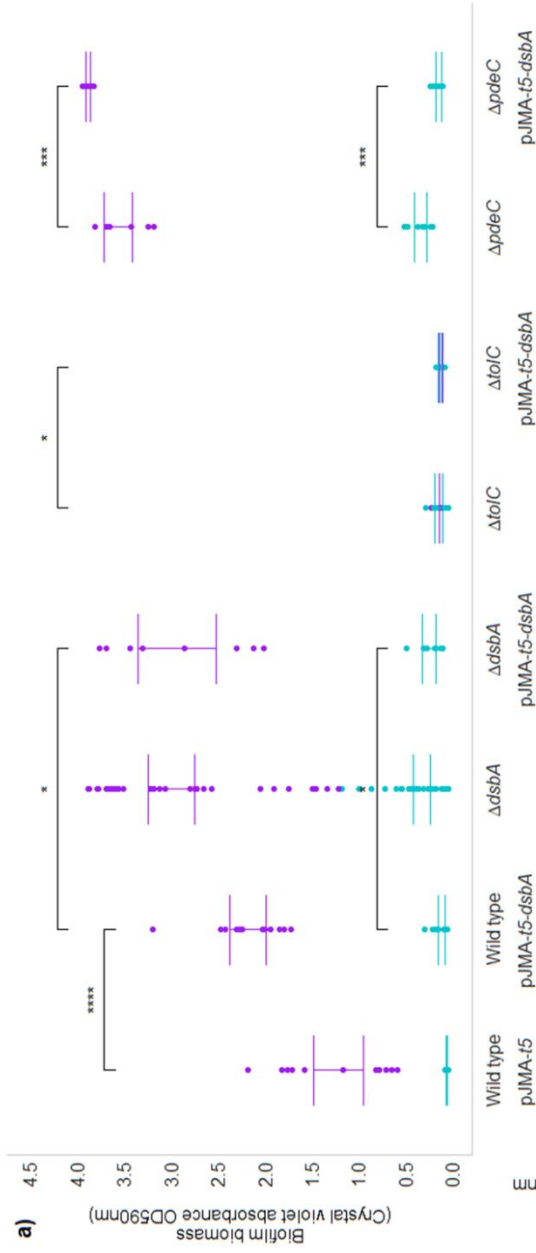


**Figure 7.4:** The effects of *dsbA* on biofilm formation, efflux activity and motility in *S. Typhimurium*. **a)** Biofilm biomass of various deletion mutants and overexpression constructs in wild type (WT) *S. Typhimurium*, measured by crystal violet staining ( $OD_{590\text{ nm}}$ ). Points show two biological and four technical replicates. **b)** Curli and cellulose biosynthesis in  $\Delta dsbA$ , the WT overexpressing *dsbA* on a plasmid,  $\Delta toIC$  and  $\Delta pdeC$ , relative to the WT. Images are representative of four independent replicates. **c)** Dye accumulation in the WT,  $\Delta dsbA$ , the WT overexpressing *dsbA* on a plasmid and an empty plasmid control. Accumulation of resazurin (excitation 544 nm, emission 580 nm) was measured over 100 minutes and the area under the curve was plotted. Points show two biological and four technical replicates. Both biofilm biomass and dye uptake were measured in stress-free conditions (purple) and with PA $\beta$ N (blue). **d)** Fold change in MICs of acriflavine, azithromycin, cefotaxime and gentamycin in  $\Delta dsbA$  relative to the WT, and the WT overexpressing *dsbA* on a plasmid relative to the plasmid control, measured by the broth dilution method. The shaded area shows an experimental error of 1-fold change and points show two independent replicates. **e)** Swimming motility of WT,  $\Delta dsbA$  and  $\Delta toIC$ , measured by the diameter of the motile disk. Points show five independent replicates. For all graphs, error bars show 95% confidence intervals and asterisks (\*) show where there was a significant difference between the strains indicated (Mann–Whitney U test, ns = not significant; \* =  $p < 0.05$ ; \*\* =  $p < 0.01$ ; \*\*\* =  $p < 0.001$ ; \*\*\*\* =  $p < 0.0001$ ).

### 7.5.3. Hypothesis 1: Disruption of *dsbA* affects outer membrane integrity

Expression of *dsbA* is induced by the CpxAR signal transduction system involved in cell envelope and outer membrane repair and maintenance (Danese and Silhavy, 1997). I predicted that disruption of efflux activity induces this system, resulting in overexpression of *dsbA* and thereby reducing curli biosynthesis. A plasmid with *dsbA* cloned downstream of an inducible promoter was inserted into *S. Typhimurium*, which found that overexpression of *dsbA* resulted in increased biofilm biomass relative to the plasmid control in *S. Typhimurium* (figure 7.4a). Biofilm biomass increased further when *dsbA* was overexpressed in a  $\Delta dsbA$  deletion mutant, both in the presence and absence of PA $\beta$ N. This was contrary to what was predicted. Deletion of *dsbA* in both *E. coli* and *S. Typhimurium* increased curli biosynthesis, and overexpression of *dsbA* restored curli biosynthesis to wild type levels in *S. Typhimurium* (figure 7.4b). This suggests that any perturbation of *dsbA* expression results in more biofilm biomass production. It is possible this use of knockout mutants and overexpression vectors results in very different levels of *dsbA* within the cell and does not mimic the curli phenotype seen in efflux-deficient mutants. Overexpression of *dsbA* in a  $\Delta tolC$  deletion mutant did not rescue biofilm biomass, and either deletion or overexpression of *dsbA* did not rescue biofilm biomass production in *S. Typhimurium* treated with PA $\beta$ N (figure 7.4a). This suggests that the activity of *dsbA* alone is not sufficient to cause the biofilm deficit seen in when efflux activity is disrupted. Further work should determine whether *dsbA* is overexpressed upon disruption of efflux activity with PA $\beta$ N or deletion of efflux-related genes *acrB* and *tolC*. Modulation of membrane permeability may affect *dsbA* expression, which affects curli biosynthesis, although this requires further investigation.

### 7.5.4. Hypothesis 2: Disruption of *dsbA* reduces c-di-GMP degradation

DsbA has been found to promote disulphide bond formation in c-di-GMP phosphodiesterase PdeC (Herbst et al., 2018), which is known to reduce c-di-GMP availability and reduce curli biosynthesis and cellulose production (Hengge, 2009). I predicted that overexpression of *dsbA* would result in increased PdeC activity and reduced biofilm biomass and curli biosynthesis through increased c-di-GMP catabolism. Deletion of either *dsbA* or *pdeC* increased curli and cellulose biosynthesis relative to the wild type (figure 7.4b). To investigate the relationship between *dsbA*, *pdeC* and curli biosynthesis, *dsbA* was overexpressed in a  $\Delta pdeC$  deletion mutant to determine whether DsbA affected biofilm biomass production through this route. Biofilm biomass increased upon overexpression of *dsbA* in the  $\Delta pdeC$  deletion mutant (figure 7.4a), suggesting that the impacts of *dsbA* on biofilm development are independent of PdeC. Multiple c-di-GMP phosphodiesterases are known to reduce curli biosynthesis (Hengge et al., 2019), and *dsbA* may affect the activity of more than one. Curli biosynthesis was reported to return to wild type levels in a  $\Delta dsbA$  mutant upon overexpression of *pdeH* or deletion of *pdeK*

(Anwar et al., 2014). Deletion of *dsbA* also increased curli biosynthesis in a *csgD* mutant, suggesting *dsbA* can affect transcription of *csgBAC* independently of *csgD*. Multiple c-di-GMP metabolic proteins have been reported to affect *csgBAC* directly (Sommerfeldt et al., 2009), further supporting the hypothesis that *dsbA* affects curli biosynthesis through c-di-GMP. Further investigation is necessary to determine how *dsbA* affects c-di-GMP metabolism, intracellular c-di-GMP concentrations and pools, and curli transcription.

## 7.6. DNA housekeeping

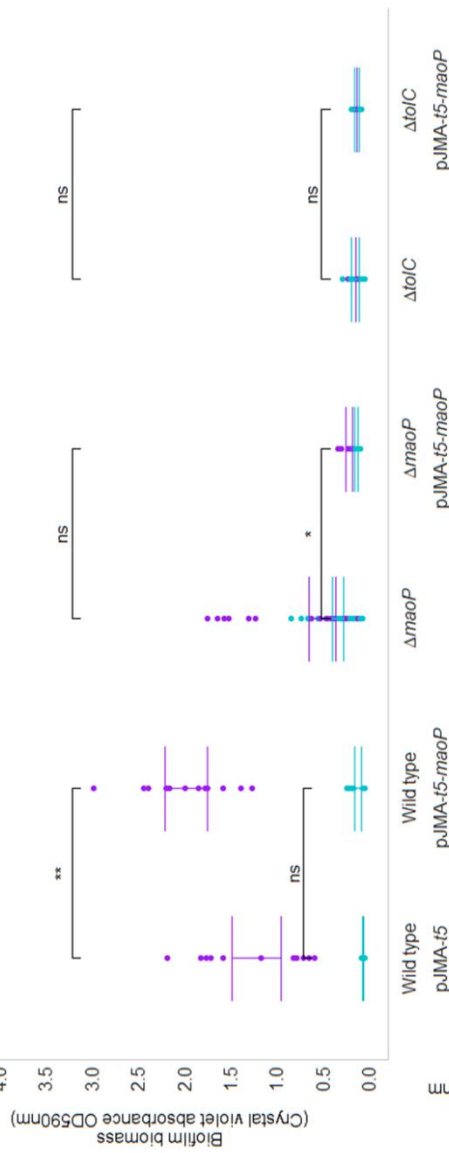
### 7.6.1. Macrodomain organiser *MaoP*

*MaoP* is involved in the organisation of the Ori macrodomain in both the *E. coli* and *S. Typhimurium* chromosomes (Valens et al., 2016). TraDIS-*Xpress* showed mutants within *maoP* thrived in biofilms after 24 hours growth relative to the planktonic control in *E. coli*. However, analysis of  $\Delta$ *maoP* deletion mutants found reduced curli biosynthesis and biofilm biomass relative to the wild type in both *E. coli* (Appendix 5) and *S. Typhimurium* (figure 7.5 a,b). Overexpression of *maoP* resulted in increased biofilm biomass production relative to the plasmid control in *S. Typhimurium* (figure 7.5a). Deletion or overexpression of *maoP* had no effect on cellulose production in *S. Typhimurium* (figure 7.5b).

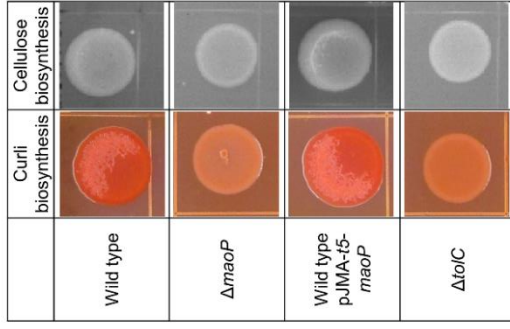
As well as predicting a role in biofilm formation, TraDIS-*Xpress* found *maoP* to be beneficial to efflux activity in *E. coli*, with fewer insertions in *maoP* seen in cultures treated with PA $\beta$ N relative to the unstressed control. Deletion of *maoP* resulted in increased dye accumulation in *E. coli*, and reduced dye accumulation in the presence of PA $\beta$ N, similar to the pattern seen in the *acrA* and *acrB* knockout mutants (figure 7.5c). Previous work found *maoP* was downregulated 16.8 fold in an *acrB* deletion mutant (Ruiz and Levy, 2013), suggesting a relationship between *maoP* and efflux activity. However, no significant change in drug susceptibility was seen when *maoP* was deleted in either *E. coli* (Appendix 5) or *S. Typhimurium* (figure 7.5d). Deletion or overexpression of *maoP* had no effect on dye accumulation with or without PA $\beta$ N in *S. Typhimurium*. Further investigation into how disruption of efflux activity affects *maoP* expression and how *maoP* interacts with efflux function in both *E. coli* and *S. Typhimurium* would strengthen our understanding of this system.



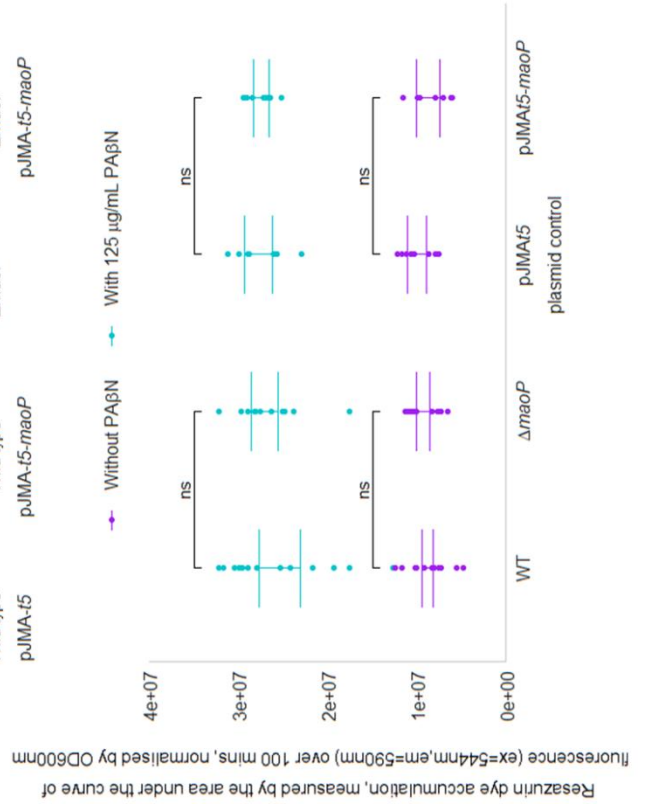
**a)**



**b)**



**c)**



**d)**

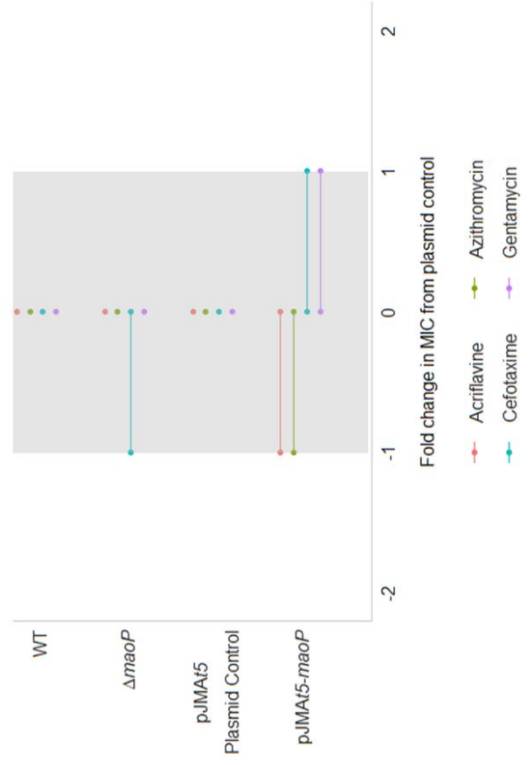


**Figure 7.5:** The effects of *maoP* on biofilm formation, efflux activity and, motility in *S. Typhimurium*. **a)** Biofilm biomass of various deletion mutants and overexpression constructs in wild type (WT) *S. Typhimurium*, measured by crystal violet (OD<sub>590 nm</sub>). Points show two biological and four technical replicates. **b)** Curli and cellulose biosynthesis in  $\Delta$ *maoP*, the WT overexpressing *maoP* on a plasmid and  $\Delta$ *toIC*, relative to the WT. Images are representative of four independent replicates. **c)** Dye accumulation in the WT,  $\Delta$ *maoP*, the WT overexpressing *maoP* on a plasmid and the empty plasmid control. Accumulation of resazurin (excitation 544 nm, emission 580 nm) was measured over 100 minutes and the area under the curve was plotted. Points show two biological and four technical replicates. Both biofilm biomass and dye uptake were measured in stress-free conditions (purple) and with PA $\beta$ N (blue). **d)** Fold change in MICs of acriflavine, azithromycin, cefotaxime and gentamycin in  $\Delta$ *maoP* relative to the WT, and the WT overexpressing *maoP* on a plasmid relative to the plasmid control, measured by the broth dilution method. The shaded area shows an experimental error of 1-fold change and points show two independent replicates. For all graphs, error bars show 95% confidence intervals and asterisks (\*) show where there was a significant difference between the strains indicated (Mann–Whitney U test, ns = not significant; \* =  $p < 0.05$ ; \*\* =  $p < 0.01$ ; \*\*\* =  $p < 0.001$ ; \*\*\*\* =  $p < 0.0001$ ).

### 7.6.2. DNA adenine methyltransferase Dam

Insertional inactivation of *dam*, encoding DNA methyltransferase (Szyf et al., 1984), was detrimental to biofilm development in *E. coli* and efflux activity in both *E. coli* and *S. Typhimurium*. Dam is involved in positive regulation of antigen 43 (*agn43/flu*) which has a strong role in aggregation and adhesion in the biofilm (Chauhan et al., 2013, Danese et al., 2000). Additionally, *dam* has an important role in drug resistance and may play a role in efflux activity (Motta et al., 2015, Adam et al., 2008). Susceptibility to acriflavine increased upon deletion of *dam* but there was no change in dye accumulation (figure 7.6). The effect of *dam* on various efflux systems and regulators was discussed in the previous chapter, and it was concluded that DAM methylation can affect drug susceptibility through many pathways, one of which may be efflux. There are conflicting reports about how *dam* expression affects *marR* (and subsequently *marA*) expression (Løbner-Olesen et al., 2003, Hughes et al., 2020, Prieto et al., 2009), and this should be further investigated to determine exactly how DAM methylation affects efflux regulation.

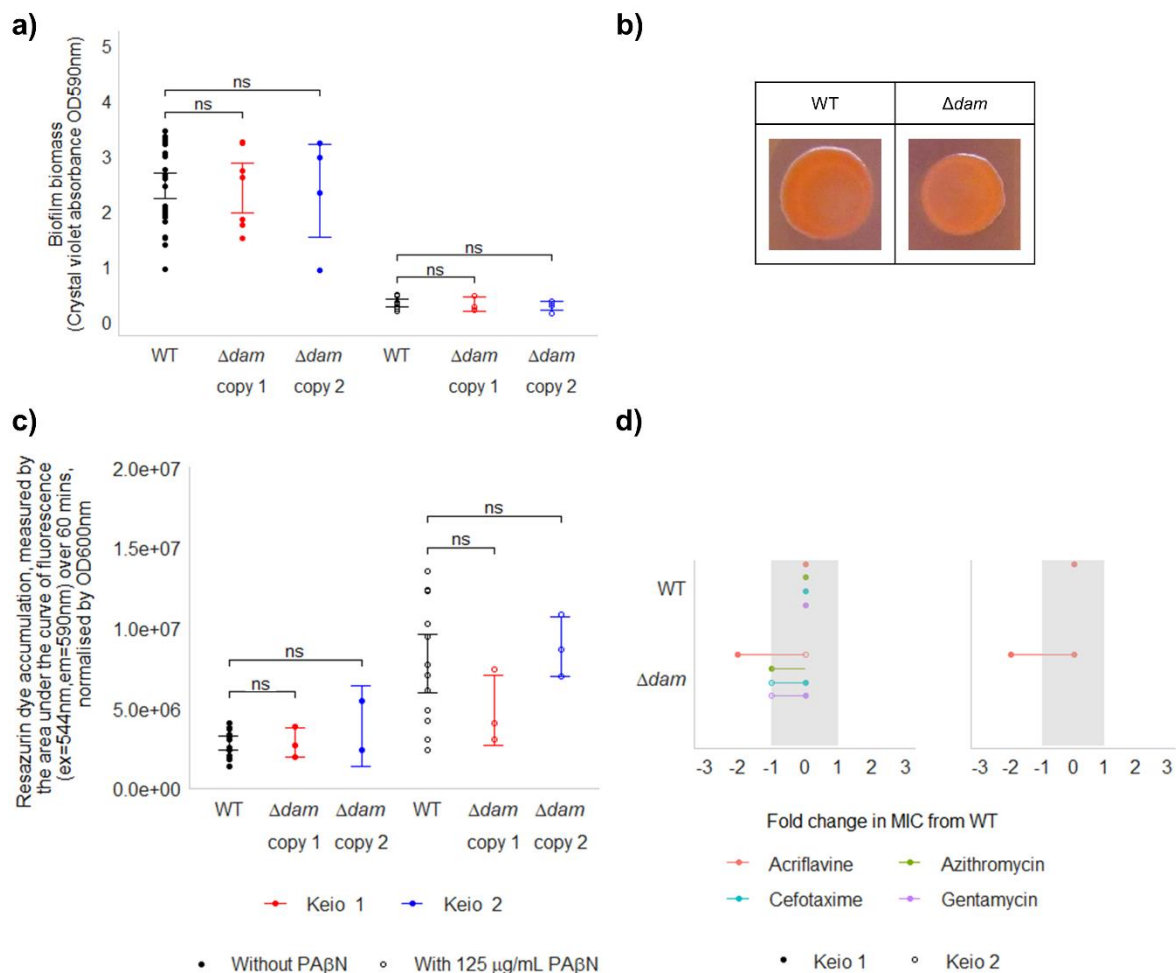


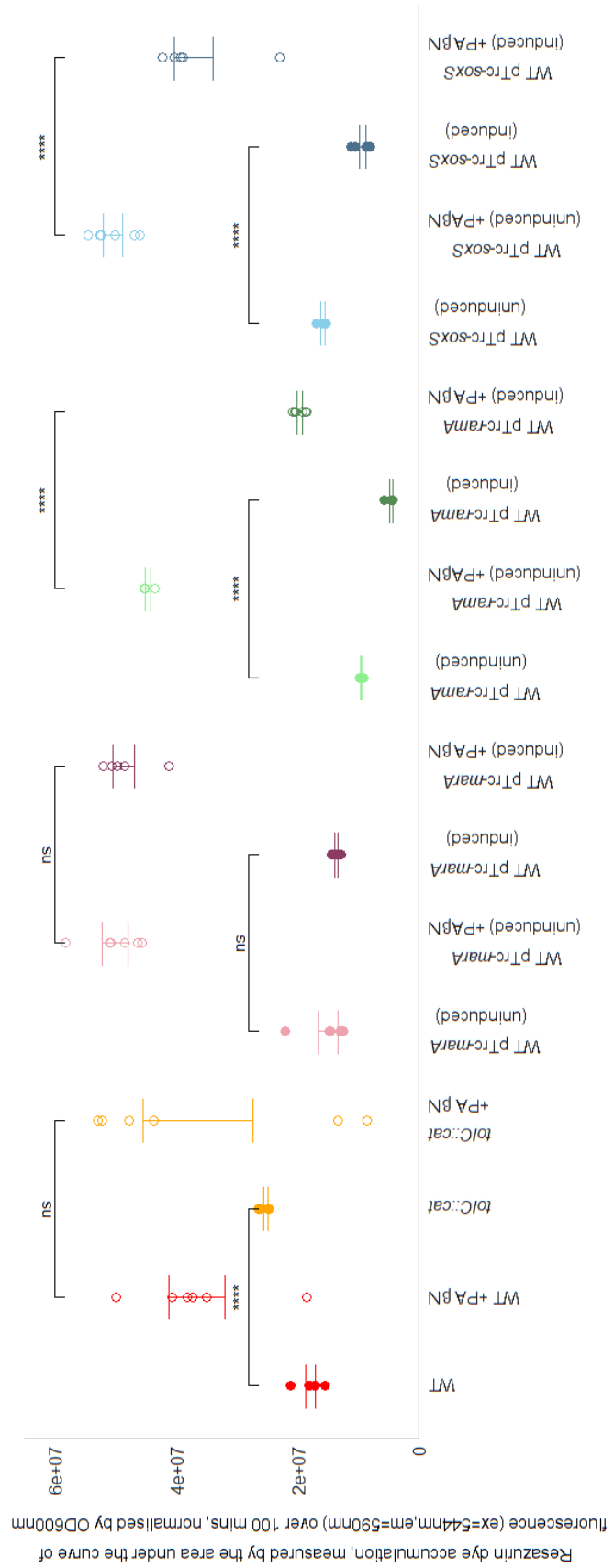
**Figure 7.6:** The effects of *dam* on biofilm formation and efflux activity in *E. coli*. **a)** Biofilm biomass of  $\Delta dam$  and the wild type (WT), measured by crystal violet staining (OD<sub>590 nm</sub>). Points show two biological and four technical replicates. **b)** Curli biosynthesis in  $\Delta dam$  relative to the WT. Images are representative of four independent replicates. **c)** Dye accumulation in  $\Delta dam$  and the WT. Accumulation of resazurin (excitation 544 nm, emission 580 nm) was measured over 60 minutes and the area under the curve was plotted. Points show two biological and four technical replicates. Both biofilm biomass and dye uptake were measured in stress free conditions (●) and with PA $\beta\text{N}$  (○). **d)** Fold change in MICs of acriflavine, azithromycin, cefotaxime and gentamycin in  $\Delta dam$  relative to the WT, measured by the broth (left) and agar (right) dilution methods. The shaded area shows an experimental error of 1-fold change and points show two independent replicates. For all graphs, error bars show 95% confidence intervals and asterisks (\*) show where there was a significant difference between the strains indicated (Mann–Whitney U test, ns = not significant; \* =  $p < 0.05$ ; \*\* =  $p < 0.01$ ; \*\*\* =  $p < 0.001$ ; \*\*\*\* =  $p < 0.0001$ ).

## 7.7. Transcription factors and regulators

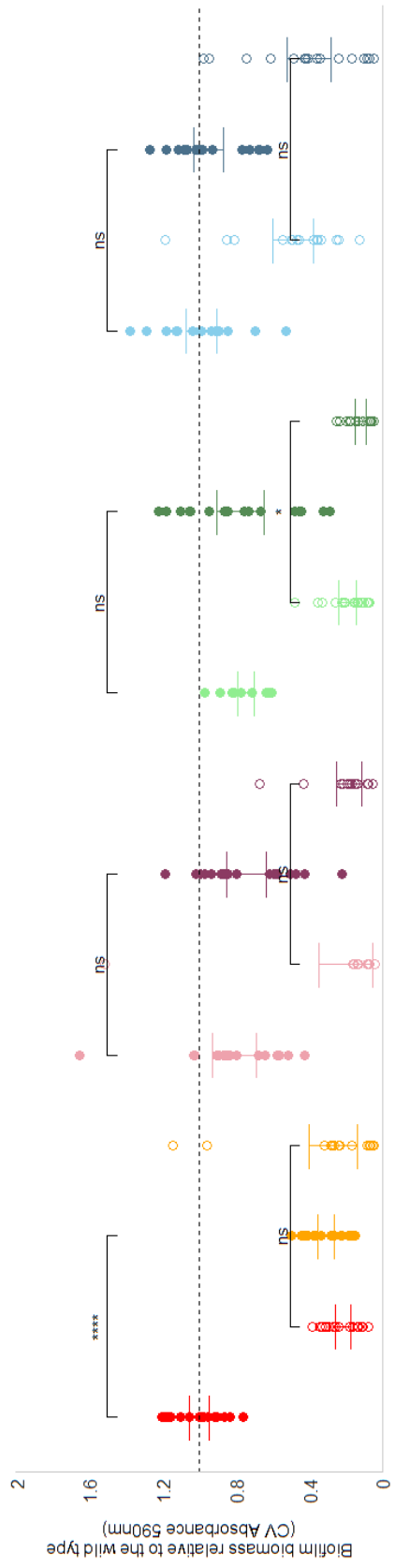
### 7.7.1. MarA, RamA and SoxS

MarR, RamR and SoxR are local negative regulators of the AraC/XylS family global transcriptional regulators MarA, RamA and SoxS, respectively, whereby deletion of *marR*, *ramR* or *soxR* results in overexpression of *marA*, *ramA* or *soxS*. Deletion of *marR* in *E. coli* and *ramR* in *S. Typhimurium* was detrimental to biofilm development but beneficial to efflux activity, according to the TraDIS-*Xpress* data. I investigated how overexpression of *marA*, *ramA* and *soxS*, affected biofilm biomass and efflux activity in *S. Typhimurium*. These genes were cloned into overexpression vector pTrc and expression was induced with IPTG. Overexpression of *ramA* lead to a slight decrease in biofilm biomass in *S. Typhimurium* relative to the uninduced plasmid control (figure 7.7a). Overexpression of the other regulators, *marA* and *soxS*, had no effect on biofilm biomass either in the presence or absence on PA $\beta$ N. Overexpression of any of *marA*, *ramA* or *soxS* has previously been reported to reduce biofilm biomass production in *S. Typhimurium* (Holden and Webber, 2020). Additionally, increased expression of *ramA* has been seen in *S. Typhimurium* when treated with incrementally increasing concentrations of PA $\beta$ N, associated with in incremental decreases in biofilm biomass (Holden and Webber, 2020). This supports the finding that modulation of these global transcriptional regulators affects biofilm development, but this may not be seen in these phenotypic assays due to compensation by functional copies of other regulators in the deletion mutants.

MarA, RamA and SoxS have a well-defined role in regulating efflux activity through activating expression of efflux systems, such as AcrAB-TolC (Holden and Webber, 2020). TraDIS-*Xpress* showed more insertions in *ramR* in *S. Typhimurium* treated with a subinhibitory concentration of acriflavine relative to the unstressed control. In *E. coli*, there were more insertions in *marR* when treated with PA $\beta$ N or subinhibitory concentrations of acriflavine relative to the unstressed control. When *E. coli* was treated with both PA $\beta$ N and acriflavine, the insertion frequency in *marR* was similar to the wild type, suggesting deletion of this gene was only beneficial to fitness when efflux was not inhibited. Overexpression of either *ramA* or *soxS* (another member of the same family of regulators) resulted in reduced dye accumulation in *S. Typhimurium* relative to the uninduced plasmid control in both the presence and absence of PA $\beta$ N, confirming increased efflux activity in these strains (figure 7.7b). It is possible that modulation of efflux activity causes overexpression of these genes, which then results in reduced biofilm biomass. However, the data suggest that overexpression of any of these genes alone cannot replicate the reduction in biofilm biomass seen in an efflux-deficient mutant, therefore this is most likely not the sole cause of this relationship.



b)



a)

**Figure 7.7:** The effects of *marA*, *ramA* and *soxS* on biofilm formation and efflux activity in *S. Typhimurium*. **a)** Biofilm biomass of *tolC::cat*, and strains overexpressing *marA*, *ramA* and *soxS* on plasmids, relative to wild type (WT) *S. Typhimurium*. Points represent two biological and eight technical replicates. **b)** Dye accumulation in the WT, *tolC::cat*, and strains overexpressing *marA*, *ramA* and *soxS* on plasmids. Accumulation of resazurin (excitation 544 nm, emission 580 nm) was measured over 100 minutes and the area under the curve was plotted. Points represent two biological and six technical replicates. Both biofilm biomass and dye uptake in strains overexpressing *marA*, *ramA* or *soxS* were compared to the plasmid controls, where expression was not induced with IPTG. Both biofilm biomass and dye uptake were measured in stress free conditions (●) and with PAβN (○). Error bars show 95% confidence intervals and asterisks (\*) show where there was a significant difference between the strains indicated (Mann–Whitney U test, ns = not significant; \* =  $p < 0.05$ ; \*\* =  $p < 0.01$ ; \*\*\* =  $p < 0.001$ ; \*\*\*\* =  $p < 0.0001$ ).

### 7.7.2. DksA and RpoS/ $\sigma^S$

DksA is a transcription factor that binds to RNA polymerase to affect transcription in response to the alarmone ppGpp, the synthesis of which is dependent on amino acid availability, growth rate or growth phase (Paul et al., 2004). Both are responsible for activating the stringent response, and one of the ways this is achieved is through inducing expression of *rpoS*, encoding sigma factor  $\sigma^S$ , which regulates the expression of genes involved in the general stress response (Brown et al., 2002). Together, DksA and ppGpp induce *rpoS* transcription through small regulatory RNAs *iraP* and *dsrA* (Girard et al., 2018).

Analysis of the TraDIS-*Xpress* data found that *dksA* in *E. coli* and *rpoS* in *S. Typhimurium* were detrimental to biofilm development and beneficial to efflux activity. Analysis of the  $\Delta$ *dksA* mutant in found increased adhesion in the early biofilm relative to wild type *E. coli*, but reduced biofilm biomass and curli biosynthesis in the mature biofilm (Appendix 5, figure 7.8 a,b). Deletion of *rpoS* has been reported to reduce curli biosynthesis in a similar manner in both *E. coli* and *S. Typhimurium* (Niba et al., 2008, Römling et al., 1998b). Previous work has shown a positive regulatory relation between *rpoS* and curli biosynthesis, where *rpoS* positively affects *mlrA* expression, which induces expression of *csgD* (Brown et al., 2001). This however does not explain why TraDIS-*Xpress* found *rpoS* to be detrimental to biofilm development in *S. Typhimurium*. It may be that *rpoS* has the same effect on biofilm development as *dksA*, where its expression is detrimental for adhesion and initial biofilm formation, but necessary for matrix production in the biofilm as it matures. Adhesion and biofilm structure through time should be compared in an  $\Delta$ *rpoS* mutant and wild type *S. Typhimurium* to investigate this further.

Both *dksA* and *rpoS* have a role in the cell's general stress response, and their expression was found to be beneficial when the cell was stressed by an efflux inhibitor or sub-inhibitory concentrations of acriflavine. Deletion of *dksA* resulted in increased dye uptake and increased susceptibility to acriflavine relative to wild type *E. coli* (figure 7.8 c,d). Previous work has found that expression of *rpoS* increased in both *E. coli* and *S. Typhimurium* (and expression of *dksA* increased in *S. Typhimurium*) following exposure to triclosan, which is also a substrate of the AcrAB-TolC efflux pump (Bailey et al., 2009). Pathways regulated by  $\sigma^S$  were seen to decrease drug susceptibility in *E. coli* mutants lacking the AcrAB and AcrEF efflux systems (Cho et al., 2021), thereby supporting the findings from TraDIS-*Xpress* that activation of the stringent response is beneficial for survival in efflux-deficient mutants. The small regulatory RNA *iraP* was also identified by TraDIS-*Xpress* to be beneficial to efflux activity in *S. Typhimurium* alongside *rpoS*, so it is likely that *dksA* activates *rpoS* expression through *iraP* (Girard et al., 2018) to confer this fitness benefit. It is unlikely that the expression of *dksA* or *rpoS* is responsible for the



deficit in curli biosynthesis seen in an efflux mutant, as these genes are overexpressed when the cell is under stress, which would in turn activate expression of *csgD* rather than reduce curli biosynthesis. Further work is therefore necessary to determine whether *dksA* and *rpoS* expression increases upon inactivation of efflux, and investigation is needed into why curli expression is transcriptionally repressed upon efflux inactivation, rather than induced by *dksA* and *rpoS* expression.

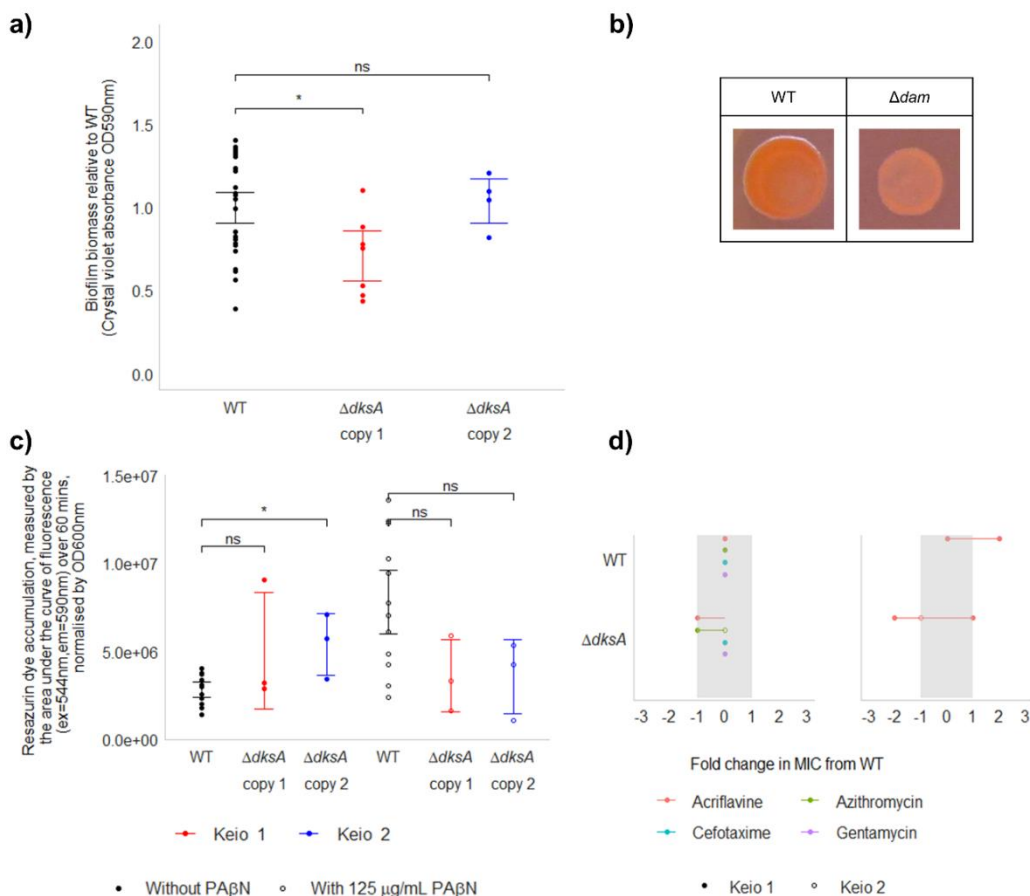


**Figure 7.8:** The effects of *dksA* on biofilm formation and efflux activity in *E. coli*. **a)** Biofilm biomass of  $\Delta dksA$  and the wild type (WT), measured by crystal violet staining (OD<sub>590 nm</sub>). Points show two biological and four technical replicates. **b)** Curli biosynthesis in  $\Delta dksA$  relative to the WT. Images are representative of four independent replicates. **c)** Dye accumulation in  $\Delta dksA$  and the WT. Accumulation of resazurin (excitation 544 nm, emission 580 nm) was measured over 60 minutes and the area under the curve was plotted. Points show two biological and four technical replicates. Dye uptake was measured in stress free conditions (●) and with PA $\beta$ N (○). **d)** Fold change in MICs of acriflavine, azithromycin, cefotaxime and gentamycin in  $\Delta dksA$  relative to the WT, measured by the broth (left) and agar (right) dilution methods. The shaded area shows an experimental error of 1-fold change and points show two independent replicates. For all graphs, error bars show 95% confidence intervals and asterisks (\*) show where there was a significant difference between the strains indicated (Mann–Whitney U test, ns = not significant; \* =  $p < 0.05$ ; \*\* =  $p < 0.01$ ; \*\*\* =  $p < 0.001$ ; \*\*\*\* =  $p < 0.0001$ ).

### 7.7.3. Antitoxin component TomB

TomB is an antitoxin to Hha, which makes a complex with H-NS to negatively regulate transcription (Fernández-García et al., 2016). Hha has been reported to reduce biofilm formation through reducing fimbriae expression and repressing rare tRNAs, and TomB is thought to rescue biofilm formation by attenuating Hha activity (Garcia-Contreras et al., 2008). Analysis of the TraDIS-*Xpress* data found *tomB* to be beneficial throughout biofilm development in *E. coli*, and deletion of *tomB* reduced cell aggregation, curli biosynthesis and biofilm biomass (Appendix 5, figure 7.9 a,b). Deletion of *tomB* was also found to reduce acriflavine susceptibility in *E. coli*, suggesting its deletion may affect efflux activity, but there was no change in dye uptake in  $\Delta tomB$  relative to wild type *E. coli* (figure 7.9 c,d). Previous work has found that insertional inactivation of *tomB* rescued biofilm biomass production in an  $\Delta mdtK$  mutant to the levels of the wild type, only partially restored biofilm biomass production in a  $\Delta toIC$  mutant and had no effect on biofilm biomass in an  $\Delta acrB$  mutant (Baugh, 2014). Contrary to this, I saw reduced curli biosynthesis when *tomB* was inactivated in an  $\Delta acrB$  mutant relative to both wild type *S. Typhimurium* and the  $\Delta acrB$  mutant (figure 7.9 b). *TomB* is chromosomally located immediately downstream of *acrB* in both *E. coli* and *S. Typhimurium*, therefore a change in *acrB* transcription may affect *tomB* transcription solely due to their colocation. Additionally, colocation can be suggestive of a functional link between genes. To investigate this, transcription of *tomB* should be investigated in the presence and absence of active efflux and *acrB* to determine whether biofilm formation is affected through this route. Additionally, the mechanism by which curli biosynthesis is affected by *tomB* has not yet been described, therefore *csgD* and *csgB* transcription, as well as the transcription of other known curli regulators, should be investigated in the *tomB* mutant relative to the wild type.

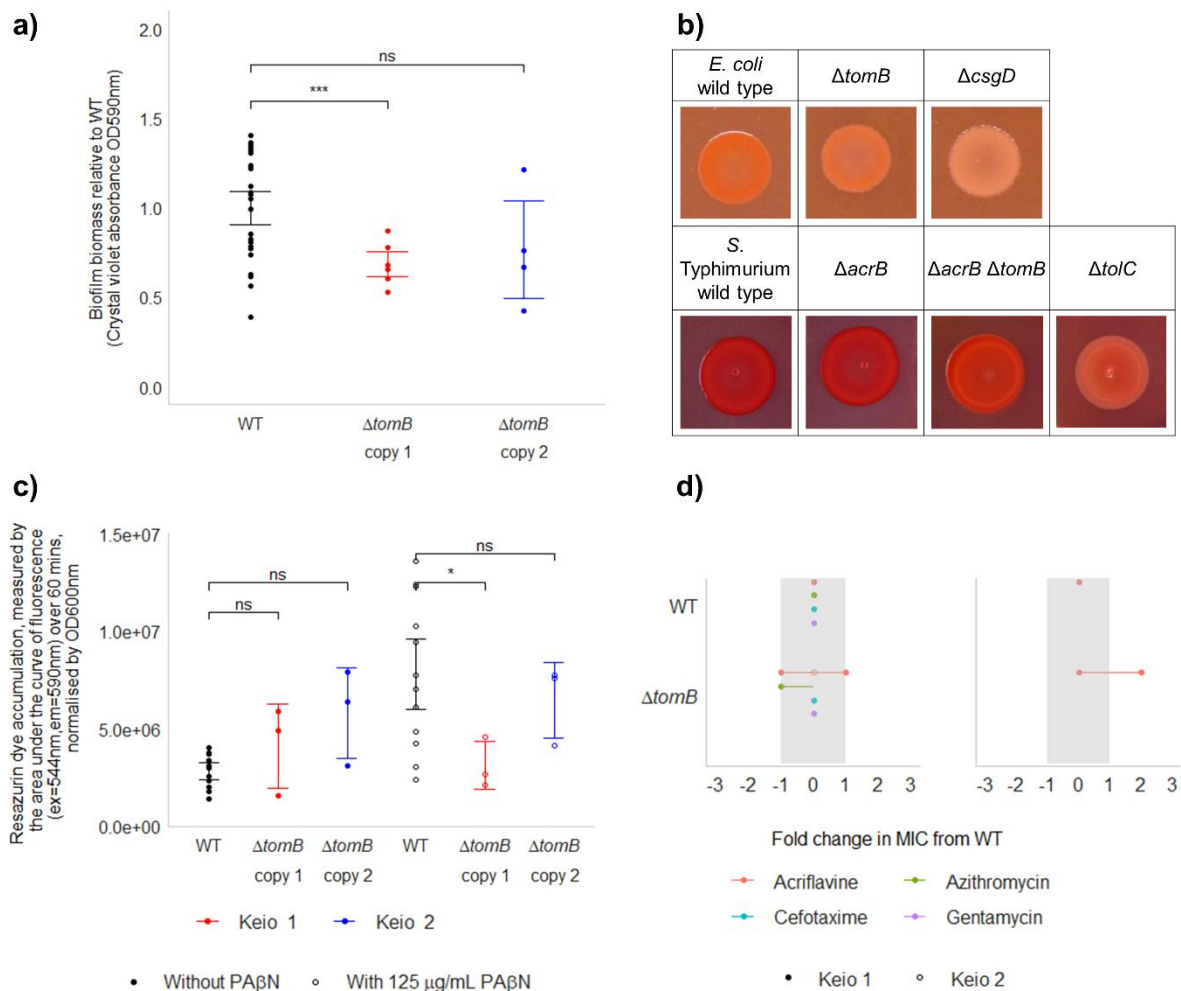


**Figure 7.9:** The effects of *tomB* on biofilm formation and efflux activity in *E. coli*. **a)** Biofilm biomass of  $\Delta tomB$  and the wild type (WT), measured by crystal violet staining (OD<sub>590 nm</sub>). Points show two biological and four technical replicates. **b)** Curli biosynthesis in *E. coli* and *S. Typhimurium* wild types and  $\Delta tomB$  mutants., *E. coli*  $\Delta csgD$  and *S. Typhimurium*  $\Delta toIC$ , are included as curli-deficient controls. Images are representative of four technical and two biological replicates. **c)** Dye accumulation in  $\Delta tomB$  and the WT. Accumulation of resazurin (excitation 544 nm, emission 580 nm) was measured over 60 minutes and the area under the curve was plotted. Points show two biological and four technical replicates. Both biofilm biomass and dye uptake were measured in stress free conditions (●) and with PA $\beta$ N (○). **d)** Fold change in MICs of acriflavine, azithromycin, cefotaxime and gentamycin in  $\Delta dksA$  relative to the WT, measured by the broth (left) and agar (right) dilution methods. The shaded area shows an experimental error of 1-fold change and points show two independent replicates. For all graphs, error bars show 95% confidence intervals and asterisks (\*) show where there was a significant difference between the strains indicated (Mann–Whitney U test, ns = not significant; \* =  $p < 0.05$ ; \*\* =  $p < 0.01$ ; \*\*\* =  $p < 0.001$ ; \*\*\*\* =  $p < 0.0001$ ).

#### 7.7.4. Acid response regulator GadW









In *E. coli*, expression of *gadW* was found to be beneficial for biofilm development in the mature biofilm grown for 48 hours, and detrimental for fitness when treated with the efflux inhibitor PA $\beta$ N. There was no difference in biofilm biomass, curli biosynthesis, dye accumulation or drug susceptibility between wild type *E. coli* and a  $\Delta$ *gadW* deletion mutant (Appendix 5). Previous work found *gadW* and other genes involved in acid resistance had a small effect on biofilm development only at 25°C, where the effect was not seen at 37°C (Mathlouthi et al., 2018). Biofilm formation was investigated at 30°C in this work, therefore the full effect of *gadW* on biofilm development may not have been picked up by these assays. Additionally, the  $\Delta$ *gadW* mutants from the Keio collection were not sequenced to confirm the construct was correct, therefore these phenotypic analyses may be flawed. Based on this work, manipulation of *gadW* expression does not appear to be sufficient to result in the biofilm deficit seen when efflux is disrupted.

#### 7.8. Cell envelope biogenesis

Genes involved in LPS biosynthesis had a strong effect on both curli biosynthesis and drug susceptibility in both *E. coli* and *S. Typhimurium*. Increased azithromycin susceptibility was seen in  $\Delta$ *waaF*,  $\Delta$ *waaG* and  $\Delta$ *waaP* mutants in *E. coli*, and decreased cefotaxime susceptibility was seen in  $\Delta$ *waaG* and  $\Delta$ *waaP* (figure 7.10d). Both drugs are substrates of the AcrAB-TolC efflux system, therefore it is most likely that these genes involved in LPS core biosynthesis affect drug susceptibility through a pathway independent of efflux activity. Increased dye accumulation was seen in a  $\Delta$ *waaG* mutant in *E. coli* (figure 7.10c). Previous work in efflux-deficient *P. aeruginosa* found that deletion of six RND efflux pumps resulted in the activation of pathways responsible for lipid A modifications and membrane protection (Adamiak et al., 2021), which supports the findings of this work that LPS biosynthesis is affected by efflux modulation. Additionally, previous work has found that *acrA*, along with other genes encoding efflux pump components, were upregulated following deletion of genes involved in LPS biosynthesis (Wang et al., 2021). Efflux regulator *ramA* has been reported to bind upstream and initiate expression of genes in the *lpx* operon involved in lipid A and LPS biosynthesis (De Majumdar et al., 2015). TraDIS-*Xpress* data from *S. Typhimurium* found that genes involved in biosynthesis of the O-antigen component of the LPS were implicated in efflux activity and acriflavine susceptibility. Deletion of *rffF* prevented survival under the concentration of resazurin used in dye accumulation assays (figure 7.10c), suggesting a role for *rffF* and O-antigen biosynthesis as a whole in preventing dye uptake.

Deletion of  $\Delta$ *waaF*,  $\Delta$ *waaG* and  $\Delta$ *waaP* resulted in a significant reduction in curli biosynthesis and biofilm biomass relative to wild type *E. coli* (figure 7.10 a,b). Previous

work has suggested that the LPS may have a role in the correct folding and export of curli (Swasthi and Mukhopadhyay, 2017). Investigation is needed into whether disruption of LPS affects curli transcription or solely protein folding and export. However, no differences were observed in LPS extracted from wild type *S. Typhimurium* and mutants lacking either *tolC* or *acrB* (Baugh, 2014), therefore LPS biosynthesis cannot be solely responsible for the biofilm deficit seen in *E. coli* or *S. Typhimurium* with reduced efflux activity. Further work should focus on characterising how genes involved in LPS biosynthesis affect the expression of genes encoding efflux systems and their regulators.

<i>E. coli</i> WT	<i>S. Typhimurium</i> WT		
$\Delta waaF$	$\Delta rfbF$		
$\Delta waaP$			
$\Delta waaG$			
$\Delta wzvB$			
$\Delta wecF$			

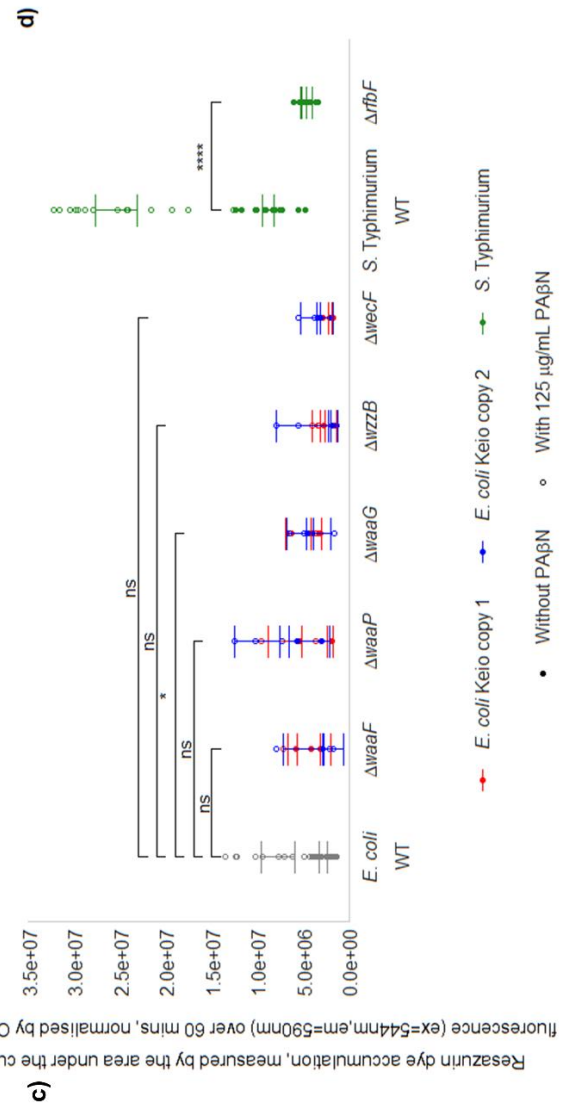
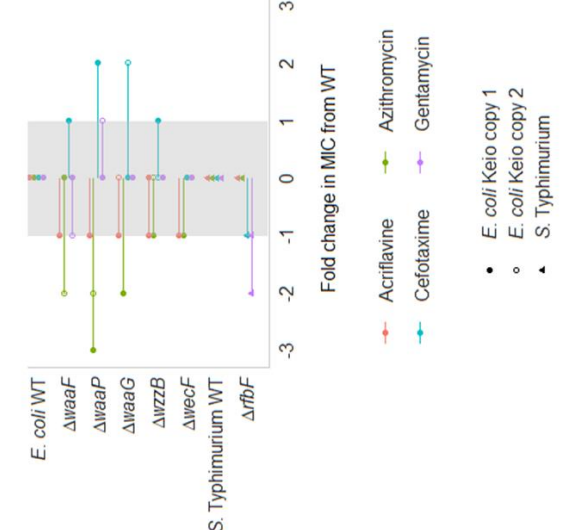
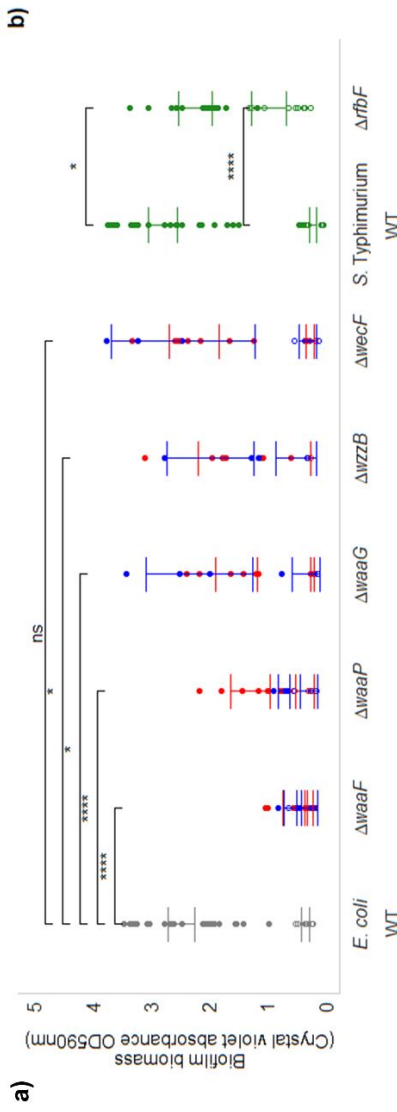


**Figure 7.10:** The effects of genes involved in LPS biosynthesis on biofilm formation and efflux activity in *E. coli* and *S. Typhimurium*. **a)** Biofilm biomass of deletion mutants and the wild type (WT) of each species, measured by crystal violet staining (OD<sub>590 nm</sub>). Points show two biological and a minimum of six technical replicates. **b)** Curli biosynthesis in deletion mutants relative to the WT of each species. Images are representative of four independent replicates. **c)** Dye accumulation in deletion mutants and the WT of each species. Accumulation of resazurin (excitation 544 nm, emission 580 nm) was measured over 60 minutes in *E. coli* and 100 minutes in *S. Typhimurium* and the area under the curve was plotted. Points show two biological and four technical replicates. Both biofilm biomass and dye uptake was measured in stress free conditions (●) and with PAβN (○). **d)** Fold change in MICs of acriflavine, azithromycin, cefotaxime and gentamycin in deletion mutants relative to the WT of each species, measured by the broth dilution method. The shaded area shows an experimental error of 1-fold change and points show two independent replicates. For all graphs, error bars show 95% confidence intervals and asterisks (\*) show where there was a significant difference between wild type and the mutant indicated (Mann–Whitney U test, ns = not significant; \* =  $p < 0.05$ ; \*\* =  $p < 0.01$ ; \*\*\* =  $p < 0.001$ ; \*\*\*\* =  $p < 0.0001$ ).

## 7.9. Intracellular signalling systems

### 7.9.1. Response regulator OmpR

OmpR is a positive regulator of the *csgD* promoter and induces curli production (Römling et al., 1998a). In concordance with this, deletion of *ompR* resulted in reduced biofilm biomass and curli biosynthesis in *E. coli*. TraDIS-*Xpress* also found a role for OmpR in efflux activity, where there were more insertions in *ompR* in *E. coli* treated with subinhibitory concentrations of acriflavine relative to the unstressed control. There was no difference in insertion frequency in *ompR* in conditions with both acriflavine and PA $\beta$ N relative to the unstressed control, which indicates expression of *ompR* is only detrimental to acriflavine susceptibility when efflux is active. Deletion of *ompR* reduced dye accumulation and decreased cefotaxime susceptibility in *E. coli*, supporting the finding from the TraDIS-*Xpress* data that its expression is detrimental to efflux activity. OmpR has a well-defined role in regulating expression of major outer membrane porins OmpF and OmpC, but the difference in dye accumulation seen in the presence and absence of efflux inhibitor PA $\beta$ N suggests that *ompR* can also affect efflux activity rather than just diffusion of dye through these porins.

OmpR is the response regulator component of a two-component system involved the sensor kinase EnvZ involved is osmoregulation (Cai and Inouye, 2002). The sensor kinase component of this system, encoded by *envZ*, was not found by TraDIS-*Xpress* to affect fitness in experiments investigating either biofilm development or efflux activity. This was unexpected, as both components are necessary for the sensory system to function. It is possible that disruption of efflux results in reduced transcription of *ompR* or phosphorylation of OmpR independent of EnvZ, thereby reducing *csgD* transcription and curli biosynthesis. This could be investigated by measuring *ompR* transcription in an  $\Delta$ *acrB* or  $\Delta$ *tolC* mutant, or when efflux is inhibited by PA $\beta$ N, relative to the wild type. Additionally, ChIP-seq analysis of the OmpR regulon found a small signal at the *acrA* promoter (Perkins et al., 2013), potentially indicating that OmpR may directly regulate expression of the AcrAB-TolC efflux system. However, further investigation is needed into this to determine whether OmpR can and does affect the transcription of genes encoding efflux pump components.

### 7.9.2. Adenylate cyclase CyaA

TraDIS-*Xpress* identified a role for *cyaA*, encoding adenylate cyclase involved in cAMP synthesis, in biofilm development and efflux activity in *S. Typhimurium*. Increased expression of *cyaA* was beneficial to fitness in biofilms grown for 24 hours relative to the planktonic control, and insertional inactivation of *cyaA* benefitted the fitness of *S. Typhimurium* treated with subinhibitory concentrations of acriflavine relative to the unstressed control. The relationship between cAMP and biofilm development has been



characterised, where cAMP positively regulates curli biosynthesis through *csgD* (Hufnagel et al., 2016). This is supported by this work, where deletion of *cyaA* resulted in significantly reduced biofilm biomass and slightly reduced curli biosynthesis relative to the wild type (figure 7.11 a,b). The relationship between cAMP and efflux activity is slightly more complex, where there was no significant difference in dye accumulation or drug susceptibility between wild type *S. Typhimurium* and the  $\Delta$ *cyaA* mutant (figure 7.11 c,d). Because of this, it is unlikely that cAMP biosynthesis through *cyaA* is solely responsible for the biofilm deficit seen in an efflux-deficient mutant. cAMP may affect efflux activity through MarA, as it has previously been reported that deletion of *cyaA* reduced *marA*-mediated multidrug resistance in *E. coli* and resulted in significantly increased susceptibility to cefoxitin, norfloxacin, chloramphenicol and minocycline in a  $\Delta$ *marRA* background relative to a  $\Delta$ *marR* background (Ruiz and Levy, 2010). Further investigation into how cAMP affects *marA*, as well as related regulators *ramA* and *soxS*, is necessary to reveal how *cyaA* affects efflux activity in *S. Typhimurium*.

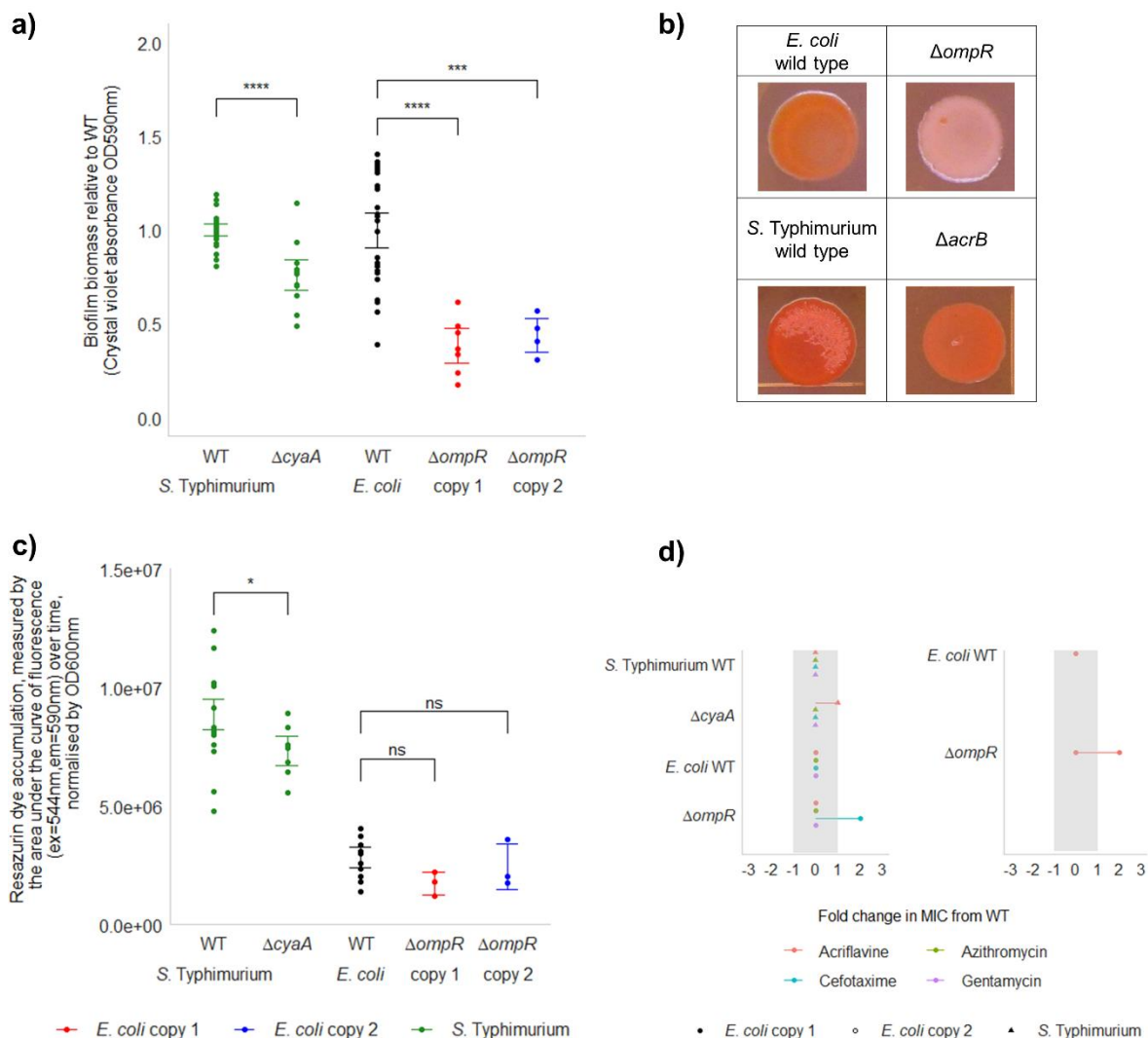


**Figure 7.11:** The effects of *ompR* and *cyxA* on biofilm formation and efflux activity in *E. coli* and *S. Typhimurium*. **a)** Biofilm biomass of  $\Delta ompR$  relative to wild type (WT) *E. coli* and  $\Delta cyxA$  relative to WT *S. Typhimurium*, measured by crystal violet staining (OD<sub>590 nm</sub>). Points show two biological and a minimum of four technical replicates. **b)** Curli biosynthesis of  $\Delta ompR$  and  $\Delta cyxA$  relative to the WT of each species. Images are representative of four technical and two biological replicates. **c)** Dye accumulation in  $\Delta ompR$ ,  $\Delta cyxA$  and the WT of each species. Accumulation of resazurin (excitation 544 nm, emission 580 nm) was measured over 60 minutes for *E. coli* and 100 minutes for *S. Typhimurium*, and the area under the curve was plotted. Points show two biological and four technical replicates. Both biofilm biomass and dye uptake were measured in stress free conditions (●) and with PA $\beta$ N (○). **d)** Fold change in MICs of acriflavine, azithromycin, cefotaxime and gentamycin in  $\Delta dksA$  relative to the WT, measured by the broth (left) and agar (right) dilution methods. The shaded area shows an experimental error of 1-fold change and points show two independent replicates. For all graphs, error bars show 95% confidence intervals and asterisks (\*) show where there was a significant difference between the strains indicated (Mann–Whitney U test, ns = not significant; \* =  $p < 0.05$ ; \*\* =  $p < 0.01$ ; \*\*\* =  $p < 0.001$ ; \*\*\*\* =  $p < 0.0001$ ).

### 7.10. Fimbriae

Genes encoding fimbriae subunits and regulators of fimbriae expression were seen to affect the fitness of both *E. coli* and *S. Typhimurium* during biofilm formation and when treated with acriflavine in the presence and absence of PA $\beta$ N. In both species, TraDIS-*Xpress* found that expression of fimbriae was beneficial at all stages of biofilm development but detrimental for survival in the presence of PA $\beta$ N or acriflavine. Genes involved in fimbriae synthesis and regulation were also found by TraDIS-*Xpress* to be detrimental for fitness in *E. coli* when treated with triclosan (Yasir et al., 2020) and fosfomycin (Turner et al., 2020b). Acriflavine, triclosan and fosfomycin can all be removed from the cell via the AcrAB-TolC efflux pump, therefore it is still unclear whether expression of fimbriae affects drug susceptibility in a manner dependent on or independent of efflux activity. Investigation into how genes encoding fimbriae subunits and regulators affect the susceptibility of *E. coli* to a non-efflux substrate, such as kanamycin or gentamycin, will determine whether fimbriae affect efflux activity or drug susceptibility through a different pathway.

### 7.11. Motility

Negative regulators of motility *hdfR* and *IrhA* were found by TraDIS-*Xpress* to be detrimental for biofilm formation and development, but beneficial for efflux activity in *E. coli*. Analysis of biofilm biomass production in these knockout mutants found reduced biomass in an  $\Delta$ *hdfR* mutant (Appendix 5), contrary to what was predicted by TraDIS-*Xpress*. Deletion of *IrhA* was beneficial for adhesion in the early biofilm, possibly due to the role of *IrhA* in reducing fimbriae expression through inducing expression of *fimE*, but deletion of *IrhA* did not affect biofilm biomass. Deletion of *hdfR* or *IrhA* was found to be detrimental for survival in the presence of PA $\beta$ N or subinhibitory concentrations of acriflavine, however no change in dye accumulation or drug susceptibility was found in these deletion mutants. Genes involved in encoding flagella subunits were not identified by TraDIS-*Xpress* in experiments investigating efflux activity, so the role of these regulators in efflux activity or drug susceptibility may be independent of their role in motility regulation. Further investigation into the regulons of *hdfR* and *IrhA* may give further insight into how these genes affect efflux activity or drug susceptibility.

### 7.12. Conclusions

Many pathways were identified to affect both biofilm development and efflux activity in *E. coli* and *S. Typhimurium*, including electron transport, protein chaperones, DNA housekeeping, transcription factors and regulators, cell envelope biogenesis and intracellular signalling systems. No one pathway was found to be the sole cause of the

deficit in biofilm biomass seen in an efflux-deficient mutant. Therefore, it is most likely that disruption of efflux activity results in multiple pathways being altered, each of which impact biofilm matrix production to some degree. It is probable that the biofilm deficit resulting from loss of efflux function is a result of this cumulative perturbation of multiple pathways rather than one single regulatory link.

Different pathways relevant to both biofilm formation and efflux activity affected each phenotype to different degrees. Deletion of the *nuo* operon was found to reduce biofilm biomass production in both *E. coli* and *S. Typhimurium* and reduce efflux activity in *S. Typhimurium*. This was further investigated in this chapter to gain a deeper understanding of how expression of the *nuo* operon affected biofilm matrix production. I determined that it is unlikely that the deficit in curli biosynthesis seen in a *nuo* mutant was mediated through disruption of purine biosynthesis. The NADH dehydrogenase encoded by the *nuo* operon has a role in creating the proton gradient necessary for powering efflux pumps, ATP synthesis and flagella rotation through proton motive force, but deleting *nuoB* in both *E. coli* and *S. Typhimurium* did not affect flagella rotation in a consistent manner in both species. This suggests that the deficit in curli biosynthesis is not mediated through disruption of the proton gradient. Further investigation is therefore necessary to determine how expression of the *nuo* operon and the function of electron transport chain affect curli biosynthesis and transcription of *csgD* and *csgB*.

In this chapter, I investigated how overexpression of various genes affected biofilm development and efflux activity, following on from the finding that deletion of these genes had a strong effect on curli biosynthesis. Deletion of *dsbA* resulted in increased curli biosynthesis in both *E. coli* and *S. Typhimurium*, and increased expression of *dsbA* in *S. Typhimurium* reduced curli biosynthesis to the levels of the wild type. Increasing expression of *dsbA* further may have reduced curli biosynthesis further, and this should be tested to confirm. Expression of *dsbA* should be measured following inactivation of efflux to determine whether it could be responsible for the reduction in curli biosynthesis seen in an efflux mutant. Additionally, expression of curli biosynthetic genes *csgD* and *csgB* should be measured in mutants overexpressing *dsbA* and those without a functional copy of *dsbA* relative to the wild type to determine whether its deletion affects transcription of the *csgDEFG* or *csgBAC* operons, or whether *dsbA* affects curli biosynthesis post transcriptionally.

Manipulation of *maoP* expression has the opposite effect on curli biosynthesis relative to *dsbA*, where deletion of *maoP* reduced curli biosynthesis and biofilm biomass. Increased expression of *maoP* restored curli biosynthesis to wild type levels and increased biofilm biomass relative to the vector control, but only when a chromosomal copy of *maoP* was

present. This suggests the chromosomal location of *maoP* is important for its activity and its relationship with biofilm development, but this requires further investigation. Deletion of *maoP* reduced efflux activity in *E. coli*, but neither deletion nor overexpression of *maoP* affected efflux activity or drug susceptibility in *S. Typhimurium*. Previous work found reduced expression of *maoP* in an *acrB* deletion mutant (Ruiz and Levy, 2013), therefore the relationship between *maoP* transcription and efflux activity warrants further investigation. As before, expression of *csgD* and *csgB* should be investigated in mutants overexpressing *maoP* and without a functional copy of *maoP* to determine through which route curli biosynthesis is affected.

Both efflux activity and biofilm formation affect the cell's susceptibility to antimicrobials. Comparing the genes involved has highlighted shared regulatory pathways that may prove to be useful targets for increasing drug susceptibility and efficacy in bacterial biofilms. Developing drugs that either silence these genes or inactivate the gene products may reduce the fitness of a pathogen in the biofilm as well as increasing its susceptibility to antibiotics, making infections easier to treat. Increasing our understanding of the genetic basis of biofilm formation under antimicrobial stress has multiple applications, both in situations where biofilm development is advantageous and disadvantageous.

## **8. CHAPTER 8: OVERALL DISCUSSION**

## 8.1. Biofilms

This study identified how gene expression contributes to fitness during biofilm formation in both *E. coli* and *S. Typhimurium*. Pathways involved in both species include type I fimbriae regulation, flagella biosynthesis, purine biosynthesis, curli production, LPS biosynthesis, sugar utilisation, transmembrane transport and various similar transcriptional regulators. After 12 hours growth, genes involved in adhesion and transcriptional regulation were beneficial for fitness in biofilm cultures relative to planktonic, and after 24 hours, genes with roles in DNA housekeeping and matrix production were important. Genes that were beneficial for fitness in biofilm cultures grown for 48 hours relative to planktonic cultures had roles in purine biosynthesis, c-di-GMP metabolism, flagella biosynthesis, transmembrane transport, transcriptional regulation and cell division. Throughout biofilm formation and development, fimbriae expression and motility regulation were extremely important, with insertion frequencies in *fimB*, *fimE*, *IrhA* and *tomB* differing between biofilm and planktonic conditions at all time points tested, rather than solely initial attachment. Additionally, this work identified that *dsbA* and *dksA* had temporal contributions to biofilm development in *E. coli*, whereby they affected fitness differently in a biofilm grown for 12 hours relative to a mature biofilm grown for 48 hours. This work built upon our existing knowledge of genes involved in biofilm formation and identified their time-specific roles in *E. coli*. The TraDIS-*Xpress* approach used in this study identified many genes already known to affect biofilm development, such as those involved in regulating curli biosynthesis, but was also able to highlight roles for novel genes. This work identified five genes that had novel roles in biofilm formation in *E. coli*, including *zapE* and *truA* involved in cell division, *maoP* in DNA housekeeping and *yigZ* and *ykgJ* of unknown function. Their effects on biofilm biomass, aggregation, matrix production and adhesion were investigated. Biofilm biomass and curli biosynthesis were severely reduced following inactivation of *maoP*. Deletion of *truA* and *ykgJ* resulted in the formation of filamented cells that reduced biofilm density after 48 hours growth on glass under flow conditions. Aggregation was significantly increased following deletion of either *zapE* or *yigZ*. Further characterisation of how these genes affect biofilm formation and development is necessary. This work has added to our understanding of important time-specific roles for known and novel genes with roles in biofilm formation in *E. coli*.

A transposon mutant library was also constructed in *S. Typhimurium* to compare the genes involved in biofilm development to those in *E. coli*. The *lac* repressor was inserted into the chromosome of *S. Typhimurium* to allow control of the transposon-located *tac* promoter essential for TraDIS-*Xpress*. There were many similarities between *E. coli* and *S. Typhimurium* in the genes that affected fitness of cells in the biofilm relative to planktonic culture, but there were also various key differences. Cellulose biosynthesis and various genes involved in amino acid biosynthesis were important for adhesion in *S.*

Typhimurium biofilms grown for 12 hours. As the biofilm matures, genes involved in DNA housekeeping were identified by TraDIS-*Xpress* to affect biofilm development after 24 hours growth in only *E. coli* and not *S. Typhimurium*. Genes involved in cAMP biosynthesis, protease activity, ribosomal modification and respiration were found to only affect the fitness of *S. Typhimurium*, and not *E. coli*, in the maturing biofilm grown for 24 or 48 hours. Deletion of the *nuo* operon (encoding the NADH dehydrogenase at the start of the electron transport chain) was identified by TraDIS-*Xpress* to reduce the fitness of the mature biofilm in *S. Typhimurium*, but analysis of knockout mutants found that inactivation of the *nuo* operon reduced biofilm biomass and curli biosynthesis in both species. This study is the first to compare the genes impacting biofilm formation over time in *E. coli* and *S. Typhimurium*, and the first to investigate the contribution of the *nuo* operon to biofilm formation in both species. I also identified 21 genes in *S. Typhimurium* that had not previously been implicated in biofilm formation, and three of these, *STM14\_1074*, *yjiG* and *tyrT*, were investigated further. All three genes were showed to have a positive effect on curli biosynthesis, and *STM14\_1074* and *yjiG* were showed to have roles in adhesion. Further work should build on this to fully characterise the role of these genes on biofilm biomass production and matrix biosynthesis in both species. This comparison of the requirements for optimal biofilm fitness between *E. coli* and *S. Typhimurium* sheds light on the species-specific differences in biofilm formation, but also deepens out understanding of the core requirements for biofilm formation across the Enterobacteriaceae family.

This work was completed in one set of lab conditions, and the same approach can be applied to a wide range of environmental conditions, strains and species, abiotic and biotic surfaces. This will provide a wider list of essential genes for biofilm formation shared amongst a majority of human pathogens, as well as substrate-, condition- and species-specific genes and pathways for specific industrial, clinical and drug-development applications. As well as temporal changes in gene expression, spatial changes have been shown to affect biofilm development (Samanta et al., 2013). Investigation into the spatial distribution of target genes in the biofilm, to assay how gene expression throughout the biofilm over time affects biofilm fitness, would be the next logical step in furthering our understanding of biofilm development.

## 8.2. Efflux

TraDIS-*Xpress* was also used to identify the genes involved in efflux activity in *E. coli* and *S. Typhimurium*. This was done by looking for changes in the data generated when bacteria were grown with the efflux substrate acriflavine in the presence and absence of the efflux inhibitor PA $\beta$ N. This facilitated the identification of genes involved in efflux activity as well as acriflavine susceptibility. Predictions were validated in several deletion



mutants in both *E. coli* and *S. Typhimurium* through measuring resazurin dye accumulation and antibiotic susceptibility. This approach identified known efflux pumps and regulators, with strong signals seen in *E. coli* for the AcrAB-TolC efflux system and global transcriptional regulatory systems MarRA and SoxRS. In *S. Typhimurium*, the efflux pump encoded by *smvA* was found to be beneficial for efflux activity, as this is a major resistance mechanism to acriflavine in this species. Additionally, TraDIS-*Xpress* suggested efflux activity was affected by genes involved in multiple other pathways, with roles in protein chaperoning, transcription, signalling, glutathione metabolism, respiration and ribosome modification. This supports previous work showing efflux regulation is complex and many cellular regulatory networks can influence efflux expression. Genes contributing to acriflavine susceptibility alone were involved in envelope biosynthesis, fimbriae expression, amino acid biosynthesis, translation and motility. Genes involved in DNA housekeeping affected both efflux activity and acriflavine susceptibility. Two genes involved in DNA housekeeping, *dam* and *maoP*, were suggested to be involved in efflux activity rather than acriflavine susceptibility. This is supported by previous work that also links the expression of *dam* (Hughes et al., 2020, Løbner-Olesen et al., 2003, Prieto et al., 2009) and *maoP* (Ruiz and Levy, 2013) to the expression of known efflux pumps and regulators. Acriflavine is a dye that binds to DNA, so it is plausible that genes involved in DNA damage response would affect acriflavine susceptibility.

These findings could be strengthened by repeating the experiment with a range of antimicrobials, using a wider range of substrates that can and cannot be removed from the cell via efflux, as this would identify mechanisms of efflux-mediated multidrug resistance and separate out drug-specific responses. Additionally, comparing the data from conditions treated with acriflavine relative to other antimicrobials with known mechanisms of action and antibacterial targets may provide further insight into mechanisms of acriflavine action and resistance. Repeating this work in a range of other clinically important pathogens would also be beneficial to our understanding of how efflux is controlled in other species and may identify drug targets to reduce the progression of reduced antibiotic susceptibility.

### **8.3. Links between biofilm formation and efflux activity**

A major aim of this work was to understand how efflux function is linked to control of biofilm formation. No one pathway was identified to cause the deficit in curli biosynthesis seen in efflux-deficient mutants in either *E. coli* or *S. Typhimurium*. Instead, many genes involved in multiple different pathways were identified that affected biofilm development and are sensitive to changes in efflux activity. Six of these are discussed below,

representing the regulatory systems with the biggest effect on both biofilm development and efflux activity that warrant further investigation.

### **8.3.1. DsbA**

The disulphide bond oxidoreductase encoded by *dsbA* was beneficial for adhesion and detrimental to biofilm matrix production in both *E. coli* and *S. Typhimurium*. Its expression is induced by membrane stress and it has a role in the correct folding of outer membrane proteins. It was predicted that disruption of efflux activity induced expression of *dsbA*, which would reduce curli biosynthesis through increasing the activity of c-di-GMP phosphodiesterases. Further work on this hypothesis should focus on quantifying *dsbA* transcription following efflux inactivation, and *csgD* transcription following *dsbA* overexpression. This would determine whether *dsbA* affects curli biosynthesis at the transcriptional or post-transcriptional level and characterise its effect on biofilm development following efflux inactivation.

### **8.3.2. MaoP**

The effect of *maoP* on biofilm formation and curli biosynthesis was first described in this study, whereby its deletion reduced biofilm biomass and curli biosynthesis in both *E. coli* and *S. Typhimurium*. Deletion of *maoP* was only seen to affect efflux activity in *E. coli* and not *S. Typhimurium*, and there was no change in drug susceptibility in either species. Expression of *maoP* has previously been found to be reduced following deletion of *acrB* in *E. coli* (Ruiz and Levy, 2013), and this could be sufficient to cause the reduction in curli biosynthesis seen in an efflux-deficient mutant, but further investigation is required to characterise how *maoP* could affect curli biosynthesis. Expression of *csgD* should be quantified in strains overexpressing *maoP* and without a function copy of *maoP*, relative to the wild type, in both *E. coli* and *S. Typhimurium* to determine whether *maoP* affects *csgD* or *csgB* transcription, or transcription of a known regulator of curli biosynthesis. Little is known about the function of *maoP* and its role in chromosomal organisation with *maoS* (Valens et al., 2016), therefore further investigation into this may reveal whether its relationship with biofilm matrix biosynthesis is separate or related to its role in chromosomal organisation.

### **8.3.3. The *nuo* operon**

Deletion of the *nuo* operon was identified to reduce the fitness of *S. Typhimurium* growing as a biofilm after 24 and 48 hours relative to growth in parallel planktonic cultures. Further investigation found that deletion of *nuoB* reduced biofilm biomass and curli biosynthesis in both *E. coli* and *S. Typhimurium*, and that the reduction in curli biosynthesis was not due to disruption of purine biosynthesis. Efflux activity was affected by deletion of the *nuo* operon in *S. Typhimurium*, resulting in reduced dye accumulation and increased

cefotaxime susceptibility. It was suspected that this was due to disruption of the proton gradient necessary to power efflux pumps driven by proton motive force. However, flagella rotation is also powered by proton motive force, and motility increased in the *nuo*-deficient mutants and decreased in *toIC*-deficient mutants relative to wild type *S. Typhimurium*. This suggests that these two genes do not have the same effect on the integrity of the proton gradient, and it is unlikely the reduction in curli biosynthesis is mediated through this pathway in both mutants. The next steps in characterising the effect of the *nuo* operon on curli biosynthesis would involve determining how *csgD* and *csgB* expression changes in the *nuo*-deficient mutants of *E. coli* and *S. Typhimurium* relative to the wild type, as well as identified whether the expression of any known regulators of *csgD* is affected by this pathway to identify how the electron transport chain affect biofilm matrix biosynthesis.

#### **8.3.4. MarA, RamA and SoxS**

Overexpression of MarA, RamA and SoxS has been shown to increase efflux activity and reduce biofilm biomass production (Holden and Webber, 2020). In *E. coli*, *marR* was found to benefit the fitness of the early biofilm grown for 12 hours, and *ramA* and *ramR* were beneficial to the mature biofilm in *S. Typhimurium* after 24- and 48-hours growth, respectively. Links between MarA and biofilm formation have previously been suggested, where expression of *marA* was found to repress *csgD* transcription via a regulatory pathway involving the *ycgZ-ymgABC* operon, the Rcs phosphorylay and the small regulatory RNA *rprA*. However, deletion of *marA* or overexpression of *marR*, which should increase curli biosynthesis according to this hypothesis, was not found to do so (Nhu et al., 2018). MarA has many binding sites throughout the genome and affects multiple systems (Sharma et al., 2017), therefore its effect on biofilm development and curli biosynthesis may be mediated through multiple pathways. The functional redundancy between MarA, RamA and SoxS (Holden and Webber, 2020) may complicate analysis of how this system affects biofilm formation, and this should be taken into consideration in future work.

#### **8.3.5. TomB**

TomB is an antitoxin that attenuates Hha, abrogating its negative effect on biofilm formation and development (Garcia-Contreras et al., 2008). In *E. coli*, deletion of *tomB* reduced cell aggregation, curli biosynthesis and biofilm biomass, and also reduced dye accumulation but not drug susceptibility. Previous work in *S. Typhimurium* found insertional inactivation of *tomB* restored curli biosynthesis in efflux-deficient mutants (Baugh, 2014). *TomB* is located immediately downstream of *acrAB* on both the *E. coli* and *S. Typhimurium* chromosomes, and therefore it was thought that manipulation of *acrAB* expression would also manipulate expression of *tomB*. However, deletion of *tomB* did not restore curli biosynthesis in an *acrB*-deficient mutant. Further investigation into this

system should focus on the relationship between Hha and TomB, as its effect on biofilm formation has only been described relative to Hha, and our TraDIS-*Xpress* findings suggest *tomB*, rather than *hha*, affects biofilm fitness. Transcription of the curli biosynthetic operons and regulators should be measured in a *tomB*-deficient and a *hha*-deficient mutant, relative to the wild type, to determine how each component of this toxin-antitoxin system affects biofilm matrix production

### **8.3.6. OmpR**

OmpR is a known positive regulator of *csgD* and biofilm matrix biosynthesis. Deletion of *ompR* was also found to reduce dye accumulation and cefotaxime susceptibility in *E. coli*, supporting the finding from the TraDIS-*Xpress* data that its expression is detrimental to efflux activity. The relationship between OmpR and efflux activity is not well understood, however ChIP-seq analysis found a small signal at the *acrA* promoter (Perkins et al., 2013), which may indicate that OmpR binds to and affects expression of the AcrAB-TolC efflux system. Expression of *ompR* and phosphorylation of OmpR should be investigated in an efflux-deficient strain relative to the wild type to determine whether its reduced expression could be responsible for the reduced curli biosynthesis seen. Additionally, expression of *acrAB*, *tolC*, other efflux systems and the regulators *marA*, *ramA* and *soxS* should be investigated in the presence and absence of both members of the EnvZ/OmpR two component signalling system to determine whether it affects their transcription or activity. This would be an important contribution to our understanding of how this signalling system affects efflux activity.

## **8.4. Looking to the future**

TraDIS-*Xpress* has been extremely effective in identifying the genes and pathways that affect fitness during biofilm development and efflux activity and has highlighted multiple pathways through which curli biosynthesis may be affected when efflux is inactivated. Further work should now focus on characterising the effect of these genes and pathways on biofilm matrix production in various knockout mutants and overexpression constructs. The next step in this project would involve investigating how the genes mentioned previously affect transcription of the curli biosynthetic operon and several known regulators of curli biosynthesis, to determine whether they affect biofilm matrix production at the transcriptional level or post-transcriptionally. Additionally, transcription of these genes in an efflux-deficient strain relative to the wild type would determine if they could be responsible for the reduction in curli biosynthesis seen.

Investigating the regulatory pathways that affect curli biosynthesis in response to efflux inactivation may reveal pathways that could be inhibited by drugs that would affect the

fitness of cells within the biofilm exposed to antimicrobials. The implications of this could be useful for reducing the ability for pathogens to form multidrug-resistant biofilm infections or could improve biofilm formation under stress for bioengineering approaches. Understanding how biofilm formation is affected by antimicrobial exposure will improve our management of biofilm development, to either help or hinder their growth.

## 9. REFERENCES

- ABOUZEED, Y. M., BAUCHERON, S. & CLOECKAERT, A. 2008. *ramR* Mutations Involved in Efflux-Mediated Multidrug Resistance in *Salmonella enterica* Serovar Typhimurium. *Antimicrobial Agents and Chemotherapy*, 52, 2428-2434.
- ADAM, M., MURALI, B., GLENN, N. O. & POTTER, S. S. 2008. Epigenetic inheritance based evolution of antibiotic resistance in bacteria. *BMC Evolutionary Biology*, 8, 52.
- ADAMIAK, J. W., JHAWAR, V., BONIFAY, V., CHANDLER, C. E., LEUS, I. V., ERNST, R. K., SCHWEIZER, H. P. & ZGURSKAYA, H. I. 2021. Loss of RND-type multidrug efflux pumps triggers iron starvation and lipid A modifications in *Pseudomonas aeruginosa*. *Antimicrobial Agents and Chemotherapy*, 0, AAC.00592-21.
- ADAMS, M. A. & JIA, Z. 2005. Structural and biochemical evidence for an enzymatic quinone redox cycle in *Escherichia coli*: identification of a novel quinol monooxygenase. *J Biol Chem*, 280, 8358-63.
- AEDO, S. J., MA, H. R. & BRYNILDSEN, M. P. 2019. Checks and Balances with Use of the Keio Collection for Phenotype Testing. *Methods Mol Biol*, 1927, 125-138.
- AHMAD, I., LAMPROKOSTOPOULOU, A., LE GUYON, S., STRECK, E., BARTHEL, M., PETERS, V., HARDT, W.-D. & RÖMLING, U. 2011. Complex c-di-GMP Signaling Networks Mediate Transition between Virulence Properties and Biofilm Formation in *Salmonella enterica* Serovar Typhimurium. *PLOS ONE*, 6, e28351.
- AHMER, B. M. M. 2004. Cell-to-cell signalling in *Escherichia coli* and *Salmonella enterica*. *Molecular Microbiology*, 52, 933-945.
- AIBA, H., MATSUYAMA, S., MIZUNO, T. & MIZUSHIMA, S. 1987. Function of *micF* as an antisense RNA in osmoregulatory expression of the *ompF* gene in *Escherichia coli*. *J Bacteriol*, 169, 3007-12.
- AIJUKA, M. & BUYS, E. M. 2019. Persistence of foodborne diarrheagenic *Escherichia coli* in the agricultural and food production environment: Implications for food safety and public health. *Food Microbiology*, 82, 363-370.
- ALAV, I., SUTTON, J. M. & RAHMAN, K. M. 2018. Role of bacterial efflux pumps in biofilm formation. *Journal of Antimicrobial Chemotherapy*, dky042-dky042.
- ALBA, B. M. & GROSS, C. A. 2004. Regulation of the *Escherichia coli* sigma-dependent envelope stress response. *Mol Microbiol*, 52, 613-9.
- ALCALDE-RICO, M., HERNANDO-AMADO, S., BLANCO, P. & MARTÍNEZ, J. L. 2016. Multidrug Efflux Pumps at the Crossroad between Antibiotic Resistance and Bacterial Virulence. *Frontiers in Microbiology*, 7, 1483.
- ALEKSHUN, M. N. & LEVY, S. B. 1999a. Alteration of the Repressor Activity of MarR, the Negative Regulator of the *Escherichia coli* *marRAB* Locus, by Multiple Chemicals In Vitro. *Journal of Bacteriology*, 181, 4669-4672.
- ALEKSHUN, M. N. & LEVY, S. B. 1999b. The *mar* regulon: multiple resistance to antibiotics and other toxic chemicals. *Trends in Microbiology*, 7, 410-413.
- ALEXEEVA, S., HELLINGWERF, K. J. & TEIXEIRA DE MATTOS, M. J. 2003. Requirement of ArcA for redox regulation in *Escherichia coli* under microaerobic but not anaerobic or aerobic conditions. *J Bacteriol*, 185, 204-9.
- ALLEN, W. J., PHAN, G. & WAKSMAN, G. 2012. Pilus biogenesis at the outer membrane of Gram-negative bacterial pathogens. *Current Opinion in Structural Biology*, 22, 500-506.
- ALPER, H. & STEPHANOPOULOS, G. 2008. Uncovering the gene knockout landscape for improved lycopene production in *E. coli*. *Applied Microbiology and Biotechnology*, 78, 801-810.
- AMORES, G. R., DE LAS HERAS, A., SANCHES-MEDEIROS, A., ELFICK, A. & SILVA-ROCHA, R. 2017. Systematic identification of novel regulatory interactions controlling biofilm formation in the bacterium *Escherichia coli*. *Scientific Reports*, 7, 16768.
- AMOS, M. R., SANCHEZ-CONTRERAS, M., JACKSON, R. W., MUÑOZ-BERBEL, X., CICHE, T. A., YANG, G., COOPER, R. M. & WATERFIELD, N. R. 2011. Influence of the *Photobacterium luminescens* Phosphomannose Isomerase Gene, *manA*, on

- Mannose Utilization, Exopolysaccharide Structure, and Biofilm Formation. *Applied and Environmental Microbiology*, 77, 776-785.
- ANRIANY, Y., SAHU, S. N., WESSELS, K. R., MCCANN, L. M. & JOSEPH, S. W. 2006. Alteration of the rugose phenotype in *waaG* and *ddhC* mutants of *Salmonella enterica* serovar Typhimurium DT104 is associated with inverse production of curli and cellulose. *Applied and environmental microbiology*, 72, 5002-5012.
- ANTON, B. P., SALEH, L., BENNER, J. S., RALEIGH, E. A., KASIF, S. & ROBERTS, R. J. 2008. RimO, a MiaB-like enzyme, methylthiolates the universally conserved Asp88 residue of ribosomal protein S12 in *Escherichia coli*. *Proc Natl Acad Sci U S A*, 105, 1826-31.
- ANWAR, N., ROUF, S. F., RÖMLING, U. & RHEN, M. 2014. Modulation of Biofilm-Formation in *Salmonella enterica* Serovar Typhimurium by the Periplasmic DsbA/DsbB Oxidoreductase System Requires the GGDEF-EAL Domain Protein STM3615. *PLOS ONE*, 9, e106095.
- ARCHER, C. D. & ELLIOTT, T. 1995. Transcriptional control of the *nuo* operon which encodes the energy-conserving NADH dehydrogenase of *Salmonella typhimurium*. *Journal of bacteriology*, 177, 2335-2342.
- BAARS, L., YTTERBERG, A. J., DREW, D., WAGNER, S., THILO, C., VAN WIJK, K. J. & DE GIER, J. W. 2006. Defining the role of the *Escherichia coli* chaperone SecB using comparative proteomics. *J Biol Chem*, 281, 10024-34.
- BABA, T., ARA, T., HASEGAWA, M., TAKAI, Y., OKUMURA, Y., BABA, M., DATSENKO, K. A., TOMITA, M., WANNER, B. L. & MORI, H. 2006. Construction of *Escherichia coli* K-12 in-frame, single-gene knockout mutants: the Keio collection. *Molecular systems biology*, 2, 2006.0008-2006.0008.
- BAHAT-SAMET, E., CASTRO-SOWINSKI, S. & OKON, Y. 2004. Arabinose content of extracellular polysaccharide plays a role in cell aggregation of *Azospirillum brasilense*. *FEMS Microbiology Letters*, 237, 195-203.
- BAILEY, A. M., CONSTANTINIDOU, C., IVENS, A., GARVEY, M. I., WEBBER, M. A., COLDHAM, N., HOBMAN, J. L., WAIN, J., WOODWARD, M. J. & PIDDOCK, L. J. V. 2009. Exposure of *Escherichia coli* and *Salmonella enterica* serovar Typhimurium to triclosan induces a species-specific response, including drug detoxification. *Journal of Antimicrobial Chemotherapy*, 64, 973-985.
- BAILEY, A. M., IVENS, A., KINGSLEY, R., COTTELL, J. L., WAIN, J. & PIDDOCK, L. J. 2010. RamA, a member of the AraC/XylS family, influences both virulence and efflux in *Salmonella enterica* serovar Typhimurium. *J Bacteriol*, 192, 1607-16.
- BANG, I. S., AUDIA, J. P., PARK, Y. K. & FOSTER, J. W. 2002. Autoinduction of the *ompR* response regulator by acid shock and control of the *Salmonella enterica* acid tolerance response. *Molecular Microbiology*, 44, 1235-1250.
- BARCHIESI, J., CASTELLI, M. E., SONCINI, F. C. & VÉSCOVI, E. G. 2008. *mgtA* Expression Is Induced by Rob Overexpression and Mediates a *Salmonella enterica* Resistance Phenotype. *Journal of Bacteriology*, 190, 4951-4958.
- BARDWELL, J. C. 1994. Building bridges: disulphide bond formation in the cell. *Mol Microbiol*, 14, 199-205.
- BARNHART, M. M. & CHAPMAN, M. R. 2006. Curli Biogenesis and Function. *Annual Review of Microbiology*, 60, 131-147.
- BARQUIST, L., MAYHO, M., CUMMINS, C., CAIN, A. K., BOINETT, C. J., PAGE, A. J., LANGRIDGE, G. C., QUAIL, M. A., KEANE, J. A. & PARKHILL, J. 2016. The TraDIS toolkit: sequencing and analysis for dense transposon mutant libraries. *Bioinformatics*, 32, 1109-11.
- BARRIOS, A. F., ZUO, R., REN, D. & WOOD, T. K. 2006. Hha, YbaJ, and OmpA regulate *Escherichia coli* K12 biofilm formation and conjugation plasmids abolish motility. *Biotechnol Bioeng*, 93, 188-200.
- BATCHELOR, E., WALTHERS, D., KENNEY, L. J. & GOULIAN, M. 2005. The *Escherichia coli* CpxA-CpxR Envelope Stress Response System Regulates Expression of the Porins OmpF and OmpC. *Journal of Bacteriology*, 187, 5723-5731.
- BAUCHERON, S., NISHINO, K., MONCHAUX, I., CANEPA, S., MAUREL, M. C., COSTE, F., ROUSSEL, A., CLOECKAERT, A. & GIRAUD, E. 2014. Bile-mediated

- activation of the *acrAB* and *tolC* multidrug efflux genes occurs mainly through transcriptional derepression of *ramA* in *Salmonella enterica* serovar Typhimurium. *J Antimicrob Chemother*, 69, 2400-6.
- BAUCHERON, S., TYLER, S., BOYD, D., MULVEY, M. R., CHASLUS-DANCLA, E. & CLOECKAERT, A. 2004. AcrAB-TolC Directs Efflux-Mediated Multidrug Resistance in *Salmonella enterica* Serovar Typhimurium DT104. *Antimicrobial Agents and Chemotherapy*, 48, 3729-3735.
- BAUGH, S. 2014. *The role of multidrug efflux pumps in biofilm formation of Salmonella enterica serovar Typhimurium*. Ph.D. Thesis, University of Birmingham.
- BAUGH, S., EKANAYAKA, A. S., PIDDOCK, L. J. & WEBBER, M. A. 2012. Loss of or inhibition of all multidrug resistance efflux pumps of *Salmonella enterica* serovar Typhimurium results in impaired ability to form a biofilm. *J Antimicrob Chemother*, 67, 2409-17.
- BAUGH, S., PHILLIPS, C. R., EKANAYAKA, A. S., PIDDOCK, L. J. & WEBBER, M. A. 2014. Inhibition of multidrug efflux as a strategy to prevent biofilm formation. *J Antimicrob Chemother*, 69, 673-81.
- BEENKEN, K. E., DUNMAN, P. M., MCALEESE, F., MACAPAGAL, D., MURPHY, E., PROJAN, S. J., BLEVINS, J. S. & SMELTZER, M. S. 2004. Global gene expression in *Staphylococcus aureus* biofilms. *J Bacteriol*, 186, 4665-84.
- BENDER, J. K., WILLE, T., BLANK, K., LANGE, A., GERLACH, R. G. & JUNIOR RESEARCH, G. 2013. LPS Structure and PhoQ Activity Are Important for *Salmonella* Typhimurium Virulence in the *Galleria mellonella* Infection Model. *PLoS ONE*, 8, e73287.
- BENNIK, M. H., POMPOSIELLO, P. J., THORNE, D. F. & DEMPLE, B. 2000. Defining a rob regulon in *Escherichia coli* by using transposon mutagenesis. *Journal of bacteriology*, 182, 3794-3801.
- BERLANGA, M. & GUERRERO, R. 2016. Living together in biofilms: the microbial cell factory and its biotechnological implications. *Microbial Cell Factories*, 15, 165.
- BESSAIAH, H., POKHAREL, P., HABOURIA, H., HOULE, S. & DOZOIS, C. M. 2019. *yqhG* Contributes to Oxidative Stress Resistance and Virulence of Uropathogenic *Escherichia coli* and Identification of Other Genes Altering Expression of Type 1 Fimbriae. *Frontiers in Cellular and Infection Microbiology*, 9.
- BIAN, Z., BRAUNER, A., LI, Y. & NORMARK, S. 2000. Expression of and Cytokine Activation by *Escherichia coli* Curi Fibers in Human Sepsis. *The Journal of Infectious Diseases*, 181, 602-612.
- BIGGER, J. W. 1944. Treatment of Staphylococcal Infections with Penicillin by Intermittent Sterilisation. *The Lancet*, 244, 497-500.
- BLAIR, J. M., RICHMOND, G. E. & PIDDOCK, L. J. 2014. Multidrug efflux pumps in Gram-negative bacteria and their role in antibiotic resistance. *Future Microbiol*, 9, 1165-77.
- BLAIR, J. M., WEBBER, M. A., BAYLAY, A. J., OGBOLU, D. O. & PIDDOCK, L. J. 2015a. Molecular mechanisms of antibiotic resistance. *Nat Rev Microbiol*, 13, 42-51.
- BLAIR, J. M. A., LA RAGIONE, R. M., WOODWARD, M. J. & PIDDOCK, L. J. V. 2009. Periplasmic adaptor protein AcrA has a distinct role in the antibiotic resistance and virulence of *Salmonella enterica* serovar Typhimurium. *Journal of Antimicrobial Chemotherapy*, 64, 965-972.
- BLAIR, J. M. A., SMITH, H. E., RICCI, V., LAWLER, A. J., THOMPSON, L. J. & PIDDOCK, L. J. V. 2015b. Expression of homologous RND efflux pump genes is dependent upon AcrB expression: implications for efflux and virulence inhibitor design. *Journal of Antimicrobial Chemotherapy*, 70, 424-431.
- BLANA, V., GEORGOMANOU, A. & GIAOURIS, E. 2017. Assessing biofilm formation by *Salmonella enterica* serovar Typhimurium on abiotic substrata in the presence of quorum sensing signals produced by *Hafnia alvei*. *Food Control*, 80, 83-91.
- BLANCO, P., HERNANDO-AMADO, S., REALES-CALDERON, J. A., CORONA, F., LIRA, F., ALCALDE-RICO, M., BERNARDINI, A., SANCHEZ, M. B. & MARTINEZ, J. L. 2016. Bacterial Multidrug Efflux Pumps: Much More Than Antibiotic Resistance Determinants. *Microorganisms*, 4, 14.
- BLOUNT, Z. D. 2015. The unexhausted potential of *E. coli*. *eLife*, 4, e05826.



- BLUMER, C., KLEEFELD, A., LEHNEN, D., HEINTZ, M., DOBRINDT, U., NAGY, G., MICHAELIS, K., EMODY, L., POLEN, T., RACHEL, R., WENDISCH, V. F. & UNDEN, G. 2005. Regulation of type 1 fimbriae synthesis and biofilm formation by the transcriptional regulator LrhA of *Escherichia coli*. *Microbiology*, 151, 3287-3298.
- BOEHM, A., KAISER, M., LI, H., SPANGLER, C., KASPER, C. A., ACKERMANN, M., KAEVER, V., SOURJIK, V., ROTH, V. & JENAL, U. 2010. Second Messenger-Mediated Adjustment of Bacterial Swimming Velocity. *Cell*, 141, 107-116.
- BOGACHEV, A. V., MURTAZINA, R. A. & SKULACHEV, V. P. 1996. H<sup>+</sup>/e<sup>-</sup> stoichiometry for NADH dehydrogenase I and dimethyl sulfoxide reductase in anaerobically grown *Escherichia coli* cells. *Journal of Bacteriology*, 178, 6233-6237.
- BONTEMPS-GALLO, S., BOHIN, J.-P., LACROIX, J.-M. & SLAUCH, J. M. 2017. Osmoregulated Periplasmic Glucans. *EcoSal Plus*, 7.
- BONTEMPS-GALLO, S., MADEC, E., DONDEYNE, J., DELRUE, B., ROBBE-MASSELOT, C., VIDAL, O., PROUVOST, A. F., BOUSSEMARY, G., BOHIN, J. P. & LACROIX, J. M. 2013. Concentration of osmoregulated periplasmic glucans (OPGs) modulates the activation level of the RcsCD RcsB phosphorelay in the phytopathogen bacteria *Dickeya dadantii*. *Environ Microbiol*, 15, 881-94.
- BOSCH, M. E., BERTRAND, B. P., HEIM, C. E., ALQARZAE, A. A., CHAUDHARI, S. S., ALDRICH, A. L., FEY, P. D., THOMAS, V. C., KIELIAN, T. & TORRES, V. J. 2020. *Staphylococcus aureus* ATP Synthase Promotes Biofilm Persistence by Influencing Innate Immunity. *mBio*, 11, e01581-20.
- BOUGDOUR, A., LELONG, C. & GEISELMANN, J. 2004. Crl, a low temperature-induced protein in *Escherichia coli* that binds directly to the stationary phase sigma subunit of RNA polymerase. *J Biol Chem*, 279, 19540-50.
- BRANDA, S. S., CHU, F., KEARNS, D. B., LOSICK, R. & KOLTER, R. 2006. A major protein component of the *Bacillus subtilis* biofilm matrix. *Molecular Microbiology*, 59, 1229-1238.
- BRAUN, T., PHILIPPSEN, A., WIRTZ, S., BORGNIA, M. J., AGRE, P., KÜHLBRANDT, W., ENGEL, A. & STAHLBERG, H. 2000. The 3.7 Å projection map of the glycerol facilitator GlpF: a variant of the aquaporin tetramer. *EMBO Rep*, 1, 183-9.
- BRINGER, M. A., ROLHION, N., GLASSER, A. L. & DARFEUILLE-MICHAUD, A. 2007. The oxidoreductase DsbA plays a key role in the ability of the Crohn's disease-associated adherent-invasive *Escherichia coli* strain LF82 to resist macrophage killing. *J Bacteriol*, 189, 4860-71.
- BROCK, M., DARLEY, D., TEXTOR, S. & BUCKEL, W. 2001. 2-Methylisocitrate lyases from the bacterium *Escherichia coli* and the filamentous fungus *Aspergillus nidulans*: characterization and comparison of both enzymes. *Eur J Biochem*, 268, 3577-86.
- BROMBACHER, E., BARATTO, A., DOREL, C. & LANDINI, P. 2006. Gene expression regulation by the Curli activator CsgD protein: modulation of cellulose biosynthesis and control of negative determinants for microbial adhesion. *Journal of bacteriology*, 188, 2027-2037.
- BROWN, L., GENTRY, D., ELLIOTT, T. & CASHEL, M. 2002. DksA affects ppGpp induction of RpoS at a translational level. *J Bacteriol*, 184, 4455-65.
- BROWN, P. K., DOZOIS, C. M., NICKERSON, C. A., ZUPPARDO, A., TERLONGE, J. & CURTISS, R., 3RD 2001. MlrA, a novel regulator of curli (AgF) and extracellular matrix synthesis by *Escherichia coli* and *Salmonella enterica* serovar Typhimurium. *Mol Microbiol*, 41, 349-63.
- BUCKLEY, A. M., WEBBER, M. A., COOLES, S., RANDALL, L. P., LA RAGIONE, R. M., WOODWARD, M. J. & PIDDOCK, L. J. 2006. The AcrAB-TolC efflux system of *Salmonella enterica* serovar Typhimurium plays a role in pathogenesis. *Cell Microbiol*, 8, 847-56.
- BYRD, B. A., ZENICK, B., ROCHA-GRANADOS, M., C., ENGLANDER, H. E., HARE, P. J., LAGREE, T. J., DEMARCO, A. M. & MOK, W. W. K. 2021. The AcrAB-TolC Efflux Pump Impacts Persistence and Resistance Development in Stationary-Phase *Escherichia coli* following Delafloxacin Treatment. *Antimicrobial Agents and Chemotherapy*, 65, e00281-21.

- CAGLIERO, C., MOULINE, C., CLOECKAERT, A. & PAYOT, S. 2006. Synergy between Efflux Pump CmeABC and Modifications in Ribosomal Proteins L4 and L22 in Conferring Macrolide Resistance in *Campylobacter jejuni* and *Campylobacter coli*. *Antimicrobial Agents and Chemotherapy*, 50, 3893-3896.
- CAI, S. J. & INOUE, M. 2002. EnvZ-OmpR interaction and osmoregulation in *Escherichia coli*. *J Biol Chem*, 277, 24155-61.
- CALVO, J. M. & MATTHEWS, R. G. 1994. The leucine-responsive regulatory protein, a global regulator of metabolism in *Escherichia coli*. *Microbiol Rev*, 58, 466-90.
- CAMACHO CARVAJAL, M. M., WIJFJES, A. H., MULDER, I. H., LUGTENBERG, B. J. & BLOEMBERG, G. V. 2002. Characterization of NADH dehydrogenases of *Pseudomonas fluorescens* WCS365 and their role in competitive root colonization. *Mol Plant Microbe Interact*, 15, 662-71.
- CAMPOLI-RICHARDS, D. M., MONK, J. P., PRICE, A., BENFIELD, P., TODD, P. A. & WARD, A. 1988. Ciprofloxacin. *Drugs*, 35, 373-447.
- CARVER, T., HARRIS, S. R., BERRIMAN, M., PARKHILL, J. & MCQUILLAN, J. A. 2011. Artemis: an integrated platform for visualization and analysis of high-throughput sequence-based experimental data. *Bioinformatics*, 28, 464-469.
- CASERTA, E., TOMŠIĆ, J., SPURIO, R., LA TEANA, A., PON, C. L. & GUALERZI, C. O. 2006. Translation Initiation Factor IF2 Interacts with the 30 S Ribosomal Subunit via Two Separate Binding Sites. *Journal of Molecular Biology*, 362, 787-799.
- CEPAS, V., BALLÉN, V., GABASA, Y., RAMÍREZ, M., LÓPEZ, Y. & SOTO, S. M. 2020. Transposon Insertion in the *purL* Gene Induces Biofilm Depletion in *Escherichia coli* ATCC 25922. *Pathogens*, 9.
- CEVALLOS-CEVALLOS, J. M., GU, G., DANYLUK, M. D. & VAN BRUGGEN, A. H. C. 2012. Adhesion and splash dispersal of *Salmonella enterica* Typhimurium on tomato leaflets: Effects of rdar morphotype and trichome density. *International Journal of Food Microbiology*, 160, 58-64.
- CHAKRABORTY, S. & KENNEY, L. J. 2018. A New Role of OmpR in Acid and Osmotic Stress in *Salmonella* and *E. coli*. *Frontiers in microbiology*, 9, 2656-2656.
- CHAUHAN, A., SAKAMOTO, C., GHIGO, J.-M. & BELOIN, C. 2013. Did I Pick the Right Colony? Pitfalls in the Study of Regulation of the Phase Variable Antigen 43 Adhesin. *PLOS ONE*, 8, e73568.
- CHEN, R. & HENNING, U. 1996. A periplasmic protein (Skp) of *Escherichia coli* selectively binds a class of outer membrane proteins. *Mol Microbiol*, 19, 1287-94.
- CHEREPANOV, P. P. & WACKERNAGEL, W. 1995. Gene disruption in *Escherichia coli*: TcR and KmR cassettes with the option of Flp-catalyzed excision of the antibiotic-resistance determinant. *Gene*, 158, 9-14.
- CHITSAZ, M. & BROWN, M. H. 2017. The role played by drug efflux pumps in bacterial multidrug resistance. *Essays Biochem*, 61, 127-139.
- CHO, H., MISRA, R. & COMSTOCK LAURIE, E. 2021. Mutational Activation of Antibiotic-Resistant Mechanisms in the Absence of Major Drug Efflux Systems of *Escherichia coli*. *Journal of Bacteriology*, 203, e00109-21.
- CHOI, E. & HWANG, J. 2018. The GTPase BipA expressed at low temperature in *Escherichia coli* assists ribosome assembly and has chaperone-like activity. *J Biol Chem*, 293, 18404-18419.
- CHOI, K. H., GAYNOR, J. B., WHITE, K. G., LOPEZ, C., BOSIO, C. M., KARKHOFF-SCHWEIZER, R. R. & SCHWEIZER, H. P. 2005. A Tn7-based broad-range bacterial cloning and expression system. *Nat Methods*, 2, 443-8.
- CISNEROS, D. A., PEHAU-ARNAUDET, G. & FRANCETIC, O. 2012. Heterologous assembly of type IV pili by a type II secretion system reveals the role of minor pilins in assembly initiation. *Molecular Microbiology*, 86, 805-818.
- CLAAS, K., WEBER, S. & DOWNS, D. M. 2000. Lesions in the *nuo* Operon, Encoding NADH Dehydrogenase Complex I, Prevent PurF-Independent Thiamine Synthesis and Reduce Flux through the Oxidative Pentose Phosphate Pathway in *Salmonella enterica* Serovar Typhimurium. *Journal of Bacteriology*, 182, 228-232.
- COHEN, N. R., ROSS, C. A., JAIN, S., SHAPIRO, R. S., GUTIERREZ, A., BELENKY, P., LI, H. & COLLINS, J. J. 2016. A role for the bacterial GATC methylome in antibiotic stress survival. *Nature genetics*, 48, 581-586.

- COHEN, S. P., HÄCHLER, H. & LEVY, S. B. 1993. Genetic and functional analysis of the multiple antibiotic resistance (*mar*) locus in *Escherichia coli*. *Journal of bacteriology*, 175, 1484-1492.
- COQUET, L., VILAIN, S., COSETTE, P., JOUENNE, T. & JUNTER, G.-A. 2006. A Proteomic Approach to Biofilm Cell Physiology. In: GUIBAN, J. M. (ed.) *Immobilization of Enzymes and Cells*. Totowa, NJ: Humana Press.
- CRAWFORD, R. W., ROSALES-REYES, R., RAMÍREZ-AGUILAR, M. D. L. L., CHAPA-AZUELA, O., ALPUCHE-ARANDA, C. & GUNN, J. S. 2010. Gallstones play a significant role in *Salmonella* spp. gallbladder colonization and carriage. *Proceedings of the National Academy of Sciences*, 107, 4353-4358.
- DA RE, S., VALLE, J., CHARBONNEL, N., BELOIN, C., LATOUR-LAMBERT, P., FAURE, P., TURLIN, E., LE BOUGUENEC, C., RENAULD-MONGENIE, G., FORESTIER, C. & GHIGO, J. M. 2013. Identification of commensal *Escherichia coli* genes involved in biofilm resistance to pathogen colonization. *PLoS One*, 8, e61628.
- DAILEY, F. E. & BERG, H. C. 1993. Mutants in disulfide bond formation that disrupt flagellar assembly in *Escherichia coli*. *Proceedings of the National Academy of Sciences*, 90, 1043.
- DANESE, P. N., PRATT, L. A., DOVE, S. L. & KOLTER, R. 2000. The outer membrane protein, Antigen 43, mediates cell-to-cell interactions within *Escherichia coli* biofilms. *Molecular Microbiology*, 37, 424-432.
- DANESE, P. N. & SILHAVY, T. J. 1997. The sigma(E) and the Cpx signal transduction systems control the synthesis of periplasmic protein-folding enzymes in *Escherichia coli*. *Genes Dev*, 11, 1183-93.
- DASSLER, T., MAIER, T., WINTERHALTER, C. & BÖCK, A. 2000. Identification of a major facilitator protein from *Escherichia coli* involved in efflux of metabolites of the cysteine pathway. *Mol Microbiol*, 36, 1101-12.
- DE MAJUMDAR, S., YU, J., FOOKES, M., MCATEER, S. P., LLOBET, E., FINN, S., SPENCE, S., MONAGHAN, A., KISSENFENNIG, A., INGRAM, R. J., BENGOCHEA, J., GALLY, D. L., FANNING, S., ELBORN, J. S. & SCHNEIDERS, T. 2015. Elucidation of the RamA Regulon in *Klebsiella pneumoniae* Reveals a Role in LPS Regulation. *PLOS Pathogens*, 11, e1004627.
- DEACON, J. & COOPER, R. A. 1977. D-Galactonate utilisation by enteric bacteria. The catabolic pathway in *Escherichia coli*. *FEBS Lett*, 77, 201-5.
- DEMPLE, B. 1996. Redox signaling and gene control in the *Escherichia coli* *soxRS* oxidative stress regulon — a review. *Gene*, 179, 53-57.
- DESAI, S. K., PADMANABHAN, A., HARSHE, S., ZAIDEL-BAR, R. & KENNEY, L. J. 2019. Salmonella biofilms program innate immunity for persistence in *Caenorhabditis elegans*. *Proc Natl Acad Sci U S A*, 116, 12462-12467.
- DILLON, S. C., ESPINOSA, E., HOKAMP, K., USSERY, D. W., CASADESUS, J. & DORMAN, C. J. 2012. LeuO is a global regulator of gene expression in *Salmonella enterica* serovar Typhimurium. *Mol Microbiol*, 85, 1072-89.
- DOMKA, J., LEE, J., BANSAL, T. & WOOD, T. K. 2007. Temporal gene-expression in *Escherichia coli* K-12 biofilms. *Environmental Microbiology*, 9, 332-346.
- DONG, J., LUCHI, S., KWAN, H.-S., LU, Z. & E. C. C., L. 1993. The deduced amino-acid sequence of the cloned *cpxR* gene suggests the protein is the cognate regulator for the membrane sensor, CpxA, in a two-component signal transduction system of *Escherichia coli*. *Gene*, 136, 227-230.
- DONG, T. & SCHELLHORN, H. E. 2009. Global effect of RpoS on gene expression in pathogenic *Escherichia coli* O157:H7 strain EDL933. *BMC Genomics*, 10, 349.
- DOREL, C., VIDAL, O., PRIGENT-COMBARET, C., VALLET, I. & LEJEUNE, P. 1999. Involvement of the Cpx signal transduction pathway of *E. coli* in biofilm formation. *FEMS Microbiol Lett*, 178, 169-75.
- DORMAN, C. J., CHATFIELD, S., HIGGINS, C. F., HAYWARD, C. & DOUGAN, G. 1989. Characterization of porin and *ompR* mutants of a virulent strain of *Salmonella typhimurium*: *ompR* mutants are attenuated in vivo. *Infect Immun*, 57, 2136-40.
- DUGUAY, A. R. & SILHAVY, T. J. 2004. Quality control in the bacterial periplasm. *Biochim Biophys Acta*, 1694, 121-34.

- DURFEE, T., NELSON, R., BALDWIN, S., PLUNKETT, G., 3RD, BURLAND, V., MAU, B., PETROSINO, J. F., QIN, X., MUZNY, D. M., AYELE, M., GIBBS, R. A., CSORGO, B., POSFAI, G., WEINSTOCK, G. M. & BLATTNER, F. R. 2008. The complete genome sequence of *Escherichia coli* DH10B: insights into the biology of a laboratory workhorse. *J Bacteriol*, 190, 2597-606.
- ECDC 2020. Salmonellosis. *ECDC Annual epidemiological report for 2017*.
- EFSA & ECDC 2018. The European Union summary report on trends and sources of zoonoses, zoonotic agents and food-borne outbreaks in 2017. *EFSA Journal*, 16, e05500.
- EFSA & ECDC 2019. The European Union One Health 2018 Zoonoses Report. *EFSA Journal*, 17, e05926.
- EICHELBERGER, K. R., SEPÚLVEDA, V. E., FORD, J., SELITSKY, S. R., MIECZKOWSKI, P. A., PARKER, J. S. & GOLDMAN, W. E. 2020. Tn-Seq Analysis Identifies Genes Important for *Yersinia pestis* Adherence during Primary Pneumonic Plague. *mSphere*, 5, e00715-20.
- EICHER, T., CHA, H. J., SEEGER, M. A., BRANDSTATTER, L., EL-DELIK, J., BOHNERT, J. A., KERN, W. V., VERREY, F., GRUTTER, M. G., DIEDERICHS, K. & POS, K. M. 2012. Transport of drugs by the multidrug transporter AcrB involves an access and a deep binding pocket that are separated by a switch-loop. *Proc Natl Acad Sci U S A*, 109, 5687-92.
- EUCAST, R. G. F. B. M. 2021. [https://www.eucast.org/ast\\_of\\_bacteria/mic\\_determination/?no\\_cache=1](https://www.eucast.org/ast_of_bacteria/mic_determination/?no_cache=1) [Online]. [Accessed].
- EVANS, MARGERY L., CHORELL, E., TAYLOR, JONATHAN D., ÅDEN, J., GÖTHESON, A., LI, F., KOCH, M., SEFER, L., MATTHEWS, STEVE J., WITTUNG-STAFSHED, P., ALMQVIST, F. & CHAPMAN, MATTHEW R. 2015. The Bacterial Curli System Possesses a Potent and Selective Inhibitor of Amyloid Formation. *Molecular Cell*, 57, 445-455.
- FAHMY, A., SRINIVASAN, A. & WEBBER, M. A. 2016. The Relationship Between Bacterial Multidrug Efflux Pumps and Biofilm Formation. In: LI, X.-Z., ELKINS, C. A. & ZGURSKAYA, H. I. (eds.) *Efflux-Mediated Antimicrobial Resistance in Bacteria: Mechanisms, Regulation and Clinical Implications*. Cham: Springer International Publishing.
- FANG, N., YANG, H., FANG, H., LIU, L., ZHANG, Y., WANG, L., HAN, Y., ZHOU, D. & YANG, R. 2015. RcsAB is a major repressor of *Yersinia biofilm* development through directly acting on *hmsCDE*, *hmsT*, and *hmsHFRS*. *Sci Rep*, 5, 9566.
- FANG, X., AHMAD, I., BLANKA, A., SCHOTTKOWSKI, M., CIMDINS, A., GALPERIN, M. Y., RÖMLING, U. & GOMELSKY, M. 2014. GIL, a new c-di-GMP-binding protein domain involved in regulation of cellulose synthesis in enterobacteria. *Molecular microbiology*, 93, 439-452.
- FANG, X. & GOMELSKY, M. 2010. A post-translational, c-di-GMP-dependent mechanism regulating flagellar motility. *Molecular Microbiology*, 76, 1295-1305.
- FATH, M. J., MAHANTY, H. K. & KOLTER, R. 1989. Characterization of a *purF* operon mutation which affects colicin V production. *J Bacteriol*, 171, 3158-61.
- FERNÁNDEZ-GARCÍA, L., BLASCO, L., LOPEZ, M., BOU, G., GARCÍA-CONTRERAS, R., WOOD, T. & TOMAS, M. 2016. Toxin-Antitoxin Systems in Clinical Pathogens. *Toxins*, 8, 227.
- FERRARI, R. G., ROSARIO, D. K. A., CUNHA-NETO, A., MANO, S. B., FIGUEIREDO, E. E. S. & CONTE-JUNIOR, C. A. 2019. Worldwide Epidemiology of *Salmonella* Serovars in Animal-Based Foods: a Meta-analysis. *Applied and environmental microbiology*, 85, e00591-19.
- FERRIÈRES, L. & CLARKE, D. J. 2003. The RcsC sensor kinase is required for normal biofilm formation in *Escherichia coli* K-12 and controls the expression of a regulon in response to growth on a solid surface. *Molecular Microbiology*, 50, 1665-1682.
- FERRIÈRES, L., HÉMERY, G., NHAM, T., GUÉROUT, A.-M., MAZEL, D., BELOIN, C. & GHIGO, J.-M. 2010. Silent mischief: bacteriophage Mu insertions contaminate products of *Escherichia coli* random mutagenesis performed using suicidal

- transposon delivery plasmids mobilized by broad-host-range RP4 conjugative machinery. *Journal of bacteriology*, 192, 6418-6427.
- FIGUEROA-BOSSI, N., UZZAU, S., MALORIOL, D. & BOSSI, L. 2001. Variable assortment of prophages provides a transferable repertoire of pathogenic determinants in *Salmonella*. *Mol Microbiol*, 39, 260-71.
- FITZGERALD, D. M., BONOCORA, R. P. & WADE, J. T. 2014. Comprehensive Mapping of the *Escherichia coli* Flagellar Regulatory Network. *PLOS Genetics*, 10, e1004649.
- FLEISCHER, R., HEERMANN, R., JUNG, K. & HUNKE, S. 2007. Purification, reconstitution, and characterization of the CpxRAP envelope stress system of *Escherichia coli*. *J Biol Chem*, 282, 8583-93.
- FLEMMING, H.-C., WINGENDER, J., SZEWCZYK, U., STEINBERG, P., RICE, S. A. & KJELLEBERG, S. 2016. Biofilms: an emergent form of bacterial life. *Nature Reviews Microbiology*, 14, 563.
- FRANCO, A. V., LIU, D. & REEVES, P. R. 1996. A Wzz (Cld) protein determines the chain length of K lipopolysaccharide in *Escherichia coli* O8 and O9 strains. *J Bacteriol*, 178, 1903-7.
- FRYE, J. G., PORWOLLIK, S., BLACKMER, F., CHENG, P. & MCCLELLAND, M. 2005. Host Gene Expression Changes and DNA Amplification during Temperate Phage Induction. *Journal of Bacteriology*, 187, 1485-1492.
- FUCHS, J. A. & WARNER, H. R. 1975. Isolation of an *Escherichia coli* mutant deficient in glutathione synthesis. *J Bacteriol*, 124, 140-8.
- FUJIKAWA, M., KOBAYASHI, K. & KOZAWA, T. 2012. Direct oxidation of the [2Fe-2S] cluster in SoxR protein by superoxide: distinct differential sensitivity to superoxide-mediated signal transduction. *The Journal of biological chemistry*, 287, 35702-35708.
- FUX, C. A., COSTERTON, J. W., STEWART, P. S. & STOODLEY, P. 2005. Survival strategies of infectious biofilms. *Trends in Microbiology*, 13, 34-40.
- GALLEGOS, M. T., SCHLEIF, R., BAIROCH, A., HOFMANN, K. & RAMOS, J. L. 1997. Arac/XylS family of transcriptional regulators. *Microbiology and molecular biology reviews : MMBR*, 61, 393-410.
- GARAVAGLIA, M., ROSSI, E. & LANDINI, P. 2012. The pyrimidine nucleotide biosynthetic pathway modulates production of biofilm determinants in *Escherichia coli*. *PloS one*, 7, e31252-e31252.
- GARCIA-CONTRERAS, R., ZHANG, X. S., KIM, Y. & WOOD, T. K. 2008. Protein translation and cell death: the role of rare tRNAs in biofilm formation and in activating dormant phage killer genes. *PLoS One*, 3, e2394.
- GARCIA, B., LATASA, C., SOLANO, C., GARCIA-DEL PORTILLO, F., GAMAZO, C. & LASA, I. 2004. Role of the GGDEF protein family in *Salmonella* cellulose biosynthesis and biofilm formation. *Mol Microbiol*, 54, 264-77.
- GARMENDIA, J., BEUZON, C. R., RUIZ-ALBERT, J. & HOLDEN, D. W. 2003. The roles of SsrA-SsrB and OmpR-EnvZ in the regulation of genes encoding the *Salmonella* Typhimurium SPI-2 type III secretion system. *Microbiology*, 149, 2385-96.
- GEMMILL, R. M., JONES, J. W., HAUGHN, G. W. & CALVO, J. M. 1983. Transcription initiation sites of the leucine operons of *Salmonella typhimurium* and *Escherichia coli*. *Journal of Molecular Biology*, 170, 39-59.
- GENNARIS, A., EZRATY, B., HENRY, C., AGREBI, R., VERGNES, A., OHEIX, E., BOS, J., LEVERRIER, P., ESPINOSA, L., SZEWCZYK, J., VERTOMMEN, D., IRANZO, O., COLLET, J.-F. & BARRAS, F. 2015. Repairing oxidized proteins in the bacterial envelope using respiratory chain electrons. *Nature*, 528, 409-412.
- GENTRY, D. R., HERNANDEZ, V. J., NGUYEN, L. H., JENSEN, D. B. & CASHEL, M. 1993. Synthesis of the stationary-phase sigma factor  $\sigma_s$  is positively regulated by ppGpp. *J Bacteriol*, 175, 7982-9.
- GEORGE, A. M., HALL, R. M. & STOKES, H. W. 1995. Multidrug resistance in *Klebsiella pneumoniae*: a novel gene, *ramA*, confers a multidrug resistance phenotype in *Escherichia coli*. *Microbiology*, 141, 1909-1920.
- GERDING, M. A., OGATA, Y., PECORA, N. D., NIKI, H. & DE BOER, P. A. 2007. The trans-envelope Tol-Pal complex is part of the cell division machinery and required

- for proper outer-membrane invagination during cell constriction in *E. coli*. *Mol Microbiol*, 63, 1008-25.
- GERSTEL, U., PARK, C. & RÖMLING, U. 2003. Complex regulation of *csgD* promoter activity by global regulatory proteins. *Molecular Microbiology*, 49, 639-654.
- GERSTEL, U. & RÖMLING, U. 2003. The *csgD* promoter, a control unit for biofilm formation in *Salmonella Typhimurium*. *Res Microbiol*, 154, 659-67.
- GERSTEL, U. & RÖMLING, U. 2001. Oxygen tension and nutrient starvation are major signals that regulate *agfD* promoter activity and expression of the multicellular morphotype in *Salmonella typhimurium*. *Environmental Microbiology*, 3, 638-648.
- GIBSON, M. M., BAGGA, D. A., MILLER, C. G. & MAGUIRE, M. E. 1991. Magnesium transport in *Salmonella typhimurium*: the influence of new mutations conferring Co<sup>2+</sup> resistance on the CorA Mg<sup>2+</sup> transport system. *Molecular Microbiology*, 5, 2753-2762.
- GIRARD, M. E., GOPALKRISHNAN, S., GRACE, E. D., HALLIDAY, J. A., GOURSE, R. L. & HERMAN, C. 2018. DksA and ppGpp Regulate the  $\sigma$ S Stress Response by Activating Promoters for the Small RNA DsrA and the Anti-Adapter Protein IraP. *Journal of Bacteriology*, 200, e00463-17.
- GIRGIS, H. S., HOTTES, A. K. & TAVAZOIE, S. 2009. Genetic architecture of intrinsic antibiotic susceptibility. *PLoS One*, 4, e5629.
- GOH, K. G. K., PHAN, M.-D., FORDE, B. M., CHONG, T. M., YIN, W.-F., CHAN, K.-G., ULETT, G. C., SWEET, M. J., BEATSON, S. A. & SCHEMBRI, M. A. 2017. Genome-Wide Discovery of Genes Required for Capsule Production by Uropathogenic *Escherichia coli*. *mBio*, 8, e01558-17.
- GOODALL, E. C. A., ROBINSON, A., JOHNSTON, I. G., JABBARI, S., TURNER, K. A., CUNNINGHAM, A. F., LUND, P. A., COLE, J. A. & HENDERSON, I. R. 2018. The Essential Genome of *Escherichia coli* K-12. *mBio*, 9, e02096-17.
- GOOSEN, N. & VAN DE PUTTE, P. 1995. The regulation of transcription initiation by integration host factor. *Molecular Microbiology*, 16, 1-7.
- GRENIER, F., MATTEAU, D., BABY, V. & RODRIGUE, S. 2014. Complete Genome Sequence of *Escherichia coli* BW25113. *Genome Announcements*, 2, e01038-14.
- GRIFFITH, K. L., FITZPATRICK, M. M., KEEN, E. F. & WOLF, R. E. 2009. Two Functions of the C-Terminal Domain of *Escherichia coli* Rob: Mediating "Sequestration–Dispersal" as a Novel Off–On Switch for Regulating Rob's Activity as a Transcription Activator and Preventing Degradation of Rob by Lon Protease. *Journal of Molecular Biology*, 388, 415-430.
- GUEST, J. R. & ROBERTS, R. E. 1983. Cloning, mapping, and expression of the fumarase gene of *Escherichia coli* K-12. *J Bacteriol*, 153, 588-96.
- GUO, X. P., REN, G. X., ZHU, H., MAO, X. J. & SUN, Y. C. 2015. Differential regulation of the *hmsCDE* operon in *Yersinia pestis* and *Yersinia pseudotuberculosis* by the Rcs phosphorelay system. *Sci Rep*, 5, 8412.
- GUY, C. P., ATKINSON, J., GUPTA, M. K., MAHDI, A. A., GWYNN, E. J., RUDOLPH, C. J., MOON, P. B., VAN KNIPPENBERG, I. C., CADMAN, C. J., DILLINGHAM, M. S., LLOYD, R. G. & MCGLYNN, P. 2009. Rep provides a second motor at the replisome to promote duplication of protein-bound DNA. *Mol Cell*, 36, 654-66.
- HALL, R. S., XIANG, D. F., XU, C. & RAUSHEL, F. M. 2007. N-Acetyl-D-glucosamine-6-phosphate deacetylase: substrate activation via a single divalent metal ion. *Biochemistry*, 46, 7942-52.
- HAMMA, T. & FERRÉ-D'AMARÉ, A. R. 2006. Pseudouridine Synthases. *Chemistry & Biology*, 13, 1125-1135.
- HAMMAR, M., BIAN, Z. & NORMARK, S. 1996. Nucleator-dependent intercellular assembly of adhesive curli organelles in *Escherichia coli*. *Proceedings of the National Academy of Sciences of the United States of America*, 93, 6562-6566.
- HARA, H., YAMAMOTO, Y., HIGASHITANI, A., SUZUKI, H. & NISHIMURA, Y. 1991. Cloning, mapping, and characterization of the *Escherichia coli* *prc* gene, which is involved in C-terminal processing of penicillin-binding protein 3. *Journal of bacteriology*, 173, 4799-4813.

- HARBORNE, N. R., GRIFFITHS, L., BUSBY, S. J. W. & COLE, J. A. 1992. Transcriptional control, translation and function of the products of the five open reading frames of the *Escherichia coli nir* operon. *Molecular Microbiology*, 6, 2805-2813.
- HARRIS, R. M., WEBB, D. C., HOWITT, S. M. & COX, G. B. 2001. Characterization of PitA and PitB from *Escherichia coli*. *J Bacteriol*, 183, 5008-14.
- HEJAIR, H. M. A., ZHU, Y., MA, J., ZHANG, Y., PAN, Z., ZHANG, W. & YAO, H. 2017. Functional role of *ompF* and *ompC* porins in pathogenesis of avian pathogenic *Escherichia coli*. *Microbial Pathogenesis*, 107, 29-37.
- HELAINÉ, S. & KUGELBERG, E. 2014. Bacterial persisters: formation, eradication, and experimental systems. *Trends in Microbiology*, 22, 417-424.
- HENGGE, R. 2009. Principles of c-di-GMP signalling in bacteria. *Nature Reviews Microbiology*, 7, 263.
- HENGGE, R. 2020. Linking bacterial growth, survival, and multicellularity – small signaling molecules as triggers and drivers. *Current Opinion in Microbiology*, 55, 57-66.
- HENGGE, R., GALPERIN, M. Y., GHIGO, J.-M., GOMELSKY, M., GREEN, J., HUGHES, K. T., JENAL, U. & LANDINI, P. 2015. Systematic Nomenclature for GGDEF and EAL Domain-Containing Cyclic Di-GMP Turnover Proteins of *Escherichia coli*. *Journal of bacteriology*, 198, 7-11.
- HENGGE, R., HÄUSSLER, S., PRUTEANU, M., STÜLKE, J., TSCHOWRI, N. & TURGAY, K. 2019. Recent Advances and Current Trends in Nucleotide Second Messenger Signaling in Bacteria. *Journal of Molecular Biology*, 431, 908-927.
- HERBST, S., LORKOWSKI, M., SARENKO, O., NGUYEN, T. K. L., JAENICKE, T. & HENGGE, R. 2018. Transmembrane redox control and proteolysis of PdeC, a novel type of c-di-GMP phosphodiesterase. *The EMBO Journal*, 37, e97825.
- HERNANDEZ-MONTALVO, V., MARTINEZ, A., HERNANDEZ-CHAVEZ, G., BOLIVAR, F., VALLE, F. & GOSSET, G. 2003. Expression of *galP* and *glk* in a *Escherichia coli* PTS mutant restores glucose transport and increases glycolytic flux to fermentation products. *Biotechnol Bioeng*, 83, 687-94.
- HERRING, C. D. & BLATTNER, F. R. 2004. Global transcriptional effects of a suppressor tRNA and the inactivation of the regulator *frmR*. *J Bacteriol*, 186, 6714-20.
- HERZBERG, M., KAYE, I. K., PETI, W. & WOOD, T. K. 2006. YdgG (TqsA) controls biofilm formation in *Escherichia coli* K-12 through autoinducer 2 transport. *J Bacteriol*, 188, 587-98.
- HICKSON, I. D., ROBSON, C. N., ATKINSON, K. E., HUTTON, L. & EMMERSON, P. T. 1985. Reconstitution of RecBC DNase activity from purified *Escherichia coli* RecB and RecC proteins. *Journal of Biological Chemistry*, 260, 1224-1229.
- HMIEL, S. P., SNAVELY, M. D., MILLER, C. G. & MAGUIRE, M. E. 1986. Magnesium transport in *Salmonella typhimurium*: characterization of magnesium influx and cloning of a transport gene. *Journal of bacteriology*, 168, 1444-1450.
- HOBMAN, J. L., PENN, C. W. & PALLEN, M. J. 2007. Laboratory strains of *Escherichia coli*: model citizens or deceitful delinquents growing old disgracefully? *Molecular Microbiology*, 64, 881-885.
- HØIBY, N., CIOFU, O. & BJARNSHOLT, T. 2010. *Pseudomonas aeruginosa* biofilms in cystic fibrosis. *Future Microbiology*, 5, 1663-1674.
- HOLDEN, E. R. & WEBBER, M. A. 2020. MarA, RamA and SoxS as mediators of the Stress Response: Survival at a Cost. *Frontiers in Microbiology*, 11, 828.
- HOLDEN, E. R., WICKHAM, G. J., WEBBER, M. A., THOMSON, N. M. & TRAMPARI, E. 2020. Donor plasmids for phenotypically neutral chromosomal gene insertions in *Enterobacteriaceae*. *Microbiology*.
- HOYLE, B. D. & COSTERTON, J. W. 1991. Bacterial resistance to antibiotics: the role of biofilms. *Prog Drug Res*, 37, 91-105.
- HUANG, C. J., WANG, Z. C., HUANG, H. Y., HUANG, H. D. & PENG, H. L. 2013. YjcC, a c-di-GMP phosphodiesterase protein, regulates the oxidative stress response and virulence of *Klebsiella pneumoniae* CG43. *PLoS One*, 8, e66740.
- HUANG, L., TSUI, P. & FREUNDLICH, M. 1990. Integration host factor is a negative effector of *in vivo* and *in vitro* expression of *ompC* in *Escherichia coli*. *Journal of Bacteriology*, 172, 5293-5298.



- HUFNAGEL, D. A., EVANS, M. L., GREENE, S. E., PINKNER, J. S., HULTGREN, S. J. & CHAPMAN, M. R. 2016. The Catabolite Repressor Protein-Cyclic AMP Complex Regulates *csgD* and Biofilm Formation in Uropathogenic *Escherichia coli*. *Journal of Bacteriology*, 198, 3329-3334.
- HUGHES, L., ROBERTS, W. & JOHNSON, D. 2020. The impact of DNA adenine methyltransferase knockout on the development of triclosan resistance and antibiotic cross-resistance in *Escherichia coli*. *Access microbiology*, 3, acmi000178-acmi000178.
- HUNG, D. L., RAIVIO, T. L., JONES, C. H., SILHAVY, T. J. & HULTGREN, S. J. 2001. Cpx signaling pathway monitors biogenesis and affects assembly and expression of P pili. *The EMBO Journal*, 20, 1508-1518.
- HYNEN, A. L., LAZENBY, J. J., SAVVA, G. M., MCCAUGHEY, L. C., TURNBULL, L., NOLAN, L. M. & WHITCHURCH, C. B. 2020. Multiple Holins Contribute to Extracellular DNA Release in *Pseudomonas aeruginosa* Biofilms. *bioRxiv*, 2020.10.28.358747.
- HYNES, M. J. & MURRAY, S. L. 2010. ATP-Citrate Lyase Is Required for Production of Cytosolic Acetyl Coenzyme A and Development in *Aspergillus nidulans*. *Eukaryotic Cell*, 9, 1039-1048.
- INOUE, T., SHINGAKI, R., HIROSE, S., WAKI, K., MORI, H. & FUKUI, K. 2007. Genome-Wide Screening of Genes Required for Swarming Motility in *Escherichia coli* K-12. *Journal of Bacteriology*, 189, 950-957.
- ISLAM, S. T. & LAM, J. S. 2014. Synthesis of bacterial polysaccharides via the Wzx/Wzy-dependent pathway. *Can J Microbiol*, 60, 697-716.
- JAISWAL, S., PAUL, P., PADHI, C., RAY, S., RYAN, D., DASH, S. & SUAR, M. 2016. The Hha-TomB Toxin-Antitoxin System Shows Conditional Toxicity and Promotes Persister Cell Formation by Inhibiting Apoptosis-Like Death in *S. Typhimurium*. *Scientific reports*, 6, 38204-38204.
- JARVIK, T., SMILLIE, C., GROISMAN, E. A. & OCHMAN, H. 2010. Short-Term Signatures of Evolutionary Change in the *Salmonella enterica* Serovar Typhimurium 14028 Genome. *J Bacteriol*, 192, 560-7.
- JIANG, X. M., NEAL, B., SANTIAGO, F., LEE, S. J., ROMANA, L. K. & REEVES, P. R. 1991. Structure and sequence of the *rfb* (O antigen) gene cluster of *Salmonella* serovar typhimurium (strain LT2). *Molecular Microbiology*, 5, 695-713.
- JONAS, K., TOMENIUS, H., KADER, A., NORMARK, S., RÖMLING, U., BELOVA, L. M. & MELEFORS, Ö. 2007. Roles of curli, cellulose and BapA in *Salmonella* biofilm morphology studied by atomic force microscopy. *BMC Microbiology*, 7, 70.
- JUBELIN, G., VIANNEY, A., BELOIN, C., GHIGO, J.-M., LAZZARONI, J.-C., LEJEUNE, P. & DOREL, C. 2005. CpxR/OmpR Interplay Regulates Curli Gene Expression in Response to Osmolarity in *Escherichia coli*. *Journal of Bacteriology*, 187, 2038-2049.
- KAASEN, I., FALKENBERG, P., STYRVOLD, O. B. & STRØM, A. R. 1992. Molecular cloning and physical mapping of the *otsBA* genes, which encode the osmoregulatory trehalose pathway of *Escherichia coli*: evidence that transcription is activated by *katF* (AppR). *Journal of Bacteriology*, 174, 889-898.
- KACHARIA, F. R., MILLAR, J. A. & RAGHAVAN, R. 2017. Emergence of New sRNAs in Enteric Bacteria is Associated with Low Expression and Rapid Evolution. *Journal of Molecular Evolution*, 84, 204-213.
- KADER, A., SIMM, R., GERSTEL, U., MORR, M. & RÖMLING, U. 2006. Hierarchical involvement of various GGDEF domain proteins in *rdar* morphotype development of *Salmonella enterica* serovar Typhimurium. *Molecular Microbiology*, 60, 602-616.
- KALMAN, M., GENTRY, D. R. & CASHEL, M. 1991. Characterization of the *Escherichia coli* K12 *gltS* glutamate permease gene. *Mol Gen Genet*, 225, 379-86.
- KANG, W. K., ICHO, T., ISONO, S., KITAKAWA, M. & ISONO, K. 1989. Characterization of the gene *rimK* responsible for the addition of glutamic acid residues to the C-terminus of ribosomal protein S6 in *Escherichia coli* K12. *Mol Gen Genet*, 217, 281-8.
- KASAHARA, M., NAKATA, A. & SHINAGAWA, H. 1992. Molecular analysis of the *Escherichia coli* *phoP-phoQ* operon. *J Bacteriol*, 174, 492-8.



- KASHIWAGI, K., MIYAMOTO, S., NUKUI, E., KOBAYASHI, H. & IGARASHI, K. 1993. Functions of potA and potD proteins in spermidine-preferential uptake system in *Escherichia coli*. *J Biol Chem*, 268, 19358-63.
- KASIMOGLU, E., PARK, S. J., MALEK, J., TSENG, C. P. & GUNSALUS, R. P. 1996. Transcriptional regulation of the proton-translocating ATPase (*atpIBEFHAGDC*) operon of *Escherichia coli*: control by cell growth rate. *Journal of bacteriology*, 178, 5563-5567.
- KAVČIČ, B., TKAČIK, G. & BOLLENBACH, T. 2020. Mechanisms of drug interactions between translation-inhibiting antibiotics. *Nature Communications*, 11, 4013.
- KEHRES, D. G., JANAKIRAMAN, A., SLAUCH, J., M & MAGUIRE, M. E. 2002. Regulation of *Salmonella enterica* Serovar Typhimurium *mntH* Transcription by H<sub>2</sub>O<sub>2</sub>, Fe<sup>2+</sup>, and Mn<sup>2+</sup>. *Journal of Bacteriology*, 184, 3151-3158.
- KEISKI, C.-L., HARWICH, M., JAIN, S., NECULAI, A. M., YIP, P., ROBINSON, H., WHITNEY, J. C., RILEY, L., BURROWS, L. L., OHMAN, D. E. & HOWELL, P. L. 2010. AlgK is a TPR-containing protein and the periplasmic component of a novel exopolysaccharide secretin. *Structure (London, England : 1993)*, 18, 265-273.
- KERN, W. V., OETHINGER, M., JELLEN-RITTER, A. S. & LEVY, S. B. 2000. Non-target gene mutations in the development of fluoroquinolone resistance in *Escherichia coli*. *Antimicrob Agents Chemother*, 44, 814-20.
- KETTLES, R. A., TSCHOWRI, N., LYONS, K. J., SHARMA, P., HENGGE, R., WEBBER, M. A. & GRAINGER, D. C. 2019. The *Escherichia coli* MarA protein regulates the *ycgZ-ymgABC* operon to inhibit biofilm formation. *Molecular Microbiology*, 0.
- KIM, T., LEE, J. & KIM, K.-S. 2013. *Escherichia coli* YmdB regulates biofilm formation independently of its role as an RNase III modulator. *BMC microbiology*, 13, 266-266.
- KINGSLEY, R. A., MSEFULA, C. L., THOMSON, N. R., KARIUKI, S., HOLT, K. E., GORDON, M. A., HARRIS, D., CLARKE, L., WHITEHEAD, S., SANGAL, V., MARSH, K., ACHTMAN, M., MOLYNEUX, M. E., CORMICAN, M., PARKHILL, J., MACLENNAN, C. A., HEYDERMAN, R. S. & DOUGAN, G. 2009. Epidemic multiple drug resistant *Salmonella* Typhimurium causing invasive disease in sub-Saharan Africa have a distinct genotype. *Genome research*, 19, 2279-2287.
- KLEMM, P. 1986. Two regulatory *fim* genes, *fimB* and *fimE*, control the phase variation of type 1 fimbriae in *Escherichia coli*. *The EMBO Journal*, 5, 1389-1393.
- KO, M. & PARK, C. 2000. H-NS-Dependent regulation of flagellar synthesis is mediated by a LysR family protein. *J Bacteriol*, 182, 4670-2.
- KRAGH, K. N., HUTCHISON, J. B., MELAUGH, G., RODESNEY, C., ROBERTS, A. E., IRIE, Y., JENSEN, P. O., DIGGLE, S. P., ALLEN, R. J., GORDON, V. & BJARNSHOLT, T. 2016. Role of Multicellular Aggregates in Biofilm Formation. *MBio*, 7, e00237.
- KRASTEVA, P. V., BERNAL-BAYARD, J., TRAVIER, L., MARTIN, F. A., KAMINSKI, P.-A., KARIMOVA, G., FRONZES, R. & GHIGO, J.-M. 2017. Insights into the structure and assembly of a bacterial cellulose secretion system. *Nature communications*, 8, 2065-2065.
- KRÖGER, C. & FUCHS THILO, M. 2009. Characterization of the myo-Inositol Utilization Island of *Salmonella enterica* serovar Typhimurium. *Journal of Bacteriology*, 191, 545-554.
- KRONER, G. M., WOLFE, M. B. & FREDDOLINO, P. L. 2019. *Escherichia coli* Lrp Regulates One-Third of the Genome via Direct, Cooperative, and Indirect Routes. *Journal of Bacteriology*, 201, e00411-18.
- KUMAR, C. G. & ANAND, S. K. 1998. Significance of microbial biofilms in food industry: a review. *International Journal of Food Microbiology*, 42, 9-27.
- KVIST, M., HANCOCK, V. & KLEMM, P. 2008. Inactivation of efflux pumps abolishes bacterial biofilm formation. *Appl Environ Microbiol*, 74, 7376-82.
- KWAN, G., PLAGENZ, B., COWLES, K., PISITHKUL, T., AMADOR-NOGUEZ, D. & BARAK, J. D. 2018. Few Differences in Metabolic Network Use Found Between *Salmonella enterica* Colonization of Plants and Typhoidal Mice. *Frontiers in microbiology*, 9, 695-695.

- LACEY, M. M., PARTRIDGE, J. D. & GREEN, J. 2010. *Escherichia coli* K-12 YfgF is an anaerobic cyclic di-GMP phosphodiesterase with roles in cell surface remodelling and the oxidative stress response. *Microbiology*, 156, 2873-2886.
- LANG, S., CRESSATTI, M., MENDOZA, K. E., COUMOUNDOUROS, C. N., PLATER, S. M., CULHAM, D. E., KIMBER, M. S. & WOOD, J. M. 2015. YehZYXW of *Escherichia coli* Is a Low-Affinity, Non-Osmoregulatory Betaine-Specific ABC Transporter. *Biochemistry*, 54, 5735-47.
- LANGRIDGE, G. C., PHAN, M. D., TURNER, D. J., PERKINS, T. T., PARTS, L., HAASE, J., CHARLES, I., MASKELL, D. J., PETERS, S. E., DOUGAN, G., WAIN, J., PARKHILL, J. & TURNER, A. K. 2009. Simultaneous assay of every *Salmonella* Typhi gene using one million transposon mutants. *Genome Res*, 19, 2308-16.
- LATASA, C., GARCÍA, B., ECHEVERZ, M., TOLEDO-ARANA, A., VALLE, J., CAMPOY, S., GARCÍA-DEL PORTILLO, F., SOLANO, C. & LASA, I. 2012. *Salmonella* Biofilm Development Depends on the Phosphorylation Status of RcsB. *Journal of Bacteriology*, 194, 3708-3722.
- LATASA, C., ROUX, A., TOLEDO-ARANA, A., GHIGO, J. M., GAMAZO, C., PENADES, J. R. & LASA, I. 2005. BapA, a large secreted protein required for biofilm formation and host colonization of *Salmonella enterica* serovar Enteritidis. *Mol Microbiol*, 58, 1322-39.
- LAZAR, S. W. & KOLTER, R. 1996. SurA assists the folding of *Escherichia coli* outer membrane proteins. *J Bacteriol*, 178, 1770-3.
- LE QUÉRÉ, B. & GHIGO, J.-M. 2009. BcsQ is an essential component of the *Escherichia coli* cellulose biosynthesis apparatus that localizes at the bacterial cell pole. *Molecular Microbiology*, 72, 724-740.
- LEE, D. J., BINGLE, L. E., HEURLIER, K., PALLAN, M. J., PENN, C. W., BUSBY, S. J. & HOBMAN, J. L. 2009. Gene doctoring: a method for recombineering in laboratory and pathogenic *Escherichia coli* strains. *BMC Microbiol*, 9, 252.
- LEE, S. J., KO, J. H., KANG, H. Y. & LEE, Y. 2006. Coupled expression of MhpE aldolase and MhpF dehydrogenase in *Escherichia coli*. *Biochem Biophys Res Commun*, 346, 1009-15.
- LEE, Y., KIM, Y., YEOM, S., KIM, S., PARK, S., JEON, C. O. & PARK, W. 2008. The role of disulfide bond isomerase A (DsbA) of *Escherichia coli* O157:H7 in biofilm formation and virulence. *FEMS Microbiol Lett*, 278, 213-22.
- LEHNEN, D., BLUMER, C., POLEN, T., WACKWITZ, B., WENDISCH, V. F. & UNDEN, G. 2002. LrhA as a new transcriptional key regulator of flagella, motility and chemotaxis genes in *Escherichia coli*. *Molecular Microbiology*, 45, 521-532.
- LEMKE, J. J., DURFEE, T. & GOURSE, R. L. 2009. DksA and ppGpp directly regulate transcription of the *Escherichia coli* flagellar cascade. *Molecular Microbiology*, 74, 1368-1379.
- LEO, V., TRAN, E., MORONA, R. & COMSTOCK, L. E. 2021. Polysaccharide Copolymerase WzzB/WzzE Chimeras Reveal that the Transmembrane 2 Region of WzzB Is Important for Interaction with WzyB. *Journal of Bacteriology*, 203, e00598-20.
- LERMAN, L. S. 1963. The Structure of the DNA-Acridine Complex. *Proceedings of the National Academy of Sciences*, 49, 94-102.
- LEWIS, M. 2005. The *lac* repressor. *Comptes Rendus Biologies*, 328, 521-548.
- LI, P., LIU, Q., HUANG, C., ZHAO, X., ROLAND, K. L. & KONG, Q. 2017. Reversible synthesis of colanic acid and O-antigen polysaccharides in *Salmonella* Typhimurium enhances induction of cross-immune responses and provides protection against heterologous *Salmonella* challenge. *Vaccine*, 35, 2862-2869.
- LI, S., LIANG, H., WEI, Z., BAI, H., LI, M., LI, Q., QU, M., SHEN, X., WANG, Y. & ZHANG, L. 2019. An Osmoregulatory Mechanism Operating through OmpR and LrhA Controls the Motile-Sessile Switch in the Plant Growth-Promoting Bacterium *Pantoea alhagi*. *Applied and Environmental Microbiology*, 85, e00077-19.
- LI, X. Z., MA, D., LIVERMORE, D. M. & NIKAIIDO, H. 1994. Role of efflux pump(s) in intrinsic resistance of *Pseudomonas aeruginosa*: active efflux as a contributing factor to  $\beta$ -lactam resistance. *Antimicrob Agents Chemother*, 38, 1742-52.

- LIAO, H., ZHONG, X., XU, L., MA, Q., WANG, Y., CAI, Y. & GUO, X. 2019. Quorum-sensing systems trigger catalase expression to reverse the *oxyR* deletion-mediated VBNC state in *Salmonella typhimurium*. *Research in Microbiology*, 170, 65-73.
- LIM, J. Y., YOON, J. & HOVDE, C. J. 2010. A brief overview of *Escherichia coli* O157:H7 and its plasmid O157. *Journal of microbiology and biotechnology*, 20, 5-14.
- LIN, F. C., BROWN, R. M., JR., DRAKE, R. R., JR. & HALEY, B. E. 1990. Identification of the uridine 5'-diphosphoglucose (UDP-Glc) binding subunit of cellulose synthase in *Acetobacter xylinum* using the photoaffinity probe 5-azido-UDP-Glc. *J Biol Chem*, 265, 4782-4.
- LØBNER-OLESEN, A., MARINUS, M. G. & HANSEN, F. G. 2003. Role of SeqA and Dam in *Escherichia coli* gene expression: a global/microarray analysis. *Proceedings of the National Academy of Sciences of the United States of America*, 100, 4672-4677.
- LOFERER, H., HAMMAR, M. & NORMARK, S. 1997. Availability of the fibre subunit CsgA and the nucleator protein CsgB during assembly of fibronectin-binding *curli* is limited by the intracellular concentration of the novel lipoprotein CsgG. *Mol Microbiol*, 26, 11-23.
- LOMOVSKAYA, O., WARREN, M. S., LEE, A., GALAZZO, J., FRONKO, R., LEE, M., BLAIS, J., CHO, D., CHAMBERLAND, S., RENU, T., LEGER, R., HECKER, S., WATKINS, W., HOSHINO, K., ISHIDA, H. & LEE, V. J. 2001. Identification and characterization of inhibitors of multidrug resistance efflux pumps in *Pseudomonas aeruginosa*: novel agents for combination therapy. *Antimicrob Agents Chemother*, 45, 105-16.
- LOPILATO, J. E., GARWIN, J. L., EMR, S. D., SILHAVY, T. J. & BECKWITH, J. R. 1984. D-ribose metabolism in *Escherichia coli* K-12: genetics, regulation, and transport. *Journal of bacteriology*, 158, 665-673.
- LU, H.-F., WU, B.-K., HUANG, Y.-W., LEE, M.-Z., LI, M.-F., HO, H.-J., YANG, H.-C. & YANG, T.-C. 2020. PhoPQ two-component regulatory system plays a global regulatory role in antibiotic susceptibility, physiology, stress adaptation, and virulence in *Stenotrophomonas maltophilia*. *BMC Microbiology*, 20, 312.
- LUCCHINI, S., MCDERMOTT, P., THOMPSON, A. & HINTON, J. C. D. 2009. The H-NS-like protein StpA represses the RpoS ( $\sigma$ 38) regulon during exponential growth of *Salmonella* Typhimurium. *Molecular Microbiology*, 74, 1169-1186.
- LUSETTI, S. L., DREES, J. C., STOHL, E. A., SEIFERT, H. S. & COX, M. M. 2004. The DinI and RecX proteins are competing modulators of RecA function. *J Biol Chem*, 279, 55073-9.
- MA, D., COOK, D. N., ALBERTI, M., PON, N. G., NIKAIDO, H. & HEARST, J. E. 1995. Genes *acrA* and *acrB* encode a stress-induced efflux system of *Escherichia coli*. *Molecular Microbiology*, 16, 45-55.
- MA, X., PRATHAPAM, R., WARTCHOW, C., CHIE-LEON, B., HO, C. M., DE VICENTE, J., HAN, W., LI, M., LU, Y., RAMURTHY, S., SHIA, S., STEFFEK, M. & UEHARA, T. 2020. Structural and Biological Basis of Small Molecule Inhibition of *Escherichia coli* LpxD Acyltransferase Essential for Lipopolysaccharide Biosynthesis. *ACS Infect Dis*, 6, 1480-1489.
- MACGREGOR, G. R., NOLAN, G. P., FIERING, S., ROEDERER, M. & HERZENBERG, L. A. 1991. Use of *Escherichia coli* (*E. coli*) *lacZ* ( $\beta$ -Galactosidase) as a Reporter Gene. In: MURRAY, E. J. (ed.) *Gene Transfer and Expression Protocols*. Totowa, NJ: Humana Press.
- MACIAG, A., PEANO, C., PIETRELLI, A., EGLI, T., DE BELLIS, G. & LANDINI, P. 2011. *In vitro* transcription profiling of the  $\sigma$ S subunit of bacterial RNA polymerase: re-definition of the  $\sigma$ S regulon and identification of  $\sigma$ S-specific promoter sequence elements. *Nucleic acids research*, 39, 5338-5355.
- MACNAB, R. M. 1992. Genetics and biogenesis of bacterial flagella. *Annu Rev Genet*, 26, 131-58.
- MADISON, K. E., ABDELMEGUID, M. R., JONES-FOSTER, E. N. & NAKAI, H. 2012. A new role for translation initiation factor 2 in maintaining genome integrity. *PLoS genetics*, 8, e1002648-e1002648.

- MADRID, C., GARCÍA, J., PONS, M. & JUÁREZ, A. 2007. Molecular Evolution of the H-NS Protein: Interaction with Hha-Like Proteins Is Restricted to *Enterobacteriaceae*. *Journal of Bacteriology*, 189, 265-268.
- MAGNUSSON, L. U., GUMMESSON, B., JOKSIMOVIĆ, P., FAREWELL, A. & NYSTRÖM, T. 2007. Identical, Independent, and Opposing Roles of ppGpp and DksA in *Escherichia coli*. *Journal of Bacteriology*, 189, 5193-5202.
- MAH, T.-F. C. & O'TOOLE, G. A. 2001. Mechanisms of biofilm resistance to antimicrobial agents. *Trends in Microbiology*, 9, 34-39.
- MAJDALANI, N. & GOTTESMAN, S. 2005. The Rcs Phosphorelay: A Complex Signal Transduction System. *Annual Review of Microbiology*, 59, 379-405.
- MALLIK, P., PAUL, B. J., RUTHERFORD, S. T., GOURSE, R. L. & OSUNA, R. 2006. DksA is required for growth phase-dependent regulation, growth rate-dependent control, and stringent control of *fis* expression in *Escherichia coli*. *Journal of bacteriology*, 188, 5775-5782.
- MANGAN, M. W., LUCCHINI, S., DANINO, V., CRÓINÍN, T. Ó., HINTON, J. C. D. & DORMAN, C. J. 2006. The integration host factor (IHF) integrates stationary-phase and virulence gene expression in *Salmonella enterica* serovar Typhimurium. *Molecular Microbiology*, 59, 1831-1847.
- MAO, X., LI, K., LIU, M., WANG, X., ZHAO, T., AN, B., CUI, M., LI, Y., PU, J., LI, J., WANG, L., LU, T. K., FAN, C. & ZHONG, C. 2019. Directing curli polymerization with DNA origami nucleators. *Nature Communications*, 10, 1395.
- MARTEYN, B. S., KARIMOVA, G., FENTON, A. K., GAZI, A. D., WEST, N., TOUQUI, L., PREVOST, M. C., BETTON, J. M., POYRAZ, O., LADANT, D., GERDES, K., SANSONETTI, P. J. & TANG, C. M. 2014. ZapE is a novel cell division protein interacting with FtsZ and modulating the Z-ring dynamics. *mBio*, 5, e00022-14.
- MATHLOUTHI, A., PENNACCHIETTI, E. & DE BIASE, D. 2018. Effect of Temperature, pH and Plasmids on In Vitro Biofilm Formation in *Escherichia coli*. *Acta naturae*, 10, 129-132.
- MAXWELL, I. H. 1967. Partial removal of bound transfer RNA from polysomes engaged in protein synthesis in vitro after addition of tetracycline. *Biochimica et Biophysica Acta (BBA) - Nucleic Acids and Protein Synthesis*, 138, 337-346.
- MAY, T., ITO, A. & OKABE, S. 2009. Induction of multidrug resistance mechanism in *Escherichia coli* biofilms by interplay between tetracycline and ampicillin resistance genes. *Antimicrobial agents and chemotherapy*, 53, 4628-4639.
- MAZUR, O. & ZIMMER, J. 2011. Apo- and cellopentaose-bound structures of the bacterial cellulose synthase subunit BcsZ. *J Biol Chem*, 286, 17601-6.
- MCCLAIN, M. S., BLOMFIELD, I. C., EBERHARDT, K. J. & EISENSTEIN, B. I. 1993. Inversion-independent phase variation of type 1 fimbriae in *Escherichia coli*. *J Bacteriol*, 175, 4335-44.
- MCCLEARY, W. R., STOCK, J. B. & NINFA, A. J. 1993. Is acetyl phosphate a global signal in *Escherichia coli*? *Journal of bacteriology*, 175, 2793-2798.
- MCKENZIE, G. J. & CRAIG, N. L. 2006. Fast, easy and efficient: site-specific insertion of transgenes into enterobacterial chromosomes using Tn7 without need for selection of the insertion event. *BMC Microbiol*, 6, 39.
- MEGANATHAN, R. & KWON, O. 2009. Biosynthesis of Menaquinone (Vitamin K2) and Ubiquinone (Coenzyme Q). *EcoSal Plus*, 3, 10.1128/ecosalplus.3.6.3.3.
- MEIER-DIETER, U., STARMAN, R., BARR, K., MAYER, H. & RICK, P. D. 1990. Biosynthesis of enterobacterial common antigen in *Escherichia coli*. Biochemical characterization of Tn10 insertion mutants defective in enterobacterial common antigen synthesis. *Journal of Biological Chemistry*, 265, 13490-13497.
- MELAUGH, G., HUTCHISON, J., KRAGH, K. N., IRIE, Y., ROBERTS, A., BJARNSHOLT, T., DIGGLE, S. P., GORDON, V. D. & ALLEN, R. J. 2016. Shaping the Growth Behaviour of Biofilms Initiated from Bacterial Aggregates. *PLoS One*, 11, e0149683.
- MIELICH-SÜSS, B. & LOPEZ, D. 2015. Molecular mechanisms involved in *Bacillus subtilis* biofilm formation. *Environmental Microbiology*, 17, 555-565.

- MIRELES, J. R., TOGUCHI, A. & HARSHEY, R. M. 2001. *Salmonella enterica* Serovar Typhimurium Swarming Mutants with Altered Biofilm-Forming Abilities: Surfactin Inhibits Biofilm Formation. *Journal of Bacteriology*, 183, 5848-5854.
- MITCHELL, A. M., SRIKUMAR, T., SILHAVY, T. J. & HULTGREN, S. J. 2018. Cyclic Enterobacterial Common Antigen Maintains the Outer Membrane Permeability Barrier of *Escherichia coli* in a Manner Controlled by YhdP. *mBio*, 9, e01321-18.
- MITRA, R., MCKENZIE, G. J., YI, L., LEE, C. A. & CRAIG, N. L. 2010. Characterization of the TnsD-attTn7 complex that promotes site-specific insertion of Tn7. *Mob DNA*, 1, 18.
- MONTEIRO, D. C. F., PATEL, V., BARTLETT, C. P., NOZAKI, S., GRANT, T. D., GOWDY, J. A., THOMPSON, G. S., KALVERDA, A. P., SNELL, E. H., NIKI, H., PEARSON, A. R. & WEBB, M. E. 2015. The structure of the PanD/PanZ protein complex reveals negative feedback regulation of pantothenate biosynthesis by coenzyme A. *Chem Biol*, 22, 492-503.
- MOORE, T. C. & ESCALANTE-SEMERENA, J. C. 2016. The EutQ and EutP proteins are novel acetate kinases involved in ethanolamine catabolism: physiological implications for the function of the ethanolamine metabolosome in *Salmonella enterica*. *Molecular Microbiology*, 99, 497-511.
- MORGAN, J. L. W., MCNAMARA, J. T. & ZIMMER, J. 2014. Mechanism of activation of bacterial cellulose synthase by cyclic di-GMP. *Nature structural & molecular biology*, 21, 489-496.
- MORGAN, J. L. W., STRUMILLO, J. & ZIMMER, J. 2012. Crystallographic snapshot of cellulose synthesis and membrane translocation. *Nature*, 493, 181.
- MORONA, R., MANNING, P. A. & REEVES, P. 1983. Identification and characterization of the TolC protein, an outer membrane protein from *Escherichia coli*. *J Bacteriol*, 153, 693-9.
- MOTTA, S. S., CLUZEL, P. & ALDANA, M. 2015. Adaptive Resistance in Bacteria Requires Epigenetic Inheritance, Genetic Noise, and Cost of Efflux Pumps. *PLOS ONE*, 10, e0118464.
- MOUSLIM, C., DELGADO, M. & GROISMAN, E. A. 2004. Activation of the RcsC/YojN/RcsB phosphorelay system attenuates *Salmonella* virulence. *Molecular Microbiology*, 54, 386-395.
- MOUSSATOVA, A., KANDT, C., O'MARA, M. L. & TIELEMAN, D. P. 2008. ATP-binding cassette transporters in *Escherichia coli*. *Biochimica et Biophysica Acta (BBA) - Biomembranes*, 1778, 1757-1771.
- MUELA, A., SECO, C., CAMAFEITA, E., ARANA, I., ORRUÑO, M., LÓPEZ, J. A. & BARCINA, I. 2008. Changes in *Escherichia coli* outer membrane subproteome under environmental conditions inducing the viable but nonculturable state. *FEMS Microbiol Ecol*, 64, 28-36.
- MÜLLER, C. M., DOBRINDT, U., NAGY, G., EMÖDY, L., UHLIN, B. E. & HACKER, J. 2006. Role of histone-like proteins H-NS and StpA in expression of virulence determinants of uropathogenic *Escherichia coli*. *Journal of bacteriology*, 188, 5428-5438.
- NAKAYAMA, S.-I. & WATANABE, H. 1998. Identification of *cpxR* as a Positive Regulator Essential for Expression of the *Shigella sonnei virF* Gene. *Journal of Bacteriology*, 180, 3522-3528.
- NENNINGER, A. A., ROBINSON, L. S., HAMMER, N. D., EPSTEIN, E. A., BADTKE, M. P., HULTGREN, S. J. & CHAPMAN, M. R. 2011. CsgE is a curli secretion specificity factor that prevents amyloid fibre aggregation. *Molecular Microbiology*, 81, 486-499.
- NENNINGER, A. A., ROBINSON, L. S. & HULTGREN, S. J. 2009. Localized and efficient curli nucleation requires the chaperone-like amyloid assembly protein CsgF. *Proceedings of the National Academy of Sciences*, 106, 900-905.
- NESPER, J., LAURIANO, C. M., KLOSE, K. E., KAPFFHAMMER, D., KRAISS, A. & REIDL, J. 2001. Characterization of *Vibrio cholerae* O1 El tor *galU* and *galE* mutants: influence on lipopolysaccharide structure, colonization, and biofilm formation. *Infect Immun*, 69, 435-45.

- NESSE, L. L., SEKSE, C., BERG, K., JOHANNESSEN, K. C. S., SOLHEIM, H., VESTBY, L. K. & URDAHL, A. M. 2014. Potentially Pathogenic *Escherichia coli* Can Form a Biofilm under Conditions Relevant to the Food Production Chain. *Applied and Environmental Microbiology*, 80, 2042-2049.
- NHU, N. T. K., PHAN, M.-D., PETERS, K. M., LO, A. W., FORDE, B. M., MIN CHONG, T., YIN, W.-F., CHAN, K.-G., CHROMEK, M., BRAUNER, A., CHAPMAN, M. R., BEATSON, S. A. & SCHEMBRI, M. A. 2018. Discovery of New Genes Involved in Curli Production by a Uropathogenic *Escherichia coli* Strain from the Highly Virulent O45:K1:H7 Lineage. *mBio*, 9, e01462-18.
- NIBA, E. T. E., NAKA, Y., NAGASE, M., MORI, H. & KITAKAWA, M. 2008. A Genome-wide Approach to Identify the Genes Involved in Biofilm Formation in *E. coli*. *DNA Research*, 14, 237-246.
- NIEHAUS, T. D., ELBADAWI-SIDHU, M., DE CRÉCY-LAGARD, V., FIEHN, O. & HANSON, A. D. 2017. Discovery of a widespread prokaryotic 5-oxoprolinase that was hiding in plain sight. *J Biol Chem*, 292, 16360-16367.
- NIKAIDO, E., SHIROSAKA, I., YAMAGUCHI, A. & NISHINO, K. 2011. Regulation of the AcrAB multidrug efflux pump in *Salmonella enterica* serovar Typhimurium in response to indole and paraquat. *Microbiology*, 157, 648-55.
- NISHINO, K., LATIFI, T. & GROISMAN, E. A. 2006. Virulence and drug resistance roles of multidrug efflux systems of *Salmonella enterica* serovar Typhimurium. *Molecular Microbiology*, 59, 126-141.
- NUCCIO, S.-P., BAÜMLER ANDREAS, J. & FINLAY, B. B. 2014. Comparative Analysis of *Salmonella* Genomes Identifies a Metabolic Network for Escalating Growth in the Inflamed Gut. *mBio*, 5, e00929-14.
- NUNN, W. D. & SIMONS, R. W. 1978. Transport of long-chain fatty acids by *Escherichia coli*: mapping and characterization of mutants in the *fadL* gene. *Proc Natl Acad Sci U S A*, 75, 3377-81.
- OBERTO, J., NABTI, S., JOOSTE, V., MIGNOT, H. & ROUVIERE-YANIV, J. 2009. The HU regulon is composed of genes responding to anaerobiosis, acid stress, high osmolarity and SOS induction. *PLoS one*, 4, e4367-e4367.
- OETHINGER, M., KERN, W. V., JELLEN-RITTER, A. S., MCMURRY, L. M. & LEVY, S. B. 2000. Ineffectiveness of Topoisomerase Mutations in Mediating Clinically Significant Fluoroquinolone Resistance in *Escherichia coli* in the Absence of the AcrAB Efflux Pump. *Antimicrobial Agents and Chemotherapy*, 44, 10-13.
- OETHINGER, M., PODGLAJEN, I., KERN, W. V. & LEVY, S. B. 1998. Overexpression of the *marA* or *soxS* regulatory gene in clinical topoisomerase mutants of *Escherichia coli*. *Antimicrobial agents and chemotherapy*, 42, 2089-2094.
- OGASAWARA, H., ISHIDA, Y., YAMADA, K., YAMAMOTO, K. & ISHIHAMA, A. 2007. PdhR (pyruvate dehydrogenase complex regulator) controls the respiratory electron transport system in *Escherichia coli*. *Journal of bacteriology*, 189, 5534-5541.
- OGASAWARA, H., ISHIZUKA, T., HOTTA, S., AOKI, M., SHIMADA, T. & ISHIHAMA, A. 2020. Novel regulators of the *csgD* gene encoding the master regulator of biofilm formation in *Escherichia coli* K-12. *Microbiology*.
- OKUSU, H., MA, D. & NIKAIDO, H. 1996. AcrAB efflux pump plays a major role in the antibiotic resistance phenotype of *Escherichia coli* multiple-antibiotic-resistance (Mar) mutants. *Journal of bacteriology*, 178, 306-308.
- OLSÉN, A., ARNQVIST, A., HAMMAR, M., RTEN, SUKUPOLVI, S. & NORMARK, S. 1993. The RpoS Sigma factor relieves H-NS-mediated transcriptional repression of *csgA*, the subunit gene of fibronectin-binding curli in *Escherichia coli*. *Molecular Microbiology*, 7, 523-536.
- ORLOWSKI, M. & MEISTER, A. 1970. The  $\gamma$ -glutamyl cycle: a possible transport system for amino acids. *Proceedings of the National Academy of Sciences of the United States of America*, 67, 1248-1255.
- OSMAN, K. M., KAPPELL, A. D., ELHADIDY, M., ELMOUGY, F., EL-GHANY, W. A. A., ORABI, A., MUBARAK, A. S., DAWOUD, T. M., HEMEG, H. A., MOUSSA, I. M. I., HESSAIN, A. M. & YOUSEF, H. M. Y. 2018. Poultry hatcheries as potential

- reservoirs for antimicrobial-resistant *Escherichia coli*: A risk to public health and food safety. *Scientific Reports*, 8, 5859.
- OTTO, K. & SILHAVY, T. J. 2002. Surface sensing and adhesion of *Escherichia coli* controlled by the Cpx-signaling pathway. *Proceedings of the National Academy of Sciences*, 99, 2287-2292.
- PARK, F., GAJIWALA, K., EROSHKINA, G., FURLONG, E., HE, D., BATIYENKO, Y., ROMERO, R., CHRISTOPHER, J., BADGER, J., HENDLE, J., LIN, J., PEAT, T. & BUCHANAN, S. 2004. Crystal structure of YIGZ, a conserved hypothetical protein from *Escherichia coli* k12 with a novel fold. *Proteins: Structure, Function, and Bioinformatics*, 55, 775-777.
- PARSEK, M. R. & GREENBERG, E. P. 2005. Sociomicrobiology: the connections between quorum sensing and biofilms. *Trends in Microbiology*, 13, 27-33.
- PAUL, B. J., BARKER, M. M., ROSS, W., SCHNEIDER, D. A., WEBB, C., FOSTER, J. W. & GOURSE, R. L. 2004. DksA: a critical component of the transcription initiation machinery that potentiates the regulation of rRNA promoters by ppGpp and the initiating NTP. *Cell*, 118, 311-22.
- PEIL, L., VIRUMÄE, K. & REMME, J. 2008. Ribosome assembly in *Escherichia coli* strains lacking the RNA helicase DeaD/CsdA or DbpA. *Febs j*, 275, 3772-82.
- PENESYAN, A., NAGY, S. S., KJELLEBERG, S., GILLINGS, M. R. & PAULSEN, I. T. 2019. Rapid microevolution of biofilm cells in response to antibiotics. *npj Biofilms and Microbiomes*, 5, 34.
- PENROD, J. T. & ROTH, J. R. 2006. Conserving a Volatile Metabolite: a Role for Carboxysome-Like Organelles in *Salmonella enterica*. *Journal of Bacteriology*, 188, 2865-2874.
- PERCIVAL, S. L., HILL, K. E., WILLIAMS, D. W., HOOPER, S. J., THOMAS, D. W. & COSTERTON, J. W. 2012. A review of the scientific evidence for biofilms in wounds. *Wound Repair and Regeneration*, 20, 647-657.
- PERERA, I. C. & GROVE, A. 2010. Molecular Mechanisms of Ligand-Mediated Attenuation of DNA Binding by MarR Family Transcriptional Regulators. *Journal of Molecular Cell Biology*, 2, 243-254.
- PÉREZ, A., POZA, M., FERNÁNDEZ, A., DEL CARMEN FERNÁNDEZ, M., MALLO, S., MERINO, M., RUMBO-FEAL, S., CABRAL, M. P. & BOU, G. 2012. Involvement of the AcrAB-TolC Efflux Pump in the Resistance, Fitness, and Virulence of *Enterobacter cloacae*. *Antimicrobial Agents and Chemotherapy*, 56, 2084-2090.
- PERKINS, T. T., DAVIES, M. R., KLEMM, E. J., ROWLEY, G., WILEMAN, T., JAMES, K., KEANE, T., MASKELL, D., HINTON, J. C. D., DOUGAN, G. & KINGSLEY, R. A. 2013. ChIP-seq and transcriptome analysis of the OmpR regulon of *Salmonella enterica* serovars Typhi and Typhimurium reveals accessory genes implicated in host colonization. *Molecular Microbiology*, 87, 526-538.
- PERRETT, C. A., KARAVOLOS, M. H., HUMPHREY, S., MASTROENI, P., MARTINEZ-ARGUDO, I., SPENCER, H., BULMER, D., WINZER, K., MCGHIE, E., KORONAKIS, V., WILLIAMS, P., KHAN, C. M. & JEPSON, M. A. 2009. LuxS-based quorum sensing does not affect the ability of *Salmonella enterica* serovar Typhimurium to express the SPI-1 type 3 secretion system, induce membrane ruffles, or invade epithelial cells. *J Bacteriol*, 191, 7253-9.
- PESAVENTO, C., BECKER, G., SOMMERFELDT, N., POSSLING, A., TSCHOWRI, N., MEHLIS, A. & HENGGE, R. 2008. Inverse regulatory coordination of motility and curli-mediated adhesion in *Escherichia coli*. *Genes Dev*, 22, 2434-46.
- PESTKA, S. 1975. Chloramphenicol. In: CORCORAN, J. W., HAHN, F. E., SNELL, J. F. & ARORA, K. L. (eds.) *Mechanism of Action of Antimicrobial and Antitumor Agents*. Berlin, Heidelberg: Springer Berlin Heidelberg.
- PETERSON, K. R., WERTMAN, K. F., MOUNT, D. W. & MARINUS, M. G. 1985. Viability of *Escherichia coli* K-12 DNA adenine methylase (*dam*) mutants requires increased expression of specific genes in the SOS regulon. *Molecular and General Genetics MGG*, 201, 14-19.
- PIFFER, V., SARENKO, O., POSSLING, A. & HENGGE, R. 2019. Genetic dissection of *Escherichia coli*'s master diguanylate cyclase DgcE: Role of the N-terminal

- MASE1 domain and direct signal input from a GTPase partner system. *PLOS Genetics*, 15, e1008059.
- PHE 2016. Salmonella data 2006 to 2015. *PHE publications gateway number: 22016581*.
- PIDDOCK, L. J. 2006a. Clinically relevant chromosomally encoded multidrug resistance efflux pumps in bacteria. *Clin Microbiol Rev*, 19, 382-402.
- PIDDOCK, L. J. 2006b. Multidrug-resistance efflux pumps - not just for resistance. *Nat Rev Microbiol*, 4, 629-36.
- POMPOSIELLO, P. J. & DEMPSEY, B. 2000. Identification of SoxS-Regulated Genes in *Salmonella enterica* Serovar Typhimurium. *Journal of Bacteriology*, 182, 23-29.
- PONTES, M. H., LEE, E.-J., CHOI, J. & GROISMAN, E. A. 2015. Salmonella promotes virulence by repressing cellulose production. *Proceedings of the National Academy of Sciences*, 112, 5183-5188.
- PRATT, L. A. & KOLTER, R. 1998. Genetic analysis of *Escherichia coli* biofilm formation: roles of flagella, motility, chemotaxis and type I pili. *Molecular Microbiology*, 30, 285-293.
- PRATT, L. A. & SILHAVY, T. J. 1998. Crl stimulates RpoS activity during stationary phase. *Molecular Microbiology*, 29, 1225-1236.
- PRIETO, A. I., HERNÁNDEZ, S. B., COTA, I., PUCCIARELLI, M. G., ORLOV, Y., RAMOS-MORALES, F., GARCÍA-DEL PORTILLO, F. & CASADESÚS, J. 2009. Roles of the Outer Membrane Protein AsmA of *Salmonella enterica* in the Control of *marRAB* Expression and Invasion of Epithelial Cells. *Journal of Bacteriology*, 191, 3615-3622.
- PRIGENT-COMBARET, C., BROMBACHER, E., VIDAL, O., AMBERT, A., LEJEUNE, P., LANDINI, P. & DOREL, C. 2001. Complex Regulatory Network Controls Initial Adhesion and Biofilm Formation in *Escherichia coli* via Regulation of the *csgD* Gene. *Journal of Bacteriology*, 183, 7213-7223.
- PROUTY, A. M. & GUNN, J. S. 2003. Comparative analysis of *Salmonella enterica* serovar Typhimurium biofilm formation on gallstones and on glass. *Infect Immun*, 71, 7154-8.
- PROUTY, A. M., SCHWESINGER, W. H. & GUNN, J. S. 2002. Biofilm formation and interaction with the surfaces of gallstones by *Salmonella* spp. *Infect Immun*, 70, 2640-9.
- PRÜSS, B. M., VERMA, K., SAMANTA, P., SULE, P., KUMAR, S., WU, J., CHRISTIANSON, D., HORNE, S. M., STAFSLIEN, S. J., WOLFE, A. J. & DENTON, A. 2010. Environmental and genetic factors that contribute to *Escherichia coli* K-12 biofilm formation. *Archives of microbiology*, 192, 715-728.
- PUTTAMREDDY, S., CORNICK, N. A. & MINION, F. C. 2010. Genome-Wide Transposon Mutagenesis Reveals a Role for pO157 Genes in Biofilm Development in *Escherichia coli* O157:H7 EDL933. *Infection and Immunity*, 78, 2377.
- QIN, R., SANG, Y., REN, J., ZHANG, Q., LI, S., CUI, Z. & YAO, Y.-F. 2016. The Bacterial Two-Hybrid System Uncovers the Involvement of Acetylation in Regulating of Lrp Activity in *Salmonella* Typhimurium. *Frontiers in microbiology*, 7, 1864-1864.
- RACZKOWSKA, A., SKOREK, K., BIELECKI, J. & BRZOSTEK, K. 2011. OmpR controls *Yersinia enterocolitica* motility by positive regulation of *flhDC* expression. *Antonie van Leeuwenhoek*, 99, 381-394.
- RACZKOWSKA, A., TRZOS, J., LEWANDOWSKA, O., NIECKARZ, M. & BRZOSTEK, K. 2015. Expression of the AcrAB Components of the AcrAB-TolC Multidrug Efflux Pump of *Yersinia enterocolitica* Is Subject to Dual Regulation by OmpR. *PloS one*, 10, e0124248-e0124248.
- RAGHUNATHAN, D., WELLS, T. J., MORRIS, F. C., SHAW, R. K., BOBAT, S., PETERS, S. E., PATERSON, G. K., JENSEN, K. T., LEYTON, D. L., BLAIR, J. M. A., BROWNING, D. F., PRAVIN, J., FLORES-LANGARICA, A., HITCHCOCK, J. R., MORAES, C. T. P., PIAZZA, R. M. F., MASKELL, D. J., WEBBER, M. A., MAY, R. C., MACLENNAN, C. A., PIDDOCK, L. J., CUNNINGHAM, A. F. & HENDERSON, I. R. 2011. SadA, a Trimeric Autotransporter from *Salmonella enterica* Serovar Typhimurium, Can Promote Biofilm Formation and Provides Limited Protection against Infection. *Infection and Immunity*, 79, 4342-4352.



- RAINA, S. & MISSIAKAS, D. 1997. Making and breaking disulfide bonds. *Annual Review of Microbiology*, 51, 179-202.
- RAMOS-MORALES, F., PRIETO, A. I., BEUZÓN, C. R., HOLDEN, D. W. & CASADESÚS, J. 2003. Role for *Salmonella enterica* Enterobacterial Common Antigen in Bile Resistance and Virulence. *Journal of Bacteriology*, 185, 5328-5332.
- REEDER, T. & SCHLEIF, R. 1991. Mapping, sequence, and apparent lack of function of *araJ*, a gene of the *Escherichia coli* arabinose regulon. *J Bacteriol*, 173, 7765-71.
- RESCH, A., ROSENSTEIN, R., NERZ, C. & GÖTZ, F. 2005. Differential Gene Expression Profiling of *Staphylococcus aureus* Cultivated under Biofilm and Planktonic Conditions. *Applied and Environmental Microbiology*, 71, 2663.
- RESCH, A., VEĆEREK, B., PALAVRA, K. & BLÄSI, U. 2010. Requirement of the CsdA DEAD-box helicase for low temperature riboregulation of *rpoS* mRNA. *RNA biology*, 7, 796-802.
- RICCI, V., TZAKAS, P., BUCKLEY, A., COLDHAM, N. C. & PIDDOCK, L. J. V. 2006. Ciprofloxacin-Resistant *Salmonella enterica* Serovar Typhimurium Strains Are Difficult To Select in the Absence of AcrB and TolC. *Antimicrobial Agents and Chemotherapy*, 50, 38.
- RÖMLING, U., BIAN, Z., HAMMAR, M., SIERRALTA, W. D. & NORMARK, S. 1998a. Curli fibers are highly conserved between *Salmonella typhimurium* and *Escherichia coli* with respect to operon structure and regulation. *Journal of bacteriology*, 180, 722-731.
- RÖMLING, U., BOKRANZ, W., RABSCH, W., ZOGAJ, X., NIMTZ, M. & TSCHÄPE, H. 2003. Occurrence and regulation of the multicellular morphotype in *Salmonella* serovars important in human disease. *International Journal of Medical Microbiology*, 293, 273-285.
- RÖMLING, U., ROHDE, M., OLSÉN, A., NORMARK, S. & REINKÖSTER, J. 2000. *AgfD*, the checkpoint of multicellular and aggregative behaviour in *Salmonella typhimurium* regulates at least two independent pathways. *Molecular Microbiology*, 36, 10-23.
- RÖMLING, U., SIERRALTA, W. D., ERIKSSON, K. & NORMARK, S. 1998b. Multicellular and aggregative behaviour of *Salmonella typhimurium* strains is controlled by mutations in the *agfD* promoter. *Molecular Microbiology*, 28, 249-264.
- ROSENBLUM, R., KHAN, E., GONZALEZ, G., HASAN, R. & SCHNEIDERS, T. 2011. Genetic regulation of the *ramA* locus and its expression in clinical isolates of *Klebsiella pneumoniae*. *International journal of antimicrobial agents*, 38, 39-45.
- ROSNER, J. L. & MARTIN, R. G. 2013. Reduction of cellular stress by TolC-dependent efflux pumps in *Escherichia coli* indicated by BaeSR and CpxARP activation of spy in efflux mutants. *J Bacteriol*, 195, 1042-50.
- ROY, A. & DANCHIN, A. 1982. The *cya* locus of *Escherichia coli* K12: Organization and gene products. *Molecular and General Genetics MGG*, 188, 465-471.
- RUAN, X., LOYOLA, D. E., MAROLDA, C. L., PEREZ-DONOSO, J. M. & VALVANO, M. A. 2012. The WaaL O-antigen lipopolysaccharide ligase has features in common with metal ion-independent inverting glycosyltransferases. *Glycobiology*, 22, 288-99.
- RUIZ, C. & LEVY, S. B. 2010. Many chromosomal genes modulate MarA-mediated multidrug resistance in *Escherichia coli*. *Antimicrobial agents and chemotherapy*, 54, 2125-2134.
- RUIZ, C. & LEVY, S. B. 2011. Use of functional interactions with MarA to discover chromosomal genes affecting antibiotic susceptibility in *Escherichia coli*. *International journal of antimicrobial agents*, 37, 177-178.
- RUIZ, C. & LEVY, S. B. 2013. Regulation of *acrAB* expression by cellular metabolites in *Escherichia coli*. *Journal of Antimicrobial Chemotherapy*, 69, 390-399.
- RUIZ, N. & SILHAVY, T. J. 2005. Sensing external stress: watchdogs of the *Escherichia coli* cell envelope. *Curr Opin Microbiol*, 8, 122-6.
- RYJENKOV, D. A., SIMM, R., RÖMLING, U. & GOMELSKY, M. 2006. The PilZ domain is a receptor for the second messenger c-di-GMP: the PilZ domain protein YcgR controls motility in enterobacteria. *J Biol Chem*, 281, 30310-4.

- SÁ-PESSOA, J., PAIVA, S., RIBAS, D., SILVA, I. J., VIEGAS, S. C., ARRAIANO, C. M. & CASAL, M. 2013. SATP (YaaH), a succinate-acetate transporter protein in *Escherichia coli*. *Biochem J*, 454, 585-95.
- SAIER, M. H., JR. & RAMSEIER, T. M. 1996. The catabolite repressor/activator (Cra) protein of enteric bacteria. *J Bacteriol*, 178, 3411-7.
- SAINI, S., PEARL, J. A. & RAO, C. V. 2009. Role of FimW, FimY, and FimZ in Regulating the Expression of Type I Fimbriae in *Salmonella enterica* Serovar Typhimurium. *Journal of Bacteriology*, 191, 3003-3010.
- SAKAI, Y., KIMURA, S. & SUZUKI, T. 2019. Dual pathways of tRNA hydroxylation ensure efficient translation by expanding decoding capability. *Nature communications*, 10, 2858-2858.
- SAMANTA, P., CLARK, E. R., KNUTSON, K., HORNE, S. M. & PRÜß, B. M. 2013. OmpR and RcsB abolish temporal and spatial changes in expression of *flhD* in *Escherichia coli* Biofilm. *BMC Microbiology*, 13, 182.
- SANTANDER, P. J., KAJIWARA, Y., WILLIAMS, H. J. & SCOTT, A. I. 2006. Structural characterization of novel cobalt corrinoids synthesized by enzymes of the vitamin B12 anaerobic pathway. *Bioorg Med Chem*, 14, 724-31.
- SANTIAGO, M., MATANO, L. M., MOUSSA, S. H., GILMORE, M. S., WALKER, S. & MEREDITH, T. C. 2015. A new platform for ultra-high density *Staphylococcus aureus* transposon libraries. *BMC genomics*, 16, 252-252.
- SANTIAGO, P., JIMÉNEZ-BELENGUER, A., GARCÍA-HERNÁNDEZ, J., ESTELLÉS, R. M., HERNÁNDEZ PÉREZ, M., CASTILLO LÓPEZ, M. A., FERRÚS, M. A. & MORENO, Y. 2018. High prevalence of *Salmonella* spp. in wastewater reused for irrigation assessed by molecular methods. *International Journal of Hygiene and Environmental Health*, 221, 95-101.
- SARKER, S. & OLIVER, D. 2002. Critical regions of *secM* that control its translation and secretion and promote secretion-specific *secA* regulation. *J Bacteriol*, 184, 2360-9.
- SASAHARA, K. C. & ZOTTOLA, E. A. 1993. Biofilm Formation by *Listeria monocytogenes* Utilizes a Primary Colonizing Microorganism in Flowing Systems. *Journal of Food Protection*, 56, 1022-1028.
- SCHEMBRI, M. A., KJÆRGAARD, K. & KLEMM, P. 2003. Global gene expression in *Escherichia coli* biofilms. *Molecular Microbiology*, 48, 253-267.
- SCHNAITMAN, C. A. & KLENA, J. D. 1993. Genetics of lipopolysaccharide biosynthesis in enteric bacteria. *Microbiological Reviews*, 57, 655-682.
- SCHNEIDER, D., KAISER, W., STUTZ, C., HOLINSKI, A., MAYANS, O. & BABINGER, P. 2015. YbiB from *Escherichia coli*, the Defining Member of the Novel TrpD2 Family of Prokaryotic DNA-binding Proteins. *The Journal of biological chemistry*, 290, 19527-19539.
- SCHNEIDER, K., DIMROTH, P. & BOTT, M. 2000. Identification of triphosphoribosyl-diphospho-CoA as precursor of the citrate lyase prosthetic group. *FEBS Lett*, 483, 165-8.
- SCHRODER, O. & WAGNER, R. 2002. The bacterial regulatory protein H-NS - a versatile modulator of nucleic acid structures. *Biol Chem*, 383, 945-60.
- SCHURR, T., NADIR, E. & MARGALIT, H. 1993. Identification and characterization of *E.coli* ribosomal binding sites by free energy computation. *Nucleic Acids Research*, 21, 4019-4023.
- SEO, S. W., KIM, D., LATIF, H., O'BRIEN, E. J., SZUBIN, R. & PALSSON, B. O. 2014. Deciphering Fur transcriptional regulatory network highlights its complex role beyond iron metabolism in *Escherichia coli*. *Nature Communications*, 5, 4910.
- SERRA, D. O. & HENGGE, R. 2019. Cellulose in Bacterial Biofilms. In: COHEN, E. & MERZENDORFER, H. (eds.) *Extracellular Sugar-Based Biopolymers Matrices*. Cham: Springer International Publishing.
- SERRA, D. O., RICHTER, A. M. & HENGGE, R. 2013. Cellulose as an architectural element in spatially structured *Escherichia coli* biofilms. *Journal of bacteriology*, 195, 5540-5554.
- SHAFQAT, J., HÖÖG, J. O., HJELMQVIST, L., OPPERMANN, U. C., IBÁÑEZ, C. & JÖRNVALL, H. 1999. An ethanol-inducible MDR ethanol dehydrogenase/acetaldehyde reductase in *Escherichia coli*: structural and

- enzymatic relationships to the eukaryotic protein forms. *Eur J Biochem*, 263, 305-11.
- SHARMA, P., HAYCOCKS, J. R. J., MIDDLEMISS, A. D., KETTLES, R. A., SELLARS, L. E., RICCI, V., PIDDOCK, L. J. V. & GRAINGER, D. C. 2017. The multiple antibiotic resistance operon of enteric bacteria controls DNA repair and outer membrane integrity. *Nature Communications*, 8, 1444.
- SHARMA, V. K. & BEARSON, B. L. 2013. Hha controls *Escherichia coli* O157:H7 biofilm formation by differential regulation of global transcriptional regulators FlhDC and CsgD. *Applied and environmental microbiology*, 79, 2384-2396.
- SHAW, R. K., LASA, I., GARCÍA, B. M., PALLÉN, M. J., HINTON, J. C. D., BERGER, C. N. & FRANKEL, G. 2011. Cellulose mediates attachment of *Salmonella enterica* Serovar Typhimurium to tomatoes. *Environmental Microbiology Reports*, 3, 569-573.
- SHEIDY, D. T. & ZIELKE, R. A. 2013. Analysis and expansion of the role of the *Escherichia coli* protein ProQ. *PLoS One*, 8, e79656.
- SHIMADA, T., BRIDIER, A., BRIANDET, R. & ISHIHAMA, A. 2011. Novel roles of LeuO in transcription regulation of *E. coli* genome: antagonistic interplay with the universal silencer H-NS. *Molecular Microbiology*, 82, 378-397.
- SHIMADA, T., KORI, A. & ISHIHAMA, A. 2013. Involvement of the ribose operon repressor RbsR in regulation of purine nucleotide synthesis in *Escherichia coli*. *FEMS Microbiol Lett*, 344, 159-65.
- SHIN, S. & PARK, C. 1995. Modulation of flagellar expression in *Escherichia coli* by acetyl phosphate and the osmoregulator OmpR. *J Bacteriol*, 177, 4696-702.
- SIMM, R., MORR, M., KADER, A., NIMTZ, M. & RÖMLING, U. 2004. GGDEF and EAL domains inversely regulate cyclic di-GMP levels and transition from sessility to motility. *Molecular Microbiology*, 53, 1123-1134.
- SIRKO, A., ZATYKA, M., SADOWY, E. & HULANICKA, D. 1995. Sulfate and thiosulfate transport in *Escherichia coli* K-12: evidence for a functional overlapping of sulfate- and thiosulfate-binding proteins. *Journal of bacteriology*, 177, 4134-4136.
- SMITH, D. R., PRICE, J. E., BURBY, P. E., BLANCO, L. P., CHAMBERLAIN, J. & CHAPMAN, M. R. 2017. The Production of Curli Amyloid Fibers Is Deeply Integrated into the Biology of *Escherichia coli*. *Biomolecules*, 7, 75.
- SOKARIBO, A. S., HANSEN, E. G., MCCARTHY, M., DESIN, T. S., WALDNER, L. L., MACKENZIE, K. D., MUTWIRI JR, G., HERMAN, N. J., HERMAN, D. J. & WANG, Y. 2020. Metabolic Activation of CsgD in the Regulation of *Salmonella* Biofilms. *Microorganisms*, 8, 964.
- SOLANO, C., GARCÍA, B., VALLE, J., BERASAIN, C., GHIGO, J.-M., GAMAZO, C. & LASA, I. 2002. Genetic analysis of *Salmonella enteritidis* biofilm formation: critical role of cellulose. *Molecular Microbiology*, 43, 793-808.
- SOMMERFELDT, N., POSSLING, A., BECKER, G., PESAVENTO, C., TSCHOWRI, N. & HENGGE, R. 2009. Gene expression patterns and differential input into curli fimbriae regulation of all GGDEF/EAL domain proteins in *Escherichia coli*. *Microbiology*, 155, 1318-1331.
- SPERANZA, B., CORBO, M. R. & SINIGAGLIA, M. 2011. Effects of Nutritional and Environmental Conditions on *Salmonella* sp. Biofilm Formation. *Journal of Food Science*, 76, M12-M16.
- SQUIRES, C. H., DE FELICE, M., WESSLER, S. R. & CALVO, J. M. 1981. Physical characterization of the *ilvHI* operon of *Escherichia coli* K-12. *J Bacteriol*, 147, 797-804.
- SRIRAMULU, D. D., LÜNSDORF, H., LAM, J. S. & RÖMLING, U. 2005. Microcolony formation: a novel biofilm model of *Pseudomonas aeruginosa* for the cystic fibrosis lung. *Journal of Medical Microbiology*, 54, 667-676.
- STANAWAY, J. D., PARISI, A., SARKAR, K., BLACKER, B. F., REINER, R. C., HAY, S. I., NIXON, M. R., DOLECEK, C., JAMES, S. L., MOKDAD, A. H., ABEBE, G., AHMADIAN, E., ALAHDAB, F., ALEMNEW, B. T. T., ALIPOUR, V., ALLAH BAKESHEI, F., ANIMUT, M. D., ANSARI, F., ARABLOO, J., ASFAW, E. T., BAGHERZADEH, M., BASSAT, Q., BELAYNEH, Y. M. M., CARVALHO, F., DARYANI, A., DEMEKE, F. M., DEMIS, A. B. B., DUBEY, M., DUKEN, E. E.,

- DUNACHIE, S. J., EFTEKHARI, A., FERNANDES, E., FOULADI FARD, R., GEDEFW, G. A., GETA, B., GIBNEY, K. B., HASANZADEH, A., HOANG, C. L., KASAEIAN, A., KHATER, A., KIDANEMARIAM, Z. T., LAKEW, A. M., MALEKZADEH, R., MELESE, A., MENGISTU, D. T., MESTROVIC, T., MIAZGOWSKI, B., MOHAMMAD, K. A., MOHAMMADIAN, M., MOHAMMADIAN-HAFSHEJANI, A., NGUYEN, C. T., NGUYEN, L. H., NGUYEN, S. H., NIRAYO, Y. L., OLAGUNJU, A. T., OLAGUNJU, T. O., POURJAFAR, H., QORBANI, M., RABIEE, M., RABIEE, N., RAFAY, A., REZAPOUR, A., SAMY, A. M., SEPANLOU, S. G., SHAIKH, M. A., SHARIF, M., SHIGEMATSU, M., TESSEMA, B., TRAN, B. X., ULLAH, I., YIMER, E. M., ZAIDI, Z., MURRAY, C. J. L. & CRUMP, J. A. 2019. The global burden of non-typhoidal salmonella invasive disease: a systematic analysis for the Global Burden of Disease Study 2017. *The Lancet Infectious Diseases*, 19, 1312-1324.
- STEENACKERS, H., HERMANS, K., VANDERLEYDEN, J. & DE KEERSMAECKER, S. C. J. 2012. *Salmonella* biofilms: An overview on occurrence, structure, regulation and eradication. *Food Research International*, 45, 502-531.
- STENBERG, F., CHOVANEC, P., MASLEN, S. L., ROBINSON, C. V., ILAG, L. L., VON HEIJNE, G. & DALEY, D. O. 2005. Protein complexes of the *Escherichia coli* cell envelope. *J Biol Chem*, 280, 34409-19.
- STEVENSON, G., NEAL, B., LIU, D., HOBBS, M., PACKER, N. H., BATLEY, M., REDMOND, J. W., LINDQUIST, L. & REEVES, P. 1994. Structure of the O antigen of *Escherichia coli* K-12 and the sequence of its *rfb* gene cluster. *J Bacteriol*, 176, 4144-56.
- SUH, S. J., SILO-SUH, L., WOODS, D. E., HASSETT, D. J., WEST, S. E. & OHMAN, D. E. 1999. Effect of *rpoS* mutation on the stress response and expression of virulence factors in *Pseudomonas aeruginosa*. *Journal of bacteriology*, 181, 3890-3897.
- SUKHAREV, S. I., BLOUNT, P., MARTINAC, B., BLATTNER, F. R. & KUNG, C. 1994. A large-conductance mechanosensitive channel in *E. coli* encoded by *mscL* alone. *Nature*, 368, 265-8.
- SULAVIK, M. C., DAZER, M. & MILLER, P. F. 1997. The *Salmonella typhimurium* *mar* locus: molecular and genetic analyses and assessment of its role in virulence. *J Bacteriol*, 179, 1857-66.
- SUN, Y., DAI, M., HAO, H., WANG, Y., HUANG, L., ALMOFTI, Y. A., LIU, Z. & YUAN, Z. 2011. The role of RamA on the development of ciprofloxacin resistance in *Salmonella enterica* serovar Typhimurium. *PLoS One*, 6, e23471.
- SUZUKI, H., NISHIMURA, Y. & HIROTA, Y. 1978. On the process of cellular division in *Escherichia coli*: a series of mutants of *E. coli* altered in the penicillin-binding proteins. *Proc Natl Acad Sci U S A*, 75, 664-8.
- SWASTHI, H. M. & MUKHOPADHYAY, S. 2017. Electrostatic lipid-protein interactions sequester the curli amyloid fold on the lipopolysaccharide membrane surface. *Journal of Biological Chemistry*, 292, 19861-19872.
- SWORDS, W. E., CANNON, B. M. & BENJAMIN, W. H., JR. 1997. Avirulence of LT2 strains of *Salmonella typhimurium* results from a defective *rpoS* gene. *Infect Immun*, 65, 2451-3.
- SZYF, M., AVRAHAM-HAETZNI, K., REIFMAN, A., SHLOMAI, J., KAPLAN, F., OPPENHEIM, A. & RAZIN, A. 1984. DNA methylation pattern is determined by the intracellular level of the methylase. *Proceedings of the National Academy of Sciences of the United States of America*, 81, 3278-3282.
- TAGLIABUE, L., MACIAG, A., ANTONIANI, D. & LANDINI, P. 2010. The *yddV-dos* operon controls biofilm formation through the regulation of genes encoding curli fibers' subunits in aerobically growing *Escherichia coli*. *FEMS Immunology & Medical Microbiology*, 59, 477-484.
- TAM, C. C., RODRIGUES, L. C., VIVIANI, L., DODDS, J. P., EVANS, M. R., HUNTER, P. R., GRAY, J. J., LETLEY, L. H., RAIT, G., TOMPKINS, D. S. & O'BRIEN, S. J. 2012. Longitudinal study of infectious intestinal disease in the UK (IID2 study): incidence in the community and presenting to general practice. *Gut*, 61, 69-77.

- TAMAE, C., LIU, A., KIM, K., SITZ, D., HONG, J., BECKET, E., BUI, A., SOLAIMANI, P., TRAN, K. P., YANG, H. & MILLER, J. H. 2008. Determination of antibiotic hypersensitivity among 4,000 single-gene-knockout mutants of *Escherichia coli*. *J Bacteriol*, 190, 5981-8.
- TANG, F. & SAIER, M. H. 2014. Transport proteins promoting *Escherichia coli* pathogenesis. *Microbial Pathogenesis*, 71-72, 41-55.
- TEMPLIN, M. F., URSINUS, A. & HÖLTJE, J. V. 1999. A defect in cell wall recycling triggers autolysis during the stationary growth phase of *Escherichia coli*. *Embo j*, 18, 4108-17.
- TETZ, G. V., ARTEMENKO, N. K. & TETZ, V. V. 2009. Effect of DNase and Antibiotics on Biofilm Characteristics. *Antimicrobial Agents and Chemotherapy*, 53, 1204.
- THÈZE, J., MARGARITA, D., COHEN, G. N., BORNE, F. & PATTE, J. C. 1974. Mapping of the structural genes of the three aspartokinases and of the two homoserine dehydrogenases of *Escherichia coli* K-12. *J Bacteriol*, 117, 133-43.
- THOMPSON, J. F. & LANDY, A. 1988. Empirical estimation of protein-induced DNA bending angles: applications to  $\lambda$  site-specific recombination complexes. *Nucleic Acids Res*, 16, 9687-705.
- THOMSON, N. M. & PALLEEN, M. J. 2020. Restoration of wild-type motility to flagellin-knockout *Escherichia coli* by varying promoter, copy number and induction strength in plasmid-based expression of flagellin. *Current Research in Biotechnology*, 2, 45-52.
- THOMSON, N. M., ZHANG, C., TRAMPARI, E. & PALLEEN, M. J. 2020. Creation of Golden Gate constructs for gene doctoring. *BMC Biotechnology*, 20, 54.
- THONGSOMBOON, W., SERRA, D. O., POSSLING, A., HADJINEOPHYTOU, C., HENGGE, R. & CEGELSKI, L. 2018. Phosphoethanolamine cellulose: A naturally produced chemically modified cellulose. *Science*, 359, 334-338.
- TOMAR, S. K., KUMAR, P. & PRAKASH, B. 2011. Deciphering the catalytic machinery in a universally conserved ribosome binding ATPase YchF. *Biochem Biophys Res Commun*, 408, 459-64.
- TRAMONTI, A., DE CANIO, M. & DE BIASE, D. 2008. GadX/GadW-dependent regulation of the *Escherichia coli* acid fitness island: transcriptional control at the *gadY-gadW* divergent promoters and identification of four novel 42 bp GadX/GadW-specific binding sites. *Molecular Microbiology*, 70, 965-982.
- TRAMPARI, E., HOLDEN, E. R., WICKHAM, G. J., RAVI, A., PRISCHI, F., DE OLIVEIRA MARTINS, L., SAVVA, G. M., BAVRO, V. N. & WEBBER, M. A. 2019. Antibiotics select for novel pathways of resistance in biofilms. *bioRxiv*, 605212.
- TRASTOY, R., MANSO, T., FERNANDEZ-GARCIA, L., BLASCO, L., AMBROA, A., PEREZ DEL MOLINO, M. L., BOU, G., GARCIA-CONTRERAS, R., WOOD, T. K. & TOMAS, M. 2018. Mechanisms of Bacterial Tolerance and Persistence in the Gastrointestinal and Respiratory Environments. *Clin Microbiol Rev*, 31.
- TREMBLAY, L. W., DUNAWAY-MARIANO, D. & ALLEN, K. N. 2006. Structure and activity analyses of *Escherichia coli* K-12 NagD provide insight into the evolution of biochemical function in the haloalkanoic acid dehalogenase superfamily. *Biochemistry*, 45, 1183-93.
- TSANG, M. J., YAKHNINA, A. A. & BERNHARDT, T. G. 2017. NlpD links cell wall remodeling and outer membrane invagination during cytokinesis in *Escherichia coli*. *PLoS Genet*, 13, e1006888.
- TSUI, H. C., ARPS, P. J., CONNOLLY, D. M. & WINKLER, M. E. 1991a. Absence of *hisT*-mediated tRNA pseudouridylation results in a uracil requirement that interferes with *Escherichia coli* K-12 cell division. *J Bacteriol*, 173, 7395-400.
- TSUI, P., HUANG, L. & FREUNDLICH, M. 1991b. Integration host factor binds specifically to multiple sites in the *ompB* promoter of *Escherichia coli* and inhibits transcription. *Journal of bacteriology*, 173, 5800-5807.
- TUCKER, D. L., TUCKER, N., MA, Z., FOSTER, J. W., MIRANDA, R. L., COHEN, P. S. & CONWAY, T. 2003. Genes of the GadX-GadW regulon in *Escherichia coli*. *J Bacteriol*, 185, 3190-201.

- TUCKERMAN, J. R., GONZALEZ, G., SOUSA, E. H., WAN, X., SAITO, J. A., ALAM, M. & GILLES-GONZALEZ, M. A. 2009. An oxygen-sensing diguanylate cyclase and phosphodiesterase couple for c-di-GMP control. *Biochemistry*, 48, 9764-74.
- TURNER, A. K., ECKERT, S. E., TURNER, D. J., YASIR, M., WEBBER, M. A., CHARLES, I. G., PARKHILL, J. & WAIN, J. 2020a. A whole-genome screen identifies *Salmonella enterica* serovar Typhi genes involved in fluoroquinolone susceptibility. *Journal of Antimicrobial Chemotherapy*, 75, 2516-2525.
- TURNER, A. K., YASIR, M., BASTKOWSKI, S., TELATIN, A., PAGE, A. J., CHARLES, I. G. & WEBBER, M. A. 2020b. A genome-wide analysis of *Escherichia coli* responses to fosfomycin using TraDIS-*Xpress* reveals novel roles for phosphonate degradation and phosphate transport systems. *Journal of Antimicrobial Chemotherapy*, 75, 3144-3151.
- TURNER, R. J., TAYLOR, D. E. & WEINER, J. H. 1997. Expression of *Escherichia coli* TehA gives resistance to antiseptics and disinfectants similar to that conferred by multidrug resistance efflux pumps. *Antimicrobial agents and chemotherapy*, 41, 440-444.
- TYPAS, A., BANZHAF, M., VAN DEN BERG VAN SAPAROE, B., VERHEUL, J., BIBOY, J., NICHOLS, R. J., ZIETEK, M., BEILHARZ, K., KANNENBERG, K., VON RECHENBERG, M., BREUKINK, E., DEN BLAAUWEN, T., GROSS, C. A. & VOLLMER, W. 2010. Regulation of peptidoglycan synthesis by outer-membrane proteins. *Cell*, 143, 1097-109.
- VALENS, M., THIEL, A. & BOCCARD, F. 2016. The MaoP/*maoS* Site-Specific System Organizes the Ori Region of the *E. coli* Chromosome into a Macrodomain. *PLoS genetics*, 12, e1006309-e1006309.
- VAN GERVEN, N., KLEIN, R. D., HULTGREN, S. J. & REMAUT, H. 2015. Bacterial Amyloid Formation: Structural Insights into Curli Biogenesis. *Trends in Microbiology*, 23, 693-706.
- VAN VLIET, F., CRABEEL, M., BOYEN, A., TRICOT, C., STALON, V., FALMAGNE, P., NAKAMURA, Y., BAUMBERG, S. & GLANSDORFF, N. 1990. Sequences of the genes encoding argininosuccinate synthetase in *Escherichia coli* and *Saccharomyces cerevisiae*: comparison with methanogenic archaeobacteria and mammals. *Gene*, 95, 99-104.
- VESTBY, L. K., MØRETRØ, T., LANGSRUD, S., HEIR, E. & NESSE, L. L. 2009. Biofilm forming abilities of *Salmonella* are correlated with persistence in fish meal- and feed factories. *BMC Veterinary Research*, 5, 20.
- VIDAL, O., LONGIN, R., PRIGENT-COMBARET, C., DOREL, C., HOOREMAN, M. & LEJEUNE, P. 1998. Isolation of an *Escherichia coli* K-12 Mutant Strain Able To Form Biofilms on Inert Surfaces: Involvement of a New *ompR* Allele That Increases Curli Expression. *Journal of Bacteriology*, 180, 2442-2449.
- VILAIN, S., PRETORIUS, J. M., THERON, J. & BRÖZEL, V. S. 2009. DNA as an Adhesin: *Bacillus cereus* Requires Extracellular DNA To Form Biofilms. *Applied and Environmental Microbiology*, 75, 2861.
- VILLAGRA, N. A., HIDALGO, A. A., SANTIVIAGO, C. A., SAAVEDRA, C. P. & MORA, G. C. 2008. *SmvA*, and not *AcrB*, is the major efflux pump for acriflavine and related compounds in *Salmonella enterica* serovar Typhimurium. *J Antimicrob Chemother*, 62, 1273-6.
- WAINWRIGHT, M. 2001. Acridine—a neglected antibacterial chromophore. *Journal of Antimicrobial Chemotherapy*, 47, 1-13.
- WALL, E., MAJDALANI, N. & GOTTESMAN, S. 2018. The Complex Rcs Regulatory Cascade. *Annual Review of Microbiology*, 72, 111-139.
- WALL, E. A., MAJDALANI, N. & GOTTESMAN, S. 2020. IgaA negatively regulates the Rcs Phosphorelay via contact with the RcsD Phosphotransfer Protein. *PLOS Genetics*, 16, e1008610.
- WANG-KAN, X., BLAIR, J. M. A., CHIRULLO, B., BETTS, J., LA RAGIONE, R. M., IVENS, A., RICCI, V., OPPERMAN, T. J. & PIDDOCK, L. J. V. 2017. Lack of *AcrB* Efflux Function Confers Loss of Virulence on *Salmonella enterica* Serovar Typhimurium. *MBio*, 8.

- WANG, F., DENG, L., HUANG, F., WANG, Z., LU, Q. & XU, C. 2020. Flagellar Motility Is Critical for *Salmonella enterica* Serovar Typhimurium Biofilm Development. *Frontiers in Microbiology*, 11.
- WANG, J., CAO, L., YANG, X., WU, Q., LU, L. & WANG, Z. 2018. Transcriptional analysis reveals the critical role of RNA polymerase-binding transcription factor, DksA, in regulating multi-drug resistance of *Escherichia coli*. *International Journal of Antimicrobial Agents*, 52, 63-69.
- WANG, J., MA, W., FANG, Y., LIANG, H., YANG, H., WANG, Y., DONG, X., ZHAN, Y. & WANG, X. 2021. Core oligosaccharide portion of lipopolysaccharide plays important roles on multiple antibiotic resistance in *Escherichia coli*. *Antimicrobial Agents and Chemotherapy*, 0, AAC.00341-21.
- WANG, X., BISWAS, S., PAUDYAL, N., PAN, H., LI, X., FANG, W. & YUE, M. 2019. Antibiotic Resistance in *Salmonella* Typhimurium Isolates Recovered From the Food Chain Through National Antimicrobial Resistance Monitoring System Between 1996 and 2016. *Frontiers in Microbiology*, 10.
- WANG, X. & QUINN, P. J. 2010. Lipopolysaccharide: Biosynthetic pathway and structure modification. *Progress in Lipid Research*, 49, 97-107.
- WANG, Z., WANG, J., REN, G., LI, Y. & WANG, X. 2015. Influence of Core Oligosaccharide of Lipopolysaccharide to Outer Membrane Behavior of *Escherichia coli*. *Marine Drugs*, 13, 3325-3339.
- WEATHERSPOON-GRIFFIN, N., YANG, D., KONG, W., HUA, Z. & SHI, Y. 2014. The CpxR/CpxA two-component regulatory system up-regulates the multidrug resistance cascade to facilitate *Escherichia coli* resistance to a model antimicrobial peptide. *The Journal of biological chemistry*, 289, 32571-32582.
- WEBBER, M. A., BAILEY, A. M., BLAIR, J. M., MORGAN, E., STEVENS, M. P., HINTON, J. C., IVENS, A., WAIN, J. & PIDDOCK, L. J. 2009. The global consequence of disruption of the AcrAB-TolC efflux pump in *Salmonella enterica* includes reduced expression of SPI-1 and other attributes required to infect the host. *J Bacteriol*, 191, 4276-85.
- WEBBER, M. A. & PIDDOCK, L. J. 2001. Absence of mutations in *marRAB* or *soxRS* in *acrB*-overexpressing fluoroquinolone-resistant clinical and veterinary isolates of *Escherichia coli*. *Antimicrob Agents Chemother*, 45, 1550-2.
- WEBBER, M. A. & PIDDOCK, L. J. V. 2003. The importance of efflux pumps in bacterial antibiotic resistance. *Journal of Antimicrobial Chemotherapy*, 51, 9-11.
- WEBBER, M. A., TALUKDER, A. & PIDDOCK, L. J. V. 2005. Contribution of Mutation at Amino Acid 45 of AcrR to *acrB* Expression and Ciprofloxacin Resistance in Clinical and Veterinary *Escherichia coli* Isolates. *Antimicrobial Agents and Chemotherapy*, 49, 4390-4392.
- WEBER, H., PESAVENTO, C., POSSLING, A., TISCHENDORF, G. & HENGGE, R. 2006. Cyclic-di-GMP-mediated signalling within the  $\sigma$ S network of *Escherichia coli*. *Molecular Microbiology*, 62, 1014-1034.
- WEIJLAND, A., HARMARK, K., COOL, R. H., ANBORGH, P. H. & PARMEGGIANI, A. 1992. Elongation factor Tu: a molecular switch in protein biosynthesis. *Mol Microbiol*, 6, 683-8.
- WEINER, J. H., SHAW, G., TURNER, R. J. & TRIEBER, C. A. 1993. The topology of the anchor subunit of dimethyl sulfoxide reductase of *Escherichia coli*. *J Biol Chem*, 268, 3238-44.
- WERNER, J., AUGUSTUS ANNE, M. & MISRA, R. 2003. Assembly of TolC, a Structurally Unique and Multifunctional Outer Membrane Protein of *Escherichia coli* K-12. *Journal of Bacteriology*, 185, 6540-6547.
- WHITCHURCH, C. B., TOLKER-NIELSEN, T., RAGAS, P. C. & MATTICK, J. S. 2002. Extracellular DNA required for bacterial biofilm formation. *Science*, 295, 1487.
- WHITNEY, J. C. & HOWELL, P. L. 2013. Synthase-dependent exopolysaccharide secretion in Gram-negative bacteria. *Trends in Microbiology*, 21, 63-72.
- WHO 2015. *WHO estimates of the global burden of foodborne diseases: foodborne disease burden epidemiology reference group 2007-2015*, World Health Organization.

- WINSTON, F., BOTSTEIN, D. & MILLER, J. H. 1979. Characterization of amber and ochre suppressors in *Salmonella typhimurium*. *Journal of Bacteriology*, 137, 433-439.
- WIRTH, T., FALUSH, D., LAN, R., COLLES, F., MENSA, P., WIELER, L. H., KARCH, H., REEVES, P. R., MAIDEN, M. C. J., OCHMAN, H. & ACHTMAN, M. 2006. Sex and virulence in *Escherichia coli*: an evolutionary perspective. *Molecular microbiology*, 60, 1136-1151.
- WONG, Y.-C., ABD EL GHANY, M., NAEEM, R., LEE, K.-W., TAN, Y.-C., PAIN, A. & NATHAN, S. 2016. Candidate Essential Genes in *Burkholderia cenocepacia* J2315 Identified by Genome-Wide TraDIS. *Frontiers in microbiology*, 7, 1288-1288.
- WOOD, T. K., GONZÁLEZ BARRIOS, A. F., HERZBERG, M. & LEE, J. 2006. Motility influences biofilm architecture in *Escherichia coli*. *Applied Microbiology and Biotechnology*, 72, 361-367.
- WU, X., HOU, J., CHEN, X., CHEN, X. & ZHAO, W. 2016. Identification and functional analysis of the L-ascorbate-specific enzyme II complex of the phosphotransferase system in *Streptococcus mutans*. *BMC Microbiology*, 16, 51.
- WUCHER, B. R., BARTLETT, T. M., HOYOS, M., PAPERFORT, K., PERSAT, A. & NADELL, C. D. 2019. *Vibrio cholerae* filamentation promotes chitin surface attachment at the expense of competition in biofilms. *Proceedings of the National Academy of Sciences*, 116, 14216-14221.
- XU, K. D., FRANKLIN, M. J., PARK, C. H., MCFETERS, G. A. & STEWART, P. S. 2001. Gene expression and protein levels of the stationary phase sigma factor, RpoS, in continuously-fed *Pseudomonas aeruginosa* biofilms. *FEMS Microbiol Lett*, 199, 67-71.
- XU, X. & HENSEL, M. 2010. Systematic analysis of the SsrAB virulon of *Salmonella enterica*. *Infect Immun*, 78, 49-58.
- YAMADA, H., MURAMATSU, S. & MIZUNO, T. 1990. An *Escherichia coli* protein that preferentially binds to sharply curved DNA. *J Biochem*, 108, 420-5.
- YAMAGUCHI, Y. & INOUE, M. 2015. An endogenous protein inhibitor, YjxX (TopAI), for topoisomerase I from *Escherichia coli*. *Nucleic Acids Res*, 43, 10387-96.
- YAMASAKI, S., NAKASHIMA, R., SAKURAI, K., BAUCHERON, S., GIRAUD, E., DOUBLET, B., CLOECKAERT, A. & NISHINO, K. 2019. Crystal structure of the multidrug resistance regulator RamR complexed with bile acids. *Scientific Reports*, 9, 177.
- YANG, X., WANG, J., FENG, Z., ZHANG, X., WANG, X. & WU, Q. 2019. Relation of the *pdxB-usb-truA-dedA* Operon and the *truA* Gene to the Intracellular Survival of *Salmonella enterica* Serovar Typhimurium. *International Journal of Molecular Sciences*, 20, 380.
- YARRANTON, G. T. & GEFTER, M. L. 1979. Enzyme-catalyzed DNA unwinding: studies on *Escherichia coli* rep protein. *Proc Natl Acad Sci U S A*, 76, 1658-62.
- YASIR, M., TURNER, A. K., BASTKOWSKI, S., BAKER, D., PAGE, A. J., TELATIN, A., PHAN, M. D., MONAHAN, L., SAVVA, G. M., DARLING, A., WEBBER, M. A. & CHARLES, I. G. 2020. TraDIS-Xpress: a high-resolution whole-genome assay identifies novel mechanisms of triclosan action and resistance. *Genome Res*.
- YASUZAWA, K., HAYASHI, N., GOSHIMA, N., KOHNO, K., IMAMOTO, F. & KANO, Y. 1992. Histone-like proteins are required for cell growth and constraint of supercoils in DNA. *Gene*, 122, 9-15.
- YEOM, J., GAO, X. & GROISMAN, E. A. 2018. Reduction in adaptor amounts establishes degradation hierarchy among protease substrates. *Proceedings of the National Academy of Sciences*, 115, E4483-E4492.
- YEW, W. S. & GERLT, J. A. 2002. Utilization of L-ascorbate by *Escherichia coli* K-12: assignments of functions to products of the *yjf-sga* and *yia-sgb* operons. *Journal of bacteriology*, 184, 302-306.
- YOSHIDA, H., MAKI, Y., FURUIKE, S., SAKAI, A., UETA, M. & WADA, A. 2012. YqjD is an inner membrane protein associated with stationary-phase ribosomes in *Escherichia coli*. *Journal of bacteriology*, 194, 4178-4183.
- ZAWADZKE, L. E., BUGG, T. D. & WALSH, C. T. 1991. Existence of two D-alanine:D-alanine ligases in *Escherichia coli*: cloning and sequencing of the *ddlA* gene and



- purification and characterization of the DdIA and DdIB enzymes. *Biochemistry*, 30, 1673-82.
- ZHANG, A., ROSNER, J. L. & MARTIN, R. G. 2008a. Transcriptional activation by MarA, SoxS and Rob of two *tolC* promoters using one binding site: a complex promoter configuration for *tolC* in *Escherichia coli*. *Molecular microbiology*, 69, 1450-1455.
- ZHANG, Y., MORAR, M. & EALICK, S. E. 2008b. Structural biology of the purine biosynthetic pathway. *Cellular and Molecular Life Sciences*, 65, 3699-3724.
- ZHENG, J., TIAN, F., CUI, S., SONG, J., ZHAO, S., BROWN, E. W. & MENG, J. 2011. Differential Gene Expression by RamA in Ciprofloxacin-Resistant *Salmonella* Typhimurium. *PLOS ONE*, 6, e22161.
- ZOGAJ, X., NIMTZ, M., ROHDE, M., BOKRANZ, W. & RÖMLING, U. 2001. The multicellular morphotypes of *Salmonella typhimurium* and *Escherichia coli* produce cellulose as the second component of the extracellular matrix. *Molecular Microbiology*, 39, 1452-1463.
- ZORRAQUINO, V., GARCÍA, B., LATASA, C., ECHEVERZ, M., TOLEDO-ARANA, A., VALLE, J., LASA, I. & SOLANO, C. 2013. Coordinated Cyclic-Di-GMP Repression of *Salmonella* Motility through YcgR and Cellulose. *Journal of Bacteriology*, 195, 417-428.
- ZORRAQUINO, V., KIM, M., RAI, N. & TAGKOPOULOS, I. 2017. The Genetic and Transcriptional Basis of Short and Long Term Adaptation across Multiple Stresses in *Escherichia coli*. *Molecular Biology and Evolution*, 34, 707-717.

## 10. APPENDICES

### 10.1. APPENDIX 1: Genes determined by TraDIS-*Xpress* to be important for biofilm formation in *E. coli* and *S. Typhimurium* (STM), and the phenotypes of deletion mutants relative to the wild type.

Bacteria	Pathway	Gene	Time point	Difference in insertions in biofilm condition relative to planktonic condition		Significantly different phenotype from wild type?					Ref
				Log fold change *	Observed change	Biomass	Aggregation	Curli production	Adhesion	Biofilm architecture	
Both <i>E. coli</i> and STM	Curli biosyntheses	<i>csgD</i>	12h (STM) 24h ( <i>E. coli</i> ), 48h (Both)	-1.4 ( <i>E. coli</i> )	Increased expression beneficial at 12h and 48h in STM, Increased expression beneficial at 24h in <i>E. coli</i> , Fewer insertions at 48h in <i>E. coli</i>	Reduced (in <i>E. coli</i> )	Reduced (in <i>E. coli</i> )	Reduced (in <i>E. coli</i> )			(Barnhart and Chapman, 2006)

	Protein modification	<i>dsbA</i>	12h (Both) 24h ( <i>E. coli</i> )	-0.7 ( <i>E. coli</i> ) 1.8 (STM) -3.0 ( <i>E. coli</i> )	Fewer insertions in <i>E. coli</i> , More insertions in STM	No change (Both)	Increased (in <i>E. coli</i> )	Increased (Both)			(Bardwell, 1994)
	Transmembrane transport	<i>tolC</i>	48h	-2.9 ( <i>E. coli</i> ) -0.7 (STM)	Fewer insertions in both	No change (in <i>E. coli</i> ) Reduced (in STM)	Reduced (in <i>E. coli</i> )	No change (in <i>E. coli</i> ) Reduced (in STM)			(Morona et al., 1983)
<i>E. coli</i>	Cell division	<i>zapE</i>	48h	-3.4	Fewer insertions	No change	Increased	No change	Reduced	No change	(Marteyn et al., 2014)
	c-di-GMP metabolism	<i>rcdA</i>	48h	-0.8	Fewer insertions	Reduced		Reduced			(Pfiffer et al., 2019)
		<i>pdeF</i>	48h	-0.3	Fewer insertions						(Lacey et al., 2010)
		<i>csgC</i>	24h, 48h	-1.6 -0.6	Fewer insertions						(Barnhart and

Curli biosynthesi s	<i>csgE</i>	12h, 48h	-2.5 -1.6	Fewer insertions	Reduced		Reduced				Chapman, 2006)
	<i>csgF</i>	48h	-4.8	Fewer insertions							
DNA housekeepi ng	<i>dam</i>	24h	-3.9	Fewer insertions	No change	Reduced	No change				(Szyf et al., 1984)
	<i>maoP</i>	24h	1.6	More insertions	Reduced	Reduced	Reduced	Reduced	Reduced density and biomass		(Valens et al., 2016)
Flagella-associated motility	<i>flhD</i>	24h, 48h	-3.9 -2.6	Increased expression beneficial	No change	No change	No change				(Fitzgerald et al., 2014)
	<i>flhC</i>	48h	-4.1	Fewer insertions	No change	Reduced	No change				
	<i>flgD</i>	24h	-3.0	Fewer insertions	No change	No change	No change				(Macnab, 1992)
	<i>fliE</i>	48h	-4.7	Fewer insertions	No change	Reduced	No change				
	<i>hdfR</i>	12h, 24h	3.8 2.4	More insertions	Reduced	No change	Reduced				(Ko and Park, 2000)

		<i>lrhA</i>	12h, 24h, 48h	2.0 3.2 2.3	More insertions	No change	Reduced	No change	Increased	Early microcolony formation, reduced in the mature biofilm	(Lehnen et al., 2002)
	LPS	<i>wzzB</i>	48h	-1.4	Fewer insertions	Reduced		No change			(Stenberg et al., 2005)
	Oxidised protein repair	<i>msrQ</i>	48h	-0.4	Fewer insertions	No change		No change			(Gennaris et al., 2015)
	Purine ribonucleotide biosynthesis	<i>purD</i>	48h	-4.3	Fewer insertions	Reduced	No change	Reduced	No change	Reduced microcolony formation	(Zhang et al., 2008b)
		<i>purE</i>	48h	-5.7	Fewer insertions	Reduced	Increased	Reduced			
		<i>purH</i>	48h	-3.2	Fewer insertions						
		<i>purL</i>	48h	-3.1	Fewer insertions						

	rRNA methyltransferase	<i>rlmI</i>	12h	-3.8	Fewer insertions	Reduced	No change	No change			(Herzberg et al., 2006)
	RNase III regulator	<i>ymdB</i>	24h, 48h	-0.5 -2.5	Fewer insertions	Reduced	Increased	No change			(Kim et al., 2013)
	Sugar metabolism and transport	<i>sgbE</i>	48h	-2.5	Fewer insertions	No change		No change			(Yew and Gerlt, 2002)
	Toxin-antitoxin system	<i>tomB</i>	12h, 24h, 48h	-0.5 -0.4 -1.6	Fewer insertions	Reduced	Reduced	Reduced	Increased	Early microcolony formation, reduced in the mature biofilm	(Garcia-Contreras et al., 2008)
	Transcriptional regulators and signalling systems	<i>dksA</i>	12h, 24h	4.4 2.9	More insertions	Reduced	Reduced	Reduced	Increased	Reduced microcolony formation	(Girard et al., 2018, Lemke et al., 2009, Mallik et al., 2006)

		<i>leuO</i>	12h, 48h	-0.6	Increased expression beneficial at 12h, Fewer insertions at 48h	Reduced	Reduced	No change	No change	Reduced microcolony formation	(Dillon et al., 2012)
		<i>marR</i>	12h	-4.1	Fewer insertions	Reduced	No change	No change			(Alekhshun and Levy, 1999a)
		<i>ompR</i>	24h, 48h	-0.8 -4.7	Fewer insertions	Reduced	Reduced	Reduced			(Cai and Inouye, 2002)
		<i>lrp</i>	48h	-5.9	Fewer insertions	Reduced	Reduced	Reduced			(Calvo and Matthews, 1994)
		<i>gadW</i>	48h	-1.1	Fewer insertions	No change	No change	No change			(Tucker et al., 2003)
		<i>rscC</i>	48h	-2.9	Fewer insertions	Reduced		No change			(Ferrières and Clarke, 2003)

	Transmembrane transport, porins and channels	<i>mscL</i>	48h	-0.9	Fewer insertions						(Sukharev et al., 1994)
		<i>ompF</i>	48h	-2.7	Fewer insertions	Reduced		No change			(Cai and Inouye, 2002)
		<i>fadL</i>	48h	-1.5	Fewer insertions						(Nunn and Simons, 1978)
	tRNA modification	<i>truA</i>	24h, 48h	-3.3 -5.9	Fewer insertions	No change	Increased	No change	No change	Increased filamentation after 24- and 48-hours growth	(Hamma and Ferré-D'Amaré, 2006)
Type 1 fimbriae	<i>fimB</i>	12h, 24, 48h	-0.4 -1.3 -2.1	Fewer insertions and increased expression beneficial at all time points	No change	Reduced	No change			(Klemm, 1986)	



		<i>fimE</i>	12h, 24, 48h	1.5 3.3 2.6	More insertions	Reduced	Reduced	No change			
		<i>fimC</i>	48h	-1.3	Fewer insertions						(Allen et al., 2012)
		<i>fimD</i>	24h, 48h	-2.3 -2.1	Fewer insertions						
	Putative fimbrial-like protein	<i>ydeR</i>	48h	-2.4	Fewer insertions						(Da Re et al., 2013)
	Unknown	<i>yigZ</i>	12h	-2.8	Fewer insertions	No change	Increased	No change	No change	No change	(Park et al., 2004)
		<i>yebB</i>	48h	-2.3	Fewer insertions						(Schurr et al., 1993, Alper and Stephanopoulos, 2008)
		<i>yedN</i>	48h	-1.7	Fewer insertions						(Goodall et al., 2018)
		<i>yjbL</i>	48h	-2.8	Fewer insertions	Reduced		No change			(Herzberg et al., 2006)

		<i>ykgJ</i>	12h		Reduced expression beneficial (increased expression of antisense mRNA beneficial)	No change	Increased	No change	No change	Increased filamentation after 24- and 48-hours growth	(Kacharia et al., 2017)
STM	Adhesin	<i>sadA</i>	12h		Increased expression beneficial						(Raghunathan et al., 2011)
	Amino acid synthesis	<i>ilvH</i>	12h	-2.5	Fewer insertions						(Squires et al., 1981)
		<i>hisC</i>	12h	-1.6	Fewer insertions						(Schembri et al., 2003)
	Biofilm matrix component	<i>bapA</i>	48h		Increased expression beneficial						(Latasa et al., 2005)
	Polysaccharide	<i>gcpA</i>	12h		Increased expression beneficial						(Garcia et al., 2004)

	biosynthesi s	<i>gcpG</i>	12h		Increased expression beneficial						
		<i>manA</i>	48h	-2.4	Fewer insertions						(Kwan et al., 2018, Li et al., 2017)
	Secondary messenger molecular metabolism	<i>cyaA</i>	24h		Increased expression beneficial	Reduced		Reduced			(Roy and Danchin, 1982)
	Curli biosynthesi s	<i>csgB</i>	48h		Increased expression beneficial						(Barnhart and Chapman, 2006)
	Ethanolami ne utilisation	<i>eutQ</i>	12h, 24h, 48h		Reduced expression beneficial (increased expression of antisense mRNA beneficial)						(Moore and Escalante- Semerena, 2016)

	Fimbriae	<i>fimY</i>	12h, 48h		Increased expression beneficial						(Saini et al., 2009)	
		<i>fimW</i>	48h	1.8	More insertions							
		<i>fimZ</i>	48h		Increased expression beneficial							
		<i>fimA</i>	12h, 48h		Increased expression beneficial						(Allen et al., 2012)	
	Flagella-associated motility	<i>flgA</i>	48h	-1.8	Fewer insertions							(Macnab, 1992)
		<i>flgB</i>	24h	-9.8	Fewer insertions							
		<i>flgF</i>	48h	-0.9	Fewer insertions							
		<i>flgN</i>	48h	-1.8	Fewer insertions							
	Iron acquisition	<i>ybaN</i>	12h	-8.6	Fewer insertions							(Seo et al., 2014)

	LPS	<i>rfaJ</i>	12h, 24h, 48h		Increased expression beneficial						(Wang et al., 2015)
		<i>rfaP</i>	24h, 48h	-1.0	Increased expression beneficial at 24h, Fewer insertions at 48h						
		<i>rfaG</i>	24h, 48h	2.2 2.2	More insertions						
		<i>rfaL</i>	48h	0.8	More insertions						
		<i>rfaJ</i>	24h	2.5	More insertions						
	Outer membrane integrity	<i>yciB</i>	48h	-4.3	Fewer insertions						(Niba et al., 2008)

	Prosthetic group biosyntheses	<i>citG</i>	12h	-2.3	Fewer insertions						(Hynes and Murray, 2010)
	Protease	<i>clpS</i>	24h	-3.6	Fewer insertions						(Yeom et al., 2018)
	Purine ribonucleotide metabolism	<i>purK</i>	24h		Increased expression beneficial						(Zhang et al., 2008b)
		<i>nagD</i>	48h	-3.6	Fewer insertions						(Tremblay et al., 2006)
	Quorum sensing	<i>STM14_2049/cat</i>	48h		Increased expression beneficial						(Liao et al., 2019)
	Respiration	<i>nuoB</i>	24h, 48h	-1.0 -5.8	Fewer insertions	Reduced		Reduced	Reduced	Reduced density and biomass	(Archer and Elliott, 1995)
		<i>nuoC</i>	24h, 48h	-2.6 -0.8	Fewer insertions						

		<i>nuoF</i>	48h	-4.4	Fewer insertions						
		<i>nuoG</i>	24h, 48h	-0.8 -2.0	Fewer insertions						
		<i>nuoH</i>	48h	-9.6	Fewer insertions						
		<i>nuoI</i>	48h	-8.8	Fewer insertions						
		<i>nuoJ</i>	24h, 48h	-2.5 -1.9	Fewer insertions						
		<i>nuoK</i>	24h, 48h	-9.0 -1.9	Fewer insertions						
		<i>nuoL</i>	24h, 48h	-1.0 -1.1	Fewer insertions						
		<i>nuoM</i>	24h, 48h	-1.8 -2.8	Fewer insertions						
		<i>menH.</i>	24h	-2.2	Fewer insertions						(Meganathan and Kwon, 2009)

		<i>fumA</i>	48h		Increased expression beneficial						(Guest and Roberts, 1983)
		<i>pdhR</i>	48h	-2.7	Fewer insertions						(Ogasawara et al., 2007)
		<i>cra</i>	48h	-7.2	Fewer insertions						(Saier and Ramseier, 1996)
		<i>ygiN</i>	24h	-2.1	Fewer insertions						(Adams and Jia, 2005)
	Sugar import & degradation	<i>ulaC</i>	48h	-3.1	Fewer insertions						(Wu et al., 2016)
	Transcription factors	<i>rpoS</i>	24h	2.4	More insertions						(Gentry et al., 1993)
		<i>ramA</i>	24h	-4.0	Fewer insertions						(George et al., 1995)
		<i>ramR.</i>	48h	-3.7	Fewer insertions						(Abouzeed et al., 2008)



		<i>rcsB</i>	24h		Increased expression beneficial						(Majdalani and Gottesman, 2005)
		<i>ybeF</i>	24h		Increased expression beneficial						
		<i>yfaX</i>	12h	-1.4	Fewer insertions						
		<i>STM14_1074</i>	12h	-5.6	Fewer insertions	No change		No change	Reduced	Mature biofilm unchanged from wild type	(Qin et al., 2016)
	Transmembrane transport, porins and channels	<i>araJ</i>	12h	-2.0	Fewer insertions						(Reeder and Schleif, 1991)
		<i>cysW</i>	48h	-2.2	Fewer insertions						(Sirko et al., 1995)
		<i>corC</i>	24h	-2.3	Fewer insertions						(Gibson et al., 1991)

		<i>ydeD</i>	24h		Increased expression beneficial						(Dassler et al., 2000)
	Translation	<i>rimO</i>	48h		Increased expression beneficial						(Anton et al., 2008)
		<i>tyrT</i>	24h		Increased expression beneficial	No change		Increased expression increased curli biosynthesis	No change	Mature biofilm unchanged from wild type	(Winston et al., 1979)
	Type 4 pili	<i>ppdC</i>	48h	-2.2	Fewer insertions						(Cisneros et al., 2012)
	Unknown	<i>orfB</i>	12h	-1.7	Fewer insertions						
		<i>ycgL</i>	48h	-2.2	Fewer insertions						
		<i>ygbA</i>	48h	-2.1	Fewer insertions						

		<i>yjiG</i>	12h	-6.2	Fewer insertions	No change		Reduced	Reduced	Mature biofilm unchanged from wild type	(Tang and Saier, 2014)
		<i>STM1_4_049_8</i>	12h	-7.9	Fewer insertions						
		<i>STM1_4_063_4</i>	12h		Increased expression beneficial						
		<i>STM1_4_065_3</i>	48h	-2.5	Fewer insertions						
		<i>STM1_4_115_7</i>	12h		Increased expression beneficial						
		<i>STM1_4_115_8</i>	12h		Increased expression beneficial						

		STM1 4_144 0	12h		Increased expression beneficial						
		STM1 4_144 5	12h		Increased expression beneficial						
		STM1 4_176 4	12h	-10.0	Fewer insertions						
		STM1 4_285 6	48h	-0.8	Fewer insertions						
		STM1 4_320 8	12h		Increased expression beneficial						
		STM1 4_386 0	48h		Increased expression beneficial						
		STM1 4_533 2	48h	-3.9	Fewer insertions						

\* Log fold change is only shown for genes where there are differences in insertion frequency inside the coding region. Where the plot files generated by BioTraDIS show a difference in insertion frequency between the biofilm and planktonic conditions upstream or downstream of a gene, log fold change cannot easily be quantified and therefore the effect has been described in the column titled 'observed change'. Significant differences in insertion frequencies have been manually verified with the plot files generated by BioTraDIS.

**10.2. APPENDIX 2: Genes determined by TraDIS-Xpress to be important for efflux activity and acriflavine susceptibility in *E. coli* and *S. Typhimurium* (STM), and the phenotypes of deletion mutants relative to the wild type.**

Bacteria	Pathway	Gene	Difference in insertions			Significantly different phenotype from wild type?			Ref
			Condition	Log fold change *	Observed change	Dye accumulation	Drug susceptibility		
								Unstressed	With PAβN
Both <i>E. coli</i> and STM	Enterobacterial common antigen	<i>wecF</i>	subMIC vs ctrl	5.9 ( <i>E. coli</i> ) 0.3 (STM)	More insertions	Reduced ( <i>E. coli</i> )	Reduced ( <i>E. coli</i> )	No change ( <i>E. coli</i> )	(Meier-Dieter et al., 1990)
	Purine biosynthesis	<i>rbsR</i>	subMIC vs ctrl	-1.7 (STM)	Fewer insertions	Reduced ( <i>E. coli</i> )	Reduced ( <i>E. coli</i> )	No change ( <i>E. coli</i> )	(Lopilato et al., 1984)
			subMIC vs subMIC+PAβN	-1.4 ( <i>E. coli</i> only)	Fewer insertions				
	Membrane signalling systems	<i>opgG</i>	PAβN vs ctrl	2.9 ( <i>E. coli</i> only)	More insertions	No change ( <i>E. coli</i> )	No change ( <i>E. coli</i> )	No change ( <i>E. coli</i> )	(Bontemps-Gallo et al., 2017)

			subMIC vs subMIC+PAβN	-1.2 (STM only)	Fewer insertions				
		<i>opgH</i>	PAβN vs ctrl	1.5 ( <i>E. coli</i> only)	More insertions	No change ( <i>E. coli</i> )	No change ( <i>E. coli</i> )	No change ( <i>E. coli</i> )	
			subMIC vs subMIC+PAβN	-1.5 (STM only)	Fewer insertions				
Transmembrane transport systems	<i>acrR</i>		subMIC vs ctrl	12.1 ( <i>E. coli</i> ) 0.4 (STM)	More insertions	No change ( <i>E. coli</i> )	Reduced ( <i>E. coli</i> )	Increased susceptibility to acriflavine ( <i>E. coli</i> )	(Ma et al., 1995)
			subMIC vs subMIC+PAβN	10.1 ( <i>E. coli</i> only)	More insertions				
			MIC vs ctrl	-1.4 ( <i>E. coli</i> only)	Fewer insertions				
	<i>acrA</i>		PAβN vs ctrl	-3.3 ( <i>E. coli</i> ) -3.7 (STM)	Fewer insertions	Increased ( <i>E. coli</i> )	Reduced ( <i>E. coli</i> )	Increased susceptibility to acriflavine and cefotaxime ( <i>E. coli</i> )	
			subMIC vs ctrl	-2.2 (STM)	Fewer insertions				
		<i>acrB</i>		PAβN vs ctrl	-2.4 ( <i>E. coli</i> ) -3.4 (STM)	Fewer insertions	Increased ( <i>E. coli</i> )	Reduced ( <i>E. coli</i> )	

			subMIC vs ctrl	-2.7 (STM)	Fewer insertions			to acriflavine ( <i>E. coli</i> )	
		<i>tolC</i>	PAβN vs ctrl	-3.2 ( <i>E. coli</i> ) -1.9 (STM)	Fewer insertions	No change ( <i>E. coli</i> ) Increased (STM)	No change ( <i>E. coli</i> ) Reduced (STM)	Increased susceptibility to acriflavine, azithromycin and cefotaxime (STM)	(Morona et al., 1983)
	Amino acid biosynthesis	<i>metL</i>	MIC vs ctrl	2.5 ( <i>E. coli</i> only)	More insertions	Reduced ( <i>E. coli</i> )	Reduced ( <i>E. coli</i> )	No change ( <i>E. coli</i> )	(Thèze et al., 1974)
			PAβN vs ctrl	0.7 (STM only)	More insertions				
	DNA housekeeping	<i>dam</i>	subMIC vs ctrl	-1.4 ( <i>E. coli</i> ) -2.2 (STM)	Fewer insertions	No change ( <i>E. coli</i> )	No change ( <i>E. coli</i> )	Increased susceptibility to acriflavine ( <i>E. coli</i> )	(Szyf et al., 1984)
			subMIC vs subMIC+PAβN	-3.8 ( <i>E. coli</i> only)	Fewer insertions				
<i>E. coli</i>	Cell envelope biosynthesis	<i>mrcA</i>	PAβN vs ctrl	-2.9	Fewer insertions	No change	Reduced	No change	(Suzuki et al., 1978)



		<i>lpoA</i>	PAβN vs ctrl	-3.8	Fewer insertions	No change	Reduced	Increased susceptibility to acriflavine	(Typas et al., 2010)
		<i>ddlB</i>	MIC vs ctrl	6.6	More insertions				(Zawadzke et al., 1991)
Sugar utilisation and respiration	<i>dgoD</i>	subMIC vs ctrl	-0.3	Fewer insertions	Increased	No change	No change		(Deacon and Cooper, 1977)
		subMIC vs subMIC+PAβN	-1.3	Fewer insertions					
	<i>prpB</i>	MIC vs ctrl	-3.9	Fewer insertions	Reduced	No change	No change		(Brock et al., 2001)
		MIC vs MIC+PAβN	-2.1	Fewer insertions					
	<i>adhP</i>	subMIC vs ctrl	-2.5	Fewer insertions	Reduced	No change	No change		(Shafqat et al., 1999)
		subMIC vs subMIC+PAβN	-2.8	Fewer insertions					
	<i>mhpF</i>	subMIC vs ctrl	-4.2	Fewer insertions	No change	Reduced	No change		(Lee et al., 2006)

		<i>glk</i>	MIC vs MIC+PAβN	5.1	More insertions	No change	Reduced	No change	(Hernandez-Montalvo et al., 2003)
Transcription factors and regulators	<i>dksA</i>	PAβN vs ctrl	-3.9	Fewer insertions	No change	Reduced	Increased susceptibility to acriflavine	(Girard et al., 2018, Lemke et al., 2009, Mallik et al., 2006)	
		subMIC vs ctrl	-4.2	Fewer insertions					
	<i>marA</i>	PAβN vs ctrl		Increased expression beneficial	No change	Reduced	Increased susceptibility to acriflavine	(Cohen et al., 1993)	
		subMIC vs ctrl	-2.1	Increased expression beneficial and fewer insertions					
	<i>marR</i>	PAβN vs ctrl	1.0	More insertions	No change	No change	Reduced susceptibility to cefotaxime		
		subMIC vs ctrl	10.0	More insertions					

			subMIC vs subMIC+PAβN	10.6	More insertions				
			MIC vs ctrl	-3.9	Fewer insertions				
			MIC vs MIC+ PAβN	-4.6	Fewer insertions				
		<i>soxS</i>	subMIC vs ctrl	-2.8	Increased expression beneficial and fewer insertions	No change	Reduced	Increased susceptibility to acriflavine	(Demple, 1996)
			MIC vs ctrl		Reduced expression beneficial (increased expression of antisense mRNA beneficial)				
		<i>soxR</i>	subMIC vs ctrl	10.5	More insertions	No change	No change	No change	

			subMIC vs subMIC+PAβN	11.1	More insertions				
			MIC vs ctrl	-1.0	Fewer insertions				
		<i>ompR</i>	subMIC vs ctrl	6.9	More insertions	Reduced	No change	Reduced susceptibility to cefotaxime	(Cai and Inouye, 2002)
			subMIC vs subMIC+PAβN	2.8	More insertions				
		<i>gadW</i>	PAβN vs ctrl	0.8	More insertions	No change	No change	No change	(Tucker et al., 2003)
		<i>gadY</i>	subMIC vs subMIC+PAβN	3.2	More insertions				(Tramonti et al., 2008)
	Transmembrane transport systems	<i>ompC</i>	PAβN vs ctrl	2.4	More insertions	No change	No change	No change	(Cai and Inouye, 2002)
		<i>gltS</i>	subMIC vs ctrl	-1.6	Fewer insertions	No change	No change	No change	(Kalman et al., 1991)
			subMIC vs subMIC+PAβN	-1.8	Fewer insertions				
		<i>gltJ</i>	subMIC vs ctrl	-3.8	Fewer insertions	No change	Reduced	No change	(Moussatova et al., 2008)

		<i>potA</i>	subMIC vs ctrl	-4.2	Fewer insertions	No change	No change	No change	
		<i>proW</i>	MIC vs ctrl		Increased expression beneficial	No change	No change	No change	
		<i>xyIH</i>	subMIC vs subMIC+PA $\beta$ N		Increased expression beneficial in subMIC+PA $\beta$ N vs subMIC				
		<i>osmF</i>	subMIC vs ctrl	-3.4	Fewer insertions	No change	Reduced	No change	(Lang et al., 2015)
			subMIC vs subMIC+PA $\beta$ N	-5.7	Fewer insertions				
		<i>satP</i>	subMIC vs ctrl	-2.5	Fewer insertions	Reduced	No change	No change	(Sá-Pessoa et al., 2013)
		<i>glpF</i>	MIC vs ctrl	4.6	More insertions	Reduced	No change	No change	(Braun et al., 2000)

	Protein folding and repair	<i>skp</i>	PAβN vs ctrl	4.1	More insertions	Increased	Reduced	Increased susceptibility to acriflavine and azithromycin	(Chen and Henning, 1996)
		<i>surA</i>	subMIC vs ctrl	6.5	More insertions	Reduced	No change	Increased susceptibility to acriflavine	(Lazar and Kolter, 1996)
	Fimbriae	<i>fimB</i>	PAβN vs ctrl	0.8	More insertions	No change	Reduced	No change	(Klemm, 1986)
			MIC vs MIC+PAβN	0.6	More insertions				
		<i>fimE</i>	PAβN vs ctrl		More insertions	No change	Reduced	No change	
			subMIC vs ctrl	-2.2	Fewer insertions				
			MIC vs ctrl	-1.0	Fewer insertions				
		<i>fimC</i>	MIC vs ctrl	1.0	More insertions				

		<i>fimD</i>	MIC vs ctrl	1.4	More insertions				
LPS	<i>wzzB</i>	subMIC vs ctrl	-4.3	Fewer insertions	Reduced	Reduced	No change	(Franco et al., 1996)	
		subMIC vs subMIC+PA $\beta$ N	-7.2	Fewer insertions					
	<i>waaP</i>	PA $\beta$ N vs ctrl	2.0	More insertions	No change	No change	Increased susceptibility to azithromycin, reduced susceptibility to cefotaxime		(Wang et al., 2015)
	<i>waaG</i>	MIC vs ctrl	2.3	More insertions	Increased	No change	Increased susceptibility to azithromycin, reduced susceptibility to cefotaxime		
	<i>waaF</i>	subMIC vs subMIC+PA $\beta$ N	-4.0	Fewer insertions	No change	No change	Increased susceptibility		

								to azithromycin	
		<i>lpxD</i>	PAβN vs ctrl		Increased expression beneficial				(Ma et al., 2020)
Motility	<i>lrhA</i>	PAβN vs ctrl	-3.0	Fewer insertions	No change	No change	No change	(Lehnen et al., 2002)	
		subMIC vs ctrl	-3.2	Fewer insertions					
	<i>hdfR</i>	PAβN vs ctrl	-6.5	Fewer insertions	No change	No change	No change		
		subMIC vs ctrl	-3.5	Fewer insertions					
Amino acid biosynthesis	<i>leuL</i>	subMIC vs ctrl	-0.1	Fewer insertions	No change	No change	No change	(Gemmill et al., 1983)	
Glutathione metabolism	<i>gshB</i>	PAβN vs ctrl	1.9	More insertions				(Fuchs and Warner, 1975)	
	<i>pxpB</i>	subMIC vs ctrl	-4.3	Fewer insertions	No change	Reduced	No change	(Niehaus et al., 2017)	
		subMIC vs subMIC+PAβN	-2.6	Fewer insertions					



	DNA Housekeeping	<i>maoP</i>	PAβN vs ctrl	-5.4	Fewer insertions	Increased	Reduced	No change	(Valens et al., 2016)
		<i>rep</i>	PAβN vs ctrl	2.4	More insertions				(Yarranton and Gefter, 1979)
		<i>ybiB</i>	PAβN vs ctrl	-1.4	Fewer insertions	No change	No change	No change	(Schneider et al., 2015)
		<i>yjhQ</i>	subMIC vs subMIC+PAβN	4.6	More insertions	No change	Reduced	No change	(Yamaguchi and Inouye, 2015)
		<i>tehB</i>	MIC vs MIC+PAβN	2.0	More insertions	No change	No change	Increased susceptibility to acriflavine	(Turner et al., 1997)
	Secondary messenger molecule metabolism	<i>pdeC</i>	MIC vs ctrl	1.2	More insertions	No change	Reduced	No change	(Hengge et al., 2015)
	Translation	<i>ychF</i>	subMIC vs ctrl	-2.4	Fewer insertions	Increased	No change	No change	(Tomar et al., 2011)
			subMIC vs subMIC+PAβN	-4.1	Fewer insertions				

		<i>rimK</i>	subMIC vs ctrl	-3.7	Fewer insertions	No change	No change	No change	(Kang et al., 1989)
		<i>ygaM</i>	subMIC vs ctrl	-3.6	Fewer insertions	No change	No change	No change	(Yoshida et al., 2012)
		<i>trhP</i>	subMIC vs ctrl	-2.1	Fewer insertions	No change	Reduced	No change	(Sakai et al., 2019)
	Prophage genes	<i>yagL</i>	MIC vs ctrl		Reduced expression beneficial (increased expression of antisense mRNA beneficial)	Increased	Reduced	No change	(Maciag et al., 2011)
	Unknown	<i>ybaA</i>	subMIC vs ctrl		Increased expression beneficial	No change	Reduced	No change	
		<i>ybbC</i>	MIC vs ctrl		Increased expression beneficial	No change	No change	No change	

		<i>ybjM</i>	subMIC vs subMIC+PAβN	-8.5	Fewer insertions	No change	No change	No change	
		<i>yhcB</i>	subMIC vs subMIC+PAβN	-4.4	Fewer insertions	No change	Reduced	No change	
		<i>ydeJ</i>	subMIC vs subMIC+PAβN	-2.7	Fewer insertions	No change	No change	No change	
STM	Cell envelope biosynthesis and homeostasis	<i>mrcB</i>	PAβN vs ctrl	-1.5	Fewer insertions				(Suzuki et al., 1978)
		<i>prc</i>	MIC vs ctrl	2.5	More insertions				(Hara et al., 1991)
		<i>ldcA</i>	PAβN vs ctrl	-1.6	Fewer insertions				(Templin et al., 1999)
		<i>nlpD</i>	PAβN vs ctrl	-1.5	Fewer insertions				(Tsang et al., 2017)
			subMIC vs ctrl	-1.8	Fewer insertions				
		<i>cvpA</i>	PAβN vs ctrl	-2.3	Fewer insertions				(Fath et al., 1989)
		<i>tolB</i>	subMIC vs ctrl	8.3	More insertions				(Gerding et al., 2007)

			MIC vs ctrl	12.2	More insertions				
		<i>tolQ</i>	MIC vs ctrl	2.7	More insertions				
		<i>tolA</i>	MIC vs ctrl	2.3	More insertions				
		<i>tolR</i>	MIC vs ctrl	10.4	More insertions				
	Cell division	<i>zapE</i>	subMIC vs ctrl	0.7	More insertions				(Marteyn et al., 2014)
	Enterobacterial common antigen	<i>wecA</i>	PA $\beta$ N vs ctrl	-2.3	Fewer insertions				(Meier-Dieter et al., 1990)
		<i>wecB</i>	PA $\beta$ N vs ctrl	-2.2	Fewer insertions				
		<i>wecC</i>	PA $\beta$ N vs ctrl	-2.6	Fewer insertions				
			subMIC vs ctrl	0.7	More insertions				
		<i>wecG</i>	PA $\beta$ N vs ctrl	-1.4	Fewer insertions				

		<i>wecE</i>	subMIC vs ctrl	1.1	More insertions				
		<i>wzxE</i>	subMIC vs ctrl	0.8	More insertions				(Islam and Lam, 2014)
			MIC vs ctrl	3.0	More insertions				
		<i>yhdP</i>	PAβN vs ctrl	-1.2	Fewer insertions				(Mitchell et al., 2018)
	Sugar utilisation and respiration	<i>nagA</i>	PAβN vs ctrl	-2.7	Fewer insertions				(Hall et al., 2007)
		<i>eutN</i>	MIC vs ctrl	-2.6	Fewer insertions				(Penrod and Roth, 2006)
		<i>rbsK</i>	subMIC vs ctrl		Increased expression beneficial				(Lopilato et al., 1984)
		<i>nirD</i>	MIC vs ctrl	-2.7	Fewer insertions	Increased	Reduced	No change	(Harborne et al., 1992)
		<i>citG</i>	MIC vs ctrl	-2.2	Fewer insertions				(Schneider et al., 2000)
			MIC vs MIC+PAβN	-2.5	Fewer insertions				

		<i>STM14_0712</i>	MIC vs ctrl	-1.0	Fewer insertions				(Weiner et al., 1993)
			MIC vs MIC+PAβN	-0.9	Fewer insertions				
Transcription factors and regulators	<i>rpoS</i>		PAβN vs ctrl	-2.7	Fewer insertions				(Gentry et al., 1993)
			subMIC vs ctrl	-2.9	Fewer insertions				
	<i>iraP</i>		PAβN vs ctrl	-1.5	Fewer insertions				(Girard et al., 2018)
			subMIC vs ctrl	-2.4	Fewer insertions				
	<i>ramR</i>		subMIC vs ctrl	2.0	More insertions				(Abouzeed et al., 2008)
	<i>crI</i>		PAβN vs ctrl	-1.5	Fewer insertions	No change	Reduced	No change	(Bougdoor et al., 2004)
			subMIC vs ctrl	-2.1	Fewer insertions				
	<i>hupA</i>		PAβN vs ctrl	-0.9	Fewer insertions				(Oberto et al., 2009)

		<i>ioIR</i>	subMIC vs ctrl	-2.0	Fewer insertions				(Kröger and Fuchs Thilo, 2009)
			MIC vs ctrl	-1.8	Fewer insertions				
		<i>ybdF</i>	subMIC vs ctrl		Increased expression beneficial				(Rosenblum et al., 2011)
		<i>STM14_1969</i>	MIC vs ctrl	-9.1	Fewer insertions				(Herring and Blattner, 2004)
			MIC vs MIC+PAβN	-9.6	Fewer insertions				
	Membrane signalling systems	<i>cpxA</i>	subMIC vs ctrl	0.7	More insertions				(Ruiz and Silhavy, 2005)
		<i>phoP</i>	PAβN vs ctrl	-1.9	Fewer insertions				(Kasahara et al., 1992)
		<i>phoQ</i>	PAβN vs ctrl	-1.3	Fewer insertions				
		<i>arcA</i>	subMIC vs subMIC+PAβN	-2.2	Fewer insertions				(Alexeeva et al., 2003)
		<i>smvA</i>	subMIC vs ctrl	-2.2	Increased expression				(Villagra et al., 2008)

	Transmembrane transport systems				beneficial and fewer insertions				
		<i>pitA</i>	subMIC vs ctrl	1.1	More insertions				(Harris et al., 2001)
		<i>corA</i>	subMIC vs ctrl	1.1	More insertions				(Hmiel et al., 1986)
		<i>potD</i>	MIC vs ctrl	-2.4	Fewer insertions				(Kashiwagi et al., 1993)
			MIC vs MIC+PAβN	-2.8	Fewer insertions				
		<i>secM</i>	MIC vs ctrl	-8.6	Fewer insertions				(Sarker and Oliver, 2002)
		<i>ybiR</i>	MIC vs ctrl	-1.6	Fewer insertions				(Kehres et al., 2002)
	Protein folding and repair	<i>secB</i>	PAβN vs ctrl	1.6	More insertions				(Baars et al., 2006)
			subMIC vs ctrl	2.1	More insertions				
		<i>degS</i>	PAβN vs ctrl	-1.1	Fewer insertions				(Alba and Gross, 2004)



	Fimbriae	<i>fimW</i>	PAβN vs ctrl	-1.7	Fewer insertions				(Saini et al., 2009)		
			subMIC vs ctrl	-1.8	Fewer insertions						
			MIC vs ctrl	-1.9	Fewer insertions						
		<i>fimZ</i>	subMIC vs ctrl	0.5	More insertions						
		<i>fimY</i>	subMIC vs ctrl		More insertions						
		<i>fimF</i>	subMIC vs ctrl	0.5	More insertions					(Allen et al., 2012)	
	LPS	<i>ppdC</i>	MIC vs ctrl	-3.3	Fewer insertions				(Cisneros et al., 2012)		
			<i>rfaL</i>	subMIC vs subMIC+PAβN	1.9	More insertions				(Wang et al., 2015)	
				<i>rfaJ</i>	subMIC vs subMIC+PAβN	1.6	More insertions				
					<i>rfaI</i>	subMIC vs subMIC+PAβN		Increased expression beneficial in			

					subMIC+PA BN vs subMIC				
	<i>rfbH</i>	PAβN vs ctrl	-4.7	Fewer insertions					
		subMIC vs ctrl	-4.4	Fewer insertions					
	<i>rfbG</i>	PAβN vs ctrl	-3.7	Fewer insertions					
		subMIC vs ctrl	-3.9	Fewer insertions					
	<i>rfbF</i>	PAβN vs ctrl	-5.3	Fewer insertions	Reduced	Reduced	Increased susceptibility to gentamycin		
		subMIC vs ctrl	-4.4	Fewer insertions					
	<i>rfbI</i>	PAβN vs ctrl	-3.0	Fewer insertions					
		subMIC vs subMIC+PAβN	1.7	More insertions					
	<i>rfbC</i>	PAβN vs ctrl	-0.5	Fewer insertions					

			subMIC vs subMIC+PAβN	1.7	More insertions				
		<i>rfbA</i>	MIC vs ctrl	2.3	More insertions				
			subMIC vs subMIC+PAβN	1.0	More insertions				
		<i>rfbK</i>	MIC vs ctrl	1.2	More insertions				
		<i>rfbM</i>	MIC vs ctrl	1.7	More insertions				
		<i>rfbN</i>	subMIC vs subMIC+PAβN	1.5	More insertions				
		<i>rfbU</i>	MIC vs ctrl	3.2	More insertions				
		<i>rfbX</i>	MIC vs ctrl	6.3	More insertions				
		<i>arnE</i>	MIC vs MIC+PAβN	-3.6	Fewer insertions				(Wang and Quinn, 2010)
	Motility	<i>yhdA/ ydiV</i>	subMIC vs ctrl	0.7	More insertions				

	Amino acid biosynthesis	<i>leuD</i>	MIC vs ctrl	-1.1	Fewer insertions				(Gemmill et al., 1983)
		<i>argG</i>	subMIC vs ctrl	0.6	More insertions				(Van Vliet et al., 1990)
	DNA Housekeeping	<i>dinI</i>	MIC vs ctrl	-2.9	Fewer insertions				(Lusetti et al., 2004)
		<i>recB</i>	MIC vs ctrl	2.6	More insertions				(Hickson et al., 1985)
		<i>recC</i>	subMIC vs ctrl	1.1	More insertions				
			MIC vs ctrl	2.5	More insertions				
	Secondary messenger molecule metabolism	<i>pdeK</i>	PA $\beta$ N vs ctrl	-1.8	Fewer insertions	No change	Reduced	No change	(Hengge et al., 2015)
		<i>cyaA</i>	subMIC vs ctrl	1.2	More insertions	No change	No change	No change	(Roy and Danchin, 1982)
	Translation	<i>tuf_1</i>	subMIC vs ctrl	1.2	More insertions				(Weijland et al., 1992)
		<i>tuf_2</i>	subMIC vs ctrl	1.5	More insertions				

		<i>deaD</i>	subMIC vs ctrl	0.7	More insertions				(Peil et al., 2008, Resch et al., 2010)
		<i>bipA</i>	subMIC vs ctrl	0.9	More insertions				(Choi and Hwang, 2018)
		<i>proQ</i>	MIC vs ctrl	2.0	More insertions				(Sheidy and Zielke, 2013)
		<i>infB</i>	subMIC vs ctrl		Increased expression beneficial	No change	No change	No change	(Caserta et al., 2006)
	ATP synthesis	<i>atpA</i>	MIC vs ctrl	3.5	More insertions				(Kasimoglu et al., 1996)
		<i>atpG</i>	MIC vs ctrl	3.1	More insertions				
	Prophage genes (Gifsy-3 prophage)	<i>STM14_1418 – STM14_1483</i>	subMIC vs subMIC+PAβN		Fewer insertions				(Figuroa-Bossi et al., 2001)
	Cofactor biosynthesis	<i>panD</i>	MIC vs ctrl	-2.1	Fewer insertions				(Monteiro et al., 2015)

		<i>cbiT</i>	MIC vs ctrl	-2.7	Fewer insertions				(Santander et al., 2006)
	Unknown	<i>yfbU</i>	MIC vs ctrl	-0.7	Fewer insertions				
		<i>STM14_0777</i>	MIC vs ctrl	-2.1	Fewer insertions				
		<i>STM14_2429</i>	MIC vs ctrl	-2.0	Fewer insertions				
		<i>STM14_2263</i>	subMIC vs subMIC+PAβN	-1.3	Fewer insertions				

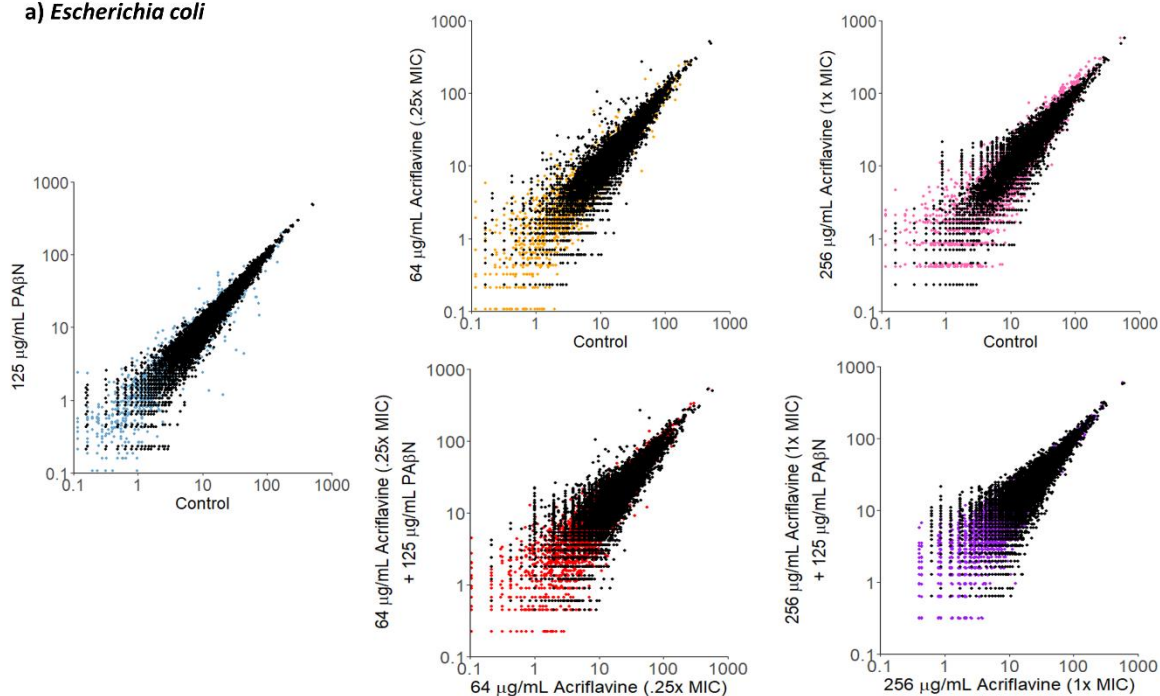
\* Log fold change is only shown for genes where there are differences in insertion frequency inside the coding region. Where the plot files generated by BioTraDIS show a difference in insertion frequency between the biofilm and planktonic conditions upstream or downstream of a gene, log fold change cannot easily be quantified and therefore the effect has been described in the column titled 'observed change'. Significant differences in insertion frequencies have been manually verified with the plot files generated by BioTraDIS.

### 10.3. APPENDIX 3: Mean insertion frequencies per gene in *E. coli* and *S.*

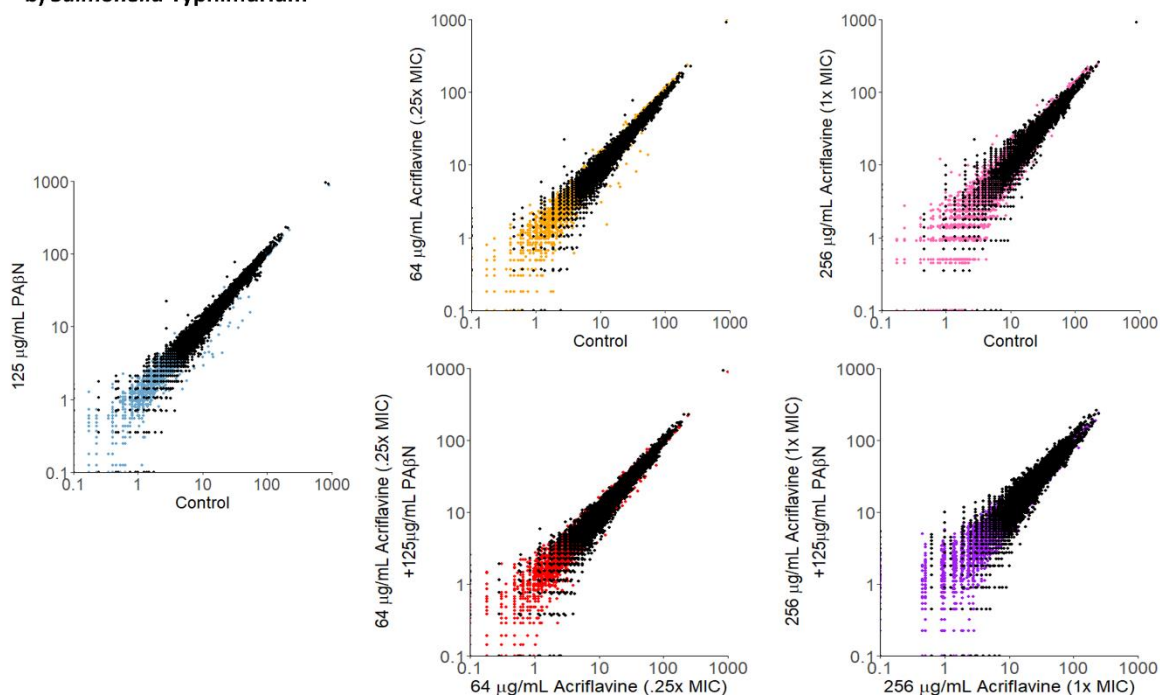
*Typhimurium* for conditions treated with PA $\beta$ N or acriflavine compared to untreated controls.

Coloured points show mean insertion frequencies per gene in conditions treated with PA $\beta$ N or acriflavine (x-axis) compared to untreated control conditions (y-axis). Black points show insertion frequencies per gene compared between identical replicates and show the experimental error. Replicates with and without promoter induction with IPTG are combined for analysis.

#### a) *Escherichia coli*



#### b) *Salmonella Typhimurium*



**10.4. APPENDIX 4: Genes implicated in both biofilm formation and efflux activity by the TraDIS-*Xpress* data and/or the phenotype of deletion mutants in *E. coli* and/or *S. Typhimurium* (STM).**

Pathway	Gene	Observed change in insertions in TraDIS- <i>Xpress</i> data in biofilm conditions	Observed change in insertions in TraDIS- <i>Xpress</i> data in efflux conditions	Biofilm phenotype of deletion mutant	Efflux phenotype of deletion mutant
Transmembrane transport	acrR	<ul style="list-style-type: none"> <li>• None</li> </ul>	<ul style="list-style-type: none"> <li>• More insertions in subinhibitory acriflavine condition vs unstressed control in <i>E. coli</i> and STM</li> <li>• More insertions in subinhibitory acriflavine condition vs condition with both acriflavine and PA<math>\beta</math>N in <i>E. coli</i></li> <li>• Fewer insertions in inhibitory acriflavine condition vs unstressed control in <i>E. coli</i></li> </ul>	<ul style="list-style-type: none"> <li>• Reduced biofilm biomass in <i>E. coli</i></li> </ul>	<ul style="list-style-type: none"> <li>• Reduced dye uptake with PA<math>\beta</math>N in <i>E. coli</i></li> <li>• Increased susceptibility to acriflavine (agar dilution) in <i>E. coli</i></li> </ul>
	acrB	<ul style="list-style-type: none"> <li>• None</li> </ul>	<ul style="list-style-type: none"> <li>• More insertions in PA<math>\beta</math>N condition vs unstressed</li> </ul>	<ul style="list-style-type: none"> <li>• Reduced biofilm biomass in <i>E. coli</i></li> </ul>	<ul style="list-style-type: none"> <li>• Increased dye uptake in <i>E. coli</i></li> </ul>



			<p>control in <i>E. coli</i> and STM</p> <ul style="list-style-type: none"> <li>• More insertions in subinhibitory acriflavine condition vs unstressed control in <i>E. coli</i> and STM</li> </ul>		<ul style="list-style-type: none"> <li>• Reduced dye uptake with PA<math>\beta</math>N in <i>E. coli</i></li> <li>• Increased susceptibility to acriflavine (broth and agar dilution) and azithromycin in <i>E. coli</i></li> </ul>
	tolC	<ul style="list-style-type: none"> <li>• Fewer insertions in 48h biofilm condition vs planktonic in both <i>E. coli</i> and STM</li> </ul>	<ul style="list-style-type: none"> <li>• Fewer insertions in PA<math>\beta</math>N condition vs unstressed control in both <i>E. coli</i> and STM</li> </ul>	<ul style="list-style-type: none"> <li>• Reduced biofilm biomass in STM</li> <li>• Reduced aggregation in <i>E. coli</i></li> <li>• Reduced curli production in STM</li> </ul>	<ul style="list-style-type: none"> <li>• Reduced dye uptake with PA<math>\beta</math>N in STM</li> <li>• Increased susceptibility to acriflavine, azithromycin and cefotaxime in STM</li> </ul>
	marR	<ul style="list-style-type: none"> <li>• Fewer insertions in 12h biofilm condition vs planktonic in <i>E. coli</i></li> </ul>	<ul style="list-style-type: none"> <li>• More insertions in PA<math>\beta</math>N condition vs unstressed control in <i>E. coli</i></li> </ul>	<ul style="list-style-type: none"> <li>• Reduced biofilm biomass in <i>E. coli</i></li> </ul>	<ul style="list-style-type: none"> <li>• Reduced susceptibility to</li> </ul>

			<ul style="list-style-type: none"> <li>• More insertions in subinhibitory acriflavine condition vs unstressed control in <i>E. coli</i></li> <li>• More insertions in subinhibitory acriflavine condition vs condition with both acriflavine and PA<math>\beta</math>N in <i>E. coli</i></li> <li>• Fewer insertions in inhibitory acriflavine condition vs unstressed control in <i>E. coli</i></li> <li>• Fewer insertions in inhibitory acriflavine condition vs condition with both acriflavine and PA<math>\beta</math>N in <i>E. coli</i></li> </ul>		cefotaxime in <i>E. coli</i>
	ramR	<ul style="list-style-type: none"> <li>• Fewer insertions in 48h biofilm condition vs planktonic in STM</li> </ul>	<ul style="list-style-type: none"> <li>• More insertions in subinhibitory acriflavine</li> </ul>	<ul style="list-style-type: none"> <li>• <i>ramRA</i> = Increased biofilm biomass with and</li> </ul>	<ul style="list-style-type: none"> <li>• Not tested</li> </ul>

			condition vs unstressed control in STM	without PA $\beta$ N in STM	
soxR	<ul style="list-style-type: none"> <li>• None</li> </ul>	<ul style="list-style-type: none"> <li>• More insertions in subinhibitory acriflavine condition vs unstressed control in <i>E. coli</i></li> <li>• More insertions in subinhibitory acriflavine condition vs condition with both acriflavine and PA<math>\beta</math>N in <i>E. coli</i></li> <li>• Fewer insertions in inhibitory acriflavine condition vs unstressed control in <i>E. coli</i></li> </ul>	<ul style="list-style-type: none"> <li>• Reduced biofilm biomass in <i>E. coli</i></li> </ul>	<ul style="list-style-type: none"> <li>• None</li> </ul>	
soxS	<ul style="list-style-type: none"> <li>• None</li> </ul>	<ul style="list-style-type: none"> <li>• Fewer insertions in subinhibitory acriflavine condition vs unstressed control in <i>E. coli</i></li> <li>• Increased expression beneficial in</li> </ul>	<ul style="list-style-type: none"> <li>• Reduced biofilm biomass in <i>E. coli</i></li> </ul>	<ul style="list-style-type: none"> <li>• Reduced dye uptake with PA<math>\beta</math>N in <i>E. coli</i></li> <li>• Increased susceptibility to</li> </ul>	

			<p>subinhibitory acriflavine condition vs unstressed control in <i>E. coli</i></p> <ul style="list-style-type: none"> <li>• Reduced expression beneficial in inhibitory acriflavine condition vs unstressed control in <i>E. coli</i></li> </ul>		<p>acriflavine (agar dilution) in <i>E. coli</i></p>
ompC & ompF	<ul style="list-style-type: none"> <li>• <i>ompF</i> = Fewer insertions in 48h biofilm condition vs planktonic in <i>E. coli</i></li> </ul>	<ul style="list-style-type: none"> <li>• <i>ompC</i> = More insertions in PA<math>\beta</math>N condition vs unstressed control in <i>E. coli</i></li> </ul>	<ul style="list-style-type: none"> <li>• Both = Reduced biofilm biomass in <i>E. coli</i></li> </ul>	<ul style="list-style-type: none"> <li>• None</li> </ul>	
potA	<ul style="list-style-type: none"> <li>• None</li> </ul>	<ul style="list-style-type: none"> <li>• Fewer insertions in subinhibitory acriflavine condition vs unstressed control in <i>E. coli</i></li> </ul>	<ul style="list-style-type: none"> <li>• Reduced biofilm biomass with and without PA<math>\beta</math>N in <i>E. coli</i></li> </ul>	<ul style="list-style-type: none"> <li>• None</li> </ul>	
proW	<ul style="list-style-type: none"> <li>• None</li> </ul>	<ul style="list-style-type: none"> <li>• Increased expression beneficial in inhibitory acriflavine condition vs unstressed control in <i>E. coli</i></li> </ul>	<ul style="list-style-type: none"> <li>• Reduced biofilm biomass in <i>E. coli</i></li> </ul>	<ul style="list-style-type: none"> <li>• None</li> </ul>	

	satP	<ul style="list-style-type: none"> <li>• None</li> </ul>	<ul style="list-style-type: none"> <li>• Fewer insertions in subinhibitory acriflavine condition vs unstressed control in <i>E. coli</i></li> </ul>	<ul style="list-style-type: none"> <li>• Reduced biofilm biomass with and without PA<math>\beta</math>N in <i>E. coli</i></li> </ul>	<ul style="list-style-type: none"> <li>• Reduced dye uptake in <i>E. coli</i></li> </ul>
	gltJ	<ul style="list-style-type: none"> <li>• None</li> </ul>	<ul style="list-style-type: none"> <li>• Fewer insertions in subinhibitory acriflavine condition vs unstressed control in <i>E. coli</i></li> </ul>	<ul style="list-style-type: none"> <li>• Reduced biofilm biomass with and without PA<math>\beta</math>N in <i>E. coli</i></li> </ul>	<ul style="list-style-type: none"> <li>• Reduced dye uptake with PA<math>\beta</math>N in <i>E. coli</i></li> </ul>
	gltS	<ul style="list-style-type: none"> <li>• None</li> </ul>	<ul style="list-style-type: none"> <li>• Fewer insertions in subinhibitory acriflavine condition vs unstressed control in <i>E. coli</i></li> <li>• Fewer insertions in subinhibitory acriflavine condition vs condition with both acriflavine and PA<math>\beta</math>N in <i>E. coli</i></li> </ul>	<ul style="list-style-type: none"> <li>• Reduced biofilm biomass in <i>E. coli</i></li> </ul>	<ul style="list-style-type: none"> <li>• None</li> </ul>
	glpF	<ul style="list-style-type: none"> <li>• None</li> </ul>	<ul style="list-style-type: none"> <li>• More insertions in inhibitory acriflavine condition vs unstressed control in <i>E. coli</i></li> </ul>	<ul style="list-style-type: none"> <li>• Reduced biofilm biomass with and without PA<math>\beta</math>N in <i>E. coli</i></li> </ul>	<ul style="list-style-type: none"> <li>• Reduced dye uptake in <i>E. coli</i></li> </ul>

Respiration	adhP	<ul style="list-style-type: none"> <li>• None</li> </ul>	<ul style="list-style-type: none"> <li>• Fewer insertions in subinhibitory acriflavine condition vs unstressed control in <i>E. coli</i></li> <li>• Fewer insertions in subinhibitory acriflavine condition vs condition with both acriflavine and PAβN in <i>E. coli</i></li> </ul>	<ul style="list-style-type: none"> <li>• Reduced biofilm biomass with and without PAβN in <i>E. coli</i></li> </ul>	<ul style="list-style-type: none"> <li>• Reduced dye uptake in <i>E. coli</i></li> </ul>
	nuo operon & nuoB	<ul style="list-style-type: none"> <li>• <i>nuoBCGJKLM</i> = Fewer insertions in 24h and 48h biofilm conditions vs planktonic in STM</li> <li>• <i>nuoFHI</i> = Fewer insertions in 48h biofilm condition vs planktonic in STM</li> </ul>	<ul style="list-style-type: none"> <li>• None</li> </ul>	<ul style="list-style-type: none"> <li>• Reduced biofilm biomass in both <i>E. coli</i> (<i>nuoB</i>) and STM (<i>nuo</i> operon and <i>nuoB</i>)</li> <li>• Reduced curli biosynthesis in both <i>E. coli</i> (<i>nuoB</i>) and STM (<i>nuo</i> operon and <i>nuoB</i>)</li> </ul>	<ul style="list-style-type: none"> <li>• Increased dye uptake with and without PAβN in STM (<i>nuo</i> operon and <i>nuoB</i>)</li> <li>• Increased susceptibility to cefotaxime in STM (<i>nuoB</i>)</li> </ul>

				<ul style="list-style-type: none"> <li>Reduced adhesion in STM (<i>nuo</i> operon)</li> </ul>	
nirD	<ul style="list-style-type: none"> <li>None</li> </ul>	<ul style="list-style-type: none"> <li>Fewer insertions in inhibitory acriflavine condition vs unstressed control in STM</li> </ul>	<ul style="list-style-type: none"> <li>Increased biofilm biomass with PAβN in STM</li> </ul>	<ul style="list-style-type: none"> <li>Increased dye uptake in STM</li> <li>Reduced dye uptake with PAβN in STM</li> </ul>	
dgoD	<ul style="list-style-type: none"> <li>None</li> </ul>	<ul style="list-style-type: none"> <li>Fewer insertions in subinhibitory acriflavine condition vs unstressed control in <i>E. coli</i></li> <li>Fewer insertions in subinhibitory acriflavine condition vs condition with both acriflavine and PAβN in <i>E. coli</i></li> </ul>	<ul style="list-style-type: none"> <li>Reduced biofilm biomass in <i>E. coli</i></li> </ul>	<ul style="list-style-type: none"> <li>Increased dye uptake in <i>E. coli</i></li> </ul>	
mhpF	<ul style="list-style-type: none"> <li>None</li> </ul>	<ul style="list-style-type: none"> <li>Fewer insertions in subinhibitory acriflavine condition vs unstressed control in <i>E. coli</i></li> </ul>	<ul style="list-style-type: none"> <li>Reduced biofilm biomass in <i>E. coli</i></li> </ul>	<ul style="list-style-type: none"> <li>Reduced dye uptake with PAβN in <i>E. coli</i></li> </ul>	

	sgbE	<ul style="list-style-type: none"> <li>Fewer insertions in 48h biofilm condition vs planktonic in <i>E. coli</i></li> </ul>	<ul style="list-style-type: none"> <li>None</li> </ul>	<ul style="list-style-type: none"> <li>None</li> </ul>	<ul style="list-style-type: none"> <li>Reduced dye uptake with and without PA<math>\beta</math>N in <i>E. coli</i></li> </ul>
DNA housekeeping	dam	<ul style="list-style-type: none"> <li>Fewer insertions in 24h biofilm condition vs planktonic in <i>E. coli</i></li> </ul>	<ul style="list-style-type: none"> <li>Fewer insertions in subinhibitory acriflavine condition vs unstressed control in <i>E. coli</i> and STM</li> <li>Fewer insertions in subinhibitory acriflavine condition vs condition with both acriflavine and PA<math>\beta</math>N in <i>E. coli</i></li> </ul>	<ul style="list-style-type: none"> <li>Reduced aggregation in <i>E. coli</i></li> <li>Reduced curli production in <i>E. coli</i></li> </ul>	<ul style="list-style-type: none"> <li>Increased susceptibility to acriflavine (broth and agar dilution) in <i>E. coli</i></li> </ul>
	maoP	<ul style="list-style-type: none"> <li>Fewer insertions in 24h biofilm condition vs planktonic in <i>E. coli</i></li> </ul>	<ul style="list-style-type: none"> <li>Fewer insertions in PA<math>\beta</math>N condition vs unstressed control in <i>E. coli</i></li> </ul>	<ul style="list-style-type: none"> <li>Reduced biofilm biomass in both <i>E. coli</i> and STM</li> <li>Increased biofilm biomass with PA<math>\beta</math>N in STM</li> </ul>	<ul style="list-style-type: none"> <li>Increased dye uptake with and without PA<math>\beta</math>N in <i>E. coli</i></li> </ul>



				<ul style="list-style-type: none"> <li>• Reduced aggregation in <i>E. coli</i></li> <li>• Reduced curli production in both <i>E. coli</i> and STM</li> <li>• Reduced adhesion in <i>E. coli</i></li> </ul>	
	ybiB	<ul style="list-style-type: none"> <li>• None</li> </ul>	<ul style="list-style-type: none"> <li>• Fewer insertions in subinhibitory acriflavine condition vs unstressed control in <i>E. coli</i></li> </ul>	<ul style="list-style-type: none"> <li>• Reduced biofilm biomass in <i>E. coli</i></li> </ul>	<ul style="list-style-type: none"> <li>• None</li> </ul>
Translation	infB	<ul style="list-style-type: none"> <li>• None</li> </ul>	<ul style="list-style-type: none"> <li>• Increased expression beneficial in subinhibitory acriflavine condition vs unstressed control in STM</li> </ul>	<ul style="list-style-type: none"> <li>• Reduced biofilm biomass in STM</li> <li>• Increased biofilm biomass with PA<math>\beta</math>N in STM</li> </ul>	<ul style="list-style-type: none"> <li>• None</li> </ul>
	truA	<ul style="list-style-type: none"> <li>• Fewer insertions in 24h and 48h biofilm conditions vs planktonic in <i>E. coli</i></li> </ul>	<ul style="list-style-type: none"> <li>• None</li> </ul>	<ul style="list-style-type: none"> <li>• Increased aggregation in <i>E. coli</i></li> </ul>	<ul style="list-style-type: none"> <li>• Increased dye uptake with PA<math>\beta</math>N in <i>E. coli</i></li> </ul>

				<ul style="list-style-type: none"> <li>Increased filamentation after 24h and 48h growth in <i>E. coli</i></li> </ul>	
rimO & rimK	<ul style="list-style-type: none"> <li><i>rimO</i> = Increased expression beneficial in 48h biofilm conditions vs planktonic in STM</li> </ul>	<ul style="list-style-type: none"> <li><i>rimK</i> = Fewer insertions in subinhibitory acriflavine condition vs unstressed control in <i>E. coli</i></li> </ul>	<ul style="list-style-type: none"> <li><i>rimK</i> = Reduced biofilm biomass in <i>E. coli</i></li> </ul>	<ul style="list-style-type: none"> <li>None</li> </ul>	
rlmI	<ul style="list-style-type: none"> <li>Fewer insertions in 12h biofilm condition vs planktonic in <i>E. coli</i></li> </ul>	<ul style="list-style-type: none"> <li>None</li> </ul>	<ul style="list-style-type: none"> <li>Reduced biofilm biomass in <i>E. coli</i></li> </ul>	<ul style="list-style-type: none"> <li>Increased dye uptake with and without PA<math>\beta</math>N in <i>E. coli</i></li> </ul>	
trhP	<ul style="list-style-type: none"> <li>None</li> </ul>	<ul style="list-style-type: none"> <li>Fewer insertions in subinhibitory acriflavine condition vs unstressed control in <i>E. coli</i></li> </ul>	<ul style="list-style-type: none"> <li>Reduced biofilm biomass in <i>E. coli</i></li> </ul>	<ul style="list-style-type: none"> <li>Reduced dye uptake with PA<math>\beta</math>N in <i>E. coli</i></li> </ul>	
yehF	<ul style="list-style-type: none"> <li>None</li> </ul>	<ul style="list-style-type: none"> <li>Fewer insertions in subinhibitory acriflavine condition vs unstressed control in <i>E. coli</i></li> </ul>	<ul style="list-style-type: none"> <li>Reduced biofilm biomass with PA<math>\beta</math>N in <i>E. coli</i></li> </ul>	<ul style="list-style-type: none"> <li>Increased dye uptake in <i>E. coli</i></li> </ul>	

			<ul style="list-style-type: none"> <li>• Fewer insertions in subinhibitory acriflavine condition vs condition with both acriflavine and PAβN in <i>E. coli</i></li> </ul>		
Signalling systems & secondary messenger molecules	ompR	<ul style="list-style-type: none"> <li>• Fewer insertions in 24h and 48h biofilm conditions vs planktonic in <i>E. coli</i></li> </ul>	<ul style="list-style-type: none"> <li>• More insertions in subinhibitory acriflavine condition vs unstressed control in <i>E. coli</i></li> <li>• More insertions in subinhibitory acriflavine condition vs condition with both acriflavine and PAβN in <i>E. coli</i></li> </ul>	<ul style="list-style-type: none"> <li>• Reduced biofilm biomass in <i>E. coli</i></li> <li>• Reduced aggregation in <i>E. coli</i></li> <li>• Reduced curli production in <i>E. coli</i></li> </ul>	<ul style="list-style-type: none"> <li>• Reduced dye uptake in <i>E. coli</i></li> </ul>
	opgG & opgH	<ul style="list-style-type: none"> <li>• None</li> </ul>	<ul style="list-style-type: none"> <li>• Both = More insertions in PAβN condition vs unstressed control in <i>E. coli</i></li> <li>• Both = More insertions in subinhibitory acriflavine condition with</li> </ul>	<ul style="list-style-type: none"> <li>• Both = Reduced curli production in <i>E. coli</i></li> </ul>	<ul style="list-style-type: none"> <li>• None</li> </ul>

			PAβN vs acriflavine alone in STM		
	pdeK/ pdeC/ pdeF	<ul style="list-style-type: none"> <li>• <i>pdeF</i> = Fewer insertions in 48h biofilm condition vs planktonic in <i>E. coli</i></li> </ul>	<ul style="list-style-type: none"> <li>• <i>pdeK</i> = Fewer insertions in PAβN condition vs unstressed control in STM</li> <li>• <i>pdeC</i> = More insertions in inhibitory acriflavine condition vs unstressed control in <i>E. coli</i></li> </ul>	<ul style="list-style-type: none"> <li>• <i>pdeK</i> = Increased biofilm biomass with PAβN in STM</li> <li>• <i>pdeF</i> = Reduced curli biosynthesis in STM</li> <li>• <i>pdeC</i> = Reduced biofilm biomass in <i>E. coli</i></li> <li>• <i>pdeC</i> = Increased curli biosynthesis in STM</li> </ul>	<ul style="list-style-type: none"> <li>• <i>pdeK</i> = Reduced dye uptake with PAβN in STM</li> <li>• <i>pdeC</i> = Reduced dye uptake with PAβN in <i>E. coli</i></li> </ul>
	cyaA	<ul style="list-style-type: none"> <li>• Fewer insertions in 24h biofilm condition vs planktonic STM</li> </ul>	<ul style="list-style-type: none"> <li>• More insertions in subinhibitory acriflavine condition vs unstressed control in STM</li> </ul>	<ul style="list-style-type: none"> <li>• Reduced biofilm biomass in STM</li> <li>• Increased biofilm biomass with PAβN in STM</li> </ul>	<ul style="list-style-type: none"> <li>• None</li> </ul>
Purine biosynthesis	rbsR	<ul style="list-style-type: none"> <li>• None</li> </ul>	<ul style="list-style-type: none"> <li>• Fewer insertions in subinhibitory acriflavine condition vs unstressed</li> </ul>	<ul style="list-style-type: none"> <li>• Reduced biofilm biomass in <i>E. coli</i></li> </ul>	<ul style="list-style-type: none"> <li>• Reduced dye uptake with and</li> </ul>

			<p>control in <i>E. coli</i> and STM</p> <ul style="list-style-type: none"> <li>• Fewer insertions in subinhibitory acriflavine condition vs condition with both acriflavine and PAβN in <i>E. coli</i></li> </ul>	<ul style="list-style-type: none"> <li>• Reduced curli production in <i>E. coli</i></li> </ul>	<p>without PAβN in <i>E. coli</i></p>
Transcription factors and regulators	dksA	<ul style="list-style-type: none"> <li>• Fewer insertions in 12h and 24h biofilm conditions vs planktonic in <i>E. coli</i></li> </ul>	<ul style="list-style-type: none"> <li>• Fewer insertions in PAβN condition vs unstressed control in <i>E. coli</i></li> <li>• Fewer insertions in subinhibitory acriflavine condition vs unstressed control in <i>E. coli</i></li> </ul>	<ul style="list-style-type: none"> <li>• Reduced biofilm biomass in <i>E. coli</i></li> <li>• Reduced aggregation in <i>E. coli</i></li> <li>• Reduced curli production in <i>E. coli</i></li> <li>• Increased adhesion in <i>E. coli</i></li> <li>• Reduced microcolony formation in <i>E. coli</i></li> </ul>	<ul style="list-style-type: none"> <li>• Reduced dye uptake with PAβN in <i>E. coli</i></li> <li>• Increased susceptibility to acriflavine (agar dilution) in <i>E. coli</i></li> </ul>

	rpoS	<ul style="list-style-type: none"> <li>• More insertions in 24h biofilm condition vs planktonic in STM</li> </ul>	<ul style="list-style-type: none"> <li>• Fewer insertions in PAβN condition vs unstressed control in STM</li> <li>• Fewer insertions in subinhibitory acriflavine condition vs unstressed control in STM</li> </ul>	<ul style="list-style-type: none"> <li>• Not tested</li> </ul>	<ul style="list-style-type: none"> <li>• Not tested</li> </ul>
	crl	<ul style="list-style-type: none"> <li>• None</li> </ul>	<ul style="list-style-type: none"> <li>• Fewer insertions in PAβN condition vs unstressed control in STM</li> <li>• Fewer insertions in subinhibitory acriflavine condition vs unstressed control in STM</li> </ul>	<ul style="list-style-type: none"> <li>• Increased biofilm biomass with PAβN in STM</li> <li>• Reduced curli biosynthesis in STM</li> </ul>	<ul style="list-style-type: none"> <li>• Reduced dye uptake with PAβN in STM</li> </ul>
	gadW	<ul style="list-style-type: none"> <li>• Fewer insertions in 48h biofilm condition vs planktonic in <i>E. coli</i></li> </ul>	<ul style="list-style-type: none"> <li>• More insertions in PAβN condition vs unstressed control in <i>E. coli</i></li> </ul>	<ul style="list-style-type: none"> <li>• None</li> </ul>	<ul style="list-style-type: none"> <li>• None</li> </ul>

	STM14_1074	<ul style="list-style-type: none"> <li>• Fewer insertions in 12h biofilm condition vs planktonic in STM</li> </ul>	<ul style="list-style-type: none"> <li>• None</li> </ul>	<ul style="list-style-type: none"> <li>• Reduced adhesion in STM</li> </ul>	<ul style="list-style-type: none"> <li>• Reduced dye uptake with PAβN in STM</li> </ul>
	leuO	<ul style="list-style-type: none"> <li>• Increased expression beneficial in 12h biofilm condition vs planktonic in <i>E. coli</i></li> <li>• Fewer insertions in 48h biofilm condition vs planktonic in <i>E. coli</i></li> </ul>	<ul style="list-style-type: none"> <li>• None</li> </ul>	<ul style="list-style-type: none"> <li>• Reduced biofilm biomass in <i>E. coli</i></li> <li>• Reduced aggregation in <i>E. coli</i></li> <li>• Reduced microcolony formation in <i>E. coli</i></li> </ul>	<ul style="list-style-type: none"> <li>• Reduced dye uptake with PAβN in <i>E. coli</i></li> </ul>
Protein chaperones	dsbA	<ul style="list-style-type: none"> <li>• Fewer insertions in 12h and 24h biofilm conditions vs planktonic in <i>E. coli</i></li> <li>• More insertions in 12h biofilm condition vs planktonic in STM</li> </ul>	<ul style="list-style-type: none"> <li>• None</li> </ul>	<ul style="list-style-type: none"> <li>• Increased biofilm biomass with PAβN in STM</li> <li>• Increased aggregation in <i>E. coli</i></li> <li>• Increased curli production in both <i>E. coli</i> and STM</li> </ul>	<ul style="list-style-type: none"> <li>• Reduced dye uptake in STM</li> <li>• Increased dye uptake in <i>E. coli</i></li> <li>• Increased susceptibility to azithromycin in <i>E. coli</i></li> </ul>

	surA	<ul style="list-style-type: none"> <li>• None</li> </ul>	<ul style="list-style-type: none"> <li>• More insertions in subinhibitory acriflavine condition vs unstressed control in <i>E. coli</i></li> </ul>	<ul style="list-style-type: none"> <li>• Reduced biofilm biomass in <i>E. coli</i></li> </ul>	<ul style="list-style-type: none"> <li>• Reduced dye uptake in <i>E. coli</i></li> <li>• Increased susceptibility to acriflavine (agar dilution) in <i>E. coli</i></li> </ul>
	msrQ	<ul style="list-style-type: none"> <li>• Fewer insertions in 48h biofilm condition vs planktonic in <i>E. coli</i></li> </ul>	<ul style="list-style-type: none"> <li>• None</li> </ul>	<ul style="list-style-type: none"> <li>• None</li> </ul>	<ul style="list-style-type: none"> <li>• Reduced dye uptake with PA<math>\beta</math>N in <i>E. coli</i></li> </ul>
Cell division	zapE	<ul style="list-style-type: none"> <li>• Fewer insertions in 48h biofilm condition vs planktonic in <i>E. coli</i></li> </ul>	<ul style="list-style-type: none"> <li>• More insertions in subinhibitory acriflavine condition vs unstressed control in STM</li> </ul>	<ul style="list-style-type: none"> <li>• Increased aggregation in <i>E. coli</i></li> <li>• Reduced adhesion in <i>E. coli</i></li> </ul>	<ul style="list-style-type: none"> <li>• Reduced dye uptake with PA<math>\beta</math>N in <i>E. coli</i></li> </ul>
Cell envelope biogenesis	rfbF	<ul style="list-style-type: none"> <li>• None</li> </ul>	<ul style="list-style-type: none"> <li>• Fewer insertions in PA<math>\beta</math>N condition vs unstressed control in STM</li> <li>• Fewer insertions in subinhibitory acriflavine</li> </ul>	<ul style="list-style-type: none"> <li>• Increased biofilm biomass with PA<math>\beta</math>N in STM</li> <li>• Reduced curli biosynthesis in STM</li> </ul>	<ul style="list-style-type: none"> <li>• Reduced dye uptake with and without PA<math>\beta</math>N in STM</li> <li>• Increased susceptibility to</li> </ul>



			condition vs unstressed control in STM		gentamycin in STM
wzzB	<ul style="list-style-type: none"> <li>Fewer insertions in 48h biofilm condition vs planktonic in <i>E. coli</i></li> </ul>	<ul style="list-style-type: none"> <li>Fewer insertions in subinhibitory acriflavine condition vs unstressed control in <i>E. coli</i></li> <li>Fewer insertions in subinhibitory acriflavine condition vs condition with both acriflavine and PA<math>\beta</math>N in <i>E. coli</i></li> </ul>	<ul style="list-style-type: none"> <li>Reduced biofilm biomass with and without PA<math>\beta</math>N in <i>E. coli</i></li> </ul>	<ul style="list-style-type: none"> <li>Reduced dye uptake with and without PA<math>\beta</math>N in <i>E. coli</i></li> </ul>	
waaF	<ul style="list-style-type: none"> <li>None</li> </ul>	<ul style="list-style-type: none"> <li>More insertions in subinhibitory acriflavine condition with PA<math>\beta</math>N vs acriflavine alone in <i>E. coli</i></li> </ul>	<ul style="list-style-type: none"> <li>Reduced biofilm biomass in <i>E. coli</i></li> </ul>	<ul style="list-style-type: none"> <li>Increased susceptibility to azithromycin in <i>E. coli</i></li> </ul>	
waaG/ rfaG	<ul style="list-style-type: none"> <li>Fewer insertions in 24h and 48h biofilm conditions vs planktonic in STM</li> </ul>	<ul style="list-style-type: none"> <li>More insertions in inhibitory acriflavine condition vs unstressed control in <i>E. coli</i></li> </ul>	<ul style="list-style-type: none"> <li>Reduced biofilm biomass with and without PA<math>\beta</math>N in <i>E. coli</i></li> </ul>	<ul style="list-style-type: none"> <li>Increased dye uptake in <i>E. coli</i></li> <li>Increased susceptibility to</li> </ul>	

				<ul style="list-style-type: none"> <li>Reduced curli production in <i>E. coli</i></li> </ul>	<ul style="list-style-type: none"> <li>azithromycin in <i>E. coli</i></li> <li>Reduced susceptibility to cefotaxime in <i>E. coli</i></li> </ul>
waaP/ rfaP	<ul style="list-style-type: none"> <li>Increased expression beneficial in 24h biofilm condition vs planktonic in STM</li> <li>Fewer insertions in 48h biofilm condition vs planktonic in STM</li> </ul>	<ul style="list-style-type: none"> <li>More insertions in PA<math>\beta</math>N condition vs unstressed control in <i>E. coli</i></li> </ul>	<ul style="list-style-type: none"> <li>Reduced biofilm biomass in <i>E. coli</i></li> <li>Reduced curli production in <i>E. coli</i></li> </ul>	<ul style="list-style-type: none"> <li>Increased susceptibility to azithromycin in <i>E. coli</i></li> <li>Reduced susceptibility to cefotaxime in <i>E. coli</i></li> </ul>	
rfaJ	<ul style="list-style-type: none"> <li>Increased expression beneficial in 12h, 24h and 48h biofilm conditions vs planktonic in STM</li> </ul>	<ul style="list-style-type: none"> <li>More insertions in subinhibitory acriflavine condition with PA<math>\beta</math>N vs acriflavine alone in STM</li> </ul>	<ul style="list-style-type: none"> <li>Not tested</li> </ul>	<ul style="list-style-type: none"> <li>Not tested</li> </ul>	

	wecF	<ul style="list-style-type: none"> <li>• None</li> </ul>	<ul style="list-style-type: none"> <li>• More insertions in subinhibitory acriflavine condition vs unstressed control in both <i>E. coli</i> and STM</li> </ul>	<ul style="list-style-type: none"> <li>• Reduced curli production in <i>E. coli</i></li> </ul>	<ul style="list-style-type: none"> <li>• Reduced dye uptake with and without PAβN in <i>E. coli</i></li> </ul>
Amino acid biosynthesis	leuL	<ul style="list-style-type: none"> <li>• None</li> </ul>	<ul style="list-style-type: none"> <li>• Fewer insertions in subinhibitory acriflavine condition vs unstressed control in <i>E. coli</i></li> </ul>	<ul style="list-style-type: none"> <li>• Reduced biofilm biomass in <i>E. coli</i></li> </ul>	<ul style="list-style-type: none"> <li>• None</li> </ul>
	metL	<ul style="list-style-type: none"> <li>• None</li> </ul>	<ul style="list-style-type: none"> <li>• More insertions in inhibitory acriflavine condition vs unstressed control in <i>E. coli</i></li> <li>• More insertions in PAβN condition vs unstressed control in STM</li> </ul>	<ul style="list-style-type: none"> <li>• Reduced biofilm biomass in <i>E. coli</i></li> </ul>	<ul style="list-style-type: none"> <li>• Reduced dye uptake with and without PAβN in <i>E. coli</i></li> </ul>
Fimbriae	+ve regulator (fimB & fimZ & fimY)	<ul style="list-style-type: none"> <li>• <i>fimB</i> = Fewer insertions in 12h, 24h and 48h biofilm conditions vs planktonic in <i>E. coli</i></li> </ul>	<ul style="list-style-type: none"> <li>• <i>fimB</i> = More insertions in PAβN condition vs unstressed control in <i>E. coli</i></li> </ul>	<ul style="list-style-type: none"> <li>• <i>fimB</i> = Reduced aggregation in <i>E. coli</i></li> </ul>	<ul style="list-style-type: none"> <li>• <i>fimB</i> = Reduced dye uptake with PAβN in <i>E. coli</i></li> </ul>

		<ul style="list-style-type: none"> <li>• <i>fimZ</i> = Increased expression in 48h biofilm condition vs planktonic in STM</li> <li>• <i>fimY</i> = Increased expression beneficial in 12h and 48h biofilm conditions vs planktonic in STM</li> </ul>	<ul style="list-style-type: none"> <li>• <i>fimB</i> = More insertions in inhibitory acriflavine condition with PA<math>\beta</math>N vs acriflavine alone in <i>E. coli</i></li> <li>• <i>fimZ</i> = More insertions in subinhibitory acriflavine condition vs unstressed control in STM</li> <li>• <i>fimY</i> = More insertions in subinhibitory acriflavine condition vs unstressed control in STM</li> </ul>		
	-ve regulator (fimE & fimW)	<ul style="list-style-type: none"> <li>• <i>fimE</i> = More insertions in 12h, 24h and 48h biofilm conditions vs planktonic in <i>E. coli</i></li> <li>• <i>fimW</i> = More insertions in 48h</li> </ul>	<ul style="list-style-type: none"> <li>• <i>fimE</i> = More insertions in PA<math>\beta</math>N condition vs unstressed control in <i>E. coli</i></li> <li>• <i>fimE</i> = Fewer insertions in subinhibitory and inhibitory acriflavine</li> </ul>	<ul style="list-style-type: none"> <li>• <i>fimE</i> = Reduced biofilm biomass in <i>E. coli</i></li> <li>• <i>fimE</i> = Reduced aggregation in <i>E. coli</i></li> </ul>	<ul style="list-style-type: none"> <li>• <i>fimE</i> = Reduced dye uptake with PA<math>\beta</math>N in <i>E. coli</i></li> </ul>

		biofilm condition vs planktonic in STM	<p>conditions vs unstressed control in <i>E. coli</i></p> <ul style="list-style-type: none"> <li>• <i>fimW</i> = Fewer insertions in PAβN condition vs unstressed control in STM <i>fimW</i> = Fewer insertions in subinhibitory and inhibitory acriflavine conditions vs unstressed control in STM</li> </ul>		
	Subunits (fimC & fimD & fimA & fimF)	<ul style="list-style-type: none"> <li>• <i>fimA</i> = Increased expression beneficial in 12h and 48h biofilm conditions vs planktonic in STM</li> <li>• <i>fimC</i> = Fewer insertions in 48h biofilm condition vs planktonic in <i>E. coli</i></li> </ul>	<ul style="list-style-type: none"> <li>• <i>fimF</i> = More insertions in subinhibitory acriflavine condition vs unstressed control in STM</li> <li>• <i>fimC</i> = More insertions in inhibitory acriflavine condition vs unstressed control in <i>E. coli</i></li> <li>• <i>fimD</i> = More insertions in inhibitory acriflavine</li> </ul>	<ul style="list-style-type: none"> <li>• Not tested</li> </ul>	<ul style="list-style-type: none"> <li>• Not tested</li> </ul>

		<ul style="list-style-type: none"> <li>• <i>fimD</i> = Fewer insertions in 24h and 48h biofilm conditions vs planktonic in <i>E. coli</i></li> </ul>	condition vs unstressed control in <i>E. coli</i>		
Motility	hdfR	<ul style="list-style-type: none"> <li>• More insertions in 12h and 24h biofilm conditions vs planktonic in <i>E. coli</i></li> </ul>	<ul style="list-style-type: none"> <li>• Fewer insertions in PA<math>\beta</math>N condition vs unstressed control in <i>E. coli</i></li> <li>• Fewer insertions in subinhibitory acriflavine condition vs unstressed control in <i>E. coli</i></li> </ul>	<ul style="list-style-type: none"> <li>• Reduced biofilm biomass in <i>E. coli</i></li> <li>• Reduced curli production in <i>E. coli</i></li> </ul>	<ul style="list-style-type: none"> <li>• None</li> </ul>
	IrhA	<ul style="list-style-type: none"> <li>• More insertions after 12h, 24h and 48h growth in <i>E. coli</i></li> </ul>	<ul style="list-style-type: none"> <li>• Fewer insertions in PA<math>\beta</math>N condition vs unstressed control in <i>E. coli</i></li> <li>• Fewer insertions in subinhibitory acriflavine condition vs unstressed control in <i>E. coli</i></li> </ul>	<ul style="list-style-type: none"> <li>• Reduced aggregation in <i>E. coli</i></li> <li>• Microcolony formation earlier compared to wild type <i>E. coli</i> but reduced over time</li> </ul>	<ul style="list-style-type: none"> <li>• None</li> </ul>

	flgD	<ul style="list-style-type: none"> <li>Fewer insertions in 24h biofilm condition vs planktonic in <i>E. coli</i></li> </ul>	<ul style="list-style-type: none"> <li>None</li> </ul>	<ul style="list-style-type: none"> <li>None</li> </ul>	<ul style="list-style-type: none"> <li>Reduced dye uptake with PA<math>\beta</math>N in <i>E. coli</i></li> </ul>
	flhC	<ul style="list-style-type: none"> <li>Fewer insertions in 48h biofilm condition vs planktonic in <i>E. coli</i></li> </ul>	<ul style="list-style-type: none"> <li>None</li> </ul>	<ul style="list-style-type: none"> <li>Reduced aggregation in <i>E. coli</i></li> </ul>	<ul style="list-style-type: none"> <li>Reduced dye uptake with PA<math>\beta</math>N in <i>E. coli</i></li> </ul>
	fliE	<ul style="list-style-type: none"> <li>Fewer insertions in 48h biofilm condition vs planktonic in <i>E. coli</i></li> </ul>	<ul style="list-style-type: none"> <li>None</li> </ul>	<ul style="list-style-type: none"> <li>Reduced aggregation in <i>E. coli</i></li> </ul>	<ul style="list-style-type: none"> <li>Reduced dye uptake with PA<math>\beta</math>N in <i>E. coli</i></li> </ul>
Biofilm matrix components	csgE	<ul style="list-style-type: none"> <li>Fewer insertions in 12h and 48h biofilm conditions vs planktonic in <i>E. coli</i></li> </ul>	<ul style="list-style-type: none"> <li>None</li> </ul>	<ul style="list-style-type: none"> <li>Reduced biofilm biomass in <i>E. coli</i></li> <li>Reduced curli production in <i>E. coli</i></li> </ul>	<ul style="list-style-type: none"> <li>Reduced dye uptake with PA<math>\beta</math>N in <i>E. coli</i></li> </ul>
	ymdB	<ul style="list-style-type: none"> <li>Fewer insertions in 24h and 48h biofilm conditions vs planktonic in <i>E. coli</i></li> </ul>	<ul style="list-style-type: none"> <li>None</li> </ul>	<ul style="list-style-type: none"> <li>Reduced biofilm biomass in <i>E. coli</i></li> <li>Increased aggregation in <i>E. coli</i></li> </ul>	<ul style="list-style-type: none"> <li>Reduced dye uptake with PA<math>\beta</math>N in <i>E. coli</i></li> </ul>

Toxin-antitoxin system	tomB	<ul style="list-style-type: none"> <li>• Fewer insertions in 12h, 24h and 48h biofilm conditions vs planktonic in <i>E. coli</i></li> </ul>	<ul style="list-style-type: none"> <li>• None</li> </ul>	<ul style="list-style-type: none"> <li>• Reduced biofilm biomass in <i>E. coli</i></li> <li>• Reduced aggregation in <i>E. coli</i></li> <li>• Reduced curli production in <i>E. coli</i></li> <li>• Increased adhesion in <i>E. coli</i></li> <li>• Microcolony formation earlier compared to wild type <i>E. coli</i> but reduced over time</li> </ul>	<ul style="list-style-type: none"> <li>• Reduced dye uptake with PA<math>\beta</math>N in <i>E. coli</i></li> </ul>
Tellurite methyltransferase	tehB	<ul style="list-style-type: none"> <li>• None</li> </ul>	<ul style="list-style-type: none"> <li>• More insertions in inhibitory acriflavine condition with PA<math>\beta</math>N vs acriflavine alone in <i>E. coli</i></li> </ul>	<ul style="list-style-type: none"> <li>• Reduced biofilm biomass in <i>E. coli</i></li> </ul>	<ul style="list-style-type: none"> <li>• Increased susceptibility to acriflavine (agar dilution) in <i>E. coli</i></li> </ul>



Glutathione metabolism	gshB	<ul style="list-style-type: none"> <li>• None</li> </ul>	<ul style="list-style-type: none"> <li>• More insertions in PA<math>\beta</math>N condition vs unstressed control in <i>E. coli</i></li> </ul>	<ul style="list-style-type: none"> <li>• Reduced biofilm biomass in <i>E. coli</i></li> </ul>	<ul style="list-style-type: none"> <li>• None</li> </ul>
Unknown	ykgJ	<ul style="list-style-type: none"> <li>• Reduced expression beneficial in 12h biofilm condition vs planktonic in <i>E. coli</i></li> </ul>	<ul style="list-style-type: none"> <li>• None</li> </ul>	<ul style="list-style-type: none"> <li>• Reduced biofilm biomass with PA<math>\beta</math>N in <i>E. coli</i></li> <li>• Increased aggregation in <i>E. coli</i></li> <li>• Increased filamentation after 24h and 48h growth in <i>E. coli</i></li> </ul>	<ul style="list-style-type: none"> <li>• Increased dye uptake in <i>E. coli</i></li> <li>• Reduced dye uptake with PA<math>\beta</math>N in <i>E. coli</i></li> </ul>
	yhcB	<ul style="list-style-type: none"> <li>• None</li> </ul>	<ul style="list-style-type: none"> <li>• More insertions in subinhibitory acriflavine condition with PA<math>\beta</math>N vs acriflavine alone in <i>E. coli</i></li> </ul>	<ul style="list-style-type: none"> <li>• Reduced biofilm biomass in <i>E. coli</i></li> </ul>	<ul style="list-style-type: none"> <li>• Reduced dye uptake with PA<math>\beta</math>N in <i>E. coli</i></li> </ul>
	ydeJ	<ul style="list-style-type: none"> <li>• None</li> </ul>	<ul style="list-style-type: none"> <li>• More insertions in subinhibitory acriflavine condition with PA<math>\beta</math>N vs</li> </ul>	<ul style="list-style-type: none"> <li>• Reduced biofilm biomass with and</li> </ul>	<ul style="list-style-type: none"> <li>• None</li> </ul>

			acriflavine alone in <i>E. coli</i>	without PAβN in <i>E. coli</i>	
ybjM	<ul style="list-style-type: none"> <li>• None</li> </ul>	<ul style="list-style-type: none"> <li>• More insertions in subinhibitory acriflavine condition with PAβN vs acriflavine alone in <i>E. coli</i></li> </ul>	<ul style="list-style-type: none"> <li>• Reduced biofilm biomass in <i>E. coli</i></li> </ul>	<ul style="list-style-type: none"> <li>• None</li> </ul>	
ybaA	<ul style="list-style-type: none"> <li>• None</li> </ul>	<ul style="list-style-type: none"> <li>• Increased expression beneficial in subinhibitory acriflavine condition vs unstressed control in <i>E. coli</i></li> </ul>	<ul style="list-style-type: none"> <li>• Reduced biofilm biomass in <i>E. coli</i></li> </ul>	<ul style="list-style-type: none"> <li>• Reduced dye uptake with PAβN in <i>E. coli</i></li> </ul>	

**10.5. APPENDIX 5: Biofilm and efflux phenotypes of all *E. coli* and *S. Typhimurium* deletion mutants relative to the wild type of each species.**

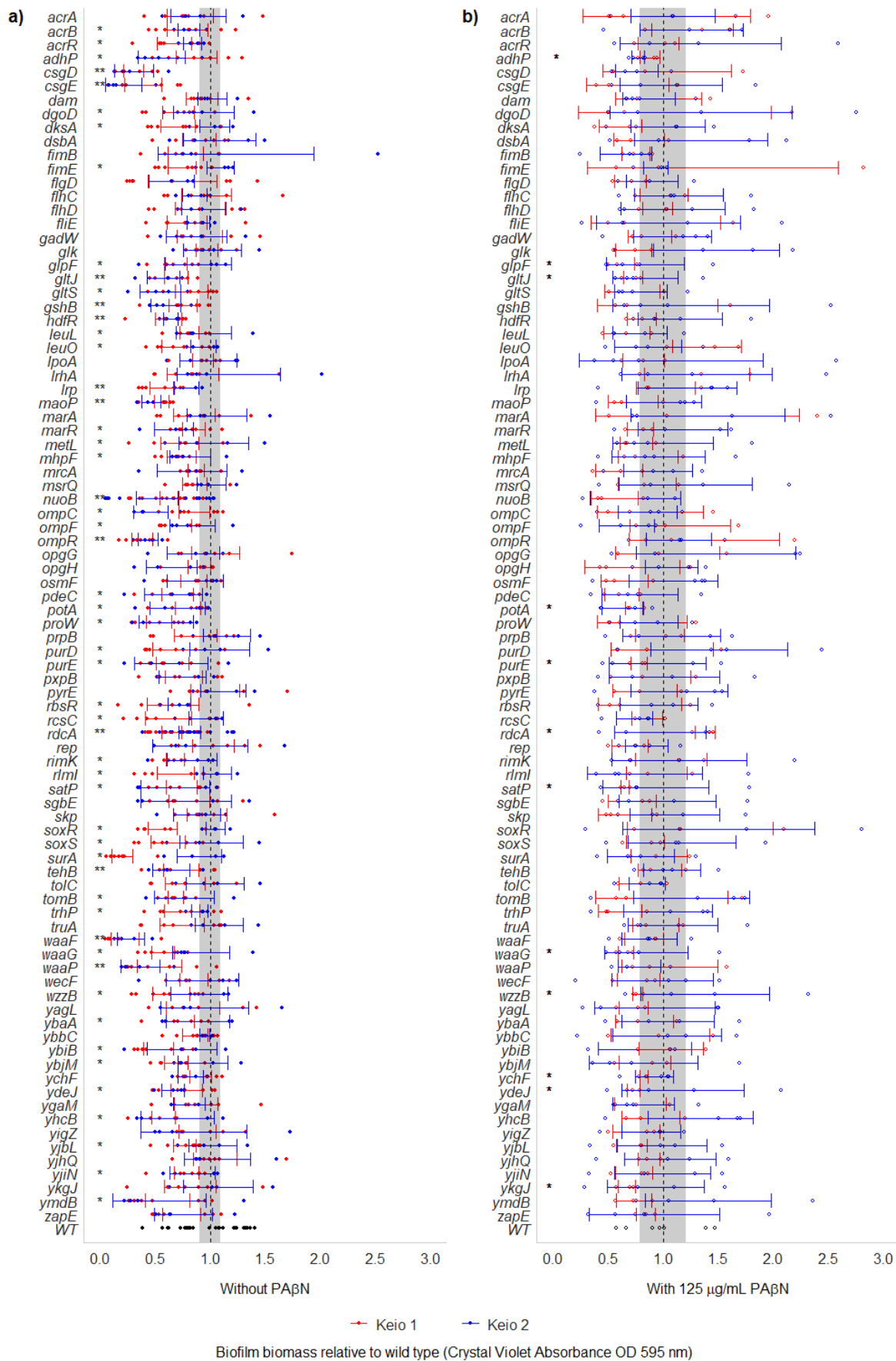


**Figure A1:** Biofilm biomass of knockout mutants relative to wild type *E. coli*, measured by crystal violet staining (OD<sub>590 nm</sub>) **a)** in stress free conditions and **b)** with PAβN, where each mutant copy is separated by colour. Two biological and a minimum of two technical replicates were performed for each mutant. Error bars show 95% confidence intervals, and the shaded area shows the 95% confidence interval of the wild type. Single asterisks (\*) represent a significant difference between one mutant copy and the wild type, and double asterisks (\*\*) denote a significant difference between both mutant copies and the wild type (Welch's *t*-test,  $p < 0.05$ ).

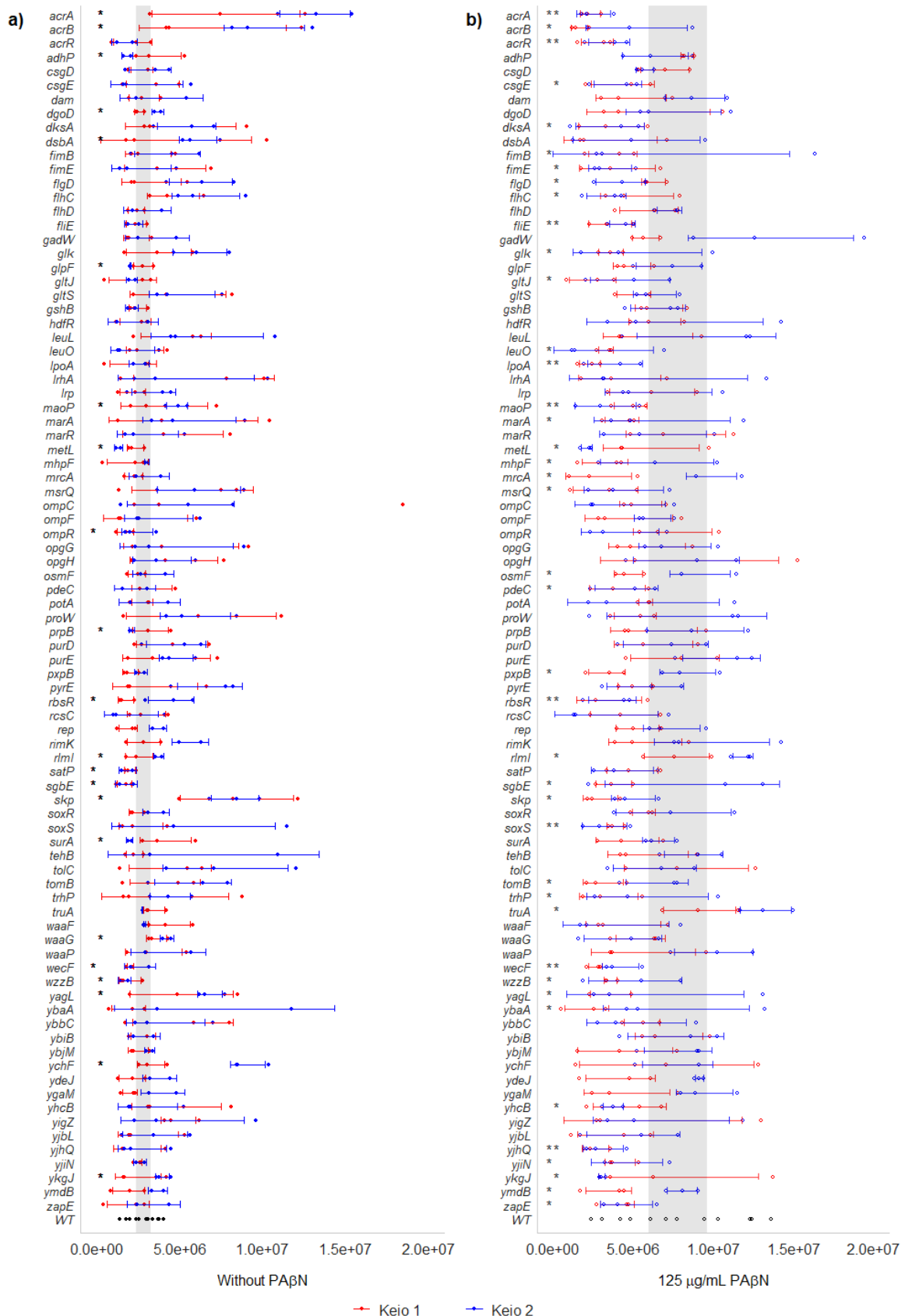


**Figure A2:** Dye accumulation in deletion mutants relative to wild type *E. coli*, where each copy of the deleted gene is separated by colour. Accumulation of resazurin (excitation 544 nm, emission 580 nm) was measured over 60 minutes and the area under the curve was plotted. Dye uptake was measured **a)** in stress-free conditions and **b)** with PA $\beta$ N. Points represent each of 3 independent replicates. Error bars show 95% confidence intervals, and the shaded area shows the 95% confidence interval of the wild type. Single asterisks (\*) represent a significant difference between one mutant copy and the wild type, and double asterisks (\*\*) denote a significant difference between both mutant copies and the wild type (Welch's *t*-test,  $p < 0.05$ ).

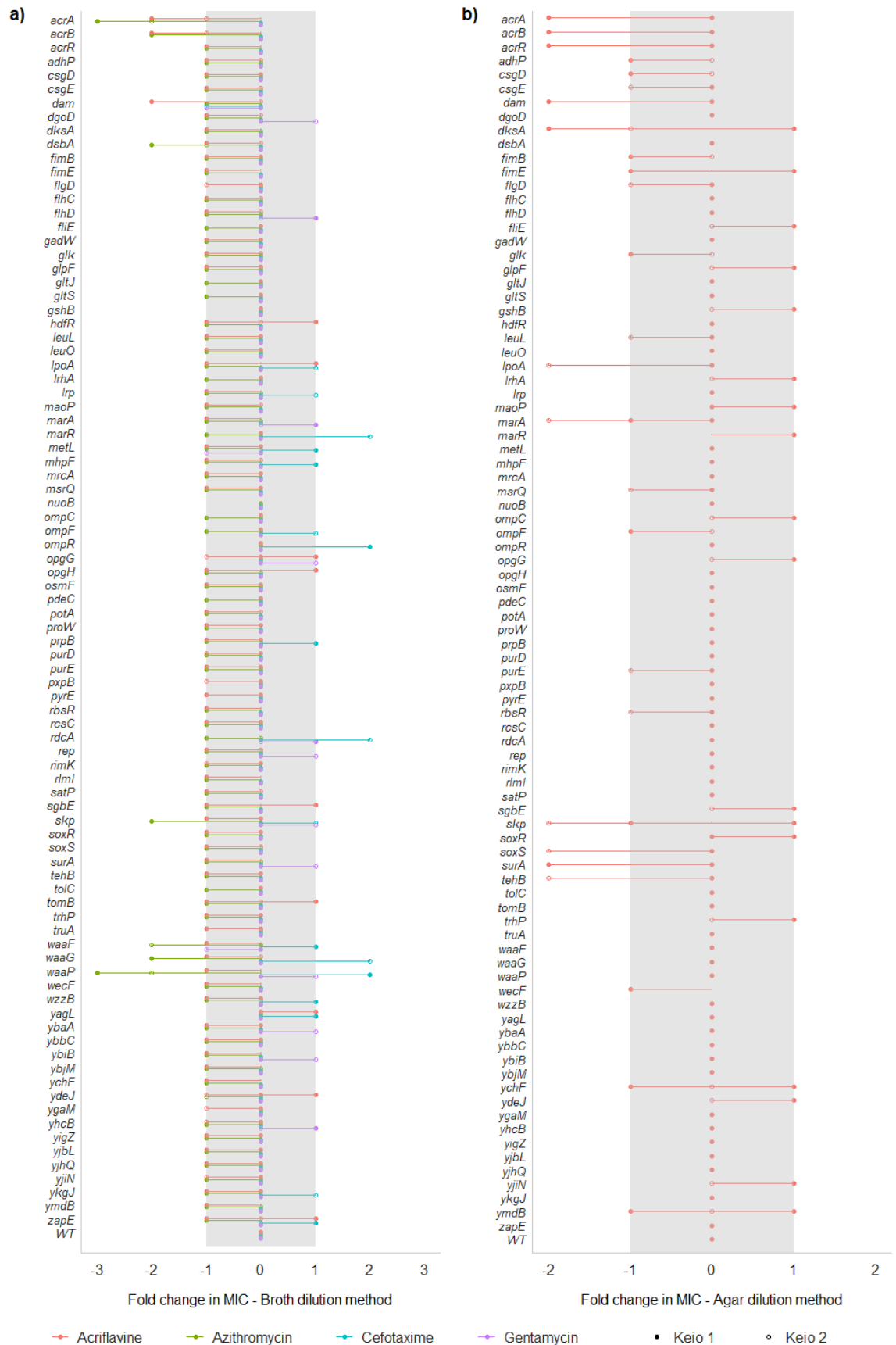


**Figure A3:** Fold change in MICs of acriflavine, azithromycin, cefotaxime and gentamycin in mutants from the Keio collection relative to wild type *E. coli*, measured by the **a)** broth and **b)** agar dilution methods. The shaded area shows an experimental error of 1-fold change and points show two independent replicates.

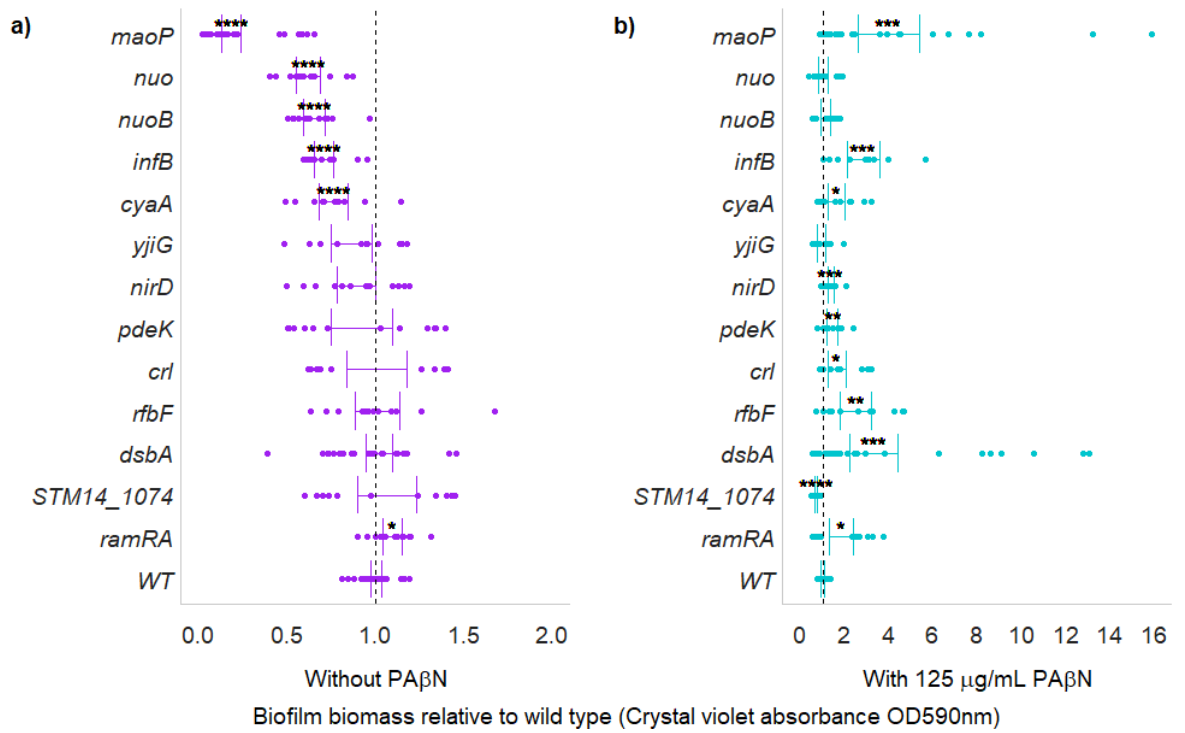
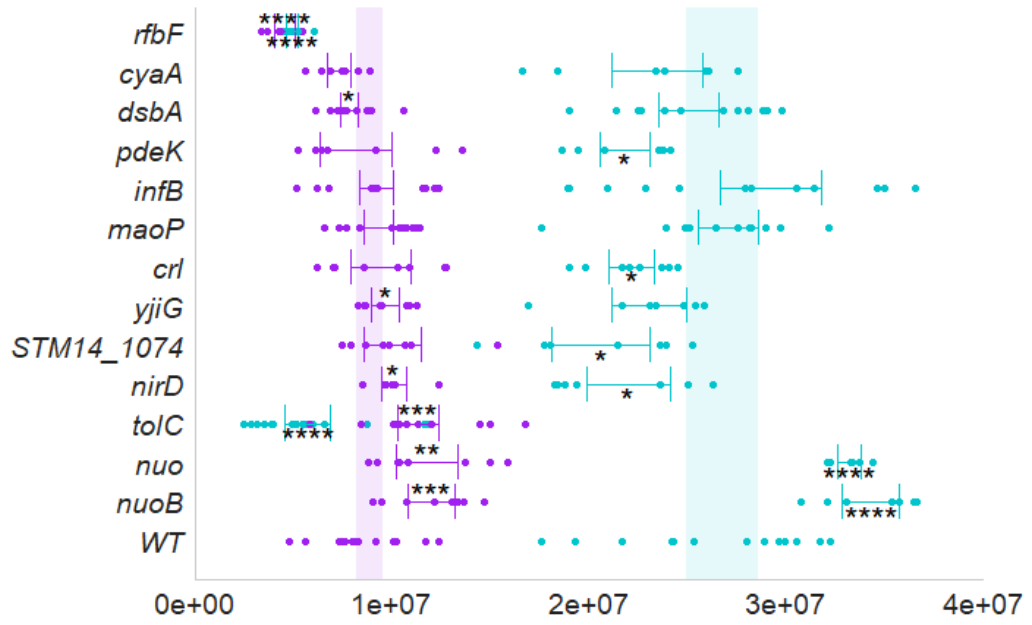


**Figure A4:** Biofilm biomass of knockout mutants relative to wild type *S. Typhimurium*, measured by crystal violet staining (OD<sub>590 nm</sub>) **a)** in stress free conditions and **b)** with PAβN. Two biological and six technical replicates were performed for each mutant. Error bars show 95% confidence intervals. Asterisks (\*) show a significant difference between the deletion mutant and the wild type (Welch's t-test, \* =  $p < 0.05$ ; \*\* =  $p < 0.01$ ; \*\*\* =  $p < 0.001$ ; \*\*\*\* =  $p < 0.0001$ ).



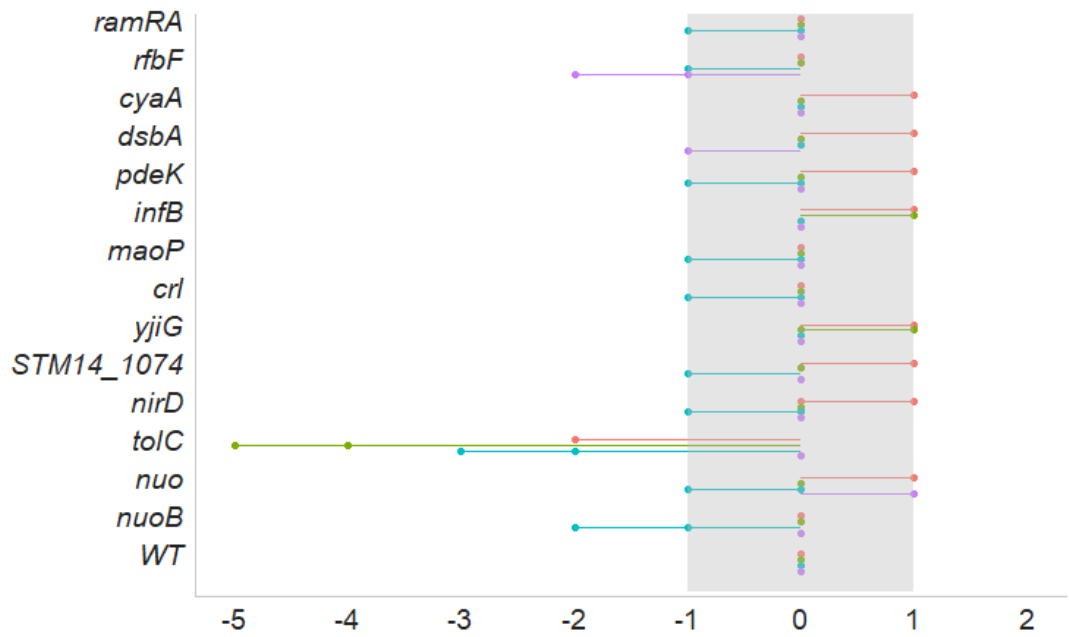
a)



Resazurin dye accumulation, measured by the area under the curve of fluorescence (ex=544nm,em=590nm) over 100 mins, normalised by OD600nm

— Without PA $\beta$ N    — With 125  $\mu$ g/mL PA $\beta$ N

b)



Fold change in MIC from WT

— Acriflavine    — Azithromycin  
— Cefotaxime    — Gentamycin

**Figure A5:** Efflux activity in *S. Typhimurium* deletion mutants and the wild type (WT) **a)** Dye accumulation in deletion mutants relative to the WT. Accumulation of resazurin (excitation 544 nm, emission 580 nm) was measured over 100 minutes and the area under the curve was plotted. Dye uptake was measured in stress-free conditions (purple) and with PA $\beta$ N (blue). Points represent each of two biological and four technical replicates. The shaded area shows the 95% confidence interval of the wild type and error bars show 95% confidence intervals of deletion mutants. Asterisks (\*) show where there is a significant difference in dye accumulation between the wild type and the deletion mutant (Welch's t-test, \* =  $p < 0.05$ ; \*\* =  $p < 0.01$ ; \*\*\* =  $p < 0.001$ ; \*\*\*\* =  $p < 0.0001$ ). **b)** Fold change in MICs of acriflavine, azithromycin, cefotaxime and gentamycin in deletion mutants relative to the WT, measured by the broth dilution method. The shaded area shows an experimental error of 1-fold change and points show two independent replicates.